Nicholas Tsoulfanidis *Editor*

Nuclear Energy

Selected Entries from the Encyclopedia of Sustainability Science and Technology

Springer

Nuclear Energy

This volume collects selected topical entries from the *Encyclopedia of Sustainability Science and Technology* (ESST). ESST addresses the grand challenges for science and engineering today. It provides unprecedented, peer-reviewed coverage of sustainability science and technology with contributions from nearly 1,000 of the world's leading scientists and engineers, who write on more than 600 separate topics in 38 sections. ESST establishes a foundation for the research, engineering, and economics supporting the many sustainability and policy evaluations being performed in institutions worldwide.

Nicholas Tsoulfanidis
Editor

Nuclear Energy

Selected Entries from the Encyclopedia of Sustainability Science and Technology

Springer

Editor
Nicholas Tsoulfanidis
Nuclear Technology Editor
Reno, NV, USA

This book consists of selections from the Encyclopedia of Sustainability Science and Technology edited by Robert A. Meyers, originally published by Springer Science+Business Media New York in 2012.

ISBN 978-1-4614-5715-2 ISBN 978-1-4614-5716-9 (eBook)
DOI 10.1007/978-1-4614-5716-9
Springer New York Heidelberg Dordrecht London

Library of Congress Control Number: 2012953698

Printed on acid-free paper

Springer is part of Springer Science+Business Media (www.springer.com)

Contents

Chapter 1
Nuclear Energy, Introduction

Nicholas Tsoulfanidis

In terms of technical progress of the human species/society, the second half of the twentieth century is marked by two developments: the computer and nuclear energy. And the two are related since progress in the development and applications of nuclear energy owes a lot to the power of computations made possible by the digital computer.

The whole twentieth century is marked by the ever-increasing use of electricity. The century started with a tiny amount of electricity use and ended with ~30% of the total energy consumed to be in the form of electricity.

Nuclear energy, unfortunately, was released in the world as a weapon. But, fortunately, after the initial shock of Hiroshima and Nagasaki, nuclear energy turned out to be of great benefit to society. First, in a "Faustian bargain," of sorts, the existence of nuclear weapons resulted in having a *cold war* between the two superpowers of the time (Soviet Union and the USA) instead of a *hot one*. Second, nuclear energy proved to be an excellent method of generating electricity and also provided the means for numerous applications in industry, science, education, and probably most of all medicine. Not even the fiercest critics of nuclear energy deny the benefits of nuclear medicine in correct diagnosis and therapy and, therefore, prolongation of life for millions of people all over the world.

Although, as mentioned above, nuclear energy touches today beneficially many aspects of our lives, the most prominent application is the generation of electricity by using nuclear fission reactors to generate heat that is used to produce steam (or hot gas) that runs a turbo generator and produces electricity. There are many advantages in using nuclear energy for the generation of electricity. Primary among them is the absence of green house gases and other pollutants such as sulfur oxides, nitrogen oxides, heavy metals (mercury etc.).

This chapter was originally published as part of the Encyclopedia of Sustainability Science and Technology edited by Robert A. Meyers. DOI:10.1007/978-1-4419-0851-3

N. Tsoulfanidis (✉)
Department of Nuclear Energy, Missouri University of Science and Technology, Rolla, MO, USA
e-mail: nucpower@sbcglobal.net

N. Tsoulfanidis (ed.), *Nuclear Energy: Selected Entries from the Encyclopedia of Sustainability Science and Technology*, DOI 10.1007/978-1-4614-5716-9_1,

Probably, the most important difference between nuclear and fossil or any renewable fuels is the concentrated energy release of the former. The fission of one U nucleus releases $\sim 200 \times 10^6$ eV; the burning of one atom/molecule in a chemical reaction releases a few eV; a ratio of many million! A single pellet of nuclear fuel, about the size of a fingertip, contains as much energy as 1,700 ft^3 of natural gas, or 1,780 lb of coal, or 149 gal of oil. As a result of this concentrated energy, the "ashes" of the process, the fission products that are radioactive, constitute a, relatively, small volume. Yes, they have to be safeguarded and be kept away from the biosphere for thousands of years, but the volume of wastes is considered manageable.

Today (2011), there are 441 nuclear power plants operating in the world amounting to a total generating capacity of 375 GWe. The top five countries, in terms of number of operating plants are the USA (104), France (58), Japan (54), Russia (32), and Korea (21). In 2010, there were 62 plants under construction amounting to a capacity of 60.2 GWe. The top countries in numbers of plants under construction are China (25), Russia (11), Korea (5), and India (4); two plants under construction are in the USA, Japan, Bulgaria, Slovakia, and Ukraine.

- Today, ~16% of the electricity worldwide is produced by nuclear power plants; that fraction will increase in the coming years as developing economies (e.g., China and India) and developed ones (Korea, Japan, and Europe) complete their announced ambitious nuclear expansion in order to satisfy their ever-increasing demand for electricity. The World Nuclear Association (WNA) projects that by 2060 at least 1,100 GWe of new nuclear capacity will be added.

What drives this "Nuclear Renaissance"? There are several factors:

1. *Increasing energy demand*: Due to an ever-increasing population and desire of the underdeveloped countries to improve their standard of living. In addition, a need for new plants materializes because old plants reach the end of their life and must be shut down (all types of electricity generating plants, not only nuclear, are designed with a finite operational life).
2. *Climate change concerns*: Increased awareness that fossil fuels release a large amount of greenhouse gases that may lead to a planetary climate change are driving decisions for new plants to be "green," that is, to emit reduced amounts of greenhouse gases and other pollutants or not at all. Nuclear power plants are the only ones generating electricity with, essentially, zero emissions.
3. *Economics*: The main cost component of a nuclear plant is its construction cost; once this cost is overcome, the other two cost components for the generation of electricity (O&M and fuel) favor nuclear over fossil plants. Experience during the past 50 years, especially in the USA, has shown that nuclear is the best plant for generation of base load electricity, both in terms of cost and reliability.
4. *Fuel price stability*: Because the fuel cost constitutes a, relatively, small fraction of the total cost of generating electricity (for nuclear the main cost is the construction cost; fuel cost is between 10% and 16% of the total cost), even if the price of fuel doubles, the effect on the cost of electricity will be minimal.

It should be noted that the cost components of the fuel are uranium, conversion, enrichment, fabrication-transportation; of these, only the uranium price fluctuated during the previous 50 years; the cost of the other components has been remarkably stable.

5. *Security of Fuel Supply*: Supply of fossil fuels (oil, gas, and coal) is vulnerable to interruptions of supply due to political turmoil, strikes, weather, etc. On the contrary, uranium is plentiful and available at reasonable prices, for the foreseeable future; more than that, since nuclear plants refuel every 2 years, it is quite likely that short-term upheavals can be settled before they have an effect on nuclear fuel supply.
6. *Nuclear Safety and Public acceptance*: The safety record of nuclear power plants during more than 50 years of operation (195702011) is outstanding. There were three accidents during that period. The TMI accident in the USA in 1979: it was a financial loss to the company operating the plant; not a single injury resulted to any person in or out of the plant and there was no contamination of the environment. The Chernobyl accident in 1986 was a very serious accident: radioactivity was released to the environment and 33 persons are known to have died, mostly firefighters. Some cancers will develop as a result of exposure to the radiation from the accident, making it a difficult task to quantify them. One should note, however, that no plant licensed anywhere today can have the Chernobyl type of accident; it is physically impossible (the Chernobyl design has been abandoned). Considerable area around the plant has been contaminated, but the reports today (2011) indicate that life is returning to normal. On March 11, 2011 a 9.1, Richter scale, earthquake hit Japan and affected the Fukushima nuclear site. There are six reactors on that site. On that day, two reactors were shut down and were not affected by what followed. When the quake hit, the four operating plants shut down, as design dictated. Shutting down means that the fission reaction is stopped; however, heat continues to be generated in the core from fission products, hence cooling must be provided. As per design, cooling continued using emergency diesel generators required by regulation and readily available for such eventuality. Then, 15–20 min later, the tsunami arrived; the waves of the tsunami swept away generators and their fuel supply and cooling of the core was lost. Fuel meltdown of the cores occurred and radioactivity was released to the environment. Two plant workers were killed by the tsunami; these are the only immediate deaths as a result of this event. The tsunami itself and the earthquake resulted in the death of ~22,000 people. The area around the site was contaminated. Definitely the accident was a tremendous financial loss to the company operating the Fukushima plants.

   As a result of the accident at Fukushima, two plant workers were killed by the tsunami; these are the only immediate deaths as a result of this event. At Chernobyl, ~33 persons, mostly firefighters, were the reported immediate deaths. Of course as a result of TMI, no deaths occurred; in fact in the USA there are zero deaths from the operation of commercial nuclear power plants from 1957 until today. Compare this, for example, to coal mining fatalities which

amount to ∼30/year in the USA; in other countries, e.g., China, the direct annual death toll from coal mining is much higher.

Without trying to deemphasize the importance of these three accidents, the net effect is that the world community still recognizes and accepts the generation of electricity using nuclear fission reactors as an indispensable component in the energy portfolio. At about 9 months after the Fukushima accident, there is no report of any country changing nuclear energy policy because of that accident (with the exception of Germany that decided to accelerate the shutdown of its nuclear fleet following a decision taken earlier by its Government). Overall acceptance of nuclear technology is the result of its excellent performance; another factor in favor of nuclear power is the lack of greenhouse gases by this technology or of any environmental effect in the vicinity of the plant. In the USA, acceptance of nuclear power by communities around the plant is ∼70% or more favorable.

The nuclear industry, especially in the USA, learned and improved a lot after the TMI accident. I have no doubt that the international nuclear community will apply the lessons learned from Fukushima to make the already safe record of this industry even safer.

This section on Nuclear Energy consists of 19 articles that cover all aspects of the nuclear enterprise. Here is a brief description of each article:

A. *Radiation sources*: It discusses radioactivity and basic radiation sources.
B. *Radiation detection devices*: One characteristic of radioactivity is the fact that it can be detected relatively easily and accurately. This article discusses the devices used to accomplish such measurements.
C. *Dosimetry* and *Health Physics*: Very early in the twentieth century (1920s), it was realized that ionizing radiation may be harmful to humans, therefore measures must be taken to protect people. These measures were based on (a) quantifying the effects of radiation exposure by establishing units of radiation dose and means to measure it and (b) establishing professional bodies that set protection standards [ICRP (1928), NCRP (1964) etc.]. The field of Health Physics was thus born resulting in great benefit for the radiation workers.
D. *Fission reactor physics*: Fission reactors are the major sources of production of radioactive materials. What are the principles of their operation? What are the foundations of their safe operation? These are two of the major items discussed in this article.
E. *Nuclear fuel cycles*: Providing nuclear fuel for a fission reactor is not a simple or straightforward task; it involves many steps (U procurement, conversion, enrichment, fuel rod and assembly fabrication). The users of the fuel are presented with choices, such as discarding the irradiated fuel as waste or reprocessing and recycling it. Also, reactor designers may affect the nuclear fuel "cycle" by building reactors that just produce electricity, or combine electricity production with generation of new fuels (breeders), or generate electricity in combination with burning some of the nasty by-products of the fission process. These are the matters discussed in this article.

F. *Uranium reserves and mining*: How much uranium is there on our planet and at what price? Where is it found? How is it extracted? These are the topics of this article.
G. *Nuclear fission power plants*: Once the fission reactor is designed and ready to operate, how is the fission energy utilized to generate electricity? The reactor core itself is not enough; plenty of other components must operate for the successful transformation of energy released in fission to electricity feeding a lightbulb. The fission reactor core makes a small part of a nuclear power plant. It is this aspect of nuclear power, components and activities outside the core, that is described in this article.
H. *Nuclear reactor materials and fuel*: For a successful and long-term safe operation of a nuclear power plant, the materials used, especially those directly tied to the fuel, must function as designed (as expected) in the very hostile environment of a nuclear fission core. This article describes the pros and cons of the various materials that have been considered and the final choices made.
I. *Nuclear safeguards and proliferation of nuclear weapons materials*: Of great concern to human kind is the acquisition of nuclear materials by groups or governments that may use them to make nuclear weapons, contrary to international treaties. This "proliferation" or rather "nonproliferation" of nuclear materials and possibly weapons is a concern that will never disappear; all that can be done by the international community of nations is to set up treaties, policies, and procedures that diminish the probability of proliferation. It is these aspects of this terrible problem facing humanity that are discussed in this article.
J. *Radiation shielding and protection*: This article is complementary to articles A–C. Having discussed radiation sources, dangers from radiation, and standards of protection, how does one provide the means for a safe radiation environment for the workers and the public? How are relevant computations performed? Measurements? How is an effective radiation shield designed? These are the questions answered in this article.
K. *Isotope separation methods for nuclear fuel*: The two elements found in nature that may be considered as fuels for fission reactors are Th and U. Unfortunately, only certain isotopes of these elements or made with the help of these elements can be manufactured into fuels. Hence, isotope separation methods must be employed for the production/concentration of the "useful isotope(s)." These methods are discussed in this article.
L. *Reprocessing of nuclear fuel*: Irradiated fuel contains many useful isotopes, primarily U and Pu. Reprocessing is the operation that extracts the useful isotopes from the irradiated (spent) fuel. The reprocessing methods used until today and those under research and development are discussed in this article.
M. *Decommissioning of nuclear facilities*: Every nuclear facility has a finite lifetime; at the end, when operations stop for good, the law says that the site must, eventually, be returned to its preoperational state in terms of the presence

of radioactivity. This is what decommissioning means. All the tasks associated with decommissioning are discussed in this article.

N. *Radioactive waste management*: Storage, transport, disposal. The operation of fission reactors results in the production of radioactive materials. Such materials, if they have no further use, they must be safeguarded for long periods of time in order that their release to the biosphere may be prevented. The method of eventual disposal of such materials considered today by their producers is placement in a geologic repository. In the meantime, radioactive wastes must be stored and transported. These activities are discussed in this article.

O. *GEN-IV reactors*: By any measure, current fission reactor designs are successful. However, there is room for improvement in terms of fuel utilization, thermal efficiency, use of the heat generated by the energy released in fission, multifunction of a nuclear plant, etc. There is considerable global effort underway to design fission reactors that will show some, if not all, of the improvements just mentioned. These new designs, collectively named as GEN-IV reactors, are described in this section.

P. *Nuclear fusion*: Fusion reactors offer many advantages over fission reactors. Unfortunately, although fusion became known to man before fission and life on earth owes its existence to a fusion reactor in the sky (our Sun), no fusion plant has been built yet; fusion reactors present some unique challenges/difficulties that have not been resolved yet. But, the world's scientific community is working as a team in an effort to resolve the issues and build an operational fusion plant sometime in the future. All the past and current efforts in fusion research and the expected future developments are presented in this article.

Q. *Nuclear power economics*: In a free market, every plant generating electricity must compete economically with all other options; nuclear is no exception, of course. Nuclear power presents some unique problems, with respect to financing, and these are the problems (and possible solutions) discussed in this article.

R. *Thorium – An excellent 'fertile' nuclear fuel*: In addition to Uranium, Thorium (Th) is the only other element found on earth that can be used as a fuel in fission reactors. The Th properties, relevant to fission reactors, resources, availability and prices are discussed in this article.

Chapter 2
Fission Reactor Physics

Michael Natelson

Glossary

Fissile	Fissile isotopes are fissionable by the capture of neutrons of any energy, but are especially easily fissioned by the capture of slow neutrons, for example, U^{233}, U^{235}, Pu^{239}, and Pu^{241}.
Fertile	Fertile isotopes may be transmuted into fissile isotopes by neutron capture. The naturally occurring fertile isotopes are Th^{232} and U^{238}.
Critical	A critical fission reactor is in a steady state, with its neutron population sustained by a chain reaction.
Reactivity	Reactivity is a dimensionless parameter, which characterizes how far from critical a fission reactor is. If zero, the reactor is critical; if positive, the reactor is supercritical and its neutron population is increasing; if negative, the reactor is subcritical.
Microscopic cross section	A microscopic cross section is a parameter, with dimensions of area, that is a measure of the probability of a particular reaction resulting from an incident particle on a target nucleus. The *macroscopic cross section* for this "particular" reaction is the microscopic cross section times the number density of the target nucleus.

This chapter was originally published as part of the Encyclopedia of Sustainability Science and Technology edited by Robert A. Meyers. DOI:10.1007/978-1-4419-0851-3

M. Natelson (✉)
Retired from the Bettis Atomic Power Laboratory, West Mifflin, PA, USA
e-mail: MNatelson@aol.com

N. Tsoulfanidis (ed.), *Nuclear Energy: Selected Entries from the Encyclopedia of Sustainability Science and Technology*, DOI 10.1007/978-1-4614-5716-9_2,

Definition of Subject

At the end of the nineteenth century and through the first half of the twentieth century, revolutionary discoveries were made in physics, and the laws of physics and our understanding of them were greatly expanded. In addition, tragic historical events led to an unprecedented concentration of intellectual talent and economic resources (the Manhattan Project) that allowed the new physics to be applied to the engineering of nuclear (fission) reactors. This entry will describe the advances in physics, which are key to fission reactor design, and how they enable this engineering practice.

Introduction

In 1900, Lord Kelvin (William Thomson) reportedly told the British Association for the Advancement of Science that "there is nothing new to be discovered in physics now. All that remains is more and more precise measurements." Whether he actually said this or not, it is reasonable to believe that many scientists and engineers of his day would have concurred. Newton's definitions and laws of mechanics and optics had long been successfully applied. Maxwell's equations, Ohm's law, etc. seemed to describe electricity and magnetism. Boltzmann and Gibbs had provided the foundations of statistical mechanics and thermodynamics. And chemists had been busy developing atomic theory, identifying 92 elements, the laws of chemical combination, the weights and sizes of atoms and molecules, and the periodic system.

With hindsight it is clear, however, that in 1900 there were many intriguing questions outstanding in the physical sciences, and there was an historically large cohort of scientists, being produced by the major universities of the day, ready to address them. The questions (and their resolutions) of prime importance to "fission reactor physics" are:

1. Does a theory of relativity apply to Maxwell's equations, and is there a unique frame of reference (ether) for the propagation of light?
2. Why are the heaviest naturally occurring elements unstable, giving off various forms of "radiation" and transmuting to different elements?
3. What does the quantization of electromagnetic radiation (required to describe black body radiation energy spectra and the photoelectric effect) mean to the laws of physics on the atomic scale?

The resolution of each of these questions will be discussed in this entry, as they are the starting points for the accumulation of knowledge needed to characterize the workings of fission reactors.

Clearly, Einstein's Theory of Relativity addressing question (1), and its identification of mass as a form of energy (1905) would, excuse the bad pun, energize

the whole effort. Already in 1914, H. G. Wells in his novel "The World Set Free" envisioned industrial atomic energy and atomic bombs used in a catastrophic world war.

At the end of the nineteenth century, electrochemists looking for heavy elements (heavier than lead and bismuth) found that "radiation" was given off by the materials they were investigating. Becqueral (1896) observed γ rays (penetrating electromagnetic radiation similar to x-rays) from uranium salts. The Curies (1898) observed α and β rays from polonium and radium. Rutherford showed that the positively charged αs were doubly ionized helium atoms. The βs are negatively charged electrons, the same particles as the cathode rays that Thomson characterized and named (1897). These "radiations" proved to be key tools for determining the structure of atoms. The α particle was shown by Rutherford (1911) and his coworkers to scatter from gold foil in a manner inconsistent with the atomic model of the day, Thomson's *raisins* (electrons) *in the pudding* (positive charge medium) model. To explain the α scattering results, an atom's positive charge and its mass, minus that of its electrons, needed to be concentrated in a small nucleus (radius $\sim 10^{-12}$ cm), with its electrons distributed over a much larger volume (radius $\sim 10^{-8}$ cm), that of the whole atom. Niels Bohr, inspired by Rutherford's work, took to determining the *distribution* of atomic electrons. His success, building off Question (3) above, led to quantum mechanics. A complete model for the atom, however, still required an explanation for the mass of the nucleus. Again bombardment of various atoms (elements) with α particles led to the answer. Chadwick (1932) proved that the "rays" produced by αs striking beryllium nuclei were neutral particles with mass slightly greater than the hydrogen nucleus, the proton. These neutral particles are the neutrons that had been hypothesized by Rutherford 12 years earlier. Heisenberg (1932) produced a detailed model of the atomic nucleus where the mass number A is the total number of elementary particles, protons plus neutrons, making up a nucleus, and the nuclear charge is Z, the number of protons. Thus, there can be various *isotopes* for a given element, more than one A for a given Z.

The discovery of the neutron marked the start of furious activity, culminating in the operation of the first fission reactor only 10 years later. Leo Szilard in 1933 recognized that a neutral neutron with modest kinetic energy could penetrate an atomic nucleus and cause a reaction releasing nuclear (mass) energy, and if, as part of the "reaction," additional neutrons were produced, a chain reaction could result. Szilard produced a patent for a reactor based on this idea and assigned it to the British Government in 1936 (before fission was discovered). In 1934, Fermi was using neutron bombardment (with neutrons of various energies) to produce nuclear transformations in many elements. Of special interest was the production of trans-uranic elements, Z greater than 92. Fermi won the 1938 Nobel Prize for this work. However, unknown at the time, he had also fissioned uranium. This was determined by electrochemical analysis of the products of neutron bombardment of uranium by Hahn and Strassmann. Subsequently, the process was identified as *fission* by Meitner and Frisch. Bohr recognized that the ease with which low energy neutrons could cause fission of uranium was due to the existence of the naturally occurring,

but low atom percent (0.72%), isotope $_{92}U^{235}$ [1] (Various notations have been used to designate a particular isotope, for example, for uranium with mass number (A) 235; $_{92}U^{235}$, U235, and $^{235}_{92}U$. The latter is in common use today. For ease of composition and for consistency with most of the references used in this entry the older standard, A as a right superscript, is used.). He and Wheeler, from their Theory of Fission [2], also recognized that the not yet produced isotope $_{94}Pu^{239}$, would also be readily fissioned by slow neutrons [3]. This was in early 1939. Bohr still did not think production of a fission bomb to be feasible.

Leo Szilard was, however, not deterred. He persuaded his friend Albert Einstein to write President Roosevelt (8/2/1939), urging government support of fission research and the stock piling of uranium. This ultimately led to the Manhattan Project. In 1940, Seaborg and McMillan synthesized the readily fissionable isotope of plutonium, $_{94}Pu^{239}$, which is produced by neutron capture in the dominant uranium isotope $_{92}U^{238}$. Wheeler credited Louis Turner [3] with pointing out that kilogram quantities of $_{94}Pu^{239}$ could be produced in a large fission chain reaction reactor. Fermi and Szilard [4] designed and built the prototype for such a reactor, a "pile" of graphite blocks containing an array of natural uranium pellets. It was constructed in a squash court under a grand stand of the University of Chicago's Stagg Field, and went *critical* (sustained a chain reaction) on December 2, 1942. The Manhattan Project built large reactors of this type for weapons material production, and also successfully pursued means of enriching uranium in $_{92}U^{235}$. Enriched uranium allows more compact, higher power density, reactor designs.

The Manhattan Project brought together extraordinary scientific and engineering talent, and immense resources to produce the weapons that ended the Second World War. It also provided the foundation for all fission reactor development that has followed. The subsequent advances in "physics," which have contributed to this development, are principally:

1. The full understanding of the interaction of neutrons with nuclei: scattering (elastic and inelastic), and capture (simple absorption, transmutation, and fission), including measuring the parameters that characterize the probabilities of these "interactions"
2. The formulation of methods to solve the neutron transport (Boltzmann) equation, which governs the behavior of the dilute "gas" of neutrons in a fission reactor

This entry will discuss the topics, pre- and post-Manhattan Project, which encompass the physics of fission reactors.

Mass–Energy Relationship

In his initial paper [5] on the theory of relativity, Einstein confronted the problem of guaranteeing that the laws of electromagnetism (Maxwell's equations) apply in all inertial reference frames, just as the laws of mechanics do. In an inertial reference

frame, an object, which is at rest, remains at rest and an object traveling with a particular velocity will maintain that velocity. Einstein asserted that there is no preferred reference frame (like stationary *ether* in space, as postulated years earlier), and that the speed of light c, in vacuum, 2.998×10^8 m/s, is the same in all inertial reference frames. From these assertions, Einstein derived transformations for various variables in the laws of physics from one inertial reference frame to another. This solved the "electromagnetism" problem and provided a firm grounding (theory) for phenomena observed when velocities approach the speed of light. For examples of the latter, see Kaplan, "Nuclear Physics" on the charge-to-mass ratio of the electron as a function velocity, and Mermin, "It's About Time," on the half-life of unstable particles as a function of their velocity. Our interest here is specifically on the relationship between mass and energy resulting from the special (not applying to gravity) theory of relativity. What is meant by the ubiquitous formula.

$$\mathrm{E} = \mathrm{Mc}^2? \tag{2.1}$$

For application to fission, an inelastic collision between two particles will be treated for relativistic conditions. The approach presented by Mermin in "It's About Time" will be used.

In an elastic collision, total momentum, $\mathbf{P} = \mathbf{p_1} + \mathbf{p_2}$, mass, $\mathrm{M} = \mathrm{m}_1 + \mathrm{m}_2$, and kinetic energy, $\mathrm{K} = \mathrm{k}_1 + \mathrm{k}_2$ are all conserved, where the mass, m, is an inherent property of a particle and is a measure of how it resists a change in its velocity. In an inelastic collision, only total momentum, **P** needs to be conserved. It needs to be conserved, however, in all inertial frames of reference. For relativistic conditions, one defines a particle's momentum (a vector [in bold face]) as

$$\mathbf{p} = \mathrm{m}\mathbf{u}/(1 - \mathbf{u}^2/\mathrm{c}^2)^{1/2}, \tag{2.2}$$

where **u** is the particle velocity. As is required for consistency between relativistic and nonrelativistic laws of mechanics, Eq. 2.2 is effectively the nonrelativistic definition of momentum for the particle speed, $\mathrm{u} << \mathrm{c}$. Now to find $\mathbf{p}'$, the particle momentum, in a frame moving with velocity **v** relative to the frame in which the particle has velocity **u**, one applies the relativistic translation law for velocities:

$$\mathbf{u}' = (\mathbf{u} - \mathbf{v})/(1 - \mathbf{u}\mathbf{v}/c^2). \tag{2.3}$$

Substituting for $\mathbf{u}'$ in the expression for $\mathbf{p}'$ (Eq. 2.2 with **p** and **u** primed), one obtains the relativistic translation law for momentum

$$\mathbf{p}' = (\mathbf{p} - p^0\mathbf{v})/(1 - \mathbf{v}^2/\mathrm{c}^2)^{1/2}, \tag{2.4}$$

where

$$p^0 = \mathrm{m}/(1 - \mathbf{u}^2/\mathrm{c}^2)^{1/2}. \tag{2.5}$$

Now, if total momentum is to be conserved in our two-particle inelastic collision in both the primed and unprimed frames, then $P^0 = p^0{}_1 + p^0{}_2$ must also be conserved. Again, using the relativistic translation law for velocities (Eq. 2.3) and the definition p^0 (Eq. 2.5), we find that

$$p^{0'} = (p^0 - \mathbf{pv}/c^2)/(1 - \mathbf{v}^2/c^2)^{1/2}. \tag{2.6}$$

And so for the *total* quantities we want to be conserved we have

$$\mathbf{P}' = (\mathbf{P} - P^0\mathbf{v})/(1 - \mathbf{v}^2/c^2)^{1/2} \quad \text{and} \tag{2.7}$$

$$P^{0'} = (P^0 - \mathbf{Pv}/c^2)/(1 - \mathbf{v}^2/c^2)^{1/2}. \tag{2.8}$$

Examining these expressions, it is clear that if $\mathbf{P}$ and P^0 are not changed after an inelastic (or elastic) collision, then neither is $\mathbf{P}'$ and $P^{0'}$.

In the limit of the speed u being much smaller than c, the difference between p^0 and m, $(p^0 - m)$, approaches $mu^2/2c^2$. This result leads to a definition of relativistic kinetic energy, k, for a particle

$$k = p^0c^2 - mc^2, \tag{2.9}$$

which has the required property of reducing to the nonrelativistic form, $mu^2/2$, in the limit of u much smaller than c.

Returning to our two-particle inelastic collision, as $\mathbf{P}$ is conserved so is P^0c^2 and thus from Eq. 2.9

$$\Delta Mc^2 = \Delta K, \tag{2.10}$$

where ΔM is the change in the masses of the inputs and outputs of the collision participants, and ΔK is the change in the kinetic energies of these "inputs and outputs." Thus, Eq. 2.10 provides insight into the meaning of "$E = Mc^2$" for the fission process. For $n + {}_{92}U^{235} \mapsto$ fission products + 202.7 MeV (the ΔK of Eq. 2.10 in unit of millions of electron volts) the percent change in mass can be estimated by dividing 202.7 MeV by the energy equivalents of the inputs (i.e., 236 amu, where 1 amu = 931.141 MeV). The result is ~0.1%, which may not appear to be large until one makes a comparison with a chemical reaction. For example, $O_2 + C \rightarrow CO_2 +$ 4.1 eV. A similar calculation indicates a 1×10^{-8}% conversion of mass to kinetic energy. Since one could not measure such a small change in total input and output masses in chemical reactants, it is not surprising that the full impact of "$E = Mc^2$" had to await demonstration in a nuclear reaction like fission. However, as will be discussed in the next three sections, the large energy release in fission, while conforming to Eq. 2.10, is due to the strength of the forces that hold a nucleus together and the charge repulsion forces that will accelerate two smaller nuclei as they are formed in the fissioning of a larger "parent" nucleus.

Heavy Elements

The "heavy elements" of particular importance to fission reactors are the radioactive nuclei, which are characterized by systematic chains of decay. In nature, there are three chains (series). In a given series, each nucleus has a *mass number*, A, governed by a simple formula with the variable the integer n (see Table 2.1), and is identified with its longest lived isotope, that is, Thorium, Uranium, and Actinium (U^{235} had not been discovered when the 4n + 3 series was identified). These *longest half-lives* are not surprisingly comparable to the age of the earth, 4.5×10^9 years. Half-life is one of three related parameters of radioactive decay processes, $T_{1/2}$, λ, and τ. The fundamental equation of radioactive decay is

$$-\mathrm{dN(t)/dt} = \lambda \mathrm{N(t)}, \tag{2.11}$$

where λ is the *decay constant*, and N(t) is the number of decaying nuclei at time t. The solution of Eq. 2.11 is

$$\mathrm{N(t)} = \mathrm{N(0)e}^{-\lambda \mathrm{t}}. \tag{2.12}$$

The time when an original inventory of decaying nuclei, N(0), is halved is

$$T_{1/2} = \ln 2/\lambda = 0.693/\lambda. \tag{2.13}$$

And as the decay process is statistical the *mean life-time*, τ, of a decaying nucleus is

$$\tau = (1/\mathrm{N(0)}) \int_0^\infty \mathrm{N(0)}\lambda \mathrm{te}^{-\lambda \mathrm{t}}\, \mathrm{dt} = 1/\lambda, \tag{2.14}$$

the reciprocal of the decay constant.

With the search for transuranic elements through the bombardment of the heaviest natural elements, primarily with neutrons, a fourth decay series was identified, the Neptunium (A = 4n + 1) series whose radioactive members are not found in *nature* (see Table 2.1).

Table 2.1 Heavy element decay series

Series name	Type	Final stable nucleus	Longest lived nucleus	Longest half-life (years)
Thorium	4n[a]	Pb^{208}	Th^{232}	1.41×10^{10}
Uranium	4n + 2	Pb^{206}	U^{238}	4.47×10^9
Actinium	4n + 3	Pb^{207}	U^{235}	7.04×10^8
Neptunium, not in *nature*	4n + 1	Bi^{209}	Np^{237}	2.14×10^6

[a]n is an integer

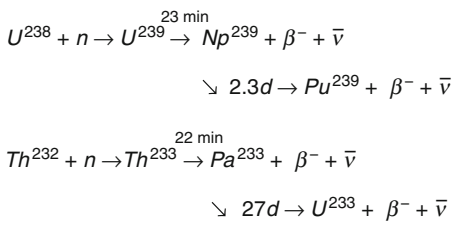

Fig. 2.1 Transmutation of fertile to fissile nuclei. ($\bar{\nu}$ is the antineutrino, the chargeless, ~zero mass particle that accompanies β emission)

Of the "heavy elements," the isotope U^{235} is key to fission reactor design. It is the only naturally occurring isotope which readily fissions when bombarded with neutrons of all energies. While its atomic percent abundance, 0.72%, is small, it is large enough to support chain reactions in reactors where neutrons born in fission are slowed down (moderated) by graphite (carbon) or by heavy water (deuterium oxide). When Uranium is enriched in U^{235} (~3–5%), it can fuel reactor designs where ordinary water moderates fission neutrons (today's pressurized water and boiling water reactors). Having U^{235} available as a reactor fuel makes it possible to exploit the two abundant *fertile* "heavy elements," U^{238} and Th^{232}. The term "fertile" refers to the fact that when these elements absorb a neutron they can be transmuted to *fissile* isotopes (Pu^{239} and U^{233} respectively), which like U^{235} readily fission when bombarded by neutrons of all energies. The transmutation processes are shown in Fig. 2.1. It is important to note that only one neutron capture is required in each of these transmutations. In a reactor design, neutron economy is the key to maintain a chain reaction and, as will be discussed in the section on Future Directions, expending one neutron with a reasonable probability of obtaining an additional fissile nucleus is a winner.

The heavy element radioactive decay series are also important to safety in fission reactor design. Each of the decay processes, α and β^- emissions and associated γs, is favorable to energy release. So any heavy elements, particularly transuranics, in a reactor's fuel system will contribute to the *decay heat* load that must be dissipated when a reactor shuts down. As will be discussed in the next section, the major short-term contributors to decay heat are *fission products*. A power reactor that shuts down following a sustained run at full rating will initially produce ~7% of that rating from decay heat, even if the chain reaction and nearly all fissioning has ceased.

For a full discussion of the radioactive decay series and the particulars of α, β^-, β^+ and γ emission, see Kaplan, and Krane, "Introductory Nuclear Physics."

Fission and Its Products

As noted in the "Introduction," fission was discovered accidentally during the search for transuranic elements. This work by Fermi and others was part of an extensive effort to understand the atomic nucleus and to duplicate the great success of quantum mechanics and the Pauli exclusion principle in providing a fully

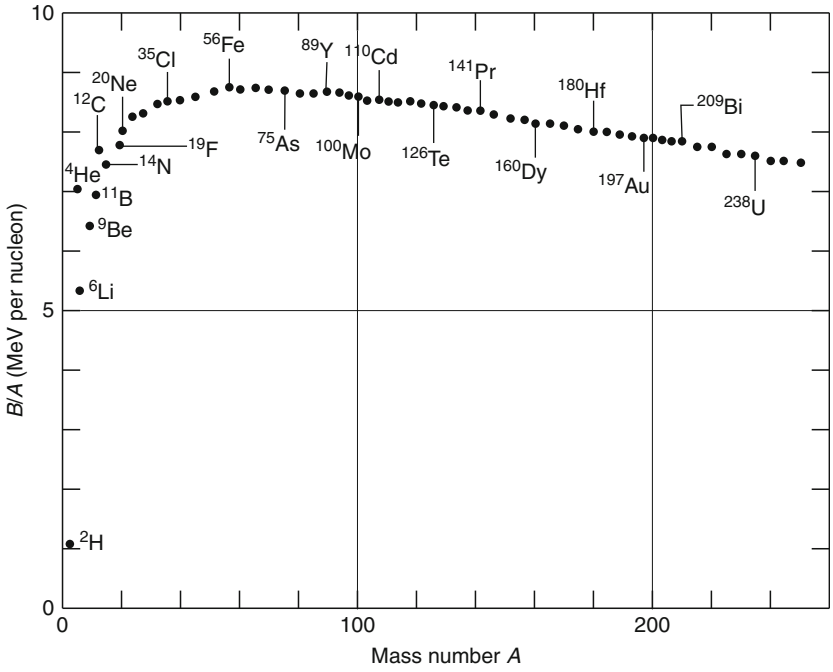

Fig. 2.2 Binding energy per nucleon (Krane)

predictive *Theory* of atomic electron structure. A comparable theory for the nucleus has not been developed, but several models (e.g., shell and liquid drop) provide insight into the trends and correlations found in the data provided by the extensive experimentation performed on the nuclei of the various elements and their isotopes.

Measurements of atomic mass ($m(X^A)$), and the mass of the electron, proton, and neutron, yields the *binding energy*, B, of a nucleus, ${}_ZX^A$, the work (energy) required to disassemble a nucleus into its neutrons and protons:

$$B = \left\{Zm_p + Nm_n - (m(X^A) - Zm_e)\right\}c^2, \tag{2.15}$$

where Z is the atomic number (the number of protons) and N = A – Z is the number on neutrons. (The binding energy of atomic electrons is ignored as negligible compared to the other factors in Eq. 2.15.)

Plotting the ratio of measured binding energies B to corresponding mass number A (Fig. 2.2) immediately makes evident the potential of energy release from fission of heavy element. Note the B/A versus A "curve" has a flat maximum in the middling A range $\sim 50 \rightarrow \sim 150$, and falls off (decreases) as A increases. Thus, there is a potential energy excess if a heavy element (isotope) can be disassembled and reassembled as two mid-range isotopes (preserving total A, Z, and N). (The behavior of the B/A curve for light elements shows the potential energy release from fusion.) Obviously fission (nor fusion) does not take occur "naturally" on earth

today (There is convincing evidence that a naturally occurring chain reaction took place in a uranium deposit in Gabon about 2×10^9 years ago, when the abundance of U^{235} would have been ~3%, high enough for a water-moderated "reactor" to operate. The higher earlier abundance is due to the shorter half-life of U^{235} (7.0×10^8 y) relative to that of U^{238} (4.4×10^9 y). See Krane for an excellent discussion of the Gabon reactor). The remainder of this section is devoted to particular requirements for fission to take place and to the discussion of the resulting fission products and their energies.

Insights provided by examining binding energies, and by additional experiments to determine nucleon–nucleon forces have led to the Shell and Liquid Drop models of the nucleus. Features of these models are incorporated in the *semiempirical mass formula* (Eq. 2.16). While a thorough discussion of the nuclear models is beyond the scope of this entry (see Kaplan or Krane), the mass formula provides key information on fission, energy release, and the relative likelihood for various nuclei.

In the semiempirical mass formula, the binding energy has five terms, which will be discussed below.

$$m\left({}_{Z}X^{A}\right) = Zm_p + Nm_n - [B_0 + B_1 + B_2 + B_3 + B_4]/c^2. \tag{2.16}$$

$B_0 = a_v A$ is the volume energy. Note in Fig. 2.2 that B/A saturates, thus B_0 has a linear dependence on A. The attractive nuclear forces between nucleons (n–n, n–p and p–p) are all equal and short range, smaller than the radius of the nucleus, $r = r_0 A^{1/3}$ where $r_0 \sim 1.2 \times 10^{-12}$ cm. If the range were larger, there would be attraction between each nucleon pair and B_0 would depend on A(A – 1).

$B_1 = -a_s A^{2/3}$, is the negative surface decrement. As the nucleon–nucleon forces are "short range," neutrons and protons on the surface of a nucleus are less tightly bound.

$B_2 = -a_c Z(Z-1)/A^{1/3}$, is the coulomb repulsion decrement. While the nuclear forces are strong enough to overcome coulomb forces, the protons in the nucleus do repel and reduce binding energy. Assuming a uniform distribution of protons in a liquid drop model of a spherical nucleus, an electrostatics calculation yields the dependence of B_2 the number of proton pair, Z(Z−1), and a measure of their spacing, $A^{1/3}$.

$B_3 = -a_a |N-Z| |N-Z|/A$, is the neutron–proton population asymmetry decrement. As nuclei become heavier, more neutrons than protons are needed to overcome coulomb repulsion. However, as the shell model of the nucleus demonstrates when nucleons, neutrons and/or protons, are added to form heavier elements and their isotopes, they fill *shells* of successively higher energy and are thus less tightly bound. This is analogous to the case of atomic electrons. Neutrons and protons have half-integral spin like the electrons, and therefore no two neutrons (or protons) can occupy the same state in a nucleus in conformance with the Pauli exclusion principle. So B_3 is negative and proportional to the neutron excess and the fraction of the nucleus the excess represents.

Table 2.2 Heavy nuclei fission

Target nucleus	Compound nucleus	E_e, Excitation energy (MeV)	E_a, Activation energy (MeV)
U^{233}	$[U^{234}]$	6.6	4.6
U^{235}	$[U^{236}]$	6.4	5.3
Pu^{239}	$[Pu^{240}]$	6.4	4.0
U^{238}	$[U^{239}]$	4.9	5.5
Th^{232}	$[Th^{233}]$	5.1	6.5

$B_4 = +\delta A^{-3/4}$ for even Z even N nuclei, = 0 for odd A nuclei, $= -\delta A^{-3/4}$ for odd Z odd N nuclei, is the pairing energy. As nucleons are added and fill *shells*, they are more tightly bound as spin up and spin down pairs. B_4 is important in determining the relative binding of isotopes of a given element and their propensity to fission.

A set of parameters for B which best fit the B/A curve (Fig. 2.2) is provided by Krane; $a_v = 15.5$ MeV, $a_s = 16.8$ MeV, $a_c = 0.72$ MeV, $a_a = 23$ MeV, and $\delta = 34$ MeV.

The potential for, and magnitude of, energy release from fission, whether as spontaneous decay or induced by particle or gamma ray capture, can be assessed with the semiempirical mass formula. As for an estimate of the magnitude of energy release, the B/A curve, as noted earlier, can be used directly. For example, the B/A for U^{238} is ~7.6 MeV. If it fissioned into two approximately equal mass nuclei (A = 119), their B/A would be ~8.5 MeV when in a ground state, and being more tightly bound than their parent (U^{238}) 214 MeV ($= 2 \times 119 \times 8.5 - 238 \times 7.6$) will be available through conservation of energy as kinetic energy of the daughter nuclei and of other fission products (neutrons, βs, γs, and neutrinos). That this energy is *available* does not mean that there is a significant probability that fission occurs. In this example, which represents spontaneous fission of U^{238}, one finds in nature that this mode of U^{238} decay competes poorly with α decay (Spontaneous fission is a significant mode of decay for some transuranic isotopes found in depleted reactor fuel, particularly Pu^{240} and Pu^{241}.). For fission fragments, daughter nuclei, to separate in spontaneous or induced fission, a potential barrier must be overcome. The height of the barrier relative to the ground state of a fission parent nucleus is called the *fission activation energy* (E_a). It can be estimated with the liquid drop model by calculating the change in the parent nucleus binding energy (B_1 and B_2) between the ground-state spherical configuration and a volume-conserving dumb-bell configuration (ref. [2] and [6]). Table 2.2 contains values of E_a for the *compound* nuclei formed by neutron capture in the fissile and fertile isotopes of primary interest in reactor design. These are compared with the *excitation energy* (E_e) provided in forming the compound nucleus.

$$E_e = \left[\left(m\left({}_ZX^A\right) + m_n\right) - m\left({}_ZX^{A+1}\right)\right]c^2. \tag{2.17}$$

Note that E_e does not include any kinetic energy contribution from the captured neutron. For the fertile target nuclei (U^{238} and Th^{232}), $E_e < E_a$ and neutron kinetic energy will be required to overcome or quantum mechanically penetrate (with high

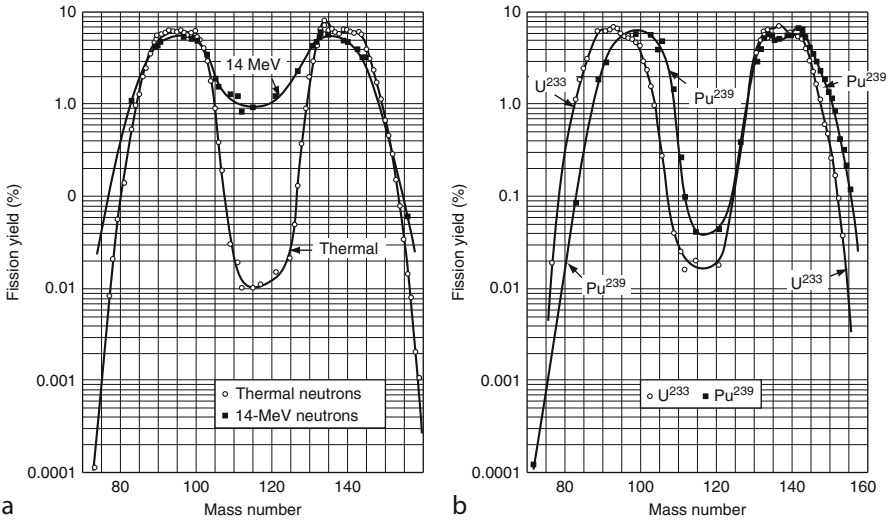

Fig. 2.3 Fission yields: (**a**) for U^{235} from fast and thermal neutrons, (**b**) for U^{233} and PU^{239} from thermal neutrons [33]

probability) the potential barrier to fission. For the fissile targets, $E_e > E_a$ and thus "slow" neutrons can initiate fission.

The high values of E_e for the fissile targets are due to the positive "pairing" contribution, B_4, to the binding energy of the compound nucleus ground states. Note ${}_{92}U^{234}$, ${}_{92}U^{236}$, and ${}_{94}Pu^{240}$ are all even Z even N nuclei and the corresponding target nuclei are even Z odd N. So, the second term in Eq. 2.17 is decreased by $\delta(A+1)^{-3/4}$, and B_4 is zero in the first term. Thus, an increase in E_e relative to the result if pairing is ignored is achieved. For fertile targets (even Z even N), roles are reversed. It is the first term in Eq. 2.17 that is decreased and B_4 is zero in the last term. Thus, E_e is lower than if pairing is ignored.

The semiempirical mass formula and the shell and liquid drop models are limited in predicting the fission process. This is best illustrated by the mass distribution of the major fission fragments (see Fig. 2.3). In the vast majority of cases, fission yields two unstable (having excess neutrons) nuclei, but not of equal mass, as in the example above used to estimate the energy available from spontaneous fission of U^{238}. The two humped curves in Fig. 2.3 are not predicted by nuclear models. To quote Krane, "surprisingly, a convincing explanation for this mass distribution has not been found."

From the nuclear models, it is not surprising that free (prompt) neutrons are emitted in fission as the daughter nuclei are so rich in neutrons, but the prediction of their number (~2.5 on average) and energy spectrum (the mean ~2 MeV, see Fig. 2.4) are still an active area of study. The decay chains of the neutron-rich, excited daughter nuclei (fission fragments) are well predicted, including the release of (delayed) neutrons when in some cases neutron decay competes

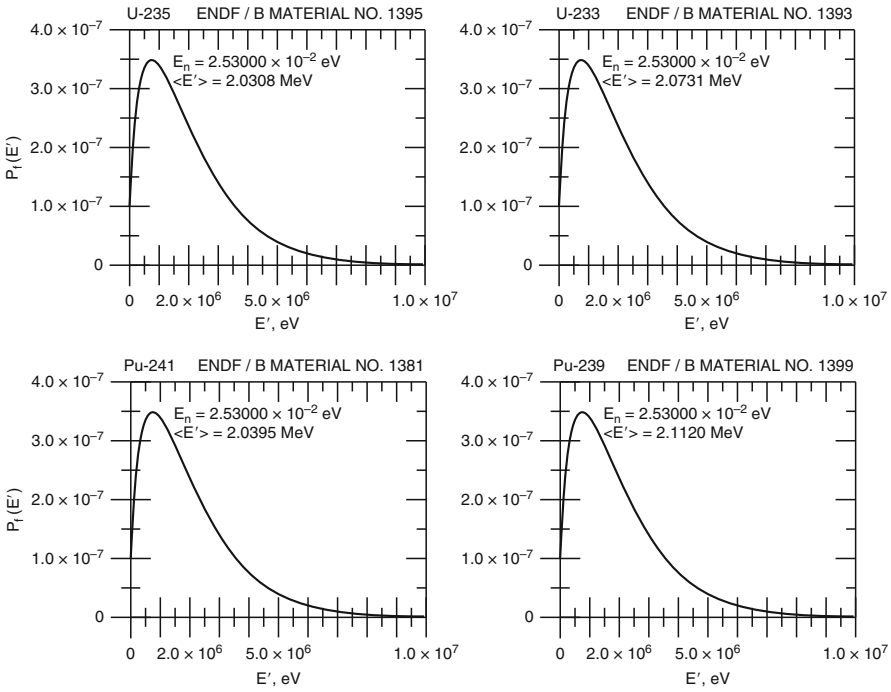

Fig. 2.4 Prompt neutron energy spectra where $P_f(E')$ is the probability per unit energy [32]

successfully with β-decay. The delayed neutrons are a small fraction of the total neutron emission (0.64% for thermal fission of U^{235}), but as will be discussed in section "Fission Reactor Performance", they are important to reactor control.

Total energy release from the various neutron-induced fissions of interest in reactor design is remarkably consistent with the simple spontaneous U^{238} fission calculation made above. Of course, the constituents are different, as displayed in Table 2.3.

In a reactor design, the total energy values in Table 2.3 are not used. First, the contribution from neutrinos is subtracted, as their range before collision is well beyond reactor boundaries. Then, the energy release per fission from neutron captures which produce βs and γs is added. The magnitude of this release is design-dependent as it is a function of the materials used, and the neutron capture rate in these materials. For plant energy balance studies, using 200 MeV/fission is satisfactory.

The problem of *decay heat* was noted in the previous section. From Table 2.3, it can be seen that fission product decay is the immediate concern when a chain reaction is terminated. Assume full power from U^{235} fissioning, when this ceases, delayed γs and βs are still being released. Thus, ∼6.3% (≃ 100 × (6.26 + 6.43)/200) of rated power, coming from fission product decay, must still be dissipated, along with energy from the decay of transuranic elements present in the reactor, for a total of ∼7%.

Table 2.3 Energy yield in MeV from fission. Thermal neutron fission of fissile isotopes; fertile isotope fission is from neutrons with energy spectrum of a light water-moderated reactor [7, 32]

	Fissile or fertile isotope†					
Energy	^{232}Th	^{238}U	^{235}U	^{233}U	^{239}Pu	^{241}Pu
Fission fragment kinetic energy	162.1 ± 1.5	170.0 ± 0.66	169.6 ± 0.7	168.7 ± 0.7	175.9 ± 0.1	175.5 ± 1.1
Prompt neutron kinetic energy	4.7 ± 0.12	5.51 ± 0.1	4.79 ± 0.07	4.9 ± 0.1	5.9 ± 0.1	5.99 ± 0.13
Delayed neutron kinetic energy	0.024 ± 0.004	0.021 ± 0.003	0.0071 ± 0.0007	0.0014 ± 0.0005	0.001 ± 0.0005	0.0074 ± 0.0015
Prompt γ rays	6.15 ± 1.75	6.28 ± 0.8	6.96 ± 0.7	7.59 ± 0.71	7.74 ± 0.45	7.86 ± 1.8
Delayed γ rays	8.01 ± 0.2	8.04 ± 0.08	6.26 ± 0.05	4.99 ± 0.04	5.16 ± 0.1	6.33 ± 0.07
β particles	8.28 ± 0.21	8.25 ± 0.08	6.43 ± 0.05	5.13 ± 0.04	5.3 ± 0.1	6.51 ± 0.04
Neutrino energy	11.1 ± 0.3	11.14 ± 0.11	8.68 ± 0.06	6.91 ± 0.05	7.15 ± 0.11	8.78 ± 0.09
Total energy yield	200.3 ± 0.5	209.3 ± 0.3	202.7 ± 0.1	198.2 ± 0.1	207.2 ± 0.3	211.0 ± 0.3

Over 800 fission fragment nuclei have been identified. Their decay must be tracked to account for *decay heat* in reactor shut-down safety analysis and for the proper handling and storage of spent fuel (where both energy release and the nature of radiation fields must be known). One hundred and two of these nuclei are delayed neutron precursors. To simplify reactor transient (kinetics) calculations, the precursors are collected into six *effective* groups, where members of a given group have similar decay constants (see Table 2.4).

The energy spectra for a given delayed group do not vary significantly with fissioning isotope. The spectra are much softer (with lower mean energies, < 1 MeV) than for prompt neutrons [7]. This means that a delayed neutron in a thermal reactor is more *important* than a prompt neutron. It is more likely to reach the low energies ($<$0.625 eV) where most fission occurs. Delayed neutrons can also result from other reactions, for example, photon capture (γ,n) (The expression (a,b) is shorthand for a nuclear reaction with an input particle "a" and output particle "b", where the target and product nuclei are understood.) and neutron activation (n,p) followed by neutron decay of the product nucleus. If important to a particular reactor design, these delayed neutrons can be included by modifying the effective delayed group structure.

The final aspect of the ~800 fission fragment nuclei that must be dealt with is their impact on neutron balance. Each of them has a probability of capturing neutrons and in some case of causing a transmutation into a nucleus with a particularly large propensity for capturing neutrons. The nuclei of greatest importance to neutron balance are listed in Table 2.5.

I^{135} is important as it is the direct precursor of Xe^{135}, an especially large absorber of thermal neutrons. The next two isotopes in the table are precursors to a decay chain with three large absorbers, Pm^{147}, Sm^{149}, and Sm^{151}. The final five, with their precursors in parentheses, are large absorbers, but not as sensitive to neutron energy spectrum and power level and history as the others. Clearly, data for the 800 fission fragments must be handled through large computer files [8]. For neutron balance, the fission fragment isotopes, which are not treated explicitly (Table 2.5), can be lumped into an effective fission product nucleus with a yield per fission and *probability* for neutron capture. How one characterizes the *probability* of nuclear reactions is the subject of the next section.

Cross Sections

The nuclear reactions of importance to fission reactor design are by *definition* governed by the postulates of quantum mechanics (i.e., they are on the dimensional scale of the nucleus). And, thus the results of the various reactions are probabilistic in nature. The probability of a particular result is characterized by a parameter, the *microscopic* cross section, σ, with, not surprisingly, the dimensions of area, and which is quoted in units of *barns*. The barn, 10^{-24} cm^2, is a reasonable measure as in some cases σ is nearly the projected

Table 2.4 Prompt and delayed neutron data. ν_p is the prompt neutron yield versus initiating neutron energy (ENDF/B-VII.0). ν_d is the total delayed yield, constant for fission initiating neutron energies between 0 and 4 MeV, and above 7 MeV. Between 4 and 7 MeV, ν_d tracks linearly [32]

The relative abundance $\gamma_I = \nu_i/\nu_d$				
Neutron E	^{233}U ν_p	^{235}U ν_p	^{239}Pu ν_p	^{241}Pu ν_p
0.0253 eV	2.4894	2.4208	2.8724	2.9251
2 MeV	2.5758	2.6366	3.171	3.1727

	$\overline{\nu}_d$			
E(MeV)	^{233}U	^{235}U	^{239}Pu	^{241}Pu
0–4	0.0074	0.0167	0.00645	0.0162
7	0.0047	0.0090	0.0043	0.0084

	^{233}U		^{235}U		^{239}Pu		^{241}Pu	
Delayed Group	Decay Constant λ_i, s^{-1}	Relative Abundance γ_i	λ_i, s^{-1}	γ_i	λ_i, s^{-1}	γ_i	λ_i, s^{-1}	γ_i
1	0.01258	0.086	0.01272	0.038	0.0129	0.038	0.0128	0.010
2	0.03342	0.274	0.03174	0.213	0.0311	0.280	0.0299	0.229
3	0.131	0.227	0.116	0.188	0.134	0.216	0.124	0.173
4	0.303	0.317	0.311	0.407	0.332	0.328	0.352	0.390
5	1.27	0.073	1.4	0.128	1.26	0.103	1.61	0.182
6	3.14	0.023	3.87	0.026	3.21	0.035	3.47	0.016

Table 2.5 Direct yield fractions ($\times 100$) for isotopes in the most important fission product chains [32]

	Fissile or fertile isotope[a]				
Fission Product	^{232}Th	^{238}U	^{235}U	^{233}U	^{239}U
^{135}I	5.238	6.548	6.349	4.860	6.303
^{135}Xe	0.0403	0.0150	0.255	1.337	1.152
^{147}Nd	3.08	2.711	2.271	1.775	2.073
^{149}Pm	0.825	1.765	1.089	0.769	1.261
^{99}Mo (^{99}Tc)	2.965	6.247	6.127	4.957	6.144
^{103}Ru (^{103}Rh)	0.164	6.336	3.137	1.707	6.991
^{131}I (^{131}Xe)	1.481	2.982	2.473	2.352	3.093
^{133}I (^{133}Cs)	3.858	6.356	6.787	5.974	6.923
^{143}Ce (^{143}Nd)	6.619	4.834	5.972	5.881	4.561

[a]The energy of the neutron initiating the fission is in the thermal range for ^{235}U, ^{233}U, and ^{239}Pu. For ^{232}Th and ^{238}U, the yields are due to fissions initiated by neutrons with a spectrum of energies typical of light water-moderated nuclear reactors.

area of a target nucleus, $4\pi R^2$, and R is $\sim 10^{-12}$ cm. Thus, envisioning a target foil of area, A, and thickness, dx (where dx is small enough to have negligible shadowing of one nucleus by another in the target foil), the probability that an incident particle in traveling a short distance (i.e., dx) will undergo a specific reaction equals $\sigma\rho A dx/A$, where ρ is the density of target nuclei (#/cm^3) in the foil. It follows that to find the reaction rate in the foil we need the number of impinging particles per second. Given the particles have a density N (#/cm^3) and are monoenergetic and monodirectional (normal to the face of the foil) with speed v, the number impinging per second equals $N \cdot (vdt) \cdot A/dt$. So the total reaction rate in the foil is $(NvA)(\rho\sigma dx)$, and the rate per cm^3 is $vN\rho\sigma$. The parameters that make up this specific rate have been reordered to reflect conventional definitions in reactor physics (In the nuclear engineering discipline, *reactor physics* refers to the portion of the field addressed in this entry):

$$vN \equiv \Psi \text{particle } \textit{flux}, \text{ and} \tag{2.18}$$

$$\rho\sigma \equiv \Sigma \textit{macroscopic} \text{ cross section.} \tag{2.19}$$

The *flux* in our simple foil example is the number of particles per cm^2 per second crossing a plan parallel to the face of the foil. Given the more general representation of particle density (which will be used in the next section):

$N(\mathbf{r},E,\mathbf{\Omega},t)dr^3dEd\Omega \equiv$ no. of particles in dr^3 about $\mathbf{r}$, with kinetic energies in dE about E, and going in the solid angle $d\Omega$ about the unit direction vector $\mathbf{\Omega}$ (see Fig. 2.5), at time t; then the corresponding definition of *flux*, $\Psi(\mathbf{r},E,\mathbf{\Omega},\mathbf{t})dsdEd\Omega$, is the no. of particles with E in dE going in direction Ω in $d\Omega$ that pass through the surface ds, which is located at $\mathbf{r}$ and is normal to $\mathbf{\Omega}$, per unit time, at time t.

The *macroscopic* cross section is the probability that a particle undergoes a reaction characterized by σ, per unit path (for small paths, dx) traversed by the particle in a homogenous material with target nucleus density, ρ. This definition

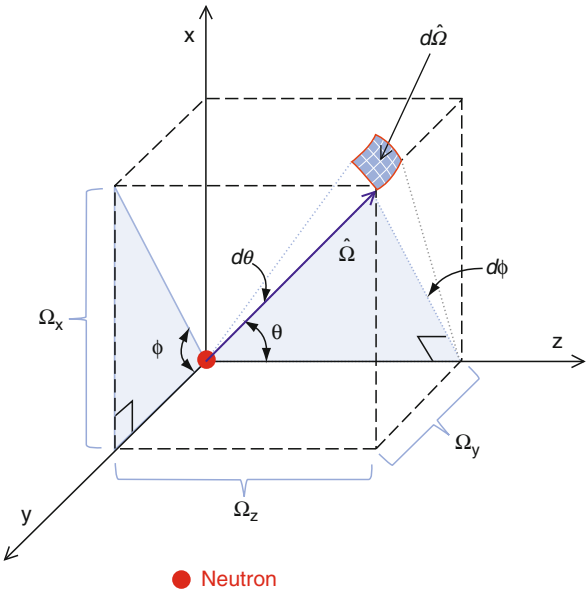

Fig. 2.5 The unit direction vector **Ω** associated with neutron velocity and the differential (small) solid angle dΩ which defines the range of directions

lends a special significance to $1/\Sigma_T$, where $\Sigma_T = \rho\sigma_T$. σ_T is the *total* microscopic cross section, the sum of the σs for all of the reactions that the initiating particle can undergo with a given target isotope. So the change in flux, where **Ω** is parallel to the x axis of a target material sample, over a small interval dx in the sample is $d\Psi = -\Psi\Sigma_T dx$. And thus, $\Psi(x) = \Psi(0)\, e^{-\Sigma_T x}$, where x is the distance into the "sample" (which has its face in the y – z plane at x = 0). So, the probability of a reaction in dx about x can be expressed as

$$P(x)dx = \Sigma_T dx \bullet (\Psi(x)/\Psi(0)) = \Sigma_T e^{-\Sigma_T x} dx. \tag{2.20}$$

And thus the *mean free path* of a particle in an incident beam (Ψ(0)) before being removed from the beam in a homogeneous target is

$$\overline{x} = \int_0^\infty dx\, xP(x) = 1/\Sigma_T. \tag{2.21}$$

or generally the *mean free path* is the average distance traveled between successive interactions.

If a homogeneous material is made up of various nuclei (elements/isotopes, indexed by j), then the macroscopic cross section for a reaction, i, is

$$\Sigma_i = \sum_j \rho_j \bullet \sigma_i^j. \tag{2.22}$$

The reactions of primary interest in fission reactor design are those initiated by neutrons and gammas. Neutron cross sections are key to determining if a chain reaction can be maintained, and that the neutron population can be controlled under various transient conditions (e.g., start-ups and shutdowns, planned and accidental), and, of course, the fission distribution in the reactor. Most of the resulting energy release, from fission fragments, is deposited locally in the fuel elements of a given design. However, gammas, from fission and neutron capture in reactor structures, have large mean free paths, and their distribution and capture rates must be determined, using gamma cross sections, to complete the knowledge of energy deposition. The subsequent engineering problem is to assure that the reactor cooling system can remove the deposited energy under normal and accident conditions. Neutron and gamma cross sections are also required for the shield design of a fission reactor.

Neutron reactions are characterized by their energy balance, the Q factor, as well as microscopic cross sections. For the simple reaction (with the target at rest),

$$n + X \rightarrow Y + y \tag{2.23}$$

the energy balance is

$$\left(E_n + m_n c^2\right) + M_X c^2 = \left(E_Y + M_Y c^2\right) + \left(E_y + m_y c^2\right), \tag{2.24}$$

and Q is defined as the difference in the kinetic energies of the inputs (here the neutron) and the outputs:

$$Q = E_Y + E_y - E_n \text{ or } = \left(M_X + m_n - M_Y - m_y\right)c^2. \tag{2.25}$$

If Q is positive, the reaction is exothermic, if negative, endothermic. For an endothermic reaction to go, for the microscopic cross section to be nonzero, enough kinetic energy must be supplied by the neutron to excite a compound nucleus, X^{A+1}, so it will decay to Y + y. As momentum must be conserved,

$$m_n v_n = (M_X + m_n)V_c \text{ or } V_c = v_n m_n/(M_X + m_n), \tag{2.26}$$

where V_c is the velocity of the compound nucleus. Then, the neutron energy supplied must be such that

$$-Q = m_n {v_n}^2/2 - (M_X + m_n){V_c}^2/2 \tag{2.27}$$

and the *threshold energy*, E_{th}, for the reaction is

$$E_{th} = m_n {v_n}^2/2 = (-Q)(1 + m_n/M_X). \tag{2.28}$$

(n, 2n) is an example of an endothermic reaction whose cross sections will exhibit an energy dependence of zero until the neutron energy E reaches an E_{th}.

The simplest, but very important, neutron reaction to be considered is a form of elastic scattering (Q = 0), where collisions can be treated with classical mechanics as hard sphere, billiard ball, interactions. For the energies of neutrons in fission reactors, 0–10 MeV, elastic scattering cross sections for most nuclei are constant and proportional to the square of the nuclear radius, ~A2/3. Assuming the target nucleus to be at rest and applying conservation of energy and momentum in the center of mass, CM, coordinate system, one determines the probability that the final energy of the scattered neutron, in the laboratory coordinate, LM, system, is E_f in dE_f:

$$\begin{aligned} P(E_i \rightarrow E_f) &= 1/(1-\alpha)E_i, \text{ for } \alpha E_i \leq E_f \leq E_i \\ &= 0 \text{ otherwise,} \end{aligned} \tag{2.29}$$

where $\alpha = ((A-1)/(A+1))2$ and E_i is the initial neutron energy. A is the mass number of the target nucleus. And, scattering is assumed to be isotropic in the CM coordinate system. This is a good assumption for the energy range of interest here, and its basis will be discussed later in this section. A full derivation of Eq. 2.29 can be found in Duderstadt and Hamilton, "Nuclear Reactor Analysis." Examining $P(E_i \Rightarrow E_f)$ one sees that a neutron scattering off a hydrogen nucleus (A = 1) can lose all its energy (as $\alpha = 0$). On average, it loses half its initial energy as

$$\overline{E}_f = \int_{\alpha E_i}^{E_i} dE_f E_f P(E_i \rightarrow E_f) = E_i(1+\alpha)/2, \text{and} \tag{2.30}$$

$$\Delta\overline{E} = E_i \rightarrow \overline{E}_f = E_i(1-\alpha)/2. \tag{2.31}$$

Given $P(E_i \rightarrow E_f)$ as in Eq. 2.29, one defines *differential* microscopic elastic scattering cross sections, $\sigma_{es}^{j}(E_i)P(E_i \rightarrow E_f)dE_f$, which are particularly useful in determining how neutrons, born in fission, are slowed down in reactors designed to take advantage of the large fission cross sections of fissile isotopes in what is conventionally defined as the *thermal* neutron energy range, less than 0.625 eV. The superscript "j" of σ_{es}^{j} refers to the nuclei of the various *moderators* (hydrogen, deuterium and carbon) that are employed in these thermal reactors.

Once neutrons have slowed to the thermal range the target nuclei can no longer be assumed to be at rest. The interaction frequency will then be

$$|\mathbf{v} - \mathbf{V}|\ \sigma(|\mathbf{v} - \mathbf{V}|)\rho, \tag{2.32}$$

where $|\mathbf{v} - \mathbf{V}|$ is the relative speed of neutron and target. For elastic scattering, $\sigma(|\mathbf{v} - \mathbf{V}|)$ is still nearly constant and an *average* cross section for *thermal* neutrons with speed v $(=(2E/m_n)1/2)$ is

$$\overline{\sigma}(\mathbf{v}) = (\sigma_{es}/\mathbf{v}\rho) \int d^3\mathbf{V}|\mathbf{v} - \mathbf{V}|\rho(\mathbf{V}), \tag{2.33}$$

where for many reactor applications the Maxwell–Boltzmann velocity distribution for ideal gases in thermal equilibrium at absolute temperature, T, can be used to represent the targets. Thus,

$$\rho(\mathbf{V}) = \rho \bullet (M/(2\pi kT))^{3/2} \exp(-MV^2/2kT), \tag{2.34}$$

where M is the mass of the target nucleus and k is the Boltzmann constant (8.6174×10^{-5} eV/K, K is degrees Kelvin).

From Eq. 2.33, one sees that for $v \gg V$ the *average* cross section is, as expected, σ_{es}. And, as the neutron speed decreases and approaches zero, the *average* cross section goes as one over the neutron speed.

For highly accurate calculations (As part of the process of evaluating nuclear data sets, very accurate calculations of integral experiments are made. Zero power *mockups* of reactors, with carefully recorded dimensions and inventories, are commonly used. Monte Carlo calculations (to be discussed in the next section) of neutron balance in the mockups are made with various data sets (e.g., cross-section libraries) to determine a recommended set. See the CESWG web site for references to such experiments.), more sophisticated treatments of scattering from moderator structures (e.g., molecules in liquids, lattices for solids) are required. The excitation of modes of vibration, and thus energy loss to phonons must be considered. This has been a fertile field of development [9] and double differential scattering cross sections for various moderators have been produced. They are of the form:

$$\begin{aligned}\sigma_s(E_i \to E_f,\ \Omega_i \to \Omega_f)dE_f d\Omega_f = (1/4\pi kT) \\ (E_f/E_i)^{1/2}\exp(-\beta/2)\sigma_{es}S(\alpha,\beta)dE_f d\Omega_f,\end{aligned} \tag{2.35}$$

where

$$\begin{aligned}\alpha \equiv (E_i + E_f - 2(E_i E_f)^{1/2})\Omega_i \bullet \Omega_f/kT \text{ and} \\ \beta \equiv (E_i + E_f)/kT.\end{aligned} \tag{2.36}$$

σ_{es} is the scattering cross section of the bound "moderating" nucleus (e.g., proton, deuteron, carbon). $S(\alpha,\beta)$, the *scattering law*, embodies the physics of the influence of the moderator structure on the scattering process. Various formulations of $S(\alpha, \beta)$ are tabulated as part of data files that document *all* the microscopic cross sections that are used in fission reactor design. These files can be found on the web site of the National Nuclear Data Center (currently, nndc.bnl.gov). The most widely used set is ENDF/B, the latest (2009) version is VII.0. In order, however, to produce the differential scattering cross sections (Eq. 2.35) for design calculations, material temperatures, T, must be identified and supplied with the corresponding ENDF files to NJOY [10], a system of computer programs which produce microscopic cross sections for use in various design programs (which will be discussed in the next section).

The remaining neutron reactions of interest all involve the formation of a compound nucleus, which will be in an excited state, $(X^{A+1})^*$, and will subsequently decay, yielding γ or γ's (neutron capture), n (elastic neutron scattering), n+γ (inelastic scattering), two n's (an (n,2n) reaction), p or α (charged particle production) or fissioning. The probabilities of these various outcomes for a given isotope, j, and incident neutron energy are characterized by the microscopic cross sections: $\sigma_c^j(E)$, $\sigma_s^j(E)$, $\sigma_{in}^j(E)$, $\sigma_{2n}^j(E)$, $\sigma_p^j(E)$, $\sigma_\alpha^j(E)$, and $\sigma_f^j(E)$. As noted above in the discussion of Q factors, for endothermic reactions, $Q < 0$, cross sections will be zero until a threshold value of E for the initiating neutron is reached. This is the case for inelastic scattering, (n,2n) and some (n,α) and (n,p) reactions. There is similar threshold behavior for fertile isotope fission cross sections (see Sect. Fission and Its Products), which when the reactions "go" are exothermic. All neutron capture reactions (n,γ) are exothermic, and thus their cross sections are nonzero over the full range of fission reactor neutron energies.

One can view the "compound nucleus reaction" cross sections as the product of a cross section for compound nucleus formation, σ_C (neutron capture by the target nucleus), times the probability of a particular decay mode of the excited compound nucleus. Both factors of this "product" depend on the nature of the target and compound nuclei, X^A and X^{A+1}, and the energy available to excite the compound nucleus, X^{A+1}. The later is the sum of the reduced mass (i.e., center of mass) kinetic energy of the initiating neutron:

$$E_C = E(M_X/(m_n + M_X)) \cong E(A/(1 + A)), \tag{2.37}$$

where X^A is assumed to be at rest and momentum is conserved; and the excitation energy, E_e (see Eq. 2.17), provided by adding a neutron to X^A. E_e is the binding energy of the "added" neutron in the compound nucleus.

The magnitude of σ_C depends on the structure of X^A. First, if neutron number N (=A–Z) is odd, σ_C is larger than its counterpart for neighboring isotopes with even neutron numbers. The opposite is true for N even. This just reflects the binding energy advantage of pairing half-integral spin Fermions in a nucleus (see the discussion of B_4 in Sect. Fission and Its Products). Second, for nuclei of various A's there are *Magic Numbers* for both Z and N (2, 8, 20, 50, 82 and 126) which can be thought of as closing shells of protons and neutrons, analogous to atomic electron shells. The reduction of σ_c for a magic number N nucleus, relative to its N + 1 isotope neighbor's σ_C, is much larger than the pairing effect.

Excited compound nuclei have mean lifetimes, τ (see Eq. 2.14) of as long as 10^{-14} s (Kaplan), much longer than the transit time for a neutron crossing a target nucleus, $\sim$2R/v. Given the nuclear diameter, $2R \sim 10^{-12}$ cm, the transit time for even a *thermal* neutron is $\sim 10^{-17}$ s (The term *thermal neutron* refers to the most probable energy of the neutrons in thermal equilibrium in a zero-power reactor (e.g., a mockup). At 20°C, this is 0.023 eV, with a corresponding neutron speed of 2,200 M/s.). Thus, the standard assumption is that the decay of an excited compound nucleus is independent of all but the input energy of the initiating neutron.

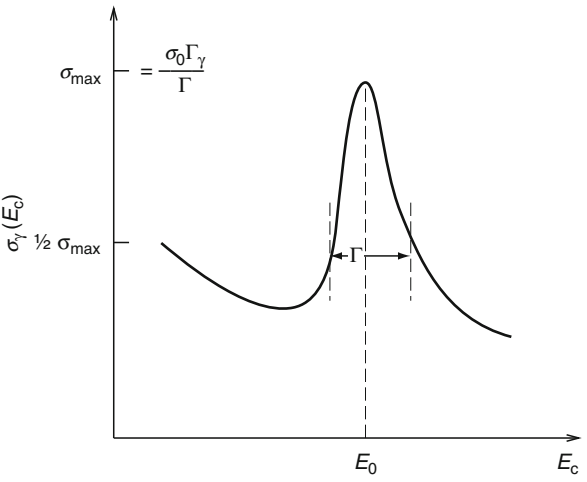

Fig. 2.6 A typical neutron capture cross section for an isolated (single) resonance whose width at half maximum is Γ, the total level width. Γ_γ is the partial width for gamma ray emission from the excited state (level). E_c is the center of mass (reduced mass) energy of the initiating neutron (Duderstadt)

The decay modes of a particular excited state, nuclear level, are characterized by a *level width*

$$\Gamma \equiv h/(2\pi\tau), \tag{2.38}$$

with dimensions of energy (h is Planck's constant, 4.135667×10^{-15} eV-s), which is based on the Heisenberg uncertainty principle. In a quantum mechanical system like our excited compound nucleus, knowledge of energy and time is governed by

$$\Delta E \Delta t \sim h/2\pi. \tag{2.39}$$

Thus, Γ can be viewed as the uncertainty in energy of an excited state (level) of a compound nucleus, and τ a measure of the "uncertainty" of the lifetime of the excited state. The microscopic neutron cross sections, which go through the compound nucleus formation process, exhibit resonance behavior (peaking) when the neutron energy and E_e (the added neutron binding energy) produce or nearly produce a well-defined excited state (i.e., having a small Γ). See Fig. 2.6.

The level width Γ can be thought of as the probability per unit time of decay of an excited state and thus the sum of partial "widths" (probabilities per unit time) for each mode of decay:

$$\Gamma = \Gamma\gamma + \Gamma_n + \Gamma_{n\gamma} + \Gamma_f + \Gamma_{2n} + \Gamma_p + \ldots, \tag{2.40}$$

(where Γ_n refers to elastic compound scattering and $\Gamma_{n\gamma}$ refers to inelastic scattering, the rest being obvious).

Therefore, a "compound nucleus reaction" cross section near an isolated resonance is

$$\sigma(n,i) = \sigma_C(n)\Gamma_i/\Gamma, \text{ for } i = \gamma, n, (n\gamma), f, 2n, p, \text{etc.} \tag{2.41}$$

The functional form of σ (n,i), its dependence on neutron energy, was derived with the principles of quantum mechanics by Briet and Wigner [11] in 1935. Their "formula" for this simple case is

$$\sigma(\mathrm{n,i}) = (\lambda^2/4\pi)\Gamma_\mathrm{n}\Gamma_\mathrm{i}/\left[(\mathrm{E}-\mathrm{E}_0)^2 + (\Gamma/2)^2\right], \tag{2.42}$$

where λ is the de Broglie wavelength of the neutron, $\mathrm{h}/(2\mathrm{m_n\,E})^{1/2}$, and E_0 is the energy of the resonance peak. Figure 2.6 is an illustration of this "form" for i = γ.

Breit and Wigner' s most impressive derivation is more general than Eq. 2.42.

First, they considered neutron energies beyond what has been found pertinent to fission reactors. When one accounts for conservation of angular momentum, the initiating neutron has classically a magnitude of angular momentum |L| equal to pb, where p is neutron momentum, $(2\mathrm{m_nE})^{1/2}$, and b is the displacement of the neutron path from a parallel axis running through the center of the target nucleus. In a quantum mechanical treatment,

$$|\mathrm{L}| = (l(l+1))^{1/2}\mathrm{h}/2\pi \text{ where } l = 0, 1, 2, 3, \ldots \tag{2.43}$$

Then, one can think of "b" as |L| (given by Eq. 2.43) divided by the neutron momentum, p, and if there is going to be a significant probability of a reaction with the target nucleus, "b" cannot be much larger than the target nucleus radius, $\mathrm{r} \cong \mathrm{A}^{1/3}(1.28 \pm 0.05) \times 10^{-13}$ cm. For this to be true for a large nucleus, for example, for U^{235}, and for nonzero angular momentum (e.g., l = 1), the neutron would have to have kinetic energy ≥ 6.6 MeV. For smaller nuclei the required energy would be greater. Given the spectrum of neutrons in fission reactors, where most neutrons are born at around 2 MeV (see Fig. 2.4), an assumption of zero angular momentum (l = 0) for the vast majority of reactions is good, and thus equation Eq. 2.42 does not include a factor involving angular momentum or spin quantum numbers. This assumption also means that decay products of an excited compound nucleus will be released isotropically in the center-of-mass coordinate system, which is reflected in the factor of 1/4π in Eq. 2.42 (the probability that the decay product i (i = n, γ, p) is released dΩ about any **Ω**). The quantum mechanical treatment of angular momentum also accounts for the statement made above that "billiard ball" elastic scattering "can be assumed to be isotropic in the center of coordinate system." This direct elastic scattering is referred to as *potential* scattering so as to be differentiated from resonance (compound nucleus) elastic scattering, that is, i = n in equation Eq. 2.42.

Second**,** Breit and Wigner recognized and treated interference between potential and resonance elastic scattering. They found that the total elastic scattering cross section dips at energies right below the resonance peak, E_0.

Finally, as they were aware that there could be multiple possible excited states of a compound nucleus they extended their "formula" to two resonances whose Γs do not over lap.

Table 2.6 Types of neutron cross section for various target element/isotope masses pertinent to fission reactor design

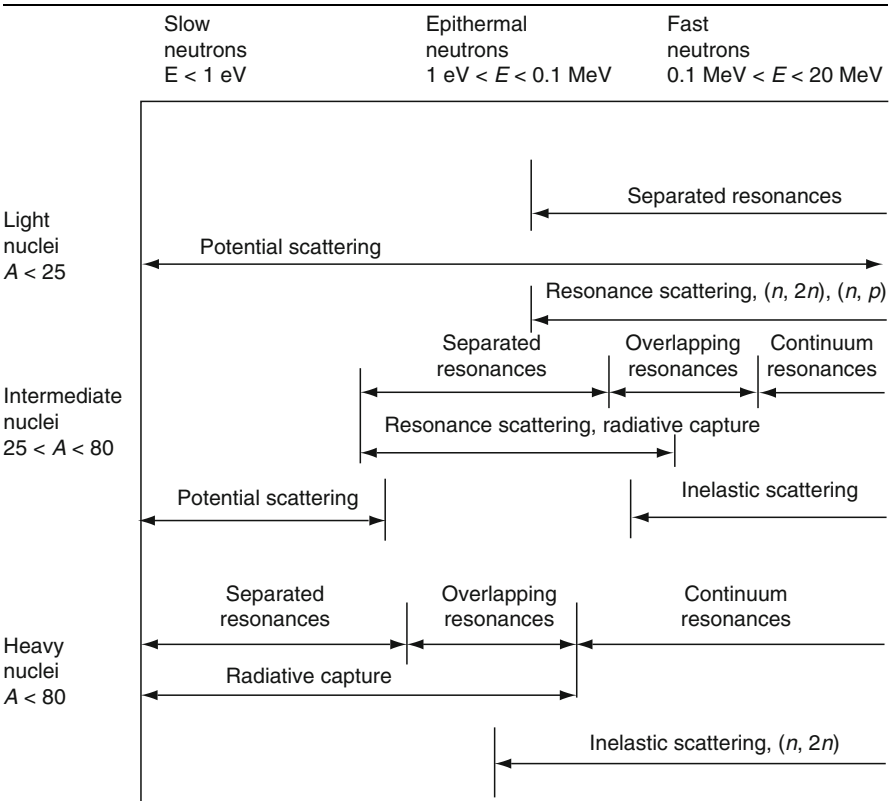

Since Breit and Wigner's original work, there has been great activity in measuring cross sections, motivated principally the desire to understand the physics of the nucleus. In the process, however, the basic parameters required for nuclear weapon and reactor design were generated. The neutron cross sections for fission reactor design are summarized in Table 2.6 [12].

In this table, the distinction is made between resonance cross sections with different densities (spacing) of resonance peaks. With intermediate and heavier nuclei the level structure grows more complex, and the number of possible excited states of a compound nucleus greatly increases. With higher neutron energy more finely spaced excited states can be reached and their level width, Γ's, increasingly overlap until measurement cannot resolve individual resonances.

In parallel with the work of nuclear spectroscopy experimentalists, theoreticians have built on Breit and Wigner's work. Resonance cross-section models [13] are key to creating Evaluated Nuclear Data Files. The Cross Section Evaluation Working Group, a cooperative effort of national laboratories, industry and universities in

the United States and Canada (see nndc.bnl.gov), sponsors reviews of the various measurements of a given cross section (target isotope and reaction) and the subsequent determination (As part of the process of evaluating nuclear data sets, very accurate calculations of integral experiments are made. Zero power *mockups* of reactors, with carefully recorded dimensions and inventories, are commonly used. Monte Carlo calculations (to be discussed in the next section) of neutron balance in the mockups are made with various data sets (e.g., cross-section libraries) to determine a recommended set. See the CESWG website for references to such experiments.) of a consensus set of parameters for an appropriate cross-section *model*. These models and their "consensus" parameters are a large part of the ENDF/B-VII.0 data files. Having the cross sections represented by an analytic model also facilitates dealing with the temperature effect on resonance cross-sections. that is, Doppler shift or broadening. The analytic process of averaging a resonance cross section (i.e., its model), over the velocity distribution of the target nuclei at a given temperature is similar to what was discussed above for reactions initiated by neutrons in thermal energy range. The process is outlined by Duderstadt and Hamilton using the single-level Breit Wigner formula as the resonance model. The effect of increasing temperature is to reduce a resonance peak while broadening its width, thus increasing its Γ. To first order, the area under the resonance is unchanged, which could led one to think that resonance "Doppler" broadening is not an import effect in a reactor application. This is true if the density of the resonance target nuclei is small (i.e., it is very dilute in the reactor), and thus its presence does not change the energy dependence of the reactor's neutron population. However, in most reactor designs, resonance absorbers are concentrated in localized reactor features (e.g., fuel elements, control rods) and there is significant self-shielding at the resonance peak. That is, neutrons with the "peak" energy will most likely be absorbed in the reactor "feature" irrespective of temperature-induced changes in the resonance microscopic cross section. But the story can be different on the wings of a resonance where the cross section is much smaller, and, thus, so is the self-shielding. An increase in temperature of the "feature" can result in a net increase in neutron absorption, with no change at the peak energy, but with increases in the wings. This phenomena can aid in insuring a *negative temperature coefficient* for a fission reactor design (*Temperature coefficients* are collective reactor parameters that reflect how neutron balance is impacted by temperature change through feedback mechanisms, for example, Doppler broadening (or narrowing) of resonances, and moderator density changes. Reactor control will be discussed in Sect. Fission Reactor Performance.). A negative temperature coefficient is a crucial reactor design safety requirement.

Dealing with temperature in producing resonance cross sections for design calculations is handled in a manner similar to the process for thermal energy range cross sections discussed above. The ENDF resonance cross-section models and appropriate material temperatures are input to NJOY, and the output are the broadened cross sections in the model format. How these cross sections are used in design calculations is addressed in the next section.

As noted at the start of this section, gamma ray (photon) cross sections are important in fission reactor design as they are required for the full treatment of energy deposition throughout a reactor (in its fuel bearing *core* and supporting structures). In the order of importance with increasing gamma energy, the mechanisms of attenuation are the photo electric effect (γ,e^-), Compton scattering (γ,γ*), and pair production (γ, e^-e^+). The photoelectric effect removes a γ when its energy, $h\upsilon$, can eject an atomic electron. Its cross section is approximately proportional to $Z^4/(h\upsilon)^3$, and has discontinuities in energy as the ionization energy of various atomic electron shells are achieved. For higher γ energies, Compton scattering interactions with atomic electrons can be treated as effectively free electron collisions. Conserving momentum and energy relativistically, one can derive expressions for energy loss and change in direction for initiating γs as a function of their incident energy. The magnitude of the cross section is proportional to Z. When γ energies reach a threshold of 1.022 MeV ($2 \times m_e c^2$) and are in the field of a target nucleus, pair production of an electron and positron is possible. The magnitude of the pair production cross section is proportional to Z^2. Of course, in tracking the γ population in a reactor, one recognizes that annihilation of a positron will produce two 0.51 MeV γ's. So pair production can be viewed as a form of inelastic scattering event. Cross sections for these three processes are tabulated in ENDF/B files, and they are described at a thorough but accessible level in the classic text by Robley D. Evans "The Atomic Nucleus."

An example plot of these cross sections for Th^{232} is provided in Fig. 2.7.

Finally, there are other gamma reactions which can take place in a reactor, for example (γ,f) and (γ,n) (the latter which we noted earlier as a source of delayed neutrons). However, these are threshold reactions for relatively high-energy gammas, and as shown in Table 2.3 the total energy available from fission from fissile isotopes for gammas is limited: <8 MeV for prompt γ's, and, <6.5 MeV for delayed γ's. Thus, these reactions are not important in determining the overall distribution of gammas in a reactor design.

Neutron Distributions

With the material provided to this point, the primary problem of reactor *theory* can be addressed: that of finding the neutron distribution in phase space ($\mathbf{r}$,E,$\mathbf{\Omega}$), of a reactor design, and subsequently the reactor's power distribution, both throughout the reactor design's lifetime. The first task is to derive the equation for the neutron density, N($\mathbf{r}$,E,$\mathbf{\Omega}$), the neutron transport equation, and auxiliary equations for the atom densities, $\rho_j(\mathbf{r},t)$, of depleting (initial inventory) isotopes and important fission products (Like reactor physics, *reactor theory* is a traditional term in the nuclear engineering discipline. It refers to the study of the neutron transport equation and the means of its solution.). A simple approach to deriving the transport equation is to consider a balance relationship for N($\mathbf{r}$,E,$\mathbf{\Omega}$,t)dEdΩdt for a time invariant volume, V, in configuration space:

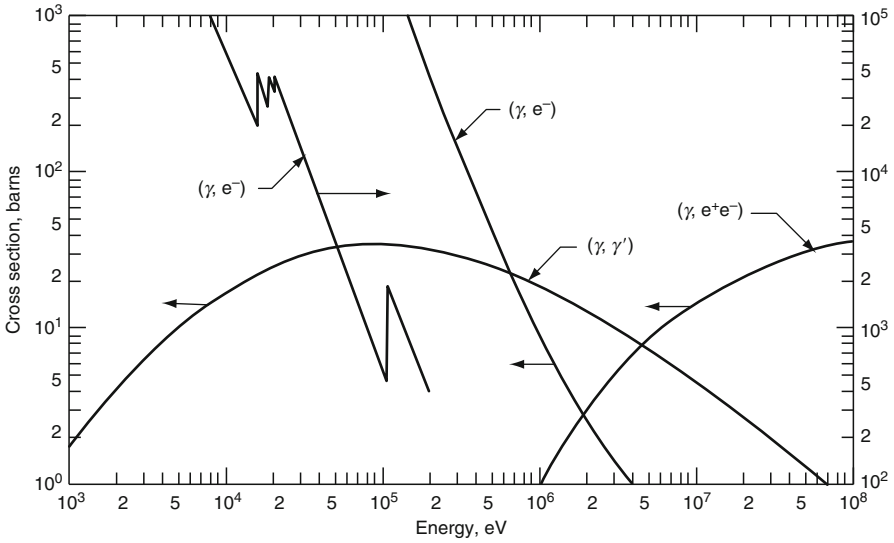

Fig. 2.7 Thorium cross section for the photo electric effect (γ,e), for Compton scattering (γ,γ‘), and pair production (γ, e + e^{-}) [32]

$$\begin{aligned} \mathrm{dEd\Omega dt}\int_{v}(\partial \mathrm{N(r,E,\Omega,t)}/\partial \mathrm{t})\mathrm{d^3r} &= -\text{loss from flow out of V} \\ &+ \#\text{ scattering into dE about E and d}\,\Omega\text{ about }\Omega \\ &+ \#\text{ produced by fission} + \#\text{ produced by other sources} \end{aligned} \tag{2.44}$$

For the “flow” term, one defines the neutron angular current $\mathbf{J}(\mathbf{r},\mathrm{E},\boldsymbol{\Omega},\mathrm{t}) \equiv \mathbf{v}\mathrm{N}(\mathbf{r}, \mathrm{E},\boldsymbol{\Omega},\mathrm{t})$, where $|\mathbf{J}(\mathbf{r},\mathrm{E},\boldsymbol{\Omega},\mathrm{t})\bullet\mathbf{n}\ \mathrm{dsdEd\Omega dt}|$ is the no. of neutrons at **r**, with energies in dE about E, traveling in dΩ about **Ω,** which cross an area ds with a unit normal vector **n** in dt at t. And thus, net flow out of V, which has a non-reentrant surface S, is:

$$\begin{aligned} &\mathrm{dEd\Omega dt}\int_{s}\mathbf{J}(\mathbf{r},\mathrm{E},\Omega,\mathrm{t})\bullet\mathbf{n}\mathrm{ds} \\ &\quad=\mathrm{dEd\Omega dt}\int_{v}\mathbf{v}\bullet\nabla\mathrm{N}(\mathbf{r},\mathrm{E},\Omega,\mathrm{t})\mathrm{d^3r}, \end{aligned} \tag{2.45}$$

where Gauss’ Theorem is applied to transform the surface integral to a volume integral.

The “reactions” in V are simply:

$$\mathrm{dEd\Omega dt}\int_{v}v\Sigma_{\mathrm{T}}(\mathbf{r},\mathrm{E},\mathrm{t})\mathrm{N}(\mathbf{r},\mathrm{E},\Omega,\mathrm{t})\mathrm{d^3r}, \tag{2.46}$$

where $\Sigma_T(\mathbf{r},E,t)$ is the total *macroscopic* cross section in V. All scattering cross sections included in Σ_T have been integrated over final energies and directions.

Scattering into V is:

$$dEd\Omega dt \int_v d^3r \int_0^\infty dE' \int d\Omega' \; v'\Sigma_s(\mathbf{r}, t, E' \rightarrow E, \Omega' \rightarrow \Omega)N(\mathbf{r}, E', \Omega', t) \tag{2.47}$$

where Σ_s is the double differential *macroscopic* scattering cross section in V (see the definition Eq. 2.65 for an example of a double differential *microscopic* scattering cross section).

The direct fission source into V is:

$$dEd\Omega dt \int_v d^3r \int_0^\infty dE' \int d\Omega'' \sum_i \nu_{pi}(E' \rightarrow E) \; \Sigma_{fi}(\mathbf{r}, E', t)\nu' N(\mathbf{r}, E', \Omega, t)/4\pi, \tag{2.48}$$

where ν_{pi} $(E' \rightarrow E)$ is the number of prompt neutrons emitted in dE about E by a fission of isotope i initiated by neutrons in dE′ about E′: the macroscopic fission cross section for isotope "i" is $\rho_i(\mathbf{r},t)\sigma_{fi}(E')$.

The delayed neutron source into V is:

$$dEd\Omega dt \sum_j X_{dj}(E) \frac{\lambda_j}{4\pi} \int_v C_j(\mathbf{r}, t) d^3r, \tag{2.49}$$

where $X_{dj}(E)/4\pi$ is the probability that the decay of delayed neutron precursor "j" will produce a neutron in dE about E and dΩ about Ω, and where λ_j and C_j are, respectively, the decay constant (see the beginning of section "Heavy Elements") and isotope density of precursor "j".

And, finally any source of neutrons in V not produced by a neutron reaction is given by:

$$dEd\Omega dt \int_v d^3r S(\mathbf{r}, E, t)/4\pi, \tag{2.50}$$

where S could characterize a source (e.g., Plutonium(238)-Beryllium(α,n) or Califonium-252 (spontaneous fission)) included in a reactor design to aid in reactor start-up or S might account for decay processes yielding neutrons due to the presence of depleted fuel incorporated from another design.

Now, if the terms on the right side of the "balance relationship," equation Eq. 2.44, are moved to the left side, and dEdΩdt and the integral operation $\int_{\mathrm{v}} \mathrm{d}^3\mathrm{r}$ is factored out of all the terms, then as the right side is now zero and the small volume V is arbitrary, the collection of expressions under the integral must equal zero. The resulting equation is the *Neutron Transport (or Boltzmann) Equation*:

$$\begin{aligned}\frac{\partial}{\partial \mathrm{t}}\mathrm{N}(\mathbf{r},\mathrm{E},\Omega,\mathrm{t}) = &-\mathbf{v}\bullet\nabla N(\mathbf{r},\mathrm{E},\Omega,\mathrm{t}) - \mathbf{v}\Sigma_T(\mathbf{r},\mathrm{E},\mathrm{t})\mathrm{N}(\mathbf{r},\mathrm{E},\Omega,\mathrm{t})\\ &+\int_0^\infty \mathrm{dE}'\int \mathrm{d}\Omega' v'\Sigma_s(\mathbf{r},\mathrm{t},\mathrm{E}'\to\mathrm{E},\Omega'\to\Omega)\mathrm{N}(\mathbf{r},\mathrm{E}',\Omega',\mathrm{t})\\ &+\int_0^\infty \mathrm{dE}'\int \mathrm{d}\Omega' v'\sum_{\mathrm{i}} \nu_{\mathrm{pi}}(\mathrm{E}'\to\mathrm{E})\Sigma_{\mathrm{fi}}(\mathbf{r},\mathrm{E}',\mathrm{t})\mathrm{N}(\mathbf{r},\mathrm{E}',\Omega',\mathrm{t})/4\pi\\ &+\sum_{\mathrm{j}} X_{\mathrm{dj}}(\mathrm{E})\lambda_{\mathrm{dj}}\mathrm{C_j}(\mathbf{r},\mathrm{t})/4\pi + S(\mathbf{r},\mathrm{E},\Omega,\mathrm{t}).\end{aligned} \tag{2.51}$$

The conditions for solutions of this partial-differential-integral equation are the continuity condition:

N(**r** + α**Ω**,E,Ω,t) must be a continuous function of α for **r** + α**Ω** in the reactor, and the

boundary condition:

$\mathrm{N}(\mathbf{r}_s,\mathrm{E},\mathbf{\Omega},\mathrm{t}) = 0$, for $\mathbf{\Omega}\bullet\mathbf{n} < 0$, where **n** is an outward unit vector normal to a non-reentrant surface chosen to define the extent of the reactor.

The auxiliary equations for number densities of delayed neutron precursors, $\mathrm{C_j}(\mathbf{r},\mathrm{t})$, and fission product poisons, depleting fissile isotopes, and *burnable* poisons, $\rho_{\mathrm{i}}(\mathbf{r},\mathrm{t})$s, are simply defined as movement of these isotopes in space can be ignored. *Burnable* poisons are elements with large neutron absorption cross sections (e.g., Boron, Hafnium, Cadmium, Erbium, Gadolinium) that can be included in reactor designs to maintain neutron balance over design lifetime.

- For delayed neutron precursors:

$$\frac{\partial}{\partial \mathrm{t}}\mathrm{C_i}(\mathbf{r},\mathrm{t}) = -\lambda_{\mathrm{i}}\,\mathrm{C_i}(\mathbf{r},\mathrm{t}) + \int_0^\infty \mathrm{d}E'\int \mathrm{d}\Omega'\sum_{\mathrm{j}}\xi_{\mathrm{ij}}\nu'\Sigma_{\mathrm{fj}}(\mathbf{r},\mathrm{E}',\mathrm{t})\mathrm{N}(\mathbf{r},\mathrm{E}',\Omega'\mathrm{t}), \tag{2.52}$$

  where ξ_{ij} is the expected number of precursors of type i produced by fission of isotope j.
- For fission product poisons (e.g., Xenon-135 and its precursors Telirium-135 and Iodine-135, and Samarium-149 and its precursors Neodimium-149 and Promethium-149):

$$\frac{\partial}{\partial t}\rho_i(\mathbf{r},t) = -\lambda_i\rho_i(\mathbf{r},t) + \lambda_{j\to i}\rho_j(\mathbf{r},t) - \int_0^\infty dE' \int d\Omega'\rho_i(\mathbf{r},t)\sigma_{c^i}(E')v'N(\mathbf{r},E',\Omega',t) + \int_0^\infty dE' \int d\Omega' \sum_k \gamma_{ik}(E')\sum_{fk}(\mathbf{r},E',t)v'N(\mathbf{r},E',\Omega',t), \quad (2.53)$$

where $\gamma_{ik}(E)$ is the expected number of poison (or poison precursor) nuclei produced by fission of isotope k induced by neutrons of energy E.

- For fissile fuel and burnable poison isotopes:

$$\frac{\partial}{\partial t}\rho_i(\mathbf{r},t) = -\int_0^\infty dE' \int d\Omega'\rho_i(\mathbf{r},t)\sigma_{a^i}(E')v'N(\mathbf{r},E',\Omega',t), \quad (2.54)$$

where the subscript "a" as applied to $\sigma_a{}^i$ conventionally refers to capture plus fission for fissile isotopes. For reactor designs containing fertile isotopes, equation Eq. 2.54 will have a source term reflecting the transmutation process leading to the fissile isotope "i" (see Fig. 2.1). Additional "auxiliary" equations may be needed to deal with transmutation of one isotope of a burnable poison to another, which has a significant neutron capture cross section (for example Hafnium, which has four naturally occurring isotopes).

Solving these "auxiliary" equations, irrespective of their number, is not a calculational challenge, given one knows the neutron density, N(**r**.E,**Ω**,t), as they are ordinary differential equations. Obviously, solving the neutron transport equation (Eq. 2.51) for N(**r**,E,**Ω**,t) is another matter. There are several features of fission reactors, however, that make this task more tractable. First, the density of neutrons needed to produce as much power as can be removed/transferred from various reactor types to do useful work is very small, $\sim 10^7$–10^9 #/cm^3, where as the density of nuclei is many orders of magnitude larger $\sim 10^{23}$ #/cm^3. Therefore, the neutrons can be viewed as a very dilute gas in the matrix of a reactor's nuclei, and thus neutron–neutron collisions can be ignored (they have not been accounted for in Eq. 2.51) (Another neutron behavior that can be ignored in formulating the transport equation is the finite lifetime of a free neutron. Its mean-life is ~11.5 min. But, as will be discussed in the next section, the lifetime of neutron in a reactor is measured in milliseconds.). Second, in the primary nuclear design calculations, where it is determined if a trial configuration, loading and geometry, of fuel, structure, moderator, coolant, control elements, and poisons, can sustain neutron balance through out the reactors lifetime objective, the time variable "t" in Eq. 2.51 can be treated in a much simplified manner. Given the initial conditions of a trial reactor configuration, it is a good assumption that the atom

densities in the various macroscopic cross sections in Eq. 2.51 can be treated as nearly constant for a significant time interval, $\Delta t \geq$ minutes. With this assumption, and no neutron–neutron collisions, Eq. 2.51 is linear in $N(\mathbf{r},E,\boldsymbol{\Omega},t)$ during Δt, and solution methods for Eq. 2.51 are greatly simplified. In addition, for the interval, Δt, Eq. 2.51 can be treated as a time-independent equation. For a *primary nuclear design* calculation, one ignores the source term $S(\mathbf{r},E,t)$ (its importance to the start-up problem will be addressed in the next section) and Eq. 2.51 becomes a linear homogeneous eigenvalue problem:

$$\begin{aligned}
&\mathbf{v}\Omega \bullet \nabla \cdot N(\mathbf{r},E,\Omega) + v\Sigma_T(\mathbf{r},E)N(\mathbf{r},E,\Omega) \\
&\quad - v\int_0^\infty dE' \int d\Omega' v'\Sigma_s(\mathbf{r},E' \rightarrow E,\Omega' \rightarrow \Omega)N(\mathbf{r},E',\Omega') \\
&\quad = \frac{1}{k}\int_0^\infty dE' \int d\Omega' v' \sum_j \Sigma_{fj}(\mathbf{r},E') \\
&\quad \left\{ v_{pj}(E' \rightarrow E) + \sum_j X_{di}(E)\xi_{ij} \right\} N(\mathbf{r},E',\Omega')/4\pi, \qquad (2.55)
\end{aligned}$$

where 1/k is the eigenvalue. It has been customary to use the inverse of "k" as the eigenvalue and to refer to k as the multiplication factor. Note that if Eq. 2.55 is integrated over the reactor volume and E and $\boldsymbol{\Omega}$, then k is equal to the ratio of neutron production to neutron loss, this is the origin of its designation as a "multiplication factor." A further simplification in Eq. 2.55 arising from the assumption of "time independence" during Δt, is that delayed neutron production can just be added to prompt neutron production. As indicated, previously delayed neutrons, though less than a percent of total neutron yield in a fission, are critical to transient reactor behavior, and, therefore, control system design, to be covered in the next section.

Before proceeding with the solution methods for Eq. 2.55, a description of how the *primary nuclear design* calculation proceeds is required for a basic understanding of reactor design, and to provide perspective on the utility of the various solution methods for the transport equation. Assuming the solution method chosen has yielded a k_i and $N_i(\mathbf{r},E,\boldsymbol{\Omega})$ for the initial time interval, Δt_i where i = 1, then one proceeds to check design requirements, and make needed modifications to the reactor's initial *trial configuration*. In general, this is an iterative process including other disciplines (i.e., heat transfer and fluid flow, structural analysis). If $k \neq 1$, inventories of fuel/poisons or the positioning of control elements will need to be altered to achieve neutron balance (*Control elements* (sometimes generically called control rods) are structures incorporating highly neutron absorbing isotopes. They have a dual role in fission reactor design: (1) assuring criticality (a controlled steady state chain reaction) throughout a reactor's design lifetime, i.e., compensating for potential excess neutron production from the initial fissile loading which must

be large enough to accommodate depletion; and (2) providing safe shut down (termination of the chain reaction) of the reactor in case of an accident condition or during a planned interruption of normal operations (e.g., for plant maintenance or refueling). The same "structures" could accomplish both functions or there could be separate structures (sometimes referred to as "shim" and "shutdown" rods respectively).). The power distribution throughout the reactor must then be determined. As N(**r**,E,**Ω**) is the solution to a homogeneous equation, its absolute magnitude is undetermined, but a normalization factor, p, can be established from the total thermal power rating, P(MWth), requirement of the design, that is from:

$$\mathbf{P} = p \int_{\text{RVol.}} \mathrm{d}^3 r \int_0^\infty \mathrm{dE} \int \mathrm{d}\Omega v \sum_{\mathrm{j}} \epsilon_{\mathrm{j}} \Sigma_{fj}(\mathbf{r}, \mathrm{E}) \mathrm{N}(\mathbf{r}, \mathrm{E}, \Omega), \tag{2.56}$$

where ε_j is the energy release per fission of isotope j (see Table 2.3). Now given pN(**r**,E,**Ω**), one can calculate the power distribution throughout the reactor

$$\mathbf{P}(\mathbf{r}) = p \int_0^\infty \mathrm{dE} \int \mathrm{d}\Omega v \sum_j \epsilon_{\mathrm{j}} \Sigma_{fj}(\mathbf{r}, \mathrm{E}) N(\mathbf{r}, \mathrm{E}, \Omega), \tag{2.57}$$

and determine peak powers in fuel elements, and average and peak heat fluxes into coolant channels. Thus, fuel element and heat removal system limits can be checked. If there are violations, the *trial configuration* must be altered and new results for k and N(**r**,E,**Ω**) found. From the power distribution and subsequent thermal analysis, one can also verify the temperatures that were assumed for the *trial configuration*, that is, the temperatures that were needed to define thermal scattering cross sections and Doppler broadened resonance cross sections. Finally, when all conditions are met for the first time interval, Δt_i, where i = 1, the *auxiliary* equations (Eq. 2.53 and Eq. 2.54) can be solved to update inventories of fuel and poisons for the next time interval, Δt_2. For a thermal reactor design, where the fission product poisons Samarium-149 and Xenon-135, are important, initial time intervals should be short (minutes) until equilibrium levels of these isotopes are achieved (~hours). Subsequent time intervals can be many hours. From this brief description of the *primary nuclear design process*, it should be clear that having accurate and efficient solution methods for the time-independent neutron transport equation is key to achieving a successful design.

There are two basic approaches to solving the time independent neutron transport equation, Eq. 2.55; the probabilistic-statistical Monte Carlo simulation method [14] where individual neutrons are traced through their life experience in a reactor, and analytic methods where the variables, **r,** E, and (sometimes) **Ω**, are made discrete, thus transforming Eq. 2.55 into a matrix equation.

Monte Carlo simulation is in principle well suited for this application because the neutron density is low so the transport equation can be treated as linear. Thus,

each "experiment," that is, neutron history, is independent of all others. Initially, a neutron is started at a randomly selected reactor location and with a randomly selected direction, $\mathbf{\Omega}$. Its initial energy is selected by treating a typical prompt neutron energy spectrum as a probability distribution:

$$P(E)dE = v_p(E)dE \Big/ \int_{E_{min}}^{E_{max}} dE v_p(E), \tag{2.58}$$

which is then "sampled" with a random number between 0 and 1. In Monte Carlo computer programs [15, 16] a sequence of random numbers is generated with an algorithm. To provide an example of "sampling," note that in this case, given a random number n, the "sampled" starting energy E is found by simply solving the transcendental equation:

$$n = \int_{E_{min}}^{E} dE' P(E') for E. \tag{2.59}$$

Now having a speed and direction, one can "sample" (with a new random number) the probability that the neutron travels a distance x before having a collision, using equation Eq. 2.20. As this probability depends on the total macroscopic cross section, $\Sigma_T(\mathbf{r},E)$, one must keep track of material boundaries. An initial sampling will be for the distance from the starting point of the neutron to the first material boundary it could cross. If the initial sampling results in the boundary being crossed, then there is a new Σ_T and a second sampling is performed to determine if another boundary is crossed. Eventually, either the neutron leaves the reactor or the location of the first collision is established. As the total cross section is the sum of capture, scattering, and possibly fission macroscopic cross sections for the various isotopes present, one can treat the relative magnitudes of the components of the sum as a probability distribution, which when "sampled" leads to the next step in our neutron's history. If capture is the result, the history ends, just as it would end if the neutron leaked (escaped) from the reactor. Either capture or leakage is recorded as a "loss." If fission is the result, the history also ends, but the number of neutrons produced (1, 2, or 3) in the fission of the "selected" isotope j, and the fission location are recorded. The number of fission neutrons is determined by "sampling" the probability distribution for fission yield of isotope j. The mean of the distribution $\overline{\nu}_j(E)$ includes delayed neutrons. The number of neutrons produced by a "history" is counted as "production." If scattering is the result of the collision then the double differential macroscopic cross section is treated as probability distribution and "sampled" to provide a new energy and direction for the neutron. Then, the process of tracking to either escape or the next collision is repeated. Thus, the "history" proceeds until it ends as either "loss" or "production", if "production" a starting point for a subsequent "history" and a location for energy deposition are also provided.

There are various strategies for carrying out Monte Carlo calculations and the evaluation of the statistical nature of the results. A standard approach, in outline, is to run successive groups of "histories" (thousands). Discard the first few groups, which are used to establish a reasonable fission neutron spatial source distribution, and then find the mean and standard deviations of the desired calculational results from the subsequent groups. It is most economical to get good statistics for the eigenvalue k, the multiplication factor, which is just "production" over "loss," quantities which are accumulated over the whole reactor. Energy deposition, that is, power distribution, results are much more costly. Hundreds of groups with millions of histories per group would be required to give good statistics (a five percent 95% confidence interval) for the number of fissions in small reactor volumes (e.g., a 1 cm length of a typical PWR fuel element which has a volume of 0.7 cm^3, out of a reactor volume of 32.8×10^6 cm^3 (for a 3,400 MWth rating)). From this discussion, one can see why, as mentioned in section Cross Sections, Monte Carlo calculations of mock-up experiments are widely used in cross-section data set evaluations, where the results of interest are changes in k, the multiplication factor. Even with the tremendous advances in computing capability which have been made to date, Monte Carlo simulation is not as yet the main line method for primary nuclear design calculations. But, as will be seen in the following description of analytic methods, it can greatly aid in improving the accuracy of the analytic methods.

When the analytic approach of making the neutron density's variables **r,** E and Ω discrete is applied, so as to make the computational errors in solving the transport equation comparable to an exhaustive Monte Carlo simulation, the computer resource requirements will challenge today's largest machines (peak speeds of $\sim 2.3 \times 10^{15}$ flops (floating point operations per second) [17]).

This can be demonstrated with the large PWR used in the Monte Carlo discussion: *First*, a spatial mesh of 65.6×10^6 points would result, assuming quarter core radial symmetry, and from using a $1 \times 1 \times 2$ cm^3 cell for averaging cross sections. (The mesh may need to be finer for highly absorbing features, e.g., fixed poisons, control elements, and can be courser in homogeneous regions.) *Second*, the energy variable can be treated with a multigroup approximation where the energy range, $0.0 \rightarrow 10$ MeV is divided into intervals (groups), for example, 24 for thermal neutrons, $0.0 \rightarrow$ 0.625 eV, and 57 for the rest of the range, with most of these groups allotted to epithermal neutrons, E = 0.625 eV $\rightarrow$ 0.1 MeV where there is a concentration of explicit resonance cross sections (see Table 2.6). A weight function f_g (**r**,E), normalized for E to unity, is required for each interval, g. These can be calculated with infinite medium problems representing various portions of the reactor; homogeneous problems with no spatial variables, or an infinite repeating array of cells (e.g., a fuel element and surrounding coolant) with radial spatial variables, but no axial, z, dependence. The power of the multigroup approximation is that it is insensitive to the choice of weight functions and thus simplifying assumptions can be made in selecting and solving the "infinite medium" problems to generate the f_g's. *Finally*, the direction variable, **Ω**, can be dealt with through a discrete ordinate approximation [18]. The unit sphere is divided into segments, the surface areas of which sum to 4π, and

a direction vector $\mathbf{\Omega}_n$ is assigned to each segment. The segment surface areas act as weight functions when the transport equation is integrated over a segment to yield an equation for the neutron density going in the direction $\mathbf{\Omega}_n$. There are various schemes for selecting ordinates and weights, the most widely known is the S_n method. All methods, however, can produce *ray effects* if "n" is too small [19]. The channeling of neutrons into a few restricted directions can produce anomalous results in reactor designs with localized neutron source regions, that is, where fissile and fertile fuel predominate in different regions (commonly referred to as seed-blanket designs). For a "highly accurate" treatment, one should let n = 16 in each octant, for a total of 128 ordinates. So for the "large PWR example," the number of unknowns to be solved for in the discretized time-independent transport equation is 170×10^9 (=16.4×10^6 (spatial mesh points) $\times$ 81 (energy groups) $\times$ 128 (ordinates)). This is clearly a formidable calculational problem. If we view the analytic approach described here as transforming Eq. 2.55 into a matrix eigenvalue equation, then the simplest solution method of matrix inversion would involve matrices of a billion by a billion. Hence, an iterative method is required [20]. Much effort in reactor *theory* has been devoted to this problem, and to simplifying the analytic approach. Iterative methods for solving matrix equations are beyond the scope of this entry, but to understand how fission reactor design is actually carried out, a description of analytic approach simplifications is needed.

The direction variable, $\mathbf{\Omega}$, received the earliest attention. Because the neutron population in a reactor can be viewed as a dilute gas, it was natural to assume that the variation of the neutron density in space could be approximated by $\nabla \bullet D(\mathbf{r},E,t)\nabla vN(\mathbf{r},E,t)$ (from Fick's Law of diffusion). When the transport equation, Eq. 2.51, is integrated over $\mathbf{\Omega}$ and the first term on the right-hand side is replaced by the Fick's Law expression, the result is the time-dependent neutron diffusion equation. Equation 55 can be treated analogously to yield the time-independent neutron diffusion equation. In either case, the limitations of the diffusion approximation only become apparent in trying to define the diffusion coefficient $D(\mathbf{r},E,t)$ (see Henry, Nuclear-Reactor Analysis). The most commonly used expression is

$$D(\mathbf{r},E,t) \equiv 1/\{3[\Sigma_t(\mathbf{r},E,t) - \overline{\mu_0}\Sigma_s(\mathbf{r},E,t)]\}, \tag{2.60}$$

where $\overline{\mu_0}$ is the average of the average cosine of the scattering angle (in the laboratory coordinate system) of each isotope making up $\Sigma_s(\mathbf{r},E,t)$. This definition (Eq. 2.60) arises from a low-order spherical harmonics expansion of $N(\mathbf{r},E,\mathbf{\Omega},t)$ in the neutron transport equation. Spherical harmonics are a complete orthonormal set of special functions on the unit sphere defined by Ω (the unit vector which is at angle θ from the z axis and projects in the x–y plane at angle φ from the x axis);

$$\begin{aligned} Y_l^m(\Omega) = H_l^m P_l^m(\mu) e^{im\varphi} \text{ for } l &= 0,1,2,3..... \\ m &= -l \le m \le l, \end{aligned} \tag{2.61}$$

where $H_l^m = \left[\frac{(2l+1)(l-m)!}{4\pi(l+m)!dm}\right]^{1/2}$, $P_l^m(\mu) = \sin^m(\mu)\frac{d^m}{d\mu^m}P_l(\mu)$ is the associated Legendre Polynomial, $P_l(\mu) = \frac{1}{2^l l!}\frac{d^l}{d\mu^l}(\mu^2-1)^l$ is the Legendre Polynomial and μ = cosθ. The spherical harmonics are normalized by the relationship:

$$\int_0^{2\pi} d\varphi \int_{-1}^{1} d\mu \; \overline{Y_l^m(\mu,\varphi)}\, Y_{l'}^{m'}(\mu,\varphi) = \delta_{mm'}\delta_{ll'}, \tag{2.62}$$

where $\overline{Y_l^m}$ is the complex conjugate of Y_l^m and the Kronecker deltas, δ, are 1 for m = m' and $l = l'$ and 0 otherwise.

The "low-order" spherical harmonics expansion, which yields the diffusion approximation, is for $l = 0$ and 1 (also referred to as the P1 approximation). The four functions in the expansion are:

$$\begin{aligned} &Y_0^0 = (1/4\pi)^{1/2}, Y_1^{-1} = (3/4\pi)^{1/2}\sin\,\theta e^{-i\varphi}, \\ &Y_1^0 = (3/4\pi)^{1/2}\mu \text{ and } Y_1^1 = -(3/4\pi)^{1/2}\sin\theta e^{-i\varphi}. \end{aligned} \tag{2.63}$$

In a Cartesian coordinate system, the expansion coefficients (for simplicity of notation the time-independent case will be treated) are N(x,y,z,E), the neutron density and N_1^{-1} (x,y,z,E), N_1^1 (x,y,z,E) and N_1^0 (x,y,z,E), which when multiplied by v (the speed corresponding to E) are the neutron currents in the x, y, and z directions. Before applying the P1 expansion to Eq. 2.55, one needs to note that the double differential scattering cross section, $\Sigma_s(E' \rightarrow E, \boldsymbol{\Omega}' \rightarrow \boldsymbol{\Omega})$ in reactor applications (where neutron polarization and Bragg scattering can be ignored) depends on $\boldsymbol{\Omega}'\bullet\boldsymbol{\Omega}$. Then, given the addition theorem for spherical harmonics,

$$P_1(\Omega'\bullet\Omega) = \sum_{m=-l}^{l}\frac{(l-m)!}{(l+m)!}P_l^m(\mu)\,P_l^m(\mu')e^{im(\varphi-\varphi')}, \tag{2.64}$$

$\Sigma_s(\mathbf{r},E' \rightarrow E, \boldsymbol{\Omega}'\bullet\boldsymbol{\Omega})$ can be expanded in terms of associated Legendre polynomials. This is done in two steps: first the double differential scattering cross section is expressed as an expansion in ordinary Legendre polynomials (which are a complete orthogonal set of functions)

$$\begin{aligned} \Sigma_s(\mathbf{r},E'\rightarrow E,\Omega'\bullet\Omega) = &\Sigma_s(\mathbf{r},E)\sum_{l=0}^{\infty}\frac{(2l+1)}{4\pi} \\ &F_1(\mathbf{r},E'\rightarrow E)\,P_1(\Omega'\bullet\Omega), \end{aligned} \tag{2.65}$$

and then Eq. 2.64 is substituted for $P_l(\boldsymbol{\Omega}'\bullet\boldsymbol{\Omega})$. (It should be remembered that Σ_s is a macroscopic cross section, and a more complete notation would show a sum over contributions from each isotope present in d^3r about $\mathbf{r}$.)

Now when the P1 expansion for N(x,y,z,E,μ,φ) is inserted in Eq. 2.55 and the resulting equation is, in turn, multiplied by the complex conjugate of each of the four spherical harmonics functions of the P1 expansion (Eq. 2.63), and integrated over μ (−1 → 1) and φ (0 → 2π), four equations result: The first is

$$\begin{aligned}&\frac{\partial}{\partial x} v N_1^{-1}(x,y,z,E) + \frac{\partial}{\partial y} v N_1^{1}(x,y,z,E) \\ &\quad + \frac{\partial}{\partial z} v N_1^{0}(x,y,z,E) = -v\Sigma_T(x,y,z,E) N(x,y,x,E) \\ &\quad + \int_0^{10Mev} dE' v' \Sigma_s(x,y,z,E') F_0(E' \to E) N(x,y,z,E') \\ &\quad + (\text{the fission term in Eq.55 with } N(\mathbf{r}, E', \Omega') \\ &\qquad \text{replaced with } N(x,y,z,E')).\end{aligned} \tag{2.66}$$

The remaining three equations are of the same form, one is provided here:

$$\begin{aligned}&\frac{1}{3}\mathbf{v}\frac{\partial}{\partial z} N(x,y,x,E) + v\Sigma_T(x,y,z,E)\, N_1^0(x,y,z,E) \\ &\quad = \int_0^{10Mev} dE' \mathbf{v} \Sigma_s(x,y,z,E') F_1(E' \to E) N_1^0(x,y,z,E')\end{aligned} \tag{2.67}$$

With these four coupled partial-differential-integral equations, there is still considerable computational complexity. To get to the standard neutron diffusion equation, one additional approximation is made:

$$F_1(E' \to E) \cong \delta(E' - E)\mu(E'), \tag{2.68}$$

where $\mu(E')$ is the average cosine of the scattering angle in the laboratory coordinate system, and energy loss (or gain) in the non-isotropic component of scattering is ignored. Substituting Eq. 2.68 in Eq. 2.67, the relationship between N_1^0 and N is a simple partial differential equation:

$$N_1^0(x,y,z,E) = -\frac{1}{3(\Sigma_T(x,y,x,E) - \mu(E)\Sigma_S(x,y,z,E))} \frac{\partial}{\partial z} N(x,y,z,E), \tag{2.69}$$

containing the diffusion coefficient D(**r**,E) (see the definition Eq. 2.60). Given the equations of the same form as Eq. 2.69 for N_1^1 and N_1^{-1}, and substituting all three into the left-hand side of Eq. 2.66. The left-hand side becomes the standard Fick's Law expression:

$$-\nabla \bullet D(r,E) \nabla N(r,E) = ... \tag{2.70}$$

As noted above, this derivation of the diffusion approximation reveals its limitations. The ability of some combination of four low-order spherical harmonic functions, Eq. 2.63, to describe the true angular distribution of the neutron density throughout a reactor will be limited to regions where the distribution is nearly isotropic, that is away from boundaries and highly absorbing features (control elements and fixed poisons). To address these limitations, special boundary conditions are used, and subsidiary calculations (to be discussed below) are made to provide "fitted" cross sections for highly absorbing features.

To make the diffusion approximation an efficient design tool, additional simplifications have been developed. The differencing of the energy variable as described above for "multigroups" can be extended to a "few group" approximation. Again, weight functions are generated using accurate solutions to small region "cell" problems, which model repeating features of a reactor. But here the weight functions are applied over much larger energy ranges, three or four to cover the energy range of 0 to 10 MeV. Furthermore, one accepts the error associated with the weight functions not perfectly representing the spatial variation of neutron density energy dependence.

The use of "cell problem" auxiliary calculations can be extended. As the core, the central fuel bearing region, of most reactor designs is made up of collections of mostly fuel elements, and possibly some fixed poison and movable control elements, assembled into modules. One can perform highly accurate (e.g., Monte Carlo or multigroup, fine spatial mess, discrete ordinate) calculations for two-dimensional (radial) repeating arrays representations of a core's various modules. Then, for each module type, a series of corresponding few-group diffusion approximation calculations can be carried out, in which key few group cross sections are adjusted ("fitted") to match reaction rates from the "highly accurate" reference calculation. One can the use these fitted cross sections in a full core three-dimensional few group diffusion calculation as part of the *principle design process*.

Of course, with depletion, as inventories of fuel, fission products, and poisons are updated, fitting calculations will have to be repeated. This approach is particularly suited to the design of thermal reactors, that is, PWRs and BWRs, where the proper treatment of epi-thermal and thermal neutrons, including the effects of self-shielding by fuel and poison inventories, is crucial.

In fast reactor design, where most fissions take place at energies above explicit resonances (liquid metals or gasses are coolants, and fissile and fertile densities and inventories are high (no effective moderators are present)) and the mean free path of fission neutrons is large ($\sim$10 cm.), the treatment of fuel, structure and coolant as an homogenized material, in formulating macroscopic cross sections, is a reasonable assumption. Treatment of the energy variable is also simpler as up-scattering is not important. As a result, multigroup, 3D discrete ordinate calculations can be used in the *principle design process* for fast reactors.

Finally, returning to thermal reactor design, there is another analytic calculational approach, which is in wide use, that should be mentioned. The general designation is Nodal Methods. There are a number of variations under this title [21], but they all have as their starting point solving 2D module array problems.

One needs to produce few group neutron distributions within each module. Each module (or depending on symmetry each half or quarter module) will be a "node." Then coupling coefficients between nodes, both radially and axially, are generated. (It is predominately in defining coupling coefficients that the various "methods" differ.) The resulting nodal equations can be solved with modest computer resources, but, to obtain power distributions and to update inventories the full reactor neutron distribution must be constructed from the module solutions and the weights found for each node. Nodal Methods have been found to be particularly useful in applying the *primary nuclear design process* to evaluating refueling options for commercial (large scale) PWRs and BWRs, where partially depleted modules are relocated, "shuffled," as new modules are added and fully depleted, "spent" modules removed during periodic refuelings. The computational economy of nodal methods also allows them to be applied to fully time-dependent problems, particularly for accident analyses. The nature of these problems will be discussed in the next section.

Fission Reactor Performance

In the previous section, the focus was the derivation of the neutron transport equation, and how it is solved in carrying out the *primary nuclear design process*. This quasi-static *process* involves a series of time-independent calculations of the neutron density, $N(\mathbf{r},E,\boldsymbol{\Omega})$, and ultimately results in the configuration and inventories (loadings) that meet design requirements for lifetime (total energy production), and normal operation thermal performance (fuel element burn-up within limits and sufficient coolant flow provided by the design pumping power allocation). There are, however, additional design requirements that involve transients, that is, $N(\mathbf{r},E,\boldsymbol{\Omega},t)$, which will be the subject here.

The simplest approach to treating transient reactor behavior is through a "point" kinetics model. If one first multiplies the time-dependent transport equation, Eq. 2.51, by a weight function, $W(\mathbf{r},E,\boldsymbol{\Omega})$, and integrates over the reactor volume, energy (the full range, $0 \rightarrow 10$ MeV), and direction ($\cos\theta$ from -1 to 1, φ from 0 to 2π); and second, multiplies the time-dependent equation for each delayed neutron precursor, Eq. 2.52 for $C_i(\mathbf{r},t)$, by $W(\mathbf{r},E,\boldsymbol{\Omega})X_{di}(E)$ and performs the same integration over reactor volume, energy, and direction, the results are the point kinetics equations:

$$\frac{dT(t)}{dt} - \frac{\rho - \beta}{\Lambda} T(t) + \sum_{l-1}^{l} \lambda_l C_l(t) + Q(t) \tag{2.71}$$

$$\frac{dC_j(t)}{dt} = \frac{\beta_j}{\Lambda} T(t) - \lambda_j C_j(t) \text{ for } j = 1, 2, \ldots I \tag{2.72}$$

where T(t) is an amplitude function;

$$T(t) \equiv \int_{\text{reactor}} dV \int_{0}^{10\text{Mev}} dE \int d\Omega W(\mathbf{r}, E, \Omega) \\ N(\mathbf{r}, E, \Omega, t). \tag{2.73}$$

In formulating the expressions for the kinetics parameters, ρ(t), β(t), and Λ(t), it is convenient to factor the neutron density into a product of "shape" and amplitude functions. The shape function is;

$$S(\mathbf{r}, E, \Omega, t) \equiv N(\mathbf{r}, E, \Omega, t)/T(t). \tag{2.74}$$

Now the weight function is defined over the same domain (space, energy, and direction) as the neutron density, and thus from the definitions Eq. 2.73 and Eq. 2.74 the normalization of S and W follows:

$$\int_{\text{reactor}} dV \int_{0}^{10\text{Mev}} dE \int d\Omega W(\mathbf{r}, E, \Omega) S(\mathbf{r}, E, \Omega, t) = 1 \text{ for all t.} \tag{2.75}$$

In order for the point kinetics equations to provide accurate solutions for small changes in reactor configuration, the weight function, $W(\mathbf{r},E,\boldsymbol{\Omega})$, is chosen to be the solution the adjoint equation corresponding to the time-independent transport equation, Eq. 2.55, for the reactor of interest adjusted to be critical (i.e., the eigenvalue k = 1). In the adjoint of Eq. 2.55, the variable pairs $(E,\boldsymbol{\Omega})$ and $(E',\boldsymbol{\Omega}')$ are interchanged in the scattering and fission terms. The solution, $N^*(\mathbf{r},E,\boldsymbol{\Omega})$, is referred to as the adjoint neutron density or the importance function. The latter name indicates the physical interpretation of N*. If the reactor described by Eq. 2.55 is at zero power (no neutrons) and a neutron is inserted at $\mathbf{r}$ with velocity $\mathbf{v}(E,\boldsymbol{\Omega})$, the neutron level will increase to a steady-state value (remember the reactor is still critical). This "level" per neutron added at $(\mathbf{r},E,\boldsymbol{\Omega})$ is $N^*(\mathbf{r},E,\boldsymbol{\Omega})$. How N*, acting as a weight function, improves the point kinetics equations will be discussed after ρ, β, and Λ are defined and their physical interpretation given. To simplify notation, the scattering and fission integral operators in Eq. 2.51 are represented by *A* and *G*:

$$A \equiv \int_{0}^{\infty} dE' \int d\Omega' \nu' \Sigma_S(\mathbf{r}, E' \rightarrow E, \Omega' \rightarrow \Omega) \bullet, \tag{2.76}$$

$$G \equiv \int_0^\infty dE' \int d\Omega' v' \sum_i \nu_i(E')\Sigma_{fi}(\mathbf{r}, E')\bullet, \tag{2.77}$$

where $\nu_i(E')$ is the total number of neutrons (prompt plus delayed) produced by fission of isotope i induced by a neutron with energy E'. In reactor kinetics, delayed neutron yields are expressed in terms of the ratio the number produced with a given half-life (i.e., a member of "delayed group," j, as noted previously, see Table 2.4) by fission of isotope, i, to the total the total yield, ν_i. These ratios are represented as β_j^i, where normally j = 1,2 . . . 6.

The parameter ρ(t) is the *reactivity* of a reactor and is a measure of how far from criticality (a steady-state chain reaction only from fission neutrons, no other neutron sources present) the reactor is at time t. This can be seen from the expression for ρ(t) that results from the derivation of Eq. 2.71 from the transport equation (where the functional dependencies on **r**, E, **Ω,** and t are understood for Σ_T, W, and S):

$$\rho(t) \equiv \frac{\int_{reactor} dV \int_0^\infty dE \int d\Omega W[-v\Omega \bullet \nabla S - v\Sigma_T S + AS + \sum_i X^i(E)GS]}{\int_{reactor} dV \int_0^\infty dE \int d\Omega W \sum_i X^i(E)GS}, \tag{2.78}$$

where $X^i(E)$ is the total fission spectrum for isotope i:

$$X^i(E) \equiv X_p^i(E)\{1 - \beta^i\} + \sum_{j=1}^{6} X_{dj}(E)\beta_j^i. \tag{2.79}$$

Now note, if both the numerator and denominator of Eq. 2.78 are multiplied by the amplitude function T(t), and W is taken as 1, then the numerator is the total neutron production rate minus loss rate for the reactor. (When the first term in the bracket in the numerator is integrated, and Gauss' theorem is applied, it yields the total neutron leakage rate from the reactor.) Similarly, the denominator is the total neutron production rate. Reactivity is a dimensionless parameter whether or not W is unity. If it is zero, the reactor is critical, if negative, subcritical and if positive, supercritical.

β_j in Eq. 2.72 is the *effective delayed neutron fraction* for the jth precursor group, and β in Eq. 2.71 is the sum of the βj's:

$$\beta_j \equiv \frac{\int_{\text{reactor}} dV \int_0^\infty dE \int d\Omega W \sum_i X^i(E)\beta_j^i GS}{\int_{\text{reactor}} dV \int_0^\infty dE \int d\Omega W \sum_i X^i(E) GS}. \tag{2.80}$$

As with the expression for reactivity, multiplying the numerator and denominator of Eq. 2.80 by T(t) and letting W = 1, one sees that in this case β_j is the fraction of total fission neutrons produced in the reactor by precursor group j.

The parameter Λ is the *prompt neutron lifetime* and is defined as:

$$\Lambda \equiv \frac{\int_{\text{reactor}} dV \int_0^\infty dE \int d\Omega WS}{\int_{\text{reactor}} dV \int_0^\infty dE \int d\Omega W \sum_i X^i(E) GS}. \tag{2.81}$$

Again multiplying the numerator and denominator by T(t) and taking W = 1, one sees that Λ equals the number of neutrons in the reactor divided by the rate of neutron production by fission. If the reactor is critical, Eq. 2.81 has the same form as the "fundamental equation of radioactive decay," Eq. 2.11, and Λ can be thought of as the "mean lifetime" of a neutron born into the reactor. In the point kinetics equations, Λ is the mean *prompt neutron lifetime,* and the timing of the appearance of delayed neutrons is treated explicitly through the behavior of their precursor, $C_j(t)$ j = 1,2 . . . . I (usually = 6).

The derivation of the point kinetics equations directly from the time-dependent neutron transport equation has been presented here to provide perspective on approximations that are normally made to make the generation of the point kinetics parameters (ρ, β, and Λ) practical. If Eq. 2.51 and its *auxiliary* equations could be readily solved for $N(\mathbf{r},E,\boldsymbol{\Omega},t)$, there would be no need for the point kinetics equations. As it turns out, however, "practical" approximations follow from the approaches described in the previous section for solving the time-independent transport equation. Henry in *Nuclear-Reactor Analysis* derives the point kinetics equations starting with the diffusion approximation (with energy a continuous variable). One could just as well start with a few group diffusion approximation which would provide a shape function (a vector) and from the adjoint of the few group diffusion equation, a weight function (also a vector). The advantage of using an adjoint weight function, irrespective of the approximation to the transport equation one starts from, is in calculating reactivity, $\rho(t)$. In transients of interest in design, $\rho(t)$ is the driver. It reflects changes in cross sections with time due to variations in temperature (coolant density, Doppler effects) and configuration (control rod motion). In whatever form Eq. 2.78 takes, given the neutron transport approximation used, if a changing cross section is represented as a starting value plus a time-varying small delta, $\delta_\Sigma(\mathbf{r},E,t)$, and the shape function is represented as a time-independent function (e.g., from the initial neutron density of the reactor,

the same problem that generates the adjoint) plus a time-dependent small delta, $\delta S(\mathbf{r},E,t)$, then the resulting calculation of $\rho(t)$ will to first order in deltas only depend on $\delta_\Sigma(t)$'s. Higher order terms can be ignored, and one does not need to calculate a time-dependent shape function. This is a classic perturbation problem. Henry (chapter 7) provides a detailed derivation.

The time dependence of $\beta_j(t)$ and $\Lambda(t)$, Eq. 2.80 and Eq. 2.81, as used in the point kinetics equations can be ignored in most applications. Measured values of β (and the β_j^i from which it is summed) can be used directly (Table 2.4). If adjoint weighting is used, the β's will be a bit larger than the physical β's in a thermal reactor due to the increased "importance" of delayed neutrons with their lower initial energies (relative to prompt neutrons). Prompt neutron lifetimes primarily depend on the reactor type; for thermal reactors they are on the order of $\sim 10^{-3}$ s, and for fast reactors as short as 10^{-7} s. They can be measured in zero power reactor mock-up experiments as ratios with β and ρ, or calculated directly from equation Eq. 2.81 with the approximations for W and S used to obtain ρ. A highly accurate calculation of Λ can be made with a Monte Carlo simulation where neutrons are introduced from the prompt neutron energy spectrum with an $S(t = 0)$ spatial distribution. Each history would be timed and terminated with neutron absorption (capture plus fission) or leakage. The "times" will yield the mean and standard deviation of the prompt neutron lifetime.

One further note on reactivity, if a perturbation of a critical reactor configuration can be viewed as nearly instantaneous, that is, a step change, then a good estimate of reactivity addition or subtraction can be found by solving the eigenvalue (time independent) problem for the perturbed reactor:

$$\rho = 1 - 1/k, \tag{2.82}$$

and if the initial reactor configuration is subcritical then the reactivity addition from a "step" perturbation can be found by performing two eigenvalue problems, the perturbed case as before, and one for the initial subcritical configuration (ignoring any nonfission source);

$$\rho = 1/k_o - 1/k, \tag{2.83}$$

where k_o (<1) is the initial subcritical eigenvalue. As reactivity is a dimensionless ratio, it is often given as a percentage or in units of β (as defined by Eq. 2.80). In the latter case, the "units" are traditionally dollars and cents. If ρ equals β, the reactivity addition is 1 dollar; if ρ equals 0.5β the reactivity addition is 50 cents. If a dollar of reactivity is added to a critical reactor, it is said to be prompt critical (critical on prompt neutrons alone) and delayed neutrons will not mitigate the resulting transient, a condition obviously to be avoided.

The motivation for the description of point kinetics provided here is best provided by Henry:

> "Since mean free paths are fairly long and since the lifetimes of neutrons in a reactor are quite short, the effects of local perturbations on" N(**r**,E,**Ω**,t) "will quickly spread throughout a reactor. The immediate consequences of perturbing a reactor locally (for example by changing a control rod slightly) is thus a readjustment of the shape of the" neutron density. In many cases this readjustment is slight and is completed in a few milliseconds; after that the readjusted shape rises or falls as a whole depending on whether the initial perturbation increases or decreases k_{eff}. For reactors in which transients proceed in this manner, merely being able to predict the change in *level* of the neutron density "is sufficient to permit a very accurate prediction of the consequences of perturbation."

With today's computer capabilities, solving point kinetics problems is not a great challenge, even with time-dependent reactivity reflecting feedback from power changes in the reactor. Henry and Duderstadt provide descriptions of applicable calculational methods (development of which inspired great ingenuity in the past). In any case, to quote Henry again, point kinetics solutions provide "very accurate predictions of the consequences of (reactor) perturbations." Thus, their utility in assuring that a reactor design satisfies fundamental transient requirements. Under normal operating conditions, a reactor must be inherently stable, that is, self-limiting. Reactivity must be reduced with increased temperature; that is, with reduced coolant density, increased mean thermal neutron energy, and Doppler broadening of resonance cross sections. These phenomena are dependent on reactor type. Clearly change in thermal neutron spectra is unimportant in a fast reactor. However, if coolant density decrease results in voiding, reactivity will dramatically decrease in a thermal reactor, but in a liquid metal cooled fast reactor increased leakage must outweigh a higher energy neutron spectrum (and an increased fission to capture ratio in fuel) to assure a negative reactivity effect. Also movement of control rods must reduce reactivity when reactor shutdown is desired. Some movable poisons, power shimming control rods, could be included in a design to flatten (make more uniform) the power distribution throughout life. (Power flattening can reduce coolant pumping power requirements. As coolant flow must meet the heat removal needs of the hottest region of the reactor, minimizing excess flow to cooler regions increases overall power plant efficiency.) But, one must assure that the operating strategy for using such rods does not compromise the speed of reactor shutdown when it is required to deal with an accident condition.

Point kinetics models can also aid in assessing *Xenon override* requirements for thermal reactors. Xe^{135} with its extremely large thermal neutron capture cross section ($\sigma_c = 2.7 \times 10^6$ b at E = 0.023 eV, for comparison $\sigma_f^{U235} = 577$ b at 0.023 eV) is the most important fission product poison. It is produced directly from fission and by decay of its precursor I^{135} (which is a direct fission product and has short-lived precursors, $Sb^{135} \rightarrow Te^{135} \rightarrow I^{135}$). Both Xe^{135} and I^{135} have half-lives measured in hours ($T_{1/2}^{Xe} = 9.14$ h, $T_{1/2}^{I} = 6.58$ h). So, a point kinetics reactor model will show that when a reactor is started up, Xe^{135} and I^{135} build up to equilibrium levels in about 30 h. Their levels, inventories, will depend on power level, that is, neutron density, and the reactor design must have enough excess reactivity (e.g., control rods that can be withdrawn, or for a PWR, a soluble poison in the coolant whose concentration can be reduced) to

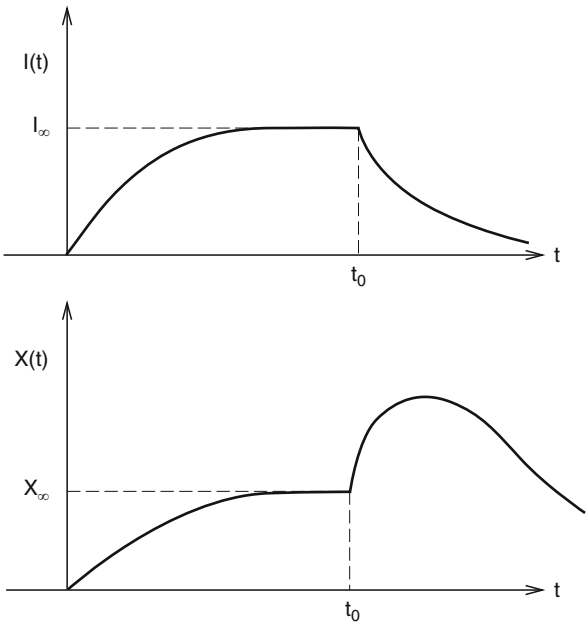

Fig. 2.8 Schematic of I^{135} and Xe^{135} inventories following an initial reactor start-up and subsequent shutdown after equilibrium levels have been reached (i.e., at t_0).(Duderstadt)

"override" the negative reactivity perturbation of neutron capture by Xe^{135} (iodine neutron capture can be ignored). In addition, when a thermal reactor is shut down, Xe^{135} builds up as loss by neutron absorption stops and decay of I^{135} continues. The Xe^{135} inventory peaks in about 10 h to approximately three times its equilibrium level and subsequently decays. It is back to its equilibrium level in $\sim$ 40 h (see Fig. 2.8).

Clearly additional "excess reactivity" is required to deal with a post-shutdown Xenon transient. Eventually, not being able to provide (and control) this excess reactivity can limit the useful lifetime of a thermal reactor design. As a historical aside, it was John Wheeler [3] who recognized the role that Xe^{135} and I^{135} could play in the operation of a thermal reactor. He explained the initial difficulties in operating the first plutonium production reactor at the Hanford Washington site.

While point kinetics can deal with most reactor design transient requirements, there are instances where significant spatial effects must be accounted for. In the normal operation of a large thermal reactor, there is the potential for spatial oscillations of Xenon concentrations, and therefore neutron density and power. These oscillations may not affect criticality and might only be observed by the reactor instrumentation system's ability to measure power distributions in core. The period of these oscillations would be many hours and thus limits on coolant channel performance and fuel temperature could be compromised for extended time intervals. Space-time calculations of neutron density have to be carried out to determine if a particular design has a propensity for these oscillations. If the design is not inherently stable, its instrumentation must provide detection and an operating

strategy must be devised to suppress any oscillation initiation. With modern computing capability, few group diffusion approximations to the time-dependent transport equation, Eq. 2.51 (with explicit spatial mesh or nodal methods), can deal with Xenon oscillation evaluations [22].

There are certain reactor plant accident scenarios, which also require space-time calculations. To deal with these, nodal methods, as described in section "Neutron Distributions", have been incorporated in safety analysis programs (see for example [23]), which model a full power plant; the reactor, its neutronics, fluid mechanics and structural integrity; and the balance of the plant, instrumentation, coolant/working fluid to power conversion, and safety systems (containment, emergency coolant injection and power supply). There are two classes of accidents where space–time effects in the reactor are important. First is "rod ejection," where a single control rod or group of control rods is rapidly withdrawn with a large reactivity addition and neutron distribution change, in no way a small perturbation in the point kinetics sense. Second is a "cold water accident" applicable to a PWR. In this case, in a plant with multiple piping "loops" carrying coolant to the reactor, if one of the loops is not functioning so that water in the loop has cooled below the normal inlet temperature of the reactor, and the loop is reactivated (its pump turned on and isolation valves (if any) opened), while the reactor is critical, there can be large asymmetric reactivity insertion, again, this is not a small perturbation problem.

Finally, there is an additional aspect of reactor neutron time variation, which has interesting *Physics*. The transport equation, derived in section "Neutron Distributions", is for the *mean* neutron density, $N(\mathbf{r},E,\boldsymbol{\Omega},t)$, but clearly as neutron interactions and production, and fission product decay are inherently probabilistic, there are fluctuations in the neutron population in a reactor (and as there are in delayed neutron precursor populations). These fluctuations were recognized early on in the Manhattan Project and are also referred to as neutron noise [24]. There are several approaches to modeling of the phenomena. The most fundamental is based on the derivation of the neutron transport equation from the quantum Liouville equation (Osborn and Yip [25]). This derivation is extended to produce an equation for the neutron doublet density, $N^{NN}(\mathbf{r},E,\boldsymbol{\Omega},\mathbf{r}',E',\boldsymbol{\Omega}',t)$, the expected number of neutrons in d^3r about **r,** with energies in dE about E, going in the solid angle $d\Omega$ about $\boldsymbol{\Omega}$ times the expected number in d^3r about $\mathbf{r}'$, and so on for E' and $\boldsymbol{\Omega}'$, where as in the transport equation neutron–neutron collisions are ignored. Additional equations for neutron–precursor and precursor–precursor doublet densities are produced to complete the set of equations needed to solve for N^{NN}. One also needs equations for the "mean" (in Osborn's nomenclature, singlet) neutron and precursor densities, which were derived in section "Neutron Distributions" (Eq. 2.51 and Eq. 2.52). Being able to solve for N^{NN} is, however, not sufficient to predict the results of neutron "noise" experiments in a reactor. Equations for doublet and singlet densities for events (D) in detectors (e.g., pulse or continuous currents in an ionization chamber) are also needed. With N^{DD} and N^{D} one can predict variance to mean ratios of counts or the power spectral density of the current in a single detector, and the cross power spectral density of currents in two detectors

[26]. These experiments are usually performed in a reactor in a steady-state condition (in the mean of course) at zero power, critical or slightly subcritical, to obtain estimates of point kinetics parameters. These experiments have the advantage of verifying expected kinetic performance without putting the reactor into a transient. They are performed at low neutron levels because as power is increased fluctuations become negligible relative to the mean. Detector noise measurements (psd and cpsd) are sometimes made at power in operating reactors to monitor for unplanned mechanical motion, or loose parts. Modeling for these measurements is deterministic.

Fluctuations in neutron populations must be considered in developing initial start-up procedures for a newly constructed reactor (In a reactor design which incorporates fuel (including fission products and transuranics) from a previously operated reactor, natural source levels will most likely be high enough to allow "fluctuations" to be ignored.). The mean neutron density before start-up depends on an external source of neutrons, $S(\mathbf{r},E)$ (not from neutron reactions, Eq. 2.50) which, as part of the design, could be adjacent or internal to the reactor. At start-up, the reactor is subcritical ($k < 1$) and the mean neutron population, in a point reactor sense, is $N = \Lambda S(k/(1–k))$. In outline, the steps to bring the reactor critical are to pull control rods up (down in most BWR designs) from their fully inserted position so as to insert some precalculated amount of reactivity and then wait for a new steady neutron level to be achieved. The subcritical neutron level is monitored by the reactor's source range detectors. A power reactor is instrumented with detectors for the full range of expected neutron levels. These pull-and-wait steps are repeated until the reactor is slightly super critical, and thus the neutron level is observed to be on a continuously increasing, but easily controlled, trajectory. A pull-and-wait procedure needs to account for neutron level fluctuations because if the observed level, due to a minimizing fluctuation, is below the expected (mean) level when the reactor is actually close to its critical configuration, then the next "pull" might produce an unacceptable rapidly increasing trajectory [27]. The simplest way to avert a problem with a pull-and-wait procedure is to assure that the sources provided in the design (In a reactor design which incorporates fuel (including fission products and transuranics) from a previously operated reactor, natural source levels will most likely be high enough to allow "fluctuations" to be ignored.) are strong enough to render subcritical neutron fluctuations negligible. Of course, one has to understand neutron level fluctuations to make this assessment [28].

Future Directions

Fission reactor development, since its inception, has progressed with advances in computing capability. Early on, analog computers were used for transient analyses, but digital computers have been the primary tool. Design codes have been adapted to advancing digital technology; scalar processing, then vector processing and now

massively parallel processing. This is an active field today and should continue to be so, particularly as the drivers for improve computer technology are universal. In section "Neutron Distributions" the two approaches to solving the neutron transport equation, Monte Carlo simulation and analytic methods (differencing variables and solving the resulting matrix equations) were described. Parallel computing would appear to be well suited to Monte Carlo as independent histories can be run on the various (1,000's of) processors simultaneously. There is, of course, the need to provide the reactor configuration (geometry, nuclide inventories, and cross sections) and the Monte Carlo code itself to each processor that runs a history. This challenge is being accepted with considerable success as exemplified by the accomplishments of the Los Alamos National Laboratory group working on the MCNP code [15] and the joint effort at the Knolls and Bettis Atomic Power Laboratories on the MC21 code [29]. Advocates of the analytic approach have, however, not accepted the ultimate triumph of Monte Carlo. This is clear in the work of a group at the Argonne National Laboratory, which has modestly named their multigroup, discrete ordinate code UNIC, for Ultimate Neutronic Investigation Code [30]. They are demonstrating impressive results for fast reactor designs. Competition in supercomputer development and in attendant codes for nuclear reactor design bodes well for better products in the future.

Physicists in their efforts to understand the atomic nucleus have made myriad measurements and only partially by design these have included the neutron and gamma cross sections, and fission product yields (and their decay mechanisms) needed for the development of fission reactors. Today, work on this reactor-related data is focused on establishing well-founded uncertainty measures. The Cross Section Evaluation Working Group of the National Nuclear Data Center refers to this effort as covariance evaluation [31]. This is particularly appropriate, for as discussed above, one expects calculational methods to improve with computer power and code development. Thus, in assigning error bounds in design, the uncertainty in basic data will become more important relative to the contribution of calculational error (e.g., Monte Carlo statistics or differencing and convergence error in analytic methods). More well-founded and hopefully smaller design error bounds can obviously be taken advantage of in future reactor development. Improving error bounds is also consistent with the approach to overall power plant safety analysis being fostered by many of the world's nuclear regulatory agencies. They favor best estimate analyses plus the assignment of rigorously defined uncertainty factors for various classes of accident conditions. Reactor design error is only a contributor to a safety analysis "uncertainty factor," but for power plant technology to advance, "reactor design" must do its part.

Much of the research for a next generation of fission reactor power plants is focused on higher operating temperatures. Today's thermal reactor plants, PWRs, BWRs, and CANDU (heavy water moderated) have outlet reactor coolant temperatures, T_H, of ~600°F, and thus thermal (Rankine cycle) efficiencies in the low 30%. Raising T_H would increase cycle efficiency and lower fuel cost, and provide high-temperature process heat (possibly for a catalytic hydrogen production process). Higher operating temperatures in a water (or heavy water)

environment present core and structural materials challenges. There likely will be a need for additional resonance cross-section data for some additives (e.g., Manganese and Chrome) to new high-temperature materials. Fast reactors (liquid metal or gas cooled) operate at much higher temperatures than thermal reactors but also require much higher fissile inventories to attain criticality. Experience with design and operation of these reactors is limited (especially for gas cooled reactors) compared to thermal reactors. Their future development with emphasis on the burning of unwanted transuranics as well their traditional mission of efficient conversion of fertile isotopes (U^{238} and Th^{232}) to fissile isotopes (Pu^{239}, Pu^{241} and U^{233}) will stimulate some cross-section work. But, both thermal and fast reactor development will most likely benefit more from advances in branches of physics other than Nuclear, particularly Condensed Matter and Fluid Mechanics. The need for nuclear power, both economic and environmental (if they can be separated?), will drive fission reactor development. While Uranium and Thorium are abundant in the earth's crust, power demand will push reactor development to most efficiently exploit the highest grade ores, which will likely lead to a mix of fast and thermal reactors. In any case, physics as well as engineering will play key roles in this development.

Bibliography

Primary Literature

1. Wheeler JA (1967) Mechanism of fission. Phys Today 20(11):49–52
2. Bohr N, Wheeler JA (1939) The mechanism of nuclear fission. Phys Rev 56:426
3. Ford KW (2009) Wheeler's work on particles, nuclei, and weapons. Phys Today 62(4):29
4. Fermi E, Szilard L (1955) Neutronic reactor. US Patent 2,708,656, 17 May 1955
5. Einstein A (1905) On the electrodynamics of moving bodies. Ann Phys 17:891–921
6. Frankel S, Metropolis N (1947) Calculations in the liquid-drop model of fission. Phys Rev 72:914
7. Kinsey R (1979) Compiler "ENDF/B Summary Doc." BNL-NCS-17541(ENDF-201), 3rd edn. ENDF/B-V, Brookhaven National Laboratory, Upton
8. England TR, Wilson WB, Stamatelatos MG (1976) Fission product data for thermal reactors. EPRI-NP-356, Los Alamos Scientific Lab., New Mexico
9. Parks DE, Nelkin MS, Wikner NF, Beyster JR (1970) Slow neutron scattering and thermalization with reactor applications. Benjamin, New York
10. MacFarlane RE (1994) The NJOY nuclear data processing system, Version 91, report #LA-12740-M, Los Alamos National Laboratory, New Mexico
11. Breit G, Wigner E (1936) Capture of slow neutrons. Phys Rev 49:519
12. Beckurts KH, Wirtz K (1964) Neutron physics. Springer, Berlin
13. Larson NM (2006) Updated user's guide for SAMMY: multilevel R-matrix fits to neutron data using Bayes' equations, ORNL/TM-9179/R7. Oak Ridge National Lab, OakRidge
14. Spanier J, Gelbard EM (1969, 2008) Monte carlo principles and neutron transport problems, Dover, New York, Addison-Wesley, Reading

15. X-5 Monte Carlo Team (2003) MCNP – A general Monte Carlo N-Particle transport code, Version 5, LA-UR-03-1987, Los Alamos National Laboratory, New Mexico
16. Ondis LA II, Tyburski LJ, Moskowitz BS (2000) RCP01 – a Monte Carlo program for solving neutron and photon transport problems in three dimensional geometry with detailed energy description and depletion capability, B-TM-1638. Bettis Atomic Power Laboratory, West Mifflin
17. TOP 500 Super Computing Sites, www.Top500.org
18. Lathrop KA (1972) Discrete-ordinates methods for the numerical solution of the transport equation. Reactor Technol 15:107
19. Lathrop KA (1971) Remedies for ray effects. Nucl Sci Eng 45(3):355–68
20. Varga RS (2000) Matrix iterative analysis, 2 Revised and Expandedth edn. Springer, Heidelberg
21. Henry A, Dias A, Frances W, Parlos A, Tanker E, Tanker Z (1986) Continued development of nodal methods for nuclear reactor analysis, MIT EL 86-002. Massachusetts Institute of Technology, Cambridge
22. Buslik AJ, Weinreich WA (1967) Variational calculation of complex natural modes of xenon oscillation, WAPD –TM-673 (LWB-LSBR Development Program). Bettis Atomic Power Laboratory, West Mifflin
23. Idaho National Laboratory (2009) RELAP5-D, www.INL.gov
24. Thie JA (1963) Reactor noise (an AEC monograph). Rowman and Littlefield, New York
25. Osborn RK, Yip S (1966) Foundations of neutron transport theory, Monograph series on nuclear technology. Gordon and Breach, New York
26. Natelson M, Osborn RK, Shure S (1966) Space and energy effects in reactor fluctuation experiments. J Nucl Energy Parts A/B 20(7):557–585
27. Hurwitz H Jr, MacMillan DB, Smith JH, Storm ML (1963) Kinetics of low source reactor startups, part I and II. Nucl Sci Eng 15:166
28. Clark WG, Harris DR, Natelson M, Walter JF (1968) Variances and covariances of neutron and precursor populations in time-varying reactors. Nucl Sci Eng 31:440–457
29. Sutton TM et al, Knolls Atomic Power Lab., Griesheimer DP et al, Bettis Atomic Power Lab. (2007) The MC21 Monte Carlo Code, LM-06K144, Proceedings (on CD-ROM) of the joint international topical meeting on M&C and supercomputing applications, Monterey
30. Palmiotti G et al, Argonne National Lab. (April 2007) UNIC Ultimate Neutronic Investigation Code, Proceeding (on CD-ROM) of the joint international topical meeting on M&C and supercomputing applications, Monterey
31. Herman M et al (2008) Covariance evaluation methodology for neutron cross sections, BNL-81525-2008. Brookhaven National Lab, Upton
32. Belle J, Berman RM (eds) (1984) Chapter 2, Natelson M, Nuclear properties of the thorium fuel cycle. In: Thorium dioxide: properties and nuclear applications, Naval Reactors Office, U. S. Department of Energy, Govt. Printing Office, Washington, DC
33. Katcoff S (1958) Fission–Product yields from U, Th and Pu. Nucleonics 16(4):78

Books and Reviews

Duderstadt JJ, Hamilton LJ (1976) Nuclear reactor analysis. Wiley, New York
Evans RD (1955) The atomic nucleus. McGraw-Hill, New York
Henry AF (1975) Nuclear-reactor analysis. MIT Press, Cambridge
Kaplan I (1962) Nuclear physics, 2nd edn. Addison-Wesley, Reading
Krane KS (1988) Introductory nuclear physics. Wiley, New York
Mermin ND (2005) It's about time, understanding Einstein's relativity. Princeton University Press, Princeton

Chapter 3
Isotope Separation Methods for Nuclear Fuel

Shuichi Hasegawa

Glossary

Isotope	Nuclei of a chemical element which have the same number of protons but different number of neutrons. Some isotopes are stable; some are radioactive.
Separation factor	A ratio of a mole fraction of an isotope of interest to that of non-interest in an enriched flow divided by that in a depleted flow from a separation unit. The factor should be larger than unity for the unit to result in isotopic enrichment.
Separation capability	A measure of separative work by a cascade per unit time.
Mean free path	An average distance of a moving gas molecule between its collisions.
Molecular flow	Low-pressure phenomenon when the mean free path of a gas molecule is about the same as the channel diameter; then a molecule migrates along the channel without interference from other molecules present.

This chapter was originally published as part of the Encyclopedia of Sustainability Science and Technology edited by Robert A. Meyers. DOI:10.1007/978-1-4419-0851-3

S. Hasegawa (✉)
Department of Systems Innovation, School of Engineering, The University of Tokyo,
7-3-1 Hongo Bunkyo-ku, Tokyo, Japan
e-mail: hasegawa@sys.t.u-tokyo.ac.jp

N. Tsoulfanidis (ed.), *Nuclear Energy: Selected Entries from the Encyclopedia of Sustainability Science and Technology*, DOI 10.1007/978-1-4614-5716-9_3,

Definition of the Subject

Isotope separation, in general, means enrichment of a chemical element to one of its isotopes (e.g., ^{10}B in B; ^{6}Li in Li, ^{157}Gd, etc). In the case of uranium, isotope separation refers to the enrichment in the isotope ^{235}U, which is only 0.711% of natural uranium; today's nuclear power plants require fuel enriched to 3–5% in ^{235}U. Uranium enrichment is the subject of this article.

Efficiencies of sorting out different isotopes of the element (separation factor) are usually very low. For practical enrichment plants, a gaseous diffusion process has been successfully employed to obtain enriched uranium. A gas centrifugation process is the preferred method of enrichment today due to reduced energy consumption. A new process using lasers, which can have a high efficiency of separation, is under development and has the potential to replace the current enrichment methods.

Introduction

The fuel used today by commercial nuclear power plants is the fissile isotope ^{235}U. Unfortunately, ^{235}U is only 0.711% of natural uranium, the rest of which is, essentially, ^{238}U. Light water reactors (LWR) operating dominantly all over the world require isotope enrichment processes because the isotopic ratio of ^{235}U for their fuels should be 3–5%. The processes used to elevate the ^{235}U content from 0.711% to 3–5% are called isotope separation or enrichment processes. Table 3.1 shows the current trends of isotope separation capabilities of the world. The main countries performing the process are Russia, France, US, and URENCO (Germany,

Table 3.1 World Enrichment capacity (thousand SWU/year) [1]

Country	2010	2015	2020
France (Areva)	8,500*	7,000	7,500
Germany, Netherlands, UK (Urenco)	12,800	12,200	12,300
Japan (JNFL)	150	750	1,500
USA (USEC)	11,300*	3,800	3,800
USA (Urenco)	200	5,800	5,900
USA (Areva)	0	>1,000	3,300
USA (Global Laser Enrichment)	0	2,000	3,500
Russia (Tenex)	23,000	33,000	30–35,000
China (CNNC)	1,300	3,000	6,000–8,000
Pakistan, Brazil, Iran	100	300	300
Total approx.	57,350	69,000	74–81,000
Requirements (WNA reference scenario)	48,890	55,400	66,535

Source: WNA Market Report 2009; WNA Fuel Cycle: Enrichment plenary session WNFC April 2011
*Diffusion

Netherland, and UK). A number of separation processes have been studied so far, but the principles of the current isotope separation processes mainly use gaseous diffusion or gas centrifugation. The diffusion process was commercialized first but the centrifugation is taking over because of less energy consumption. This article following mainly [2, 3] describes the principles of the two processes and cascade theory, which explains why it is required to repeat the process many times (using successive stages/cascades) to obtain a certain desired enrichment fraction such as 3–5% because a single step provides only a small incremental enrichment. The new enrichment technology using lasers will be described at the end.

Principles of the Separation Processes

Gaseous Diffusion

Figure 3.1 shows the schematic diagram of the gaseous diffusion process. Consider a chamber divided into two compartments by a porous membrane. When dilute gases are introduced into the bottom compartment of the chamber, the pores of the membrane (membrane) make dependency of the transmission of the gases on their molecular masses.

If we have a mixture of two molecules in a gas with the same kinetic energy (kinetic energy is determined by kT, k = Boltzmann constant; T = temperature in K; $(1/2\ mv^2 \sim kT)$), the lighter molecule is faster than the heavier one. Therefore, their frequencies of hitting the membrane is higher for the lighter than for the heavier molecule. However, the mass preference phenomena occur only when the mean free path of the gas molecule is longer than the diameter of the pores $2r$ and the thickness of the membrane l. The mean free path, λ of the molecule can be written as [2]

$$\lambda = \frac{kT}{4\sqrt{2}\pi\sigma^2 p} \tag{3.1}$$

where k is the Boltzmann constant, T is the absolute temperature, σ is the radius of the molecule, and p is the gas pressure in the chamber. In this condition, a molecule

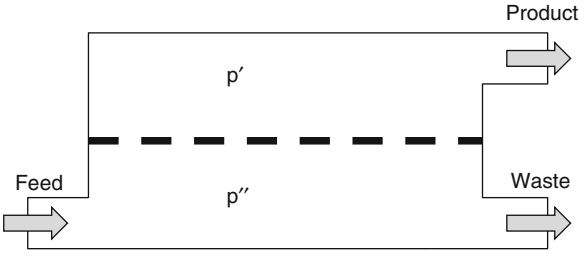

Fig. 3.1 A single gaseous diffusion stage

cannot collide with others during the transmission through the membrane so that its dynamics can be considered as a single molecule process. This process is called molecular flow. The flux of the molecular flow through the flow path with circular cross section is derived by Knudsen as [3]

$$G_{mol} = \frac{8r\Delta p}{3l\sqrt{2\pi mRT}} \tag{3.2}$$

where G_{mol} is the molecular flow velocity, m is the molecular mass, R is the gas constant, and $\Delta p = p'' - p'$ is the pressure difference between the bottom and top compartments of the chamber. Equation 3.2 shows that the flow velocity depends on the mass of the gas molecules so that the ratio of the molecules in the mixture transmitted to the upper compartment of the chamber is changed compared with that of the feeding gas. The opposite condition where flows do not depend on the molecular mass is called viscous flow.

We will derive the ideal separation factor in the case of $^{235}UF_6$ and $^{238}UF_6$ [3], the gas molecules used for uranium enrichment. On the ideal condition where p'' is very small and p′ can be neglected compared with p'', when we have a binary mixture of gases which consist of $^{235}UF_6$ (molecular mass: m_{235} = 349, mole fraction: x) and $^{238}UF_6$ (molecular mass: m_{235} = 352, mole fraction: $1 - x$), the molecular flow velocities of $^{235}UF_6$ and $^{238}UF_6$ are

$$G_{235} = \frac{ap''x}{\sqrt{m_{235}}}, \quad G_{238} = \frac{ap''(1-x)}{\sqrt{m_{238}}} \tag{3.3}$$

where the constant a includes factors in Eq. 3.2. The ratio of the molecular flow of $^{235}UF_6$ to the whole can be written as

$$\mathrm{s} = \frac{G_{235}}{G_{235}+G_{238}} = \frac{\frac{x}{\sqrt{m_{235}}}}{\frac{x}{\sqrt{m_{235}}}+\frac{1-x}{\sqrt{m_{238}}}} = \frac{\frac{x}{1-x}}{\frac{x}{1-x}+\sqrt{\frac{m_{235}}{m_{238}}}} \tag{3.4}$$

Therefore, the ideal separation factor α_0 of the gaseous diffusion process can be derived as the separation factor of the molecular flow of the porous media

$$\alpha_0 = \frac{\frac{s}{1-s}}{\frac{x}{1-x}} = \sqrt{\frac{m_{238}}{m_{235}}} = \sqrt{\frac{352}{349}} = 1.00429 \tag{3.5}$$

The separation factor depends on the ratio of the molecular masses so that this method is more effective for the isotope separation of lighter elements. For heavier elements, a larger number of repeated processes is required to obtain sufficiently enriched products.

However, in reality, the real value of the separation factor is smaller than that given by Eq. 3.5 due to reverse molecular flow from the upper compartment to the

bottom one and viscous flow not depending on the molecular mass; these two phenomena work in a direction negating the enrichment process. Furthermore operating conditions (porous media performance, working pressures, etc.) affect the value of the separation factor. The energy consumption to run the process is very high due to pressure controlling of the gases, small separation factors and so on (see discussion about Separative Work Unit). Because of the relatively high energy consumption, uranium enrichment by gaseous diffusion is on the way out and is replaced by the gas centrifugation method.

Gas Centrifugation

The principle of gas centrifugation is based upon centrifugal forces that are created inside a rotating cylinder containing two different gas molecules, forces that depend on the molecular mass. Let's see how it works in detail [2]. When we have a mixture of two gas molecules in a rotating cylinder (centrifuge), pressure gradients develop with respect to the radial direction. The pressures can be written as

$$\frac{dp}{dr} = \omega^2 r\rho \tag{3.6}$$

where p is the pressure, r is the radial distance, ω is the angular frequency of rotation, and ρ is the density of the gases. By substituting the equation of state $\rho = pm/RT$ into the differential equation, we can derive the following equation,

$$\frac{dp}{p} = \frac{m\omega^2}{RT} r dr \tag{3.7}$$

When we integrate this differential equation from the radial distance r (pressure p_r) to the inner radius of the cylinder a (pressure p_a), we can obtain this expression,

$$\frac{p_r}{p_a} = \exp\left[-\frac{1}{2}\frac{mv_a^2}{RT}\left\{1 - \left(\frac{r}{a}\right)^2\right\}\right] \tag{3.8}$$

where the speed of the outer circumference of the cylinder $v_a = \omega a$ This equation shows that the ratio of the pressure at radius r to that of radius a depends on the molecular mass of the gases.

If we have the gases which consist of $^{235}UF_6$ (molecular mass: $m_{235} = 349$, mole fraction: x) and $^{238}UF_6$ (molecular mass: $m_{235} = 352$, mole fraction: $1 - x$), their ratios of the partial pressures at the radius r to the radius a can be derived as

$$\frac{p_r x_r}{p_a x_a} = \exp\left[-\frac{1}{2}\frac{m_{235}v_a^2}{RT}\left\{1 - \left(\frac{r}{a}\right)^2\right\}\right] \tag{3.9}$$

Table 3.2 The local separation factor of $^{235}UF_6$ and $^{238}UF_6$ at r/a with T = 300K, υ_a = 700m/s

r/a	0	0.5	0.8	0.9	0.95	0.98	0.99	1.0
α	1.343	1.247	1.112	1.058	1.029	1.012	1.006	1.0

$$\frac{p_r(1-x_r)}{p_a(1-x_a)} = \exp\left[-\frac{1}{2}\frac{m_{238}v_a^2}{RT}\left\{1-\left(\frac{r}{a}\right)^2\right\}\right] \tag{3.10}$$

Therefore, the local separation factor at radial distance r of radius a is given by

$$\alpha = \frac{\dfrac{x_r}{1-x_r}}{\dfrac{x_a}{1-x_a}} = \exp\left[\frac{(m_{238}-m_{235})v_a^2}{2RT}\left\{1-\left(\frac{r}{a}\right)^2\right\}\right] \tag{3.11}$$

which depends on the difference of their molecular masses, $\Delta m = m_{238} - m_{235} = 3$. Values of the local separation factor of $^{235}UF_6$ and $^{238}UF_6$ with T = 300 K and v_a = 700 m/s are given in Table 3.2. This feature is superior to the gaseous diffusion method when the difference of the masses is large, (e.g., for heavier elements). The separation factor increases as the speed of the outer circumference increases. However, the maximum speed $v_{\max}$ is limited by stresses created to the cylinder from the force of the centrifugation and can be written as [2]

$$v_{max} = \sqrt{\frac{\sigma}{\rho}} \tag{3.12}$$

where ρ is the density of the material of the cylinder, and σ is the tensile strength. Although most molecular gases are localized at $\frac{r}{a} \approx 1$ because of the centrifugation, the values of the separation factor could be higher than those obtained from the gaseous diffusion method. These values can be enhanced if we make use of a countercurrent flow in the vertical direction. Figure 3.2 shows the schematic diagram of countercurrent centrifugation method. Gernot Zippe performed pioneering work on the development of the centrifugation first in the Soviet Union during 1946–1954, and from 1956 to 1960 at the University of Virginia. The countercurrent flow can be induced by heating and cooling centrifuges, or pipes drawing off flows in centrifuges. The temperature control can adjust the flow deliberately but the equipment becomes more complicated than that of the flow control by the pipes (Fig. 3.2). This countercurrent flow makes enrichment of the lighter isotopes at inner radius as the flow descending along the axis direction, and the heavier isotopes are being enriched at the circumference as the flow ascending. These enriched gases are collected at different radial positions of the both ends (at outer radius for heavier isotope and at inner radius by baffle for lighter isotope). When the centrifuge has a length L, the maximum separative power δU_{max} can be derived as [2, 4]

$$\delta U_{max} = \frac{\pi}{2} L\rho D\left(\frac{\Delta m v_a^2}{2RT}\right)^2 \tag{3.13}$$

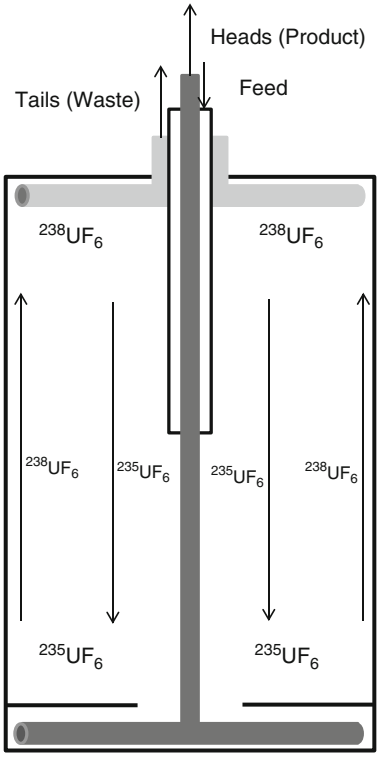

Fig. 3.2 Schematics of gas centrifuge with countercurrent flow

where D is diffusion coefficient. The maximum separative power is proportional to the height of the centrifuge. It is preferable to have a taller centrifuge in the vertical direction, but the length is imposed on the resonant vibration of the centrifuge. The resonant conditions can be written as [3]

$$\left(\frac{L}{a}\right)_i = \sqrt{\lambda_i}\sqrt[4]{\frac{E}{2\sigma'}} \quad \lambda_i = 22.0, 61.7, 121.0, 200.0, 298.2, \cdots \tag{3.14}$$

where E is coefficient of elasticity. A taller centrifuge can give a larger separative power although excellent mechanical properties are required to overcome the resonant conditions.

Cascade Theory

The present isotope separation plants make use of these principles of enrichment with small separation factors. In order to obtain high enrichment ratios, cascade theory is necessary [3]. According to the theory, we can enhance the ratios by iterating a single physical stage many times. Figure 3.3 shows a simple scheme

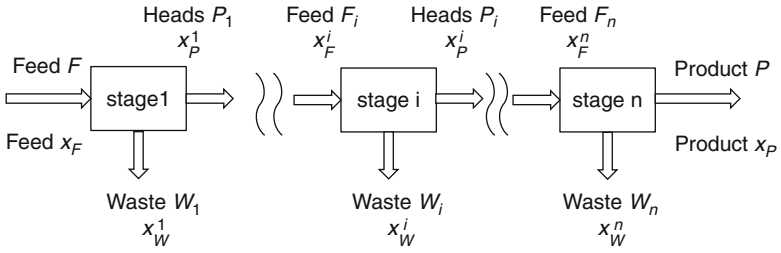

Fig. 3.3 Simple scheme of the cascade

of a cascade. An original material "feed" is provided to the system. The isotope of interest is enriched as going through many separation stages and a final output "product" is obtained. Another output which mainly contains unnecessary isotopes is called "waste." Each flow F, P and W should have the following equation

$$F = P + W \tag{3.15}$$

and with mole fractions of the isotope of interest in each flow x_F, x_P, x_W, we can obtain

$$Fx_F = Px_P + Wx_W \tag{3.16}$$

In this system, we have four independent parameters to define. In order to obtain necessary flow of Product "P" and mole fraction "x_P" of the isotope of interest, we need the design methodology to construct stages of separation units. The product of a single stage (unit) is called heads and the waste of that is tails. The ratios of the isotope of interest in the product are usually most important. If, for instance, we have two isotopes "1" and "2," and want to enrich the "1" isotope, we would focus on the variation of the mole fraction ratio of the two isotopes, $\frac{x_1}{x_2}$, which can be rewritten as $\frac{x_1}{1-x_1}$. The capability of each enrichment unit is described as separation factor α. This factor is defined as the ratios of the isotopes of interest to that of not-interest in the heads (product) divided by those in the tails (waste)

$$\alpha = \frac{\dfrac{x_P}{1-x_P}}{\dfrac{x_W}{1-x_W}} \tag{3.17}$$

In a similar way, we can define the ratio of the heads (product) to the feed as heads separation factor β, and that of the feed to the tails as tails separation factor γ,

$$\beta = \frac{\dfrac{x_P}{1-x_P}}{\dfrac{x_F}{1-x_F}},\ \gamma = \frac{\dfrac{\mathrm{x_F}}{1-\mathrm{x_F}}}{\dfrac{\mathrm{x_W}}{1-\mathrm{x_W}}} \text{ and } \alpha = \beta\gamma \tag{3.18}$$

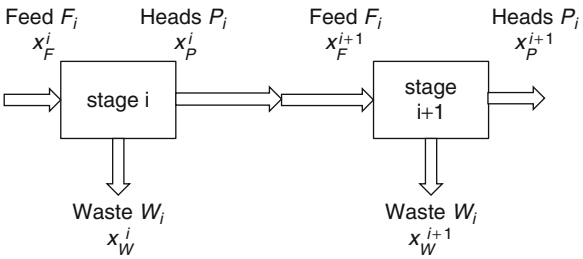

Fig. 3.4 Simple cascade of the i and i + 1 th stages

The ratio of the product to the feed is called "cut" θ and defined as

$$\theta \equiv \frac{P}{F} = \frac{x_F - x_w}{x_P - x_W} \tag{3.19}$$

The simplest design to accomplish enrichment is to accumulate separation stages in a single line such as Fig. 3.4. This scheme is called simple cascade.

Simple Cascade

In this scheme, the heads and the mole fraction of the i th stage are equal to the feed flow and the mole fraction of the i + 1 th stage (Fig. 3.4).

$$F_{i+1} = P_i, \quad x_F^{i+1} = x_P^i \tag{3.20}$$

This cascade disposes of the tails of all stages so that the total amount of the isotope of interest in the waste should be given sufficient attention. This can be evaluated by means of the recovery rate of the i th stage r_i

$$r_i = \frac{P_i x_P^i}{F_i x_F^i} = \theta_{\mathrm{i}} \frac{x_P^i}{x_F^i} = \frac{x_F^i - x_W^i x_P^i}{x_P^i - x_W^i x_F^i} = \frac{1 - \dfrac{x_W^i}{x_F^i}}{1 - \dfrac{x_W^i}{x_P^i}} = \frac{\alpha_i - \beta_i}{\alpha_i - 1} \tag{3.21}$$

When we have n stages in the cascade, the total recovery rate r can be expressed as

$$r = \frac{P x_P}{F x_F} = \frac{P_n x_P^n}{F_1 x_F^1} = \frac{P_1 x_P^1 P_2 x_P^2}{F_1 x_F^1 F_2 x_F^2} = \frac{P_n x_P^n}{F_n x_F^n} = r_1 r_2 \cdots r_n \tag{3.22}$$

The over-all separation factor of the cascade ω can be derived as

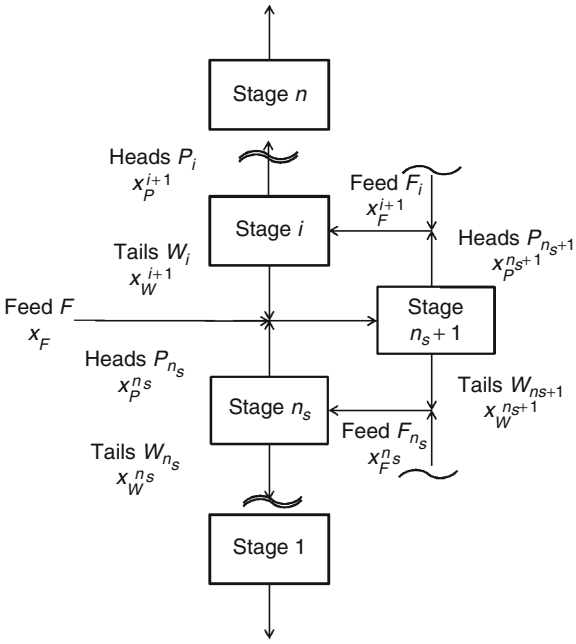

Fig. 3.5 Countercurrent recycle cascade

$$\omega = \frac{\dfrac{x_P^n}{1-x_P^n}}{\dfrac{x_F^1}{1-x_F^1}} = \beta_1 \beta_2 \cdots \beta_n \tag{3.23}$$

Therefore, if α, β do not depend on each stage, the total recovery rate can be rewritten as

$$r = \left(\frac{\alpha-\beta}{\alpha-1}\right)^n = \left(\frac{\alpha-\omega^{\left\{\frac{1}{n}\right\}}}{\alpha-1}\right)^n \tag{3.24}$$

When the feed itself is available without any special cost, the simple cascade is effective. But in case the wastes from each stage should not be disposed because, for instance, it is valuable or the recovery rate has to be increased, the waste flows are recycled as feed flow, which is called countercurrent recycle cascade (Fig. 3.5).

Countercurrent Recycle Cascade

Since the simple cascade cannot improve the recovery rate, the tail flow is recycled into either stage to use it efficiently, which is called recycle cascade (Fig. 3.5). If β (heads separation factor) is equal to γ (tails separation factor) in all stages, we can obtain $x_W^{i+2} = x_F^{i+1} (= x_P^i)$. So the tails flow of the $i+2$ th stage can be merged to the

heads flow of the i th stage and fed into the $i + 1$ th stage without any mixing loss. We will consider the case that the tails flow of the second upper stage is refluxed to the i th stage.

The flows and the fractions of the isotope of interest in each stage of enriching sections should have the following relationships.

$$P_i = W_{i+1} + P, \quad P_i x_P^i = W_{i+1} x_w^{i+1} + P x_P \tag{3.25}$$

In a similar way, those in stripping sections can be expressed as

$$W_{j+1} = P_j + W, \quad W_{j+1} x_W^{j+1} = P_j x_P^j + W x_W \tag{3.26}$$

Let's estimate the number of stages. From these equations, we can derive

$$x_P^i - x_W^{i+1} = \frac{x_P - x_P^i}{\frac{W_{i+1}}{P}} \tag{3.27}$$

At total reflux, where the reflux ratio is infinity,

$$\frac{W_{i+1}}{P} \to \infty \tag{3.28}$$

the mole fraction of the heads flow at the i th stage x_P^i becomes equal to that of the tails flow at the i + 1 th stage x_W^{i+1} and the number of the stages is minimal.

$$\frac{x_P^{i+1}}{1 - x_P^{i+1}} = \alpha \frac{x_W^{i+1}}{1 - x_W^{i+1}} = \alpha \frac{x_P^i}{1 - x_P^i} = \alpha^2 \frac{x_P^{i-1}}{1 - x_P^{i-1}} = \cdots \tag{3.29}$$

gives the following equation,

$$\frac{x_P}{1 - x_P} = \alpha^n \frac{x_W}{1 - x_W} \tag{3.30}$$

and the minimum number of the stages at total reflux can be derived as

$$n = \frac{1}{\ln \alpha} \ln\left(\frac{x_P}{1 - x_P} \frac{1 - x_W}{x_W}\right) \tag{3.31}$$

On the contrary, the reflux ratio becomes minimum when the mole fraction of the heads at the i + 1 th stage is equal to that of the heads at the i th stage ($x_P^{i+1} = x_P^i$).

Ideal Cascade

Ideal cascade satisfies the condition that the values of β (heads separation factor) at all stages are constant and the mole fraction of the heads flow at the $i+1$ th stage is equal to those of the tails flow at the $i-1$ th stage and of the feed flow at the i th stage $\left(x_p^{i+1} = x_W^{i-1} = x_F^i\right)$. In this instance, each separation factor satisfies the following relationship.

$$\beta = \sqrt{\alpha} = \gamma \tag{3.32}$$

In a similar way to the previous section, we can obtain the total number of the stages for an ideal cascade

$$\begin{aligned} n &= \frac{1}{\ln \beta} \ln \left(\frac{x_P}{1-x_P} \ \frac{1-x_W}{x_W} \right) - 1 \\ &= \frac{2}{\ln \alpha} \ln \left(\frac{x_P}{1-x_P} \ \frac{1-x_W}{x_W} \right) - 1 \end{aligned} \tag{3.33}$$

The number of stages in stripping n_S and enriching $n_E = n - n_S$ sections can be derived as

$$n_S = \frac{1}{\ln \beta} \ln \left(\frac{x_F}{1-x_F} \ \frac{1-x_W}{x_W} \right) - 1 \tag{3.34}$$

$$n_E = n - n_S = \frac{1}{\ln \beta} \ln \left(\frac{x_P}{1-x_P} \ \frac{1-x_F}{x_F} \right) \tag{3.35}$$

The reflux ratio Eq. 3.27 can be rewritten using $x_P^i = x_F^{i+1}$ and β as

$$\frac{W_{i+1}}{P} = \frac{x_P - x_P^i}{x_P^i - x_W^{i+1}} = \frac{1}{\beta - 1} \left\{ \frac{x_P}{x_W^{i+1}} - \frac{\beta(1-x_P)}{1-x_W^{i+1}} \right\} \tag{3.36}$$

Mccabe–Thiele Diagram

It is useful to draw McCabe–Thiele diagram to investigate the design of the cascade, the mole fractions of the stages and so on. Figure 3.6 shows a typical McCabe–Thiele diagram. In this graph, the horizontal and vertical axes correspond to the mole fractions of the heads flow x_P^i and of the tails flow x_W^i, respectively.

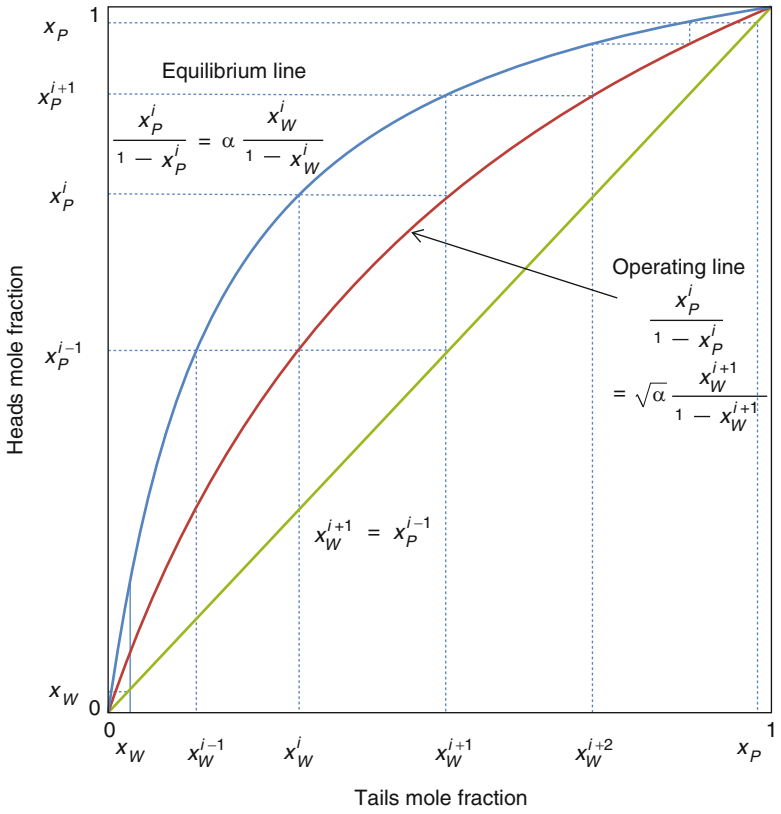

Fig. 3.6 McCabe-Thiele diagram

First, the following equation is satisfied at the enrichment process of the i th stage because of the definition of the separation factor

$$\frac{x_P^i}{1-x_P^i} = \alpha \frac{x_W^i}{1-x_W^i} \text{(Equilibrium line)} \tag{3.37}$$

Second, the condition that the tail (waste) flow at the i + 1 th stage is the feed of the i th stage ($x_F^i = x_W^{i+1}$) defines the relationship between the mole fractions of the tail (waste) and head (product) flows at different stages as follows

$$\frac{x_P^i}{1-x_P^i} = \beta \frac{x_F^i}{1-x_F^i} = \sqrt{\alpha} \frac{x_W^{i+1}}{1-x_W^{i+1}} \text{(Operating line)} \tag{3.38}$$

And third, the feed flow at the i th stage consists of the tails flow of the i + 1 th stage and the heads flow of the i − 1 th stage and their mole fractions are the same.

$$x_W^{i+1} = x_P^{i-1} \tag{3.39}$$

These three formulae can be shown in the McCabe–Thiele diagram as shown in Fig. 3.6. We can estimate the number of necessary stages, mole fractions of the stages, and overview the total processes through the graphical construction.

Separative Work Unit

The total flow in the cascade can be derived as

$$\sum_i (P_i + W_i) = \frac{\beta + 1}{(\beta - 1)\ln \beta}\left[W(2x_W - 1)\ln\left(\frac{x_W}{1 - x_W}\right) + P(2x_P - 1)\ln\left(\frac{x_P}{1 - x_P}\right) - F(2x_F - 1)\ln\left(\frac{x_F}{1 - x_F}\right)\right] \tag{3.40}$$

The first term of Eq. 3.40 including β indicates the difficulty of the separation and increases as the value of β approaches to unity. The second term corresponds to the amount of work for separation, and it has the same dimension as flow rates and is called separative capacity or separative power. This value is important because it is considered to be proportional to the initial cost of the plant. When we use the unit of the amounts of material (mole, kg, etc.) instead of flow rates, this is called separative work. The sum of the annual investment and operation costs can be expressed by the product of the separative work *SW* (kg SWU/year) and unit price of separative work c_s ($/kg SWU). SWU is the abbreviation of Separative Work Unit. The separative work is defined as

$$SW = W\phi(x_W) + P\phi(x_P) - F\phi(x_F) \tag{3.41}$$

where $\phi(\mathrm{x_i})$ is called separation potential and written as

$$\phi(x_i) = (2x_i - 1)\ln\frac{x_i}{1 - x_i} \tag{3.42}$$

When we use kg SWU/year for the separative work, the unit of W, P, and F should be kg/year.

For operating the plant, we need the raw materials, the amount of which is F (kg/year) and unit price of the raw materials c_F ($/kg). The total cost per year c ($) can be written as

$$c = SWc_S + Fc_F \tag{3.43}$$

When the amount of the product per year is P (kg), the unit cost of the product $c_P = \frac{c}{P}$. could be derived as

$$c_P = \frac{SWc_s}{P} + \frac{Fc_F}{P} = \left\{ (\phi(\mathrm{x_P}) - \phi(\mathrm{x_F})) - (x_P - x_F)\frac{\phi(\mathrm{x_F}) - \phi(x_W)}{x_F - x_W} \right\} c_s + \left(\frac{x_P - x_W}{x_F - x_W}\right) c_F \tag{3.44}$$

Example

With the ideal cascade of the gaseous diffusion method (α = 1.00429), the mole fraction of the feed flow 0.711% ($x_F = 0.00711$) would be enriched to 3% ($x_P = 0.03$) and the mole fraction of the waste is planned to be 0.3% ($x_W = 0.003$). In this case, the necessary moles of the feed and the waste to obtain the product of 1 [mol] are

$$F = \frac{P(x_P - x_W)}{x_F - x_W} = \frac{1 \times (0.03 - 0.003)}{0.00711 - 0.003} = 6.569[mol]$$

$$\mathrm{W} = \frac{P(x_P - x_F)}{x_F - x_W} = \frac{1 \times (0.03 - 0.00711)}{0.00711 - 0.003} = 5.569(= 6.569 - 1)[mol]$$

The total number of stages n and the number of stages in stripping section n_S and in enriching section n_E are calculated as

Stripping Section

$$n_S = \frac{2}{\ln\alpha} \ln\left(\frac{x_F}{1 - x_F} \frac{1 - x_W}{x_W}\right) - 1 = \frac{2}{\ln 1.00429} \ln\left(\frac{0.00711}{1 - 0.00711} \frac{1 - 0.003}{0.003}\right) - 1 = 404$$

Enriching Section

$$n_E = \frac{2}{\ln \alpha} \ln \left(\frac{x_p}{1 - x_p} \ \frac{1 - x_F}{x_F} \right)$$
$$= \frac{2}{\ln 1.00429} \ln \left(\frac{0.03}{1 - 0.03} \ \frac{1 - 0.00711}{0.00711} \right) = 683.5$$

The total number of stages

$$n = \frac{2}{\ln \alpha} \ln \left(\frac{x_p}{1 - x_p} \ \frac{1 - x_W}{x_W} \right) - 1$$
$$= \frac{2}{\ln 1.00429} \ln \left(\frac{0.03}{1 - 0.03} \ \frac{1 - 0.003}{0.003} \right) - 1 = 1087.5$$

The heads flow rate in the enriching section can be written as

$$P_i = P + W_{i+1}$$
$$= P + \frac{P}{\beta - 1} \{ x_p (1 - \beta^{i-n}) + (1 - x_p) \beta (\beta^{n-i} - 1) \}$$

and that in the stripping section

$$P_i = \frac{W}{\beta - 1} \left\{ x_W \beta (\beta^i - 1) + (1 - x_W)(1 - \beta^{-i}) \right\}$$

These flows as a function of the number of the stages can be shown as Fig. 3.7 in this example.

When we need higher concentration, such as 5%, $F = 11.436[mol]$, $W = 10.436$ $[mol]$, $n = 1336$ and $n_E = 932$.

Laser Isotope Separation (LIS)

The photon absorbing frequencies of isotopes show small differences caused by shifts of atomic electron energies due to the differences in the number of neutrons among isotopes. This is called isotope shift. The invention and development of lasers enable to resolve the isotope shift sufficiently and make isotope-selective photo-chemical reaction possible. Laser Isotope Separation may lead to almost 100% isotope separation in a single stage. Mainly, two methods such as Atomic Vapor Laser Isotope Separation (AVLIS) and Molecular Laser Isotope Separation (MLIS) were intensively studied. AVLIS uses uranium atomic vapor that is struck by lasers of such wavelength that only ^{235}U atoms are excited and then ionized;

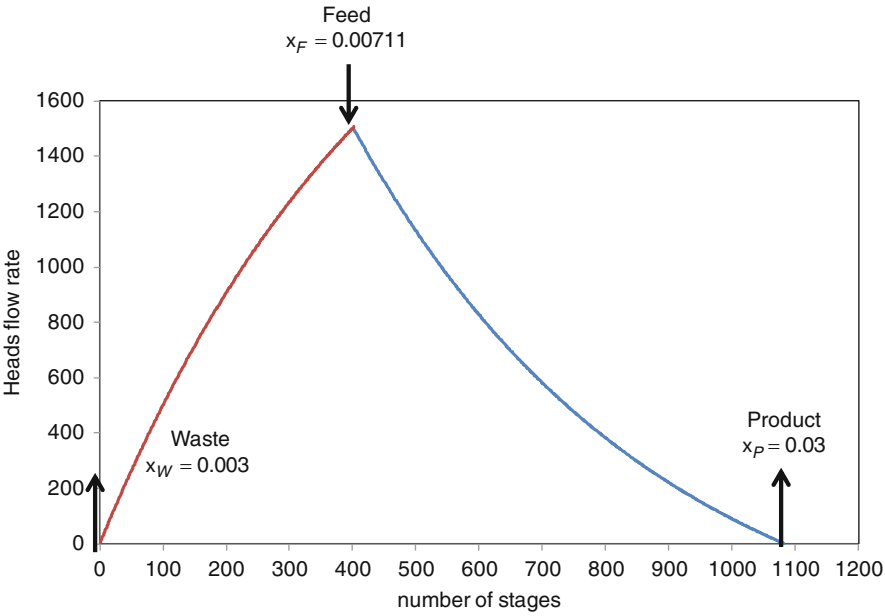

Fig. 3.7 Heads flow rate

once ionized, the ^{235}U ions are collected by an electromagnetic field. MLIS uses UF_6, and vibrationally excites and multiphoton-dissociates only $^{235}UF_6$ into $^{235}UF_5$ by infrared lasers. The research to commercialize them has faded on a global scale.

A new process called Separation of Isotopes by Laser Excitation (SILEX) is under development. All details are not out in the open yet; but SILEX is considered to be a kind of molecular LIS using UF_6. The method only isotope-selectively excites but not dissociates $^{235}UF_6$. The separation factor announced by the company has been 2–20 [5]. Silex Systems Ltd was originally established as a subsidiary of Sonic Healthcare Limited of Australia in 1988. In 2007, the SILEX Uranium Enrichment project was transferred to GE's nuclear fuel plant in the United States. Global Laser Enrichment (GLE) was formed as a subsidiary of GE-Hitachi in 2008 [5]. In June 2009, GE-Hitachi submitted a license application to construct a commercial laser enrichment plant in Wilmington, NC. The NRC staff is currently reviewing that application. They announced that they succeeded the initial measurement program at Test Loop in 2010 and proceeded to evaluate the program to decide the commercialization of the process [6].

Future Directions

As of today, the gaseous diffusion and centrifuge processes have been used on a commercial scale. For the future, it seems that laser enrichment (the SILEX process) may be the successor to current enrichment methods. Preliminary results, based on enrichment by lasers, are encouraging. However, considerable improvements are needed before this method achieves commercial competitive status. Every uranium enrichment process is linked to nuclear proliferation issues. It would be very beneficial for the world if a method of enrichment is devised which inherently offers non- proliferation safeguards for nuclear materials.

Bibliography

1. World Nuclear Association, Uranium Enrichment, World Enrichment capacity - operational and planned. http://www.world-nuclear.org/info/inf28.html
2. Villani S (1976) Isotope separation. American Nuclear Society, Hillsdale
3. Benedict M, Pigford TH (1957) Nuclear chemical engineering. Mcgraw-Hill, New York; Benedict M, Pigford TH, Levi HW (1981) Nuclear chemical engineering (second edn.), (trans: by Kiyose R into Japanese)
4. Kemp RS (2009) Gas centrifuge theory and development: a review of U.S. programs. Science and Global Security 17, 1; Wood HG, Glaser A, Kemp RS (2008) The gas centrifuge and nuclear weapons proliferation. Physics Today 40
5. Silex Systems Limited home page. http://www.silex.com.au/
6. World Nuclear News (2010) Initial Success from SILEX test loop, 12 April 2010. http://www.world-nuclear-news.org/NN-Initial_success_from_SILEX_test_loop-1204104.html

Chapter 4
Nuclear Fission Power Plants

Ronald Allen Knief

Glossary

Blanket	Region surrounding the fuel core of a breeder reactor that contains fertile material to increase production of new fuel.
Brayton cycle	Method used to transfer fission heat energy to gas (e.g., helium or superheated carbon dioxide) for use in a gas turbine to generate electricity.
Breeder	Reactor that produces new fuel from fertile material at a faster rate than it bums fuel for energy production.
Converter	Reactor that produces less new fuel from fertile material than it burns for energy production.
Coolant	Liquid or gaseous medium used to remove fission heat from a reactor core.
Core	Region within a reactor occupied by the nuclear fuel that supports the fission chain reaction.
Critical	Condition where a fission chain reaction is stable with neutron production balancing losses at a nonzero power level.
Electron volt (eV)	1 eV is the kinetic energy obtained by an electron moving across 1 V of electric potential 1 eV = 1.602×10^{-19} J. Common multiples are 1 keV = 1,000 eV and 1 MeV = 10^6 eV. Neutron energies from less than an eV through about 10 MeV are important in nuclear fission power plants.

This chapter was originally published as part of the Encyclopedia of Sustainability Science and Technology edited by Robert A. Meyers. DOI:10.1007/978-1-4419-0851-3

R.A. Knief (✉)
Sandia National Laboratories, PO Box 5800, Albuquerque, NM 87185-1141, USA
e-mail: raknief@sandia.gov

N. Tsoulfanidis (ed.), *Nuclear Energy: Selected Entries from the Encyclopedia of Sustainability Science and Technology*, DOI 10.1007/978-1-4614-5716-9_4,

Fast neutrons	Neutrons of high energy, particularly those produced directly by the fission reaction (~0.1–10 MeV).
Fertile	Material, not itself fissile, capable of being converted to fissile material following absorption of a neutron.
Fissile	Material capable of sustaining a fission chain reaction.
Fissionable	Nuclei capable of fission by neutrons and of participation in a fission chain reaction (category includes fissile nuclides).
Fission	Process in which a heavy-metal nucleus splits into two or more large fragments, releases energy, and emits neutrons and gamma radiation.
Isotopes	Different nuclides of the same chemical element, e.g., ^{235}U and ^{238}U are two of the isotopes of uranium.
Moderator	Material of low atomic mass included in a reactor for the purpose of reducing the kinetic energy of neutrons.
Multiplication factor	Ratio of neutron production rate to neutron loss rate value is unity for a critical system.
Nuclide	Atomic nucleus with a specified number of neutrons and protons, e.g., the uranium-235 [$^{235}_{92}$U] nuclide has atomic mass number 235, 92 protons (atomic number), and 235–92 = 143 neutrons.
Reactivity	Fractional change in neutron multiplication referenced to the critical condition value is zero for a critical system.
Reactor	Combination of fissile and other materials in a geometric arrangement designed to support a neutron chain reaction.
Steam cycle	Method used to convert fission heat energy to steam that drives a turbo-generator, thus, generating electricity.
Thermal neutrons	Low-energy neutrons at or near thermal equilibrium with their surroundings produced by slowing down or moderating the fast neutrons produced by fission. (Equilibrium thermal energy, e.g., is 0.25-eV at 20°C).

Definition of the Subject

Nuclear fission power plants – or nuclear power reactors – are the instruments for commercial use of nuclear energy, relying on a sustained neutron chain reaction from the fission process. Nuclear fission – splitting of heavy-metal nuclei, most importantly ^{235}U and ^{239}Pu – produces an enormous amount of energy.

Fission was discovered in 1938 on the eve of World War II. The magnitude of the energy release was recognized immediately. However, it was not until after the attack on Pearl Harbor in late 1941 that the USA began serious efforts to develop this energy source for military purposes. Germany conducted research along these same lines, but ultimately was unsuccessful in development efforts.

The USA's ensuing "Manhattan Project" [1] included monumental basic research, development of nuclear reactors for research and nuclear-material production, design of nuclear explosives, and ultimately testing of a nuclear explosive device and development of the two nuclear weapons credited with ending the war. Post war, the next use of nuclear energy was for propulsion in submarines, first by the USA, then other countries. Subsequently nuclear propulsion has been extended to surface vessels as well. About 85% of the world's nuclear electricity is generated by reactors derived from designs originally developed for naval use [2].

Nuclear power for nonmilitary, peaceful uses began in earnest in 1956 with the startup of the world's first full-scale nuclear electric generating plant, at Calder Hall in England, followed in the USA a year later by the initial operation of a 60-MW unit at Shippingport, Pennsylvania [3]. By the middle of the 1960s, there was a growing optimism on the part of US utilities toward nuclear power as well as substantial activity worldwide. Electric generation using nuclear steam-supply systems was economically competitive with fossil-fuel fired plants. The passage in mid-1964 of a US law providing for private ownership of nuclear fuel was hailed as paving the way for an independent nuclear power industry.

By 1970, the combined capacity of US nuclear plants in service, under construction, and on order was over 64 GW, more than twice the total for all other nations combined. Widespread enthusiasm for nuclear power had reached its high-water mark.

Subsequently nuclear technology suffered "growing pains." High interest rates affected the capital-cost-intensive reactors. Then in 1979 came the accident at Three Mile Island. As a result of the accident – and that at Chernobyl in 1986 [4] – over 100 orders for new reactors were cancelled and no new orders were placed in the ensuing three decades.

Despite residual public misgivings over Three Mile Island and Chernobyl, the industry has learned its lessons and established a solid safety record during the past two decades. Meanwhile efficiency and reliability of nuclear plants have climbed to record levels [5]. By 2010, 104 nuclear reactors were producing a fifth of the USA's total electric output.

"Nuclear power supplies a sixth of the world's electricity. Along with hydropower (which supplies slightly more than a sixth), it is the major source of 'carbon-free' energy today" [4]. "Nuclear power now accounts for 73% of the emission-free generation in the USA and is the only technologically mature, non-emitting source of power that is positioned to deliver large-scale CO_2 reduction in the decades ahead" [6].

Growing concern about global warming – and the associated likelihood that greenhouse gas emissions will be regulated in some fashion – has led power providers in the USA and elsewhere, and their governments [4], to recognize that nuclear reactors produce electricity without atmospheric discharge of carbon dioxide, pollutants such as nitrogen oxides, and smog-causing sulfur compounds [5]. With the world demand for energy projected to rise by about 50% by 2030 and to nearly double by 2050, building nuclear power plants appears to be increasingly viable and attractive.

The fossil-fuel alternatives have their drawbacks. Oil and natural-gas supplies are shrinking and their use can have unwanted political consequences [3]. Natural gas – attractive because it has the lowest carbon content of the fossil fuels and advanced power plants have low capital costs – has electricity costs which are very price-sensitive and can be volatile. Although abundant, coal is difficult to recover, deliver, and burn [3, 4]. As the most carbon-intensive source of electricity, coal's long-term viability will depend on capture and sequestration of carbon dioxide – which is both costly and yet to be demonstrated and introduced on a large scale [4].

Solar, geothermal, wind, and tidal power, while attractive, cannot be expected to supply energy in the vast amounts required in the immediate future. Conservation and tight management of energy consumption are necessary, but not sufficient, parts of the equation [3].

With the future uncertain, energy realists see nuclear power as indispensable for electric generation well past the mid twenty-first century. It can fill uniquely a gap in the spectrum of electricity generation methods.

Designers are adopting novel approaches for new nuclear systems. They are evaluating systems in terms of their sustainability – meeting present needs without jeopardizing the future generations. "It is a strategy that helps to illuminate the relation between energy supplies and the needs of the environment and society. This emphasis on sustainability can lead to the development of nuclear energy-derived products besides electric power, such as hydrogen fuel for transportation. It also promotes the exploration of alternative reactor designs and nuclear fuel-recycling processes that could yield significant reductions in waste while recovering more of the energy contained in uranium" [5].

There are indications of a possible nuclear revival. More than 20,000 megawatts of nuclear capacity have come on-line globally in the early years of the twenty-first century, mostly in the Far East. Nuclear plants have demonstrated remarkable reliability and efficiency recently. The world's ample supply of uranium could fuel a much larger fleet of reactors than exists today throughout their 40- to 50-year life span [4]. The nuclear power industry has been developing and improving reactor technology for more than five decades and is starting to build the next generation of nuclear power reactors to fill orders now materializing [2]. The first firm order for new reactors in the USA was placed in 2009. Nearly 20 more considered "firmly planned" are expected to follow. There are even more prospects worldwide, most notably in pacific-basin countries [7].

Wide-scale deployment of nuclear power technology would seem to offer substantial advantages over other energy sources. However, there also are challenging questions to be addressed regarding the best way to make it fit into the future. These include achievement of economic viability, improved operating safety, efficient waste management and resource utilization, as well as weapons nonproliferation, all of which are influenced by the design of the nuclear reactor system that is chosen and the fuel cycle followed [4, 5].

Introduction

The current nuclear power reactors produce electricity using a steam cycle in much the same way as conventional fossil-fuel power plants. However, special design and operating features are required to address the unique characteristics of the fission-energy source and its associated radiation environment. A wide variety of reactor concepts have been developed to this purpose [8]. (The other major nuclear reaction for energy production, *fusion*, offers the prospect as a future energy source. See Nuclear Fusion).

Fission

Fission reactions occur when a neutron strikes a nucleus of specific heavy-metal isotopes of uranium and plutonium – most notably ^{235}U or ^{239}Pu – and causes splitting into two or more fission fragments, emits additional neutrons and other radiations, and releases a relatively large amount of energy. The energy release from a single fission is between five and six orders of magnitude greater than that from a single chemical reaction (e.g., combustion of carbon and oxygen). This large amount of energy per unit mass of fuel is a major advantage of fission as an energy source. The emission of extra neutrons is a necessary feature to support a sustained chain reaction with steady or accelerated energy release.

The fission reaction also has unique problems in the form of particulate and electromagnetic radiations emitted at the time of fission and from the long-lingering radioactivity (i.e., emission of radiations over time) of the fission fragments and their products. Protection against the effects of these radiations requires shielding and removal of the associated heat.

The fission process produces several hundred different fission fragments, each of which is radioactive and undergoes successive decays prior to reaching stability. Each species has a different characteristic lifetime, described in terms of its unique *half-life* – the average time required for one half of a mass of the radioactive material to decay. The resulting overall radiation levels are substantial, having an energy equivalent to about 7.5% of the total fission output at the time a reactor is shut down, and decreasing roughly inversely as the one-fifth power with time (i.e., $t^{-1/5}$). Handling this lingering decay heat load is a principal consideration in the safe operation of nuclear reactors. Containment of the radioactive material requires both near-term and long-term nuclear waste management strategies. (See Health Physics, Fission Reactor Physics, and Radioactive Waste Management: Storage, Transport, Disposal.)

Fission Chain Reaction

When the chain reaction exactly balances the rates of neutron production from fission with non-fission absorption and leakage from the system boundaries, it is steady and said to be *critical*. When production exceeds losses, it is *supercritical* and power increases. When losses exceed production, the chain reaction is *subcritical* and power decreases, down to and including being shut down. All three states of criticality are necessary to nuclear power reactor operation. These states are quantified with an *effective multiplication factor* k_{eff} or k, defined as

$$k_{\text{eff}} = k = \text{production}/[\text{absorption} + \text{leakage}]$$

or by the change in multiplication, *reactivity* ρ, defined as

$$\rho = (k - 1)/k.$$

Thus, $k = 1$ and $\rho = 0$ constitute the critical condition; $k > 1$ and $\rho > 0$ supercritical; and $k < 1$ and $\rho < 0$ subcritical.

The mathematical equations associated with the neutron balance are quite complex since the reaction rates are a strong function of both material (composition, location, and irradiation history) and neutron population (position, direction, and energy) characteristics. Neutron energy is a particularly important parameter. Neutrons emitted in fission are in the 0.1–10 MeV range with an average energy of about 2 MeV. The probability for fission increases dramatically if the neutron energy falls below 1 eV.

For this reason, a *moderator* material of low mass may be added to enhance the slowing down. (The closer the mass of the moderator nuclei to that of the neutron, the larger the potential energy loss in a single collision; thus, hydrogen with essentially the same mass is best in this regard, although it may not be selected for other reasons.) (See Nuclear Reactor Materials and Fuels.)

Fissionable Materials

The heavy metals uranium and plutonium each have isotopes that can be caused to fission by neutrons, i.e., that are *fissionable*. Fission occurs under different circumstances among the isotopes.

Fissile nuclides can fission with neutrons of energy, all the way down to essentially zero. The principal fissile materials are those containing significant quantities of ^{233}U, ^{235}U, ^{239}Pu, and/or ^{241}Pu. A fission reactor core contains fissile as well as non-fissile and other materials.

Other isotopes of U, Pu, and Th can be fissioned by neutrons, but only by neutrons with kinetic energy above a minimum threshold. Particularly important

examples of such *fissionable* nuclides are ^{238}U, ^{232}Th, and ^{240}Pu. The latter nuclides also have the unique characteristic that upon absorbing a neutron in a non-fission reaction, they will convert to fissile nuclides either directly or via a multi-step process. These *fertile* nuclides produce the new fissile as follows:

$$^{238}\text{U} \rightarrow ^{239}\text{Pu}:$$
$$^{232}\text{Th} \rightarrow ^{233}\text{U}: \text{ and}$$
$$^{240}\text{Pu} \rightarrow ^{241}\text{Pu}.$$

(See Fission Reactor Physics)

Reactor Classifications

Nuclear power reactors are designed to achieve a self-sustained chain reaction with a combination of fissile, fertile, and structural materials. The current generation of reactors uses the heat produced by fissions in the core to produce steam and then electricity, employing a variety of fuel forms, coolants, moderators, and other materials.

Common characteristics useful for classifying reactors are:

1. *Coolant* – principal heat-removal medium.
2. *Steam cycle* – number and configuration of separate coolant "loops" for producing steam to turn a turbine generator and produce electricity.
3. *Moderator* – material (if any) used to "slow down" the neutrons produced by fission.
4. *Neutron energy* – general energy range (typically fast [fission-energy] or thermal) for the neutrons that cause most of the fissions.
5. *Fuel production* – system is referred to as a *breeder* if it produces (i.e., changes from fertile to fissile) more fuel than it consumes; it is said to be a *converter* otherwise.

The first two features relate to the current practice of converting fission energy first to heat and then to electric energy by employing a steam cycle. Coolants include water, heavy water, gases (e.g., CO_2 or helium), and liquid metal (e.g., sodium). The steam cycles may employ from one to three separate loops, including one for primary coolant circulation and one (not necessarily separate from the first) for steam generation. It may be noted that next-generation reactors could bypass steam in favor of direct use of a coolant for electricity, process heat, or hydrogen production.

As mentioned earlier, neutrons emitted from fission are of high energy. However, very low energy neutrons have a higher likelihood of causing fission reactions. Thus, many systems employ a moderator to "slow down" these neutrons. The best moderators are of low mass, allowing maximum energy transfer through neutron

collisions (e.g., the limiting case of potentially total energy transfer between a moving cue ball and a stationary billiard ball of equal mass). Typical materials used for this purpose are hydrogen, deuterium (heavy hydrogen), and carbon/graphite. The moderator and coolant may be the same (e.g., water or heavy water) or may be separate (e.g., water, heavy water, or a gas coolant with heavy water or solid graphite moderator). Neutrons with low enough energies to be roughly in thermal equilibrium (<1 eV) with the surrounding materials are said to be *thermal neutrons*. Neutrons at or near fission energies (averaging ~2 MeV) are *fast neutrons*. Fast reactors avoid the use of moderators, such as with a metal coolant like sodium, instead of one of the moderating materials identified above.

All nuclear power reactors contain fertile ^{238}U or ^{232}Th and, thus, produce some amount of new fissile fuel. The ubiquitous light-water reactors (LWR) have slightly enriched uranium fuel which is up to 5 wt% ^{235}U with the remaining 95 wt% ^{238}U. Thus, they produce plutonium during routine operation. Producing about 60% as much new fuel as used for operation, the LWR units are considered to be *converter* reactors. By contrast, a reactor producing more new fuel than it uses is called a *breeder*.

The world's six principal types in the current generation of nuclear power reactors are:

1. Boiling-water reactor (BWR)
2. Pressurized-water reactor (PWR)
3. Heavy-water-moderated reactor (HWR)
4. Gas-cooled reactor (GCR)
5. Light-water-cooled graphite-moderated reactor (LWGR)
6. Fast breeder reactor (FBR)

The section labeled "General" in Table 4.1 classifies one or more versions of each of these six reactor types in terms of the five categories identified at the beginning of this section [8]. For example, the GCR variation known as the high-temperature gas-cooled reactor (HTGR) is a double-loop, helium-cooled, graphite-moderated, thermal, converter reactor.

Principles for Design and Operation

Nuclear power reactors are complex systems whose design represents a balance among conflicting requirements. Principal among these requirements are nuclear design, materials, thermal design, economics, and control and safety [8, 9].

The nuclear (physics) design seeks to match fissile and fertile constituents with appropriate coolants and moderators (if any) to optimize specific (per unit mass of fuel) fission-energy output and production of new fuel or meet alternative design goals. Materials concern focus on chemical compatibility of components, thermal and radiation stability, and overall mechanical strength. One especially important

Table 4.1 Characteristics for six representative nuclear steam-supply systems

	BWR	PWR	PHWR	PTGR	HTGR	LMFBR
	Manufacturer					
	General Electric	Westinghouse	Atomic Energy of Canada, Ltd.	(Former) Soviet Union	General Atomic	Novatome
	System (Station)					
	BWR/6	(Sequoyah/SNUPPS)	CANDU 600	RBMK-1000	(Fulton)	(Superphénix)
General						
Steam cycle						
Loops	1	2	2	1	2	3
Primary coolant	H_2O	H_2O	D_2O	H_2O	He	Liq. Na
Secondary coolant	–	H_2O	H_2O	–	H_2O	Liq. Na/H_2O
Moderator	H_2O	H_2O	D_2O	Graphite	Graphite	–
Neutron energy	Thermal	Thermal	Thermal	Thermal	Thermal	Fast
Fuel production	Converter	Converter	Converter	Converter	Converter	Breeder
Energy conversion						
Gross thermal power, MWt	3,579	3,411	2,180	3,200	3000	3,000
Net electric power, MWe	1,178	1,150	638	950	1,160	1,200
Efficiency,%	32.9	33.7	29.3	31.2	38.7	40
Heat transport						
Primary loops and pumps	2	4	2	2/6 + 2	6	4
Intermediate loops	–	–	–	–	–	8
Steam generators	–	4	4	–	6	8
Steam-generator type	–	U-tube	U-tube	–	Helical coil	Helical coil
No. turbine generators	1	1	1	2	1	2
Fuel						

(continued)

Table 4.1 (continued)

	BWR	PWR	PHWR	PTGR	HTGR	LMFBR
	Manufacturer					
	General Electric	Westinghouse	Atomic Energy of Canada, Ltd.	(Former) Soviet Union	General Atomic	Novatome
	System (Station)					
	BWR/6	(Sequoyah/SNUPPS)	CANDU 600	RBMK-1000	(Fulton)	(Superphénix)
Particles	Short, cyl. pellets	Short, cyl. pellets	Short, cyl. pellets	Short, cyl. pellets	Coated microspheres	Short, cyl. pellets
Chemical form	UO_2	UO_2	UO_2	UO_2	UC/ThC	Mixed UO_2/PuO_2
Fissile (% by wt.)	2–4% ^{235}U	2–4% ^{235}U	Natural uranium	Natural uranium	93% ^{235}U	10–20% Pu (core)
Fertile	^{238}U	^{238}U	^{238}U	^{238}U	Thorium	^{238}U (core + blanket)
Pins	Pellet stacks in Zr-alloy tubes	Pellet stacks in Zr-alloy tubes	Pellet stacks in Zr-alloy tubes	Pellet stacks in Zr-alloy tubes	Microspheres in graphite stick	Pellet stacks in SS tubes
Assembly	8 × 8 sq. pin array	17 × 17 sq. pin array	37-pin concentric circles	18-pin concentric circles	Hex. graphite block with fuel sticks	271-pin hex. array
Core						
Axis	Vertical	Vertical	Horizontal	Vertical	Vertical	Vertical
Assys on axis	1	1	12	2	8	1
Assys radially	748	193	380	1,661	493	364 (core), 233 (blanket)
Performance						
Equil. burnup, MWD/T	27,500	27,500	7,500	18,500	95,000	100,000
Refueling sequence	1/4 per year	1/3 per year	Continuous, on-line	On-line	1/4 per year	Variable
Thermal hydraulics						
Primary system						

Pressure, MPa	7.17	15.5	10.0	7.2	4.90	~0.1
Inlet temp., °C	278	292	267	270	318	395
Avg. out. temp., °C	288	325	310	284	741	545
Core flow, Mg/s	13.1	18.0	7,6	10.4	1.42	16.4
Volume, L	–	3.36×10^5	1.20×10^5	4.0	(9,550 kg)	(3,200 Mg) Na/H_2O
Secondary system						
Pressure, MPa	–	6.89	4.7	54	17.2	~0.1/17.7
Inlet temp., °C	–	227	187	29	188	345/235
Outlet temp., °C	–	285	260		513	525/487
Power density						
Core avg., kW/L	54.1	105	12	4.0	8.4	280
Fuel avg., kW/L	54.1	105	60	54	44	280
Linear heat rate						
Core avg., kW/m	19.0	17.8	25.7	29	7.87	29
Core max., kW/m	44.0	42.7	44.1		23.0	45
Design peaking factors						
Radial	1.4		1.21			
(Total)		(2.5)			(2.9)	(1.55)
Axial	1.6		1.41			
Moderator						
Volume, L	(Same as primary coolant)	(Same as primary coolant)	2.17×10^6	(Graphite)	(Graphite in fuel blocks)	–
Inlet temp., °C			43			–
Outlet temp., °C			71			–
Reactivity control						
Control rods						

(continued)

Table 4.1 (continued)

	BWR	PWR	PHWR	PTGR	HTGR	LMFBR
	Manufacturer					
	General Electric	Westinghouse	Atomic Energy of Canada, Ltd.	(Former) Soviet Union	General Atomic	Novatome
	System (Station)					
	BWR/6	(Sequoyah/SNUPPS)	CANDU 600	RBMK-1000	(Fulton)	(Superphénix)
Geometry	Cruciform	Rod clusters	Rods	Rods	Rod pairs	Hex. pin bundle
Absorber material	B_4C	Ag In Cd	Various	B_4C	B_4C/graphite	B_4C
Burnable poison	Gd. in fuel pellets	Borosilicate glass	–		B_4C/graphite	–
Other systems	Voids in coolant	Soluble boron	H_2O, various		Reserve shutdown	Three bundle secondary
Reactor vessel						
Inside dimension, m	6.05D × 21.6 H	4.83D × 13.4 H	7.6D × 4 L	0.08ID × 8 H tubes	11.3D × 14.4 H	21D × 19.5 H
Wall thick., mm	152	224	28.6	4.0	(4.72 m min.)	25
Material	SS-clad carbon steel	SS-clad carbon steel	Stainless steel	Zr-Nb alloy	Prestressed concrete	Stainless steel
Other features			Pressure tubes	Pressure tubes	Steel liners	Pool-type

Data summarized from [8]. Appendix IV. (Appendix also includes parameters for PWR designs from US manufacturers B&W and CE, France's Framatome, and the former Soviet Union's unique VVER)

requirement for reactors that refuel only while shutdown – which is the majority – is that the fuel maintains its general structural integrity throughout up to 4 years or more of in-core residence; unlike other energy production cycles, the fuel is not literally "burned up" with wastes discarded along the way.

Thermal design is concerned with heat removal for effective energy production and maintaining the integrity of the fuel, cladding, and other materials for operational and safety purposes. Reactor thermal operating limits are determined by the most extreme postulated local conditions – to avoid damage anywhere in the reactor core. Temperature limits are established to prevent fuel melting and/or clad damage during power excursions and loss of cooling. Other limits address avoiding coolant-clad temperature mismatch that could lead to local loss of fuel integrity. Both types of limits are established in terms of peak (local)-to-average core conditions. Such factors vary with power level, time in core life, and other parameters.

The primary economic consideration is to minimize overall costs, i.e., initial capital outlay, operating and maintenance costs, and fuel charges. Increasing electric-generation reliability and thermal conversion efficiency are particularly important throughout lifetime.

Power reactor controls must be capable of maintaining the critical condition, increasing and decreasing power, and adjusting to long-term changes such as the conflicting effects from breeding new fuel, depleting existing fuel and burnable neutron poisons, and building in radioactive fission- and transuranic-product neutron poisons. The desired neutron balance is maintained predominately by adjusting neutron absorption using materials designed to remove neutrons from, or "poison," the chain reaction. Methods may include a combination of solid moveable control rods, soluble poisons in the coolant or moderator (PWR), and fixed burnable poisons designed to deplete or be "burned out" by the continuing neutron population. Some reactor designs also change neutron production by on-line fuel exchange. Fission products whose poisoning effects are sensitive to operating conditions also must be subject to control.

Routine control strives to make the power density as uniform as possible throughout the core, while allowing for power changes. In most designs, control-rod movement is used with groups selected for symmetry to maintain uniform, i.e., avoid highly asymmetric, power distribution. Measures are instituted to restrict the speed of movement and reactivity effect of individual rods or groups of rods to prevent excessively rapid power increase. Similarly, the design intends to minimize the likelihood of inadvertent control-rod withdrawal which could lead to unplanned supercritical conditions.

Safety concerns are addressed through a protective system whereby the control rods may be inserted into the core – dropped down or pushed up – into the core quickly; i.e., they "scram" or "trip" the reactor through gravity drop or gas pressure, respectively, when certain predetermined parameter limits (e.g., on pressure, temperature, flow, or power levels) are exceeded.

Reactor safety is enhanced with inherent negative feedback mechanisms, where a power increase tends to be self-limiting. Fuels are designed to have such feedback, with their reactivity decreasing with escalating temperature. Expansion of the

coolant and/or moderator (such as with increased temperature) provides negative reactivity feedback in light-water reactors. Reactors with positive reactivity feedback in certain operating regimes may be difficult to control. The essentially instantaneous feedback contributions, along with some long-term ones (such as from time-dependent changes in concentrations of xenon and samarium fission-product poisons), affect the stability of the chain reaction, may limit the ability to change the power level, and are a major consideration in overall reactor safety design.

A fundamental safety feature for all power rectors is multiple-barrier containment of fission products. As may be observed for each reactor type described in the remainder of this article, these barriers include the fuel particles, surrounding cladding, the coolant system boundary, and a containment structure.

An important example of tradeoffs among the design goals is seen in thermal-reactor fuel assemblies (e.g., subsequent Figs. 4.3 and 4.8) whose pin arrangement determines the characteristics of the chain reaction, economics, and heat removal [9]. The chain reaction is enhanced by optimum spacing of the fuel in "lumps" with moderator interspersed so that neutrons from fission will undergo a number of scattering collisions for slowing down prior to reentering the fuel; too little and too much spacing can both be detrimental. The extent of slowing down also determines the amount of conversion of fertile to fissile material and the overall energy production possible from a given amount of fuel. Spacing and coolant flow rate establish heat-removal characteristics (including temperature feedback effects on the fuel's reactivity). Final dimensions generally represent a best-estimate balance among these and other competing concerns.

Reactor Systems

The major nuclear power reactor types were identified at the end of the section "Introduction" noting that characterization of each is provided in the "General" section of Table 4.1. More detailed descriptions of each of these systems as implemented in the present generation of reactors follow. (As explained in detail in the section "Advanced Reactors," several generations of reactors are commonly distinguished. Of interest here, Generation I (GEN-I) reactors were developed in the 1950s–1960s, while Generation II (GEN-II) reactors are typified by the present US fleet and most in operation elsewhere.) Parameters for selected specific present reactor designs are detailed in the remainder of Table 4.1.

The main focus of these nuclear power plant descriptions is on the steam cycle, fuel assemblies, reactivity control, and the protective system [8]. General safety-related functions are summarized separately in the section "Nuclear Reactor Safety Features."

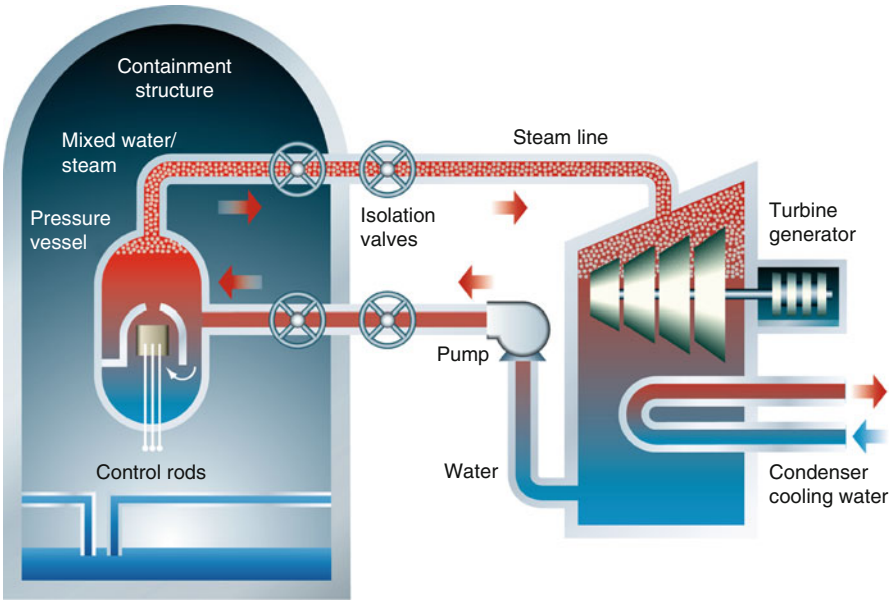

Fig. 4.1 Steam cycle for boiling-water reactor (BWR) (Courtesy of Atomic Industrial Forum/ Nuclear Energy Institute)

Light-Water Reactors

Two light-water reactor (LWR) systems – boiling-water reactor (BWR) and pressurized-water reactor (PWR) – employ ordinary ("light") water as coolant and moderator. The former design produces steam through a direct cycle (Fig. 4.1), while the latter uses an intermediate steam-generator heat exchanger to maintain an all-liquid primary loop and produce steam in a separate secondary loop (Fig. 4.2).

The nature of the water coolant/moderator results in similarities between the two LWR designs. The fuel is uranium dioxide pellets enriched to 2–5 wt% ^{235}U; initial core loadings typically span this range with reload cores distinctly at the upper end of the enrichment range. The pellets are clad in sealed zirconium-alloy tubes. Fuel assemblies consist of rectangular arrays of fuel pins with regular spacing (see also Modern Nuclear Fuel Cycles).

Since the LWR designs rely on liquid water for moderating neutrons, maximum operating temperatures must remain well below the 706°F (374°C) critical temperature at which pressure increases dramatically and liquid cannot exist regardless of pressure. They, thus, cannot operate at the "modern steam conditions" – nominally 1,000°F (540°C) – typical of fossil-fueled plants. The LWR's saturated steam–water mixture requires a special, more costly "wet steam" turbine.

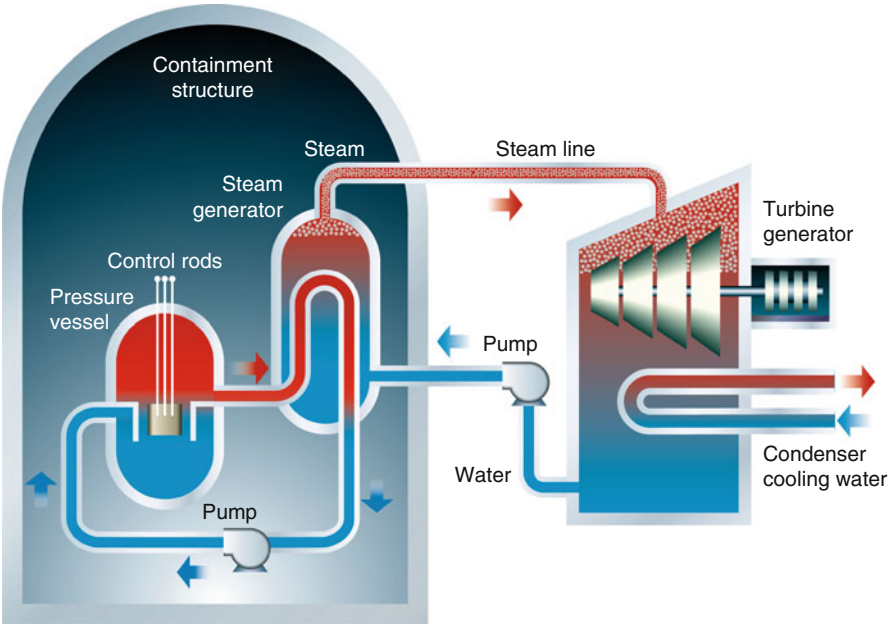

Fig. 4.2 Steam cycle for pressurized-water reactor (PWR) (Courtesy of Atomic Industrial Forum/ Nuclear Energy Institute)

Boiling-Water Reactors

The direct-cycle boiling-water reactor (BWR) was developed in the USA by General Electric and was followed by designs in Western Europe and Japan. It may be noted that the current designs for BWR and other reactors are increasingly characterized by multinational joint ventures. See also the section "Advanced Reactors." For details on historical, current, and proposed units of this and the other designs, see Refs. [7, 8, 10, 11].

Employing the cycle shown in concept by Fig. 4.1 and in more detail in Fig. 4.3, feedwater enters the steel reactor vessel, is heated by the fission chain reaction occurring in the fuel pins, and leaves the vessel as steam. The high- and low-pressure turbine stages are employed in concert with the multiple heaters and condensers to enhance energy-conversion efficiency. The more recent BWR designs use jet pumps to recirculate a fraction of the feedwater flow for better control.

Fuel assemblies for the BWR appear as shown in Fig. 4.4. The 7×7 to 9×9 square arrays of fuel pins is surrounded by a metal fuel channel, which prevents the water–steam mixture from moving between assemblies (and potentially resulting in inadequate cooling (steam–water mixture) in some assemblies). Fuel assemblies may contain pins of several different enrichments (Fig. 4.5). The reactor fuel core consists of up to 800 fuel assemblies.

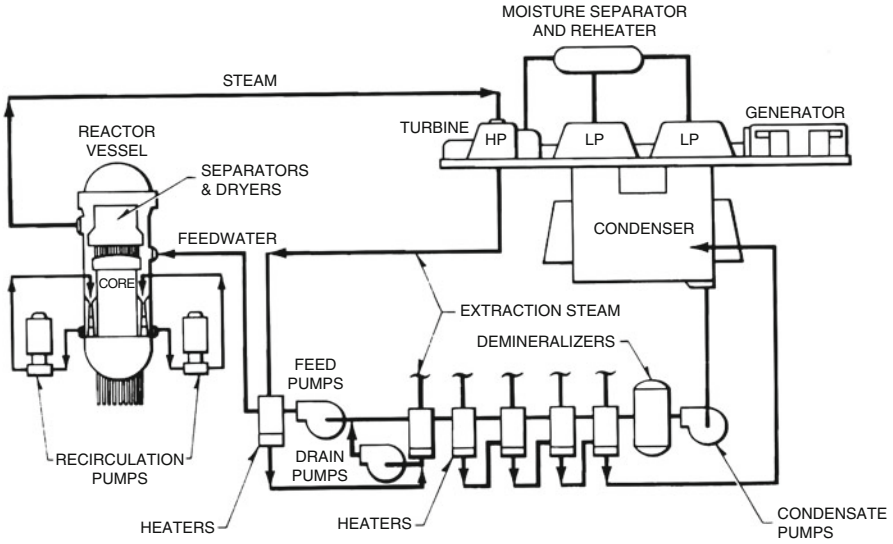

Fig. 4.3 Representative steam cycle schematic diagram for a boiling-water reactor (BWR) (Courtesy of General Electric Company)

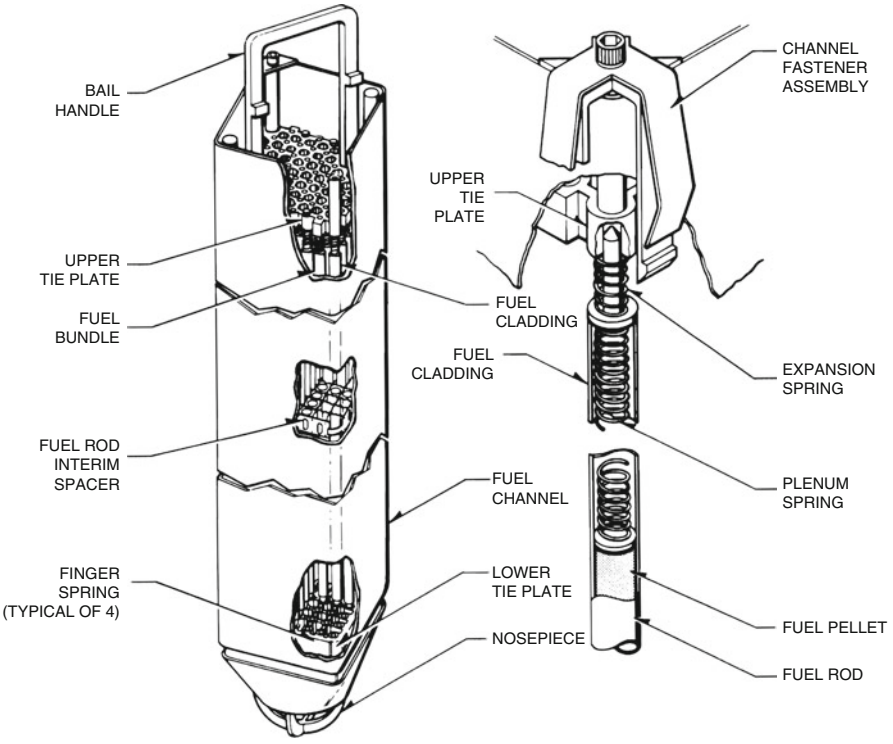

Fig. 4.4 Representative fuel assembly for boiling-water reactor (Courtesy of General Electric Company)

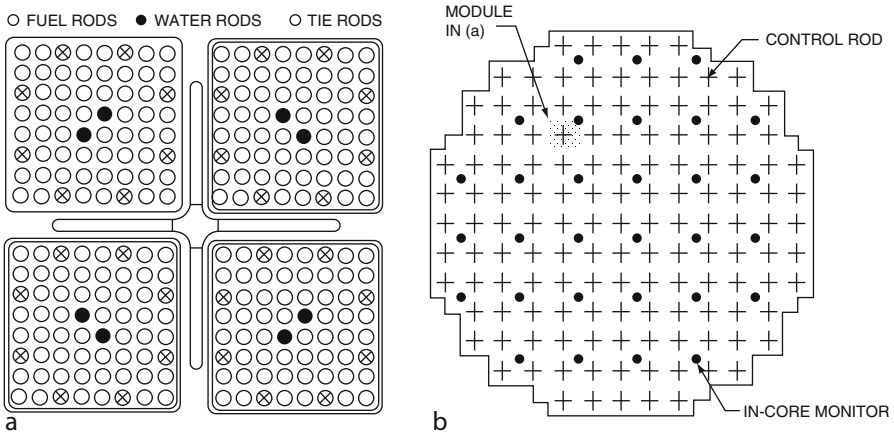

Fig. 4.5 Core fuel module (**a**) and control-rod pattern (**b**) for representative boiling-water reactor (Courtesy of General Electric Company)

Reactivity control for routine operation is implemented through a combination of control rods and coolant flow adjustment. The bottom-mounted control rods (indicated below the reactor vessel in Fig. 4.3) are made of long boron carbide–filled pins in a cruciform ("cross") shape that fits between four fuel assemblies as shown in Fig. 4.5.

Flow adjustment can provide another effective control method, since the water density changes with temperature. At low temperature, the dense water is very effective at moderating neutrons, and thereby encourages fission. With increased temperature, the density decreases (or, equivalently, void content increases as steam is being produced), causing a reduction in moderation and fission rate. Thus, if flow rate is increased, energy removal can be increased without a net change in coolant temperature with a resulting increase in power generation. In practice, power-level changes of up to 40% may be accomplished by flow control. (BWR operational practices are described further in the section "Boiling-Water Reactor.")

Longer-term reactivity control is accomplished using burnable poisons (e.g., "curtains" containing boron placed between fuel assemblies or gadolinium poisons fabricated into the fuel itself) and gradually withdrawing inserted control rods over core lifetime. Reactor shutdown – scram or trip – is accomplished by using gas pressure to insert all of the bottom-mounted control rods into the core.

Table 4.1 contains parameters for a large BWR and other reactor types. Advanced BWRs are addressed in the section "Advanced Reactors."

Pressurized-Water Reactor

The two-loop pressurized-water reactor (PWR) was developed in the USA by Westinghouse Electric Corporation. Other somewhat similar designs have been

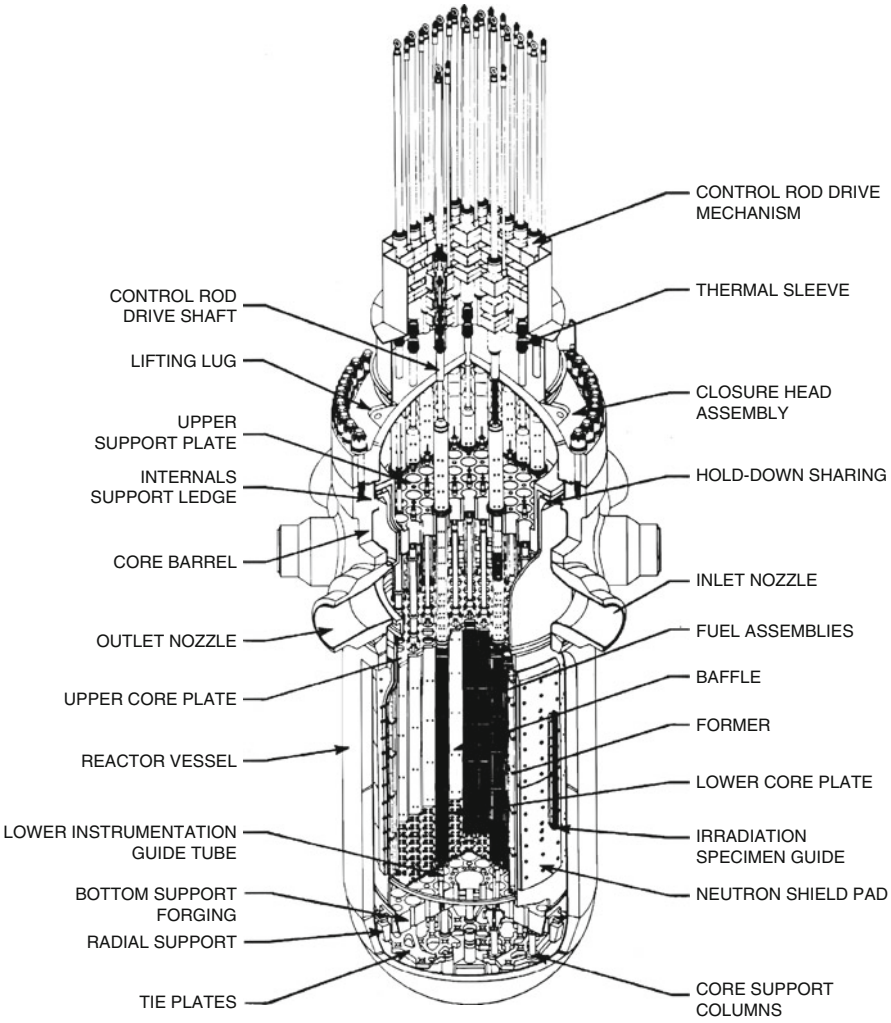

Fig. 4.6 Reactor pressure vessel for a representative pressurized-water reactor (Courtesy of Westinghouse Electric Company)

developed by a pair of US organizations, as well as by others in Western Europe, Japan, and South Korea. A particular unique version has come from the Soviet Union (now by Russia). Water in the primary loop (Fig. 4.2) is maintained as liquid by using high pressure. The water enters the reactor vessel (Fig. 4.6) at the inlet nozzle, flows downward along the inner vessel wall, is distributed at the lower vessel plate, flows up through the fuel assemblies removing heat energy, and exits at the outlet nozzle – still as a liquid.

Energy from the primary loop is extracted and converted to steam by two to four U-tube (Fig. 4.7), once-through, or horizontal (Russian design) steam generators.

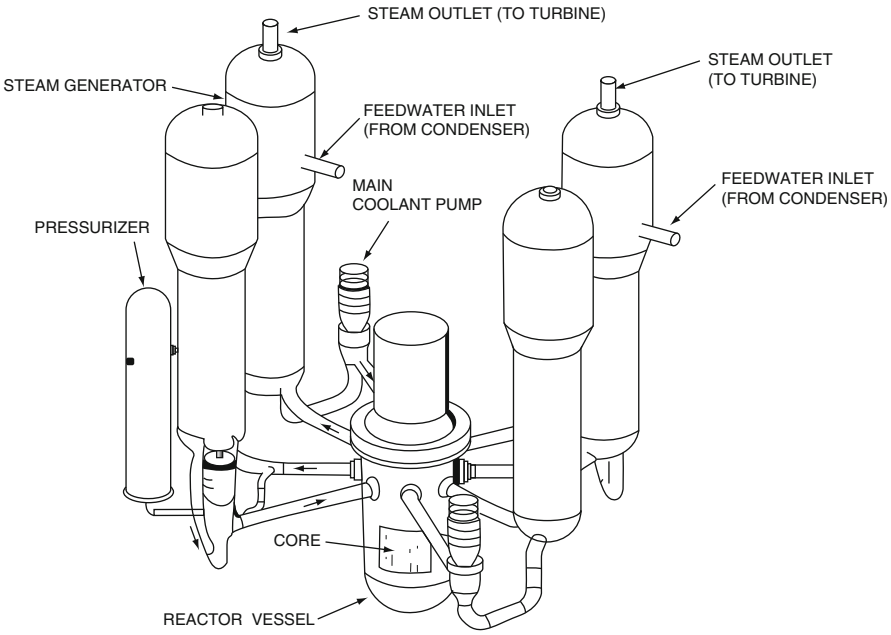

Fig. 4.7 Four U-tube steam-generator primary loop configuration for a pressurized-water reactor (Courtesy of Westinghouse Electric Company)

Multiple turbine stages, heaters, and a condenser are employed as for the BWR (Fig. 4.3). A *pressurizer* with a steam–water interface is used to maintain the sensitive pressure/temperature balance in the primary system by using heaters to boil water, increase the amount steam, and thus raise the pressure; conversely spraying "cooler" ("less hot") water condenses steam and reduces the pressure.

Fuel assemblies for the PWR are of 14 × 14 to 17 × 17 square fuel pin arrays (Fig. 4.8) or a hexagonal array of up to 331 pins (Russian VVER). They are not enclosed in a fuel channel (in part because the single-phase primary fluid is better behaved than the BWR's boiling coolant). These assemblies also have unoccupied pin locations, which can accommodate control rods, burnable poisons, or instruments. The large PWR reactor cores consist of 150–200 or more fuel assemblies.

Like the BWR, the PWR uses control and burnable-poison rods for reactivity control. Uniquely, it also uses the soluble neutron poison, boric acid, for long-term control. The boric acid concentration is adjusted to match general changes from fuel burnup, conversion of fertile material into fissile, and depletion of burnable poisons.

Insertion of control-rod assemblies from the top of the core (by contrast with the bottom-mounted BWR control rods) provides short-term, routine reactivity control. These assemblies consist of 5–24 "fingers," made of boron carbide or of a silver–indium–cadmium mixture, which move in channels within the fuel assemblies (e.g., as shown in Fig. 4.8). A small group of rods in a symmetric

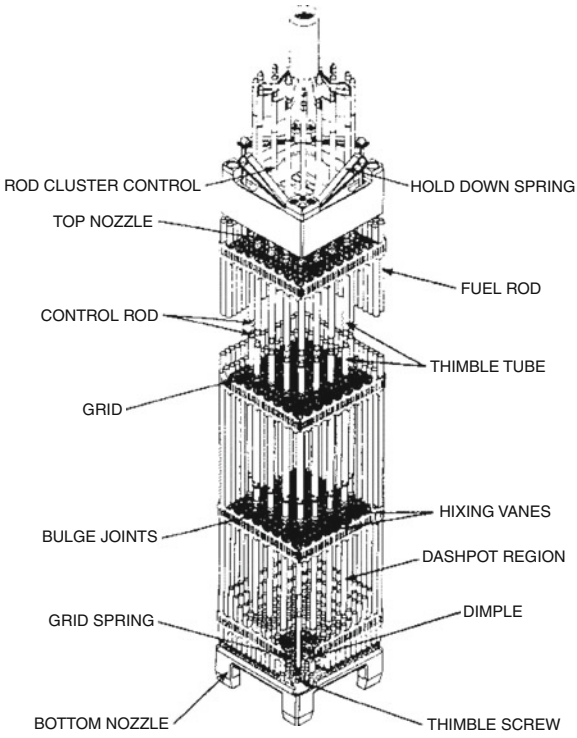

Fig. 4.8 Representative fuel assembly for a pressurized-water reactor (Courtesy of Westinghouse Electric Corporation)

pattern is inserted partially into the fuel (typically >25%) and then moved as needed to compensate for routine power fluctuations. Significant power changes up to an including startup and shutdown invoke other, larger groups of control rods. (PWR operational practices are described further in the section "Pressurized-Water Reactor.")

Scram/trip is accomplished in the PWR by dropping the top-mounted control rods (Figs. 4.6 and 4.8) into the core under the influence of gravity. The rods are mounted to their drives by electromagnets so that interruption of the current (from power failure or indication that a specific parameter is outside of a predetermined range) causes the rods to fall.

Fig. 4.9 is a cutaway drawing (wallchart) of a representative PWR unit. Other than for the reactor "nuclear island" – also known as the nuclear steam-supply system (NSSS) – the drawing shows features common to the other reactor units, all of which have turbine generator(s), and containment, auxiliary, and support buildings. (Reference [12] contains a Web link to this wallchart, as well as to charts for over 100 other reactors.)

Table 4.1 contains parameters for a representative PWR and other reactor types. Advanced PWRs are addressed in the section "Advanced Reactors."

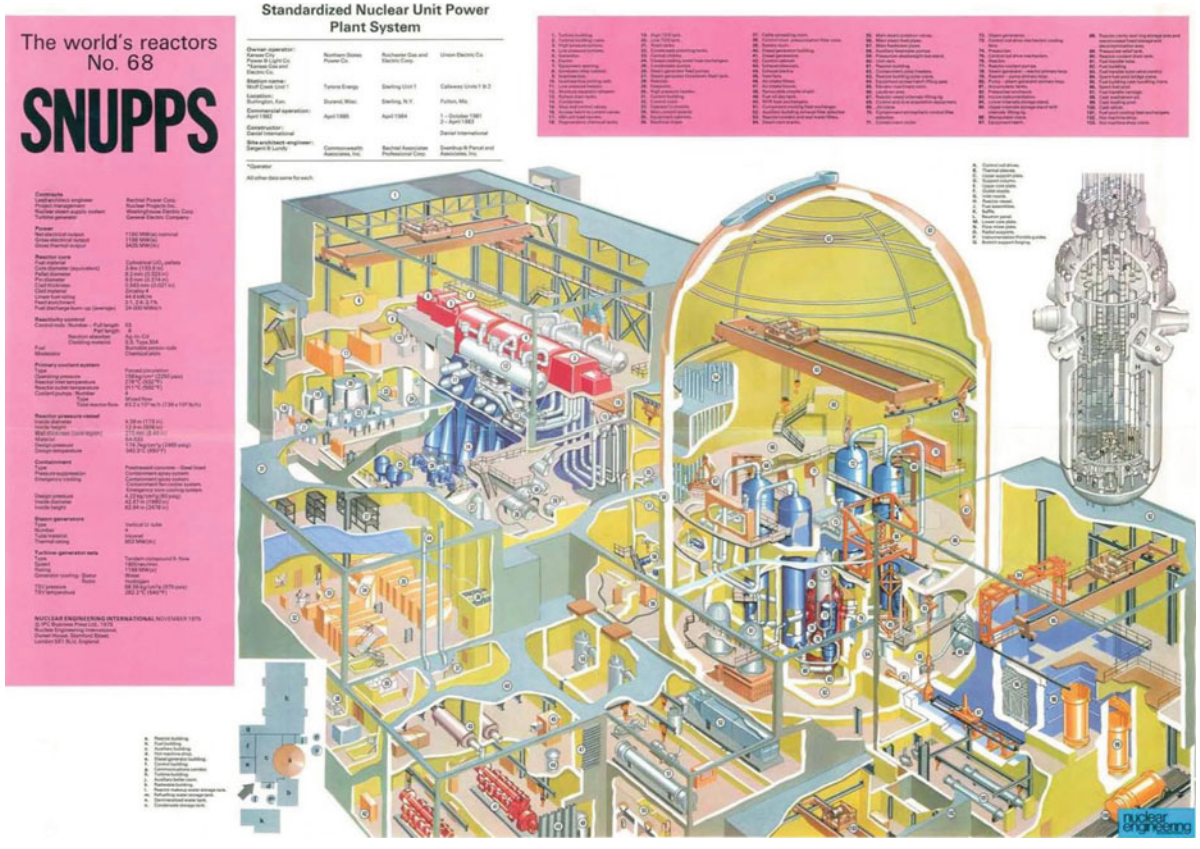

Fig. 4.9 Cutaway of a representative PWR station – Standardized Nuclear Unit Power Plant System (SNUPPS) (Courtesy of Nuclear Engineering International)

Heavy-Water Reactors

Ordinary hydrogen in the form of water is the most effective material for reducing neutron energy, but it also absorbs some of the neutrons that could otherwise participate in the chain reaction. Thus, deuterium as heavy water, which requires more collisions for a given energy change but exhibits much less absorption, is a better moderator in some ways, e.g., allowing use of natural- or other low-enrichment uranium fuel. Deuterium, existing in nature in a ratio of 1:400 with ordinary hydrogen, requires isotopic enrichment prior to use (as does ^{235}U in uranium for many of the reactor applications).

Heavy-water reactors (HWR) have been developed in Canada – their signature CANDU (for Canadian deuterium-uranium) – the UK, West Germany, India, Japan, and South Korea. Pressure-vessel designs (with similar hardware configurations to the PWR) employ the same heavy water volume as coolant and moderator. Pressure-tube designs use heavy water in a separate moderating volume generally with pressurized heavy-water (PHW) coolant, sometimes boiling light-water coolant, and potentially with an organic liquid. The example of a CANDU-PHW is considered further below.

The CANDU-PHW steam cycle has two loops (Fig. 4.10), like the PWR, with the primary pressurized heavy-water loop transferring heat energy to a loop of ordinary water for steam production. A major difference, however, is that the primary fluid is distributed among several hundred pressure tubes which pass through a large calandria vessel (Fig. 4.11) containing the separate heavy-water moderator. The coolant is actually collected in two separate loops, with the fluid in adjacent tubes flowing in opposite directions.

The fuel assemblies consist of natural (i.e., 0.711 wt% ^{235}U) uranium dioxide fuel pellets in zirconium clad, similar to LWR fuel. However, short, cylindrical bundles of fuel pins (Fig. 4.12) allow a unique on-line fueling scheme whereby a machine attaches to each end of a single coolant tube and inserts one fuel assembly while in effect pushing out another.

A major portion of the reactivity control is accomplished by on-line fueling, which is required to compensate for the low reactivity inherent in the natural uranium fuel. Routine operating adjustments and power shaping are accomplished with neutron-poison control rods, or by introduction of ordinary water (which absorbs more neutrons than heavy water) into special chambers. Other control rods are available for reactor scram/trip. The separation of the coolant and moderator volumes also provides the possibility for moderator "dumping" as an emergency shutdown method.

Table 4.1 contains parameters for a large CANDU-PHW and other reactor types. Advanced HWRs are addressed in the section "Advanced Reactors."

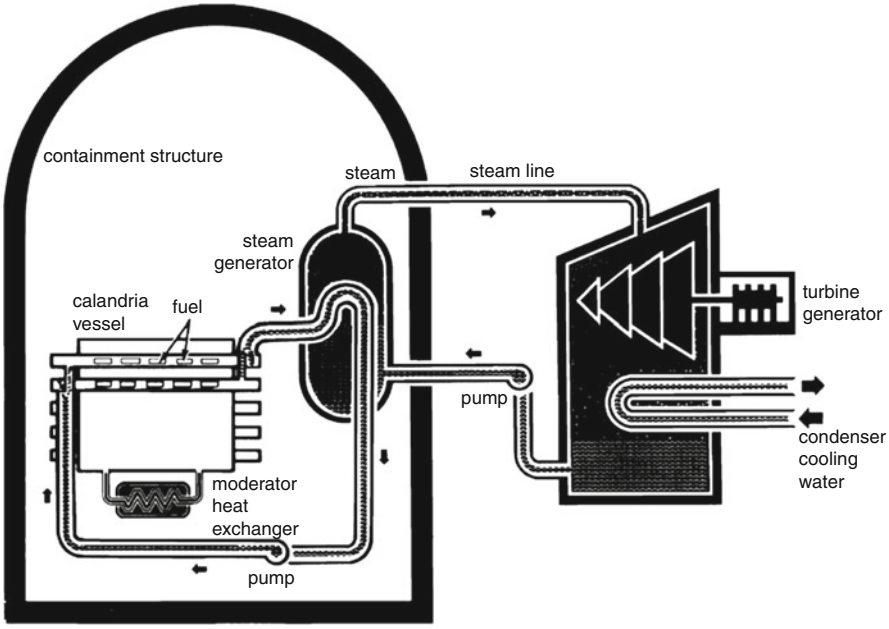

Fig. 4.10 Steam cycle for CANDU pressurized heavy-water reactor (Courtesy of Atomic Industrial Forum/Nuclear Energy Institute)

Gas-Cooled Reactors

The world's first research reactor used natural uranium fuel, graphite moderator, and natural-circulation air cooling. Subsequent systems have also used graphite moderator with natural or enriched uranium and with carbon dioxide or helium coolant. Various commercial gas-cooled reactors (GCR) have operated in France, the UK, the USA, and Germany. Two versions of the helium-cooled high-temperature gas-cooled reactor (HTGR) developed by the USA and Germany are described below. (Both are prototypical designs at ~1,000 MWe described for the purpose of comparison with other current large commercial reactors in this section. Evolutionary units of this heritage are addressed in the section "Advanced Reactors".)

The HTGR steam cycle (Fig. 4.13) employs a primary loop of helium, heat exchangers, and pumps contained within a prestressed concrete reactor vessel (PCRV) – two versions of which are shown in Fig. 4.14 – and a steam loop. Since the coolant is a single-phase gas, no pressurizer is required (in contrast to the two-loop water-cooled designs). The nature of the coolant also provides the prospect for direct conversion through a gas turbine, e.g., employing a Brayton thermodynamic cycle.

Fuel for the HTGR consists of small microspheres of uranium or thorium carbide (UC/ThC) with coatings of graphite and/or silicon carbide (Fig. 4.15a). The uranium microspheres, enriched to 20–93 wt%, may be mixed with separate thorium microspheres to an effective fissile enrichment of about 5 wt%.

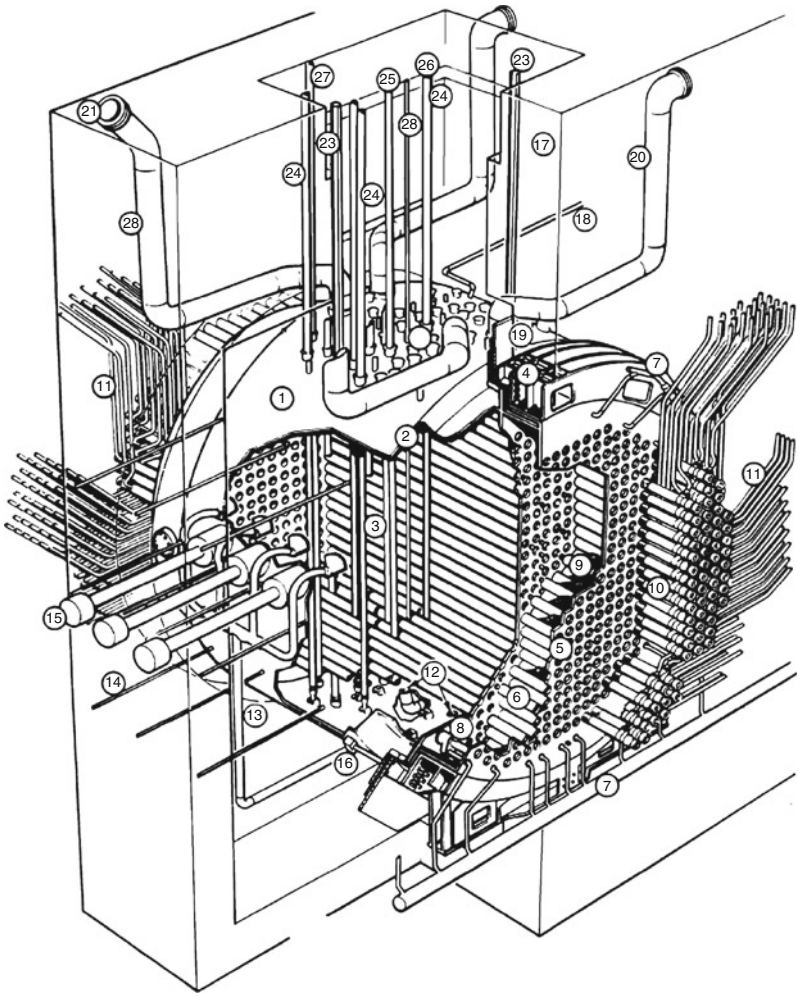

1 CALANDRIA
2 CALANDRIA SHELL
3 CALANDRIA TUBES
4 EMBEDMENT RING
5 FUELLING TUBESHEET
6 END SHIELD LATTICE TUBES
7 END SHIELD COOLING PIPES
8 INLET OUTLET STRAINER
9 STEEL BALL SHIELDING
10 END FITTINGS
11 FEEDER PIPES
12 MODERATOR OUTLET
13 MODERATOR INLET
14 FLUX DETECTOR AND LIQUID INJECTION NOZZLE
15 ION CHAMBER
16 EARTHQUAKE RESTRAINT
17 VAULT WALL
18 MODERATOR EXPANSION TO HEAD TANK
19 CURTAIN SHIELDING SLABS
20 PRESSURE RELIEF PIPES
21 PRESSURE RELIEF DISC
22 REACTIVITY CONTROL ROD NOZZLES
23 VIEWING PORT
24 SHUTOFF ROD
25 ADJUSTER ROD
26 CONTROL ABSORBER ROD
27 ZONE CONTROL ROD
28 VERTICAL FLUX DETECTOR

Fig. 4.11 Calandria vessel and pressure tube of CANDU pressurized heavy-water reactor (Courtesy of Atomic Energy of Canada Limited)

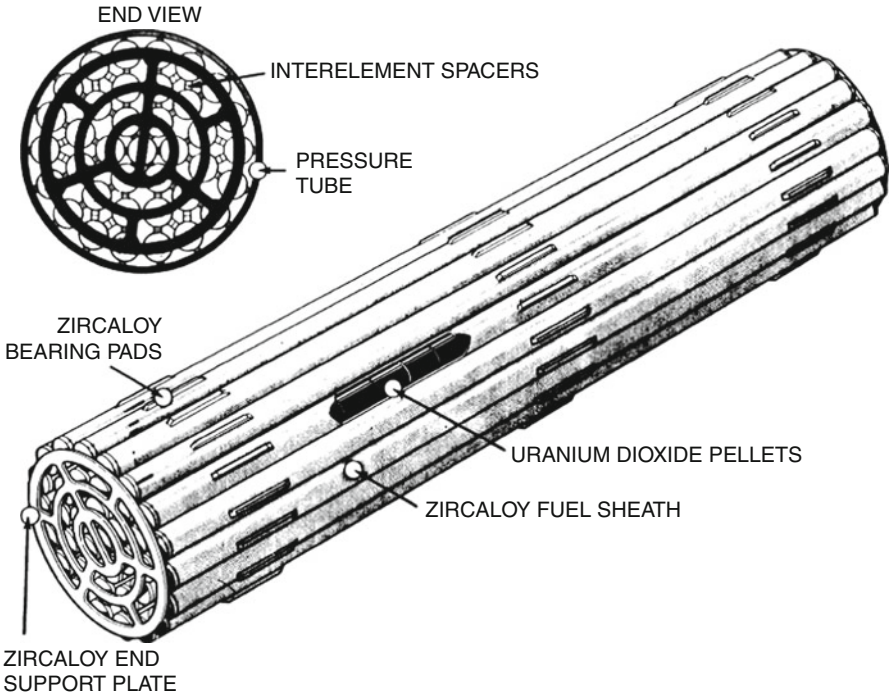

Fig. 4.12 Fuel assembly for CANDU pressurized heavy-water reactor (Courtesy of Atomic Energy of Canada Limited)

In the US "prismatic" – hexagonal-block – HTGR system, the microsphere mixture is formed into roughly finger-sized sticks with a carbon-resin binder. The sticks are then loaded into large hexagonal graphite blocks with interspersed coolant holes (Fig. 4.15b). The blocks are stacked several high and in a roughly cylindrical arrangement to form the reactor core (Fig. 4.14a). Another version of the HTGR – the thorium high-temperature reactor (THTR) – forms the microspheres into a spherical shape and coats them with hard, thick graphite layers into a 6-cm-diameter "pebble" (Fig. 4.15c). The reactor core is then formed by loading these fuel units into a hopper in a PCRV (Fig. 4.14b), from which fueling and defueling can be accomplished on-line. This THTR design feature leads to the alternative designation of the reactor as "pebble bed."

Reactivity control in the prismatic design depends on boron control rods for routine and shutdown functions. Burnable poisons may be used for long-term reactivity control. A reserve shutdown system consisting of small boron-carbide balls backs up the primary systems.

The THTR requires minimal excess reactivity due to its ability to change fuel on-line. Control rods inserted into the pool of pebbles provide the means for routine operational adjustments.

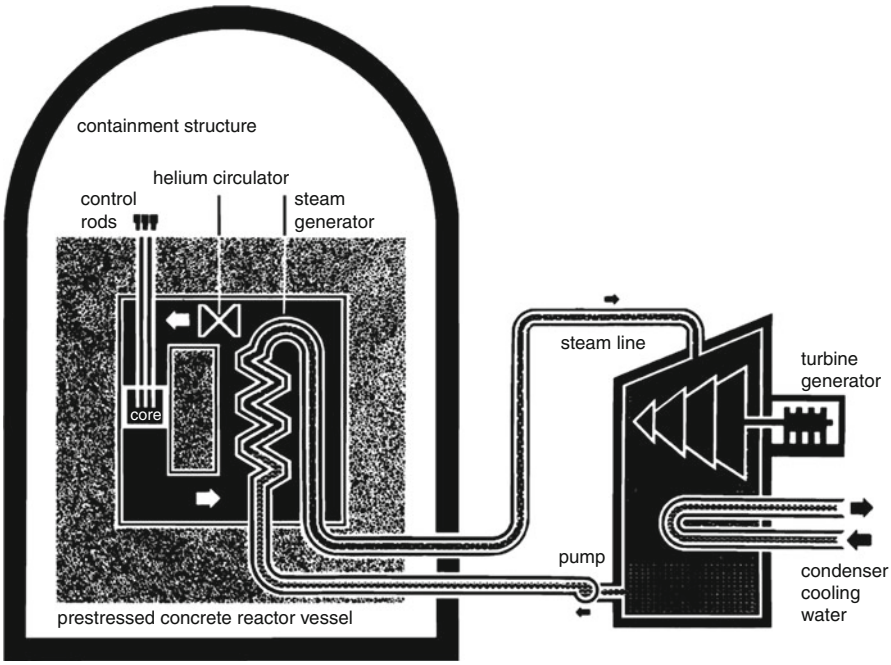

Fig. 4.13 Steam cycle for high-temperature gas-cooled reactor (HTGR) (Courtesy of Atomic Industrial Forum/Nuclear Energy Institute)

Table 4.1 contains parameters for a large prismatic HTGR and other reactor types. Advanced GCRs – prismatic and pebble bed – are addressed in the section "Advanced Reactors."

Light-Water Graphite Reactors

Light-water-cooled graphite-moderated reactors (LWGR)/pressure-tube graphite reactors (PTGR) were among the first systems used for purposes of research, plutonium production, and electric power generation. The Soviet Union credits a small unit of this type with generating the first commercial electricity. Current commercial use is limited to the Soviet RBMK pressure-tube graphite reactors (PTGR). The Chernobyl reactor – the site of the catastrophic 1986 accident – was of this type.

The RBMK uses a direct steam cycle (Fig. 4.16) with boiling-water coolant like the BWR (Fig. 4.1). However, its complex pressure-tube design with separate coolant and moderator also has similarities to the CANDU-HWR (Fig. 4.11).

The RBMK reactor (Fig. 4.17) consists of nearly 1,900 vertical pressure tubes – each accommodating a pair of fuel assemblies or a control rod. The pressure tubes

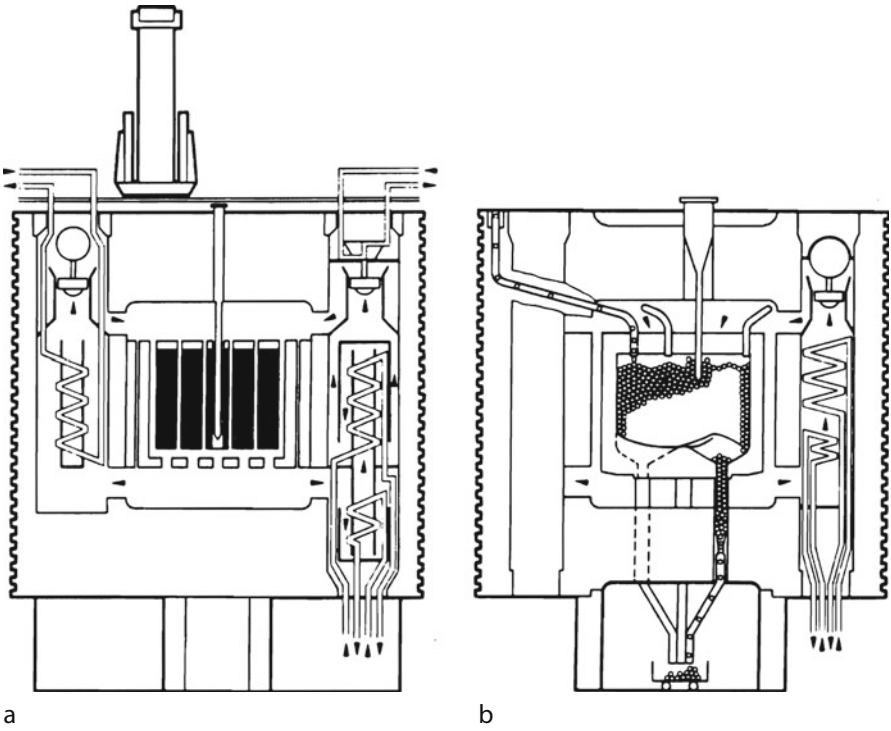

Fig. 4.14 Prestressed concrete reactor vessels (PCRV) for (**a**) prismatic high-temperature gas-cooled reactor and (**b**) thorium high-temperature ("pebble-bed") reactor (Courtesy of Oak Ridge National Laboratory)

are surrounded by an array of long, square graphite blocks – which serve as the system's neutron moderator – set together, side-by-side vertically approximating a cylinder of roughly 12 m diameter and 7 m height. Water introduced at the bottom of the core enters pressure tubes, and then boils in the process of removing fission heat from the fuel pins. Steam is drawn from each tube through a stainless-steel pipe for use in one of two turbine generators.

A steel reactor vessel serves primarily as structural support for the graphite-moderator blocks. This vessel with the pressure tubes and piping constitute the primary-system boundary.

The RBMK fuel assemblies (Fig. 4.18) each contain two stacked subassemblies of 18 zirconium-clad fuel pins of UO_2 enriched to 1.8 wt% in ^{235}U. Stacked one atop the other, a pair fills a pressure tube to facilitate the on-line refueling paradigm that adjusts reactivity and facilitates plutonium production. Various groups of control rods are moved for routine power adjustment and for full-insertion core shutdown.

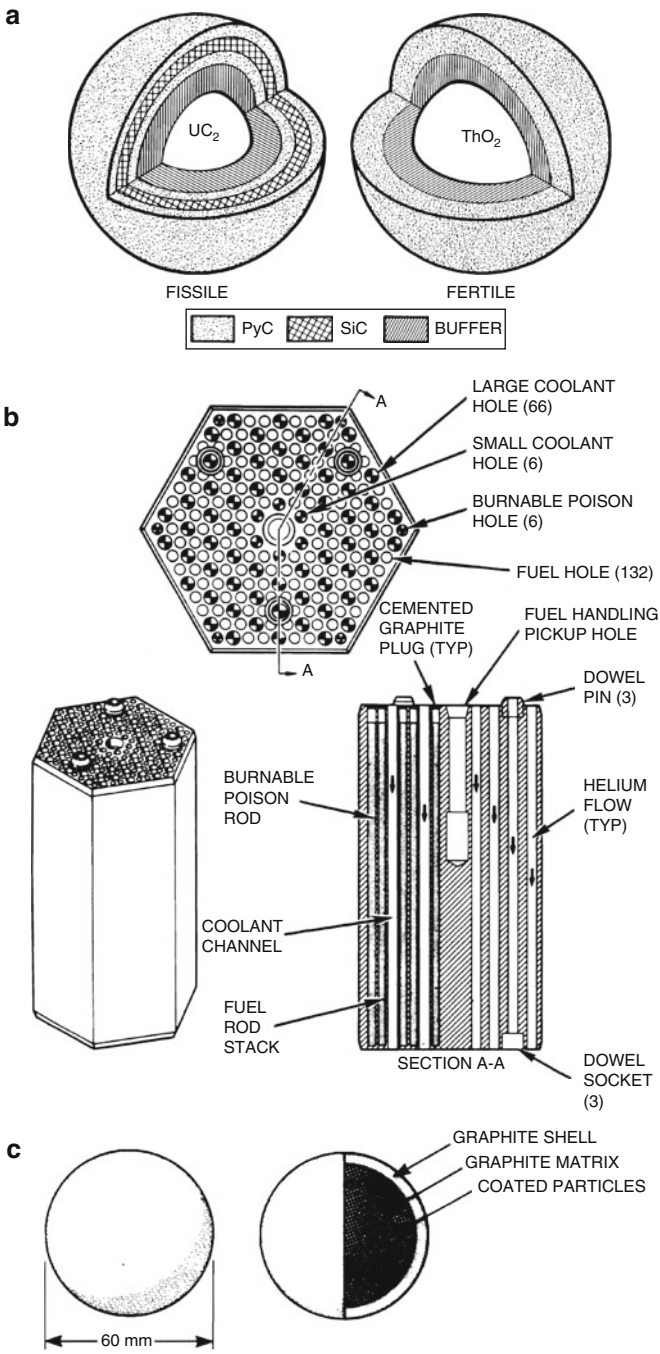

Fig. 4.15 Fuel-assembly components for high-temperature gas-cooled reactors: (**a**) microspheres, (**b**) prismatic fuel block (Courtesy of GA Technologies), and (**c**) fuel sphere ("pebble") [8]

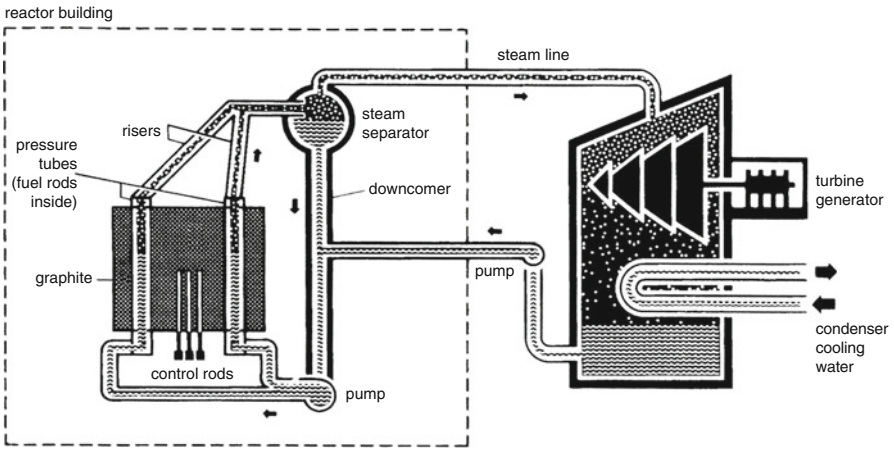

Fig. 4.16 Steam cycle for pressure-tube graphite reactor (PTGR) (Courtesy of Atomic Industrial Forum/Nuclear Energy Institute)

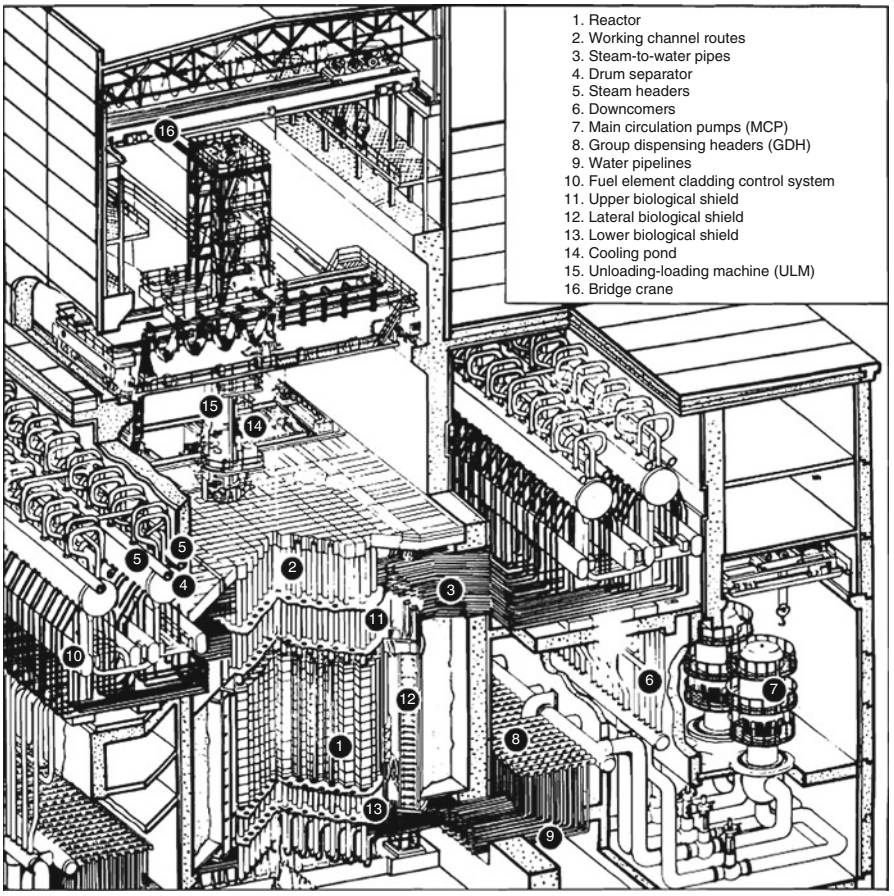

Fig. 4.17 Sectional view of a Soviet pressure-tube graphite reactor (PTGR) (From [23])

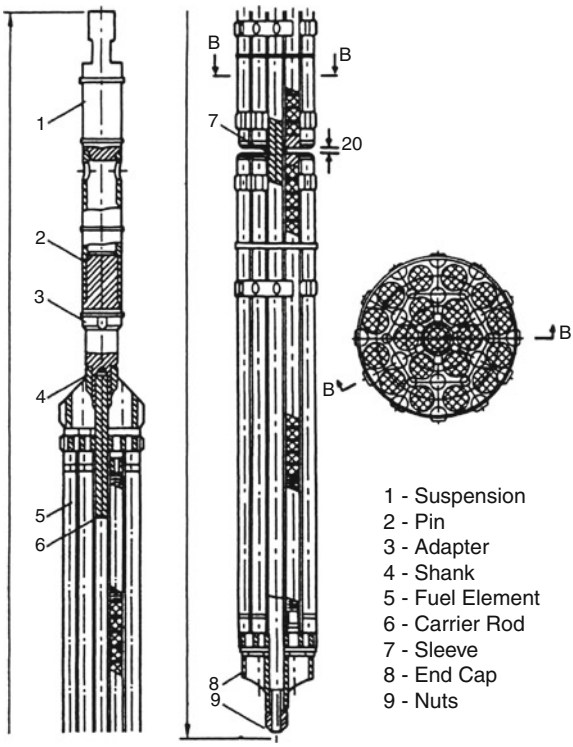

Fig. 4.18 Fuel assembly for a Soviet RBMK pressure-tube graphite reactor (PTGR) (From NUREG-1250 [1987])

Table 4.1 contains parameters for a large PTGR/RBMK unit and other reactor types. Advanced LWGR/PTGRs, if any, will be of totally different design.

Fast Breeder Reactors

The fast-neutron-spectrum breeder reactor (FBR) design concepts are predicated on breeding more new fuel than that used to sustain the neutron chain reaction (section "Reactor Classifications"). For this purpose, fissile plutonium (^{239}Pu and ^{241}Pu) and fertile ^{238}U (natural or depleted uranium with, respectively, 0.711 wt% and 2–3.5 wt% in ^{235}U) fuel with a fast-neutron spectrum are most effective. An FBR optimized for breeding, thus, can utilize uranium at least 60 times more efficiently than a normal LWR reactor. (Note that some fast-spectrum reactors – see the section "Advanced Reactors" – may not have actual breeding as a design specification.)

The liquid-metal fast breeder reactor (LMFBR) keeps neutron energy high (in the upper keV to MeV range) by using (non-moderating) liquid sodium as a coolant.

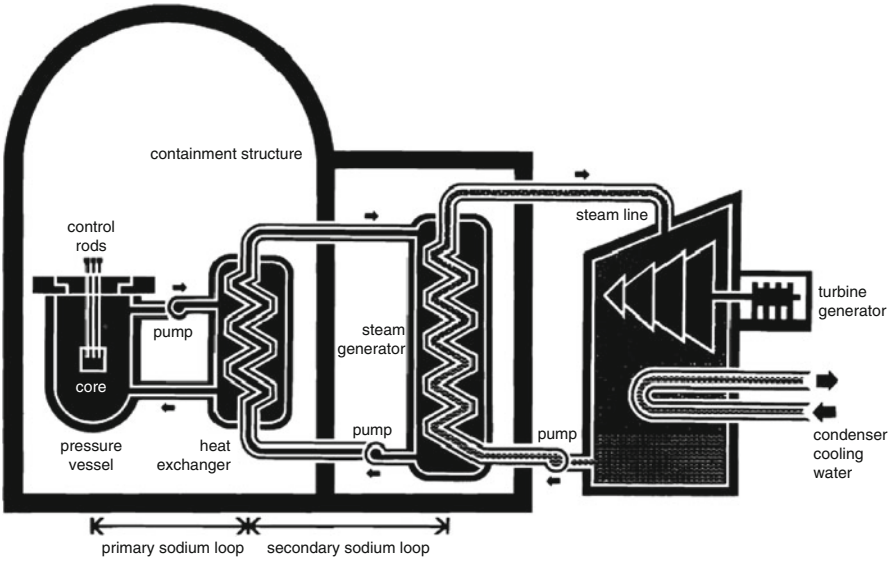

Fig. 4.19 Steam cycle for liquid-metal fast breeder reactor (LMFBR) (Courtesy of Atomic Industrial Forum/Nuclear Energy Institute)

The liquid sodium, although not the heaviest coolant available is not too light, has favorable heat transfer properties, and is not an excessively strong absorber of neutrons compared to other choices.

Although experimental fast breeder reactors have operated in the USA since the late 1950s, and subsequently as prototypes in Western Europe, most recent activity has been in Russia, Japan, and India.

The steam cycle has three loops (Fig. 4.19) with the first two of sodium and the third of water. The intermediate sodium loop is present to isolate the primary from possible direct contact with water in the steam generator. The primary sodium becomes radioactive from neutron absorption and also can pick up fission-product radionuclides from the fuel. If this sodium were to come in contact with water, it would not only precipitate an exothermic reaction but also spread radioactive contamination.

LMFBRs have been implemented in two main configurations – loop-type and pool-type. The former is essentially as shown in Fig. 4.19 and similar paradigm to LWR and HTGR. The pool-type LMFBR has the reactor vessel, heat exchanger, and associated piping – entire primary loop – immersed in a large pool of sodium. The now shutdown SuperPhenix was a pool-type LMFBR of similar capacity to the current large commercial reactors. The SuperPhenix reactor vessel and layout are shown in Fig. 4.20.

Fuel for the LMFBR consists of mixed-oxide (PuO_2-UO_2) fuel pellets, which typically combine about 10–30 wt% fissile plutonium with natural or depleted uranium – the remnants of the enrichment process. As shown in Fig. 4.21a, for

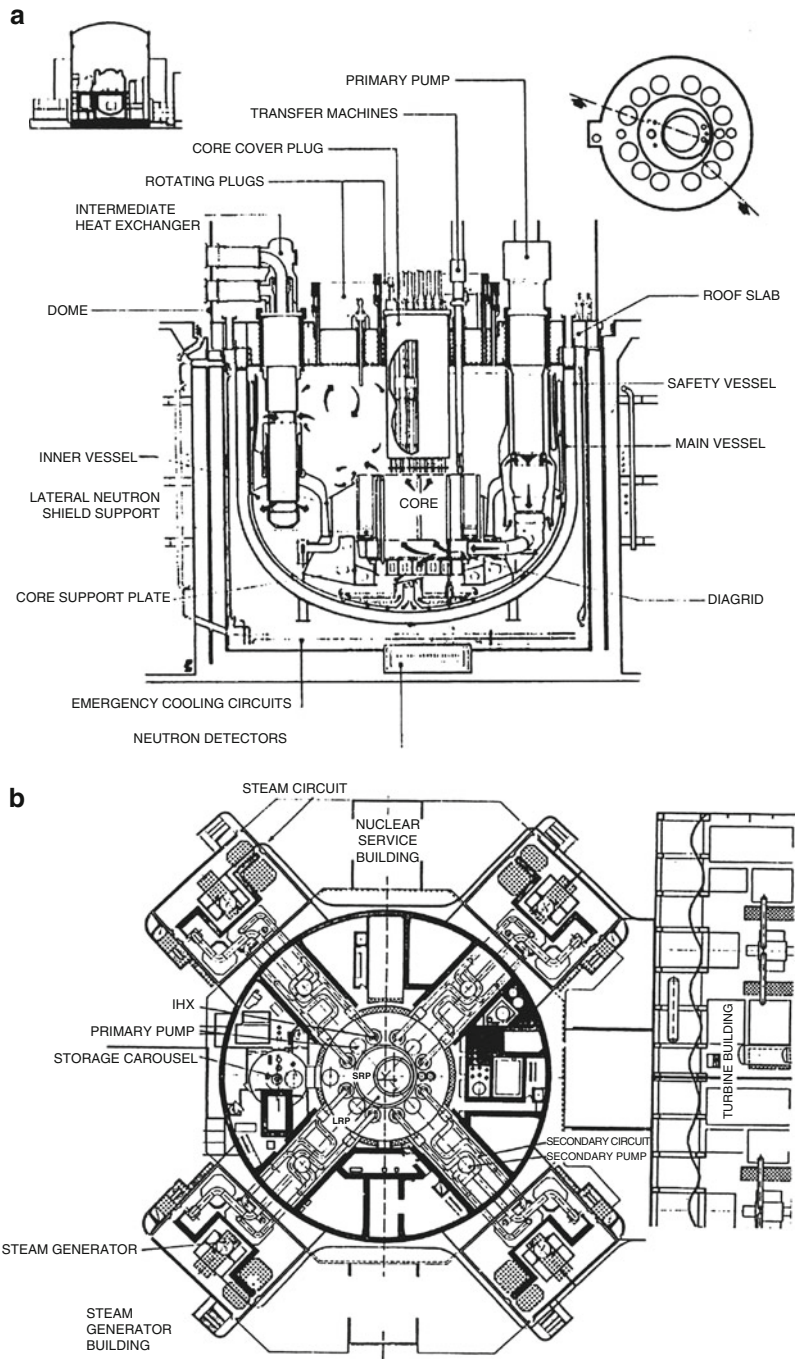

Fig. 4.20 Basic features of the pool-type SuperPhenix (**a**) reactor and (**b**) plan-view layout (Reprinted with permission of NOVATOME, a division of Framatome)

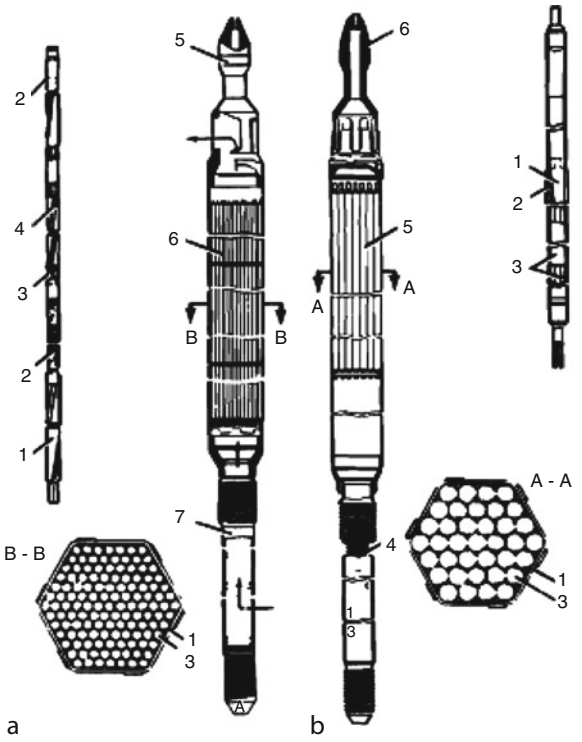

Fig. 4.21 Fuel assembly for a representative liquid-metal fast breeder reactor. (**a**) Fuel assembly: *1*, pin cladding; *2*, slugs of depleted uranium; *3*, fuel pellets; *4*, wire-wrapped pin; *5*, fuel assembly head; *6*, fuel-pin assembly; *7*, stem. (**b**) Radial blanket assembly: *1*, pin cladding; *2*, wire-wrapped fin; *3*, depleted uranium; *4*, blanket assembly stem; *5*, blanket pin assembly; *6*, blanket assembly head (Courtesy of *Nuclear Engineering International*)

a reactor other than SuperPhenix, pellets are loaded into thin stainless-steel cladding tubes, and hence into hexagonal-array subassemblies. Breeding is optimized by surrounding the mixed-oxide core with a *blanket* of depleted uranium. The axial blankets above and below the core are created by loading pellets of natural or depleted uranium at either end of the core fuel pins. The surrounding radial blanket consists of separate subassemblies (Fig. 4.21b) of natural or depleted uranium, where the pins may be of larger diameter because the power density in the blanket is much lower than it is in the core.

LMFBR reactivity control is accomplished through use of neutron-poison control rods. Since the breeder produces more fuel than it uses, however, the core reactivity does not decrease with fissile burnup and fission-product buildup as dramatically as in the in thermal-neutron-energy converter reactors described previously. This is fortunate, because the traditional neutron poisons are not very effective for fast neutrons.

Rapid shutdown may be implemented with either of two independent sets of control rods. It is typical for one set to consist of solid neutron-poison rods, top-mounted and inserted by gravity – the traditional approach for most of the world's reactors. The second system – providing full redundancy should the first fail – often has features allowing for operation even if core distortion has occurred, e.g.,

through use of oversized channels and segmented rods. Table 4.1 contains parameters for a large LMFBR and other reactor types. Advanced fast-neutron reactors are addressed in the section "Advanced Reactors."

Worldwide Perspective

Worldwide nuclear power reactor status is shown in Table 4.2 as a snapshot circa 2009 of the ever-changing landscape. Reactor data are from Ref. [7], which also provides significant information on essentially each nuclear reactor ever built or even ordered.

The table also shows nuclear generation performance – as both TWe-hr generated and percentage of total national electric energy production – for 2009 and, as a comparison, a decade and a year earlier. It is apparent, e.g., that the USA and many other countries experienced a decade of stagnation at the same as the Pacific-basin nations produced impressive growth.

Other Reactor Concepts

In addition to the nuclear power reactor designs described above, a wide variety of other possibilities have been built for power production or research purposes. Still others have been researched "on paper." The major approach is to look at viable combinations of fuel, coolant, and moderator. A few examples are identified here and in the section "Advanced Reactors."

CANDU reactors could also be operated with fuel assemblies of enriched uranium, plutonium, ^{233}U/thorium, or a mixture thereof. Potential coolants other than heavy water include light water and organic liquid.

The gas-cooled fast breeder reactor (GCFBR) uses helium coolant and plutonium fuel in a concept similar to the HTGR, except with no graphite moderator. The molten-salt breeder reactor (MSBR) concept includes liquid fuel that circulates through a graphite-block core region in a closed primary loop. The fuel is processed on-line to remove fission products and ^{233}U bred from thorium in the salt.

Many other novel designs that stress enhanced safety and/or compact size also have been proposed. A wide variety of such concepts are identified in the section "Advanced Reactors."

Table 4.2 Worldwide nuclear generating capacity by reactor type[a] and summary of reactor performance

	Reactors operable		Reactors under construction		Reactors under contract and [planned][b,c]		1998 reactor performance[d]		2009 reactor performance[e]	
Country[c]	No.	MWe	No.	MWe	No.	MWe	TWe-hr	% of Electric	TWe-hr	% of Electric
Argentina							6.9	10.0	7.6	7.0
PHWR	2	1,005	1	745						
Armenia							1.42	24.7	2.3	45
VVER	1	408			1	1,060				
Belgium							43.9	55.2	45	51.7
PWR	7	6,192								
Brazil							3.3	1.1	12.2	3.0
PWR	2	2,007	1	1,309						
Bulgaria							15.5	41.5	14.2	35.9
VVER	2	2,000								
Canada							67.5	12.4	85.3	14.8
PHWR	17	12,969			[5]	4,800				
China							13.5	1.2	65.7	1.9
PWR	7	5,558	21	23,000	5/[42]					
VVER	2	2,000			[4]					
PHWR	2	1,500								
HTGR	1	2	1	195						
FBR					[3]					
	12		22	23,195	5/[49]					
Cuba										
PWR			2	880 suspend						
Czech Republic							28.5	20.5	25.7	33.8
VVER	6	3,892			[2]					
Finland							21.0	27.4	22.6	32.9
VVER	2	1,020								

BWR	2	1,780								
EPR PWR			1	1,600						
Unspecified					[3]					
TOTAL	4	2,800	1	1,600	[3]					
France							368.4	75.8	391.7	75.2
PWR	58	63,134	1	1,650	[1]	[1 650]				
Germany							145.2	28.3	127.7	26.1
PWR	11	14,783								
BWR	4	4,526								
	12	19,309								
Hungary					[2]		13.1	35.6	14.3	43
VVER	4	2,000								
PWR										
India							10.2	2.5	14.8	2.2
PWR					[4]					
EPR PWR					[6]					
BWR	2	320			[8]					
PHWR	16	4,140			[4]					
VVER			2	2,000	[4]					
FBR					[1]					
	18	4,460			[27]					
Iran										
VVER			1	1,000						
Japan							306.9	35.9	263.1	28.9
PWR	24	20,278			2	3,076				
BWR	25	23,221	1	1,373	[1][3]					
FBR					[1]	660				
ABWR					2	2,746				
					[6][1]					

(continued)

Table 4.2 (continued)

	Reactors operable		Reactors under construction		Reactors under contract and [planned][b,c]		1998 reactor performance[d]		2009 reactor performance[e]	
Country[c]	No.	MWe	No.	MWe	No.	MWe	TWe-hr	% of Electric	TWe-hr	% of Electric
APWR					2	1,590				
	49	43,499	1	1,373	6 [12]					
Kazakhstan							0.1	0.2		
VVER					[3]	1,920				
(Korea, North)										
PWR					[2] cancel	1,000				
Korea, South							85.2	41.4	141.1	34.8
PWR	16	15,643	6	6,800	[2]	2,800				
PHWR	3	2,189								
	19	17,832								
Lithuania							12.3	77.2	10	76.2
RBMK	2 s/d	2,600								
Unspecified					[1]					
Mexico							8.8	5.4	10.1	4.8
BWR	2	1,364								
Netherlands							3.6	4.1	4.0	3.7
PWR	1	515								
Unspecified					[1]			1,000–1,600		
Pakistan							0.3	0.7	2.6	2.7
PHWR	1	137								
PWR	1	325	1	325						
Unspecified					[1]	600				
	2	462								
Romania							4.9	10.4	10.8	20.6
PHWR	2	1,411			[2]	1,412				

Russian Federation							95.4	13.1	152.8	17.8
VVER	16	12,594	4	4,600	4 [6][19]	4,600				
RBMK	11	11,000	1	1,000						
LWGR (EGP)	4	48			[3]					
KLT (Floating)			2	70						
FBR	1	600	1	880						
BWR (heat)					[4]					
VBER (PWR)					[6]					
	32	14,242	8	6,550	4 [38]	4,600				
Slovakia							11.4	43.8	13.1	53.5
VVER	4	1,896	2	880						
Slovenia							4.8	38.3	5.5	37.9
PWR	1	730								
South Africa							13.6	7.25	11.6	4.8
PWR	2	1,880			[1]	110				
HTGR										
Spain							56.7	31.7	50.6	17.5
PWR	6	5,912								
BWR	2	6,177								
	8	12,089								
Sweden							70.0	45.8	50.0	34.7
PWR	3	3,002								
BWR	7	6,559								
		9,561								
Switzerland							24.4	41.1	26.3	39.5
PWR	3	1,795								
BWR	2	1,610								
		3,405								
Taiwan									(39.3)	(17.1)
PWR	2	1,914								

(continued)

Table 4.2 (continued)

	Reactors operable		Reactors under construction		Reactors under contract and [planned][b,c]		1998 reactor performance[d]		2009 reactor performance[e]	
Country[c]	No.	MWe	No.	MWe	No.	MWe	TWe-hr	% of Electric	TWe-hr	% of Electric
BWR	4	3,276	2	2,700						
	6	5,190								
Turkey										
VVER					[2]					
Ukraine							70.6	45.4	77.9	48.6
VVER	15	13,835	2	2,000						
United Arab Emirates										
PWR					2	2,000				
UK							91.1	27.1	62.9	17.9
PWR	1	1,250								
Magnox GCR	4	1,540								
AGR GCR	14	9,112								
EPR PWR					[4]	6,600				
Unspecified					[4]					
	19	11,902			[8]					
USA							673.7	18.7	798.7	20.2
PWR	69	70,388	1	1,218						
BWR	35	35,903								
AP1000					2 [12]	2,500				
ESBWR					[2]					
ABWR					[2]					
US-EPR PWR					[6]					
US-APWR					[2]					
Unspecified					[6]					
	104	106,291			2 [30]	2,500				

TOTAL[f]					
PWR	214	215,306	31	34,302	9 + [53]
EPR PWR					[10]
US-EPR PWR					[6]
APWR					[2]
US-APWR					[2]
AP1000					[12]
VVER	52	39,645	11	10,480	7 + [40]
VBER					[6]
BWR	84	84,736	3	4,073	[12]
ABWR					2 + [9]
ESBWR					[2]
BWR (Heat)					[4]
PHWR	43	23,351	1	745	[11]
HTGR	1	2	1	195	[1]
Magnox	4	1,540			
AGR	14	9,112			
RBMK	11	11,000	1	1,000	
LWGR (EGP)	4	48			[3]
FBR	1	600	1	800	[5]
KLT-Float			2	70	
Unspecified					[17]
TOTAL	**414**	**385,340**	**51**	**51,665**	**18 + [139]**

[a]Reactor data current through 2009. Source: *2010 World Nuclear Industry Handbook*, from the publishers of Nuclear Engineering International magazine, www.neimagazine.com. (Note: Reference also contains details on essentially every reactor built or planned)

[b]The source document includes several categories of planned reactors, essentially ranging from very firm to highly speculative. As used in this table, the author's designation "[Planned]" excludes the more speculative categories

[c]World Nuclear Association reported reactors also "planned" and/or "proposed" by Bangladesh, Belarus, Egypt, Indonesia, Israel, Italy, Jordan, Malaysia, Poland, and Thailand – http://www.world-nuclear.org/info/reactors.html – August 1, 2010 (updated periodically)

[d]From *Nuclear Engineering International World Nuclear Industry Handbook 1999*, November 1998

[e]From World Nuclear Association – http://www.world-nuclear.org/info/reactors.html – August 1, 2010 (updated periodically)

[f]Not all countries reporting status distinguished between traditional reactors (e.g., PWR or BWR) and advanced versions (e.g., APWR or ESBWR) thereof

Operation, Maintenance, and Control Practices

Specific characteristics of the fission process and the design of reactors and their fuel result in unique features which affect operations, maintenance, and plant control. With over 50 years of experience for nuclear reactors in general and 30 or more years of experience with the more mature system technologies, an increasingly solid basis for good operating practices is becoming available [13]. Uniformly excellent nuclear plant availability is a key indication of this.

Operation

Routine power operations reflect characteristics of the reactor design – fuel, moderator, coolant, geometry. The BWR, with water boiling in the core, and PWR, with pressurized liquid water in the core – the two plant types dominating the world circa 2010 – show quite different operational characteristics.

Boiling-Water Reactor

Startup of a boiling-water reactor begins with running the coolant pumps at minimum speed. The control rods are withdrawn from their initial fully inserted position one at a time in a preset sequence that keeps the power distribution reasonably uniform. The reactor is brought to critical, and then made slightly supercritical to heat the coolant slowly to the boiling point where steam formation begins to pressurize the vessel. Initially, the steam is dumped to the main condenser (Figs. 4.1 and 4.3). When operating temperature and pressure are reached and the steam flow is about 20% of full capacity, the turbine is started and the generator synchronized to the electric power grid. Power level is increased by control-rod withdrawal, flow increase, or a combination (e.g., with flow set for 20% power, rod withdrawal takes the power to 50% and then the pumps are used to achieve full power).

Once at power, an automatic control system is used to change coolant flow for the reactor to *load follow* the turbine steam demand. The control rods are still under operator control. For continued steady power operation, control-rod withdrawal or coolant flow changes can be made manually within predetermined power-to-flow limits. Control rods are withdrawn systematically to match fuel-assembly burnup.

Tripping – initiating a scram – of the control rods to shutdown a reactor causes thermal-mechanical stress. Thus, the preferred method for shutdown is essentially the reverse of the startup process. When the power drops too low for production of electricity, the steam is again dumped to the condenser. This is continued until the fission-product-decay heat load is small enough to be handled by a specifically designed residual-decay-heat-removal system.

BWR refueling is similar to that for the PWR – as described in the next subsection. One important difference is that the control rods do not need to be removed with the vessel head (because they are bottom mounted).

Pressurized-Water Reactor

Startup of a pressurized-water reactor begins with alignment of support systems and pressurization of the primary reactor coolant system (Figs. 4.6 and 4.7). All shutdown (or "safety") rods are "cocked" (i.e., withdrawn fully) to be available for reactor trip if necessary. Designated regulating rods remain fully inserted. The main reactor coolant pumps are started with their inherent heat generation producing a slow heat-up of the reactor coolant system that minimizes mechanical stress. As operating temperatures are approached, a "bubble" (i.e., steam volume) is drawn in the pressurizer, volume control is established, steam may be drawn to warm the steam generators, and final adjustments are made to the reactor coolant system chemistry and the soluble boron concentration. Steady withdrawal of the regulating control rods first takes the core critical and then supercritical to increase the power level at a predetermined rate. The turbine is started and the generator is synchronized to the grid. Manual control of the reactor, turbine, and steam-generator feedwater is maintained until about 15% power when transfer is made to an automatic mode for escalation to full power. In general, the turbine is matched to the reactor's (or actually steam generator's) steaming rate, a *reactor following* mode of operation. (Note: In practice for a PWR the reactor leads turbine, while for a BWR the reactor follows the turbine.)

During routine full-power operation, small movements of the first regulating group balance normal power fluctuations. Larger insertions change the power level.

Boric acid concentration is adjusted to match fuel burnup and allow control-rod positions to remain consistent with the power-dependent insertion limits. This concentration may be as high as 2,000 ppm (parts-per-million) in a fresh core and be reduced to 100 ppm or less by the end of the core's lifetime.

Planned shutdown involves insertion of the rods (with additional boration if cold shutdown, e.g., for defueling, is desired). Decay heat is removed initially by one-pump or natural-circulation operation of the steam generators with the steam dumped to the condenser. When the bulk coolant temperature falls sufficiently, cooling is shifted to a dedicated residual-decay-heat-removal system and the pressurizer bubble is collapsed.

Within a day or two of reactor shutdown, the decay-heat load decreases sufficiently for reactor coolant system depressurization and refueling. The reactor cavity is flooded with highly borated water to a height of 10 m or more so that the vessel head (with all control rods attached) and the fuel assemblies can be removed while still having enough water above them to provide radiation shielding for operating personnel. Individual spent-fuel assemblies are extracted remotely from the core and moved to a spent-fuel storage rack, usually in a separate building. Fuel not

discharged is "shuffled" to new locations. Fresh assemblies are brought in from a fuel handling building.

Refueling itself for an LWR requires only about 4 days. However, "refueling outages" often last up to a month or more when including cool-down and advance preparations, maintenance (corrective and preventive), minor plant modifications, vessel reassembly, and preoperational testing.

Operation Features

Four key goals of operations for nuclear power plants – the first two unique and the other two common to all power plants – relate to: (1) nuclear safety, (2) communications, (3) technical results, and (4) operating and fuel costs. Nuclear safety, i.e., prevention of accidents, underlies both technical and economic performance. Good, reliable communications with the public, staff, and company are necessary to counterbalance unfounded fears that may be associated with nuclear energy.

Technical results are judged according to performance indicators, an important one being availability. As for any power plant, availability is enhanced by reducing the length of planned shutdowns and the frequency of unplanned shutdowns. Because reactor fuel assemblies are added and replaced as units, adjustment of cycle length (typically between 1 and 2 years) can affect both availability and reasonable operating and fuel costs.

Where possible, nuclear units run base-loaded due to both high plant capital costs and difficulties in making rapid power-level changes (based on the behavior of certain fission products that poison the chain reaction). France, however, with its large fraction of nuclear electricity (e.g., see Table 4.2) has developed technical ability to facilitate daily load following variations. The latter is also a valued attribute in a number of advanced reactors (e.g., units considered in the section "Advanced Reactors.")

The hazard of nuclear power associated with the large fission-product inventory and the potential severe accident consequences leads to special attention to operator training and to emergency response capabilities. Operators are provided with extensive technical training including substantial use of high-fidelity, plant-referenced control-room simulators which allow practice on routine, anticipated upset, and emergency operating scenarios. Emergency preparedness includes developing procedures, establishing communications, preparing equipment and facilities, and designating an emergency response team personnel.

Maintenance

Due to the presence of fission products and other indirect sources of radioactivity from the neutron chain reaction, many important maintenance and other activities

must be conducted in a manner that minimizes the hazards associated with radiation. This has led to the development of remote and other sophisticated radiological control methods. In performing hands-on work, it is challenging to hold radiation exposures of personnel within specified limits on quarterly, annual, and lifetime doses. Overall, however, the requirement that all exposures be kept "as low as reasonably achievable" (ALARA) has resulted in extensive preplanning of all radiological work activities.

Gaseous and liquid wastes are held for as long as practicable to allow maximum radioactive decay. Then, they may be diluted and dispersed to the environment so long as applicable limits for liquid and airborne discharges are not exceeded. Otherwise, solidification, containment, and disposal are required.

Nuclear reactors, like all power plants, require corrective and preventive maintenance that balance the conflicting goals of maximizing short-term profits by deferring work and reducing intervals between regular maintenance activities to assure top performance. The amount of corrective maintenance depends primarily on the initial quality of components and systems, control of operating conditions, and the effectiveness of the preventive maintenance program.

Preventive maintenance for the reactor coolant system (including reactor vessel, reactor coolant pumps, control rod drive mechanisms, instrumentation, and in applicable systems pressurizer and steam generators) must account for neutron irradiation effects on components and systems. The nuclear industry is using methods of reliability-centered maintenance increasingly as sufficient operating experience and data are collected to provide useful statistical reference. In France, where a single utility operates a sizeable number of each of several standardized units, maintenance is considered a lifetime project with integrated goals to guarantee safety, ensure efficiency, assess impact of changes in operating conditions, minimize maintenance cost increases, and establish an optimum decommissioning policy (i.e., definition of the end of a reactor's safe and economic lifetime).

Plant Control Systems

Plant instrumentation and control systems are divided among those for normal operation, regulation of parameters through analog or digital technologies, and protection of personnel and equipment by reactor trip and safety feature actuation. Examples of control requirements in the first category may be inferred from discussions earlier in this subsection of operation of boiling- and pressurized-water systems. Specific safety features are described in the next subsection.

Reactors in the USA have tended to continue use of older analog systems for routine reactor control, lacking incentive – and, in some sense, having a *disincentive* associated with time and costs associated with being among the first to develop, test, and license a process – to upgrade to state-of-the-art digital systems. However,

significant government-sponsored research and development support in the first decade of the twenty-first century offers the prospect of near-term progress.

Data acquisition and display technology, by contrast, has been upgraded substantially, especially in the aftermath of the accident at the Three Mile Island, Unit 2 reactor. Should the control room become uninhabitable, a remote shutdown panel will allow operators to implement the emergency response functions necessary for safe shutdown of the plant.

France, with its large, dynamic development program, has upgraded controls in early units and developed new systems. Their current and near-future reactor generations have particularly sophisticated reactor operating consoles with state-of-the-art digital systems for control, data acquisition, operator support, and emergency response. Control systems facilitate process monitoring, exchange of information, and self-monitoring and self-diagnosis. Automatic protection systems are designed for reliability with redundancy and diversity (e.g., one of which includes four redundant data acquisition and processing units coupled with two independent safeguard logic units for automatic actuation of the engineered safety features) and include testing and simulation capabilities. Data processing systems are designed to give operators full information on the present state of the reactor, monitor data, store event scenarios and other data changes in memory, and perform calculations. Advanced reactor controls may facilitate functions such as automatic turbine load shedding, steam level control, (nonreactor, non-safety-related) and trip avoidance – and the consequent thermal-mechanical disruption, and postaccident monitoring and control.

Nuclear Reactor Safety Features

An operating nuclear power reactor accumulates an enormous inventory of radioactive products. Each reactor system has been designed with a multiple-barrier approach to retention of this radioactivity [8]. The first three of these barriers – fuel pellet, metal cladding, and reactor-primary-system – were described in the section "Reactor Systems." The fourth barrier is a containment building supported by safety systems.

A "defense-in-depth" design approach to maintaining the effectiveness of barriers seeks first of all to prevent accidents. But absent this, protective actions – identification and correction – and mitigative actions – long-term response to and control of consequences are provided. Safety analyses address the variety of reactor-related energy sources and their roles in operational abnormalities and in design-basis and more severe accidents. The results of the analyses also define requirements for the engineered safety systems.

Energy Sources

Five distinct energy sources may contribute to an accident in a nuclear power reactor:

1. Stored energy – fuel, coolant, and structures store thermal energy at all times during reactor power operation; redistribution may result in immediate damage and/or prolonged problems.
2. Nuclear transients – positive insertion of reactivity, from configuration or material changes, may add a transient energy source resulting in from an increased power level to a large power pulse.
3. Decay heat – heat from fission-product decay, as high as 7.5% of operating power at the time of shutdown from a lengthy run, dies out slowly, and can be a large energy contribution after dissipation of stored energy and shutdown of the neutron chain reaction; with inadequate heat removal, it may be sufficient to cause fuel melting or other damage.
4. Chemical reactions – fuel, cladding, and coolant materials selected to be essentially unreactive with each other under normal operating conditions at elevated temperatures that may be produced by nuclear transients and/or decay heat may experience energetic chemical reactions.
5. External events – natural (floods, hurricanes, tornadoes, and earthquakes) and man-made (aircraft impacts and industrial explosions) events external to the reactor system have the potential to initiate or otherwise contribute to accidents.

The magnitude and timing of contributions from each category are important to accident progression. Understanding each is necessary to accident prevention and mitigation.

Nearly 98% of all radioactive products are retained by the fuel assemblies when sufficient cooling is provided to prevent fuel melting. Thus, major objectives of nuclear reactor operation and safety are to provide adequate heat removal and control of the energy released in the system to prevent overheating and, in the most severe case, melting of the fuel.

Design-Basis Accidents

Design-basis accidents involve the postulated failure of one or more important systems and an analysis based on conservative assumptions (e.g., pessimistic estimates of fission-product release). The radiological consequences must be shown to be within preestablished limits. In this sense, the accidents serve as the *basis* for assessing the overall acceptability of a particular reactor *design*. Design-basis accidents for light-water reactors (and, by extension, other reactor types) are often classified according to the following general characteristics:

1. Overcooling – excessive heat removal from steam withdrawal, perhaps through a steam-line break or steam-generator overfeeding (PWR and other multi-loop systems).
2. Undercooling – inadequate heat removal occurring when steam flow is decreased, e.g., following a turbine trip or reduction in feedwater flow; a complete *loss of heat-sink accident* (LOHA) – up to and including total loss of heat-removal capability – is the most extreme case of undercooling.
3. Overfilling – increase in reactor coolant inventory, e.g., from malfunction of the volume control system or inadvertent emergency core cooling system (ECCS) – see the section "Safety Systems" – actuation during power operation.
4. Loss of flow (accident (LOFA)) – decrease in reactor coolant system (RCS) flow rate, e.g., follow failure of main reactor coolant pump(s).
5. Loss of coolant (accident (LOCA)) – decrease in reactor coolant inventory resulting from breaches in the reactor coolant pressure boundary; the "classic" LOCA involves rupture of major primary piping, but *steam-generator tube rupture* and inadvertent opening of a relief or safety valve – the proximate cause of the reactor accident at Three Mile Island – are also included.
6. Reactivity-core reactivity and power distribution anomalies – unplanned control-rod withdrawal, other maloperation, and ejection (in a PWR) or drop (in a BWR) of one or more control-rod assemblies; also increased BWR coolant flow rate, and decreased PWR boron concentration, or misleading of a fuel assembly.
7. Anticipated transient without scram (ATWS) – failure to trip (or shutdown) the reactor following a transient such as inadvertent control-rod withdrawal, turbine trip, or loss of feedwater.
8. Spent-fuel and waste system-radioactivity release from a spent-fuel assembly or reactor subsystem or component – events outside of the reactor-primary system.
9. External events-natural or human-caused events that can effect plant operating and safety systems – sequence initiated by an "external event" as identified in the section "Energy Sources."

More severe accidents, sometimes referred to as beyond-design-basis accidents, where multiple safety systems fail to function (or, as in the Chernobyl accident, are disabled), are sometimes considered to evaluate overall responses.

Safety Systems

Safety systems for accident mitigation are highly design-dependent (e.g., based on design and operational differences among fuel form: coolant – water, gas, liquid metal; neutron energy; and other features. The common goals, however, are to prevent overheating, fuel melting and other damage, and subsequent large-scale dispersal of fission products. Reliability is enhanced through redundancy in subsystem function and location.

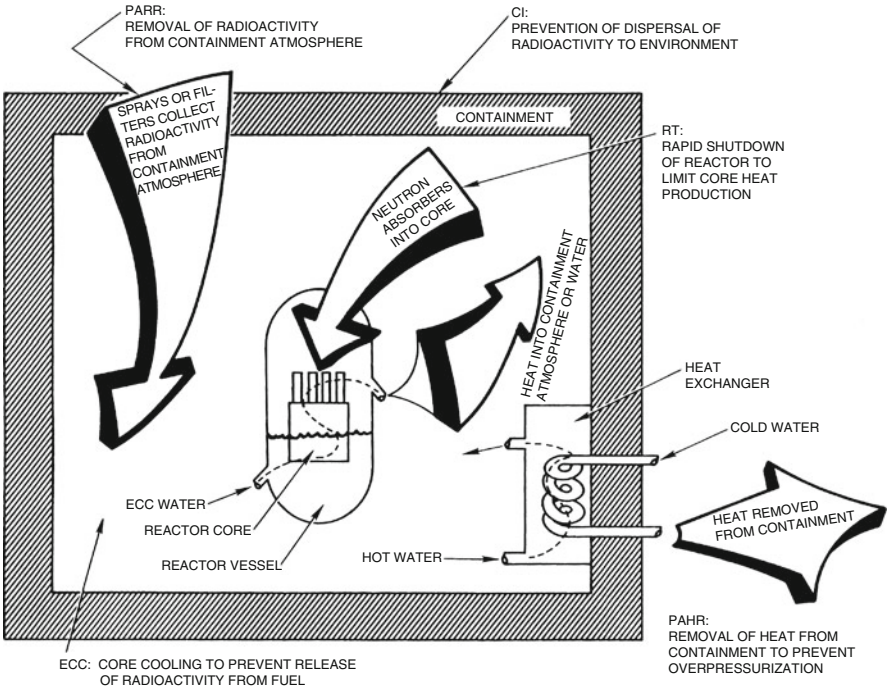

Fig. 4.22 Functions of safety systems for light-water reactors (Adapted from WASH-1400 [14], courtesy of US Nuclear Regulatory Commission)

Reactor safety systems – for the dominant loss-of-coolant accident, but with more general applicability as well – may be classified according to function as:

1. Reactor trip (RT)
2. Emergency core cooling (ECC)
3. Postaccident heat removal (PAHR)
4. Postaccident radioactivity removal (PARR)
5. Containment integrity (CI)

Their basic functions are summarized by Fig. 4.22 for light-water reactors. The same basic functions apply to all reactor systems, even if in somewhat different form.

Reactor trip for each of the reactor types described in the section "Reactor Systems" includes neutron poison control rods, which can be inserted rapidly into the fuel core to shut down the fission chain reaction. These rods are supplemented by alternative shutdown means including injection of soluble boric acid poison (LWRs); moderator dump (CANDU-PHWR); reserve shutdown spheres (HTGR); and a redundant, independent set of rods (LMFBR).

Emergency core cooling for the light-water, and most other water-cooled, reactors is implemented by injection of borated water – the same medium that provides for emergency reactor trip – into the coolant-starved core region following a LOCA event.

Multiple trains of separate systems typically can inject water at high, intermediate, or low pressure to coincide with various needs during the time-history and/or magnitude of the event. The recirculation of coolant that collects in the reactor building sump provides a long-term coolant supply after the initial inventories have been exhausted.

The CANDU-PHWR system also has a unique safety-related design feature with two separate flow circuits configured so that adjacent pressure tubes (Fig. 4.11) receive coolant from a different source. Thus, a break in a specific pressure tube can affect no more than half of the fuel and no large core volumes are left uncooled. Additionally, the separate moderator volume provided by the calandria vessel provides a huge heat sink for energy removal.

Emergency cooling for the HTGR design is predicated largely on the very high heat capacity of the graphite fuel, supported by auxiliary helium circulation and containment afforded by a steel-lined prestressed concrete reactor vessel (PCRV). The LMFBR, by contrast with the water-cooled reactors, has low-pressure, high-boiling liquid-sodium coolant which would not be voided even during a serious primary-system breach. Thus, long-term, natural-circulation cooling capability is uniquely available. Postaccident heat removal has two components – coolant temperature reduction and containment-building pressure control. The first is accomplished through heat exchangers for ECC water recirculation in the water reactors. For the gas- and liquid-sodium-cooled reactors, continued use of the steam generators can serve a similar function in the primary coolant loops. Pressure control may be accomplished with containment-atmosphere coolers. In water reactors this may be supplemented with steam-condensing water sprays.

Postaccident radioactivity removal of chemically active iodine and aerosol/particulate constituents is accomplished with filtration. The nonreactive noble-gas constituents can only be contained – or released in a controlled manner.

Water-cooled reactors also have provision for containment sprays to remove radioactivity. Although the water sprays used for pressure reduction naturally remove much of the chemically reactive radioactive material, additives such as sodium hydroxide or thiosulfate increase removal, especially of elemental iodine.

Containment integrity is the last line of defense against fission-product release. Common features of water reactor containments are a leak-tight steel liner surrounded by thick reinforced concrete, including, e.g., that for the pressurized-water and boiling-water reactors in Figs. 4.23 and 4.24, respectively. The structure of the HTGR's prestressed concrete vessel (Fig. 4.14) serves a similar purpose.

Another major element of containment integrity is the ability to isolate penetrations using remotely operated valves or other means. These typically actuate on the predetermined indication of excessive pressure, radiation level, or other related parameters.

Integrity of even the most robust containment, however, depends on having all – or at least a reasonable subset – of the other safety features function as intended. Otherwise there can be excessive pressure buildup and/or severe fuel melting with subsequent dire consequences. The complete lack of a leak-tight containment structure at the Chernobyl PTGR (Fig. 4.17) was a major contributor to the consequences of the 1986 accident there.

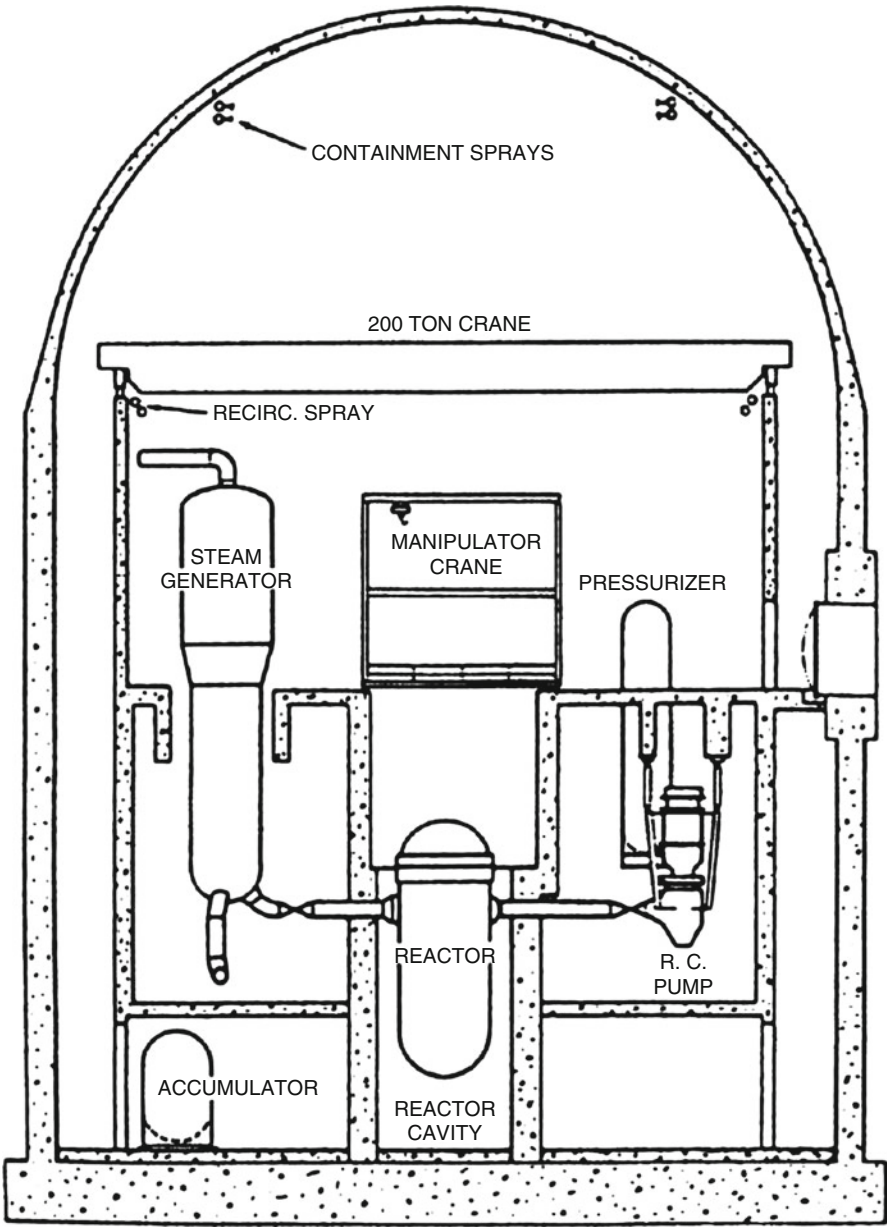

Fig. 4.23 Containment structure for a representative pressurized-water reactor (From NUREG-1150 [15], courtesy of US Nuclear Regulatory Commission)

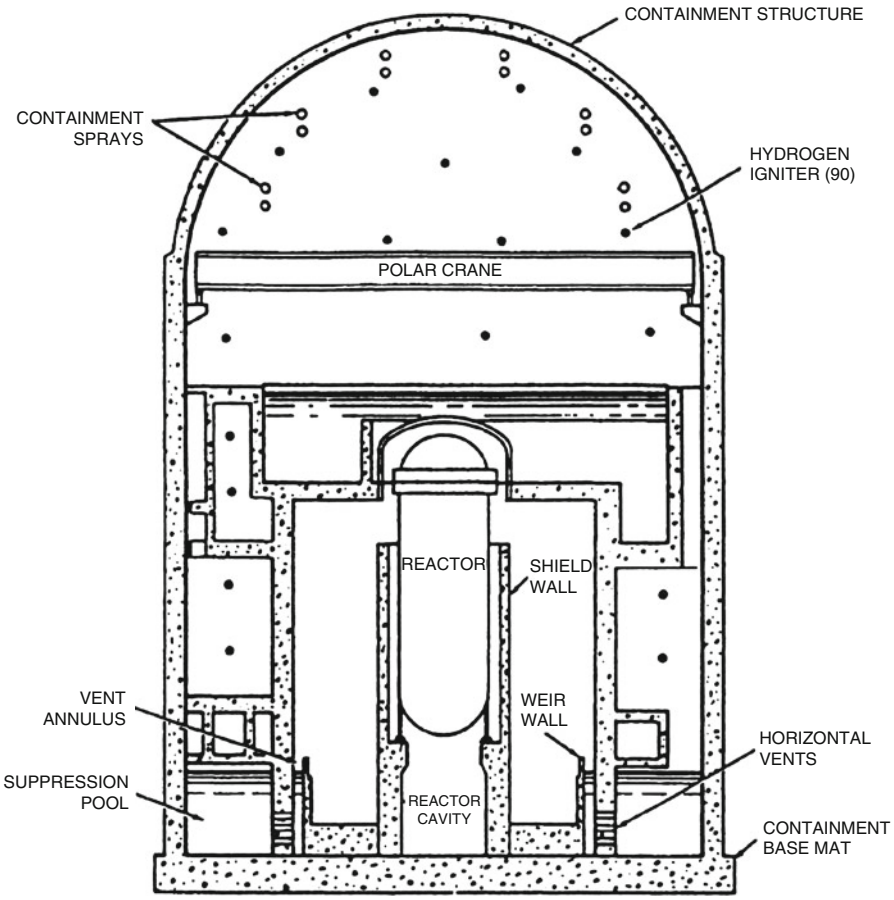

Fig. 4.24 Containment structure for a representative boiling-water reactor (From NUREG-1150 [15], courtesy of US Nuclear Regulatory Commission)

Defense-in-Depth

The previous descriptions of the defense-in-depth approach to nuclear safety have a strong technical emphasis. However, nuclear safety also depends on preventive measures, only a few of which include testing and inspection, safety assessment, deficiency analysis and correction, training, and quality assurance. Protection and mitigation require transient operating guidelines and procedures and detailed emergency planning.

Increasingly important is free and open international exchange of knowledge and experience with proper feedback to reactor design, maintenance, and operation – the need for which was highlighted dramatically by the TMI-2, Chernobyl-4, and other accidents. Regulatory controls and voluntary peer oversight – e.g., by the US

Institute for Nuclear Power Operations (INPO) and the World Organization of Nuclear Operators (WANO) – provide independent verification of safety aspects, but do not replace responsibility of the owner/operators.

Nuclear-Power Regulation

The inherent hazard associated with the radioactive material in reactor systems has led to the nuclear industry being the most regulated in the world [8, 13, 16]. Regulatory bodies include: the US Nuclear Regulatory Commission (NRC); French Commissariat à l'Énergie Atomique et aux Énergies Alternatives (CEA) – up until late 2009, Commissariat à l'Energie Atomique, now with added regulation of alternative energies; Canadian Nuclear Safety Commission (CNSC) – known as Atomic Energy Control Board (AECB) prior to 2000; and the UK Nuclear Installations Inspectorate (NII). Every other nation that operates nuclear-fission reactors also has established a regulatory authority. Requirements for reactor design and operation are established and their implementation is evaluated and monitored. Regulations with the force of law, licenses, or other methods are developed for reactor operation by such bodies, often with significant political and/or public input to the process.

The somewhat recent advent of advanced nuclear power reactors (section "Advanced Reactors") has led to changes in the NRC licensing process. Newly instituted generic certifications are valid for 15 years. Using an exhaustive public process, safety issues within the scope of the certified designs are fully resolved and, hence, will not be open to legal challenge during licensing for specific plants. US utilities will be able to obtain a single NRC reactor license to both construct and operate – as opposed to separate ones previously – before construction begins. A number of reactor types have received design certification [2].

Overall, certification of designs is on a national basis, and is safety based. In Europe, there are moves toward harmonized requirements for licensing. Reactors there may also be certified according to compliance with European Utilities Requirements (EUR) [2].

Quality assurance (QA) requirements focus on methods and procedures to assure proper design, construction, and operation of safety-related components and subsystems. Other requirements address issues from acceptable personnel radiation exposures to analysis methods and acceptance criteria for consequences of design-basis accidents and, in some cases beyond-design-basis accidents.

The accident at the Three Mile Island Unit 2 (TMI-2) PWR in 1979 led to seminal changes in the regulatory process – and nuclear industry as a whole – in the USA and elsewhere in the world. Some of these changes relate to the design, quality assurance, and inspection of modifications to plant safety systems; development and use of preapproved procedures for operation, maintenance, and other activities; administration, including staffing, training, and documentation; emergency

planning; technical support, including accident and root-cause analysis; and support services such as radiological controls, chemistry, and maintenance [8, 17].

Training and qualification, in particular, permeates essentially all of the changes. Content for control-room operators and other specialties is developed systematically and formally beginning with intensive job-analysis and moving on through feedback of operating experience. It also represents collaboration among training specialists, incumbents, supervision, management, and subject-matter expertise. Of special significance, operator training is augmented greatly by availability for each reactor of a high-fidelity, replica control-room simulator.

The disastrous 1986 accident at the Chernobyl Unit 4 in the former Soviet Union occurred with a reactor system not used elsewhere in the world. However, it did serve to reinforce many of the designs, operations, and management lessons from the earlier TMI-2 accident. It also provided unprecedented insights into severe-accident behavior and served as a catalyst for completion of post-TMI-2 "action plans," significantly enhanced international cooperation and collaboration in research initiatives and nuclear-power-plant operation and management [8].

Advanced Reactors

The nuclear power industry has been developing and improving reactor technology for more than five decades. Some of the *advanced – next generation* – reactors, which provide hope for revitalizing the nuclear-power option, are starting to be built [2, 3].

Four generations of reactors are commonly distinguished. *GEN-I* reactors were developed in the 1950s–1960s with only a few in the UK still running today. *GEN-II* reactors are typified by the present US fleet and most operated elsewhere worldwide (including those described the section "Reactor Systems" with examples in Table 4.1). The second-generation nuclear power units have been found to be safe and reliable, but they are being superseded by better designs [2].

GEN-III are the initial "advanced reactors" – the first are in operation in Japan and others are under construction or ready to be ordered. The more cutting-edge units may be termed GEN-III+. Safety-based certification of designs is on a national basis. Many are now under licensing review at the US Nuclear Regulatory Commission with some having received Design Certification. In Europe there is some movement toward harmonized requirements for licensing.

GEN-IV reactors are "still on the drawing board." They will not be operational before 2020 at the earliest [2]. (See the section "Generation IV Nuclear Reactors").

GEN-III reactors include, conceptually [2]:

- A standardized design for each type which is intended to expedite licensing, reduce capital cost and reduce construction time, and ultimately compete economically with coal-fired and other generation alternatives

- A simpler and more rugged design, making them easier to operate and less vulnerable to operational upsets
- Higher availability and longer operating life – typically 60 years
- Further reduced risk of serious reactor accidents
- Resistance to serious damage that would allow radiological release from an aircraft impact
- Higher fuel burnup lifetime, reduced outage time, and reduced amount of radioactive waste

The signature difference for GEN-III plants is a strong focus on passive, inherent safety features – e.g., gravity, natural convection, or resistance to high temperatures – which require no active controls or operational intervention to avoid accidents in the aftermath of a serious malfunction. This is in contrast to the more traditional (GEN-II, e.g., in the section "Reactor Systems") reactor safety systems which are "active" in the sense of involving electric or mechanical operation on command. Certainly some current features of GEN-II reactors are passive, e.g., negative reactivity feedback and mechanical pressure relief valves which function absent operator action or auxiliary power. However, parallel redundant systems are also necessary. The advanced reactors emphasize inherent or full passive safety depending only on physical phenomena, not on electric power and functioning engineered components. This emphasis is to the extent that some are referred to, probably inappropriately, as *inherently safe*. (See the next section "Conceptual Advanced Reactors" for three distinctly different examples).

Conceptual Advanced Reactors

Since the early 1990s, advanced reactor concepts using light-water, helium, and liquid-sodium coolants have been under development from the experience base of the current "parent" reactors. An early, conceptual version of each is described here. All include enhanced negative power feedback mechanisms to assist in obtaining shutdown and passive postaccident/post-shutdown cooling mechanisms.

Advanced Light-Water Reactor

The conceptual advanced light-water reactors differ from the traditional ones (section "Light-Water Reactors) primarily through reduction or elimination of active emergency system components, including large pumps and diesel generators, and implementation of passive features, from reactor control to emergency core cooling functions [18].

Both GEN-III PWR and BWR versions (section "Light-Water Reactor") use conventional uranium-oxide fuel assemblies with negative temperature feedback mechanisms. All combat core damage in the aftermath of a loss-of-coolant accident

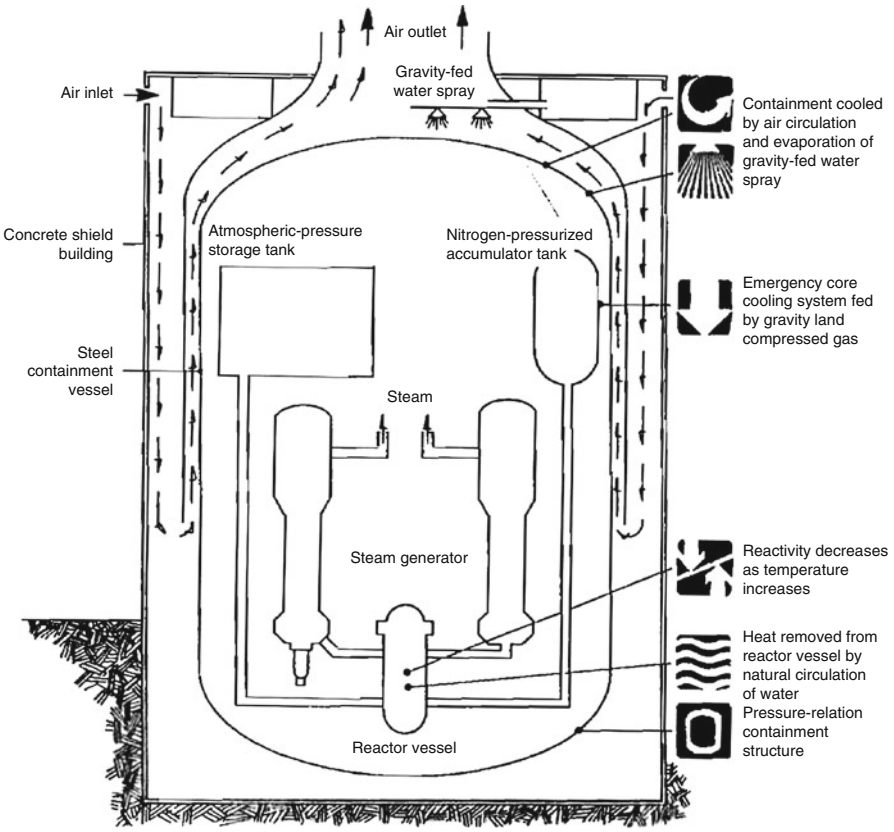

Fig. 4.25 Conceptual advanced PWR (Electric Power Research Institute)

(LOCA) by flooding the core with sufficient water to last for at least several days – as compared to the current tens of minutes – without further operator action.

An advanced PWR concept (Fig. 4.25) features passive emergency core cooling systems (ECCS) with water stored in large tanks above the core. During a large LOCA, injection of water into the core from two of the tanks is initiated by pressurized nitrogen even before the reactor coolant system has a chance to depressurize. Subsequent to depressurization, more water from a massive tank inside the containment structure can flow downward into the core under the influence of gravity alone. Neither of these two ECCS options requires pumps or emergency electric power. If the steam generators are not operable, however, natural circulation of water transfers core thermal energy to a large water storage tank located above the reactor vessel.

Post shutdown, decay heat is ordinarily removed through the steam generators. Heat removal from the steel containment shell is facilitated by a gravity-fed water

spray. Natural circulation of air, directed by large baffles, provides passive flow, i.e., without using the large fans and coolers typical of current PWRs.

The passive safety systems also simplify overall plant design. Compared with the active safety systems of a current plant, e.g., there are only half as many large pumps and 40% as much in terms of building volume designed to nuclear-grade seismic standards, number of valves, and amount of piping.

Gas-Cooled Reactors

The reference HTGR (section "Gas-Cooled Reactors") combines helium coolant, microsphere fuel, and graphite-moderator blocks to provide uniquely robust safety characteristics. A smaller *modular high-temperature gas-cooled reactor* (MHTGR) design was built upon these same features. The basic MHTGR (Fig. 4.26) is a 400–600 MWe module intended to be used in groups of four with a pair of turbine generators.

The graphite and fuel core operates at low power density, has a large inherent heat sink, and is very slow to overheat. Even with depressurization of the primary system, fuel failure would be unlikely. Operator response time, thus, is essentially unlimited.

The helium coolant is circulated through the steel – rather than HTGR's prestressed concrete – reactor vessel by an electric blower. It operates at high temperature for high steam cycle electric-generation efficiency or, potentially, a variety of industrial processes including coal gasification, chemical manufacturing, petroleum refining, or desalination of sea water.

Each reactor vessel and steam generator is enclosed in an underground silo (Fig. 4.26). Natural air circulation is sufficient to provide passive silo cooling. Even if said circulation were blocked, direct heat loss to the surrounding earth would keep fuel temperatures well below the melting point. Thus, as with the classic HTGR, an LWR-type containment is unnecessary.

Liquid-Metal Reactor

Traditionally, liquid-metal reactors have focused on LMFR-like features (section "Light-Water Graphite Reactors"). The power reactor inherently safe module (PRISM) is a small liquid-metal-cooled module (Fig. 4.27) which could be used in groups of three connected to a common steam turbine.

Each PRISM module has a pool-type configuration with the liquid-sodium coolant circulated through the core to an intermediate heat exchanger by a pair of pumps. As in an LMFBR, a secondary sodium loop connects to a steam generator.

If pumps fail, sodium flows through the PRISM core by natural convection. If the secondary flow is interrupted, the primary sodium continues to cool the core by carrying heat to the containment vessel.

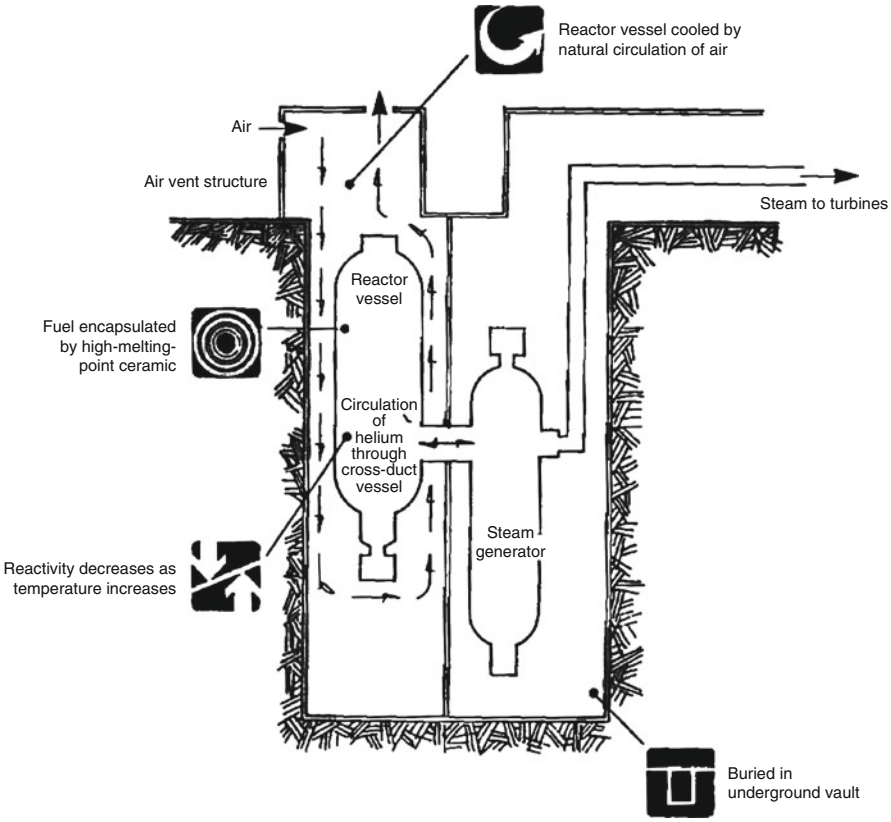

Fig. 4.26 Conceptual advanced reactor MHTGR (Electric Power Research Institute)

Fuel assemblies are made of a pyrometallurgical alloy. Reactor experiments have demonstrated that with loss of liquid-sodium flow, temperature feedback will shut down the neutron chain reaction core and natural circulation of the coolant can remove the decay heat sufficiently to prevent fuel melting.

The PRISM reactor vessel is surrounded by a guard vessel to catch leaking sodium. Both vessels are placed in an underground concrete silo. Air, allowed to circulate freely between the silo wall and guard vessel, can remove core decay heat passively to the outside environment, if necessary. Due to PRISM's passive stability, LWR-type containment is not included in the design.

Generation-III Reactors

The nuclear industry is developing a full product line touted as of clean, safe, secure carbon-free energy sources. Several advanced designs can be ready to meet USA's

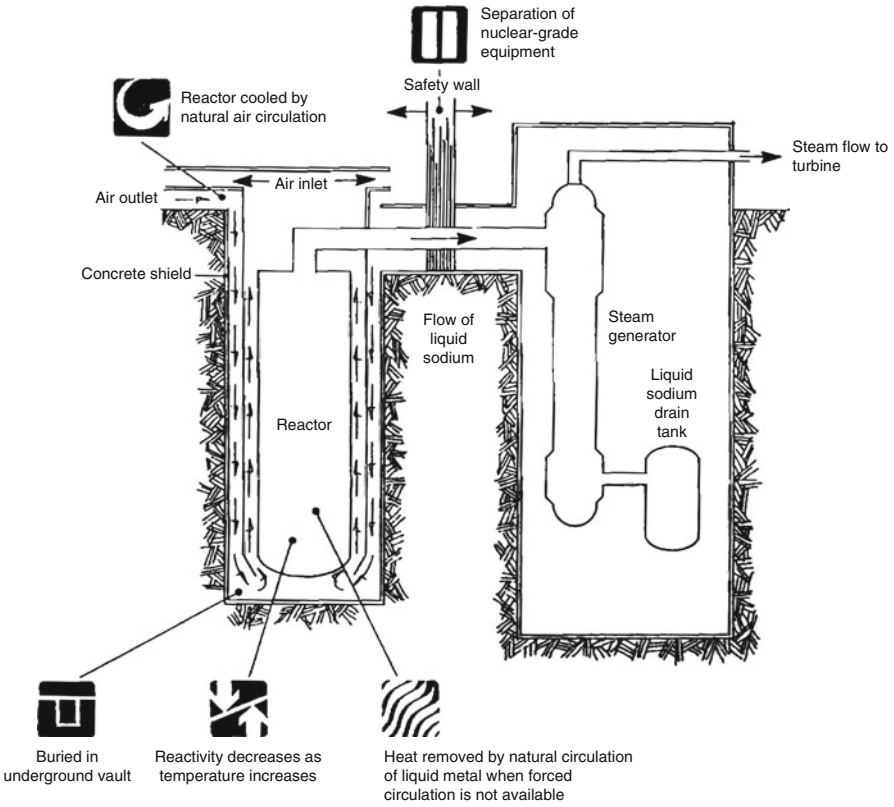

Fig. 4.27 Conceptual advanced reactor LMR (Electric Power Research Institute)

generating needs by 2015. These fall into the category of "evolutionary," i.e., modifications of existing systems building directly on the experience of operating reactors in the USA, Japan, and Western Europe. These reactors tend to be as large as, or larger than, their predecessors [2, 10].

The industry also is developing more highly advanced nuclear reactors based on new technologies, ready for commercial use by 2020 or later. A revolutionary generation of smaller, passively stable reactors is envisioned [19]. Some could replace older fossil-fired power stations of similar size – and their associated carbon emissions. The infrastructure, cooling water, rail, and transmission facilities already exist at such facilities.

Alternatively, these same small reactors can be a "right size" match for utilities or countries entering the nuclear arena for the first time. They also could be used to generate electricity for remote locations and/or provide process heat for diverse industrial applications. The designs are poised to capitalize on the benefits of modular construction, ease of transportation, and reduced financing. Modules can

be added as needed. Units could operate anywhere from 2 to 10 years on an initial fuel load, depending on the design.

Whether the advanced reactor designs are evolutionary or revolutionary, or something in between, almost all involve multi-organizational, multinational collaboration. By the end of 2006, e.g., three major Western-Japanese alliances had formed to dominate much of the world reactor supply market. Subsequently there have been a number of other international collaborative arrangements initiated among reactor vendors and designers. Circa 2010, reactor suppliers in North America, Japan, Europe, Russia, and elsewhere are marketing a dozen new thermal-neutron reactor designs as summarized in Table 4.3. Others designs, including a number of them based on fast-neutron chain reactions, are, respectively, in advanced planning stages or still in research and development.

Light-Water Reactors

Many of the advanced reactors are light-water reactor designs [2]. (See, e.g., Table 4.3) In the USA, two advanced light-water reactors fall into the category of large "evolutionary" designs, building directly on operating experience in USA, Japan, and Western Europe. Advanced boiling-water reactors (ABWR) derived from a general electric design (section "Boiling-Water Reactors") are in commercial operation and/or under construction in Japan and Taiwan, with others planned in Japan and the USA. It, and the System 80+ advanced PWR, received final design certification from US-NRC in May 1997, noting that they exceeded NRC "safety goals by several orders of magnitude." The ABWR has also been certified as meeting European requirements for advanced reactors. Although the System 80+ itself is not now being promoted for sale, eight System 80 reactors in South Korea incorporate many of its design features and are the basis of the Korean's APR-1400 which has enhanced safety and seismic robustness, and is expected to be in operation by 2013 and is being marketed worldwide.

Another, more innovative US advanced reactor is the smaller AP600 (AP = Advanced Passive) at 600 MWe with highly evolved passive safety features compared to those described in concept in the section "Advanced Light-Water Reactor" (and in concert with Fig. 4.25). Projected core-damage frequency is nearly 1,000 times less than today's NRC requirements. In 1999, it was the first to gain NRC generic final design certification. Said certifications are valid for 15 years and will allow US utilities to obtain a single NRC license to both construct and operate a reactor before construction begins.

The scaled-up AP1000 was the first GEN-III+ type reactor to receive NRC final design certification from the NRC in December 2005. It also is under active consideration for building in Europe and USA. In comparison to current plants for the same size, AP1000 is about one quarter the size with concrete and steel requirements are less by a factor of five. It is designed for unique modular construction. A single unit has 149 structural modules of five kinds, and 198 mechanical modules of four kinds – equipment, piping and valve, commodity,

Table 4.3 Advanced thermal-neutron reactors being marketed

Country (developer)	Reactor	Size (MWe)	Design progress	Main features (improved safety in all)
USA-Japan (GE Hitachi, Toshiba)	ABWR	1,300	Commercial operation in Japan since 1996–1997. In USA: NRC certified 1997, FOAKE	• Evolutionary design • More efficient, less waste • Simplified construction (48 months) and operation
South Korea (KHNP, derived from Westinghouse)	APR-1400 (PWR) from System80+	1,450	Design certification 2003, first units expected to be operating c. 2013	• Evolutionary design • Increased reliability • Simplified construction and operation
USA(Westinghouse)	AP-600 AP-1000 (PWR)	600 1,100	AP-600: NRC certified 1999, FOAKE AP-1000 NRC certification 2005, under construction in China, many more planned there	• Simplified construction and operation • 3 years to build • 60-year plant life
USA(GE Hitachi)	ESBWR	1,550	Developed from ABWR, under certification in USA, likely construction there	• Evolutionary design • Short construction time
Japan(Utilities, Mitsubishi)	APWR US-APWR EU-APWR	1,530 1,700 1,700	Basic design in progress, planned for Tsuruga US design certification application 2008	• Hybrid safety features • Simplified construction and operation
France-Germany (Areva NP)	EPR US-EPR (PWR)	1,600	Future French standard French design approval Being built in Finland, France, and China Under certification in USA	• Evolutionary design • High fuel efficiency • Flexible operation
Germany (Areva NP)	SWR-1000 (BWR)	1,200	Under development, pre-certification in USA	• Innovative design • High fuel efficiency
Russia (Gidropress)	VVER-1200 (PWR)	1,200	Under construction at Leningrad and Novovoronezh plants	• Evolutionary design • High fuel efficiency • 50-year plant life
Canada (AECL)	Enhanced CANDU-6	750	Improved model licensing approval 1997	• Evolutionary design • Flexible fuel requirements
Canada (AECL)	ACR	700 1,080	Undergoing certification in Canada	• Evolutionary design • Light-water cooling • Low-enriched fuel
China (INET, Chinergy)	HTR-PM	2 × 105 (module)	Demonstration plant due to start building at Shodaowan	• Modular plant, low cost • High temperature • High fuel efficiency
USA-Russia et al. (General Atomics – OKBM)	GT-MHR	285 (module)	Under development in Russia by multinational joint venture	• Modular plant, low cost • High fuel efficiency • Direct cycle gas turbine

Source: Adapted from World Nuclear Association – http://www.world-nuclear.org/info/inf08.html

and standard service modules. These comprise one third of all construction and can be built off site in parallel with the on-site construction. China has four AP-1000 units under construction, with many more to follow.

GE Hitachi Nuclear Energy's ESBWR is a GEN-III+ BWR technology that utilizes passive safety features and natural-circulation principles. It is essentially a larger evolution from a predecessor SBWR.

Mitsubishi's large – advanced – APWR was developed in collaboration with four utilities. It is a simpler four-loop design which combines both active and passive cooling systems. The first two are planned for Japan to come on-line from 2016 and will be the basis for the next generation of Japanese PWRs. US-APWR and EU-APWR versions, respectively, are being developed for USA and European markets.

In Europe, several designs are being developed to meet the European Utility Requirements (EUR) of French and German utilities, which have stringent safety criteria. European pressurized-water reactor (EPR) developed from French and German designs has four separate, redundant safety systems rather than passive safety. The first EPR unit is being built in Finland, with two other slated for France, and another for China. US-EPR – now known as the Evolutionary PWR (EPR) – was submitted for US design certification.

Another evolutionary design, the SWR 1000, is a Siemens BWR now known as Kerena. It is simpler overall and has many passive safety features.

In Russia, several advanced PWR designs with passive safety features have been developed. Late-model VVER-1000 units (see the section "Pressurized-Water Reactor") – one considered GEN-III with enhanced safety – are being built in India and China with two more planned for Bulgaria. A third-generation standardized VVER-1200 reactor is an evolutionary development from the VVER-1000 with longer life, greater power, and greater efficiency. They have enhanced safety including that related to earthquakes and aircraft impact with some passive safety features, double containment, and low core-damage frequency. A Europe-tailored reactor design, MIR-1200 – Modernized International Reactor – has some Czech involvement.

Russia also has a number of other novel small reactor designs [2, 19]. Several *VBER* PWR variations developed from naval power plants may be floating or land-based, modular construction, and/or provide cogeneration. VK-300 – with fuel elements similar to the VVER – have been developed specifically for cogeneration of both power and district heating or heat for desalination. Cooling (by convection) and all safety systems are passive. It has been announced that six would be built in Russia's far east.

Heavy-Water Reactors

A pair of GEN-III HWRs are under development based directly on CANDU reactors. Each is to be configured for flexible fuel requirements including standard

natural uranium, slightly enriched LWR-like uranium, and mixed-oxide (U and Pu) fuel and from a variety of potential sources, e.g., PWR spent-fuel or even military down-sizing.

Such fuel innovations, combined with the experiences of South Korea and China, suggest that an Enhanced CANDU-6 (EC6) could have a 4.5-year construction and 60-year plant life. This design is under consideration for new build in Canada.

The Advanced CANDU Reactor (ACR) is a more innovative concept using a low-pressure heavy-water moderator with PWR-like light-water cooling for higher thermal efficiency. The resulting compact core would reduce capital cost – an ACR-700 is physically much smaller, simpler, and more efficient as well as 40% cheaper. A larger ACR-1000 – the current focus of attention – has more fuel channels; is designed to run on low-enriched uranium ($\sim$ 1.5–2.0 wt% ^{235}U) with high burnup, MOX fuel, thorium-^{233}U fuels; and extends the fuel life by about three times reducing high-level waste volumes accordingly. Other features include small negative reactivity feedback, other passive safety features, two independent and fast shutdown systems; and prefabricated modules to cut construction time to 3.5 years. The CANDU X or SCWR – a GEN-IV ACR variant with supercritical light-water coolant – would operate at very high pressure and temperature, and, thus, high thermal efficiency. (See the section "Generation IV Nuclear Reactors".)

Table 4.3 summarizes key characteristics for the advance HWRs and other advanced reactor types.

For the longer term, India is developing the Advanced Heavy Water Reactor (AHWR) to utilize its plentiful reserves of thorium. The AHWR is a 300-MWe reactor moderated by heavy water in a calandria vessel with about 450 *vertical* pressure tubes. The coolant is boiling light water circulated by convection. A "gravity-driven water pool" near the top of the reactor building with 7,000 cubic meters of water is proposed as a novel heat sink. A unique fuel paradigm calls initially for fuel assemblies each consisting of a mixture of oxide pins of Th-^{233}U and Pu-Th, respectively, with resulting very high net fuel utilization. Once fully operational, the fuel pins would be arranged in three concentric rings each "zoned" with a specific equivalent fissile content based on adjusting Th, ^{233}U, and Pu fractions. The content of ^{233}U – with inherent ^{232}U and its unique high-gamma-active daughter products – is considered to confer a substantial proliferation resistance (i.e., high-capacity fabrication of ^{233}U fuel must be done remotely, a feature not necessary for either ^{235}U or plutonium). (See also the chapter on Modern Nuclear Fuel Cycles.)

In 2009, an export version named AHWR-LEU was announced. The major difference is use of low-enriched uranium (LEU) – in lieu of Pu – plus thorium as a fuel. Plutonium production will differ from that in light-water reactors – the fissile proportion will be less and the ^{238}Pu (non-fissile with high radioactivity and associated heat) portion three times as high – giving inherent proliferation resistance. The net result is described as a reactor "manageable with modest industrial infrastructure within the reach of developing countries."

High-Temperature Gas-Cooled Reactors

The advanced high-temperature gas-cooled reactors (HTGR) use helium as a coolant at up to 950°C, which for electric generation either makes steam conventionally or directly drives a gas turbine for electricity and a compressor to return the gas to the reactor core. They also are especially well-suited for providing process heat for industrial applications, including hydrogen production and could be used in the development of tar sands, oil shale, and coal-to-liquid applications, reducing the life cycle carbon footprint of all these activities.

The fuel is in the conventional HTGR form of microsphere particles arranged in blocks as hexagonal "prisms" of graphite, or in billiard ball-sized "pebbles" of graphite encased in silicon carbide (Fig. 4.15) each providing containment for fission products which is stable to 1,600°C or more. Other features are similar to those in Fig. 4.26.

China's HTR-PM is to have two reactor modules of 105 MWe each and use a steam cycle to drive a single steam cycle turbine at about 40% thermal efficiency. It is expected to pave the way for an 18-unit full-scale power plant also using the steam cycle.

A larger US design, the Gas Turbine–Modular Helium Reactor (GT-MHR), is planned as modules of 285 MWe each directly driving a gas turbine (Brayton cycle) at 48% thermal efficiency. The cylindrical core consists of 102 prism blocks (Fig. 4.15b) with channels for helium and control rods. It is being developed by General Atomics in partnership with Russia, and supported by Japan. Initially it was to be used to burn pure ex-weapons plutonium in Russia. The preliminary design stage was completed in 2001, but the program has stalled since. Areva's Antares also is based on the GT-MHR.

Table 4.3 summarizes key characteristics for the first two of the advanced HTGRs and for other advanced reactor types.

South Africa's Pebble Bed Modular Reactor (PBMR) draws on German THTR (section "Gas-Cooled Reactor" and Fig. 4.14b) expertise. Production units would be 165 MWe, ultimately using a direct-(Brayton) cycle gas-turbine generator with thermal efficiency of about 41%. Power would be adjusted by changing the pressure in the system.

Up to 450,000 fuel pebbles (Fig. 4.15a and c) recycle through the reactor continuously (about six times each) until they are expended. The reactor will use about 13 fuel loads in a 40-year lifetime. The on-line refueling can facilitate operational cycles with as long as 6 years between shutdowns.

Fast-Neutron Reactors

The classic fast-neutron reactor has been the fast breeder reactor (FBR). Current interest centers on their ability to provide unique nuclear fuel-cycle services, such as breeding new fuel, consuming recycled nuclear waste as fuel, and supporting

government-sponsored nonproliferation efforts by consuming material from former nuclear weapons [10].

About 20 liquid-metal fast breed reactors (LMFBR), mainly research units, have accumulated some significant operating experience. Several countries have research and development programs for improving their current designs, but generally less as GEN-III efforts and more as a bridge to new GEN-IV reactors [2, 20].

The consummate LMFBR, France's SuperPhenix (section "Light-Water Graphite Reactors"), was optimized to run on plutonium fuel and to "breed" even more plutonium fuel with a depleted uranium blanket around the core. The LMFBRs, however, are expensive to build and could only be justified economically if uranium prices were to rise dramatically above market price circa 2010. For this reason, research work almost ceased for some years. Closure of the SuperPhenix after very little operation over 13 years especially set back developments.

Primarily to address nonproliferation concerns, there apparently are no plans to build any more plutonium-fueled fast reactors with blanket assemblies. Fast-reactor concepts slated for the GEN-IV program simply have a core where both plutonium production and consumption occur [20].

In Russia, the BN-600 – a fast breeder reactor with a conventional core-blanket configuration – has supplied electricity to the grid since 1981 (and has had the best operating and production record of all of the nation's nuclear power units). Its evolutionary BN-800 counterpart originally was fueled with uranium-oxide fuel, but reconfigured to burn the plutonium from military stockpiles. Two BN-800 units have been sold to China with construction slated to start in 2012. Further development of the BN-series is slated to be with an integrated core to meet GEN-IV nonproliferation goals. Russia also has interest in developing lead- and lead-bismuth fast-neutron-reactor designs, having used these coolants in submarines.

Japan is continuing with development of the FBR. The Japan Standard Fast Reactor (JSFR) is a breeder-like concept, but having a breeding ratio less than unity.

Meanwhile in the USA, the modular liquid-metal-cooled inherently safe reactor – PRISM (See the section "Liquid-Metal Reactors" and Fig. 4.27) – is continuing to receive attention. It is a compact modular pool-type reactor with passive cooling for decay heat removal. PRISM is considered a potential GEN-IV solution to closing the fuel cycle in the USA.

Korea's KALIMER (Korea Advanced LIquid MEtal Reactor) also is pool-type sodium-cooled fast reactor. Having evolved from a smaller unit, it has a core designed to transmute transuranic species and no breeding blanket. Future development of KALIMER for GEN-IV is envisaged.

Research continues in India including on the unique track of using thorium – which it has in abundance – in a breeding scheme with fissile ^{233}U. The Kalpakkam reactor is fueled with uranium-plutonium carbide and has a thorium blanket to breed the ^{233}U.

Generation IV Nuclear Reactors

The GEN-IV International Forum (GIF) was initiated in 2000 as an international collective committed to joint development of the next generation of nuclear technology. Currently six nuclear reactor technologies are under development for deployment between 2020 and 2030 [21, 22].

All six technologies represent advances in sustainability, economics, safety, reliability, and proliferation resistance. Most employ a closed fuel cycle to maximize the resource base and minimize high-level wastes that will need to be sent to a repository.

Collectively, the reactors include thermal-, epithermal-, or fast-neutron spectra. Coolants are light water, helium, sodium, lead-bismuth, and fluoride salt. Temperatures range from 510°C to 1,000°C – compared with less than 330°C for today's LWRs. At the higher temperatures, thermochemical hydrogen production is envisioned. Power ratings range all the way from 20 to 1,500 MWe (or equivalent thermal).

At least four of the systems already have significant operating experience in most respects of their design. This provides a good basis for further research and development and prospects for commercial operation well before 2030.

Table 4.4 provides a comparison. (See also the following section "Future Directions".) Although six technologies were chosen, development on one of them has gone in two different directions resulting in seven being listed in the table. Summary descriptions of each are provided in the remainder of this section.

Supercritical water-cooled reactors (SWCR) use water coolant at extremely high temperatures and pressures – thermodynamically in the "supercritical" fluid regime. Such fluids are those above the thermodynamic critical point, defined as the highest temperature and pressure at which gas and liquid phases can coexist in equilibrium. They have properties between those of gas and liquid. For water the critical point is at 374°C and 22 MPa, giving it a "steam" density one third that of the liquid so that it can drive a turbine in a similar way to normal steam. A fleet of over 400 supercritical coal-fired plants operating worldwide provides a solid experience base for reactor application [21].

Supercritical water obviates the need for a secondary steam system and drives a turbine generator directly at 44% (and potentially up to 50%) efficiency. Designs call for a high power level and include BWR-like pressure-vessel and CANDU-variant pressure-tube options. Each will have passive safety features with fewer components (e.g., none related to steam separator/driers) and relatively low capital cost. Neutron-spectrum and fuel-cycle options combine in an interesting manner to provide the potential for:

1. Thermal reactors with enriched uranium-oxide fuel and an open fuel cycle
2. Fast reactors with full actinide-element recycle and conventional reprocessing

Table 4.4 Generation IV nuclear reactors

	Neutron spectrum (fast/thermal)	Coolant	Temperature (C)	Pressure[a]	Fuel	Fuel cycle	Size(s) (MWe)	Uses
Supercritical water-cooled reactors (SCWR)	Thermal or fast	Water	510–625	Very high	UO_2	Open		(thermal)
300–700	Electricity							
						Closed (fast)	1,000–1,500	
Very high temperature gas reactors (VHTR)	Thermal	Helium	900–1,000	High	UO_2 prism or pebbles	Open	250–300	Hydrogen and electricity
Gas-cooled fast reactors (GFR)								
Sodium-cooled fast reactors (SFR)	Fast	Sodium	550	Low	U-238 and MOX	Closed	30–150 300–1,500 1,000–2,000	Electricity
Lead-cooled fast reactors (LFR)	Fast	Lead or Pb-Bi	480–800	Low	U-238[b]	Closed, regional	20–180[c] 300–1,200 600–1,000	Electricity and hydrogen
Molten salt fast reactors (MSFR)	Fast	Fluoride salts	700–800	Low	UF in salt	Closed	1,000	Electricity and hydrogen
Molten salt advanced high-temperature reactors (AHTR)	Thermal	Fluoride salts	750–1,000		UO_2 particles in prism	Open	1,000–1,500	Hydrogen

Source: Adapted from World Nuclear Association – http://www.world-nuclear.org/info/inf77.html

[a]High 7–15 MPa

[b]With some U-235 or Pu-239

[c]"Battery" model with long cassette core life (15–20 years) or replaceable reactor module

Very high-temperature gas reactors (VHTR) are thermal-neutron systems with graphite moderator and helium coolant. Fuel can be (1) stacks of prism blocks or (2) a pebble bed (section "Gas-Cooled Reactors" and Fig. 4.15). The "very high" temperatures result in high thermodynamic efficiency which can be applied for thermochemical hydrogen production with electricity cogeneration or direct high-efficiency driving of a gas turbine (Brayton cycle). Essentially complete passive safety, low operation and maintenance costs, and modular construction are envisioned based on the HTGR (section "Gas-Cooled Reactors") and PBR (section "High-Temperature Gas-Cooled Reactors") heritage.

Gas-cooled fast reactors (GFR) are the fast-neutron counterparts of the VHTR – absent graphite moderator – described above. The design includes a thick steel reactor pressure vessel and helium coolant. It is well suited for conventional steam-electric generation, helium direct-drive gas turbine (Brayton cycle), and thermochemical hydrogen production or other process heat. With the fast-neutron spectrum, fuel of Pu, ^{238}U, and Th can support a blanket-less breeding paradigm.

Sodium-cooled fast reactors (SFR), using liquid-sodium coolant, are progeny of the LMFBR (section "Light-Water Graphite Reactors"). Configurations could be loop-type or pool-type. Passive safety features are augmented by the coolant's low pressure and inherent natural-convection tendency. An initial core plus blanket configuration is likely to be displaced by new core-only breeding designs with depleted uranium integral to the fuel matrix. High-temperature operation is consistent with electricity generation or a supercritical CO_2 turbine. Fuel-related variants include: (1) U-Pu metal fuel with actinide retention and on-site pyrometallurgical processing and (2) conventional mixed Pu-U "mixed-oxide" (MOX) fuel and advanced aqueous reprocessing elsewhere in central facilities.

Lead-cooled fast reactors (LFR) have similarity to the SCFR in terms of fast-neutron spectrum, as well as liquid-metal coolant – here Pb or Pb-Bi eutectic – with low pressure and natural convection. Russia has had multi-decade experience with this technology in its nuclear submarine program. Design power levels range from relatively small for modular units to large for single plants. A novel concept is for a factory-built "battery" unit of 20–180 MWe with 15–20 year life for small grids or developing countries. Operating temperatures are slated to be sufficient for thermochemical hydrogen production. Fuel would be Pu and depleted uranium – with an option to introduce thorium – in metal or nitride form.

Molten-salt reactors (MSR) – the most novel of the technologies – use uranium dissolved in sodium (or zirconium) fluoride salt which serves as both the fuel and the coolant. When the salt circulates through graphite core channels, the neutrons are moderated to epithermal (i.e., average above, or faster than, thermal) energies and can support a critical chain reaction. Outside of the core and absent proximity to moderator, the salt is very highly subcritical. Similar to the metal-cooled reactors, the molten salt has the inherent safety feature of operating at very low pressure. An appropriately designed secondary loop can provide for electricity generation or thermochemical hydrogen production.

The MSR fuel requires no fabrication per se. Fissile inventory can be kept to a minimal level as the plutonium, depleted uranium, and/or thorium fuel constituents can be inserted at any time as needed. Actinides from outside sources, e.g., to be transmuted by neutron irradiation to less hazardous form, can also be added. Simultaneously, on-line and continuous removal of fission products and recycle of self-generated actinides can be implemented.

There are two separate baseline MSR concepts. One is the (Molten Salt) Advanced High-Temperature Reactor (AHTR) which has a graphite core similar to that of the VHTR (and HTGR Fig. 4.15b). Use of a neutron-moderating, molten-salt coolant, instead of helium, supports a much higher power density The other version is the Molten Salt Fast Neutron Reactor (MSFR) with a graphite-free "core tank with no internals" and molten-salt compositions which provide less moderation.

Future Directions

The future of nuclear power as a world energy source is a complex part of an overall energy picture, a few aspects of which were summarized in the section "Definition of the Subject." Two recent studies – sponsored, respectively, by the Massachusetts Institute of Technology (MIT) and the Electric Power Research Institute (EPRI) – shed light on both future prospects and problems.

The Future of Nuclear Power

The MIT study, *The Future of Nuclear Power* (2003 report and 2009 update) – in its own words – was "the most comprehensive, interdisciplinary study ever conducted on the future of nuclear energy," and concluded that "The nuclear option should be retained precisely because it is an important carbon-free source of power" [4].

The study examines a growth scenario – characterized as "not a prediction, but rather a study case in which nuclear power would make a significant contribution to reducing CO_2 emissions" – with the current deployment of 360 GWe of nuclear capacity worldwide expanded to 1,000 GWe (1 Terawatt) of "carbon-free" power by mid-century, keeping nuclear's fraction of the electricity market about constant. Correspondingly, the USA would triple its nuclear deployment from about 100 GWe to 300 GWe. (See also the subsequent section "New Nuclear Installations".)

The credibility of such a scenario – and nuclear energy as an option – will be largely determined in the forthcoming decade by the extent to which significant progress is made on four unresolved problems:

1. High relative construction costs
2. Perceived adverse safety, environmental, and health effects

3. Potential security risks stemming from proliferation
4. Unresolved challenges in long-term management of nuclear wastes

The up-front costs associated with nuclear power are higher than those for fossil-fueled plants. However, the study was optimistic about ways to mitigate the costs, and noted that, over time, the societal and environmental price of carbon emissions could dramatically improve the competitiveness of nuclear power. The goal of 1 terawatt of "carbon-free" nuclear power by 2050 is certainly challenging, requiring deployment of about 2,000 MW a month with an associated capital investment of $2 trillion over several decades.

One key economic incentive has been a limited production tax credit – a provision in the 2005 Energy Policy Act – to "first mover" private sector investors who successfully build new nuclear plants. This tax credit is extendable to other carbon-free electricity technologies and is not paid unless the plant operates. The study also suggested the industry-wide cost-reduction options of placing near-term emphasis on the once-through fuel cycle and delaying expensive development projects pending progress on near-term deployments.

Public acceptance turns on the perception of safety, environmental, health effects. Thus, performance, cost, and environmental acceptability of the technology must be demonstrated to the public, political leaders, and investors. Having the government develop enhanced capabilities to analyze life-cycle health and safety impacts of fuel-cycle facilities is also recommended. It also is essential that NRC regulations are developed and enforced diligently.

Security risks can be addressed by encouraging countries to forego the proliferation-risky nuclear technologies – enrichment and reprocessing – by offering "a preferred position to receive nuclear fuel and waste management services from nations that operate the entire fuel cycle." Near-term emphasis on the once-through fuel cycle also supports this scenario.

Long-term management of nuclear wastes is a huge problem, the solution for which is key to public acceptance. Key to the resolution of this task is the capability of the government to start moving spent fuel from reactor sites and to develop long-term waste management research and development programs. (See also the following section "New Nuclear Installations" with respect to spent-fuel management.)

According to a 2009 MIT update report [4], the initial 2003 study in the years following its publication was credited with a significant impact on the public debate both in the USA and abroad, including influence on the US Department of Energy's (DOE) nuclear energy research and development (R&D) program. Unfortunately, in this same time frame, the challenges to greater nuclear-power deployment were found to have remained largely the same – especially with no new US plants under construction and insufficient progress on waste management – leading to: "The sober warning. . .that if more is not done, nuclear power will diminish as a practical and timely option for deployment at a scale that would constitute a material contribution to climate change risk mitigation."

New Nuclear Installations

An EPRI summer seminar in 2007 entitled "Electricity Solutions for a Carbon-Constrained Future" addressed "New Nuclear Installations" [6]. Whereas the MIT study [4] focused primarily on policy, the EPRI nuclear effort provides a valuable counterpoint on implementation.

At the time, nuclear power accounted for 73% of the emission-free generation in the USA and was described as the only technologically mature, non-emitting source of power that positioned to deliver large-scale CO_2 reduction in the upcoming decades. Employing a study target of 64 GW of new nuclear by 2030 – considered ambitious but achievable – key challenges were identified so as to:

1. Keep the current nuclear power plants running safely and reliably for 60–80 years.
2. Build out the next generation of plants starting around 2015.
   The existing fleet of light-water reactor (LWR) technology – generating approximately 20% of the nation's electricity and operating at an average capacity of 90% – establishes a platform of confidence for the nation to proceed with further life extension of existing plants and to considerably expand the fleet using advanced LWR designs.
3. Achieve consensus on a long-term strategy for spent fuel.

Almost all of the US operating plants have had, or are in the process of having, their operating licenses extended from the initial 40–60 years. It is a reasonable assumption that all units will be granted a 20-year life extension by about 2016.

Even while these life extensions are being finalized, the technical basis must be laid for an additional 20-year extension – from 60 to 80 years – by confirming that "…with sufficient maintenance, refurbishment, and upgrades, today's plants could [continue to] operate quite safely …." "Ultimately, extending the life of our current fleet an additional 20 years will be a business decision, which means that both continued high safety performance and continued economic competitiveness must be addressed." Key among a wide variety of important milestones are assessing the ability of passive components to continue safe performance, upgrading instrumentation and controls to modern digital technology, and developing of higher-performance fuels to extend the time between refueling outages and reduce spent-fuel volumes.

Design development and prelicensing have produced advanced light-water reactor (ALWR) designs (section "Advanced Reactors") that are approaching the "essentially complete design" status which will enable new plant orders to be based on detailed cost and schedule estimates. ALWRs are already in operation today or under construction around the world. At least fifteen US companies stated their intent to file for NRC combined construction and operating licenses. Of a total

of 30 reactors under consideration, most were slated for sites that have existing units and were developed with such expansion in mind.

The first commercial operation of ALWRs in the USA could begin shortly after 2015. "The first new plants out of the box must be done very, very well. . .. They must be executed thoughtfully, deliberately, and with the highest level of skill." The challenge is daunting. Then, the industry must sustain a much higher build rate out to 2050 and beyond. The research, development, and demonstration (RD&D) – with particular emphasis on the latter – focus for new advanced reactors should/must include:

- Completing, in the short term, engineering work necessary for detailed cost and schedule estimates for plant construction, and resolution of any remaining regulatory issues
- Beginning now to lay the foundation for the high build rates, including bringing capital costs and construction times down, addressing shortfalls in both physical and workforce infrastructure, and dealing with a plethora of other issues
- Helping the US federal government advance the capabilities of the high-temperature gas-cooled reactor (HTGR) from construction of an operational prototype to enabling commercially available units, e.g., to take advantage of the ability to produce electricity, provide process heat for industrial applications, and – especially – cost-effectively generate hydrogen by emission-free methods

Finally, sustained expansion of nuclear generation ultimately requires the resolution of spent-fuel management concerns. Although on-site interim storage in concrete silos has been effective and safe for over two decades, imperatives of economics, security, and sustainability will require establishing an integrated fuel management system for the longer term, i.e., including centralized interim storage, long-term geologic storage, and eventually, a closed fuel cycle. A well-thought-out, deliberate consensus strategy on nuclear fuel storage is needed. Such a consensus will allow for advanced reprocessing and separation technologies, reconditioning, fuel manufacturing facilities, and effective application of GEN-IV fast-reactor technologies.

Notes

Sandia National Laboratories is a multi-program laboratory managed and operated by Sandia Corporation, a wholly owned subsidiary of Lockheed Martin Corporation, for the U.S. Department of Energy's National Nuclear Security Administration under contract DE-AC04-94AL85000.

Bibliography

Primary Literature

1. Rhodes R (1986) The making of the atomic bomb. Simon and Schuster, New York
2. Advanced nuclear power reactors – World Nuclear Association – http://www.world-nuclear.org/info/inf08.html. Accessed 6 July 2011
3. Knief RA (1997) Nuclear steam supply systems. In: Elliott T et al (eds) Standard handbook of power plant engineering, 2nd edn. McGraw-Hill Book, New York
4. Ansolabehere S et al (2003) The future of nuclear power – an interdisciplinary MIT study. Massachusetts Institute of Technology. http://web.mit.edu/nuclearpower/). [Summarized in Deutch JM, Moniz EJ (2006) The nuclear option. Sci. Am, September 2006.] Also "Update of the MIT 2003 future of nuclear power study," Massachusetts Institute of Technology, 2009 – http://web.mit.edu/nuclearpower/pdf/nuclearpower-update2009.pdf
5. Lake JA, Bennett RG, Kotek JF (2009) Next generation nuclear power. Sci Am 286(1):72–79
6. New nuclear installations (from EPRI's 2007 Summer seminar: electricity solutions for a carbon-constrained future), EPRI J (Fall 2007):26–28
7. 2010 World nuclear industry handbook, from the publishers of Nuclear Engineering International magazine, www.neimagazine.com
8. Knief RA (1992) Nuclear engineering – theory and technology of commercial nuclear power, 2nd edn. Taylor & Francis, Washington, DC (Reprinted by American Nuclear Society, 2008; 3rd edition in preparation)
9. Sesonske A (1973) Nuclear power plant design analysis. U.S. Atomic Energy Commission, TID-26241, Washington, DC
10. Nuclear Energy Institute – http://www.nei.org/keyissues/newnuclearplants/ – http://www.nei.org. Accessed 6 July 2011
11. World Nuclear Association – http://www.world-nuclear.org/. Accessed 6 July 2011
12. UNM (University of New Mexico) CEL (Centennial Engineering Library) Nuclear Engineering Wallcharts – http://econtent.unm.edu/cdm4/browse.php?CISOROOT=/nuceng – Nuclear Engineering International – http://www.neimagazine.com/story.asp?storyCode=2055665. Accessed 6 July 2011
13. Rahn FJ, Adamantiades AG, Kenton JE, Braun C (1984) A guide to nuclear power technology: a resource for decision making. Wiley-lnterscience, New York
14. U.S. Nuclear Regulatory Commission (1975) Reactor safety study: an assessment of risks in U. S. commercial nuclear power plants. U.S. Nuclear Regulatory Commission, WASH-1400 (NUREG-74/014), Washington, DC
15. U.S. Nuclear Regulatory Commission (1989) Severe accident risks: an assessment for five U.S. nuclear plants. U.S. Nuclear Regulatory Commission, NUREG-1150, Washington, DC
16. Nuclear Engineering International magazine – http://www.neimagazine.com/. Accessed 6 July 2011
17. Walker SJ (2004) Three Mile Island – a nuclear crisis in perspective. University of California Press, Berkeley
18. Catron J (1989) New interest in passive reactor designs. EPRI J 14(3):4–13
19. Small Nuclear Power Reactors – World Nuclear Association – http://www.world-nuclear.org/info/inf33.html. Accessed 6 July 2011
20. Fast Neutron Reactors – World Nuclear Association – http://www.world-nuclear.org/info/inf98.html. Accessed 6 July 2011
21. Generation IV Nuclear Reactors – World Nuclear Association – http://www.world-nuclear.org/info/inf77.html. Accessed 6 July 2011

22. Generation IV Nuclear Energy Systems – U.S. Department of Energy – http://www.ne.doe.gov/genIV/neGenIV1.html. Accessed 6 July 2011
23. Seminov BA (1983) Nuclear power in the Soviet Union. IAEA Bull 25(2):47–59

Books and Reviews

Agnew HM (1981) Gas-cooled nuclear power reactors. Sci Am 244:55–63
American Nuclear Society (+ Nuclear News). www.ans.org
Benedict M, Pigford TH, Levi HW (1981) Nuclear chemical engineering, 2nd edn. McGraw-Hill, New York
Cochran RG, Tsoulfanidis N (1990) The nuclear fuel cycle – analysis and management. American Nuclear Society, La Grange Park
Douglas J (1994) Reopening the nuclear option. EPRI J 19(8):6–17
Electric Power Research Institute (EPRI). http://my.epri.com. Accessed 6 July 2011
Fishetti MA (1987) Inherently safe reactors: they'd work if we'd let them. IEEE Spect 24(4):28–33
Framatome (1992) P4: the 1300 MWe PWR Series. Paris, France, April 1992
Glasstone S, Sesonske A (1994) Nuclear reactor engineering (volume 1: reactor design basics and volume 2: reactor systems engineering), 4th edn. Chapman & Hall, New York
Golay MW, Todreas NE (1990) Advanced light water reactors. Sci Am 262(4):82–89
Hore-Lacy I (2009) Nuclear energy in the 21st century, 2nd edn. World Nuclear University Press, London
International Atomic Energy Agency (IAEA). http://www.iaea.org
Lewis HW (1980) The safety of fission reactors. Sci Am 242:53–65
Lish KC (1972) Nuclear power plant systems and equipment. Industrial Press, New York
Marcus GH (2010) Nuclear firsts: milestones on the road to nuclear power development. American Nuclear Society, La Grange Park
Marshall W (ed) (1983) Nuclear power technology – volumes 1, 2, and 3. Clarendon Press, Oxford
Mclntyre MC (1975) Natural uranium heavy-water reactors. Sci Am 233:17–27
MIT: the future of nuclear power. http://web.mit.edu/nuclearpower/. http://web.mit.edu/nuclearpower/pdf/nuclearpower-update2009.pdf. Accessed 6 July 2011
Murray RL (2008) Nuclear energy, 6th edn. Butterworth-Heinemann, Oxford
Nero AV Jr (1979) A guidebook to nuclear reactors. University of California Press, Berkeley
Nuclear Engineering International Special Publications (1989) French PWR technology. Nuclear Engineering International Special Publications, Sutton
Organisation for Economic Co-Operation and Development (OECD) – Nuclear Energy Agency (NEA). http://www.nea.fr/
Rogovin M, Frampton GT Jr (1980) Three Mile Island: a report to the Commissioners and to the public. U. S Nuclear Regulatory Commission, Washington, DC
Todreas NE, Kazimi MS (1990) Nuclear systems (vol 1: Thermal hydraulic fundamentals and vol 2: Elements of thermal hydraulic design). Taylor & Francis/Hemisphere, New York
U.S. Department of Energy (1987) Overall plant design descriptions VVER water-cooled, water-moderated energy reactor. DOE/NE0084, Rev. 1, October
U.S. Department of Energy (DOE) – Office of Nuclear Energy (NE). www.ne.doe.gov. Accessed 6 July 2011
U.S. Nuclear Regulatory Commission (1975) Reactor safety study: an assessment of risks in U.S. commercial nuclear power plants, WASH-1400 (NUREG-74/014). U.S. Nuclear Regulatory Commission, Washington, DC

U.S. Nuclear Regulatory Commission (1987) Report on the accident at the Chernobyl nuclear power station, NUREG-1250, rev.1. U.S. Nuclear Regulatory Commission Washington, DC
U.S. Nuclear Regulatory Commission (1989) Severe accident risks: an assessment for five U.S. nuclear plants, NUREG-1150. U.S. Nuclear Regulatory Commission, Washington, DC
U.S. Nuclear Regulatory Commission (NRC). www.nrc.gov. Accessed 6 July 2011
Vendryes GA (1977) Superphénix: a full-scale breeder reactor. Sci Am 236:26–35
World Nuclear Association (WNA). http://www.world-nuclear.org/info/reactors.html; Advanced Nuclear Power Reactors. http://www.world-nuclear.org/info/inf08.html; Generation IV Nuclear Reactors. http://www.world-nuclear.org/info/inf77.html; Fast Neutron Reactors. http://www.world-nuclear.org/info/inf98.html; Small Nuclear Power Reactors. http://www.world-nuclear.org/info/inf33.html. Accessed 6 July 2011

Chapter 5
Nuclear Fuel, Reprocessing of

Michael F. Simpson and Jack D. Law

Glossary

Actinides	All elements including and beyond actininium ($Z > 89$) in the periodic table. In spent fuel, the major actinides of interest are uranium, plutonium, neptunium, americium, and curium.
Cathode processor	A high-temperature vacuum distillation furnace used to separate salt from metallic actinides deposited on an electrorefiner cathode.
Centrifugal contactors	Liquid–liquid extraction equipment used for aqueous solvent extraction that consists of a spinning rotor to intensely mix the different phases.
Ceramic waste	The glass-bonded sodalite matrix used to encapsulate waste salt from electrorefiner operation.
COEX™	French process for coextracting uranium and plutonium using extraction methods similar to PUREX.
Electrorefiner	An electrochemical system used to separate actinides from spent fuel using a molten salt electrolyte.

This chapter was originally published as part of the Encyclopedia of Sustainability Science and Technology edited by Robert A. Meyers. DOI:10.1007/978-1-4419-0851-3

M.F. Simpson (✉) • J.D. Law
Fuel Cycle Science and Technology Division, Idaho National Laboratory,
Idaho Falls, ID 83415, USA
e-mail: Michael.Simpson@INL.gov; Jack.Law@INL.gov

N. Tsoulfanidis (ed.), *Nuclear Energy: Selected Entries from the Encyclopedia of Sustainability Science and Technology*, DOI 10.1007/978-1-4614-5716-9_5,

Experimental Breeder Reactor-II	A sodium-cooled, fast test reactor operational at Argonne National Laboratory-West from 1963 to 1994.
Geologic repository	A permanent nuclear waste disposal site located deep within a geological formation.
Metal waste	The stainless steel–zirconium matrix used to encapsulate cladding hulls and noble metals left in anode baskets after U electrorefining is completed.
Mixer-settler	Liquid–liquid extraction equipment used for aqueous solvent extraction requiring a relatively large footprint.
Minor actinides	Actinide elements other than U and Pu. In spent fuel, the primary minor actinides of concern are Np, Am, and Cm.
Noble metals	Elements found in spent nuclear fuel that have chloride forms that are thermodynamically less stable than uranium chloride.
Pulsed columns	Liquid–liquid extraction equipment used for aqueous solvent extraction involving a single column consisting of trays of perforated plates to promote interphase mass transport.
Pyroprocessing	Nuclear fuel treatment technology that uses electrochemical reactors with molten salt electrolytes to separate actinides from fission products.
PUREX	Nuclear reprocessing technology that separates actinides from the spent fuel via liquid–liquid extraction involving acidic aqueous and organic liquid phases.
Spent fuel	Nuclear fuel that has gone through at least one irradiation cycle in a nuclear reactor. It contains a mixture of actinides and fission products.
Solvent extraction	A separations method for extracting species from a liquid phase. In this entry, it refers to a process for removing uranium from spent fuel that utilizes dissolution in acid followed by liquid–liquid extraction between aqueous and organic liquid phases.
UREX	A variant of the PUREX process that separates uranium from spent fuel without recovering pure plutonium

V-blender	A v-shaped vessel that is designed to efficiently blend two or more different kinds of powders with or without applied heat.

Objective

The objective of this entry is to give a basic overview of the technology elements behind nuclear fuel reprocessing. It should serve as a starting point for more detailed study with the aid of the Bibliography section to obtain more technical details on this subject. Several more process concepts have been proposed, tested, and demonstrated other than those listed in this entry. For the sake of conciseness, only two fundamentally different technologies have been described here – aqueous and pyrochemical fuel reprocessing. In the case of pyrochemical fuel reprocessing, focus has been placed on the LiCl-KCl electrorefining technology developed originally at Argonne National Laboratory. The overall scope of nuclear fuel reprocessing technology is too broad to cover in this entry.

Introduction

Nuclear reprocessing is the chemical treatment of spent fuel involving separation of its various constituents. Principally, it is used to recover useful actinides from the spent fuel. Radioactive waste that cannot be reused is separated into streams for consolidation into waste forms. The first known application of nuclear reprocessing was within the Manhattan Project to recover material for nuclear weapons. Currently, reprocessing has a peaceful application in the nuclear fuel cycle. A variety of chemical methods have been proposed and demonstrated for reprocessing of nuclear fuel. The two most widely investigated and implemented methods are generally referred to as aqueous reprocessing and pyroprocessing. Each of these technologies is described in detail in Sect. 3 with numerous references to published articles.

Reprocessing of nuclear fuel as part of a fuel cycle can be used both to recover fissionable actinides (primarily U and Pu isotopes) and to stabilize radioactive fission products into durable waste forms. It can also be used as part of a breeder reactor fuel cycle that could result in an almost 70-fold increase in energy utilization per unit of natural uranium [1]. Reprocessing can also impact the need for geologic repositories for spent fuel. The volume of waste that needs to be sent to such a repository can be reduced by first subjecting the spent fuel to reprocessing. The extent to which volume reduction can occur is currently under study by the US Department of Energy via research at various national laboratories and universities. Reprocessing can also separate fissile and nonfissile radioactive elements for transmutation.

The current known reserves of uranium that can be economically harvested are 5.5 million metric tons U at a maximum market price of about $80/lb. At the current usage rate of 65,000 metric tons U/year, this quantity of uranium will last for about 85 years [2]. However, nuclear power expansion in India, China, and other countries will soon lead to a substantial increase in the global usage rate for uranium. Increased investment in uranium exploration will undoubtedly reveal additional recoverable resources. And the inevitable increase in cost of uranium will lead to a higher fraction of economically recoverable resources. Reprocessing of spent fuel and use in light water reactors can also serve to improve efficiency of uranium resource utilization. Estimates range from about 10% to 30% for reduction of natural uranium usage as a result of reprocessing spent fuel and reuse in nonbreeding reactors.

Reprocessing Technology

Aqueous Reprocessing

General Description

With this technology, nuclear fuel is dissolved into an acidic solution. The resulting solution is then chemically processed to separate the metals of interest, typically uranium and/or plutonium. Minor actinides as well as other fission products may also be separated using advanced aqueous processes. Specific unit operations utilized in the past primarily consist of precipitation and liquid–liquid extraction. Precipitation was the primary method used in the defense industry initially for the production of plutonium. Liquid–liquid extraction was later developed as an improved method for reprocessing in the defense industry and also became the primary method of reprocessing of commercial nuclear fuel internationally. Since the vast majority of aqueous reprocessing applications continue to utilize liquid–liquid extraction, this will be the primary focus of discussion in this entry.

Liquid–liquid extraction (also called solvent extraction) was initially utilized in the petroleum industry beginning in the 1930s. It has since been utilized in numerous applications including petroleum, hydrometallurgical, pharmaceutical, and nuclear industries. Liquid–liquid extraction describes a method for separating components of a solution by exploiting an unequal distribution of the component(s) between two immiscible liquid phases. In most cases, this process is carried out by intimately mixing the two immiscible phases, allowing for the selective transfer of solute(s) from one phase to the other, then allowing the two phases to separate. Typically, one phase will be an aqueous solution, usually containing the component (s) to be separated, and the other phase will be an organic solvent, which has a high affinity for some specific components of the solution. The process is reversible by contacting the solvent loaded with solute(s) with another immiscible phase that has

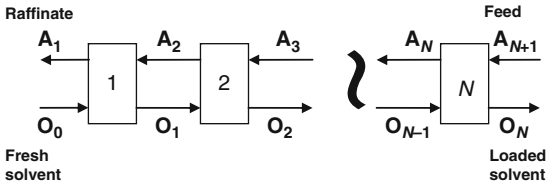

Fig. 5.1 Countercurrent multistage extraction process flow diagram

a higher affinity for the solute than the organic phase. The transfer of solute from one phase into the solvent phase is referred to as extraction and the transfer of the solute from the solvent back to the second (aqueous) phase is referred to as back-extraction or stripping. The two immiscible fluids must be capable of rapidly separating after being mixed together, and this is primarily a function of the difference in densities between the two phases.

While limited mass transfer can be completed in a single, batch equilibrium contact of the two phases, one of the primary advantages of liquid–liquid extraction processes is the ability to operate in a continuous, multistage countercurrent mode. This allows for very high separation factors while operating at high processing rates. Countercurrent operation is achieved by repeating single-stage contacts, with the aqueous and organic streams moving in opposite directions as shown in Fig. 5.1.

In this flow diagram, the aqueous feed stream containing the solute(s) to be extracted enters at one end of the process (A_{N+1}), and the fresh solvent (organic) stream enters at the other end (O_0). The aqueous and organic streams flow countercurrently from stage to stage, and the final products are the solvent loaded with the solute(s), O_N, leaving stage N and the aqueous raffinate, A1, depleted in solute(s) and leaving stage 1. In this manner, the concentration gradient in the process remains relatively constant. The organic at stage O_0 contains no solute(s), while the raffinate stream is depleted of solute(s). Streams A_{N+1} and O_N contain the highest concentration of the solute(s).

For the process to be economical, the solvent must be recycled. In order to recycle the solvent, the solute is subsequently stripped from the solvent, and the solvent is then recycled back to the countercurrent extraction process. This allows the solvent to be recycled indefinitely, until it has degraded (due to acid hydrolysis or radiolytic degradation) or the solvent composition has changed due to solubility in the aqueous phase and/or evaporation.

History of Aqueous Separation Technology

Aqueous separations processes for nuclear reprocessing evolved from early US defense programs for the separation of Pu for weapons manufacture. The bismuth phosphate process began operation at the Hanford Nuclear Reservation in 1944 for the separation of Pu from irradiated slugs from the B reactor [3]. The first continuous solvent extraction reprocessing plant replaced the bismuth phosphate process at Hanford in 1952. This facility used the reduction oxidation (REDOX) process to separate Pu. The REDOX process utilized methyl isobutyl ketone as an extractant.

In the REDOX process, uranium and plutonium nitrate is preferentially extracted from the fission products in a high salting strength aqueous solution [4, 5]. The uranium and plutonium are then selectively stripped from the solvent by adjusting the valence state of the Pu to back-extract it and use a low salting strength strip solution to back-extract U. Additional cycles of extraction were used to decontaminate the products. General Electric's Knolls Atomic Power Laboratory developed the PUREX process in the 1950s. PUREX-based operations at Savannah River F Canyon began in 1954 and replaced the REDOX process at Hanford in 1956 [3]. The PUREX process became the standard method of reprocessing used nuclear fuel throughout the world.

PUREX Process Technology

PUREX-based reprocessing consists of leaching the spent fuel from the cladding using a nitric acid solution, chemical adjustment and filtration of the resulting feed solution, several cycles of solvent extraction to separate and purify the uranium and plutonium, solidification of the resulting uranium and/or plutonium product, as well as the waste solutions. The plutonium oxide product, with or without uranium, is then recycled as mixed oxide (MOX) fuel. This resulting MOX fuel can be used as an alternative to low-enriched uranium in light water reactors. MOX fuel is widely used in Europe, and there are plans for use in Japan. About 40 reactors in Europe (Belgium, Switzerland, Germany, and France) are licensed to use MOX fuel [6]. Existing aqueous commercial reprocessing facilities throughout the world utilize, primarily, the PUREX solvent extraction process or a variant of this process to accomplish the separation of U and Pu. Pure plutonium can also be separated with this process and used to make nuclear weapons.

The front end of the PUREX process involves mechanical chopping of the spent nuclear fuel assemblies into small pieces (1 cm long) followed by leaching of the spent fuel in a nitric acid solution. The chopped pieces of the pins, as well as spacers and other fittings, must then be separated from the leached fuel solution. This has been performed through the use of perforated baskets that hold the hardware, such as in the batch operations performed at the THORP facility in the UK, or through the use of a continuous dissolver, such as the wheel dissolver at the UP2 and UP3 plants in France which holds the hardware in buckets formed in sections of the wheel as the wheel rotates through the nitric acid solution [7]. The dissolver solution, after further clarification and feed adjustment, is then processed through the use of the PUREX technology to separate and purify the uranium and plutonium from the dissolver product solution.

The PUREX process utilizes 20–40 vol% tributyl phosphate in a hydrocarbon diluent to extract uranium and plutonium from the acidic solution resulting from the dissolution of spent nuclear fuel. In general, metals in the +4 and +6 oxidation state are extracted in the PUREX process. The chemical equilibria for U (VI) in a nitrate media is

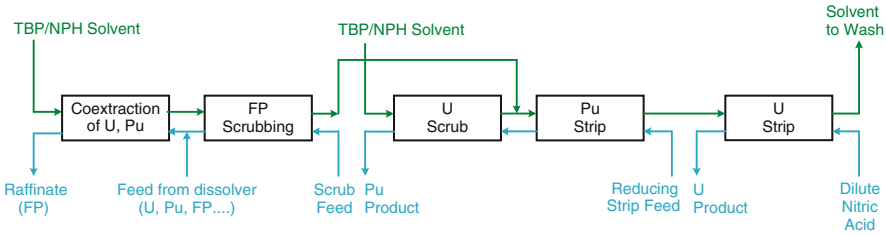

Fig. 5.2 Typical PUREX first cycle flowsheet

$$UO_2{}^{2+} + 2NO_3{}^{-} + 2TBP \Leftrightarrow UO_2(NO_3)_2 \cdot 2TBP \tag{5.1}$$

The chemical equilibria for the actinides in the +4 oxidation state is

$$An^{4+} + 4NO_3{}^{-} + 2TBP \rightleftharpoons An(NO_3)_4 \cdot 2TBP \tag{5.2}$$

Plutonium maintained in the +4 oxidation state is, therefore, coextracted with the U. Pu (III) and other actinides and lanthanides in the +3 or lower oxidation state are not extracted in the PUREX Process. Neptunium, if maintained in the +6 oxidation state, can be coextracted with the U and Pu. The strong extraction of the +4 and +6 oxidations states, along with the weak extraction of the other oxidations states, results in the effective use of the PUREX process for separation of uranium and plutonium from nearly all of the other metals present in the spent nuclear fuel.

A typical PUREX process first extraction cycle is provided in Fig. 5.2. The solution resulting from the dissolution of the spent nuclear fuel is the feed to the coextraction section of the flowsheet. The aqueous feed flows countercurrent to the PUREX solvent, and the U and Pu are extracted by the TBP into the normal paraffin hydrocarbon (NPH) organic phase. The loaded organic phase enters the fission product (FP) scrub section in which a nitric acid scrub solution (approx. 2 M HNO_3) is used to remove coextracted fission products, such as Zr and Ru, from the solvent. The scrub solution containing the Zr and Ru combines with the feed solution entering the extraction section. The solvent then enters a Pu strip section in which the Pu is back-extracted from the organic phase. This is accomplished by reducing the Pu from the extractable +4 oxidation state to the inextractable +3 state. A strip solution containing a reductant, such as hydroxylamine nitrate, U (IV), or ferrous sulfamate, is typically used [8].

Reduction and back-extraction of the Pu also results in back-extraction of a portion of the uranium. The strip product from the Pu strip section therefore enters a uranium scrub section in which the Pu strip solution is contacted with a fresh solvent feed to reextract this uranium into the organic phase. The organic phase containing the reextracted U combines with the loaded solvent from the extraction section which enters the Pu strip section. Once the Pu has been back-extracted from the PUREX solvent, the solvent enters the uranium strip section, which utilizes dilute nitric acid (typically 0.01 M HNO_3) at elevated temperature to back-extract the U into the aqueous phase.

The resulting solutions from the first cycle PUREX extraction process include a solvent solution that is washed with a carbonate or hydroxide solution to remove degradation products and recycled back to the extraction section, a raffinate stream which is depleted of the U and Pu and disposed of as waste, and the Pu and U product streams. The U and Pu product streams are typically further processed with additional PUREX cycles to purify these streams [9].

PUREX Process Waste Treatment

The separation of the Pu and U from spent nuclear fuel results in a high-level waste (HLW) requiring immobilization and storage. The immobilization technology currently in use in the UK, France, and Japan is vitrification of the waste to form a stable borosilicate glass waste form suitable for long-term storage [10]. The glass waste produced is poured into canisters and are stored until long-term geological storage is available. Appropriate geological repositories are currently being pursued in these countries. Low (LLW) and intermediate-level wastes (ILW) are also generated from aqueous reprocessing and require treatment and disposal.

Advanced Aqueous Separations Process Technology

Advanced aqueous separations processes are being developed throughout the world including the USA, France, UK, Japan, Russia, and China. The goals of the development of advanced aqueous processes include closing the nuclear fuel cycle and reducing the proliferation risk of the technologies. Reduction in proliferation risk is being addressed through development of modified PUREX processes which do not separate pure plutonium. In addition, advanced separation processes are being developed to separate the actinides for reactor recycle to close the fuel cycle.

Advanced Aqueous Reprocessing Strategies

Numerous strategies are being developed internationally for advanced aqueous reprocessing processes. The goals of these processes typically are to accomplish separations beyond the Pu and U that is separated with the PUREX process in order to reduce the volume, radiotoxicity, and heat generation of the spent nuclear fuel. The components targeted include the minor actinides as a group, the short-lived fission products (Cs and Sr), and/or individual actinides, such as Am. The minor actinides or Am separated from the spent fuel would be recycled for burning in a fast reactor. If separated, the Cs and Sr could be placed into decay storage.

A wide variety of advanced processes are currently being developed to accomplish these advanced separations. Major research efforts on advanced processing are ongoing in France, Japan, UK, USA, China, and Russia [11–17]. These technologies are at various stages of maturity, and none have been implemented into full-scale reprocessing facilities to date.

Advanced aqueous processing has the potential to significantly reduce the volume, heat load (long and short-term), and radiotoxicity of HLW requiring disposal in a geological repository [18]. These processes, however, will result in the generation of a significant quantity of LLW requiring treatment and disposal. These wastes include spent solvent, solvent treatment solutions, and decontamination solutions, among others. Additionally, solid waste is generated from facility operations (e.g., gloves, shoe covers, cleaning supplies, filters) and will require treatment and disposal.

The primary focus of recent development of advanced PUREX processes is to prevent the separation of pure Pu, thus reducing proliferation risk, as well as controlling Np and Tc chemistry to allow for the extraction of these metals.

In France, the COEX™ process is being developed which coextracts the U and Pu and produces a Pu/U product instead of a pure Pu product [19]. This is accomplished by adjusting the chemistry of the PUREX process to allow some U to be back-extracted from the solvent with the Pu. The process also uses a coconversion process to produce a (Pu, U) oxide product. Coextraction of Np is also being evaluated with the COEX™ process to produce a (Pu, U, Np) oxide product [19]. The Rokkasho reprocessing plant in Japan, which has been constructed and is currently undergoing operational testing, also uses a PUREX process that has been modified to combine uranium with the separated plutonium in a 50/50 mix prior to denitration [20]. In the USA, the uranium extraction (UREX) process has been developed which separates the uranium from spent nuclear fuel. The UREX process is a modification of the PUREX process in which the Pu is prevented from extracting with the U by adding acetohydroxamic acid as a reductant/complexant [21, 22].

Aqueous Reprocessing Equipment

The solvent extraction equipment utilized for industrial-scale aqueous reprocessing must enable continuous processing at high throughputs while efficiently mixing and separating the two phases. In the nuclear industry, specific constraints, such as remote operation and maintenance, must be considered, since the solutions processed are highly radioactive. There are three basic types of equipment used in industrial-scale nuclear solvent extraction processes: mixer-settlers, columns, and centrifugal contactors. A detailed description of the three types of equipment follows.

Mixer-Settlers. This equipment consists of a small mixing chamber followed by a larger gravity-settling chamber as shown in Fig. 5.3. Each mixer-settler unit provides a single stage of extraction. The two phases enter the mixing section where they are mixed using an impeller. The two-phase solution flows into the settling section where the phases are allowed to separate by gravity due to their density differences. Typical mixer settlers have mixing times on the order of a few minutes and settling times of several minutes. The separate phases exit the settling section by flowing over a weir (less dense phase – typically organic) or through an underflow then over a weir (more dense phase – typically aqueous). The

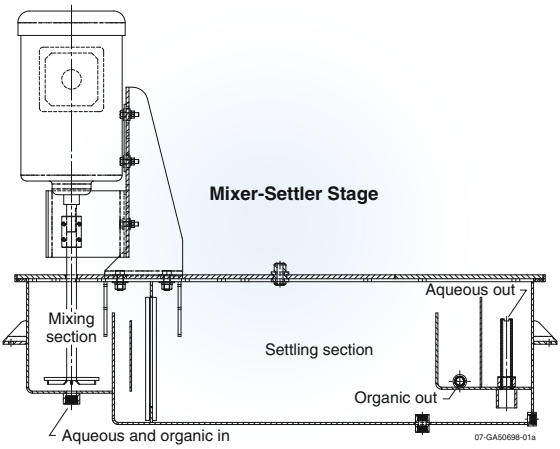

Fig. 5.3 Diagram of a mixer-settler

separation interface is controlled by the height of the weirs on the outlets of the settler section. Only minimal instrumentation is required, and mechanical maintenance is limited to occasional mixing motor replacement. In a countercurrent process, multiple mixer settlers are installed with mixing and settling chambers located at alternating ends for each stage (since the outlet of the settling sections feed the inlets of the adjacent stage's mixing sections).

Mixer-settlers are best suited for use when a process requires longer residence times and when the solutions are easily separated by gravity. They require a large facility footprint, but do not require much headspace and need limited remote maintenance capability for occasional replacement of mixing motors [23, 24].

Columns. There are two basic types of columns employed industrially, packed columns and pulse columns with plates or trays. Packed columns are filled with some type of packing material, such as Raschig rings, to create a tortuous path for the two solutions as they flow through the column (typically aqueous feed downward and solvent upward), ensuring that the two phases are in constant contact. Packed columns have no moving parts and are relatively simple to operate, but they are not very efficient. Since columns do not have discrete stages, such as mixer-settlers or centrifugal contactors, the number of stages is determined by the height equivalent of a theoretical stage (HETS) [25]. For most packed columns, this HETS of extraction is usually several feet, meaning that a countercurrent process utilizing several stages to effect a given separation factor would require very tall columns. To reduce the height of a theoretical stage in the column, other packing (trays or perforated plates) is used and mechanical energy is applied to force the dispersed phase into smaller droplets, improving mass transfer. The most common type of column used today, particularly in the nuclear industry, is the pulse column.

In a pulse column, liquids are continuously fed to the column and flow counter – currently, as is done with a packed column; but mechanical energy is applied to pulse the liquids in the column up and down. This is normally done by injecting

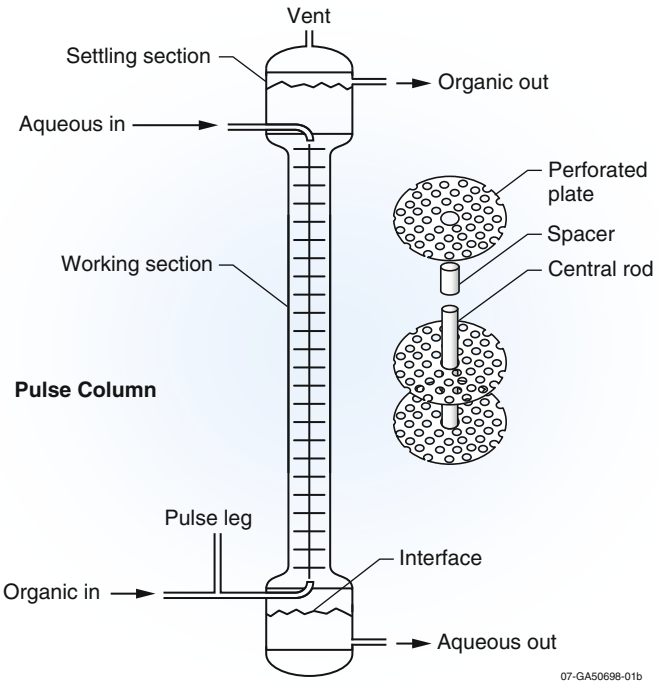

Fig. 5.4 Pulse column with perforated plates

pressurized air into a pulse leg that pushes liquid into the column, then venting the pulse leg to fill the pulse leg with solution from the column. The pulse action lifts and lowers the solution in the column, usually only a few inches. The column is filled with perforated plates or other plates to promote droplet formation as the dispersed phase is pushed through the plates. This pulsing action reduces droplet size of the dispersed phase and improves mass transfer. A perforated plate pulse column is shown in Fig. 5.4. There are a number of plate designs used. Early pulse columns used sieve plates, which are flat plates with holes drilled into them. A more effective plate is the nozzle plate, which has different contours on the top and bottom of the plate (making it directional, in that, it must be configured according to the continuous phase in the column). The French and Japanese pulse columns employ a disk and doughnut configuration, where the plates are solid (no openings) but the alternating plates enable effective contacting of the phases [25].

The separation interface is controlled during column operation using bubble probes in the disengaging section. The probes are interfaced to a controller that drains heavy phase from the bottom of the column. The bubble probes allow operators to monitor the weight of the column, which gives them a good indication of column performance, by determining the ratio of heavy and light phases in the column. In addition, pulsing devices and pulse speed controllers are required as

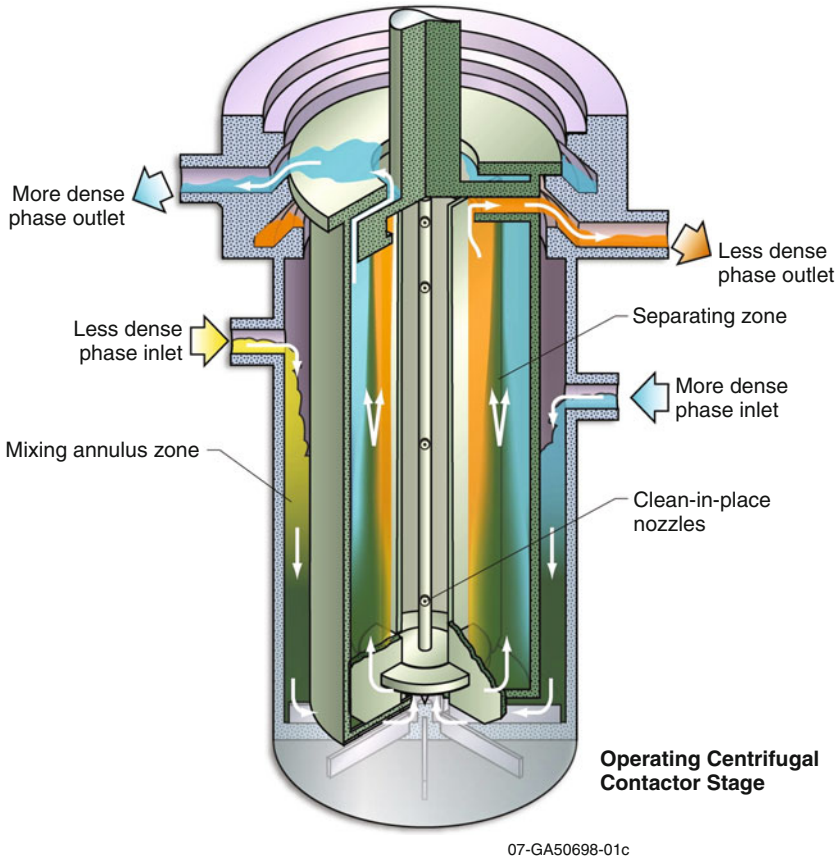

Fig. 5.5 Cutaway view of an operating centrifugal contactor

pulse frequency and amplitude must be controlled during operation. Periodic maintenance is required only for the pulsing equipment, which is located out of cell, above the columns. Pulse columns are used when a process requires intermediate residence times, as adjusting flow rate easily varies residence time. They require a small facility footprint, but do require much headspace (typically 40–50 ft). Pulse columns do not need remote maintenance capability, as all moving parts (pulser equipment) are located outside the shielded cell. Extensive literature has been published on pulse columns [9, 27–29]. Pulse columns are the primary type of aqueous separation equipment utilized in the nuclear industry today.

Centrifugal Contactors. Centrifugal contactors, like mixer-settlers, are discrete-stage units, providing one stage of extraction per unit and are readily linked together as each rotor pumps separated fluids to the next stage inlet in each direction. The primary difference between a centrifugal contactor and a mixer-settler is the separation of the two-phase mixture. Centrifugal contactors employ a spinning rotor that intensely mixes the two phases and separates the two phases inside the rotor where the centrifugal forces can be as high as 300 g. This results in

efficient and fast phase separation. The separated phases exit the contactor by overflow and underflow weirs, similar to a mixer-settler. A cutaway view of an operating centrifugal contactor is shown in Fig. 5.5.

Centrifugal contactors have high single-stage efficiency (routinely greater than 95% of theoretical for chemical processes with rapid kinetics). Process flow interruptions cause no loss of process concentration profiles if centrifugal contactor rotors are kept spinning. Thus centrifugal contactor-based processes can be paused for a period of time sufficient to reestablish flow or even replace a motor without significant loss of product or rework. Centrifugal contactors require minimal instrumentation for process operation. Computer control via commercial software allows monitoring of motor amperage, rotor rpm, inlet flow rates, temperatures, and many other process parameters. Centrifugal contactors are used when a process requires short residence times, on the order of several seconds. They require a small facility footprint and minimal headspace, but they do require remote maintenance capability for periodic removal of the motor and/or rotor.

Centrifugal contactors have been the subject of much recent development work over the past 40 years, while the designs of pulse column and mixer-settlers has changed little over the same time period [30–32]. Early designs included a paddle wheel to mix the phases below the spinning rotor [33]. This precluded removal of the rotor assembly. The annular centrifugal contactor was subsequently developed, which allowed the motor and rotor assembly to be easily removed [34]. Other designs included multistage units, units for low-mix applications (higher phase separation), and clean-in-place units that have an array of internal spray nozzles to facilitate solids removal as necessary [35–37]. Design of remote operation and maintenance capabilities has also continued, resulting in more efficient remote handling [38, 39].

Pyroprocessing

General Description

Pyroprocessing is currently considered an alternative reprocessing technology to the more commonly used aqueous processing technology. Pyroprocessing accomplishes separations by way of high-temperature electrorefining. It is yet to be implemented on a large scale, limited to date to laboratory-scale and engineering-scale experimentation and demonstration. Much of the current state of the art for pyroprocessing was developed during the Integral Fast Reactor (IFR) program, which was carried out at Argonne National Laboratory from about 1984 to 1995 [40, 41]. With the shutdown of Experimental Breeder Reactor-II in 1995, the IFR program was converted into a spent fuel treatment program to safely treat the 25 metric tons of heavy metal from that reactor [42]. Pyroprocessing utilizes molten salt electrolytes as the media rather than acidic aqueous solutions and organic solvents [43]. These electrolytes are principally used to support electrochemical separations such as uranium electrorefining and electrolytic reduction of oxide fuel.

The process includes vacuum furnaces that accomplish salt/metal separations and melt metal deposits into ingots for either waste disposal or fuel fabrication. Ceramic and metal waste streams are generated that immobilize fission products and, optionally, plutonium and minor actinides into high-level waste forms. For eventual commercial implementation, it is expected that plutonium and minor actinides will be recycled and used for fast reactor fuel fabrication. While this technology is yet to reach the commercialization stage, it has been the subject of extensive, government-funded research and development worldwide in addition to the EBR-II spent fuel treatment work in the USA. For example, the Republic of Korea is currently pursuing a strategy of developing pyroprocessing technology for treatment of spent fuel from their commercial light water reactors to minimize volume of HLW and possibly extract fissile actinides for eventual fabrication of fast reactor fuel [44, 45]. Russia has already demonstrated production of MOX based on pyroprocessing and plans to develop a closed fuel cycle using the technology by 2020.

While PUREX and related aqueous reprocessing technology has superior maturity, pyroprocessing does have unique benefits that make it a credible alternative and in some cases a preferred alternative. This includes use of process liquids that are more stable than organics in the presence of high radiation fields, improved criticality safety due to the lack of neutron moderators in the process, and waste processing that is integrated with the separations flowsheet.

Process Technology

There are many variants of the pyroprocessing flowsheet, but the IFR scheme shown in Fig. 5.6 can be used as a reference, as it contains all of the key unit operations.

The electrorefiner is at the center of the flowsheet and is used to perform the primary separation of actinides from fission products [46, 47]. It contains a molten salt electrolyte – typically LiCl-KCl-UCl_3 maintained at 450–500°C. The eutectic composition of LiCl-KCl (44.2 wt% LiCl, 55.8 wt% KCl) is maintained to keep the melting point at approximately 350°C. The UCl_3 content varies depending on desired operating conditions from about 0.5–10 wt%. It is used as a charge carrier for electrotransport through the electrolyte. After the spent fuel is chopped into segments, it is loaded into anode baskets, and the baskets are lowered into the electrorefiner. As current is passed between the anode and cathode, U metal is oxidized to U^{3+} at the anode and reduced back to metallic form at the steel cathode. The deposit contains high purity uranium and is typically dendritic. An example of a U cathode deposit is shown in Fig. 5.7.

Transuranic (TRU) elements and active metal fission products are oxidized electrochemically or via reaction with uranium chloride in the salt and enter the electrolyte. Under normal conditions, Pu and minor actinides cannot deposit at the cathode, because their back-reaction with UCl_3 is thermodynamically spontaneous. However, codeposition of U and TRU can be achieved via a combination of elevating the TRU to U ratio in the salt and utilizing a liquid cadmium cathode (LCC). In the molten cadmium phase, TRU elements have a very low activity

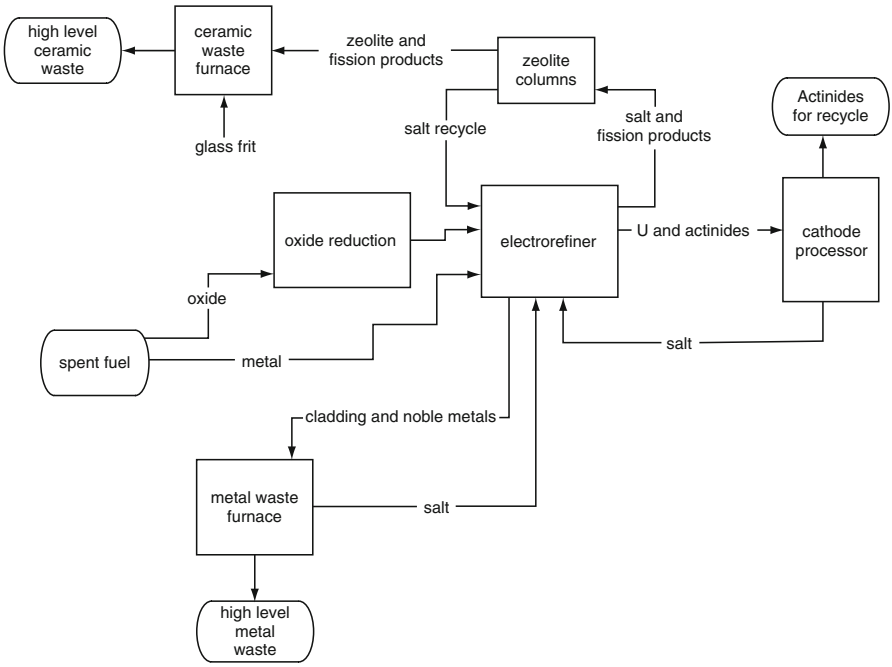

Fig. 5.6 Fuel Processing Flowsheet for the Integral Fast Reactor Program

coefficient compared to U. This allows for TRU metals to be present in quantities comparable to that of uranium in the cadmium. Alternative methods are currently being investigated to corecover U and TRU without the need for an LCC.

Fission product elements segregate between the anode basket and the molten salt during the electrorefining process. Noble metals such as Tc, Ru, and Rh remain with the cladding hulls in the anode basket. Active metals that typically include Group I and II elements in addition to lanthanides are oxidized to chloride form and accumulate in the salt. If sodium metal is used as a bonding agent, as in the case of EBR-II fuel, this sodium is oxidized to sodium chloride, which accumulates in the ER electrolyte.

Note in Fig. 5.6 that both metal fuel and oxide fuel can be treated via pyroprocessing. Treatment of metallic fuel is relatively straightforward due to the fact that it is already in a state compatible with the ER. Oxide fuel must first be converted to metallic form. This can be accomplished in an oxide reduction step. Various methods have been investigated for reducing spent oxide fuel. Early efforts were focused on chemical reduction via lithium. Similar to electrorefining, a molten salt is used for carrying out this reaction. In this case, it is LiCl saturated with lithium metal at 650°C. The lithium reduction reaction is as follows [47].

$$4Li + UO_2 \rightarrow 2Li_2O \tag{3}$$

Fig. 5.7 Dendritic uranium deposit on electrorefiner cathode

More recently, a similar process based on electrochemical reactions has been favored for development. It also uses a vessel containing molten LiCl at 650°C, but it contains lithium oxide in the salt rather than lithium metal. The reactions for the electrolytic process are shown below [49].

$$UO_2 + 4e^- \rightarrow U + 2O^{2-} 2O^{2-} \rightarrow O_2 + 4e^- \tag{5.4}$$

The generated oxygen bubbles out of the salt as a gas and can be sent to an off-gas treatment system to remove any entrained or volatile contaminants. The advantages of the electrolytic method based on the above reactions are that lithium oxide concentration in the molten salt can be kept low (1 wt%), and there is no need for a separate vessel to regenerate lithium metal from lithium oxide.

U or U/TRU product deposited on the cathode in the electrorefiner is transferred to a cathode processor, which is essentially a vacuum distillation furnace. The salt is separated from the metals and recycled to the electrorefiner. The purified metals can be fed into a process for fabricating metallic fuel for fast reactors. For the case of the EBR-II Spent Fuel Treatment process, the cathode processor operates at a temperature up to 1200°C and achieves pressures less than 1 torr.

After an electrorefining run, the anode basket contains the cladding hulls, undissolved actinides, inert fuel matrix material such as zirconium, adhering salt, and noble metal fission products such as Tc, Mo, Rh, and Ru. All of this material is removed from

the anode baskets and loaded into an inductively heated vacuum distillation furnace that is used to distill adhering salt and consolidate the metals into an ingot. The metal ingot becomes a waste form that has been tested and shown to be suitable for disposal in an HLW repository [50, 51].

Electrorefiner salt becomes progressively more contaminated with fission product chlorides as well as sodium chloride in the process of treating fuel. Once the contamination level has exceeded a predetermined limit, the salt must be removed from the electrorefiner and either disposed or processed through a purification step and returned to the electrorefiner. The basis for that limit can be fission product decay heat, salt melting point, or criticality limits. Another potential limiting factor is contamination of the metallic actinide products recovered in the cathode processor. High concentrations of rare earth fission products in the salt, for example, have been shown to lead to high rare earth contamination levels in the actinide product. The process flow sheet shown in Fig. 5.6 includes zeolite ion exchange columns for achieving this salt purification. Zeolite-A has been shown to exhibit selectivity for the fission product ions when in contact with molten chloride salt [52–55]. Other alternatives that have been considered for treating the salt to remove fission products and other contaminants include selective precipitation, zone freeze refining, and adsorption by nonzeolitic materials [56].

The current baseline technology for dealing with the salt waste from electrorefining EBR-II spent fuel is to nonselectively immobilize the salt into a ceramic waste form consisting of glass-bonded sodalite [57, 58]. In this process, salt is removed from the electrorefiner, sized via crushing and milling to a fine particulate, and absorbed into zeolite-4A in a high-temperature blending operation. A V-blender capable of heating and mixing particulate material to 500°C is used for this absorption step. Prior to being loaded into the V-blender, it is necessary to dry the zeolite to less than 1 wt% water. This drying is used to maximize salt absorption in the zeolite while minimizing evolution of water vapor in a high-temperature, corrosive environment. Drying the zeolite should also minimize pores in the final ceramic waste form. Zeolite drying is accomplished via mechanically fluidizing the zeolite under vacuum at temperatures up to 550°C [57, 58]. Heating the zeolite-4A to temperatures of 600°C or higher has been determined to cause structural damage that inhibits its ability to absorb salt [59]. Final consolidation into the ceramic waste form occurs after borosilicate glass binder has been mixed with the salt-loaded zeolite, loaded into a steel canister, and heated to a maximum temperature of 915–950°C. During the process of consolidation, the zeolite-A phase converts to sodalite. In the glass-bonded sodalite waste form, the fission products are distributed between the glass and sodalite phases [60].

If an ion exchange process with zeolite-A has been used to selectively remove fission products from the salt, the resulting fission product-loaded zeolite-A can be similarly converted into a glass-bonded sodalite ceramic waste form. Zeolite-A used for ion exchange is typically in pelletized form and must be milled to a fine particulate prior to blending with additional dried zeolite-4A and borosilicate glass. The flowsheet shown in Fig. 5.6 includes zeolite ion exchange followed by conversion of this zeolite into the ceramic waste form.

Future Directions

In the USA, the current focus is on research and development into both aqueous reprocessing and pyroprocessing technology to support a future decision on closing the fuel cycle. The US Department of Energy (2009) has established the Fuel Cycle Research and Development program for carrying out this research in national laboratories and universities. At this time, there are no large-scale demonstration projects planned. Meanwhile, plans to open a geologic repository for spent nuclear fuel and waste in Nevada's Yucca Mountain have been suspended. The government has commissioned a study to evaluate alternative options for disposal of the spent fuel and waste.

In Japan, the main option for reprocessing spent nuclear fuel is based on aqueous process technology. The Rokkasho plant based on such technology is currently operational with a design capacity of 800 tons of spent light water reactor fuel per year, extracting up to 8 tons of plutonium per year for MOX fuel production. Pyroprocessing is considered an option for fast reactors once they have been included in the Japanese energy fleet. A commercial fast reactor is not planned for completion in Japan until about 2050.

In France, advanced aqueous processing technologies are being developed and assessed to support future recycling of Am and Cm or the minor actinides together with U and Pu to fast reactors. Pilot-scale demonstration is planned within the next decade with a goal of industrial deployment to support the deployment of Generation IV fast reactors. France is also in the process of selecting a site for a geological repository for disposal of HLW with a goal to open the repository in 2025. Research related to the study of geological formations and the capacity as a deep geological repository for HLW is being conducted at the Meuse/Haute Marne Underground Research Laboratory located in Bure, France.

Russia is currently reprocessing spent fuel from civilian power reactors as well as spent HEU fuel from naval and other reactors at Mayak's RT-1 aqueous reprocessing plant. The Experimental-Demonstration Center (EDC), which will be a 100 metric tons/year pilot facility for evaluation of the fuel cycle based on modified PUREX extraction technology, is currently being designed. This facility will also be used to develop other advanced processing technologies for processing used fuel from thermal reactors. The current goal is to support completion of a new aqueous reprocessing facility around 2025. Research is also actively being performed relative to pyroprocessing technologies for the processing of spent fuel from future fast reactors. To this end, the Multipurpose Pyroprocessing Complex (MPC) is being designed at the Research Institute of Atomic Reactors (RIAR) to support molten salt processing development at a capacity of up to 2,500 kg fast reactor used fuel per year.

In South Korea (Republic of Korea), on-site wet storage capacity for spent nuclear fuel at its twenty operating nuclear power plants is rapidly approaching current limits. In December 2008, Atomic Energy Commission of South Korea decided to develop a closed fuel cycle associated with pyroprocessing and sodium

fast reactors (SFR) with metallic fuels. A demonstration SFR is planned to operate from 2030 initially with U-Zr metal fuels and later with recycled U/TRU/Zr metal fuels produced from pressurized water reactor (PWR) spent nuclear fuel in a pyroprocessing facility that is planned to be operated from 2025. Pyroprocessing technology research and development continues at Korea Atomic Energy Research Institute with plans to build an engineering scale facility by 2016. Aqueous reprocessing technology is currently not being actively studied and is not considered a candidate for commercialization in the Republic of Korea. The lack of a high-level waste repository is another problem faced by the country due to severely limited land resources. Waste minimization is, thus, a major objective with pyroprocessing technology research and development in South Korea.

Bibliography

1. Cochran RG, Tsoulfanidis N (1993) The nuclear fuel cycle: analysis and management, 2nd ed. American Nuclear Society, Washington, p. 214
2. OECD, IAEA (2008) Uranium 2007: resources, production, and demand. Nuclear Energy Agency, Washington, June 2008
3. Gray LW (1999) From separations to reconstitution – A short history of plutonium in the US and Russia. Lawrence Livermore National Laboratory, UCRL-JC-133802
4. Evans TF, Tomlinson RE (1954) Hot semiworks REDOX studies, Hanford Atomics Products Operations, HW-31767
5. (1951) REDOX technical manual, Hanford Works, HW-18700
6. Hore-Lacy I (2009) Mixed oxide fuel (MOX). World Nuclear Association (Content Partner); Cutler J Cleveland (Topic Editor). In: Cutler J (ed) Encyclopedia of earth. Environmental Information Coalition, National Council for Science and the Environment, Cleveland/ Washington, DC
7. Denniss IS, Jeapes AP (2001) Reprocessing irradiated fuel. In: Wilson PD (ed) The nuclear fuel cycle: from ore to wastes. Oxford University Press, Oxford, p 120
8. Poczynajlo A (1988) Studies on reductive back extraction of plutonium in PUREX process. J Radioanal Nucl Chem 125(2):445–465
9. Long JT (1967) Engineering for nuclear fuel reprocessing. Gordon Breach Sci Publ, New York
10. Petitjean V, Fillet C, Boen R, Veyer C, Flament T (2002) Development of vitrification process and glass formulation for nuclear waste conditioning, Proceedings of Waste Management 2002. Tucson, AZ USA
11. Spent Fuel Reprocessing Options (2008) International Atomic Energy Administrations, IAEA-TECDOC-1587, Vienna, Austria 2008
12. Boullis B (2008) Future nuclear fuel cycles: prospects and challenges. In: Bruce Moyer (ed) Solvent Extraction: fundamentals to industrial applications, Proceedings of ISEC 2008 International Solvent Extraction Conference, vol 1., pp 29–42
13. Nash K (2008) Key features of the TALSPEAK and similar trivalent actinide-lanthanide partitioning processes. In: Bruce Moyer (ed) Solvent extraction: fundamentals to industrial applications, Proceedings of ISEC 2008 International Solvent Extraction Conference, vol 1., pp 511–519
14. Laidler J (2008) An overview of spent-fuel processing in the Global Nuclear Energy Partnership. In: Bruce Moyer (ed) Solvent extraction: fundamentals to industrial applications, Proceedings of ISEC 2008 International Solvent Extraction Conference, vol 1., pp 695–701

15. Riddle C, Baker J, Law J, McGrath C, Meikrantz D, Mincher B, Peterman D, Todd T (2005) Development of a novel solvent for the simultaneous separation of strontium and cesium from acidic solutions. Sovent Extr Ion Exch 23(3):449–461
16. Christiansen B, Apostolidis C, Carlos R, Courson O, Glatz JP, Malmbeck R, Pagliosa G, Römer K, Serrano-Purroy D (2004) Advanced aqueous reprocessing in P&T strategies: process demonstrations on genuine fuels and targets. Radiochim Acta 92:475–480
17. Miguirditchian M, Chareyre L, Hérès X, Hill C, Baron P, Masson M (2007) GANEX: adaptation of the DIAMEX-SANEX process for the group actinide separation, Proceedings of GLOBAL 2007 Advanced Nuclear Fuel Cycles and Systems. Bosie, Idaho
18. Wigeland R, Bauer T, Fanning T, Morris E (2006) Separations and transmutation criteria to improve utilization of a geologic repository. Nuclear Technol 154(1):95–106
19. Drain F, Emin JL, Vinoche R, Baron P (2008) COEX process: cross-breeding between innovation and industrial experience. Proceedings from Waste Management 2008, Tucson, AZ
20. Katsuta T, Suzuki T (2009) Japan's spent fuel and plutonium management challenge. Energy Policy doi: 10.1016/j.enpol.2009.05.075
21. Pereira C, Vandegrift G, Regalbuto M, Bakel A, Bowers D, Gelis A, Hebden A, Maggos L (2007) Lab-scale demonstration of the UREX+1a process using spent fuel. Proceedings from Waste Management 2007, Tucson, AZ
22. Nuñez L, Vandegrift G (2000) Evaluation of hydroxamic acid in uranium extraction process: literature review, Argonne National Laboratory, ANL00/35.
23. Colven, TJ Jr, (1956) Mixer-Settler development-operating characteristics of a large-scale mixer-seller. Savannah River Laboratory, DP-140
24. Davidson JK, Shafer AC, Haas WO (1957) Application of Mixer-Settlers to the PUREX Process. In: The Symposium on the Reprocessing of Irradiated Fuels, Book 1. United States Atomic Energy Commission, TID-7534
25. Benedict M, Pigford TH, Levi HW (1981) Nuclear chemical engineering. McGraw-Hill, New York, p 210
26. Milot JF, Duhamet J, Gourdon C, Casamatta G (1990) Simulation of a pneumatically pulsed liquid-liquid extraction column. The Chemical Engineering Journal 45:111–122
27. Sege G, Woodfield FW (1954) Chem Eng Progress 50(8)
28. Geier RG (1954) Application of the Pulse Column to the PUREX Process. USACC, Report TID-7534
29. Richardson GL, Platt AM (1961) Progress in nuclear energy, Series IV, Technology engineering and safety, vol 4. Pergammon Press, New York
30. Leonard RA (1988) Recent advances in centrifugal contactor design. Separation Sci Technol 23:12–13
31. Jubin RT et al (1988) Developments in centrifugal contactor technology. Oak Ridge National Laboratory, ORNL/TM-10768
32. Meikrantz DH, et al (2001) Annular Centrifugal Contactors for Multiple Stage Extraction Processes. Chem Eng Comm 188: 115–127
33. Watts C (1977) Solvent Extraction Equipment Evaluation Study – Part 2. Battelle Northwest Laboratory, BNWL-2186 Pt. 2
34. Bernstein GL et al (1973) A high-capacity annular centrifugal contactor. Nuclear Technol 20
35. Drain F et al (2003) Forty years of experience with liquid-liquid extraction equipment in the nuclear industry. Proceedings from Waste Management Conference 2003, Tucson, AZ
36. Meikrantz DH et al (1996) Rotor sleeve for a centrifugal separator. U.S. Patent # 5,571,070
37. Macaluso LL, Meikrantz DH (1999) Self-cleaning rotor for a centrifugal separator. U.S. Patent # 5,908,376
38. Garn, TG, Meikrantz DH, Law JD (2008) Remote evaluation of a three-stage 5 cm annular centrifugal contactor remote module at the INL. Idaho National Laboratory, INL/EXT-08-13670

39. Meikrantz DH, Garn TG, Law JD, Macaluso LL (2009) Evaluation of a new remote handling design for high throughput annular centrifugal contactors. Idaho National Laboratory INL/EXT-09-16824
40. Chang YI (1989) The integral fast reactor. Nuclear Technol 188(2):129–138
41. Till CE, Chang YI, Hannum WH (1997) The integral fast reactor – an overview. Prog Nuclear Energy 31(1–2):3
42. Benedict RW (1997) EBR-II spent fuel treatment demonstration project. Trans Amer Nuclear Soc 77:75–76
43. Ackerman JP (1991) Chemical basis for pyrochemical reprocessing of nuclear fuel. Industrial Eng Chem Res 30(1):141–145
44. Lee SY et al (2007) A preliminary study on the safeguardability of a Korean Advanced Pyroprocessing Facility (KAPF). Proceedings of Global 2007, Boise, Idaho
45. Lee HS, Hur JM, Ahn DH, Kim IT, Lee JH (2009) Development of Pyroprocessing Technology at KAERI. Proceedings of Global 2009, Paris, France
46. Willit JL, Miller WE, Battles JE (1992) Electrorefining of uranium and plutonium – a literature review. J Nuclear Mater 195(3):229–249
47. Goff KM, Benedict RW (2005) Electrorefining Experience for Pyrochemical Reprocessing of Spent EBR-II Fuel. Proceedings of Global 2005, Tsukuba, Ibaraki (Japan)
48. Karell EJ, Gourishankar KV, Smith JL, Chow LS, Redey L (2001) Separation of actinides from LWR fuel using molten-salt-based electrochemical processes. Nuclear Technology 136:342–353
49. Gourishankar K, Redey L, Williamson M (2002) Electrochemical Reduction of Metal Oxides in Molten Salts. Light Metals 2002, TMS
50. Westphal BR, Keiser DD, Rigg RH, Laug DV (1994) Production of Metal Waste Forms from Spent Fuel Treatment. Proceedings of the DOE Spent Nuclear Fuel Meeting: Challenges and Initiatives, Salt Lake City, Utah; December 13–16, 1994
51. Abraham DP, McDeavitt SM, Park J (1996) Metal waste forms from the electrometallurgical treatment of spent nuclear fuel. Proceedings of the Embedded Topical Meeting on DOE Spent Nuclear Fuel and Fissile Material Management, Reno, Nevada, June 16–20, 1996
52. Pereira C, Hash MC, Lewis MA, Richmann MK, Basco J (1999) Incorporation of Radionuclides from the Electrometallurgical Treatment of Spent Fuel into a Ceramic Waste Form. Materials Research Society Symposium Proceedings 556 (1999), 115–120
53. Ahluwalia RK, Geyer HK, Pereira C, Ackerman JP (1998) Modeling of a zeolite column for the removal of fission products from molten salt. Ind Eng Chem Res 37:145
54. Lexa D, Johnson I (2001) Occlusion and Ion Exchange in the Molten (Lithium Chloride-Potassium Chloride-Alkali Chloride) Salt + Zeolite 4A System with Alkali Metal Chlorides of Sodium, Rubidium, and Cesium. Metallurgical Mater Trans 32B:429
55. Phongikaroon S, Simpson MF (May 2006) two site equilibrium model for ion exchange between multivalent cations and Zeolite-A in a molten salt. AIChE J 52(5):1736–1743
56. Kim EH, Park GI, Cho YZ, Yang HC (2008) A new approach to minimize pyroprocessing waste salts through a series of fission product removal process. Nuclear Technol 162(2):208–218
57. Simpson MF, Sachdev P (2008) Development of electrorefiner waste salt disposal process for the EBR-II spent fuel treatment project. Nuclear Eng Technol 40(3), April 2008
58. Simpson MF, Goff KM, Johnson SG, Bateman KJ, Battisti TJ, Toews KL, Frank SM, Moschetti TL, O'Holleran TP (2001) A description of the ceramic waste form production process from the demonstration phase of the electrometallurgical treatment of EBR-II spent fuel. Nuclear Technol 134:263–277
59. Thomas JL, Mange M, Eyraud C (1971) Molecular Sieve Zeolites-I., R.F. Gould, Ed., Amer Chem Soc (1971), 101:443–449
60. Ebert WE (2005) Testing to evaluate the suitability of waste forms developed for electrometallurgically treated spent sodium-bonded nuclear fuel for disposal in the Yucca Mountain repository. Argonne National Laboratory, ANL-05/43, September 2005

Chapter 6
GEN-IV Reactors

Taek K. Kim

Glossary

Breeding ratio	Ratio of fission atom production to fissile atom destruction during a certain time interval in a nuclear system.
Closed fuel cycle (full recycle)	One of the nuclear fuel cycle options, in which all actinides in the used nuclear fuel are separated and recycled to reduce the radiotoxicity of a geological repository while enhancing uranium utilization.
Energy sustainability	Ability to meet the energy needs of the present generation while enhancing the ability of the future generation. In GEN-IV, the sustainability is measured by utilization of uranium resource without creating any weakness in economics and environmental goals.
GFR	Gas-cooled Fast Reactor, which features a fast reactor and closed fuel cycle.
GIF	Generation IV international forum, which is a cooperative international endeavor organized to carry out the R&D needed to establish the feasibility and performance capabilities of GEN-IV nuclear systems.
LFR	Lead-cooled Fast Reactor, which features a fast reactor and closed fuel cycle.
MSR	Molten Salt Reactor, which features thermal, epithermal, or fast reactor and closed fuel cycle.

This chapter was originally published as part of the Encyclopedia of Sustainability Science and Technology edited by Robert A. Meyers. DOI:10.1007/978-1-4419-0851-3

T.K. Kim (✉)
Nuclear Engineering Division, Argonne National Laboratory, 9700 South Cass Avenue, Argonne, IL 60439, USA
e-mail: tkkim@anl.gov

N. Tsoulfanidis (ed.), *Nuclear Energy: Selected Entries from the Encyclopedia of Sustainability Science and Technology*, DOI 10.1007/978-1-4614-5716-9_6,

Open fuel cycle (once-through cycle)	One of the nuclear fuel cycle options, in which the used nuclear fuel discharged from a nuclear system is stored for some period of time and disposed in a geological repository isolating from environment.
Pyroprocessing	The complete set of operations developed in USA. Integral Fast Reactor program based on the pyrometallurgical and electrochemical processes for recovering actinide elements from the used nuclear fuel and recycling them.
SCWR	Supercritical Water Reactor, which features either thermal or fast reactor and open or closed fuel cycle.
SFR	Sodium-cooled Fast Reactor, which features a fast reactor and closed fuel cycle.
Uranium utilization	Ratio of uranium mass used in a nuclear system for energy generation to the uranium mass required by the nuclear system in a nuclear fuel cycle option.
VHTR	Very-High-Temperature Reactor, which features a thermal reactor and open fuel cycle.

Definition of the Subject

Generation-IV reactors are a set of nuclear reactors currently being developed under international collaborations targeting sustainability, safety and reliability, high economics, proliferation resistance, and physical protection of nuclear energy. Nuclear systems have been developed over a number of decades and have evolved to the third generation from the first generation of prototypes constructed in 1950s and 1960s, via the second generation of the commercial reactors operated world-wide after 1970s. While the third generation nuclear systems are currently proposed to the potential customers and under constructions with significant evolutionary in economics and safety based on lessons learnt through plenty reactor operations, nuclear experts from around the world began formulating the requirements for a generation IV of nuclear systems concerning over energy resource availability, climate change, air quality, and energy security. Six systems have been selected for further R&D as generation IV nuclear systems by Generation IV International Forum (GIF), which is a cooperative international endeavor organized to carry out the R&D needed to establish the feasibility and performance capabilities of Generation IV systems. The six systems are Gas-cooled Fast Reactor, Lead-cooled Fast Reactor, Molten Salt Reactor, Sodium-cooled Fast Reactor, Supercritical-Water Reactor, and Very-High-Temperature Reactor.

Introduction

Nuclear energy systems have evolved up to the third generation: a first generation of prototypes constructed in 1950 and 1960; a second generation of commercial nuclear power plants built from 1970, most of which are in operation today; and a third generation of advanced nuclear reactors, called Generation III/III+, which incorporate technical progress based on lessons learnt through more than 10,000 reactor-years of operation. While the generation III/III+ nuclear systems are currently proposed to the potential customers and under constructions with significant evolutionary in economics and safety, nuclear experts from around the world indicated that further advances in nuclear energy systems are required to better meet the rapid growth of environment friendly, highly economic, and secure nuclear energy in both industrialized and developing countries. In particular, it is now globally recognized that the nuclear energy is the practically available massive energy source without greenhouse gas emission among numerous options. To meet these needs, the international nuclear community has engaged in a wide-range discussion on the development of next generation nuclear energy systems known as *Generation IV* (GEN-IV) targeting the deployment around 2030. Figure 6.1 shows the evolution of the nuclear energy systems.

Nine countries, Argentina, Brazil, Canada, France, Japan, the Republic of Korea, the Republic of South Africa, the UK, and the USA, have initially joined together to form the Generation IV International Forum (GIF) [1] for developing GEN-IV nuclear systems that can be licensed, constructed, and operated in a manner that will provide competitively priced and reliable energy products while satisfactorily addressing nuclear safety, waste, proliferation, and public perception concerns. Now, the GIF consists of 13 membership countries added by China, Euratom, Russia, and Switzerland, and two permanent observers of International Atomic Energy Agency (IAEA) and the Organization for Economic Cooperation and Development Nuclear Energy Agency (OECD/NEA).

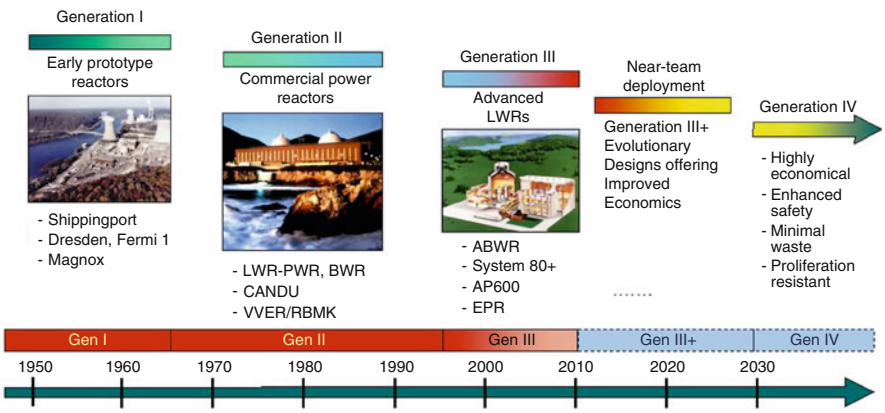

Fig. 6.1 Evolution of nuclear systems

Table 6.1 Goal for generation IV nuclear energy systems

Sustainability 1	Generation IV nuclear energy systems will provide sustainable energy generation that meets clean air objectives and promotes long-term availability of systems and effective fuel utilization for worldwide energy production.
Sustainability 2	Generation IV nuclear energy systems will minimize and manage their nuclear waste and notably reduce the long-term stewardship burden, thereby improving protection for the public health and the environment.
Economics 1	Generation IV nuclear energy systems will have a clear life-cycle cost advantage over other energy sources.
Economics 2	Generation IV nuclear energy systems will have a level of financial risk comparable to other energy projects.
Safety and Reliability 1	Generation IV nuclear energy systems operations will excel in safety and reliability.
Safety and Reliability 2	Generation IV nuclear energy systems will have a very low likelihood and degree of reactor core damage.
Safety and Reliability 3	Generation IV nuclear energy systems will eliminate the need for off-site emergency response.
Proliferation Resistance and Physical Protection 1	Generation IV nuclear energy systems will increase the assurance that they are a very unattractive and the least desirable route for diversion or theft of weapons-usable materials, and provide increased physical protection against acts of terrorism.

Beginning in 2000, more than 100 of nuclear experts from the countries constituting the GIF began to discuss for development of the GEN-IV technology roadmap in order to select the GEN-IV nuclear systems. As the first effort in the technology roadmap project [2], eight goals for the GEN-IV were defined in the four broad areas as shown in Table 6.1.

Since the eight goals are all equally important, the promising GEN-IV systems should ideally advance each and not create a weakness in one goal to gain strength in another. Under this central feature of the technical roadmap project, a series of GIF meeting was held in 2002 to conduct the selection process of the GEN-IV nuclear energy systems. The candidate systems were screened by the GIF expert group and six nuclear systems were selected on a consensus of the GIF membership countries such that the systems are the most promising and worthy of collaborative developments. The selected six systems for further R&D are alphabetically

- Gas-cooled Fast Reactor System (GFR),
- Lead-cooled Fast Reactor System (LFR),
- Molten Salt Reactor System (MSR),
- Sodium-cooled Fast Reactor System (SFR),
- Supercritical-water-cooled Reactor System (SCWR),
- Very-High-Temperature Reactor System (VHTR).

GEN-IV Nuclear Systems

In Table 6.2, the primary characteristics of the GEN-IV nuclear systems are summarized. In the roadmap project, it was recognized that the GIF countries would have perspectives on their priority missions for GEN-IV nuclear systems, which can be summarized as electricity generation, hydrogen production, and high-level radioactive material management. All six GEN-IV nuclear systems have electricity applications, while the high temperature and fast neutron spectrum are required for the hydrogen generation and high-level radioactive material management, respectively. The high temperature systems such as VHTR, GFR, LFR, and MSR have potential applications in hydrogen production. By reprocessing and recycling of actinides, the fast reactor systems such as SFR, GFR, and LFR would provide a significant reduction in radiotoxicity of all wastes.

GFR – Gas-cooled Fast Reactor

The Gas-cooled Fast Reactor system features a fast-spectrum helium-cooled reactor and closed fuel cycle. Figure 6.2 shows the schematic of the GFR, which uses a direct-cycle helium turbine for electricity. Like thermal-spectrum helium-cooled reactors such as the Gas Turbine-Modular Helium Reactor (GT-MHR [3]) and the Pebble Bed Modular Reactor (PBMR [4]), the high outlet temperature of the helium coolant makes it possible to deliver not only electricity, but also process heat for hydrogen production with a high conversion efficiency. Through the combination of a fast-neutron spectrum and closed fuel cycle options, the GFR can manage the high-level radioactive waste isotopes.

The technology base for the GFR includes a number of thermal-spectrum gas reactor plants, as well as a few fast-spectrum gas-cooled reactor designs. Past pilot and demonstration projects include decommissioned reactors such as the Dragon Project [5] built and operated in the UK, the AVR [6] and the Thorium High-Temperature Reactor (THTR [7]) built and operated in Germany, and Peach Bottom and Fort St Vrain [8] built and operated in the USA. Ongoing demonstrations include the High-Temperature engineering Test Reactor

Table 6.2 Summary of GEN-IV nuclear systems

	Coolant	Neutron spectrum	Coolant exit temp. (°C)	Fuel cycle	Size (MWe)
GFR	Helium	Fast	850	Closed	1,200
LFR	Lead	Fast	480–800	Closed	50–1,200
MSR	Fluoride salt	Fast/thermal	700–800	Closed	1,000
SFR	Sodium	Fast	550	Closed	30–2,000
SCWR	Water	Thermal/fast	510–625	Open/closed	300–1,500
VHTR	Helium	Thermal	900–1,000	Open	250–300

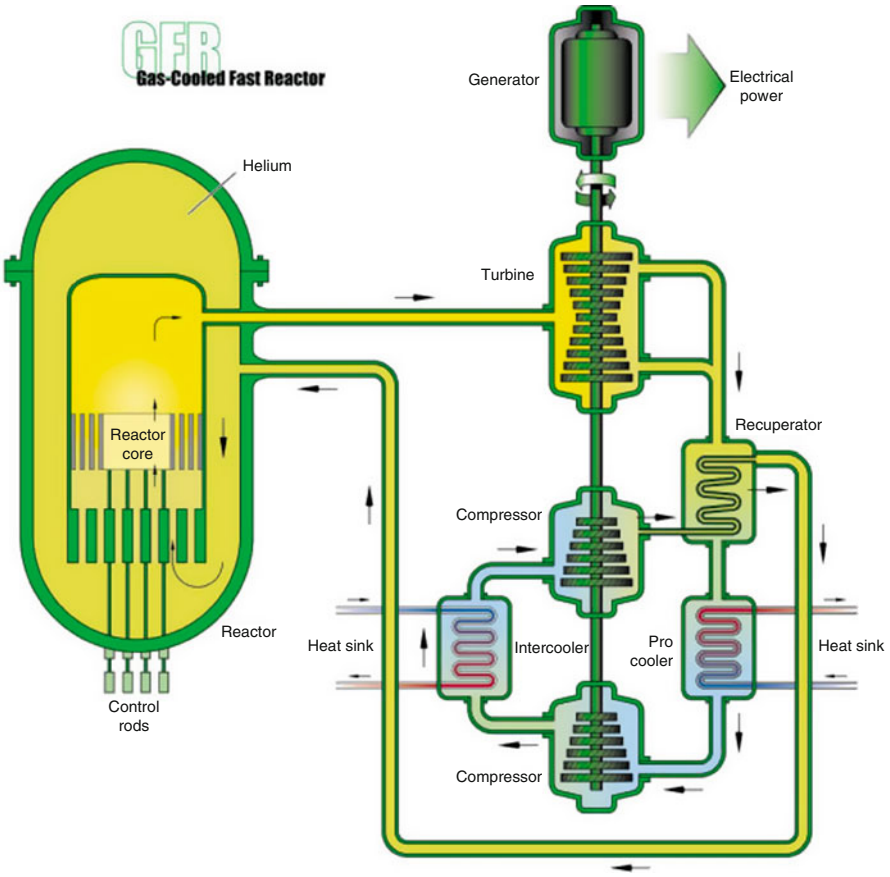

Fig. 6.2 Gas-cooled fast reactor

(HTTR [9]) in Japan, which reached full power (30 MWth) using prismatic fuel compacts in 1999, and the High-Temperature Gas-cooled Reactor (HTR-10 [10]) in China, which reached 10 MWth in 2002 using pebble fuel.

A 300-MWth pebble bed modular demonstration plant is being designed by PBMR Pty for deployment in South Africa and a consortium of Russian institutes is designing a 300-MWth GT-MHR in cooperation with General Atomics. The design of the PBMR and GT-MHR reactor systems, fuel, and materials are evolutionary advances of the demonstrated technology, except for the Brayton-cycle helium turbine and implementation of modularity in the plant design. The GFR may benefit from development of these technologies, as well as development of innovative fuel and very-high-temperature materials for the VHTR.

Spent fuel treatment for the GFR can be accomplished with aqueous processes similar to those of the SFR but qualified for the unique GFR fuel form. A composite ceramic–ceramic fuel (CERCER) with closely packed, coated (U, Pu)C kernels or

fibers is considered as the primary option for fuel development. Alternative fuel options for development include fuel particles with large (U, Pu)C kernels and thin coatings, or ceramic-clad, solid-solution metal (CERMET) fuels. The need for a high density of heavy metal elements in the fuel leads to actinide-carbides as the reference fuel and actinide-nitrides with 99.9% enriched nitrogen as the backup.

The reference material for the structure is reinforced ceramic comprising a silicon carbide composite matrix ceramic. The fuel compound is made of pellets of mixed uranium-plutonium-minor actinide carbide. A leaktight barrier made of a refractory metal or of Si-based multilayer ceramics is added to prevent fission products' diffusion through the clad.

Neither experimental reactors nor prototypes of the GFR system have been licensed or built; therefore, the construction and operation of a first experimental reactor – 50 MWth Experimental Technology Demonstration Reactor (ETDR [11]) – is proposed with an extended performance phase to qualify key technologies. A technology demonstration reactor would qualify key technologies and could be put into operation by 2025.

Unlike the VHTR, which uses its considerable thermal mass to limit the rise of core temperature during transients, the GFR requires the development of a number of unique subsystems to provide defense in depth for its considerably higher power density core. These include a robust decay heat removal system with added provisions for natural circulation heat removal, such as a low-pressure-drop core. The secondary circuit uses a He–N2 gas mixture with an indirect combined (Brayton and bottoming steam) power cycle to achieve more than 45% thermal efficiency.

A gastight envelope acting as additional guard containment is provided to maintain a backup pressure in case of large gas leak from the primary system. It is a metallic vessel, initially filled with nitrogen slightly over the atmospheric pressure to reduce air ingress potential. This unique component limits the consequence of coincident first and second safety barrier rupture (i.e., the fuel cladding and the primary system). Dedicated loops for decay heat removal (in case of emergency) are directly connected to the primary circuit using cross duct piping from the pressure vessel and are equipped with heat exchangers and blowers.

Many of the structural materials and methods are being adopted from the VHTR, including the reactor pressure vessel, hot duct materials, and design approach. The pressure vessel is a thick metallic structure of martensitic chromium steel, ensuring negligible creep at operating temperature. The primary system is comprised of three main loops of 800 MWth, each fitted with compact intermediate heat exchangers and a gas blower enclosed in a single vessel.

As a high-temperature and high-power density system, the GFR gives special attention to safety and materials management for both economics and nonproliferation. During the viability phase that is underway now, there is special interest in examining the use of pin-type fuel with a small diameter, fuel and core performance optimized for a simplified GFR having no minor actinide recycle, but with limited Pu breeding and low fuel burnup, core outlet temperature optimized to balance efficiency with materials limits, and the potential of prestressed concrete vessel technology to replace the guard vessel.

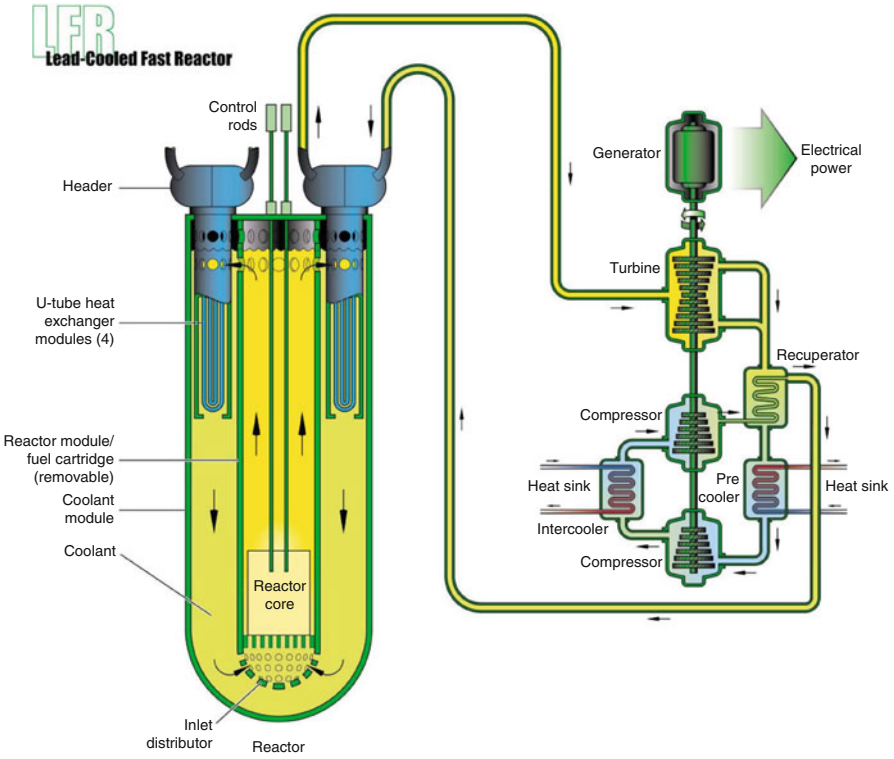

Fig. 6.3 Lead-cooled fast reactor

LFR – Lead-cooled Fast Reactor

The Lead-cooled Fast Reactor is similar to the sodium-cooled fast reactor in terms of neutron spectrum, fuel cycles, and the missions, but the coolant materials are changed to lead (Pb) or lead–bismuth (Pb–Bi). The lead coolant exhibits very low parasitic neutron absorption in fast neutron spectral environment, and this enables the sustainability and fuel cycle benefits traditionally associated with SFR. However, lead does not react readily with air, water, or carbon dioxide, which can eliminate the concerns about vigorous exothermic reactions. It has a high boiling temperature. The need to operate under high pressure and the prospect of boiling or flashing in case of pressure reduction are eliminated. Figure 6.3 shows the schematic of the LFR.

There are several potentials for advances compared to state-of-the-art liquid metal fast reactors. Innovations in heat transport and energy conversion are a central feature of the LFR options. Innovations in heat transport are afforded by natural circulation, lift pumps, in-vessel steam generators, and other features. Innovations in energy conversion are afforded by rising to higher temperatures

than liquid sodium allows, and by reaching beyond the traditional superheated Rankine cycle to supercritical Brayton cycle or process heat applications such as hydrogen production and desalination. The favorable neutronics of coolant enable low power density, natural circulation-cooled reactors with fissile self-sufficient core designs that maintain criticality over 15-year refueling interval. For modular and large units, more conventional higher power density, forced circulation, and shorter refueling intervals are used, but these units benefit from the improved heat transport and energy conversion technology. The favorable properties of lead coolant and nitride fuel, combined with high-temperature structural materials can extend the reactor coolant outlet temperature up to 800°C, which is potentially suitable for hydrogen manufacture and other process heat applications.

Two types of LFR reactors were used in Russian submarines of the 1970s with the 155 MWth LFR reactors, OK-550 and BM-440. Recently, Russian joint venture AKME Engineering announced to develop a commercial LFR called SBVR-100 [12]. The core is based on the former LFR reactors used in the submarines and will produce 100 MWe electricity from gross thermal power of 280 MWth, about twice that of the submarine reactors. The coolant is 495°C and 16.5% enriched uranium oxide fuel is used with the refueling schedule of 7–8 years. The small lead-cooled fast reactor concept known as the small secure transportable autonomous reactor (SSTAR [13]) has been under ongoing development as part of the US advanced nuclear energy systems programs (see Fig. 6.4). It is a system designed to provide energy security to developing nations while incorporating features to achieve nonproliferation goals. A 600 MWe European Lead-cooled system (ELSY [14]) has been under development since 2006. The ELSY project aims at the demonstration that it is possible to design a competitive and safe fast power reactor using simple technical engineered features.

The LFR is mainly envisioned for electricity and hydrogen production and high-level radioactive material management. The proposed LFR options include a long refueling interval battery ranging from 50 to 150 MWe, a modular system from 300 to 400 MWe, and a large monolithic plant at 1,200 MWe. The LFR battery option (like SSTAR) is a small factory-built turnkey plant operating on a closed fuel cycle with very long refueling interval (15–20 years) cassette core or replaceable reactor module. Its features are designed to meet market opportunities for electricity production on small grids, and for developing countries that may not wish to deploy an indigenous fuel cycle infrastructure to support their nuclear energy systems. Its small size, reduced cost, and full support fuel cycle services can be attractive for these markets. It had the highest evaluations to the GEN-IV goals among the LFR options, but also the largest R&D needs and longest development time.

The options in the LFR class may provide a time-phased development path: the nearer-term options focus on electricity production and rely on more easily developed fuel, clad, and coolant combinations and their associated fuel recycle and refabrication technologies. The longer-term option seeks to further exploit the inherently safe properties of lead and raise the coolant outlet temperature sufficiently high to enter markets for hydrogen and process heat, possibly as merchant plants.

The technologies employed are extensions of those currently available from the Russian submarine lead-bismuth alloy-cooled reactors, from the Integral Fast

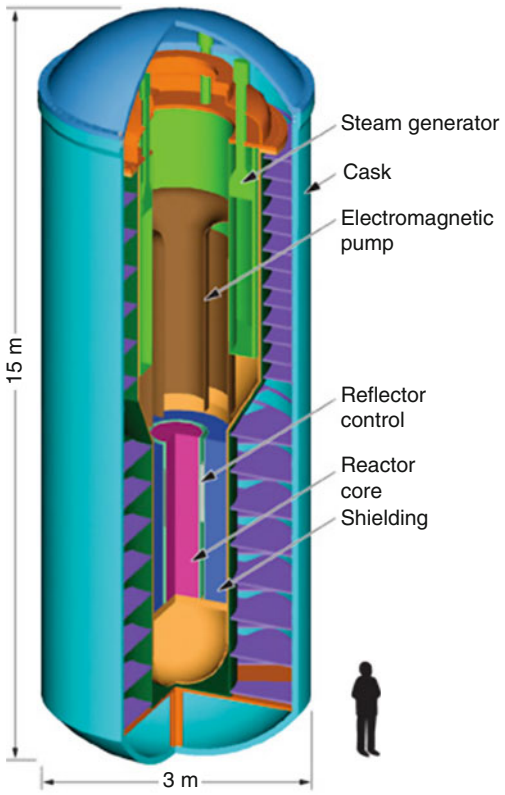

Fig. 6.4 SSTAR–A US lead-cooled fast reactor

Reactor (IFR [15]) metal alloy fuel recycle and refabrication development, and from the Advanced Liquid Metal Reactor (ALMR [16]) passive safety and modular design approach. Existing ferritic stainless steel and metal alloy fuel, which are already significantly developed for sodium fast reactors, are adaptable to lead-bismuth-cooled reactors at reactor outlet temperatures of 550°C.

Corrosion of structural materials in lead is one of the main issues for the LFR. Recent experiments confirm that corrosion of steels strongly depends on the operating temperature and dissolved oxygen. Indeed, at relatively low oxygen concentration, the corrosion mechanism changes from surface oxidation to dissolution of the structural steel. Moreover, relationships between oxidation rate, flow velocity, temperature, and stress conditions of the structural material have been observed as well. The compatibility of ferritic and austenitic steels with lead has been extensively studied and it has been demonstrated that generally below 450°C, and with an adequate oxygen activity in the liquid metal, both types of steels build up an oxide layer which behaves as a corrosion barrier. However, above about 500°C, corrosion protection through the oxide barrier appears to fail and is being addressed with various candidate materials. The prospects for extending much above this temperature are not proven at this time.

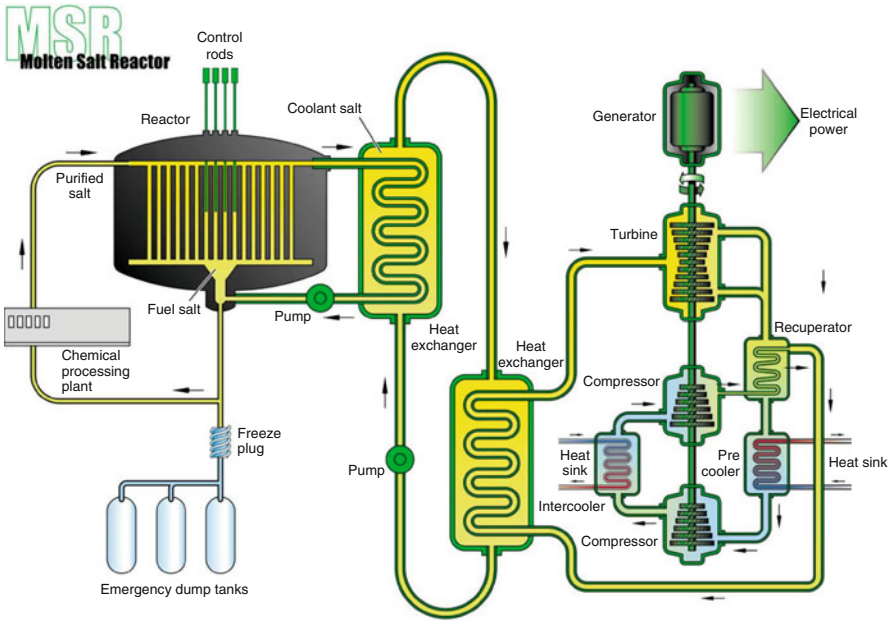

Fig. 6.5 Molten salt reactor

MSR – Molten Salt Reactor

The Molten Salt Reactor uses a molten salt mixture as a primary coolant. Systematic analysis of parameters such as reprocessing time, moderation ratio, core size, and content of heavy nuclei in the salt has resulted in several attractive reactor configurations, in thermal, epithermal, or fast neutron spectrum. The use of a molten salt coolant in a solid-fuel system has been investigated, known as the Advanced High-Temperature Reactor (AHTR [17]), which adapts VHTR fuel form and heat exchanger technology. However, in most MSRs, the fuel is dissolved in the molten salt coolant. Thus, the MSR has unique characteristic compared to other GEN-IV systems: i.e., online refueling and reprocessing are allowed without reactor shutdown because the fuel can move. In addition, the MSR have the following characteristics, which may afford advances: good neutron economy and alternatives for actinide burning or conversion, potential for hydrogen production with high operating temperature, low stresses on the vessel and piping with a very low vapor pressure, enhanced safety by fail-safe drainage, passive cooling, and a low inventory of volatile fission products, etc. Fig. 6.5 shows the schematic of the MSR concept with dissolved fuel.

The MSR was first developed in the late 1940s and 1950s for aircraft propulsion. The Aircraft Reactor Experiment (ARE [18]) was a 2.5 MWth nuclear reactor experiment designed to attain a high-power density for use as an engine in a nuclear powered

bomber. One experiment used the molten fluoride salt NaF-ZrF_4-UF_4 (53-41-6 mol%) as fuel, was moderated by beryllium oxide, used liquid sodium as a secondary coolant, and had a peak temperature of 860°C. It operated for a 1,000 h cycle in 1954. The 8 MWth Molten Salt Reactor Experiment (MSRE [19]) was operated from 1965 to 1969 to demonstrate many features, including lithium/beryllium fluoride salt, graphite moderator, stable performance, off-gas systems, and use of different fuels such as U-233, U-235, and plutonium.

Recently, two MSRs were proposed: Thorium Molten Salt Reactor (TMSR [12]), and FUJI mini-MSR [12]. Figure 6.6 shows the 1,000 MWe TMSR with graphite moderator. Its operating temperature is 630°C and its thermodynamic efficiency is 40%. The salt used is a binary salt, LiF-$(HN)F_4$, with the $(HN)F_4$ content set to 22%, corresponding to a melting temperature of 565°C. The U-233 enrichment is about 3%. A graphite radial blanket surrounds the core to improve breeding performance. The reprocessing time of the total salt volume is specified to be 6 months, with external storage of the Pa and complete extraction of the fission products and TRU. It is assumed that the U-233 produced in the blanket is also extracted every 6 months. The FUJI mini-MSR is a 100 MWe molten-salt-fueled thorium fuel cycle thermal breeder reactor being developed internationally by Japanese, Russian and US consortium. Like all molten salt reactors, the core is chemically inert under low pressures to prevent explosions and toxic releases.

There are four fuel cycle options: (1) maximum breeding ratio (up to 1.07) using a Th and U-233 fuel cycle, (2) denatured Th and U-233 converter with minimum inventory of nuclear material suitable for weapons use, (3) denatured once-through actinide burning (Pu and minor actinides) fuel cycle with minimum chemical processing, and (4) actinide burning with continuous recycling. The fourth option with electricity production is favored for the GEN-IV MSR. Fluoride salts with higher solubility for actinides such as NaF/ZrF4 are preferred for this option. Salts with lower potential for tritium production would be preferred if hydrogen production was the objective. Lithium and beryllium fluorides would be preferred if high conversion was the objective. On-line processing of the liquid fuel is only required for high conversion to avoid parasitic neutron loses of Pa-233 that decays to U-233 fuel. Off-line fuel salt processing is acceptable for actinide management and hydrogen or electricity generation missions.

The reactor can use U or Th as a fertile fuel dissolved as fluorides in the molten salt. Due to the thermal or epithermal spectrum of the fluoride MSR, Th achieves the highest conversion factors. However, before sufficient fissile is bred for maintaining the criticality, the MSR requires low-enriched uranium or other fissile materials. The operating temperature ranges from the melting point of eutectic fluorine salts (about 450°C) to below the chemical compatibility temperature of nickel-based alloys (about 800°C).

The R&D will focus on fuel salt cleanup, including pyrochemical separation technologies, extraction of gaseous fission products and noble metals by gas bubbling, tritium speciation and control, and conversion of various waste streams into final waste forms. The research will gradually advance from laboratory scale to larger and more integrated demonstrations. MSR burner and breeder fuel cycles will

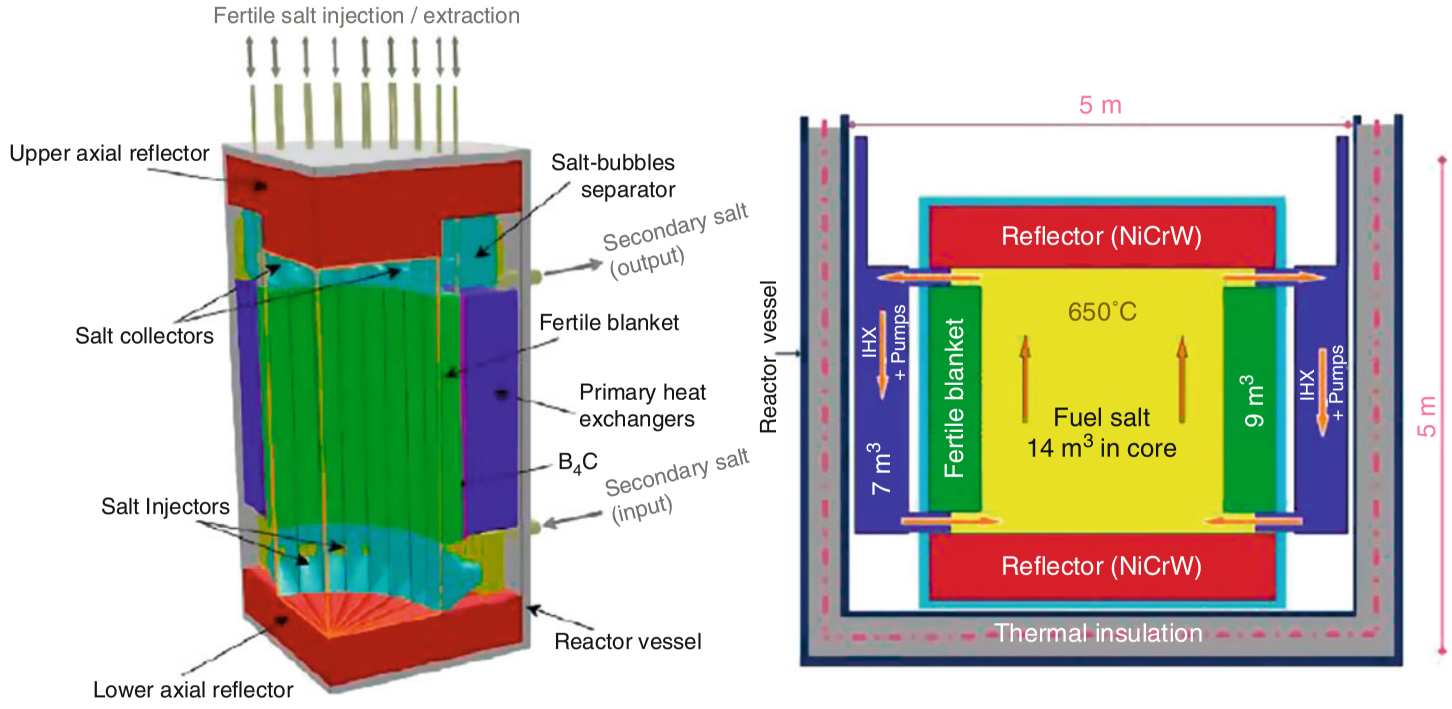

Fig. 6.6 Thorium molten salt reactor

be evaluated and compared with other nuclear systems. This includes examination of the burning of actinides from other nuclear systems, startup of MSRs on various actinides, avoidance of the generation of most actinides by use of thorium fuel cycles, and alternative breeder reactor fuel cycles.

The MSR also addresses research related to the compatibility of fuel and coolant salts with core and structural materials and challenging MSR subsystem integrity: reactor components and reprocessing unit regarding mechanical and corrosion resistance. The high temperature, salt reduction-oxidation potential, radiation fluence, and energy spectrum pose a serious challenge for any structural alloy in an MSR. The design of a practical system demands the selection of salt constituents such as LiF, NaF, BeF_2, UF_4, ThF_4, and PuF_3 that are not appreciably reduced by available structural metals and alloys whose component Fe, Ni, and Cr can be in near equilibrium with the salt. Small levels of impurities in the salt may also aggressively corrode the metallics.

Circulating fuel raises challenges within the core such as the loss of delayed neutrons, temperature differences between the salt, reflectors, and moderator, which requires the coupling between neutronics, thermal-hydraulics, salt composition, and properties of the MSR.

SFR – Sodium-cooled Fast Reactor

The Sodium-cooled Fast Reactor features a fast-spectrum reactor and closed fuel-recycle system. Including electricity generation, the primary mission for the SFR could be either enhancement of the uranium resource utilization or high-level radioactive material management, which depends on the SFR designs. Historically, the enhancement of the uranium resource utilization was the primary mission of the SFR by achieving a high breeding ratio, but the mission was recently shifted for consuming transuranics (plutonium and other long-lived radioactive material) in a very low breeding ratio core. The latter has been studied under the Global Nuclear Energy Partnership (GNEP), which was initiated to seek worldwide consensus on enabling expanded use of economical carbon-free nuclear energy to meet growing electivity demand. The GNEP adopted a fully closed nuclear fuel cycle option that enhances energy security while improving proliferation risk management. One of the major goals of the GNEP is to design and demonstrate a SFR for actinide management like the Advanced Burner Reactor (ABR, [20]).

Based on the arrangement of the primary coolant pump and intermediate heat exchanger (IHX), there are two options for the SFR systems: pool type and loop type (see Figs. 6.7 and 6.8). The primary pump and IHX are placed inside the reactor vessel in the pool type, while these two components are located outside reactor vessel by connecting them trough pipes. A hybrid option [21] of the pool and loop types has also been proposed.

The experiences on design, construction, and operation provide important input into the design process and have the potential to influence the maturity of the

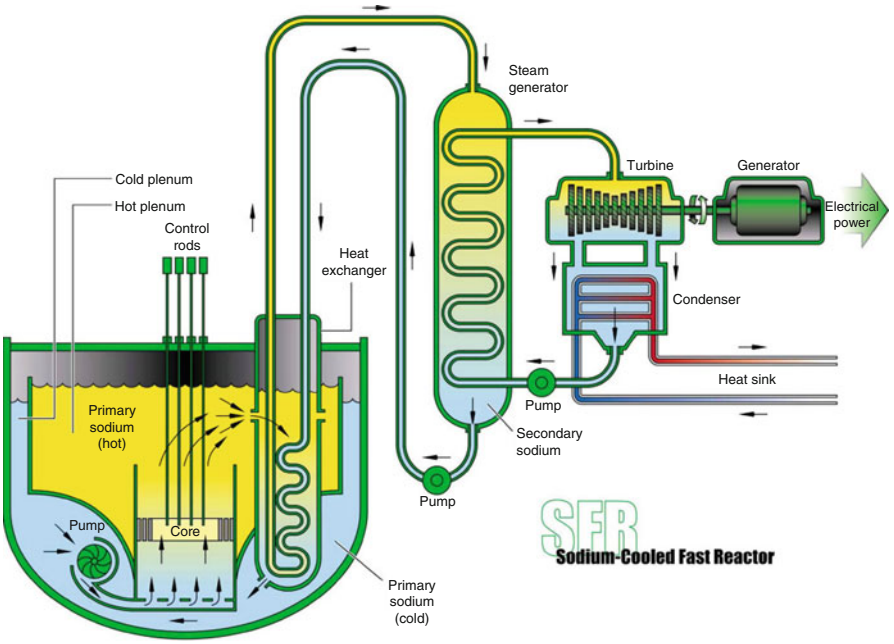

Fig. 6.7 Pool-type sodium-cooled fast reactor

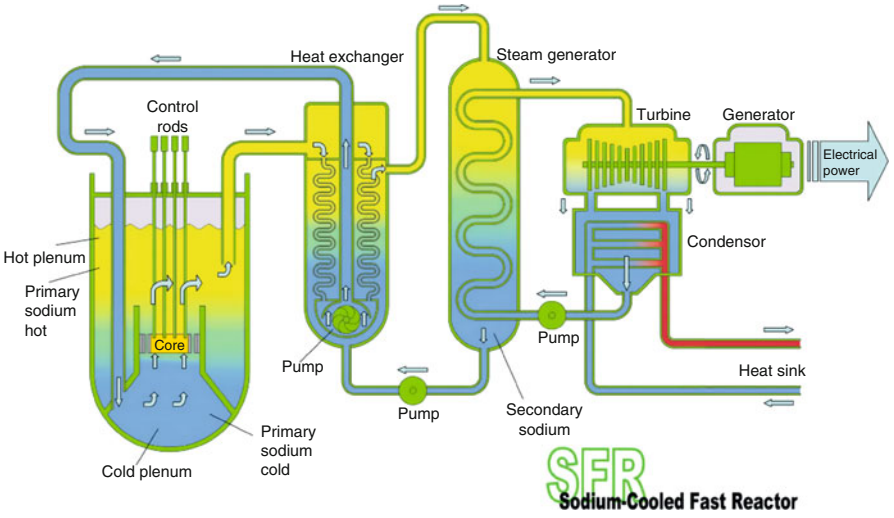

Fig. 6.8 Loop-type sodium-cooled fast reactor

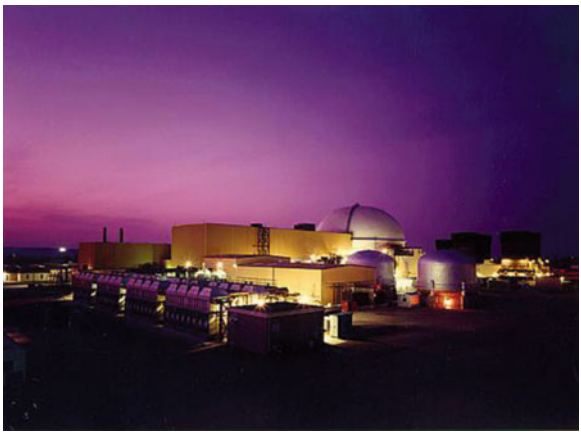

Fig. 6.9 Fast Flux Test Facility

various fast reactor concepts. The greater the number of operating experience years, the greater the opportunity to modify the design based on operating lessons learned. The SFR relies on technologies already developed and demonstrated for sodium-cooled reactors and associated fuel cycles that have successfully been built and operated in worldwide fast reactor programs. Overall, approximately 300 reactor years of operating experience have been logged on SFRs including 200 years on smaller test reactors and 100 years on larger demonstration or prototype reactors. Thus, the technical readiness level, which indicates how soon a system could be deployed, of the SFR is most matured among the six GEN-IV systems.

In the USA, the SFR technology was employed in the 20 MW-electric Experimental Breeder Reactor II (EBR-II [22]) that operated from 1963 to 1994. EBR-II R&D included development and testing of metal fuel and passive safety tests. The 400 MWth Fast Flux Test Facility (FFTF [23]) was completed in 1980 (Fig. 6.9). The FFTF operated successfully for 10 years with a full core of mixed oxide (MOX) fuel and performed SFR materials, fuels, and component testing. The US SFR development program stalled with cancellation of the Clinch River demonstration reactor in 1983, although US-DOE research for advanced SFR technology continued until 1994. The SFR experience also extends to the commercial sector with the operation of Detroit Edison's FERMI-1 plant from 1963 to 1972.

Significant SFR research and development programs are being conducted in China, France, India, Japan, Russia, and Republic of Korea. The most modern fast reactor construction project was the 280 MWe MONJU (Japan) that was completed in 1990, which will be restarted soon. The construction of 20 MWe Chinese Experimental Fast Reactor (CEFR) and coolant sodium loading was completed in 2009, and the full power operation is expected in 2010. India operates 40 MWth Fast Breeder Test Reactor (FBTR) since 1985 and 500 MWe Prototype Fast Breeder Reactor (PFBR) is under construction. The only current fast reactor for electrical generation is the Russian BN-600 that has reliably operated since 1980, and the BN-800 is under construction.

A range of plant size options are available for the SFR, ranging from a battery type systems of a hundred MW-thermal to large monolithic reactors of 3,500 MW-thermal. The sodium coolant outlet temperature is limited by the material properties. Coolant outlet temperatures are typically less than 550°C; however, further increase is considered.

A large margin to coolant boiling is achieved by design, and is an important safety feature of these systems. Another major safety feature is that the primary system operates at essentially atmospheric pressure, pressurized only to the extent needed to move fluid. Sodium reacts chemically with air, and with water, and thus the design must limit the potential for such reactions and their consequences. To improve safety, a secondary sodium system acts as a buffer between the radioactive sodium in the primary system and the steam or water that is contained in the conventional Rankine-cycle power plant.

Metallic and oxide fuel forms are available for the SFR. The metallic fuel was originally chosen in the early fast reactor programs because of its high density, compatibility with the liquid metal coolant, relative easiness to fabricate, and excellent thermal conductivity. In the late 1960s, before the full potential of metallic fuels were established, the interest worldwide for fast reactor fuel turned toward the oxide fuel, because the achievable burnup is limited by a large irradiation swelling. However, the development and irradiation test of metallic fuels continued though the 1970s and it was discovered that the metallic fuel can achieve a high burnup by allowing room for fuel to swell. In addition, the metallic fuel was focused again in the recent fast reactor programs because of its potential passive safety benefits.

The high burnup potential, rich experiences in commercial water-cooled reactors, and the existence of established industry for manufacturing were the critical factors that motivated interest in oxide fuel for the liquid-metal-cooled fast reactors. However, the low heavy metal density and low thermal conductivity are the principal disadvantages of the oxide fuel. The low density is unfavorable to implement a compact core and increase the breeding ratio or cycle length. The low thermal conductivity leads to high temperature gradient from fuel to coolant. As a result, the oxide fuel stores significant amount of Doppler reactivity in the normal operation condition and it provides the unfavorable positive reactivity feedback during an unprotected severe accident.

Recently, the mixed carbide and nitride fuels have been given attention as the alternative fuels for sodium-cooled fast reactor on the basis of their high density, compatibility with sodium coolant, high melting temperature, and excellent thermal conductivity although they are ceramic fuel like a mixed oxide fuel.

The SFR require a closed fuel cycle to enable their advantageous actinide management and fuel utilization features. There are two primary fuel cycle technology options: an advanced aqueous process and the pyroprocess [15] which derives from the term, pyrometallurgical process. Both processes have similar objectives: recovery and recycle of more than 99.9% of the actinides, inherently low decontamination factor of the product, making it highly radioactive, and never separating plutonium at any stage for nonproliferation. These fuel cycle technologies are

adaptable to thermal spectrum fuels in addition to serving the needs of the SFR. Thus, the reactor technology and the fuel cycle technology are strongly linked.

Due to the flexibility of the conversion ratio depending on the core design options, the SFR can be operated in three distinct fuel cycle roles. A conversion ratio less than 1 ("burner") can reduce long-lived radioactive waste. A conversion ratio near 1 can increase the uranium utilization without feeding additional enriched uranium. A conversion ratio greater than 1 ("breeder") affords a net creation of fissile materials. An appropriately designed fast reactor has flexibility to shift between these operating modes; the desired actinide management strategy will depend on a balance of waste management and resource extension considerations.

Regarding economics, the reduction of the plant capital costs is crucial. A number of innovative SFR design features have been proposed: configuration simplifications, improved Operations & Maintenance (O&M) technology, advanced reactor materials, advanced energy conversion systems, fuel handling, etc.

With regard to reactor safety, technology gaps center around two general areas: assurance of passive safety response and techniques for evaluation of bounding events. The advanced SFR designs exploit passive safety measures to increase reliability. The system behavior will vary depending on system size, design features, and fuel type. R&D for passive safety will investigate phenomena such as axial fuel expansion and radial core expansion, and design features such as self-actuated shutdown systems and passive decay heat removal systems. The ability to measure and verify these passive features must be demonstrated. Associated R&D will be required to identify bounding events for specific designs and investigate the fundamental phenomena to mitigate severe accidents.

Finally, the development of SFR technology provides the opportunity to design modern safeguards directly into the planning and building of new nuclear energy systems and fuel cycle facilities. Incorporating safeguards into the design phase for new facilities will facilitate nuclear inspections conducted by the International Atomic Energy Agency (IAEA). The goal of this oversight is to always have an accurate grasp of the current inventory through the utilization of advanced technologies to verify the characteristics of the security system (accountancy, detection, and promptness) and the physical protection characteristics (physical protection measures, the monitoring level, and security measures) and for ensuring robust design to guarantee these characteristics. It is also necessary to maintain transparency and openness in terms of information to more effectively and efficiently monitor and verify nuclear material inventories.

SCWR – Supercritical Water-cooled Reactor

The Supercritical Water-cooled Reactor is a water-cooled reactor like Light Water Reactor (LWR) operated commercially, but the SCWR is operated above the thermodynamic critical point of water (374°C, 22.1 MPa). Figure 6.10 shows the SCWR system.

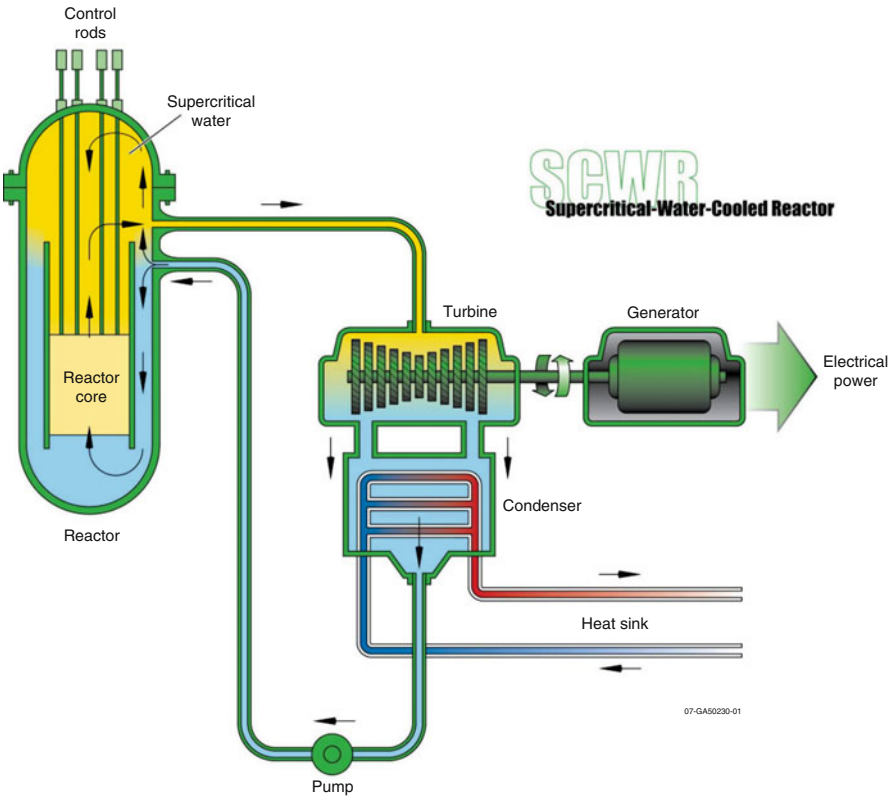

Fig. 6.10 Supercritical water-cooled reactor

The specific heat increases drastically and the water density decreases without boiling of water around the thermodynamic critical point. As a result, the SCWR has unique features that may offer advantages compared to state-of-the-art PWRs: Higher plant thermal efficiency compared to LWRs due to the higher operating temperature. Low density of water without boiling allows the direct cycle like Boiling Water Reactor (BWR), but steam dryers, steam separators, recirculation pumps, and steam generators are not necessary, and as a result, the SCWR can be a simpler plant with fewer major components. Lower-coolant mass flow rate per unit core thermal power results from the high heat capacity of the supercritical water. This offers a reduction in the size of the reactor coolant pumps, piping, and associated equipment, and a reduction in the pumping power. Lower-coolant mass inventory results from the once-through coolant path in the reactor vessel and the lower-coolant density. This opens the possibility of smaller containment buildings. No boiling crisis (i.e., departure from nucleate boiling or dry out) exists due to the lack of a second phase in the reactor, thereby avoiding discontinuous heat transfer regimes within the core during normal operation.

The SCWR systems may have a thermal [24], fast [25], or mixed-neutron spectrum [26] depending on the core design. The Japanese supercritical light water reactor (SCLWR) with a thermal spectrum has been the subject of the most development work in the last 10–15 years. The SCLWR reactor vessel is similar in design to a PWR vessel (although the primary coolant system is a direct-cycle, BWR-type system). High-pressure (25.0 MPa) coolant enters the vessel at 280°C. The inlet flow splits, partly to a downcomer and partly to a plenum at the top of the core to flow down through the core in special water rods. This strategy provides moderation in the core. The coolant is heated to about 510°C and delivered to a power conversion cycle, which blends LWR and supercritical fossil plant technology; high-, intermediate-, and low-pressure turbines are employed with two reheat cycles.

The SCWR can also be designed to operate as a fast reactor. The difference between thermal and fast versions is primarily the amount of moderator material in the SCWR core. The fast spectrum reactors use no additional moderator material, while the thermal spectrum reactors need additional moderator material in the core. The mixed-spectrum SCWR was proposed not only to achieve all advantages of SCWR but also the actinide management. The core uses two coolant flow paths: outer zone with high density water and inner zone with low density water (see Fig. 6.11). Thus, the inner zone features fast neutron spectrum, while the outer zone features thermal spectrum. By recycling TRU in the fast zone, the mixed-spectrum SCWR is capable of keeping all TRU in the reactor.

Much of the technology base for the SCWR can be found in the existing LWRs and in commercial supercritical-water-cooled fossil-fired power plants. However, there are some relatively immature areas. There have been no prototype SCWRs built and tested. For the reactor primary system, there has been very little in-pile research done on potential SCWR materials or designs, although some SCWR in-pile research has been done for defense programs in Russia and the United States. Limited design analysis has been underway over the last decade in Japan, Canada, and Russia. For the balance of plant, there has been development of turbine generators, piping, and other equipment extensively used in supercritical-water-cooled fossil-fired power plants.

The ability to use proven uranium oxide fuel greatly simplifies the application of fuel and fuel cycle technology to the SCWR. However, the supercritical water is known to challenge the corrosion/erosion performance of current cladding technology, and R&D is focused on advanced cladding materials.

There are several unique components needed for the SCWR, including the reactor pressure vessel or pressure tubes and its internal structural components, moderator channels, control rods and drives, the condenser and high-pressure pumps, valves, and seals. The reactor pressure boundary must operate above the high pressure (22.1 MPa) of supercritical water. This may be addressed with thicker sections, and thermal stresses can be avoided with a thermal sleeve for the outlet nozzle.

Zirconium-based alloys, common in water-cooled reactors, may not be a viable material without thermal and/or corrosion-resistant barriers. Based on available data for other alloy classes, there is no single alloy that has received enough study to

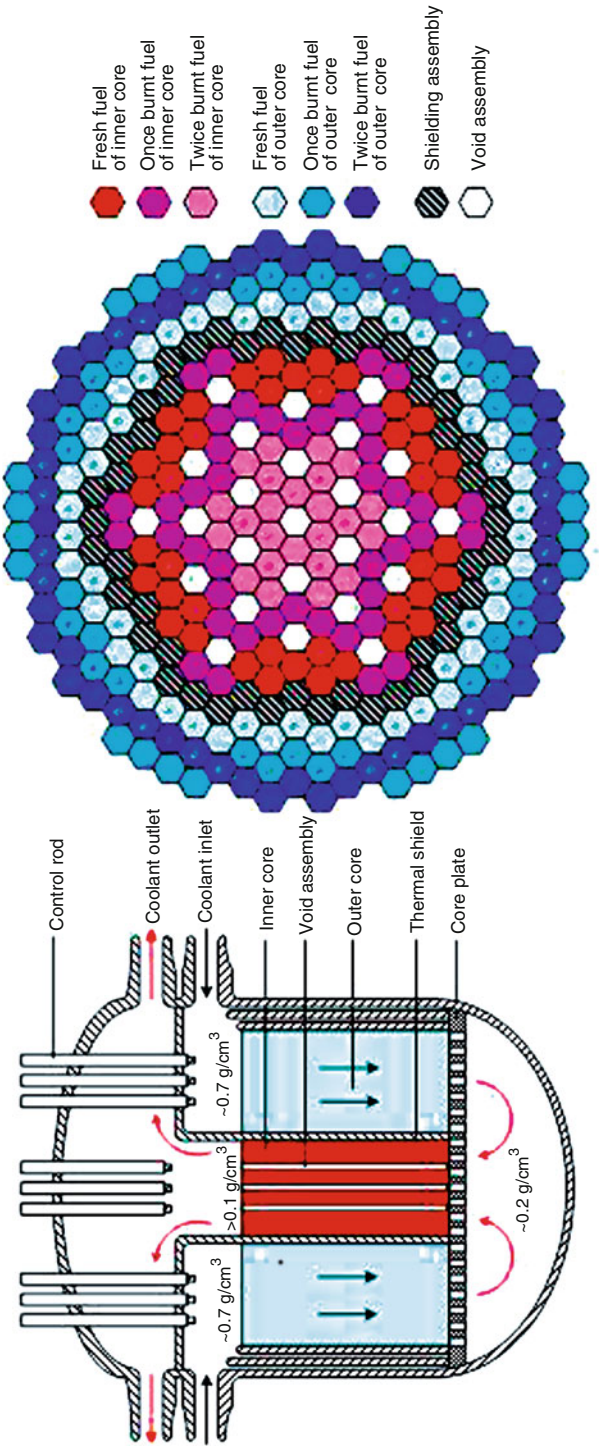

Fig. 6.11 Core layout of mixed-spectrum supercritical water reactor

unequivocally ensure its performance in an SCWR. Another key need of this system will be an enhanced understanding of the chemistry of supercritical water. Water above its critical point is accompanied by dramatic changes in chemical properties. Its behavior and degradation of materials is further accelerated by in-core radiolysis, which preliminary studies suggest is markedly different than what would have been predicted by simplistic extrapolations from conventional reactors.

The approach to development of materials and components will build on evaluation of candidate materials with regard to corrosion and stress corrosion cracking, strength, embrittlement and creep resistance, and dimensional and microstructural stability; the potential for water chemistry control to minimize impacts as well as rates of deposition on fuel cladding and turbine blades; and measurement of performance data in an in-pile loop. All of these are critical to establishing viability of the SCWR.

The SCWR leads the way among GEN-IV systems in the development of advanced materials for water coolant. In fact, the diffusion of this technology into current generation light and heavy water reactors seems assured. However, much remains to be done: the thermal-hydraulic performance during normal and off-normal operation, as well as postulated accidents, needs to be addressed both with advances in the design and safety approach as well as the analysis tools. Issues to be addressed include the basic thermal-hydraulic phenomenon of heat transfer and fluid flow of supercritical water in various geometries, critical flow measurements, the strong coupling of neutronic and thermal-hydraulic behavior, leading to concerns about flow stability and transient behavior, validation of computer codes that reflect these phenomena, and definition of the safety and licensing approach as distinct from current water reactors, including the spectrum of postulated accidents, flow instability, etc.

VHTR – Very-high-temperature Reactor

The Very-high-temperature Reactor is a graphite-moderated, helium-cooled reactor like GT-MHR and PBMR capable of generating electricity, but the coolant output temperature is significantly increased up to 1,000°C. In Fig. 6.12, the schematic of the VHTR is depicted. The higher temperatures of this reactor open the door for industrial heat processing opportunities, in particular, for hydrogen production. The annual US demand for hydrogen is over 12 million tons, and expected to grow to over 30 million tons by 2030. Industry uses hydrogen for fossil fuel refining, treating metals, and food processing. Hydrogen is currently produced primarily from steam methane reforming using fossil fuel as a heat source. Hydrogen can also be produced by various processes using a high-temperature gas-cooled reactor as the primary energy source.

Use of nuclear energy as the heat source of a large-scale hydrogen production operation would result in substantially lower carbon emissions over a natural

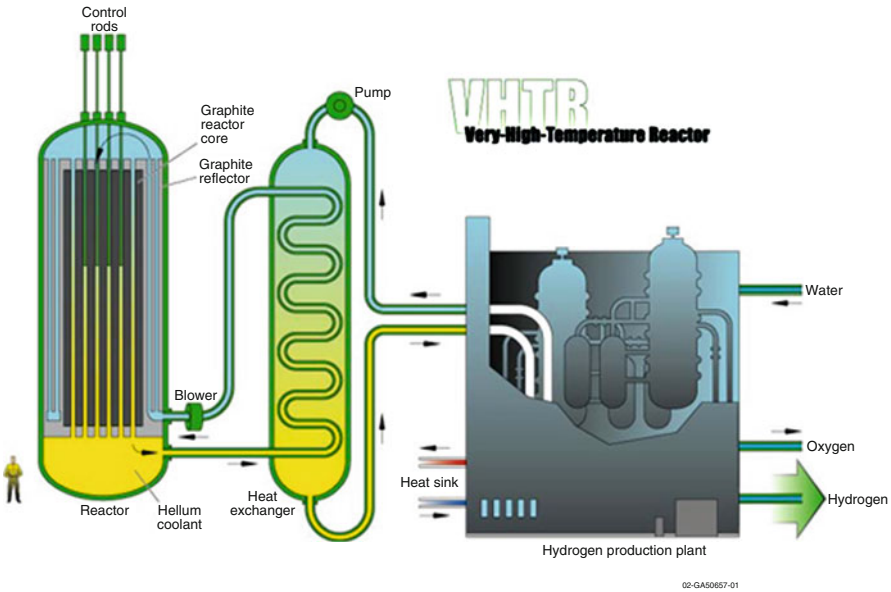

Fig. 6.12 Very-high-temperature reactor

gas-fired steam methane reforming operation. A 600 MWth VHTR dedicated to hydrogen production can yield over 2 million normal cubic meters per day. The VHTR can also generate electricity with high efficiency, over 50% at 1,000°C.

The VHTR has been evolved from gas-cooled reactor experiences and extensive international databases that can support its development. The basic technology for the VHTR has been well established in former gas-cooled reactors, such as DRAGON, Peach Bottom, AVR, THTR, and Fort St Vrain, and is being advanced in concepts such as the GT-MHR and PBMR. The ongoing 30-MWth HTTR project in Japan is intended to demonstrate the feasibility of reaching outlet temperatures up to 950°C coupled to a heat utilization process, and the HTR-10 in China will demonstrate electricity generation at a power level of 10 MWth. The former projects in Germany and Japan provide data relevant to the VHTR development.

The VHTR core uses TRISO particles to form a pebble bed or prismatic fuel element (see Fig. 6.13). The TRISO particle, which has a small diameter of less than 1.0 mm, has a fuel kernel in the form of uranium oxide. The enrichment of the uranium is dependent on the core design purposes. The kernel is subsequently coated with a porous carbon layer (to hold fission gases), a dense pyrolytic carbon layer, a silicon carbide layer, and finally another pyrolytic carbon layer. The coatings surrounding the kernel of TRISO particles produce a very robust fuel form by acting as the containment boundary for the radioactive material. These coatings work in much the same way as the massive reinforced concrete structure surrounding the light water reactors currently in service.

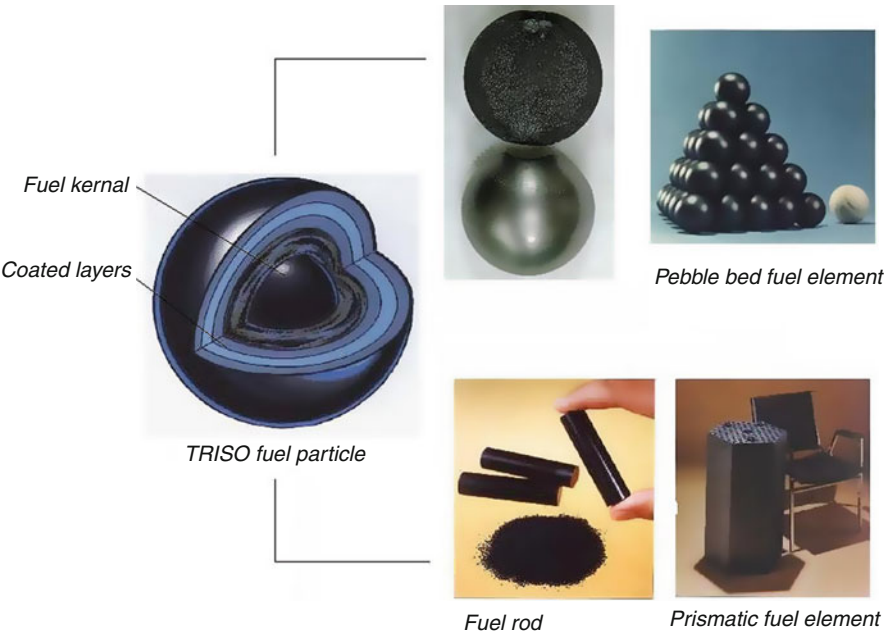

Fig. 6.13 VHTR fuel elements

The reactor core type of the VHTR can be a prismatic block core such as GT-MHR and Japanese HTTR, or a pebble-bed core such as PBMR and Chinese HTR-10. Despite of the alternate fuel element designs (pebble bed versus prismatic), the two baselines have many technologies in common that allow for a unified R&D approach. The well-known TRISO particle fuel with a UO_2 kernel and SiC/PyC coating may be used in either, or it may be enhanced with a different fuel kernel form such as UCO or an advanced ZrC coating through additional research. For electricity generation, the helium gas turbine system can be directly set in the primary coolant loop, which is called a direct cycle. For nuclear heat applications such as process heat for refineries, petro-chemistry, metallurgy, and hydrogen production, the heat application process is generally coupled with the reactor through an intermediate heat exchanger (IHX), which is called an indirect cycle.

The fuel cycle will initially be a once-through fuel cycle specified for high burnup (15–20 atom-%) using low enriched uranium. The operation with a closed fuel cycle will be assessed and solutions to better manage the fuel cycle back end will be developed. The possible use of TRU as a fuel will be studied conceptually for actinide management [27].

The primary emphasis in fuel development is on its performance at high burnup, power density, and temperature. The R&D broadly addresses its manufacture and characterization, irradiation performance, and accident behavior. Irradiation tests will provide data on coated particle fuel and fuel element performance under irradiation as necessary to support fabrication process development, to qualify the

Table 6.3 Anticipated deployment of GEN-IV systems

	Deployment timelines		
System	Viability phase	Performance phase	Demonstration phase
GFR	2012	2020	2025
LFR	2014	2020	2025
MSR	2013	2020	2025
SFR	2006	2015	2020
SCWR	2014	2020	2025
VHTR	2010	2015	2020

fuel design, and to support development and validation of models and computer codes on fission product transport. They will also provide irradiated fuel and materials samples for postirradiation and safety testing. The performance expected for the fuel must be verified for all normal, transient, or accident conditions as well as certain severe accident conditions (beyond design basis). A key claim of the fuel is its ability to retain fission products in the fuel particles under a range of postulated accidents with temperatures up to 1,600°C.

Future Directions

The objective for Generation IV nuclear energy systems is to have them available for wide-scale deployment before the year 2030. The anticipated deployment dates for the six GEN-IV systems are provided in Table 6.3 in terms of R&D phases. The deployment dates of the SFR and VHTR are expected to be earlier than other GEN-IV systems because of their matured technical readiness level.

In the viability R&D phase, the feasibility of key technologies of the GEN-IV systems will be examined. The performance R&D activities undertake the development of performance data and optimization of the system. Assuming the successful completion of viability and performance R&D, the demonstration R&D phase activities involve the licensing, construction, and operation of a prototype or demonstration system in partnership with industry and perhaps other countries. Thus, the detailed design and licensing of the system will be performed during the demonstration phase. The R&D projects and milestones anticipated in each phase were defined in GEN-IV roadmap project [2].

Bibliography

Primary Literature

1. Generation IV International Forum. http://www.gen-4.org
2. US-DOE Nuclear Energy Research Advisory Committee and GIF (2002) A technical roadmap for generation IV nuclear energy systems: ten nations preparing today for tomorrow's energy needs. Generation IV International Forum. http://www.gen-4.org

3. Potter PC (1996) Gas turbine-modular helium reactor (GT-MHR) conceptual design description report. General Atomics GA-910720
4. Koster A, Matzer HD, Nicholsi DR (2003) PBMR design for the future. Nucl Eng Des 222:231–245
5. Simon R (2005) The primary circuit of the DRAGON high temperature reactor experiment. 18th International conference of structural mechanics in reactor technology (SMiRT 18), Beijing
6. Moormann R (2008) A safety re-evaluation of the AVR pebble bed reactor operation and its consequences for future HTR concepts. Institute for Energy Research, Switzerland
7. Wachholz W (1988) The present state of the HTR concept based on experience gained from AVR and THTR. International Working Group on Gas-cooled Reactors International Atomic Energy Agency IWGGCR-19, Vienna
8. Brown JR et al (1987) Physics testing at Fort St. Vrain: a review. Nucl Sci Eng 97:104
9. Yamashita K et al (1996) Nuclear design of the high-temperature engineering test reactor (HTTR). Nucl Sci Eng 122:212
10. Seker V, Colak U (2003) HTR-10 full core first criticality analysis with MCNP. Nucl Eng Des 222:263–270
11. Stainsby R, Peers K, Mitchell C, Poette C, Mikityuk K, Somers J (2009) Gas cooled fast reactor research and development in the European Union. Sci Technol Nucl Installations 2009:1–7
12. IAEA (2007) Status of small reactor designs without on-site refueling. International Atomic Energy Agency IAEA-TECDOC-1536, Vienna
13. Smith C, Halsey WG, Brown NW, Sienicki JJ, Moisseytsev A, Wade DC (2008) SSTAR: the US lead-cooled fast reactor (LFR). J Nucl Mater 376:255–259
14. Cinotti L, Smith CF, Sienicki JJ, Abderrahim HA, Benamati G, Locaelli G, Monti S, Wider H, Stuwe D, Orden A (2007) The potential of LFR and ELSY project. 2007 International congress on advances in nuclear power plants, Nice
15. Hannum WH (1997) The technology of Integral Fast Reactor and its associated fuel cycle. Prog Nucl Energy 31:1–217
16. Boardman CE (2000) A description of the S-PRISM plant. 8th International conference on nuclear engineering, Baltimore
17. Ingersoll T et al (2004) Status of pre-conceptual design of the Advanced High-Temperature Reactor (AHTR). Oak Ridge National Laboratory, Oak Ridge, ORNL/TM-2004/104
18. Bettis ES, Cottrell WB, Mann ER, Meem JL, Whitman GD (1957) The aircraft reactor experiment: operation. Nucl Sci Eng 2:841–853
19. Haubenreich PN, Engel JR (1970) Experience with the molten-salt reactor experiment. Nucl Appl Technol 8:118–136
20. Kim TK, Yang WS, Grandy C, Hill RN (2009) Core design studies for a 1000 MWt advanced burner reactor. Ann Nucl Energy 36:331–336
21. Zhao H, Zhang H (2007) An innovative hybrid loop-pool design for sodium cooled fast reactor. Idaho National Laboratory INL/CON-07-12657
22. Koch L (2000) Experimental breeder reactor-II. Argonne National Laboratory, Chicago
23. Lash T (1997) Fast flux test facility (FFTF) briefing book 1: summary. Pacific Northwest National Laboratory PNNL-11778
24. Oka Y (2000) Design concept of once-through cycle supercritical pressurized light water reactors. The first International symposium on supercritical water-cooled reactors, SCR-2000, Tokyo
25. Macdonald P (2000) Feasibility study of supercritical light water cooled fast reactor for actinide burning and electric power production. Idaho National Laboratory INEEL/EXT-02-01330
26. Kim TK, Wilson PH, Hu P, Jain R (2004) Feasibility and configuration of a mixed spectrum supercritical water reactor. International topical meeting on the Physics of Fuel Cycles and Advanced Nuclear Systems (PHYSOR-2004), Chicago
27. Kim TK, Taiwo TA, Yang WS, Hill RN, Assessment of deep burnup concept based on graphite moderated gas-cooled thermal reactor. International topical meeting on the Physics of Fuel Cycles and Advanced Nuclear Systems (PHYSOR-2006), Vancouver

Book and Reviews

A Strategy for nuclear energy research and development. Electric Power Research Institute (ERPI)
Bouchard JB (2008) Generation IV advanced nuclear energy systems. Nucl Plant J 26
Kim WJ et al (2006) Supercritical carbon dioxide Brayton power conversion cycle design for optimized battery-type integral reactor system. International congress on advances in nuclear power plants, Reno
MacDonald PE et al (2003) NGNP preliminary point design – results of initial neutronics and thermal-hydraulic assessment. INEEL/EXT-03-00870 Rev. 1. Idaho National Engineering and Environmental Laboratory, September 2003
Sienicki JJ et al (2006) Status report on small secure transportable autonomous reactor (SSTAR)/ lead-cooled fast reactor (LFR) and supporting research and development. Argonne National Laboratory ANL-GenIV-089
Schultz RR (2008) Next generation nuclear plant methods research and development technical program plan. Idaho National Laboratory INL/EXT-06-11804
The US Generation IV Implementation Strategy (2003) US Department of Energy office of Nuclear Energy, Science and Technology
The US Generation IV Fast Reactor Strategy (2006) US Department of Energy office of Nuclear Energy

Chapter 7
Nuclear Reactor Materials and Fuels

James S. Tulenko

Glossary

Austenitic stainless steel	Austenitic steels contain alloys of chromium and nickel (sometimes manganese and nitrogen), structured around the Type 302 stainless steel composition of iron, 18% chromium, and 8% nickel. Austenitic steels are not hardenable by heat treatment. The most common austenitic stainless steel is type 304.
Burnup	A measurement of the energy generated by fuel atoms that undergo fission. It is normally quoted in megawatt–days per metric ton of uranium metal or its equivalent (MWd/MTU).
Core plate	In a reactor the upper and lower core plates supports the fuel, channels the cooling water into the fuel bundle, and assures each fuel bundle is maintained equidistant from each other.
Fertile fuel	A material capable of creating a fissile fuel upon capture of a neutron. Examples are U^{238} and Th^{232}, which create Pu^{239} and U^{233} respectively.
Fissile fuel	Capable of undergoing fission by thermal neutrons. The four primary nuclides are U^{233}, U^{235}, Pu^{239}, and Pu^{241}.

This chapter was originally published as part of the Encyclopedia of Sustainability Science and Technology edited by Robert A. Meyers. DOI:10.1007/978-1-4419-0851-3

J.S. Tulenko (✉)
Laboratory for Development of Advanced Nuclear Fuels and Materials, University of Florida, Gainesville, FL 32611, USA
e-mail: tulenko@ufl.edu

N. Tsoulfanidis (ed.), *Nuclear Energy: Selected Entries from the Encyclopedia of Sustainability Science and Technology*, DOI 10.1007/978-1-4614-5716-9_7,

Fissionable fuel	A material capable of undergoing fission, via the absorption of a neutron with kinetic energy above a certain level. Examples are U^{238} and Th^{232}.
Half-life	The time it takes for the mass of a substance undergoing decay to decrease by half.
Inconel	Refers to a family of austenitic nickel-chromium-based high performance alloys trademarked by the Special Metals Corporation. Inconel metal is typically used in high temperature applications and is generally known for its resistance to oxidation and a superior ability to maintain integrity in high temperature conditions.
Isotopes	Isotopes are different forms of atoms (nuclides) of the same chemical element, each having a different number of neutrons. Isotopes differ in mass number (the number of neutrons plus protons in the nucleus) but not in atomic number (total number of protons). All isotopes of an element have the same chemical properties, but frequently they have very different nuclear properties.
Martensitic or ferritic steels	The major alloying addition in martensitic stainless steels is chromium in the range of 11–17%. The carbon levels can vary from 0.10% to 0.65% in these alloys. The high carbon enables the material to be hardened by heating to a high temperature, followed by rapid cooling (quenching). Martensitic steels offer a good combination of corrosion resistance and superior mechanical properties, offering maximum hardness, strength, and resistance to abrasion and erosion.
Neutron capture cross section	The neutron cross section of an isotope is a measure of the probability of neutron capture by that element. It is the effective area that a particular atom of that isotope presents to absorb a neutron, and is measured by a unit (of area) called "barn," which is 10^{-24} cm^2.
Nuclear fuel clad or cladding	The outer layer of the fuel rods, a barrier between the coolant and the nuclear fuel. It is made of a corrosion-resistant metal that has a low absorption cross section for thermal neutrons. In today's modern commercial reactors, cladding is made usually of Zircaloy.
Passivating layer	In the context of corrosion, passivation is the formation of a nonreactive surface film which inhibits further corrosion.
Plutonium (Pu)	Man-made element with atomic number 94. Of the many Pu isotopes, the most noteworthy is ^{239}Pu because is a fissile isotope and may also be used to make a nuclear weapon. ^{238}Pu has found a great application in space missions powering electronic equipment.

Thermal conductivity	Property of a material that describes its ability to conduct heat.
Thorium (Th)	Naturally occurring element with atomic number 90; the only isotope found in nature is ^{232}Th. Th is more abundant than U. Upon capture of a neutron and subsequent radioactive decay, it forms ^{233}U, which is a fissile isotope.
Uranium (U)	Naturally occurring element with atomic number 92; three isotopes are found in nature: U^{238}, U^{235}, and U^{234} with an abundances respectively, of 99.28%, 0,711%, and 0.00057%. The isotope ^{235}U is the only naturally occurring fissile isotope.
Uranium dioxide (UO_2)	An oxide of uranium; a black mildly radioactive, crystalline material that is used in nuclear fuel rods in nuclear reactors.
Zircaloy	Is a group of alloys, mostly consisting of zirconium, with minor additions of tin (often about 1.5%), iron and chromium, used as a fuel rod clad material in light water thermal reactors.

Definition of the Subject: Nuclear Reactor Materials and Fuels

Nuclear reactor materials and fuels can be classified into six categories:

- Nuclear fuel materials
- Nuclear clad materials
- Nuclear coolant materials
- Nuclear poison materials
- Nuclear moderator materials
- Nuclear structural materials

The materials unique to nuclear reactors are the nuclear fuel materials. All the other materials are used in other applications. Because nuclear fuel materials are radioactive, they require specialized handling. Additionally, because of the connection of nuclear energy with the atom bomb, security in its tightest form is required for nuclear fuel.

Introduction to Nuclear Reactor Materials and Fuels

The first nuclear reactor was the famous “Chicago Pile” (CP-1) which was built under the west stands of Stagg Field at the University of Chicago on a squash court and went critical on December 2, 1942. The first nuclear materials were uranium in

both a metal and an oxide form as the fuel, carbon in a graphite form as the moderator, atmospheric air as the coolant (since the reactor power was essentially zero), cadmium as the control material, and wood as the structural material. Nuclear power plant designs have come a long way since then, particularly with regard to cooling. However, the fuel form remains basically the same.

Nuclear Fuel Materials

There are three basic nuclear fuel materials which can be utilized in many different forms: uranium, plutonium, and thorium. The most utilized fuel material is uranium and it is most often utilized in the oxide form in pellet form (see Fig. 7.1). That one pellet held in the tweezers has the energy equivalent of 1 t of coal. Natural uranium is composed of uranium 238 (99.3%) and uranium 235 (0.7%). Uranium 238 is classified as a fertile material, which produces the fissile Plutonium 239 when it captures a neutron. It is necessary to enrich the uranium in the uranium 235 isotope in order to run the light water reactors (LWRs). The uranium for commercial power reactors is normally enriched to ~5% U^{235}. The methods used to enrich the uranium are the gaseous diffusion process in which the isotopes of different molecular weights diffuse differently through a porous barrier and the gaseous centrifuge process, where the different masses are centrifuged in a fast rotating cylinder with the heavier molecules moving toward the periphery of the centrifuge, thus separated from the lighter ones. For both processes a gaseous compound is necessary, that compound is uranium hexafluoride (UF_6) which is a solid at room temperature but becomes a gas at 56.4°C. As a gas, uranium hexafluoride becomes very suitable for a variety of processes to enrich the material in uranium 235. Lastly, and still in development, the laser method where laser radiation is used to excite, ionize, or dissociate one isotopic species without affecting the other may be used for enrichment. The current favored method of enrichment is the gaseous centrifuge.

Uranium as a fuel is also utilized in the metallic form as an alloy with either zircaloy or aluminum in Sodium Fast Reactors (SFRs) and in research reactors. Experimental developmental work is researching the carbide and nitride forms of uranium as a useful fuel form for SFR reactors and Gas Cooled Reactors (GCRs) because of their excellent thermal conductivity properties and higher uranium density. Research is also under way to utilizing uranium or plutonium in either the oxide or metal form with materials such as silicon carbide or zircaloy to form inert matrix fuel forms with improved thermal conductivity properties. Uranium dioxide (UO_2) is a good fuel because it has a high melting point (2,865°C) and does not dissolve in water. However, in an oxidizing environment UO_2 can be oxidized to U_3O_8, which does dissolve in water. The major drawback of uranium dioxide as a fuel form is that it has a relatively low thermal conductivity, which continues to decrease with temperature until approximately 2,000°C. Additionally, the thermal conductivity of uranium also decreases with burnup as the fuel produces power.

Fig. 7.1 Uranium dioxide (UO_2) fuel pellet (Courtesy AREVA)

Table 7.1 Comparison between UO_2, UZr, UC, and UN fuel for key material characteristics

Fuel comparison	Uranium oxide (UO_2)	Metallic fuel (UZr)	Carbide fuel (UC)	Nitride fuel (UN)
Density (g/cm^3)	9.75	14	13.58	13.53
Melting point (°C)	2,750	1,080	2,420	2,780
Thermal conductivity (W/mK)	2.9	14	16.5	14.3

Since the Nuclear Regulatory Commission does not permit reactors to operate in a condition where centerline melting of the fuel pellet may occur, the high melting temperature of the uranium dioxide does tend to offset its low thermal conductivity. However, the high temperatures in the uranium oxide pellet during operation does lead to thermal stresses, which result in cracking in the pellet both in the radial and circumferential directions. The uranium carbide (UC) and uranium nitride (UN) fuel forms have the benefits of a very high thermal conductivity and a higher density than UO_2 of uranium. However, they dissolve in water and therefore cannot be considered for use in the water cooled reactors. The metal fuel form has a higher thermal conductivity and a higher density of uranium than UO_2, but does have a lower melting temperature. The material properties of the various uranium fuel forms are shown in Table 7.1.

Plutonium does not exist in nature, but is a totally man-generated fuel. Plutonium 239 is a fissile isotope generated from a neutron being captured in U^{238} and has a larger fission cross section than that of uranium 235. However, plutonium 239 has a smaller half-life of 24,200 years versus the half-life of uranium 235 of 7.04×10^8 years, so it is far more radioactive and cannot be handled like uranium. Additionally, plutonium 239 in reactor forms a whole family of fertile and fissionable isotopes: Pu^{240}, Pu^{241}, and Pu^{242}. These isotopes have similar short half-lives of 6,537 years for Pu^{240}, 14.4 years for Pu^{241}, and a long half-life of 376,000 years for Pu^{242}. Plutonium metal melts at approximately 640°C, a much

lower temperature than uranium, and has a thermal conductivity at 300 K of 6.74 W/mK versus a value of 27.5 W/mK for uranium metal. Plutonium fuel is normally used as an oxide and is mixed with natural or depleted uranium oxide. This mixed oxide fuel form is termed MOX.

Thorium is a fertile fuel containing only the single thorium isotope Th^{232}, which upon capture of a neutron forms Th^{233}. Th^{233} is transmuted by beta decay with a half-life of 22.3 min into Pa ^{233}, which beta decays with a half-life of 27 days into the fissile uranium isotope U^{233}. Thorium dioxide's advantage over uranium dioxide as a fuel form is that it has both a higher thermal conductivity ($\sim$5.25 $Wm^{-1}K^{-1}$ at 800 K), a higher melting point (3,350°C), 80°C higher than uranium, and is insoluble in water under all conditions, having only the single oxidation state (O_2). Thorium oxide with enriched uranium oxide was the fuel in the very first full-scale nuclear power reactor (the Shippingport Atomic Power Station), which was built by Admiral Rickover for the Duquesne Light Company. This reactor went critical on December 12, 1957.

Nuclear Clad Materials

The clad materials, which enclose the nuclear fuel, are really the first line of defense to retain the radioactive materials within its boundaries and to protect the fuel from the moderator. In additional to these tasks, the clad also provides structural integrity for the fuel assembly and a surface for heat transfer from the fuel to the coolant. The fuel clad and the guide tubes, which connect the upper and lower end fittings of the fuel assembly, are normally made of the same material. The cladding material must be chemically compatible with the fuel and it must be corrosion resistant with the coolant material. Additionally, it is important that the cladding and the guide tube material have a very small neutron capture cross section so as to not interfere with the fission process. Stainless steel has excellent corrosion properties and an excellent resistance to neutron irradiation. However, it has a relatively high thermal neutron absorption cross section. Until a material could be developed which had a low neutron absorption cross section and good corrosion and structural properties under irradiation, stainless steel was used as both the cladding material and the guide tube for both thermal and fast reactors. However, in thermal reactors, the stainless steel neutron absorption cross section is relatively large and the resulting penalty in neutron economy forced a search for a replacement material which would have the required mechanical strength, corrosion resistance in the water moderator, and a low neutron absorption cross section. This search lead to the development of zircaloy, a zirconium alloy material made with minor additions of tin, oxygen, iron, and chromium. The zircaloy family of materials was developed out of the US Naval Reactors program and was quickly picked up by the commercial industry to replace stainless steel as a cladding material and guide tube material (and shroud for BWR reactors) both

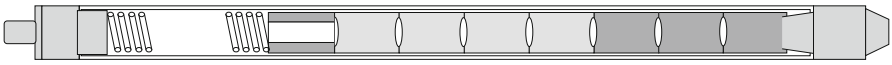

Fig. 7.2 Schematic representation of a fuel rod showing fuel pellets, upper fuel spacer, fuel clad, fuel hold down spring, and upper and lower fuel end plugs

for pressurized and boiling water reactors. The Shippingport Reactor, mentioned earlier, utilized zircaloy clad for its fuel rods. It should be noted that the light water reactor (LWR) concept was developed for the nuclear navy be Admiral H. Rickover and that he helped to shape the nuclear industry. Zircaloy had the required mechanical strength, a small neutron cross section, and good corrosion resistance. While zircaloy reacts with oxygen, it does form a passivating layer that protects the remaining zircaloy from further oxidation. Recent zircaloy alloy developments have added niobium and eliminated the chromium to give better oxidizing and hydriding resistance. Zircaloy is still the material of choice for the nuclear commercial industry. The upper and lower end fittings are made either of stainless steel or of inconel, since they are outside of the active nuclear portion of the core. Different inconels have widely varying compositions, but all are predominantly nickel, with chromium as the second element and iron as the third element. Nickel has a large thermal capture cross section for neutrons. The spacer grids which hold the fuel rods in place were originally either inconel or stainless steel, but were subsequently also changed to zircaloy. Fig. 7.2 displays a schematic of a nuclear fuel rod showing the fuel pellets, top insulator pellet, and the fuel hold down spring which keeps the fuel pellets from moving during shipping and handling. Fig. 7.3 shows a fuel assembly structure with end fittings, guide tubes, and spacer grids, but no fuel rods. The fuel guide tubes provide the vertical structure for the fuel assemblies and serve as channels for the control rods to enter into the fuel assemblies. The spacer grids provide the horizontal structure for the fuel assemblies. Fig. 7.4 shows a fuel assembly with fuel rods in place.

Stainless steel continues to be used as the cladding for fast reactors, since stainless steel tends to have low capture cross sections in the fast neutron energy region. However, even here, as coolant temperatures have been increasing in reactor designs in order to obtain ever higher thermal efficiencies, improved steel alloys have been required to be developed. First, austenitic stainless steels replaced the 304 stainless, and now oxide dispersion strengthened (ODS) martensitic or ferritic steels are under development to replace the austenitic stainless steels. Even more recently, silicon carbide cladding has been being researched as a cladding for the future. The silicon carbide cladding is made from a silicon carbide weave which is then impregnated with a silicon carbide vapor and in the latest designs a metal liner is placed on the inner surface of the clad. As a ceramic, silicon carbide would be resistant to oxidation and would have an extremely high melting temperature, so as to render the loss of coolant accident (LOCA) a nonevent.

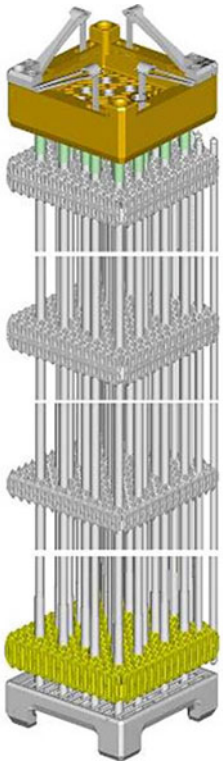

Fig. 7.3 Pressurized water nuclear fuel assembly structure showing upper and lower end fittings, fuel guide tubes, and fuel spacer grids – without fuel rods in place (Courtesy AREVA)

Fig. 7.4 Shows a fuel assembly with fuel rods in place (Courtesy AREVA)

Nuclear Moderator Materials

With the advent of nuclear reactors, the nuclear fission process was found to proceed more easily if the neutrons were moderated in energy into the thermal range ($E < 1.0$ eV). The ideal moderator would have a very low thermal neutron capture cross section and a low atomic number in order to increase the neutrons energy loss on each collision. The very first nuclear reactors used graphite (carbon) to slow the fission neutrons down to the thermal energy regime. Carbon had a very small neutron absorption cross section and an atomic weight of 12. With the advent of the power reactors, water was used as both the moderating and the coolant material. Hydrogen, with an atomic weight of 1, equal to that of a neutron, could slow the neutrons down with very few collisions, and moreover, water is inexpensive. However, hydrogen does have a relatively high thermal neutron capture cross section, turning the hydrogen into deuterium. This capture cross section of ordinary water requires that light water reactors must use enriched uranium as a fuel. Deuterium oxide, or heavy water, would be an ideal moderator and coolant because of its very low capture cross section for neutrons. However, its very high price makes it a very expensive material to use. The Canadians utilize heavy water as their moderator and coolant in their Canadian-Deuterium-Uranium (CANDU) reactors. The extremely low absorption cross section of deuterium allows the CANDU to construct and operate nuclear power plants without the need for enrichment, utilizing natural uranium fuel. But they had to build plants to separate the heavy water (deuterium) out of ordinary water. Hydrogen has also been used in solid form in zirconium hydride (ZrH) as a moderator for space applications and for the TRIGA (*T*raining, *R*esearch, *I*sotopes, *G*eneral *A*tomics) research reactors of General Atomics. Lithium, a liquid metal, can also be used as a moderator. Beryllium has been used as a moderator in research reactors and in many ways is superior to graphite and lithium. However, beryllium is a very toxic material which limits its usefulness because of Environmental Protection Agency restrictions on its use.

Nuclear Coolant Materials

Nuclear coolant materials should be marked by a low melting temperature and a high boiling point. The obvious coolant which has been used in fossil boilers for years is water or steam. However, its low boiling point requires that it be pressurized to allow for a high heat content. Thus, the pressurized water reactor (PWR) has a system pressure of approximately 2,200 psi and the Boiling Water Reactor (BWR) has a pressure of approximately 1,100 psi. As mentioned earlier, the Canadians utilize heavy water as their coolant in the CANDU reactor. However, the Canadians are developing new reactors which utilize ordinary water as the coolant, while retaining heavy water as the moderator. The British for their reactors went with graphite as the moderator and pressurized carbon dioxide (CO_2) as the

coolant in their Advanced Gas Reactor (AGR). The United States has researched using pressurized helium cooled, graphite moderated reactors at the Peach Bottom Reactor (in Pennsylvania) and the Fort Saint Vrain Reactor (in Colorado). The fast reactors utilize either sodium or helium as a coolant. Various experimental reactors have utilized exotic coolants such as fluoride salts, lithium, sodium-potassium alloy (NAK), and a lead-bismuth eutectic. Lead-bismuth (Pb-Bi) eutectic has a low melting point, a high boiling point, and does not react with water or oxygen. The Russians have operated lead cooled reactors in their nuclear navy. The heavy density of lead may generate erosion in its container pipes, particularly bends in its flow path. Molten salts have the advantage of having a very high boiling point and containing the fuel right in the molten salt mixture, thereby doing away with a need to fabricate the fuel.

Nuclear (Neutron) Poison Materials

Nuclear engineers use the term "poison" to describe any material that steals neutrons away from the fission process. Nuclear reactors use poison materials to control the fission chain reaction. These poison materials must have a high neutron capture cross sections. Poison materials are of two types: burnable and nonburnable. In the burnable poison type, the poison material upon capturing a neutron, loses its large neutron capture cross section. In the nonburnable poison type, the poison materials, upon capturing a neutron, convert into a similar high-absorbing neutron cross section material. Three typical control materials used in control rods are (1) hafnium, (2) an alloy of silver, indium, cadmium, and (3) boron. Boron is not a nonburnable poison, like the other control materials, because the main neutron-absorbing isotope ^{10}B, upon capturing a neutron, converts to ^{4}He and ^{7}Li. Boron control rods must be replaced at regular intervals, unlike control rods made with hafnium or the alloy of silver, indium, and cadmium. Soluble boron is added as a poison material into the coolant of pressurized water reactors, where it can be adjusted to keep the reactor in a critical condition. When used in the coolant, the boron is called a chemical shim or "chem shim." The use of boron in the coolant allows pressurized water reactors to keep the control rods out of the core during operation. In a PWR, control rods are used only to shut down the reactor. Boiling water reactors cannot use boron in the coolant because of the boiling action which would lead to boron plate ousting and also that the boron could reach the turbines and ruin the blades. For these reasons, they must utilize control rods in the core during operation in order to control the reactivity of the core.

Boron is also used as a burnable poison in burnable poison rod assemblies (BPRAs), which are inserted into the unoccupied control rod guide tubes and changed at each refueling. The boron is depleted during the cycle, such that at end of cycle the poison effect has been exhausted. Boron is also placed inside the fuel rods in Westinghouse reactors where a thin layer of zirconium diboride (ZrB_2) is

coated on the fuel pellets. Gadolinium and erbium are also used as burnable poison materials and are mixed with the uranium dioxide (UO_2) fuel when forming the fuel pellets. BWR reactors use gadolinium extensively in the fuel in order to control the reactivity because of their inability to utilize boron in the coolant. The advantage of the burnable poison in the fuel, as opposed to BPRAS, is that there is less nuclear waste and the displacement of the water in the guide tube by the BPRAs does result in an end-of-cycle reactivity penalty for the BPRAs.

Nuclear Structural Materials

As mentioned, the very first reactor (CP-1) used wood as the structural material. However, today the nuclear structural materials are steel and concrete. The nuclear-fueled core is contained inside a steel vessel which has steel core support plates, top and bottom, upon which the core is held in place. The steel vessel is approximately 6 in. thick. In new designs, the steel vessel may be inside a concrete shield wall. In pressurized water reactors, steel baffles surround the core and separate the incoming colder water in the down comer from the heated water in the open core. In the boiling water reactor, each fuel assembly is contained in a zircaloy fuel shroud that isolates the water being heated in each fuel assembly. In both the PWR and the BWR, the steel pressure vessel is contained inside a steel reinforced concrete containment structure with a steel liner. Fig. 7.5 shows a PWR reactor vessel with the fuel core, upper core internals, and upper and lower grid assemblies.

Future Directions

For light water reactors, the future directions for the thermal reactors include the development of a crushable fuel pellet design and a ceramic cladding, such as the silicon carbide clad mentioned. This crushable pellet is needed because ceramic clad materials do not do well in tension. Thus, it is necessary for the pellet to give when interacting with the cladding, to prevent creating excessive tension forces on the clad. This development would also eliminate concerns regarding the pellet clad interaction (PCI) which currently limits power-transitions during operation of light water reactors.

The successful development of the molten salt reactor would offer many benefits by eliminating the fuel fabrication step, allowing for online reprocessing and fueling, and also allowing for higher temperature operation with a resultant increase in thermal efficiency. In the long run, future reactors will most likely be fast breeder reactors, either using sodium or helium as the coolant, and fueled with uranium carbide and clad with silicon carbide.

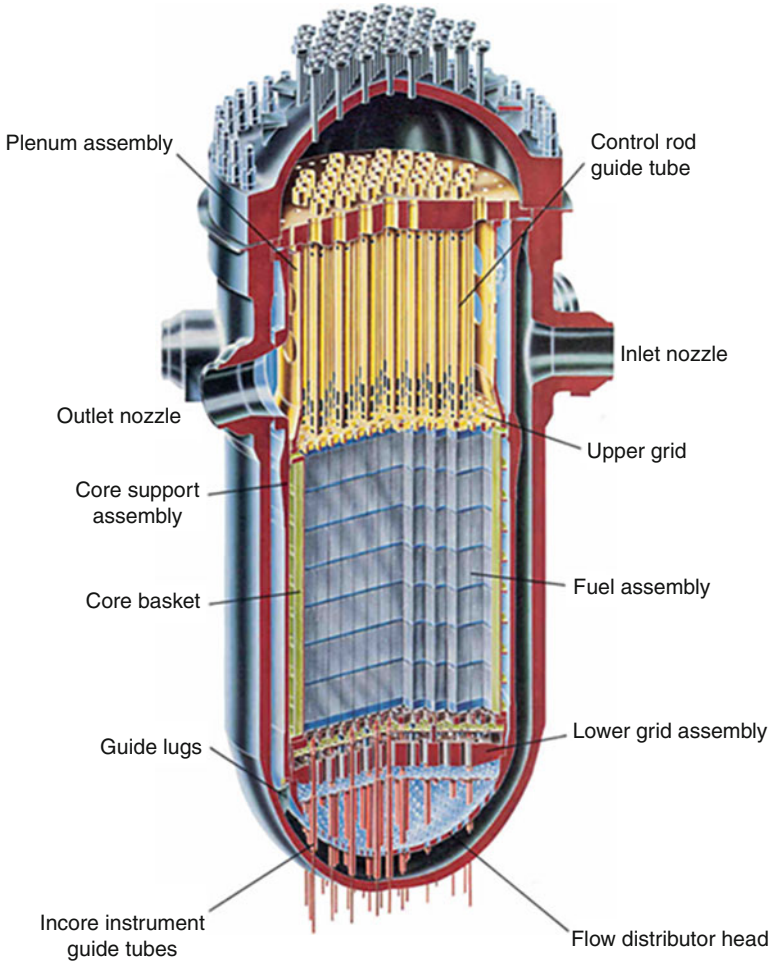

Fig. 7.5 Pressurized water reactor vessel showing fuel core, upper and lower grid assembly, and core internals (Courtesy AREVA)

Bibliography

1. Cochran RG, Tsoulfanidis N (1999) The nuclear fuel cycle: analysis and management, 2nd edn. American Nuclear Society, La Grange Park. ISBN 0-89448-451-6
2. Knief R (1992) Nuclear engineering: theory and technology of commercial nuclear power, 2nd edn. Hemisphere, Washington, DC. ISBN 978-0-89448-458-2
3. Glasstone S, Sesonske A (1994) Nuclear reactor engineering: reactor design basics, vol 1. Chapman & Hall, New York. ISBN 0-442-20057-9

Chapter 8
Modern Nuclear Fuel Cycles

James S. Tulenko

Glossary

Uranium	Occurs in most rocks in concentrations of 2 (sedimentary rocks) to 4 (granite) ppm.
Thorium	More readily available nuclear fuel than uranium, being four times more abundant than uranium in the earth's crust.
Uranium dioxide (UO_2)	An insoluble oxide of uranium which is the form commonly used in commercial nuclear fuel.
Pitchblende	An ore with a very high UO_2 content of up to 70%. Pitchblende also contains radium, thorium, cerium, and lead.
The United States Nuclear Regulatory Commission	Regulatory body for radioactive materials and nuclear power plants.
The department of energy	Required by law to be responsible for the spent fuel and collects a fee of 1 mill/kWh of nuclear electricity for disposal.
MWD/MTU (mega watt days of energy produced per metric ton of uranium contained)	Energy produced per metric ton of uranium (fuel) contained. Current Nuclear Regulatory Commission limits for nuclear power plant fuel is 60,000 MWD/MTU. Normal lifetime of a fuel assembly is 55,000 MWD/MTU.

This chapter was originally published as part of the Encyclopedia of Sustainability Science and Technology edited by Robert A. Meyers. DOI:10.1007/978-1-4419-0851-3

J.S. Tulenko (✉)
Laboratory for Development of Advanced Nuclear Fuels and Materials, University of Florida, 202 Nuclear Science Center, Gainesville, FL 32611-8300, USA
e-mail: tulenko@ufl.edu

N. Tsoulfanidis (ed.), *Nuclear Energy: Selected Entries from the Encyclopedia of Sustainability Science and Technology*, DOI 10.1007/978-1-4614-5716-9_8,

Definition of the Subject

The Nuclear Fuel Cycle describes the entire process followed to convert uranium or thorium ore to its useful state in nuclear power reactors, and its ultimate and current disposal. The cycle has been followed since the 1960s to produce electrical power safely, and without emissions of environmentally endangering carbon gases.

Introduction

Madame Marie Curie, a pioneer in the field of radioactivity and the first person honored with two Nobel Prizes, discovered radioactivity in 1898, and since then many radioactive elements have seen various uses. One in particular, uranium, has been used for its fissionable properties. When a uranium (or plutonium) atom fissions, it releases approximately 200 MeV of energy. The burning of a carbon (coal) atom releases merely 4 eV. The difference between the two – a 50 million-times advantage in nuclear energy release – shows the tremendous advantage in magnitude between chemical and nuclear energy. This advantage is used for common good in nuclear power reactors around the world. Currently, the United States lags France in the use of nuclear power with the United States obtaining ~20% of its electrical energy from nuclear power plants, while France obtains ~80% of its electrical energy from nuclear power plants. Worldwide, approximately 18% of all electrical energy is produced by nuclear power plants.

The Nuclear Fuel Cycle

The nuclear fuel cycle uses two naturally occurring elements, uranium and thorium, which are both relatively common metals. Both materials are obtained by mining the earth. Uranium occurs in most rocks in concentrations of 2 (sedimentary rocks) to 4 (Granite) ppm. Uranium also occurs in seawater in a concentration of 0.003 ppm, which corresponds to approximately 4 billion tons of uranium in the oceans. Uranium (1.8 g/t) is more abundant than common materials such as silver (0.07 g/t), tungsten (1.5 g/t) and Molybdenum (1.5 g/t) [1]. It is 800 times more abundant than gold. Natural (as mined) uranium contains in atomic abundance 99.2175% Uranium-238 (U-238); 0.72% Uranium-235 (U-235); and 0.0055% Uranium-234 (U-234). Uranium has atomic number 92, meaning all uranium atoms contain 92 protons, with the rest of the mass number being composed of neutrons. All uranium isotopes are radioactive. This radioactive property makes the detection of uranium deposits relatively easy, even allowing for prospecting by air. Uranium-238 has a half-life of 4.5×10^9 years (4.5 billion years), U-235 has a half-life of 7.1×10^8 years (710 million years), and U-234 has a half-life of 2.5×10^5 years (250,000 years). All the U-234 currently

present comes from the decay chain of U-238. Uranium-235 is the only fissile isotope available in nature. Uranium can be a fissionable fuel as mined in pressurized heavy water reactors designed by the Atomic Energy of Canada Limited (AECL). These reactors are termed CANDU for CANada Deuterium Uranium. As a by-product of the operation of a nuclear reactor, uranium-238 absorbs a neutron to form, through radioactve decay, the fissile fuel, plutonium-239. Another fissile isotope, uranium-233 comes from the naturally occurring thorium 232 when it captures a neutron. Finally, as part of the plutonium chain, plutonium-241 is also produced. It is important to note that it is the four odd number isotopes: 233, 235, 239, and 241, which are fissionable.

Thorium is an even more readily available nuclear fuel than uranium, being four times more abundant than uranium in the earth's crust. Thorium is the 39th most common element in the earth's crust and is about as common as lead. Thorium is present in the earth's crust with an average concentration of about 9.6 ppm. Thorium must be converted to a fissile fuel in a nuclear reactor by absorption of a neutron, forming through radioactive decay, the fissionable fuel, uranium-233. Thorium has only one naturally occurring isotope, thorium-232, which is radioactive with a half-life of 1.3×10^{10} years. India, which has large thorium deposits, has been a leader in utilizing thorium to breed uranium-233 to serve as a nuclear fuel. Other countries having major deposits of thorium are Australia, Norway, and the United States.

Uranium History

Uranium was discovered in 1789 by Martin Heinrich Klaproth, a German chemist, in the mineral pitchblende, which is primarily a mix of uranium oxides. No one could identify this new material he isolated, so in honor of the planet Uranus that had just been discovered, he called his new material Uranium. Although Klaproth, as well as the rest of the scientific community, believed that the substance he extracted from pitchblende was pure uranium, it was actually uranium dioxide (UO_2). It was not until 1842 that Eugene-Melchoir Peligot, a French chemist, noticed that "pure" uranium reacted oddly with uranium tetrachloride (UCl_4). He then proceeded to isolate pure uranium by heating the uranium dioxide with potassium in a platinum crucible. Radioactivity was first discovered in 1896 when the French scientist Henri Becquerel accidentally placed some uranium salts near some paper-wrapped photographic plates and discovered the natural radioactivity of uranium.

Uranium compounds have long been used for centuries to color glass. Uranium trioxide (UO_3) was used in the manufacture of a distinctive orange Fiestaware dinnerware. In 1938, Otto Hahn (1879–1968), Lise Meitner (1878–1968), and Fritz Strassmann (1902–1980) were the first to recognize that the uranium atom under bombardment by neutrons, actually split, or fissioned.

When a uranium or plutonium atom is fissioned, it releases approximately 200 MeV of energy, while the burning of a carbon (coal) atom releases 4 eV.

This difference of 50 million times in energy release shows the tremendous difference in magnitude between chemical and nuclear energy.

Thorium was discovered in 1829 by the Swedish chemist Jons Jacob Berzelius, who named the element after the Thor, the mythical Scandinavian god of war. He also was the first to isolate cerium, selenium, silicon, and zirconium. Thorium and thorium compounds have the properties of having very high melting temperatures. As a result, it was used for high-temperature application such as coatings on tungsten filaments in light bulbs and for high-temperature laboratory equipment. However, its use outside the nuclear fuel cycle has been greatly diminished because of state and federal laws concerning the handling and disposal of radioactive materials. Thorium is found in the minerals monazite and thorianite.

History of Uranium

The earliest recovery of uranium was from pitchblende, an ore with a very high UO_2 content of up to 70%. Pitchblende also contains radium, thorium, cerium, and lead. It is mostly found with deposits that contain phosphates, arsenates, and vanadates. Uranium exists in nature in two valence states, U^{6+} and U^{4+}. These properties are key to the geological distribution of uranium. U^{6+} is soluble in water, but changes to the insoluble U^{4+} in a reducing environment. The occurrence of reducing environments in riverbeds and seas have led to the formation of rich uranium deposits. A rich uranium deposit contains 2% uranium and economic deposits are as low as 0.1%. Once the ore is mined, it is sent to a mill, which is really a chemical plant that extracts the uranium from the ore. The ore arrives via truck and is crushed, leached, and approximately 90–95% of the uranium is recovered through solvent extraction. During the processing a large waste stream called tails is formed, which contains approximately 98–99.9% of the material mined. Because this waste stream or tails contains all the radioactive daughter products of uranium, such as radon and radium, this waste stream must be carefully controlled and stabilized. The tailings pile must have a cover designed to control radiological hazards for a minimum of at least 200 years and designed for 1,000 years, to the greatest extent reasonably achievable. It must also limit radon (^{222}Rn) releases to 20 $pCi/m^2/s$ averaged over the disposal area. The end uranium product of the milling process is U_3O_8, better known as "yellowcake," because of its color.

Uranium Conversion and Enriching

The U_3O_8 concentrate must be both purified and converted to uranium hexafluoride (UF_6), which is the form required for the enriching process. At the conversion facility, the uranium oxide is combined with anhydrous HF and fluorine gas in a series of chemical reactions to form the chemical compound UF6. The product

UF6 is placed into steel cylinders and shipped as a solid to a gaseous diffusion or gaseous centrifuge plant for enrichment. UF6 is a white crystalline solid at room temperature (its triple point is 64°C (147.3°F) and it sublimes at 56.5°C (133.8°F) at atmospheric pressure). The liquid phase only exists under pressures greater than about 1.5 atmospheres and at temperatures above 64°C. At the enrichment plant, the solid uranium hexafluoride (UF_6) from the conversion process is heated in its container until it becomes a gas. The container becomes pressurized as the solid melts UF_6 gas fills the container. The gaseous diffusion process is based on the difference in rates at which the fluorides of U-235 and U-238 diffuse though barriers. The uranium that has penetrated the barrier side is now slightly enriched in U-235 is withdrawn and fed into the next higher enrichment stage, while the slightly depleted material inside the barrier is recycled back into the next lower stage. It takes many hundreds of stages, one after the other, before the UF_6 gas contains enough uranium-235 to be used as an enriched fuel in reactor. Each barrier has millions of holes per square inch with each hole approximately 10^{-7} in. in diameter. This gaseous diffusion enrichment process is very energy intensive, as the gas is compressed and expanded at each stage.

The other commercial enriching process, which uses an order of magnitude less energy, is the gaseous centrifuge process. The gas centrifuge uranium enrichment process uses a large number of rotating cylinders in series and parallel formations. Centrifuge machines are interconnected to form trains and cascades. In this process, UF_6 gas is placed in a cylinder and rotated at a high speed. This rotation creates a strong centrifugal force so that the heavier gas molecules (containing U-238) move toward the outside of the cylinder and the lighter gas molecules (containing U-235) collect closer to the center. The stream that is slightly enriched in U-235 is withdrawn and fed into the next higher stage, while the slightly depleted stream is recycled back into the next lower stage. At each stage of the gaseous diffusion process the U-235 is enriched by a factor of 1.004, where at each stage of the gaseous centrifuge process the stage enrichment factor is 1.2. For 1 kg of uranium enriched to 5% U-235, 9.4 kg of natural uranium feed are required and 8.4 kg of depleted uranium (tails) with a U-235 isotope content of approximately 0.2% are produced as a waste stream. The US Nuclear Regulatory Commission has decided that depleted uranium is a low level waste. The Department of Energy has over 560,000 mt stockpile of uranium tails stored as UF_6 in steel cylinders. The tails uranium has minor uses as a shields for radioactive sources, as the penetrator in armor piercing shells, as a yacht hold ballast, and as a weight for the balancing of helicopter rotor tips and passenger aircraft.

Nuclear Fuel Fabrication

The enriched UF_6 is transported to a fuel fabrication plant where the UF_6, in solid form in containers, is again heated to its gaseous form, and the UF_6 gas is chemically processed to form uranium dioxide (UO_2) powder. This powder is then

pressed into pellets, sintered into ceramic form, loaded into Zircaloy tubes, pressurized with helium and sealed. The fuel rods are then placed into an array (17 × 17) which is bound together with guide tubes, spacer grids and top and bottom end fittings, all of which forms the nuclear fuel assembly. Depending on the type of light water reactor, a fuel assembly may contain up to 264 fuel rods and have dimensions of 5–6 in. square by about 12 ft long. The fuel is placed into containers and is trucked to the nuclear fuel plants to generate electricity. A single pressurized water fuel assembly contains about 500 kg of enriched uranium and can produces 200,000,000 kWh of electricity. Since the average national electrical yearly use per person is 11,867 kWh, a single nuclear fuel assembly gives 5,562 people their yearly electric needs during its 3 years of operation.

Nuclear Fuel Operation and Disposal

Every 12–24 months, US nuclear power plants are shut down and the oldest fuel assemblies are removed (approximately ⅓–½) and replaced with new fuel assemblies. The power production of a fuel assembly is measured in MWD/MTU or mega watt days of energy produced per metric ton of uranium (fuel) contained. Currently the normal lifetime of a fuel assembly is 55,000 MWD/MTU and the maximum lifetime currently allowed by the Nuclear regulatory commission is 60,000 MWD/MTU. At the end of its useful life, the spent fuel assembly is placed in a cooled borated water storage pond to allow for removal of the radioactive decay heat. After approximately 5 years of wet storage, the decay heat has been sufficiently decreased that the fuel assembly can be removed to dry storage in concrete or steel containers. Since only approximately 5% of the uranium fuel is destroyed, in Europe and Asia the spent fuel is reprocessed and the 95% of uranium remaining is recycled, with the 5% of radioactive waste products sent to waste storage. At the current time, the United States policy was to store the spent fuel in a waste repository being built at Yucca Mountain in Nevada. Most recently this site has become part of a political struggle and the current administration has moved to halt all licensing of the Yucca Mountain site and to convene a high level committee to revisit the question of nuclear waste disposal. The Department of Energy is required by law to be responsible for the spent fuel and collects a fee of 1 mill/kWh of nuclear electricity delivered, which is paid by consumers of nuclear-generated electricity. The one assembly described above would generate approximately $200,000 in the waste fund for its disposal.

There is enough uranium and thorium in the world to produce the required amount of fuel to allow nuclear plants to produce the current rate of electrical energy usage for the next 1,000 years.

Future Directions

(A discussion including potential impacts on the development of certain areas of science.) With the dawn of the environmental awareness and new economies of energy production, the nuclear fuel cycle also is undergoing change. Research efforts are continuing to find new and more efficient ways to use the fissionable atom. Also, currently operating nuclear plants are becoming more efficient and cost beneficial. With no greenhouse gases to speak of, nuclear energy is bound to play a role in the nation's future energy needs. More than 100 nuclear reactors nationwide now provide almost 20% of our energy production. The large, proven-safe nuclear plants produce electricity best when running at full power, 24/7.

Bibliography

1. Cochran RG, Tsoulfanidis N (1999) The nuclear fuel cycle: analysis and management. American Nuclear Society, La Grange Park
2. Wilson PD (1996) The nuclear fuel cycle: from ore to waste. Oxford Science Publications, Oxford

Chapter 9
Nuclear Facilities, Decommissioning of

David R. Turner

Glossary

Decommissioning	Nuclear decommissioning is a term used to describe the process of removing a nuclear facility or site safely from service and reducing residual radioactivity to a level that permits (1) release of the property for unrestricted use and termination of the license or (2) release of the property under restricted conditions and termination of the license. Although waste classification and management is an important aspect of decommissioning, the details of radioactive waste management and disposal are not addressed in this article.
Decontamination	The removal of undesired residual radioactivity from facilities, soils, or equipment, prior to the release of a site or facility and termination of a license. Also known as remediation, remedial action, and cleanup.
Exposure pathway	The route by which radioactivity travels through the environment to eventually cause radiation exposure to a person or group.
Financial assurance	A guarantee or other financial arrangement that ensures funds for decommissioning will be available when needed.

This chapter was originally published as part of the Encyclopedia of Sustainability Science and Technology edited by Robert A. Meyers. DOI:10.1007/978-1-4419-0851-3

D.R. Turner (✉)
Geosciences and Engineering Division, Southwest Research Institute, P.O. Drawer 28510, San Antonio, TX 78228-0510, USA
e-mail: dturner@swri.edu

N. Tsoulfanidis (ed.), *Nuclear Energy: Selected Entries from the Encyclopedia of Sustainability Science and Technology*, DOI 10.1007/978-1-4614-5716-9_9,

Institutional controls	Administrative and physical measures to control access to a site and minimize disturbances to engineered measures established to control the residual radioactivity.
Monitoring	The measurement of radiation levels, concentrations, surface area concentrations, or quantities of radioactive material and the use of the results of these measurements to evaluate potential exposures and doses.
Nuclear fuel cycle	Consists of the different stages necessary to produce nuclear power. Specific stages include (1) the *front end* of the nuclear fuel cycle where uranium is mined and fuel is prepared, (2) the *service period* in which the fuel is used during reactor operation, and (3) the *back end*, which involves safe management, containment, and either reprocessing or disposal of spent nuclear fuel. Because uranium fuel is the most common type of nuclear fuel, this article focuses on the uranium nuclear fuel cycle.
Radiological survey	An evaluation of the radiological conditions and potential hazards at a site related to the production, use, transfer, release, disposal, or presence of radioactive material or other sources of radiation. Radiological surveys can be used to provide the basis for acquiring necessary technical information to develop, analyze, and select appropriate cleanup techniques.
Residual radioactivity	Radioactivity in structures, materials, soils, groundwater, and other media at a site resulting from activities under the licensee's control, excluding background radiation.

Definition of the Subject

The process of safely shutting down, dismantling, cleaning up, and monitoring nuclear facilities is collectively known as nuclear decommissioning. Nuclear power has been used as a source of energy for more than 50 years, and more than 500 nuclear reactors have been constructed and operated worldwide [1]. In addition to power plants, the nuclear fuel cycle requires different types of facilities to mine uranium, produce fresh nuclear fuel, and manage spent nuclear fuel and associated radioactive wastes after the fuel can no longer be effectively used to produce power. Many of the facilities associated with the nuclear fuel cycle that supports these reactors, as well as the reactors themselves, have either reached or are approaching the end of their planned service life. Also, some countries such as Belgium and Germany have initiated national policies to phase out nuclear power over time [2, 3]. Owners and operators of nuclear facilities, as well as government agencies responsible for their regulation, must evaluate economic and public policy considerations to determine whether to renew facility

licenses or to permanently remove facilities from service, and decommission them to release the sites for other potential uses.

Definitions of nuclear decommissioning, radiological dose limits for site release, and even terminology can vary from country to country depending on the nature of the laws and regulations that govern the nuclear fuel cycle. The International Atomic Energy Agency (IAEA) defines decommissioning as "...the administrative and technical actions taken to allow the removal of some or all of the regulatory controls from a facility" [4]. Similarly, the Nuclear Energy Agency (NEA) broadly defines decommissioning as covering "all of the administrative and technical actions associated with cessation of operation and withdrawal from service" [1]. The World Nuclear Association (WNA) defines the two main objectives of decommissioning as rendering the site permanently safe and restoring it, "as far as practicable," for reuse for nuclear or non-nuclear activities. Reuse can apply to different components of a nuclear facility, including land, water bodies, buildings, equipment, and materials [5].

Some early nuclear facilities were developed without explicit consideration of decommissioning, and these "legacy" sites continue to be identified and cleaned up – often at public expense. As it is currently practiced in most nations with a robust legal and regulatory framework, the decommissioning process begins when a facility is removed from service. Planning for decommissioning should begin at the design stage, before a facility enters operation [4, 6]. For example, early decisions about construction materials, site layout, spill prevention and control measures, waste management, and financial assurance can all influence decommissioning activities at the end of a facility's life cycle and may be made (or be required) before a facility receives an operating license. Similarly, some national nuclear regulatory programs require that decommissioning plans be submitted with the initial license application and periodically reevaluated and updated during the operating life of the facility [6, 7]. Decommissioning is generally considered complete when the facility is removed from regulatory control (e.g., the license is terminated) and the site is made available for reuse.

The processes and technologies are similar to those used for other industrial facilities, but because of the nature of the materials used in the nuclear fuel cycle, nuclear decommissioning tends to be a regulated process that requires special procedures to handle and dispose of radioactive materials safely. The specific methods used in nuclear decommissioning vary widely, depending on factors such as the type, size, age, operational history, and design of a given nuclear facility. National policies differ on detailed objectives, and individual countries are likely to have different issues of concern such as the future use of nuclear power, the continued availability of trained staff, socioeconomic effects on surrounding communities that may result from shutting down a large facility, and financial issues associated with funding decommissioning activities.

For these reasons, there is no unique or preferred "one size fits all" approach to the nuclear decommissioning process. The intent of this article is neither to endorse any particular approach, nor to describe all potential aspects of nuclear decommissioning in detail, but rather to provide a broad overview of generally applicable principles. Further, this article focuses on decommissioning facilities associated with the commercial-scale production of nuclear power. Other processes

that use or generate nuclear materials such as military programs, nuclear medicine, and industrial operations that produce radioactive materials as a byproduct are beyond the intended scope of this discussion. The reader is referred to the references identified in the Bibliography for further information and more detailed discussion of the processes described here.

Introduction

In 2007, nuclear reactors provided slightly more than 14% of the world's electricity, with ranges as high as 76.8% in France [8]. Currently (July 2009), 436 nuclear power reactors are in operation, with 5 reactors in long-term shutdown and 48 new reactors under construction [9]. In addition to nuclear reactors, generating nuclear power requires different types of facilities to support the nuclear fuel cycle. For example, as of August 2003, the IAEA reported that there were 423 operating nuclear fuel cycle facilities, with 19 more under construction. Eventually, decisions will need to be made with regard to closing and decommissioning these facilities in a safe manner and potentially returning the land to other uses.

More than 50 years after the first nuclear power reactor went on line, many of the facilities associated with commercial-scale nuclear power generation are now approaching the end of their planned service life. For example, the European Union estimates that at least one-third of the 152 nuclear power plants operating in its member countries will need to be decommissioned by 2025 [2], and the IAEA reported that 297 nuclear fuel cycle facilities were shut down or in the process of being decommissioned worldwide as of August 2003 [4]. An even larger number of manufacturing and research facilities (about 1,600) that use radioactive material will need to be decommissioned "over the coming decades" [10].

At the same time, increased global energy demand, coupled with a growing concern about the effects of carbon emissions from traditional fuel sources, has sparked renewed interest in nuclear power generation. As an example, the U.S. Nuclear Regulatory Commission (USNRC), the agency responsible for licensing and regulating commercial nuclear activities in the United States, received a total of 17 applications to construct and operate 26 new commercial nuclear reactors during 2007–2008 [11]. Although some countries are deemphasizing nuclear power, other countries in Europe and Asia have indicated a renewed interest in nuclear power as a component of their overall energy portfolio [3, 8, 12].

Together, these developments indicate that all stages of the commercial nuclear fuel cycle will continue to be active or will be expanded in the foreseeable future. For this reason, methods to safely take these facilities out of service and decommission them will continue to be an important component of energy policy. It is these methods that are the subject of this article.

Although primarily developed for nuclear power plants, there are three basic types of alternative decommissioning strategies that may be applicable to other nuclear facilities:

- A strategy of immediate decontamination and dismantlement [1, 7] (also defined as DECON [11, 13]) begins soon after the nuclear facility closes.
- Safe storage [1], deferred or delayed decontamination [7], or SAFSTOR [14, 15] refer to decommissioning strategies where a nuclear facility is left intact after closing, placed in a stable condition, and maintained and monitored until subsequent dismantlement and decommissioning. Similarly, uranium production facilities (mines and mills) may be placed on standby status when uranium prices are low and deposits cannot be produced at a profit.
- A strategy of entombment [1, 7] or ENTOMB [14, 15] involves encasing radioactive materials onsite in a long-lived, structurally sound material such as concrete.

The first two strategies may also be combined. For example, some facilities at a site may be immediately dismantled while other structures are placed in safe storage. Generally, decommissioning activities are anticipated to be completed in a period of decades from the end of operations [14, 15].

Once the decommissioning strategy is selected for a given facility, general activities associated with nuclear decommissioning may include:

- Characterizing the features of the site and conducting radiological surveys to determine radiation background and residual radiation levels
- Developing a site-specific decommissioning plan
- Estimating cost
- Conducting safety and performance assessments
- Decontaminating structures, equipment, and components for reuse or recycling
- Dismantling and removing buildings, structures, and equipment from the site
- Remediating contaminated soils and groundwater
- Performing waste management and disposal
- Conducting final inspections and surveys
- Reclaiming disturbed lands
- Implementing active institutional controls and monitoring

Specific decommissioning activities and technologies are determined on a case-by-case basis and can depend on many things at a given site, such as the duration, type, and scale of operations; the geologic setting of the site; socioeconomic considerations; and the regulatory policies of the government. In addition, a key part of a decommissioning plan is estimating decommissioning costs to establish financial arrangements that ensure resources are available to complete the decommissioning process.

Types of Nuclear Facilities

As described in the "Introduction" section, generating electricity from nuclear power plants is only part of the nuclear fuel cycle [16] and decisions will need to be made with regard to the safe closure and decommissioning of each of these

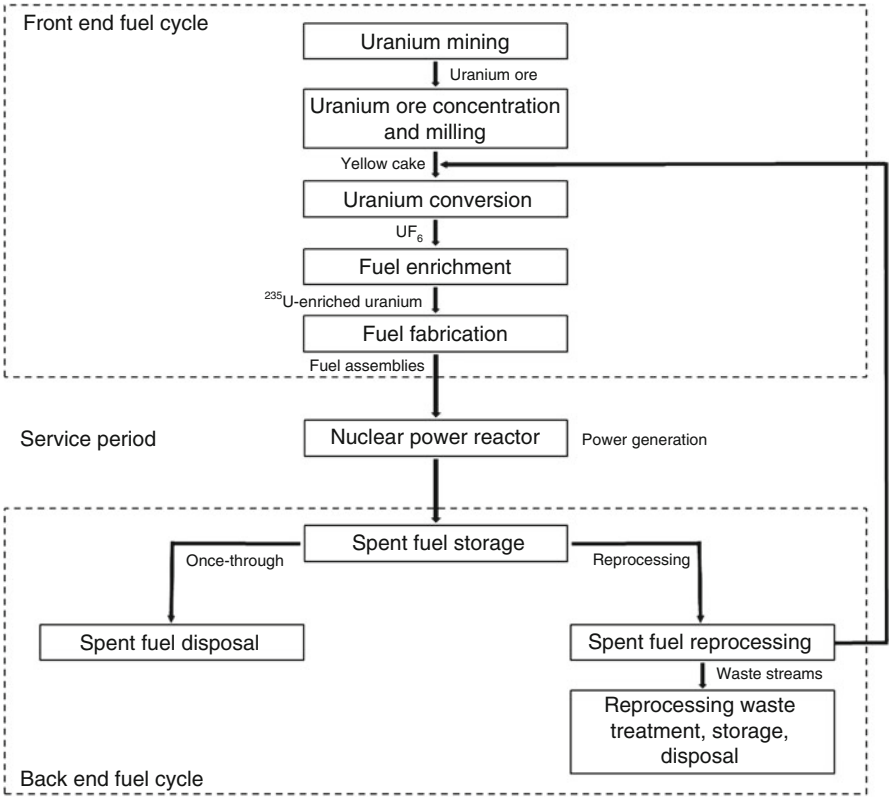

Fig. 9.1 Simplified diagram representing the nuclear (uranium) fuel cycle

facilities. To understand any unique aspects that will need to be addressed during nuclear decommissioning, it is important to describe the general nature of the activities that are conducted at each type of facility in the nuclear fuel cycle. Because uranium fuel is the most common type of nuclear fuel, this article focuses on the uranium nuclear fuel cycle (Fig. 9.1).

To support the nuclear fuel requirements of commercial power-generating facilities, there are facilities that

- Produce uranium by mining
- Mill ore to concentrate the uranium and package it for transportation
- Purify and transform the uranium concentrate into a form suitable for fuel manufacture through a process called uranium conversion
- Enrich the uranium in isotopes (^{235}U) that produce sustainable nuclear reactions
- Fabricate reactor fuel components and fuel assemblies

These facilities are part of the "front end" of the nuclear fuel cycle. Decommissioning issues for the front end of the fuel cycle are typically associated

Table 9.1 Material balance for the annual operation of a 1,000 MWe nuclear power reactor [17]

Type of nuclear facility	Material balance[a]
Mining	20,000 metric tons (22,000 t) of 1% uranium ore
Milling	230 metric tons (250 t) uranium oxide concentrate (U_3O_8) containing 195 metric tons (215 t) of uranium
Uranium conversion	288 metric tons (317 t) uranium hexafluoride (UF_6)
Fuel enrichment	35 metric tons (39 t) UF_6, containing 24 metric tons (27 t) enriched uranium (4% U-235), 11 metric tons (12 t) depleted uranium (0.25% U-235) tails
Fuel fabrication	27 metric tons (30 t) UO_2, containing 24 metric tons (30 t) enriched uranium
Reactor operation	8,640 million kilowatt-hour electricity at full output (assuming 100% load factor)
Spent nuclear fuel	27 metric tons (30 t) spent nuclear fuel containing 23 metric tons (25 t) uranium (0.8% U-235 as UO_2), 240 kg (529 lb) plutonium, 720 kg (1,587 lb) fission products, and transuranic elements

[a]Assuming enrichment to 4% U-235 with 0.25% tails assay; core load 72 metric tons (79 t) U, refueling so that 24 metric tons (26 t) U/year replaced; operation – 45,000 MWday/t (45 GWday/t) burn-up, 33% thermal efficiency

with naturally occurring radioactivity, such as uranium and radium, and hazards associated with the chemical processing of natural uranium-bearing ores [5].

After the nuclear fuel is used in a commercial reactor to produce electrical power during the service period, the management of the spent nuclear fuel at the "back end" of the nuclear fuel cycle can include facilities that

- Reprocess the fuel to extract nuclear materials and recycle uranium back into the front end of the fuel cycle
- Store or permanently dispose of spent nuclear fuel

At the back end of the fuel cycle, high-level sources of radioactivity and direct irradiation from spent nuclear fuel are decommissioning concerns in addition to natural radioactivity and chemical processing hazards [5]. An example of the typical material balance for the annual operation of a 1,000 Megawatt electric (MWe) nuclear power reactor [17] is included in Table 9.1.

Each of these facilities will require nuclear decommissioning at the end of its life cycle. Usually, the operator of a facility develops a decommissioning plan (see "Developing a Site-Specific Decommissioning Plan") to identify specific activities, estimate costs, and lay out a schedule [18–21]. The plan is submitted to the regulatory agency to ensure that it complies with the applicable regulations. Once it is approved, the initial decommissioning plan is periodically updated and becomes more detailed as the facility evolves during its operational life. At the end of the facility life cycle, the decommissioning plan serves as a blueprint for the nuclear decommissioning process. During decommissioning, the regulatory agency may periodically inspect the site to ensure that the decommissioning plan is being implemented correctly.

The following sections introduce the types of nuclear facilities associated with generating nuclear power and identify features that may influence nuclear decommissioning decisions and activities. The listing is not intended to be exhaustive, nor is it intended to provide a detailed discussion of the complex regulatory controls that may apply for a given type of nuclear facility. The reader is referred to the references identified in the Bibliography for further reading.

Front End Fuel Cycle Facilities

Uranium Mining

At the start of the nuclear fuel cycle, uranium mining focuses on extracting natural uranium ore from the earth. Uranium mining may be done through a conventional process of excavation by open pit or underground mining techniques. During excavation, uranium ore is segregated from waste rock or overburden, and shipped to a uranium mill for further processing (see "Uranium Milling"). Open pit and underground uranium mines are typically decommissioned and reclaimed in accordance with regulations applicable to the mining industry in general [22]. In many ways, decommissioning a uranium mine is subject to challenges similar to those faced in cleaning up mining operations for other resources such as coal and metals. For example, excavations may need to be backfilled, pit walls and disturbed surfaces recontoured, and revegetated to meet applicable mine reclamation standards. Groundwater contamination plumes with elevated levels of uranium and associated heavy metals (e.g., arsenic, selenium) need to be remediated and monitoring systems installed, as appropriate.

Alternatively, uranium recovery may be through a process called in situ leaching (ISL), where chemical fluids are injected through a series of wells into the subsurface to dissolve uranium from ore minerals. The now uranium-enriched solution is pumped back to the surface for subsequent extraction and processing [13, 22–24]. Decommissioning of ISL uranium facilities is different from cleaning up conventional uranium mining operations. For example, because there are no large-scale excavations associated with the ISL uranium recovery technology, surface land disturbance is much less than with conventional mining methods, and large amounts of waste rock are not generated. This can simplify the reclamation effort, but impacts to groundwater are potentially greater, and restoration of groundwater quality to premining levels tends to be a focus in decommissioning ISL facilities [13]. In addition, although the surface facilities such as well heads and pump houses necessary to support ISL uranium mining may be small compared to conventional operations, the well fields themselves may be very large. For example, the permitted areas for U.S. ISL operations in Wyoming and Texas may be as large as 6,500 ha (16,000 acres) and individual well fields may contain hundreds to thousands of wells [13].

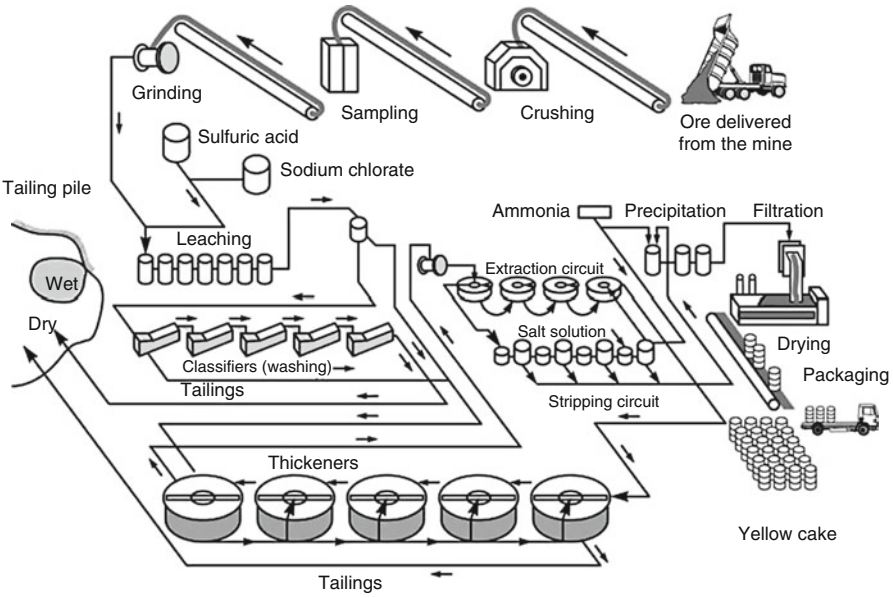

Fig. 9.2 A typical conventional uranium mill [22]

Uranium Milling

While varying depending on the deposit and the type of ore, uranium ores typically have a concentration of about 1% or less uranium (U_3O_8) by weight, although it can be as high as 20%. Decommissioning uranium milling facilities is generally concerned with naturally occurring radioactive elements such as uranium, thorium, and radium. For conventional uranium mining and milling operations (Fig. 9.2), uranium is concentrated through milling (crushing, grinding, separation) and subsequent chemical processing of the ore using alkaline or acid leaching solutions to produce a product called "yellow cake," a coarse powder that is approximately 70% or more U_3O_8 by weight. Milling operations are similar for ISL uranium, but because the mill input is uranium-bearing solutions instead of solid ore, the crushing and grinding, and leaching circuits are not necessary.

Depending on the economics of the operation, a mill may be colocated with a uranium mine, or it may be separate, charging a "toll" to accept and mill ore (conventional) or uranium-bearing solutions (ISL) from nearby uranium mines. Because of the throughput of uranium-bearing solutions and the handling of yellow cake, some of the buildings, pipes, and equipment in the mill may become radioactively contaminated with natural radioactive elements over time and will need to be decontaminated and/or disposed of during decommissioning. Spills and unintentional releases of uranium-rich solutions can lead to soil and groundwater contamination that may need to be remediated during decommissioning. In addition, during conventional milling, large quantities of waste solids are

produced by the crushing, grinding, and leaching circuits. These waste solids, or "tailings," are placed in large impoundments that will also need to be decommissioned at the end of the mill's operational life. ISL facilities do not treat solid rock and therefore produce no tailings. Because these facilities handle large volumes of uranium-rich solutions, however, they may have one or more evaporation ponds that will eventually need to be decommissioned. Although specific activities will vary depending on size, age, operational conditions, and design, decommissioning of a uranium mill (both for conventional and ISL facilities) includes general activities described in the "General Methodologies for Decommissioning" section.

Uranium Conversion

Although natural uranium ores are concentrated and purified during milling to produce yellow cake, the uranium must be further purified and converted to a gas state to produce nuclear fuel. The nature of these chemical processes and the size and complexity of these uranium conversion facilities strongly influence the decommissioning process. Uranium conversion facilities are designed to remove impurities from the yellow cake and convert solid uranium into uranium hexafluoride (UF_6), the only uranium compound that exists as a gas at suitable temperatures [4, 17]. The UF_6 gas is then pressurized and cooled to a liquid state [4]. The liquid is stored in cylinders and allowed to solidify for shipment to a fuel enrichment plant (see "Fuel Enrichment"). Some uranium conversion facilities also recycle uranium scrap that may come from manufacturing facilities or other production plants [4].

The uranium conversion process involves strong acids and alkali agents to dissolve the yellow cake powder. As with mining and milling, the operational risks associated with uranium conversion are chemical as well as radiological, and the safe removal and disposal of hazardous chemicals used in the conversion process must be taken into consideration as part of the decommissioning process. Because it is predominantly an industrial chemical facility, the types of decommissioning issues for a uranium conversion facility are similar to those described in the "Uranium Milling" section for buildings, equipment, and land reclamation at uranium mills. No tailings are produced during uranium conversion. Groundwater and soil contamination from spills and leaks are possible and will need to be identified, remediated, and monitored in accordance with applicable regulations [19]. The size and complexity of uranium conversion plants can lead to significant decommissioning costs. For example, alternative decommissioning options for the 243-ha (600-acre) Sequoyah Fuels uranium conversion plant site in Gore, Oklahoma, varied from about US $19 to US $254 million (2006 dollar value), depending on the option selected for disposal of contaminated materials [25].

Fuel Enrichment

Natural uranium is composed of ^{238}U (99.274%) and ^{235}U (0.711%) and contains trace amounts of ^{234}U (<0.01%). Nuclear reactor fuel requires increasing (or enriching) the fissionable ^{235}U above these natural levels to sustain the nuclear reactions. During the fuel enrichment process, gaseous UF_6 is gradually enriched in ^{235}U to about 3–5% – levels that are sufficient for fabricating commercial reactor fuel [26, 27]. One product of the enrichment process of special concern during decommissioning is depleted uranium tails, where the ^{235}U content has been reduced to below natural levels (about 0.2–0.35%) [28]. This waste stream is commonly stored at the site in gas cylinders of UF_6, although it may also be converted to solid form such as uranium oxide. Depleted uranium emits low levels of radiation and is also a toxic heavy metal, so during decommissioning, this waste must be managed and disposed in accordance with both radiological and hazardous waste criteria [27, 29].

Gaseous diffusion is the process most widely used for nuclear fuel enrichment. The gaseous diffusion process takes advantage of the different diffusion rates that result from the slight differences in mass for ^{238}U and ^{235}U. Gaseous UF_6 is pumped through a permeable porous barrier media. The lower molecular weight ^{235}U has a higher diffusion rate and moves through the barrier media more readily than the higher molecular weight ^{238}U; the UF_6 gas that passes through the media is therefore slightly enriched in ^{235}U [30]. The process is repeated through many barriers until the desired enrichment levels are achieved.

These types of plants are large industrial facilities, with a footprint of about 300–600 ha (750–1,500 acres) that contains a large amount of piping and pumps required to move the UF_6 gas through the permeable barrier system [4]. During operations, the primary hazards in gaseous diffusion plants that may influence subsequent decommissioning include the chemical and radiological hazard of a UF_6 release [31]. There is also a potential for mishandling the enriched uranium, which could create a criticality accident (inadvertent nuclear chain reaction). Because these are large facilities, decontamination and decommissioning of inactive buildings and areas may occur while other parts of the facility continue to operate. Surveillance, maintenance, and security will continue for active parts of the facility. Depending on the operating history of the plant, including spills and unintentional releases, decommissioning and cleanup activities at fuel enrichment facilities may include assessing and remediating soil or groundwater and waste management activities, such as disposing of contaminated materials. The size and complexity of a gaseous diffusion plant can lead to large costs for full decommissioning of all facilities. For example, the U.S. Government Accountability Office (GAO) estimated that cleanup activities at three fuel enrichment plants (Paducah, Kentucky; Oak Ridge, Tennessee; Portsmouth, Ohio) cost US $2.7 billion (in 2004 dollars) from 1993 through 2003, and total costs through final decommissioning in 2044 would exceed revenues into the Uranium Enrichment Decontamination and Decommissioning Fund by about US $3.2–6.2 billion (in

2007 dollars) [32]. Newer technologies such as gas centrifuge and laser separation are being considered for the next generation of fuel enrichment facilities, and the decommissioning issues are likely to be different, with perhaps less waste generated during operation [26].

Fuel Fabrication

For a typical commercial light water reactor, nuclear fuel is the solid form of uranium oxide (UO_2). Fuel fabrication facilities use chemical processes to convert the ^{235}U-enriched UF_6 into UO_2 in the form of a fine powder [28]. Because many of the materials (such as UF_6) are the same, specific factors that may influence the decommissioning of fuel fabrication facilities will be similar to those identified for uranium conversion and fuel enrichment facilities (see "Uranium Conversion" and "Fuel Enrichment"). This powder is then compacted and sintered (heated at a high temperature to fuse the particles together) to produce fuel pellets. These pellets are loaded into metal tubes to produce fuel rods. Hardware is then used to configure the fuel rods into fuel assemblies of the appropriate dimensions and design for a nuclear power reactor. Although this article focuses on the uranium nuclear fuel cycle, other nuclear fuels can also be fabricated, including mixed oxide (MOX) fuels formed from combining uranium and plutonium oxides, thorium fuels based on the ^{232}Th decay chain with ^{233}U as the fissile fuel element, uranium metal alloy fuels, and microsphere fuel particles [28].

Heavy water (water that contains more than the natural proportion of the hydrogen isotope deuterium, ^{2}H) is used as a moderator in some types of nuclear reactors. Heavy water is extracted from normal water through several chemical processes, the most common of which is distillation through electrolysis or isotopic exchange [24].

Chemical, radiological, and criticality hazards at fuel fabrication facilities are similar to hazards at enrichment plants. Most at risk from these hazards are the plant workers. These facilities generally pose a low risk to the public.

Service Period: Nuclear Power Plants

As indicated, the three decommissioning strategies described in the "Introduction" section were initially developed for nuclear reactors and power plants. The principal concerns during the decommissioning of these reactors and power plants are the safe cessation of operation; the safe management, storage, and disposition of highly irradiated spent nuclear fuel; draining and treatment of water and other fluids from the reactor cooling systems; and the decontamination and disposal of equipment, materials, and other systems that may contain contamination or activation products at the site.

At a very basic level, most nuclear reactors operating today use the heat from the controlled fission of ^{235}U (and perhaps ^{239}Pu in the case of MOX fuel) to boil water that turns a turbine and produces electrical power. As described previously, there are 436 nuclear power reactors operating worldwide, with 48 new reactors under construction. In addition, there are 287 (as of August 2003) research and test reactors and critical assemblies (i.e., producing little or no power), predominantly located at research universities and government facilities, that are used for research, education, and training purposes [4, 33].

There is no single design that is representative of all reactors. Of the operating nuclear power reactors, about 400 are water cooled and moderated (Energy Information Administration, 2006) and are predominantly pressurized water reactors (PWR), boiling water reactors (BWR), and pressurized heavy water reactors (PHWR). For example, all of the 104 operating commercial nuclear reactors in the United States are either BWR (35 reactors) or PWR (69 reactors) types [34]. Other operating reactor types include gas-cooled reactors, graphite-moderated reactors, and fast breeder reactors.

Early prototype nuclear reactors are sometimes called Generation I reactors. The current nuclear reactor designs are sometimes called Generation II (large central nuclear power plants) and Generation III (advanced LWR) reactors [28, 35]. Current research and development efforts are focused on designing the next generation, or Generation IV reactors, with a goal to provide more efficient and safe nuclear power generation that is also more resistant to nuclear proliferation [28, 36–38]. In the United States, the Next Generation Nuclear Program initiated with the Energy Policy Act of 2005 focuses on developing a very-high-temperature gas-cooled reactor (VHTR) operating at temperatures greater than 950°C for the production of electricity, process heat, and hydrogen [37]. Other designs are also being considered for the next generation of nuclear reactors, predominantly those based on gas-cooled (such as pebble bed modular reactors), water-cooled (super-critical water-cooled reactors), and fast-spectrum technologies (cooled by sodium, lead, or inert gases) [28, 35].

The different current and future design types and sizes of reactors make decommissioning inherently a site- and reactor-specific process. Each current and future reactor design will have its own design-specific decommissioning requirements that must be taken into consideration.

Back End Fuel Cycle Facilities

After the nuclear fuel is irradiated in a reactor and the useful energy has been extracted, it is called spent nuclear fuel. The removal of spent nuclear fuel from the reactor is generally considered part of the transition from the operational phase of the power plant, and not as part of the decommissioning process. The back end of the nuclear fuel cycle consists of facilities that handle spent nuclear fuel. Currently, most commercial nuclear power is based on an open, or “once through” uranium fuel cycle, where the fuel is used in a power plant one time and then removed as spent nuclear fuel [39].

Fuel Reprocessing Facilities

When the spent nuclear fuel is removed from the reactor, it is predominantly composed of uranium oxide (96%), other actinides like plutonium and americium (1%), and other fission products such as cesium and strontium (3%) [30]. The spent nuclear fuel must be cooled both thermally and radioactively in a water-filled spent fuel pool and later placed in dry cask storage at the reactor site.

Fuel reprocessing facilities are designed to recover materials such as uranium and plutonium from irradiated spent nuclear fuel. After sufficient cooling, the spent nuclear fuel is dissolved using solvents and the usable components (mostly uranium and plutonium) are separated from waste materials such as other actinides and fission products [4, 40]. The recovered uranium and plutonium are recycled into the front end of the nuclear fuel cycle and refabricated to produce new nuclear fuel (such as MOX) or used for defense purposes. Waste materials, in the form of sludges, salt cake, or calcined wastes, and the reprocessing solutions are collected for disposal. Liquid wastes are generally not suitable for disposal, and decommissioning and cleanup may include vitrification to solidify waste solutions in the form of borosilicate glass.

Because of the high radiological dose rates and contamination levels associated with irradiated spent nuclear fuel, human access is limited for major parts of the facility. This leads to decontamination and decommissioning that is more complicated than facilities such as uranium mills and fuel fabrication facilities at the front end of the nuclear fuel cycle. Facilities tend to be very large, and large volumes of liquid wastes are produced and stored for subsequent disposal.

Examples of fuel reprocessing facilities in the United States include U.S. Department of Energy (USDOE) facilities at Hanford, Washington, and the Savannah River site in South Carolina. The only commercial fuel reprocessing facility in the United States, located at West Valley, New York, ceased operations in 1972. The Carter administration elected to defer reprocessing of commercial nuclear fuel in 1977, and there are no commercial fuel reprocessing facilities currently operating in the United States. The USDOE has completed vitrification of the liquid wastes at West Valley, storing the borosilicate glass logs on site [41, 42]. Decommissioning activities at West Valley are ongoing. Large reprocessing facilities are also located at Sellafield in the United Kingdom and La Hague in France.

Waste Management and Disposal

As with many aspects of nuclear decommissioning, the nature and amount of waste produced during cleanup activities will depend on the age and size of a given facility, as well as the nature and history of operations at the site. As described in IAEA [43], four different types of waste or "waste streams," each with different disposal options, are typically produced during nuclear decommissioning. The first three are types that include radioactive waste:

- Primary waste is generated during dismantling activities and may include internal plant components such as a reactor pressure vessel and associated piping, equipment such as pumps and valves, special facilities such as glove boxes and radiation hot cells, and building materials. These components of the primary waste streams may be radioactive through activation by both short- and long-lived radionuclides during plant operations, or by surface contamination. Primary wastes can include a variety of materials, but typically metal and concrete rubble are the largest component by volume of this waste stream [43].
- Secondary wastes are generated during different steps in decontamination and dismantling. These may include solutions, absorbents, and filters used to treat surfaces to reduce radioactive contamination.
- Tools and equipment, such as cutting equipment and protective gear for personnel use during decontamination and dismantling, may become contaminated. To minimize costs and waste volumes, some equipment may be decontaminated so that it can continue to be used.

In addition to these radioactive wastes, decommissioning can potentially produce large volumes of non-radioactive wastes, such as construction debris, sanitary wastes, hazardous chemicals, and asbestos. These wastes are similar to those that might be encountered during the decommissioning of a typical, nonnuclear industrial facility. Some of these materials like furniture, nonirradiated scrap metal, and office equipment can be reused and recycled. The remainder of this waste stream typically has a well-established disposal path through municipal landfills and sanitary disposal systems.

Radioactive waste can occur in a variety of forms, including gases, liquids, and solids, with radiological characteristics that depend on the concentration and half-lives of the different radionuclides. For these reasons, classification of waste is particularly important, as it will determine the methods to be used in handling, segregating, conditioning, packaging, and transporting wastes. Waste classification also establishes the applicable acceptance criteria for different waste storage and disposal options, which in turn can have a strong effect on decommissioning planning and implementation, and ultimately, the total cost of decommissioning [43].

Although it varies from country to country, classification of radioactive waste is typically based on some combination of the types of processes from which the waste was generated, the radionuclide content of the waste, the timing of the waste generation (e.g., legacy wastes generated prior to developing a robust licensing process), as well as chemical, physical, and biological properties of the waste [30, 43, 44]. The following sections provide general descriptions based on waste classifications proposed in IAEA [45]. Note, however, that specific classification of waste streams and the methods for their management, treatment, and disposal are defined by the policies, laws, and regulations that a nation applies to commercial-scale nuclear power generation and subsequent nuclear decommissioning and waste management activities. For these reasons, waste classification is complex and may vary from country to country [44]; the descriptions presented here are for informational purposes only and are not an endorsement of a particular radioactive waste classification system.

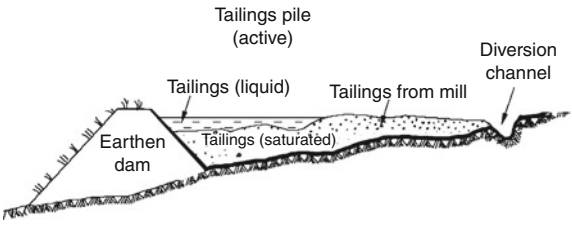

Fig. 9.3 Schematic cross section of a tailings impoundment [22]

Uranium Mill Tailings and Groundwater Restoration

For conventional mining and milling operations, processing the ore results in a waste stream of solid waste material, sands, fine-grained slurries (sometimes called slimes), and processing liquids. These materials are collectively referred to as tailings and are pumped from the mill to a tailings impoundment for disposal (see Figs. 9.2 and 9.3).

Generally, there are a number of tailings impoundments and evaporation ponds at each mill site [22], and the total volume can be quite large. The amount and nature of the tailings, however, depend on the capacity of the mill and the length of time the facility is in operation. For example, the former Climax Uranium Company mill in Grand Junction, Colorado, produced 2 million metric tons (2.2 million tons) of tailings that were placed in a 46-ha (114-acre) tailings impoundment [46]. The nature of the material in each impoundment or pond varies, depending on which part of the mill process produced the tailings. In addition, with the approval of the regulatory agency, operators may use tailings impoundments for onsite disposal of wastes associated with decommissioning and dismantling buildings, structures, and equipment, as well as for soils, pond liners, and sludges that have been radiologically contaminated.

Tailings have become a major focus in regulating active uranium mining and milling operations, as well as cleaning up legacy tailings from older, inactive sites. For example, in 1978, the U.S. Congress enacted the Uranium Mill Tailings Radiation Control Act (UMTRCA) to provide government funds to clean up and stabilize tailings from inactive legacy mills [22]. In a 1995 summary study of UMTRCA sites, the USDOE noted that tailings reclamation was the costliest aspect of the decommissioning process for conventional uranium mills [22]. During reclamation planning, the operator typically uses computer models to evaluate geotechnical stability. Although site-specific tailings reclamation methods are established in a reclamation plan that is evaluated for compliance with the government regulations that govern the cleanup [22, 24, 47, 48], general steps include:

- Shaping and recontouring the tailings pile and installing drainage diversion systems to minimize erosion hazards from surface runoff.
- Allowing the tailings to settle and dehydrate.
- Establishing survey monuments so that settling can be monitored.

- Installing a low permeability engineered cover to minimize water infiltration into the pile and radon emissions from the tailings. Generally this cover consists of clays and/or geotextiles.
- Installing a final cover for erosion protection.
- Establishing a monitoring system to ensure that the design and construction of the reclaimed tailings work as expected. Long-term stewardship during a period of institutional controls may include active measures to maintain and repair the tailings covers.

For active operations, regulations typically call for lining tailings impoundments and installing monitoring systems to prevent migration of contaminants (e.g., radionuclides and associated heavy metals) from the tailings into underlying aquifers [24, 48]. For older and inactive operations, however, the tailings impoundments may not be lined. This can lead to contaminants leaching into the underlying groundwater system over time; these contaminants need to be remediated when the tailings are reclaimed. Depending on the importance of local groundwater resources to nearby communities and the site and design of the impoundment, the level of effort needed to clean up groundwater may be extensive and long term.

Because uranium milling at an ISL facility does not produce tailings, the amount of material at the surface to be decommissioned and ultimately reclaimed is significantly less. Because there are no large tailings impoundments associated with ISL facilities, contaminated decommissioning wastes (e.g., equipment, building components, soils, evaporation pond sludges, and liners) must either be transported to a licensed disposal facility, or an onsite disposal cell will need to be built.

The ISL process does, however, alter groundwater chemistry in the production well fields. After uranium extraction from the ore deposit is no longer economically feasible, the groundwater quality is restored to pre-extraction conditions through a series of treatment steps [13, 49]. As with tailings reclamation, site-specific methods are determined with approval of the regulatory agency, but general steps for groundwater restoration include:

- Groundwater sweep, where groundwater is pumped from the production zone to draw in surrounding natural groundwater. The pumped groundwater may be treated to remove contaminants and reinjected.
- Reverse osmosis, where groundwater is pumped from the production zone and passed through a pressurized, semipermeable membrane (reverse osmosis) system to remove dissolved chemicals. The cleaner water is then reinjected, and the more concentrated brines are pumped to evaporation ponds or disposed of by injection in deep wells.
- Stabilization, where chemicals such as hydrogen sulfide may be injected into the production zone to establish chemical conditions that cause dissolved chemicals to precipitate out as minerals.
- Monitoring, where the groundwater quality is tested to ensure that conditions have stabilized and meet the restoration criteria.

Groundwater restoration occurs when the economics for producing a well field are no longer favorable. Because ISL facilities typically have more than one well field, it is common for groundwater restoration to begin in one well field while other well fields are still actively producing uranium [13, 49].

After groundwater restoration, the physical components of the well field are then restored. Piping, well casing, and pipeline materials are hauled to a licensed disposal facility. Surface facilities such as tanks and buildings are dismantled, removed, and disposed. Pumps are removed for reuse in other well fields, and the wells are filled with cement, plugged, and abandoned. Any soils contaminated by well field spills are removed and disposed, and the disturbed land is graded, recontoured, and revegetated.

Spent Nuclear Fuel and High-Level Waste

As described previously in "Fuel Reprocessing Facilities" section, after the economic energy has been extracted from nuclear fuel, the fuel is removed from the reactor. At this point, it is referred to as spent nuclear fuel. Spent nuclear fuel is highly radioactive because of the decay of fission and activation products that result from the nuclear reactions that occur when the fuel is inside the reactor core. Although it is no longer hot enough to generate electricity, it is well above ambient temperatures.

For these reasons, spent nuclear fuel must be carefully handled, stored, and shielded to provide both radiation protection to workers and the public, and to manage the thermal heat generated by the cooling fuel. In most cases, spent nuclear fuel is stored at or near the reactor, either in dedicated spent fuel pools that use water to provide both cooling and radiation protection or in air-cooled concrete and steel dry casks [13].

As described in "Fuel Reprocessing Facilities" section, after spent nuclear fuel has been cooled and radioactivity has decreased through decay of short-lived radionuclides, spent nuclear fuel may be reprocessed. The fuel reprocessing process typically produces a liquid waste stream that contains fission and activation products that remain after potentially valuable radioactive elements such as plutonium and uranium are removed. This liquid waste stream is typically stored in large tanks for subsequent treatment. Treatment may include processing the liquid wastes into different forms such as sludges, salt cake, or a calcined solid. These forms still produce radiation and must be shielded to provide protection to workers. Current practice in countries such as France, Japan, the United Kingdom, and the United States involves using high temperature furnaces to vitrify liquid wastes into a solid glass waste form.

In most countries in Europe, Asia, and North America, the ultimate disposal path for spent nuclear fuel and reprocessing high-level radioactive waste (HLW) is permanent geologic disposal in an underground repository [50]. At present, a large number of different geologic settings are under consideration. No country has licensed and constructed a geologic repository, however, and spent nuclear fuel and reprocessing HLW are typically managed through onsite interim storage.

Intermediate-Level Waste

Intermediate-level radioactive waste (ILW) is defined in IAEA [45] as "... waste which, because of its radionuclide content requires shielding but needs little or no provision for heat dissipation during its handling and transportation." This waste may be further classified into components consisting of short-lived radionuclides that will decay to low levels during a period on the order of hundreds of years in which institutional controls such as fencing or access restrictions can be considered to be effective in minimizing radiological dose [45]. Conversely, long-lived ILW is dominated by radionuclides that will not decay to sufficiently low levels. The ILW classification is not used in the United States.

In the United States, a transuranic (TRU) waste stream includes man-made alpha radiation-emitting radionuclides with an atomic number greater than that of uranium (i.e., 92) and a half-life longer than 20 years [51]. TRU is produced during reactor fuel assembly, weapons fabrication, and fuel chemical processing operations [15]. Specifically, TRU is that portion of the waste stream that is not classified as spent nuclear fuel, HLW, or low-level radioactive waste (LLW) [30, 51].

A wide variety of storage options exists for the storage and disposal of ILW and TRU. Storage may be through retrievable burial, underground bunkers, concrete caissons, aboveground concrete pads, and inside buildings [30]. Since 1999 in the United States, the USDOE has been disposing TRU waste in a bedded salt deposit about 700 m (2,300 ft) below the ground surface at the Waste Isolation Pilot Plant (WIPP) in Carlsbad, New Mexico [30].

Low-Level Waste

LLW has low radionuclide content. Similar to ILW, IAEA [45, 52] suggests that LLW be further divided on the basis of whether it consists predominantly of short-lived or long-lived radionuclides. LLW tends to be defined by what it is not (i.e., not HLW, ILW, or TRU) rather than what it is, so it can include a broad range of materials and radioactivity levels [30, 51]. For example, LLW may contain small amounts of radioactivity spread through a large volume of material or it may contain sufficiently high levels of radioactivity to require shielding for its safe handling [15, 30, 53]. LLW wastes generated during nuclear decommissioning may involve a wide range of materials including rags, papers, filters, ion exchange resins, discarded protective clothing, contaminated soils and construction rubble, piping, and tanks.

Because of the generally low levels of radioactivity, LLW is typically disposed using near-surface burial. Depending on its physical and chemical properties, LLW may be packaged in drums, casks, special boxes, or other sealed containers [30]. Contaminated soil and construction debris may be disposed directly into the cell without a container. Some large components such as pipes and tanks may be cut up or flattened to reduce the volume.

LLW disposal facilities may be either commercial or government operations, although commercial facilities are still typically governed by government regulation. Similar to municipal landfills, LLW disposal cell designs may include a liner, and an engineered cover system may be installed to reduce water infiltration into the underlying groundwater system [15]. Monitoring systems and institutional controls are installed to ensure waste isolation (air, water, and soil) and to limit access to the disposal facility [51].

Hazardous and Mixed Wastes

Depending on their age and size, decommissioning of nuclear facilities may involve management and disposal of hazardous wastes that result from the processes employed during facility operations, or from building standards used during the initial construction of the plant. For example, hazardous chemicals such as acidic, alkaline, and organic solutions used during uranium milling or fuel reprocessing may require special handling, treatment, and segregation prior to disposal. In addition, hazardous materials such as asbestos may be encountered when older buildings are dismantled and may require special treatment and disposal. If these hazardous wastes are free from radioactive contamination, their ultimate disposal path would be based on hazardous waste regulations.

Radioactive wastes may also be mixed with hazardous wastes. The management and disposal of these wastes can be complicated, as there may be more than one agency with jurisdiction and more than one set of waste handling criteria may apply. For example, in the United States, the U.S. Environmental Protection Agency (USEPA) has authority over hazardous waste through the Resource Conservation and Recovery Act, and the USNRC and USDOE have regulatory authority over radioactive wastes through the Atomic Energy Act. In this case, the management and disposal options to be considered for decommissioning wastes may need to comply with both hazardous and radiation safety requirements [54].

Uncontaminated Wastes

As with other industrial operations, nuclear facilities may also produce wastes that contain little or no radioactive contamination. If the radioactivity of these wastes falls below levels established by the applicable regulations and statutes, they may require no additional nuclear regulatory control. Also, as described in "Safety and Performance Assessment" section, some decommissioning wastes can be decontaminated below the applicable "clearance" levels and released from regulatory control [55]. IAEA [45] identifies these as "exempt" wastes and notes that they can be disposed of using conventional methods and systems.

As structures are dismantled and steel, concrete, and other surfaces (e.g., parking lots) are removed, large volumes of construction debris may be generated during

nuclear facility decommissioning. Because some of these structures are not associated with nuclear-related activities, construction debris of this nature may meet the requirements of exempt waste. The specific levels of radioactivity that establish the criteria to be used in identifying exempt wastes will typically differ from country to country. As a result, the volume of exempt waste and disposal paths will also vary.

General Methodologies for Decommissioning

Specific decommissioning activities and technologies, as well as the sequence of their application, will vary depending on size, age, operational conditions, and design of a nuclear facility, and on the regulatory framework that governs decommissioning. As indicated previously, this article provides a general discussion of typical decommissioning activities. This discussion is not a recommendation of particular approaches or technologies, and the reader is referred to the references identified in the Bibliography for further reading.

Developing a Site-Specific Decommissioning Plan

Nuclear decommissioning is perhaps most effective when the process is laid out in a decommissioning plan. For the lead organization (either commercial or government) with responsibility for decommissioning, the plan provides the opportunity to develop a strategy that, among other things, identifies specific decommissioning issues at a given site, determines the types of processes and methodologies to be used, specifies the desired end state of the facility, and establishes the schedules and financing mechanisms for decommissioning. For large, complex commercial nuclear fuel cycle facilities such as a power plant or a fuel enrichment plant, the decommissioning plan is an extensive document that is supported by a large number of underlying technical and policy reports and references. Although the specific contents of a decommissioning plan can depend on the type of facility, the regulatory framework, and other policy issues, some of the general topics to be covered include [18]:

- Facility Description and Operational History
- Radiological Status
- Alternate Decommissioning Strategies and Selection of a Preferred Alternative
- Project Management
- Decommissioning Activities
- Surveillance and Maintenance During Decommissioning
- Waste Management
- Cost Estimate and Funding Mechanisms
- Safety and Performance Assessment

- Environmental Impact Assessment
- Health and Safety for Workers and the Public
- Quality Assurance
- Emergency Planning
- Physical Security and Safeguards
- Final Radiation Survey

Typically, a site-specific decommissioning plan is developed and refined in stages. An initial plan describing major structures, systems, and features is developed as the facility is designed and constructed. The initial plan is designed to provide basic information and establish project baselines prior to facility startup. The initial decommissioning plan is also intended to provide a framework for cost estimates (see "Estimates of Decommissioning Costs") to ensure that the necessary funds will be in place to cover decommissioning when the facility ceases operation. During the operational life of the facility, the initial decommissioning plan is periodically updated to reflect the operator's experience and understanding of the site. As with any large industrial facility, nuclear facilities may change as technology or regulatory oversight develops, or as the economics of the plant change. As the plant approaches the end of its operational life, the decommissioning plan becomes more detailed. The final decommissioning plan is developed just prior to a facility ceasing operations. The regulatory agency typically reviews this plan and must approve it before the operator can implement the decommissioning strategy [18]. Once the decommissioning plan is approved, it then becomes the basis for subsequent activities, although it may continue to be revised throughout a decommissioning process that can extend over decades.

Site Characterization

Site characterization provides the context for nuclear decommissioning. Ideally, site characterization includes a description of the size and location of the facility, buildings and systems, and the operational history of the site, as well as a description of spills or other releases that may affect the decommissioning process. Nonradiological hazardous process chemicals and other materials like asbestos that require special treatment and disposal may also be identified in the site characterization survey.

One objective in undertaking site characterization is to establish the preoperational baselines and background values that may be used to determine criteria for successful decommissioning. For example, an understanding of background water quality is used to establish site-specific levels for groundwater restoration, as well as action levels for monitoring. Site characterization should identify the geographical and geological context of the facility in relationship to important resources for the area such as critical habitat or historical and cultural areas. In addition, site characterization may include a discussion of the

socioeconomic impacts of the facility, because this may be an important consideration in selecting among different decommissioning strategies [1]. The site characterization and radiological surveys are intended to be of sufficient detail to provide data for planning the decommissioning effort, including selection of specific remediation techniques, establishing decommissioning schedules, estimating costs and waste volumes, and identifying important health and safety considerations to be considered during decommissioning [20].

For the purposes of nuclear decommissioning, site characterization pays special attention to the radiological status of the site, focusing on establishing the extent to which buildings, systems, equipment, soils, and water may contain residual activity [18]. These radiological "hot spots" can be determined using historical information (e.g., location of historic spills, known storage locations, sites identified by ongoing monitoring during operations), conducting surveys with radiation detection equipment, and collecting soil and water samples for subsequent analysis [18, 20, 56, 57].

A key component of site characterization is locating and maintaining existing records [58, 59]. A lack of information on past activities has been a special challenge for decommissioning Cold War legacy sites.

Selecting a Decommissioning Strategy

The reasons for taking a nuclear facility out of service may be based on economics, national policy decisions about the suitability of nuclear power, safety, or obsolescent technology [60]. As described in "Introduction" section, decommissioning strategies for nuclear facilities generally fall into one of three categories:

- A strategy of immediate decontamination and dismantlement [1, 7, 61, 62] (also defined as DECON [14, 15]) begins soon after the nuclear facility closes. For nuclear reactors, spent nuclear fuel is removed, stored, and cooled, pending permanent disposal or reprocessing, and equipment, buildings, structures, and portions of the facility that contain radioactive contaminants are either removed or decontaminated to meet regulatory requirements for releasing the property. In general, this strategy imposes the largest requirements for resources (funding) and personnel in the short term. It takes advantage of the existence of a trained workforce with experience in operating the facility.
- Safe storage [1, 61], deferred or delayed decontamination [7, 62], or SAFSTOR [14, 15], refer to decommissioning strategies where a nuclear facility is left intact after closing, placed in a stable condition, and maintained and monitored until subsequent dismantlement and decommissioning. One purpose in choosing this strategy is to allow radioactivity to decay during a period of safe storage, perhaps on the order of decades, potentially reducing the radiological hazards and the quantity of nuclear waste that must be disposed. This strategy may also benefit from continuing developments in decommissioning technology and waste management options.

This approach places a premium on knowledge management, as the operations workforce may not be available when decommissioning begins years after the end of operations. This decommissioning strategy may be the only option if there are insufficient funds available to cover the costs of immediate decontamination and dismantlement, or if some aspects of the regulatory framework, such as a spent nuclear fuel disposal site, are not available when operations cease [7, 63]. Safe storage may allow one part of a large facility to be closed while the rest of the facility completes its life cycle. For example, one reactor unit at a nuclear power plant may be closed and the fuel removed while the remaining reactor units continue to produce electricity. When the decision is made to close the remaining portions, all of the components can then be decommissioned together, with accompanying potential benefits from optimizing the use of staff and specialized equipment for decommissioning. An example of this approach is the Peach Bottom Unit 1 reactor in York County, Pennsylvania, which was shut down in 1974 and placed in SAFSTOR. Reactor Units 2 and 3 continue to operate and are scheduled for shutdown in 2034, at which point final decommissioning will begin [64].

- A strategy of entombment [1, 7, 61, 62] or ENTOMB [14, 15] involves encasing radioactive materials onsite in a long-lived, structurally sound material such as concrete. The entombment structures are maintained and monitored as appropriate, with institutional controls (e.g., fencing, security personnel) to limit access. For some facilities, the intent of entombment is permanent encapsulation [7], and computer models are used to simulate performance for thousands of years [19]. Because entombment effectively creates a surface waste disposal site, it is not generally a suitable decommissioning strategy for facilities associated with fuel enrichment, fuel fabrication, and fuel reprocessing [62]. In addition, an entombment strategy may also limit the options for releasing the site for reuse.

The first two decommissioning strategies may also be combined. For example, some facilities at a site may be immediately dismantled while other structures are placed in safe storage. For large sites like fuel enrichment plants, nuclear decommissioning activities may be occurring at some facilities at the same time as active operations [4]. Generally, it is anticipated that decommissioning activities will be completed in a period of decades from the end of operations [14].

Because of the wide variety of nuclear facilities, there is no unique approach to decontamination and decommissioning. Several factors may be considered in selecting the decommissioning strategy [1, 7, 62] for a specific site, including:

- The status of the policies and regulatory framework that establish, among other things, the national direction of the nuclear industry and legal requirements for nuclear decommissioning
- The financial costs (both direct and indirect) associated with a given decommissioning strategy and the amount of funding available
- The availability of waste management and disposal facilities for the types and volumes of waste to be generated during decommissioning
- Risks to health and safety of both workers and members of the public

- Potential environmental impacts associated with a given decommissioning strategy
- Knowledge management concerns and the availability of trained and experienced personnel to conduct the decommissioning activities
- The desired end state for the site, and potential socioeconomic impacts to local communities and other stakeholders, including options for release and reuse of the site after decommissioning is complete

These factors need to be considered within the context of the specific site before selecting the preferred alternative. As described previously, the reasons for selecting one alternative as opposed to another should be discussed in the decommissioning plan.

Estimates of Decommissioning Costs

The facility owner is generally responsible for ensuring that there are sufficient resources to cover activities associated with decommissioning a nuclear facility. These activities may include decontamination, decommissioning, reclamation, and groundwater restoration, as well as surveillance and monitoring that may be necessary for long-term stewardship. Cleanup of government facilities and legacy sites that were established prior to the development of a regulatory framework for nuclear decommissioning are generally the responsibility of the national (or state/provincial) governments. Funds for these government responsibilities may be raised by general appropriations (taxes) or user fees imposed on the beneficiaries of nuclear power.

Methods used to accumulate and manage funds for decommissioning commercial nuclear facilities vary from country to country [1]. One common method to establish a decommissioning fund is to impose a requirement that a portion of business revenues be set aside for decommissioning and waste management. Typically, the types of financial mechanisms that are acceptable for estimating, creating, and maintaining a decommissioning fund are either established by the regulatory agency responsible for the facility license or directly by legislation [1, 21].

In countries with a robust regulatory framework, the owner/operator is commonly required to present estimates for the cost of decommissioning activities as part of the license application. A detailed discussion of estimating decommissioning costs is contained in USNRC [21]. In general, cost estimates are specific to the size, type, and location of the facility, and they incorporate assumptions about:

- The transition between operations and facility shutdown, and the work associated with that process, such as postoperational cleanout
- The definition for the end state of the decommissioning process (e.g., unrestricted release, restricted release)

Table 9.2 Estimated costs associated with decommissioning different nuclear facilities [4]

Type of nuclear facility	Estimated decommissioning cost (min to max [median] in US $ million, 2003 value)	Operational life (years)	Time to decommission (years)
Uranium milling	0.800	25	1
Uranium conversion/ recovery	150	30	3
Uranium enrichment	600	30	10
Fuel fabrication	250	30	2
Nuclear power reactor[a]	250–500 (350)	40	10 (after 5-year transition period)
Fuel reprocessing	800	30	15
Industrial facilities	0.050–3 (0.200)	20	1

[a]Cost estimates for decommissioning nuclear power reactors do not include the processing of operational waste, removal and disposition of spent nuclear fuel, the draining of operational systems, or the development of a waste disposal facility

- The availability and suitability of established approaches to decommissioning methods versus the need for unique and perhaps untested technologies
- Availability and capacity of facilities for managing or disposing of residual spent fuel and radioactive waste

Once the regulatory agency or governing body evaluates and accepts the proposed cost estimates, the type and amount of the financial surety (e.g., letter of credit, prepaid cash, government bond) is established and administered in accordance with government regulations. The regulatory agency (as in Canada, United States, and Sweden) or a waste management body (as in Belgium and Spain) then reviews the fund on a regular basis, generally between 1 and 5 years [1, 21]. As identified during the review, the decommissioning fund may be updated and the amount adjusted either upwards or downwards to account for inflation, changes in technology, or completed decommissioning activities.

As noted previously, the actual costs of nuclear decommissioning can vary substantially. The IAEA provided estimates for median decommissioning costs associated with various types of nuclear facilities based on a combination of expert judgment and decommissioning experience and using assumptions with respect to operating life and time to decommission [4]. These estimates (in US $, 2003 value) are summarized in Table 9.2. Because the cost of decommissioning will depend strongly on site-specific issues such as local geology, facility age and design, and operational history, the actual costs for a given site may fall outside these ranges.

The estimates reported in IAEA [4] are general in nature and are not intended to bound all potential costs, particularly for very large government facilities. One general conclusion that can be made from these estimates is that management of spent nuclear fuel and radioactive wastes can represent a significant proportion of the total costs of decommissioning. For example, estimated costs for decommissioning the Sequoyah Fuels uranium conversion site near Gore,

Oklahoma, varied from US $19 million for the no-action alternative of long-term stewardship, to about US $36 million for onsite disposal of most contaminated wastes, to as much as US $254 million for transportation and offsite disposal of all contaminated wastes [25]. These cost issues indicate the importance of accurately characterizing a site and identifying appropriate opportunities to decontaminate, recycle, and reuse materials.

Safety and Performance Assessment

Safety is among the highest priority issues in nuclear decommissioning. Safety assessments, typically developed by both operators and regulators, are engineering analyses that involve calculations and computer simulations to evaluate potential radiological doses. The purpose of the safety assessment is to identify and evaluate potential hazards to ensure that nuclear decommissioning can be done in a manner that is safe for workers, members of the public, and the environment [65].

In general, the safety assessment should be systematic and be linked to relevant safety criteria, taking into consideration potential radiological doses to workers and members of the public, discharges to the environment, and exposure to chemical and other nonradiological hazards [18, 57, 65, 66]. To meet these objectives, a safety assessment consists of:

- Estimates of system performance for all the situations selected
- Evaluation of the level of confidence in the estimated performance
- Overall assessment of compliance with safety requirements

The standards and criteria to be used in developing these assessments vary from country to country depending on the regulatory framework that is in place. Also, the nature of the safety assessment may vary depending on the complexity of the decommissioning strategy needed for a given nuclear facility. A general framework proposed by the IAEA [64] includes:

- The scope of the assessment, based on the physical state of the nuclear facility
- The objectives of the assessment
- The applicable safety requirements and criteria to be used in evaluating potential exposures to workers, members of the public, and the environment
- Outputs from the safety assessment, generally in the form of doses that can be compared to the relevant safety requirements and criteria
- A description of the approach used to implement the safety assessment, whether through simplified calculations or complicated computer models, and a discussion of how the approach is appropriate to the magnitude and time frames of the potential hazards
- Time frames for all phases of the decommissioning activities considered in the safety assessment

- A definition of all phases of nuclear decommissioning and the anticipated end points for each phase
- A definition of the final end state of the facility that is anticipated after all decommissioning activities are complete

In practice, a safety assessment starts with a description of the facility and all of the anticipated decommissioning activities that comprise the decommissioning strategy (see "Selecting a Decommissioning Strategy"). To evaluate off-normal scenarios, a safety assessment also includes identification of potential hazards and initiating events (both natural events such as earthquakes and human-made events such as fire), and potential exposure pathways. These are screened, usually on the basis of probability of their occurrence and the resulting consequence should they occur. Plausible scenarios are developed and used in the engineering analysis to quantify the likelihood and magnitude of potential radiological and safety consequences. In addition, the safety assessment should identify relevant experience and lessons learned from the decommissioning of similar facilities, if available.

For disposing of longer lived radionuclides, some regulatory frameworks and decommissioning strategies use a performance assessment that provides a quantitative evaluation of potential releases of long-lived radionuclides over time periods of hundreds to thousands of years or longer. Similar to safety assessments, but with a much longer time horizon, performance assessments typically involve computer simulations based on site-specific features, events, and processes (biological, physical, and chemical) that may affect the long-term performance of engineered barrier systems. A performance assessment also simulates the release of radionuclides from any engineered barrier system and their subsequent migration through the geosphere surrounding the facility. Finally, future potential radiological doses may be calculated for a hypothetical receptor group located away from the facility [38]. Because of the long time frame, it is not possible to include all potential conditions that might affect performance, so simplified models, or abstractions, are used to simulate important aspects of the engineered and geological systems. This can introduce uncertainty into the calculations that should be characterized and evaluated to determine whether there is sufficient confidence that the applicable regulatory criteria will be met [19, 38].

In essence, the idea of safety and performance assessments is intended to answer these questions: What can go wrong? How likely is it? What are the consequences? [38]. Where there is uncertainty in conceptual models of the system or in the model parameters, simplifying assumptions should be chosen in such a way that ensures the models will be transparent, conservative, and not underestimate potential radiological doses. Statistical analysis and sensitivity studies can help to characterize the nature and relative importance of the uncertainty. Depending on the results of the safety and/or performance assessment, the planned decommissioning activities may be modified to reduce risks, or compensate for uncertainty or limited information [66].

Decontaminating Structures, Equipment, and Components for Reuse or Recycling

The objectives of decontamination include reducing the potential radiological exposure of workers and members of the public during decommissioning; minimizing the volume of radioactive waste; and increasing the potential for reusing and recycling equipment, material, and land at the site of a nuclear facility [67].

Although specific technologies to be used during decommissioning activities will vary depending on size, age, operational conditions, and design, general decontamination methods include [68–70]:

- Chemical methods that use agents such as acids, oxidants, or chemical foams and gels to remove contamination fixed to surfaces. The nature of the chemical agent may be determined based on the properties of the surface to be decontaminated. Chemical decontamination methods may generate a liquid waste stream that requires further treatment to remove radioactive wastes (and generate subsequent secondary waste streams).
- Mechanical methods that rely on cutting, grinding, or other physical techniques to remove contaminated surfaces or layers.

The techniques used for decontamination will vary by material and from site to site, depending on issues such as the operational history of the facility, the level of contamination, and the type of material to be decontaminated [67, 69]. For example, chemical decontamination methods may not be appropriate for porous materials such as concrete, where fluids may migrate into the material.

In addition to technical feasibility, other considerations in selecting decontamination techniques may include the applicable clearance criteria and the potential doses to workers or members of the public to reach these levels. The selection process may also include evaluating the cost of decontamination versus the cost of disposal without decontamination, taking into account estimates of the volume, nature, category, and activity of any primary and secondary wastes that might result. For example, decontamination methods should be selected in such a way as to minimize the amounts of secondary wastes (e.g., cutting fluids or washdown fluids) produced. It is also important to ensure that selected decontamination methods are compatible with and do not compromise existing or planned key treatment, conditioning, storage, and disposal systems [67]. For example, high-pressure jets may not be an appropriate method for cleaning liquid waste storage tanks that are decades old and have experienced some corrosion.

Dismantling and Removing Buildings, Structures, and Equipment from the Site

Equipment removed from buildings (Fig. 9.4) during the cleanup process is typically categorized as (1) salable for unrestricted use after radiation checks and

Fig. 9.4 A steam generator is removed from a reactor building [76]

Fig. 9.5 Demolition of a reactor containment building [76]

decontamination; (2) potentially contaminated, but may be salvageable for sale to other nuclear facilities; and (3) contaminated and must be disposed. The responsible regulatory authority generally establishes the levels of contamination for these different categories.

Dismantling and removing buildings, foundations, structures, and equipment from a nuclear facility is sometimes referred to as "construction in reverse," and similar types of heavy equipment (e.g., trucks, cranes, earthmoving equipment) are used during dismantling (see Figs. 9.4 and 9.5). In addition, cutting equipment and even demolition explosives may be needed to break large structures down into smaller pieces that can be handled and transported more easily (Figs. 9.5 and 9.6). For high-radiation areas, remote techniques such as underwater cutting may be necessary to provide for worker radiation protection [67].

Where salvage is not economically or technically feasible, larger pieces of equipment (e.g., pipes, tanks) may be cut up and flattened, and building materials reduced to rubble to minimize waste volume and make handling for subsequent disposal easier. How much volume needs to be reduced may depend on the

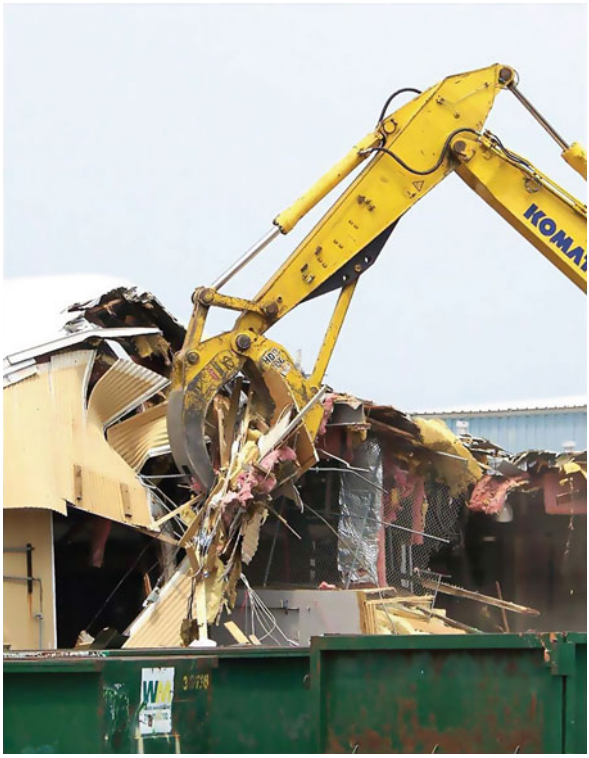

Fig. 9.6 Dismantling industrial buildings at a nuclear facility [42]

available waste disposal capacity and regulations that govern transportation and disposal. Pavement in roads and parking lots may also be removed for disposal as construction debris.

Remediating Contaminated Soils and Groundwater

Remediating residual radioactivity in soils and water generally uses technologies that are well established in the environmental industry. Evaluating and selecting a specific technique is an important part of decommissioning and depends on many site-specific issues such as the physical and chemical state of the residual radioactive material, the availability of equipment and a trained workforce, the availability of appropriate waste disposal capacity, and stakeholder sentiment. The following discussion is intended only as a brief summary of commonly available methods for remediation.

The most common remediation method used for contaminated soils involves excavating the soil for disposal in a LLW facility (Fig. 9.7). If the contamination layer is not deep, this may be an economically viable approach. If the contamination is widespread, however, the volume of material to be disposed in this fashion may be

Fig. 9.7 Removing uncontaminated soil and debris for offsite disposal [42]

quite large and may increase the costs of waste disposal. Alternatively, the soil may be excavated and treated using physical and chemical separation techniques to isolate and reduce the volume of contaminated material [27]. For example, in some cases, residual radioactivity may be more closely associated with fine clay-sized particles in the soil that can be separated by using screens or other physical separation methods. Chemical extraction methods use solutions such as organic acids to bind to the contamination and remove it from the soil. After separation of the contaminated and uncontaminated soil fractions, the uncontaminated soils are used as clean fill, and contaminated soils are treated further or processed for disposal. If chemical methods are used, the leachate may be treated to remove the dissolved radionuclides to meet water standards.

Contaminated surface water and groundwater typically require treatment to meet applicable standards. Widely available technologies for contaminated groundwater include pumping and treating to pull the contaminant plume back toward the extraction well. The contaminated water is then treated through a process such as ion exchange and is either injected back into the aquifer or discharged to a suitable surface water disposal system. A more recent technology for treating contaminated groundwater is the construction of a passive permeable reactive barrier or slurry wall system (Fig. 9.8). Built below the ground surface so that they intercept the groundwater plume, the reactive materials in the barrier are selected to chemically react with the contaminants and immobilize them in the subsurface. Reactive materials that may be used to remove uranium from groundwater include different

Fig. 9.8 Building a slurry wall to remediate contaminated groundwater [42]

forms of iron, such as metallic (zero-valent) or amorphous ferrihydrite [27]. The contamination will remain in place until the barrier is excavated, and barrier longevity and long-term performance are important engineering issues.

Other technologies rely on in place or in situ methods to reduce or immobilize soil and water contamination. For soils, contamination may be reduced or immobilized through mixing in amendments such as apatite or phosphate that will chemically react with the contamination. Alternatively, soil contamination may be immobilized in place by grouting or capping. Bioremediation is a collection of more recent technologies that use biological organisms to preferentially extract or otherwise break down toxic and radiological contamination from both soils and groundwater [71]. For example, sunflowers have been demonstrated to take up uranium from waste at a site in Ashtabula, Ohio, and at a small pond contaminated with uranium near the Chernobyl nuclear power plant site in Pripyat, Ukraine [27, 71].

In addition to active remediation technologies, monitored natural attenuation of contaminated soils and groundwater may be also be applicable, if it can be demonstrated to meet applicable criteria in a reasonable timeframe [72]. This method relies on monitoring soils and groundwater while the natural physical, chemical, or biological processes already occurring at the site contain and reduce volume, mass, and toxicity of the contamination in place. Where site conditions

such as soil type and groundwater flow are favorable, monitored natural attenuation can be an attractive option because it is typically less disruptive and costly than more active remediation measures. However, because it can be perceived by stakeholders as "doing nothing," monitored natural attenuation is generally proposed as one part of a broader remediation strategy and combined with active remediation measures [72]. For example, a contamination source may be excavated and removed while monitored natural attenuation is implemented for the associated groundwater contaminant plume.

Waste Management and Disposal

As described in "Waste Management and Disposal" section, decommissioning wastes can fall into several different classes. Waste classification ultimately depends on the type of historical operations at the site and will influence the decommissioning strategy and waste management options that are selected for a facility. Once the physical, chemical, and radiological properties are characterized and the waste is classified and the applicable criteria are determined, the basic options for waste management are either onsite storage/disposal or transport offsite to an approved waste disposal facility.

For nuclear power plants, one of the final phases of operations before decommissioning is to remove the fuel from the reactor (defuel) and place the spent nuclear fuel in interim storage, either in pools or dry casks. This step would be necessary regardless of the decommissioning strategy selected [69]. As they are generated during operations, other wastes may be collected, segregated, chemically adjusted, and decontaminated onsite, and then placed in temporary monitored storage onsite until a final disposition path is determined [44]. A partial list of examples of the types of wastes that may be encountered during the decommissioning of nuclear facilities is presented in Table 9.3.

Waste may be treated to prepare it for final disposal. Treatment concepts include volume reduction and separation and removal of radionuclides and other hazardous wastes [44]. Some treatment options include incineration or compaction to reduce volume, and evaporation or ion exchange to remove radionuclides from liquid wastes. Some of these techniques can generate secondary wastes such as liquids, sludges, and filters that need to be managed as well.

Radioactive wastes may also be conditioned to produce a form that is more suited for handling, transportation, storage, and disposal. Low-level and intermediate-level wastes may be immobilized by mixing with grouts, cements, and bitumen, while liquid high-level wastes from fuel reprocessing may be vitrified into a glass waste form or otherwise modified to produce a solid waste form. These wastes are placed in packages or specially designed containers for interim storage, transportation, and subsequent offsite disposal (Fig. 9.9). This may be at a licensed disposal site, a specially constructed disposal cell, or an existing tailings impoundment that

Table 9.3 Partial list of the types of waste materials for different nuclear facilities

Type of nuclear facility	Examples of waste materials
Uranium mine	Waste rock
	Fuels and lubricants
	Contaminated soils and groundwaters
Uranium mill	Drums
	Insoluble waste and filter materials
	Liquid effluent
	Tailings and sludges
	Liquid nitrates
	Ion exchange resins
	Tanks, pipes, and equipment
	Contaminated soils and groundwater
Uranium conversion	Solid CaF_2
	CaF_2 sludges with/without minor uranium
	Non-radiological chemical waste
	Tanks, pipes, and equipment
	Contaminated soils and groundwaters
Uranium enrichment	Depleted uranium tails
	Tanks, pipes, and equipment
	Contaminated soils and groundwaters
Fuel fabrication	Uranium scrap material
	Filters
	Wash water and decontamination/cleaning solutions
	Waste oils
	Spent acids and solvents
	Equipment
	Contaminated soils and groundwaters
Nuclear power plants	Reactor vessel and internal components
	Coolant system equipment and components
	Activated concretes and steels
	Evaporator concentrates
	Tanks, pipes, and equipment
	Contaminated debris and soils
Spent fuel reprocessing	Filters
	Activated and contaminated metal components
	Spent solvents, decontamination and metal cleaning agents
	Fuel cladding
	Laboratory analytical equipment and solutions
	Tanks, pipes, and equipment
	Contaminated debris, soils, and groundwater

is being reclaimed and used as a disposal cell. The materials must meet waste acceptance criteria for the disposal facility.

Alternatively, waste may be disposed in place with monitoring and an engineered system for long-term disposal [42]. Onsite waste management,

Fig. 9.9 Low-level radioactive waste packages for offsite disposal [42]

including a decommissioning strategy of entombment, must comply with applicable regulations for near- surface storage and disposal facilities [62]. In this case, a performance assessment (see "Safety and Performance Assessment") may be used to evaluate both engineered and natural barrier performance over long times. Depending on the nature of the waste and the site-specific conditions, different design options (backfill, concrete vaults, engineered covers) may be evaluated along with a combination of long-term monitoring and institutional controls [44]. Institutional controls such as fencing, signage, and physical security are generally assumed to be effective only for a period on the order of hundreds of years, while the performance of engineered and natural barriers is evaluated over periods as long as 10,000 years [19, 20].

Conducting Final Inspections and Surveys

During decommissioning, the national regulatory agency will typically conduct onsite reviews and inspections to ensure that the approved decommissioning plan is

being followed [19] and the decommissioning activities are being conducted in a safe manner that complies with applicable regulations. After decommissioning is complete, there should be a final survey to evaluate the residual radioactivity that remains at the site. The specific goal of this survey is to determine the extent to which the site complies with the criteria set by the governing regulatory authority for subsequent reuse and/or release of the site [57, 67] – one of the objectives of decommissioning (see "Definition of the Subject").

This survey may be carried out in phases, as decommissioning work is completed, to enable parts of the site to be released from regulatory control. The final survey data are submitted to the regulatory authority, including a description of the applicable reuse/release criteria, the methods and procedures used, and the measurement results. Typically, the sampling and surveys will be focused on areas such as previous waste burial sites or spill locations identified as contaminated during the site characterization survey. These areas are sometimes called Class 1 areas [57], and sampling and surveys will be more extensive. Areas that are less likely to be contaminated, called Class 2 and Class 3 areas, receive lesser surveying and sample coverage. The results typically include an analysis to demonstrate the statistical significance of the results as compared to natural background radiation levels [20, 56, 57, 67].

Reclaiming Disturbed Land

After decommissioning and dismantlement of buildings and structures is complete, the decommissioning strategy may call for reclaiming disturbed land to preoperational condition. This is generally accomplished by adding clean topsoil, installing drainage and erosion controls if necessary, regrading and recontouring the surface to match the surrounding topography, and revegetating with native vegetation (Fig. 9.10). In addition, land reclamation efforts should include monitoring to ensure that drainage and erosion controls are functioning as intended, revegetated areas are stable, and invasive species have not become established. Many of these techniques are similar to those used to reclaim surface mines [73].

The amount of disturbed land to potentially reclaim can vary significantly for different nuclear facilities, especially conventional uranium mining and milling operations that produce significant quantities of waste rock and tailings covering tens to hundreds of hectares (acres). The type of reclamation will depend, in part, on the intended use of the land once the license is terminated. For example, a site intended for unrestricted release as a recreation area may have a more extensive land reclamation program than a site that will ultimately be released for future industrial uses.

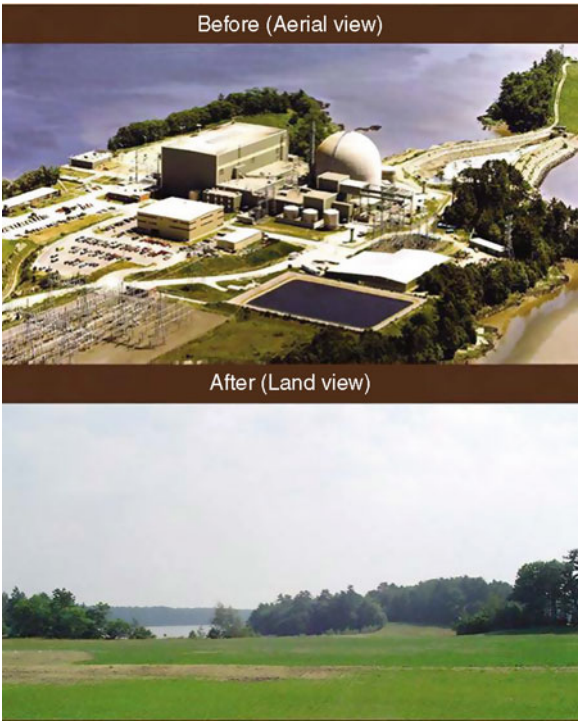

Fig. 9.10 Reclamation and revegetation of site after decommissioning a commercial nuclear power plant [77]

Status of Decontamination and Decommissioning

Because commercial nuclear fuel cycle facilities and nuclear power plants are governed at the national level using different policy, statutory, and regulatory frameworks, the status of nuclear decommissioning around the world is difficult to estimate [4]. A brief summary based on the estimates of international nuclear organizations such as the IAEA, NEA, and WNA is provided here and in Table 9.4.

- The leading countries for uranium production include Canada, Kazakhstan, and Australia, followed by Namibia, Russia, Niger, Uzbekistan, and the United States [40]. Uranium has been mined for decades, and some of the older mines are small and not well documented. The WNA estimates that more than 100 mines have been "retired from operations," although decommissioning is not complete at all of them [5].
- Uranium mills exist in countries with known uranium ore reserves. As of August 2003, the IAEA reported that 294 uranium mills were operating worldwide, with 231 plants shut down or in decommissioning and 149 fully decommissioned. Eight additional uranium mills were under construction [4].
- Uranium conversion plants to produce UF_6 operate in the United States, Canada, France, United Kingdom, China, and Russia. As of August 2003, the IAEA

Table 9.4 Decommissioning status for nuclear fuel cycle facilities as of August 2003 ([4], Table 9.3)

Type of nuclear facility	Operating	Under construction	Shut down /being commissioned	Decommissioned
Uranium milling	294	8	231	149
Uranium conversion/recovery	29	1	14	2
Uranium enrichment	21	2	7	5
Fuel fabrication/heavy water production	66	5	27	23
Fuel reprocessing	13	3	18	13

reports that 29 uranium conversion facilities were operating worldwide, with 14 plants shut down or in decommissioning and 2 fully decommissioned. One additional uranium conversion facility was under construction [4].

- Major enrichment plants are operated in the United States, France, and Russia, with smaller plants located in the United Kingdom, Netherlands, Germany, Japan, and China [28]. As of August 2003, the IAEA reports that 21 fuel enrichment facilities were operating worldwide, with 7 plants shut down or in decommissioning and 5 fully decommissioned. Two additional fuel enrichment plants were under construction [4].
- Fuel fabrication and/or heavy water production facilities operate in most countries with nuclear programs. As of August 2003, the IAEA reports that 66 fuel enrichment and heavy water production facilities were operating worldwide, with 27 plants shut down or in decommissioning and 23 fully decommissioned. Five additional fuel enrichment plants were under construction [4].
- At present, 436 commercial nuclear reactors are operating worldwide in many countries in North America, Europe, and Asia [9]. A total of 112 nuclear reactors have been placed in long-term shut down, and 14 have been completely decommissioned [4, 9]. Russia has the largest number of research and test reactors, followed by the United States, Japan, France, Germany, and China. In addition, research and test reactors are also located in developing countries in Africa, South America, and Asia. After peaking in the mid-1970s at about 370 reactors in 55 countries, the number of research and test reactors worldwide has declined sharply. As of August 2003, the IAEA reported that there were about 287 research and test reactors and critical assemblies in operation worldwide, with 8 more under construction. A total of 214 research and test reactors were shut down or being decommissioned, and 173 were reported as being decommissioned [4].
- As of August 2003, the IAEA reports that 13 fuel reprocessing plants were operating worldwide, with 18 plants shut down or in decommissioning and 13 fully decommissioned. Three additional fuel reprocessing plants were under construction [4].

Future Directions

As noted previously, interest in commercial nuclear power has been revived as a result of concerns with carbon emissions from traditional fossil fuels. As a result, many nations have reported an increase in proposed construction projects for new reactors. Although many of these proposed projects will use current Generation II and III reactor designs, there are research and development programs focused on designing the Next Generation IV reactors [37].

The different current and future design types and sizes of reactors will make decommissioning inherently a site- and reactor-specific process. Each current and future reactor design will have its own design-specific decommissioning requirements that must be taken into consideration. In addition, changes in reactor design or the use of nuclear fuels based on MOX or thorium may lead to different fuel requirements that will change the nature of decommissioning at the front end of the nuclear fuel cycle.

Much of the decommissioning experience gained to date is focused on an open, or "once through" uranium fuel cycle. Current programs such as the Global Nuclear Energy Partnership are evaluating the potential of a closed fuel cycle, where fuel is reprocessed and used more than once to generate power [39]. This approach, along with changes in ongoing nuclear reactor operations, would change the amount and characteristics of spent nuclear fuel for handling, storage, and disposal. In addition, closing the fuel cycle would require new nuclear fuel cycle facilities and change the waste streams produced at the back end of the fuel cycle. For these reasons, a change from an open to a closed nuclear fuel cycle may need new waste disposal options that will influence the selection of the decommissioning strategy for these types of facilities.

Although new decontamination techniques are continually being developed [27, 69], existing technology that has been previously applied with demonstrated success may continue to be preferred by stakeholders (members of the public, government agencies) to an untried method, particularly if trained staff and specialized equipment are readily available. As decommissioning costs and potential benefits are better understood, newer techniques may be applied more. In addition, many nations are looking at extending the service life of existing nuclear facilities and reactors. At the same time, the nuclear workforce is aging, placing a premium on knowledge management and recordkeeping to ensure valuable information and experience is not lost [58, 74, 75]. Decommissioning decisions are perhaps many decades in the future, but should be taken into consideration as designs are developed for advanced reactors and the nuclear facilities that support them.

Bibliography

Primary Literature

1. NEA (2002) The decommissioning and dismantling of nuclear facilities. Paris, France. Status, approaches, challenges. Report No. NEA 3714. Nuclear Energy Agency/Organisation for Economic Co-Operation and Development, Issy-les-Moulineaux. http://www.nea.fr/html/rwm/reports/2002/3714-decommissioning.pdf. Accessed 28 Apr 2009
2. Commission of the European Communities (Oct 2007) Communication from the commission to the council and the European parliament. Nuclear illustrative programme. Presented under Article 40 of the Euratom Treaty for the Opinion of the European Economic and Social Committee. Commission of the European Communities, Brussels
3. NEA (2009) NEA annual report 2008. Nuclear Energy Agency, Issy-les-Moulineaux. http://www.nea.fr/html/pub/activities/ar2008/AR2008.pdf. Accessed 20 May 2009
4. IAEA (Aug 2004) Status of the decommissioning of nuclear facilities around the world. IAEA, Vienna. http://www-pub.iaea.org/MTCD/publications/PDF/Pub1201_web.pdf. Accessed 20 May 2009
5. WNA (Sept 2006) Safe decommissioning of civil nuclear industry sites. World Nuclear Association, London. http://www.world-nuclear.org/reference/position_statements/decommissioning.html. Accessed 20 May 2009
6. O'Sullivan P, Pescatore C, Tripputi I (2009) Applying decommissioning experience to the design and operation of new nuclear power plants. NEA News 27:13–15, http://www.nea.fr.html/pub/newsletter/2009/applying-decommissioning.pdf. Accessed 8 July 2009
7. IAEA (Nov 2005) Selection of decommissioning strategies: issues and factors. Report by an expert group. IAEA-TECDOC-1478. IAEA, Vienna. http://www-pub.iaea.org/MTCD/publications/PDF/TE_1478_web.pdf. Accessed 20 May 2009
8. IAEA (2008) International atomic energy agency annual report 2007: 50 years of atoms for peace. IAEA, Vienna. http://www.iaea.org/Publications/Reports/Anrep2007/anrep2007_ full.pdf. Accessed 20 May 2009
9. IAEA (2009) Latest news related to the power reactor information system and the status of nuclear power plants. IAEA, Vienna. http://www.iaea.org/cgi-bin/db.page.pl/pris.main.htm. Accessed 12 June 2009
10. Reisenweaver D, Laraia M (2000) Preparing for the end of the line. Radioactive residues from nuclear decommissioning. IAEA Bull 42:51–54
11. USNRC (2009) Expected new nuclear power plant applications: updated 4 Feb 2009. U.S. Nuclear Regulatory Commission, Washington, DC. http://www.nrc.gov/reactors/new-reactors/new-licensing-files/expected-new-rx-applications.pdf. Accessed 20 May 2009
12. IAEA (2008) Energy, electricity and nuclear power estimates for the period up to 2030. Reference data series no. 1. IAEA, Vienna. http://www-pub.iaea.org/MTCD/publications/PDF/RDS1-28_web.pdf. Accessed 12 June 2009
13. USNRC (June 2009) Generic environmental impact statement for in-situ leach uranium milling facilities. Final report. NUREG-1910, vols 1 and 2. U.S. Nuclear Regulatory Commission, Washington, DC. http://www.nrc.gov/reading-rm/doc-collections/nuregs/staff/sr1910/. Accessed 5 June 2009
14. USNRC (July 2000) Regulatory guide 1.184. Decommissioning of nuclear power reactors. U.S. Nuclear Regulatory Commission, Washington, DC
15. USNRC (June 2000) Staff responses to frequently asked questions concerning decommissioning of nuclear power reactors. Final report. NUREG-1628. U.S. Nuclear Regulatory Commission, Washington, DC
16. NEA (2005) Decommissioning of nuclear power facilities. It can and has been done. Issy-les-Moulineaux, Nuclear Energy Agency. http://www.nea.fr/html/rwm/reports/2004/nea5728-decom.pdf). Accessed 28 May 2009

17. WNA (Jan 2009) The nuclear fuel cycle. World Nuclear Association, London. http://www.world-nuclear.org/info/inf03.html. Accessed 10 June 2009
18. IAEA (Nov 2005) Standard format and content for safety related decommissioning documents. Safety reports series no. 45. IAEA, Vienna. http://www-pub.iaea.org/MTCD/publications/PDF/Pub1214_web.pdf. Accessed 20 May 2009
19. USNRC (Sept 2006) Consolidated decommissioning guidance. decommissioning process for materials licensees. Final report. NUREG-1757, vol 1, Rev 2. U.S. Nuclear Regulatory Commission, Washington, DC. http://www.nrc.gov/reading-rm/doc-collections/nuregs/staff/sr1757/v1/sr1757v1r2.pdf. Accessed 20 May 2009
20. USNRC (Sept 2006) Consolidated decommissioning guidance. Characterization, survey, and determination of radiological criteria. Final report. NUREG-1757, vol 2, Rev 1. U.S. Nuclear Regulatory Commission, Washington, DC. http://www.nrc.gov/reading-rm/doc-collections/nuregs/staff/sr1757/v2/sr1757v2r1.pdf. Accessed 20 May 2009
21. USNRC (Sept 2003) Consolidated NMSS decommissioning guidance. Financial assurance, recordkeeping, and timeliness. Final report. NUREG-1757, vol 3. U.S. Nuclear Regulatory Commission, Washington, DC. http://www.nrc.gov/reading-rm/doc-collections/nuregs/staff/sr1757/v3/sr1757v3.pdf. Accessed 20 May 2009
22. USDOE (Feb 1995) Decommissioning of U.S. uranium production facilities. DOE/EIA-0592. U.S. Department of Energy, Energy Information Administration, Washington, DC
23. Taylor G, Farrington V, Woods P, Ring R, Molloy R (Aug 2004) Review of environmental impacts of the acid in-situ leach uranium mining process. CSIRO land and water client report. Commonwealth Scientific and Industrial Research Organisation, Clayton South
24. IAEA (Aug 2004) The long term stabilization of uranium mill tailings. Final report of a co-ordinated research project, 2000–2004. IAEA-TECDOC-1403. IAEA, Vienna. http://www-pub.iaea.org/MTCD/publications/PDF/TE_1403_web.pdf. Accessed 20 May 2009
25. USNRC (May 2008) Environmental impact statement for the reclamation of the sequoyah fuels corporation site in Gore, Oklahoma. Final report. NUREG-1888. U.S. Nuclear Regulatory Commission, Washington, DC. http://www.nrc.gov/reading-rm/doc-collections/nuregs/staff/sr1888/sr1888-intro-chaptr11.pdf. Accessed 5 June 2009
26. USNRC (June 2009) Fact sheet: Uranium enrichment. U.S. Nuclear Regulatory Commission, Washington, DC. http://www.nrc.gov/reading-rm/doc-collections/fact-sheets/enrichment.pdf. Accessed 5 June 2009
27. USEPA (Dec 2006) Depleted uranium technical brief. EPA-402-R-06-011. Office of Air and Radiation, U.S. Environmental Protection Agency, Washington, DC. http://www.epa.gov/radiation/docs/402-r-06-011.pdf. Accessed 2 July 2009
28. Bodansky D (2004) Nuclear energy. Principles, practices, and prospects, 2nd edn. Springer/LLC, New York
29. USDOE (Apr 1999) Final programmatic environmental impact statement for alternative strategies for the long-term management and use of depleted uranium hexafluoride. DOE/EIS-0269. U.S. Department of Energy, Office of Nuclear Energy, Science, and Technology, Washington, DC
30. Interstate Technology and Regulatory Council (Jan 2008) Decontamination and decommissioning of radiologically contaminated facilities. Interstate Technology and Regulatory Council, Washington, DC. http://www.itrcweb.org/Documents/RAD5.pdf. Accessed 5 June 2009
31. USNRC (June 2007) Uranium enrichment. U.S. Nuclear Regulatory Commission, Washington, DC. http://www.nrc.gov/materials/fuel-cycle-fac/ur-enrichment.html. Accessed 5 June 2009
32. GAO (Nov 2007) Uranium enrichment: extension of decontamination and decommissioning fund may be needed to cover projected cleanup costs. GAO-08-277T. U.S. Government Accountability Office, Washington, DC. http://www.gao.gov/new.items/d08277t.pdf. Accessed 12 June 2009

33. IAEA (Oct 2004) Research reactors worldwide. IAEA, Vienna. http://www-naweb.iaea.org/napc/physics/ACTIVITIES/Research_ Reactors_Worldwide.htm. Accessed 14 June 2009
34. USNRC (Aug 2008) Power reactors. U.S. Nuclear Regulatory Commission, Washington, DC. http://www.nrc.gov/reactors/power.html. Accessed 14 June 2009
35. Lake JA, Bennett RG, Kotek JF (Jan 2003) Next generation nuclear power. new, safer, and more economical nuclear reactors could not only satisfy many of our future energy needs but could combat global warming as well. Sci Am http://www.scientificamerican.com/article.cfm?id=next-generation-nuclear. Accessed 14 June 2009
36. USDOE (Nov 2008) Next-generation nuclear energy. Generation IV program fact sheet. U.S. Department of Energy, Office of Nuclear Energy, Washington, DC. http://nuclear.energy.gov/pdfFiles/factSheets/NextGenerationNuclearEnergy.pdf. Accessed 14 June 2009
37. USDOE (Aug 2008) Next generation nuclear plant licensing strategy. A report to Congress. U.S. Department of Energy, Office of Nuclear Energy, Washington, DC. http://nuclear.energy.gov/pdfFiles/NGNP_reporttoCongress.pdf. Accessed 14 June 2009
38. USNRC (2009) Performance assessment for waste disposal and decommissioning. Updated 11 Feb 2009. U.S. Nuclear Regulatory Commission, Washington, DC. http://www.nrc.gov/about-nrc/regulatory/performance-assessment.html. Accessed 15 May 2009
39. USDOE (Oct 2008) Draft global nuclear energy partnership programmatic environmental impact statement. DOE/EIS-0396. U.S. Department of Energy, Office of Nuclear Energy, Washington, DC. http://www.gc.energy.gov/NEPA/1003.htm. Accessed 8 July 2009
40. WNA (June 2009) World uranium mining. World Nuclear Association, London. http://www.world-nuclear.org/info/inf23.html. Accessed 5 June 2009
41. Andrews A (27 Mar 2008) Nuclear fuel reprocessing: U.S. policy development. CRS report for Congress, Order code RS22542. Congressional Research Service, Washington, DC. http://www.fas.org/sgp/crs/nuke/RS22542.pdf. Accessed 1 July 2009
42. USDOE (Nov 2008) Revised draft environmental impact statement for decommissioning and/or long-term stewardship at the West Valley demonstration project and Western New York nuclear service center. DOE/EIS-0226-D. U.S. Department of Energy, West Valley
43. IAEA (Dec 2007) Disposal aspects of low and intermediate level decommissioning waste. Results of a coordinated research project 2002–2006. IAEA-TECDOC-1572. IAEA, Vienna. http://www-pub.iaea.org/MTCD/publications/PDF/TE_1572_web.pdf. Accessed 24 June 2009
44. IAEA (Apr 2000) Radioactive waste management profiles: a compilation of data from the waste management database no. 3. IAEA, Vienna. http://www-pub.iaea.org/MTCD/publications/PDF/rwmp-3/RWMP-V3.pdf. Accessed 24 June 2009
45. IAEA (Apr 1994) Classification of radioactive waste. A safety guide. Safety series no. 111-G-1.1. IAEA, Vienna. http://www-pub.iaea.org/MTCD/publications/PDF/Pub950e_web.pdf. Accessed 24 June 2009
46. Environmental Law Institute (1999) Institutional controls case study: Grand junction. Environmental Law Institute, Washington, DC. http://www.elistore.org/Data/products/d9.14.pdf. Accessed 23 June 2009
47. USNRC (2003) Standard review plan for the review of a reclamation plan for mill tailings sites under title II of the Uranium Mill Tailings Radiation Control Act of 1978. Final report. NUREG-1620, Rev 1. U.S. Nuclear Regulatory Commission, Washington, DC
48. USNRC (Nov 2008) Design, construction, and inspection of embankment retention systems at uranium recovery facilities. Regulatory guide 3.11. U.S. Nuclear Regulatory Commission, Washington, DC
49. IAEA (May 2005) Guidebook on environmental impact assessment for *in situ* leach mining projects. IAEA-TECDOC-1428. IAEA, Vienna. http://www-pub.iaea.org/MTCD/publications/PDF/TE_1428_web.pdf. Accessed 20 May 2009
50. National Research Council (2001) Disposition of high-level waste and spent nuclear fuel. The continuing societal and technical challenges. National Academy Press, Washington, DC

51. USDOE (Jan 2007) Radioactive waste management manual. DOE M 435.1-1. U.S. Department of Energy, Office of Environmental Management, Washington, DC. http://www.directives.doe.gov/pdfs/doe/doetext/neword/435/m4351-1c1.pdf. Accessed 24 June 2009
52. IAEA (1999) Near surface disposal of radioactive waste safety requirements. IAEA safety standards series, Safety guide no. WS-R-1. IAEA, Vienna. http://www-pub.iaea.org/MTCD/publications/PDF/P073_scr.pdf. Accessed 29 June 2009
53. IAEA (2008) Managing low radioactivity material from the decommissioning of nuclear facilities. Technical reports series no. 462. IAEA, Vienna. http://www-pub.iaea.org/MTCD/publications/PDF/trs462_web.pdf. Accessed 12 June 2009
54. League of Women Voters Education Fund (1993) The nuclear waste primer. The League of Women Voters Education Fund, Washington, DC
55. IAEA (2004) Application of the concepts of exclusion, exemption and clearance. IAEA safety standards series, Safety guide no. RS-G-1.7. IAEA, Vienna. http://www-pub.iaea.org/MTCD/publications/PDF/Pub1202_web.pdf. Accessed 29 June 2009
56. USNRC (June 2001) Multi-Agency Radiation Survey and Site Investigation Manual (MARSSIM). NUREG-1575, Rev 1/EPA 402-R-97-016, Rev 1/DOE/EH-0624, Rev 1. U.S. Nuclear Regulatory Commission, Washington, DC. http://www.epa.gov/radiation/marssim/obtain.html. Accessed 29 June 2009
57. NEA (2006) Releasing the sites of nuclear installations. A status report. Report no. NEA 6187. Nuclear Energy Agency, Issy-les-Moulineaux
58. IAEA (2008) Long term preservation of information for decommissioning projects. Technical reports series no. 467. IAEA, Vienna, Austria. http://www-pub.iaea.org/MTCD/publications/PDF/trs467_web.pdf. Accessed 12 June 2009
59. IAEA (2002) Record keeping for the decommissioning of nuclear facilities: guidelines and experience. Technical reports series no. 411. IAEA, Vienna. http://www-pub.iaea.org/MTCD/publications/PDF/TRS411_scr.pdf. Accessed 12 June 2009
60. Energy Information Administration (June 2006) When do commercial reactors permanently shut down? The recent record. Energy Information Administration, U.S. Department of Energy, Washington, DC. http://www.eia.doe.gov/cneaf/nuclear/closures/closure16.html. Accessed 14 June 2009
61. European Commission (2009) Decommissioning in short. European Commission, Brussels. http://www.eu-decom.be/about/decominshort/whatis.html. Accessed 7 July 2009
62. IAEA (2007) Decommissioning strategies for facilities using radioactive material. Safety reports series no. 50. IAEA, Vienna. http://www-pub.iaea.org/MTCD/publications/PDF/Pub1281_ web.pdf. Accessed 12 June 2009
63. IAEA (2002) Safe enclosure of nuclear facilities during deferred dismantling. Safety reports series no. 26. IAEA, Vienna. http://www-pub.iaea.org/MTCD/publications/PDF/Pub1142_scr.pdf. Accessed 12 June 2009
64. USNRC (2009) Peach Bottom—Unit 1. Updated 16 Apr 2009. U.S. Nuclear Regulatory Commission, Washington, DC. http://www.nrc.gov/info-finder/decommissioning/power-reactor/peach-bottom-atomic-power-station-unit.html. Accessed 12 June 2009
65. IAEA (2008) Safety assessment for the decommissioning of facilities using radioactive material. IAEA safety standards series, Safety guide no. WS-G-5.2. IAEA, Vienna. http://www-pub.iaea.org/MTCD/publications/PDF/Pub1372_web.pdf. Accessed 29 June 2009
66. Interstate Technology and Regulatory Council (Apr 2002) Determining cleanup goals at radioactively contaminated sites: case studies. Interstate Technology and Regulatory Council, Washington, DC. http://www.itrcweb.org/Documents/RAD5.pdf. Accessed 5 June 2009
67. IAEA (1999) Decommissioning of nuclear power plants and research reactors. IAEA safety standards series, Safety guide no. RS-G-2.1. IAEA, Vienna. http://www-pub.iaea.org/MTCD/publications/PDF/P079_scr.pdf. Accessed 29 June 2009
68. USEPA (Apr 2006) Technology reference guide for radiologically contaminated surfaces. EPA-402-R-06-003. Office of Air and Radiation, U.S. Environmental Protection Agency, Washington, DC

69. IAEA (1999) State of the art technology for decontamination and dismantling of nuclear facilities. Technical reports series no. 395. IAEA, Vienna. http://www-pub.iaea.org/MTCD/publications/PDF/TRS395_scr/D395_Part1_scr.pdf. Accessed 12 June 2009
70. NEA (1999) Decontamination techniques used in decommissioning activities. Nuclear Energy Agency/Organisation for Economic Co-Operation and Development, Issy-les-Moulineaux
71. USEPA (Apr 2004) Radionuclide biological remediation resource guide. EPA-905-B-04-001. Region 5, Superfund Division, U.S. Environmental Protection Agency, Washington, DC. http://clu-in.org/download/remed/905b04001.pdf. Accessed 29 June 2009
72. USEPA (Apr 1999) Use of monitored natural attenuation at superfund, RCRA corrective action, and underground storage tank sites. Office of Solid Waste and Emergency Response (OSWER), Directive no. 9200.4-17P. Office of Solid Waste and Emergency Response, U.S. Environmental Protection Agency, Washington, DC. http://www.epa.gov/swerust1/directiv/d9200417.pdf. Accessed 29 June 2009
73. Pennsylvania Department of Environmental Protection (Oct 1998) Coal mine drainage prediction and pollution prevention in Pennsylvania. Pennsylvania Department of Environmental Protection, Harrisburg. http://www.dep.state.pa.us/dep/deputate/minres/Districts/CMDP/main.htm. Accessed 8 July 2009
74. IAEA (2009) Nuclear safety knowledge management. IAEA, Vienna. http://www-ns.iaea.org/coordination/knowledge-mng.htm. Accessed 23 July 2009
75. IAEA (2004) Planning, managing, and organizing the decommissioning of nuclear facilities. IAEA-IECDOC-1394. IAEA, Vienna
76. USNRC (Jan 2008) Decommissioning nuclear power plants. Fact sheet. U.S. Nuclear Regulatory Commission, Washington, DC. http://www.nrc.gov/reading-rm/doc-collections/fact-sheets/decommissioning.pdf. Accessed 14 June 2009
77. USNRC (Jan 2005) U.S. nuclear regulatory commission's decommissioning program. NUREG/BR-0325. U.S. Nuclear Regulatory Commission, Washington, DC. http://www.nrc.gov/reading-rm/doc-collections/nuregs/brochures/br0325/br0325.pdf. Accessed 14 June 2009

Books and Reviews

ASTM International (2005) Standard guide for nuclear facility decommissioning plans. ASTM E1281-89(2005). ASTM International, West Conshohocken

National Research Council (1998) A review of decontamination and decommissioning technology development programs at the department of energy. National Academies Press, Washington, DC

National Research Council (2001) Research opportunities for deactivating and decommissioning department of energy facilities. National Academies Press, Washington, DC

Taboas A, Moghissi A, LaGuardia T (2004) The decommissioning handbook. American Nuclear Society, LaGrange

USDOE (Jan 2000) Decommissioning handbook. Procedures and practices for decommissioning. DOE/EM-0383. USDOE, Office of Environmental Management, Washington, DC

Till JE, Meyer HR (eds) (Sept 1983) Radiological assessment. A textbook on environmental dose analysis. NUREG/CR-3332. U.S. Nuclear Regulatory Commission, Washington, DC

USNRC (Aug 1988) Final generic environmental impact statement on decommissioning of nuclear facilities. NUREG-0586. U.S. Nuclear Regulatory Commission, Washington, DC. http://www.nrc.gov/reading-rm/doc-collections/nuregs/staff/sr0586/initial/index.html

USNRC (Nov 2002a) Generic environmental impact statement on decommissioning of nuclear facilities. Regarding the decommissioning of nuclear power reactors. NUREG-0586, suppl 1, vol 1. U.S. Nuclear Regulatory Commission, Washington, DC. http://www.nrc.gov/reading-rm/doc-collections/nuregs/staff/sr0586/s1/v1/index.html

USNRC (Nov 2002b) Generic environmental impact statement on decommissioning of nuclear facilities. Regarding the decommissioning of nuclear power reactors. NUREG-0586, suppl 1, vol 2. U.S. Nuclear Regulatory Commission, Washington, DC. http://www.nrc.gov/reading-rm/doc-collections/nuregs/staff/sr0586/s1/v2/index.html

Websites

Argonne National Laboratory (USA). Decontamination and decommissioning. http://www.dd.anl.gov/
Atomic Energy Canada Limited. Sustainable development: decommissioning and waste management. http://www.aecl.ca/Development/SD-WMD.htm
Decontamination and Decommissioning Science Consortium (USA). http://www.orau.gov/ddsc/
IAEA. Decommissioning. http://www-ns.iaea.org/tech-areas/waste-safety/decommissioning.htm
IAEA. Nuclear energy handbook. Technologies for the decommissioning of installations and restoration of sites. http://www.iaea.org/inisnkm/nkm/ws/d3/r2531.html
NEA Working Party on Decommissioning and Dismantling (WPDD) http://www.nea.fr/html/rwm/wpdd.html
Nuclear Decommissioning Authority (UK). http://www.nda.gov.uk/
U.S. Department of Energy (USA). Deactivation and decommissioning. http://www.em.doe.gov/EM20Pages/DD.aspx
U.S. Nuclear Regulatory Commission (USA). Decommissioning. http://www.nrc.gov/about-nrc/regulatory/decommissioning.html
World Information Service on Energy Uranium Project. http://www.wise-uranium.org/index.html

Chapter 10
Radioactive Waste Management: Storage, Transport, Disposal

Audeen W. Fentiman

Glossary

Fission	Process by which a nucleus splits into two smaller nuclei, emitting two or three neutrons and energy.
Half-life	The time required for half of the nuclei in a sample of a radioactive isotope to emit radiation and be transformed to another isotope.
High-level radioactive waste (HLW)	Used nuclear fuel or the highly radioactive materials that are generated when used nuclear fuel is reprocessed.
Low-level radioactive waste (LLW)	Radioactive waste that is not high-level radioactive waste, used nuclear fuel, or mill tailings.
Transuranic waste (TRU)	Wastes that are not classified as high-level waste and contain more than 100 nCi/g of alpha-emitting transuranic isotopes ($Z > 92$) with half-lives of more than 20 years.
Used nuclear fuel or spent nuclear fuel (SNF)	Terms used to designate nuclear fuel that has been irradiated in a reactor to produce power.

This chapter was originally published as part of the Encyclopedia of Sustainability Science and Technology edited by Robert A. Meyers. DOI:10.1007/978-1-4419-0851-3

A.W. Fentiman (✉)
School of Nuclear Engineering, Purdue University, West Lafayette, IN 47907, USA
e-mail: fentiman@purdue.edu

N. Tsoulfanidis (ed.), *Nuclear Energy: Selected Entries from the Encyclopedia of Sustainability Science and Technology*, DOI 10.1007/978-1-4614-5716-9_10,

Definition of the Subject

Radioactive materials are widely used in our society, and when they are, radioactive wastes can be produced. In addition to being used to generate about 20% of the electricity used in the USA and 17% of the electricity used worldwide, radioactive materials are important in medicine, industry, and research. For example, radioactive materials are used to help diagnose and treat disease, as thickness gages in manufacturing, as components of some smoke detectors, to kill bacteria in food, to trace the movement of nutrients through plants, and to power spacecraft leaving the solar system. Just as there are many uses of radioactive materials, there are many types of radioactive waste, each of which must be stored for a time, treated (prepared either for disposal or recycling), transported, and ultimately disposed of in a licensed facility. Some radioactive materials are utilized in weapons production, an activity which also results in generation of radioactive wastes, although this chapter shall focus on civilian uses of radioactive materials. Proper management of radioactive wastes is essential to ensure that society continues to realize the benefits of radioactive materials without undue risk to human health or the environment, and all aspects of radioactive waste management are highly regulated.

Introduction

This chapter addresses four types of radioactive waste, used nuclear fuel, high-level radioactive waste (HLW), low-level radioactive waste (LLW), and transuranic waste (TRU). Used nuclear fuel (sometimes called spent nuclear fuel) is fuel that has reached the end of its useful life and has been taken out of a nuclear power plant. It is highly radioactive. High-level waste is a category of radioactive waste that includes used nuclear fuel and the highly radioactive wastes that are generated when used nuclear fuel is reprocessed. These two materials are expected to be disposed of in the same facility and thus are lumped together in one category. As the name implies, this waste is highly radioactive. Low-level radioactive waste is material that is not HLW or TRU; LLW typically consists of items with low concentrations of radioactive materials with relatively short half-lives ($<$100 years). There are several categories of low-level radioactive material, and the category assigned to any particular container of low-level waste depends on the type and amount of contamination on the waste material. Finally, transuranic waste is a very specialized type of waste containing materials that have an atomic number greater than that of uranium. One section of this chapter is devoted to each type of waste, and within each section, methods for storing, treating, transporting, and disposing of the waste will be discussed.

High-level Radioactive Waste – Including Used (Spent) Nuclear Fuel (SNF)

One hundred and four nuclear power plants in the USA generate about 20% of the electricity used each year [1]. Worldwide, over 435 nuclear power plants generate about 17% of the electricity [2]. Some countries rely heavily on nuclear power. For example, over 75% of the electricity in France is generated by nuclear power plants, and over 40% of the electricity in Sweden, Belgium, and Slovakia is from nuclear power [3].

The fuel for the nuclear power plants is uranium dioxide (UO_2), which is typically pressed into ceramic pellets. About 5% of the uranium in the fuel is ^{235}U which fissions, releasing energy that is ultimately converted to electricity. The other 95% of the uranium in the fuel is ^{238}U which is mostly inert although a small fraction of the ^{238}U atoms is converted to plutonium while the reactor is operating and another small fraction fissions. The ceramic UO_2 pellets are small cylinders about 0.6 in. long and 0.4 in. in diameter [4]. Stacks of pellets are sealed in zircaloy tubes about 12 ft long, and a 17 × 17 array of rods constitutes one typical fuel assembly. About 180 fuel assemblies are loaded into an average-sized pressurized water reactor. The other type of nuclear reactor commonly used in the USA, the boiling water reactor, is fueled with about 500–750 smaller fuel assemblies.

As the reactor operates, ^{235}U nuclei fission, after they absorb a neutron, breaking into two smaller nuclei. A small number of neutrons emitted during fission strike other ^{235}U atoms, causing more fissions, and releasing more energy. This process is known as a chain reaction. Eventually, most of the ^{235}U atoms in a fuel assembly have fissioned, and there are not enough of those atoms remaining to sustain the chain reaction. At that point, about one third of the fuel assemblies is removed from the reactor and fresh ones inserted in their place. Most nuclear power plants operate for 18–24 months before they need to be refueled. The fuel assemblies that are removed during refueling are referred to as used nuclear fuel or spent nuclear fuel.

The composition of the used nuclear fuel is shown in Table 10.1. Approximately 95% of the used nuclear fuel is ^{238}U. Less than 1% of the used fuel is plutonium. Some plutonium isotopes, primarily ^{239}Pu, fission and can be incorporated into new fuel rods. The reminder of the used fuel consists of fission products, that is, the atoms created when the ^{235}U atoms split, and minor actinides which were formed

Table 10.1 Composition of used nuclear fuel [5]

Material	Percent of used fuel (%)
Uranium (^{235}U and ^{238}U)	95.6
Plutonium (all isotopes)	0.9
Minor actinides	0.1
Stable fission products	2.9
Radioactive fission products	0.5

when some ^{238}U atoms absorbed neutrons. Many fission products are highly radioactive and emit penetrating gamma rays.

When the used nuclear fuel is removed from the reactor, it is transferred to the spent fuel pool in a structure adjacent to the reactor building. The spent fuel pool is an in-ground, concrete, steel-reinforced, stainless steel-lined pool that is filled with at least 20 ft of water [6]. Used fuel assemblies are placed vertically in the pool. Water in the pool cools the fuel assemblies and serves to shield workers and equipment in the area of the pool from the radiation emitted by the fuel assemblies.

Perhaps surprisingly, the spent fuel pool at a nuclear power plant is not designed to be large enough to hold all of the used fuel that will be discharged from the nuclear power plant over its lifetime. A nuclear power plant's initial license is for 40 years. By early 2010, over half of the nuclear power plants in the USA had been granted license extensions of 20 years [7]. Thus, nuclear power plants are expected to operate at least 60 years, and it will be necessary to store some used fuel outside of the spent fuel pool. At the time the first nuclear power plants were built in the 1960s, it was presumed that used nuclear fuel would be reprocessed and recycled after the fuel assemblies had cooled for several years. Thus there was no need to build a spent fuel pool to hold all of the discharged fuel. In April 1977, US policy on reprocessing was changed when President Carter issued a statement that the USA would "defer indefinitely the commercial reprocessing and recycling of plutonium" [8]. The Nuclear Waste Policy Act of 1982 mandated construction of a geologic repository for permanent disposal of used nuclear fuel and required the Department of Energy to begin disposing of the used nuclear fuel not later than January 31, 1998 [9]. Once again, it did not appear that the spent fuel pool would need to hold all of the used nuclear fuel from a nuclear power plant, since there would be a place to send the used fuel for disposal. However, the geologic repository has not been built, and spent fuel pools at many of the older nuclear power plants are full or nearly full.

Many power plants are now moving some of their older used fuel assemblies that have been cooling in the spent fuel pool for many years to dry storage casks to make room in the pool for more fuel coming out of the reactor. The typical dry storage cask is a cylinder about 19 ft high and 8 ft in diameter made of concrete or steel. Dry storage casks come in different sizes, but they usually hold approximately 30 fuel assemblies and weigh about 100 t when loaded [10]. Spent fuel assemblies are sealed in an inner canister which is then placed in the dry storage cask. Some of the dry storage casks are designed to sit vertically on a concrete pad near the reactor building. In other dry storage systems, the casks are placed horizontally into a concrete bunker near the reactor building.

Across the USA, as of 2010, there are about 60,000 t [11] of used nuclear fuel stored either in spent fuel pools or dry storage casks at the nuclear power plants where it was generated. (Because uranium is a very dense material (19.05 g/cm^3), denser even than lead (11.35 g/cm^3), a ton of used fuel does not occupy much space. If all of the used fuel assemblies that have been discharged from US nuclear power plants since they began to operate were stacked on a football field 100 yards long and 53⅓ yards wide, the stack would be about 6½ yards high.) The Nuclear Regulatory Commission which is responsible for overseeing safety at the nuclear

power plants has said that the used fuel can be safely stored at the power plant where it was generated for up to 100 years [12].

Ultimately, the used nuclear fuel must be disposed of permanently or reprocessed with as many of the constituents as possible being recycled and reused and the remainder being disposed of permanently. Until a decision about the final disposition of used nuclear fuel is made, the used fuel will continue to be stored either at the power plants where it was generated or at central storage facilities. Regardless of where the fuel is stored or whether it is reprocessed or buried, a system for transporting the used nuclear fuel will be required. Regulations governing the transportation system have been in place for decades, and some used fuel has been moved in licensed transportation casks. The next several paragraphs will describe recent US policy for disposing of used nuclear fuel, the options for central storage of used fuel if the fuel currently in dry storage casks is moved from the reactors to a central location, and the transportation system in place to move that used fuel.

Current US policy for disposal of used nuclear fuel was set by the Nuclear Waste Policy Act of 1982 and its 1987 amendments which provided for permanent disposal of used nuclear fuel in a deep geologic repository. The repository was to hold 70,000 t of used nuclear fuel and vitrified high-level waste from Department of Energy (DOE) facilities. The DOE was responsible for designing, building, and operating the repository, and the DOE was to begin taking used fuel from nuclear power plants by January 31, 1998. The Office of Civilian Radioactive Waste Management was established within DOE to manage both the repository and the transportation system for used nuclear fuel. In addition, the law required a monitored retrievable storage facility (MRS) where used fuel from reactors throughout the USA could be stored temporarily and then put into standard packages for disposal. The bill also established the Nuclear Waste Fund to pay for the design, construction, and operation of the used nuclear fuel management system. A charge of one mill (one tenth of a cent) for every kilowatt hour of electricity generated by a nuclear power plant is the source of money for the Nuclear Waste Fund. Between 1982 and 2007, $27.3 billion dollars were collected for the Nuclear Waste Fund [13].

Three possible sites for the deep geologic repository were identified, and each was to be characterized to determine whether it was an appropriate location for nuclear waste disposal. The sites were in (1) Deaf Smith County, Texas, (2) Richland, Washington, on the Hanford Site, and (3) Yucca Mountain, Nevada, near the Nevada Test Site where nuclear weapons had been tested underground. Each of the three sites offered a different type of rock in which the repository would be located. The Texas site was in salt, the Washington site in basalt, and the Nevada site in tuff. Local opposition to construction of a nuclear waste repository was strong in all three locations, and efforts to characterize the sites were often thwarted. Little progress was made toward identifying the best location for the repository.

In 1987, the US Congress passed the Nuclear Waste Policy Amendments Act. This law identified the Yucca Mountain site in the Nevada desert as the location of the nation's deep geologic repository. The law established a position of Nuclear Waste Negotiator to find a volunteer site for the MRS since the site in Tennessee identified pursuant to the 1982 Nuclear Waste Policy Act was rejected.

The geologic repository for used nuclear fuel was required to be licensed by the Nuclear Regulatory Commission (NRC). Following passage of the 1987 law, work began at the Nevada site to gather scientific evidence required to prepare an application for a license to construct and operate the geologic repository. Information required for the license application is specified in 10 CFR Part 60, Disposal of High-Level Radioactive Wastes in Geologic Repositories [14]. Scientists working on the application needed to show that they understood not only the characteristics of each of the components of the repository, but also how the components would interact and perform over time. Since the repository was to accommodate both used nuclear fuel from commercial nuclear power plants and vitrified high-level waste from nuclear weapons programs, data on composition of both waste forms as well as chemical and physical properties were required. Information required on packages that confined the waste included proposed materials, dimensions, and response to heat, pressure, radiation, water, and other possible corrosive chemicals in the rock and soil. Detailed information on the design of the engineered repository was required. DOE had to show that the repository would be safe for workers while the waste was being emplaced, that any specific container of buried waste could be retrieved for 50 years after it had been emplaced, and that the repository would confine the waste over a specified period. Data required for the site, itself, included characteristics of the rocks and soil, groundwater speed and direction, and an inventory of flora and fauna species in the area of the repository.

Between 1987 and 2007, the team of scientists characterizing Yucca Mountain spent approximately $7 billion gathering data on the site and preparing the required documents including an environmental impact statement and the license application. The repository design called for a network of tunnels approximately 1,200 ft below the surface. Each tunnel was to be reinforced with steel supports to keep the rock from collapsing onto the waste packages. Rails on the floor of each tunnel would allow casks to be moved into place. Casks designed to hold about 30 used fuel assemblies or half a dozen cylinders of vitrified waste from DOE facilities would be made of thick steel. An inverted U-shaped titanium shield was proposed to cover the casks in each tunnel to divert any water that might reach the repository from the desert above.

On June 3, 2008, DOE delivered to the Nuclear Regulatory Commission the application for a license to construct and operate the nuclear waste repository at Yucca Mountain. According to the Nuclear Waste Policy Act, the NRC had 3 years to review the application but could request an additional year. Following the presidential election in 2008, funding for the Yucca Mountain Project was reduced, and March 2010, the DOE withdrew its application for a license for a nuclear waste repository at Yucca Mountain "with prejudice." At almost the same time, the DOE created the Blue Ribbon Commission on America's Nuclear Future. The charter of this Commission was "to conduct a comprehensive review of policies for managing the back end of the nuclear fuel cycle, including all alternatives for the storage, processing, and disposal of civilian and defense used nuclear fuel, high-level waste, and materials derived from nuclear activities." The Commission is to complete its report in 24 months.

The Blue Ribbon Commission is likely to consider both direct disposal of used nuclear fuel assemblies in a deep geologic repository and reprocessing of used nuclear fuel followed by recycling of many of the components and utilization, treatment, or disposal of the remaining materials. Direct disposal in a geologic repository was discussed earlier. Reprocessing of used nuclear fuel is briefly addressed here.

Reprocessing of used nuclear fuel currently involves chopping up the used fuel rods, dissolving the fuel in a concentrated nitric acid solution, and chemically separating the various elements in the used fuel. The uranium and plutonium, which constitute about 96% of the used fuel, can be recycled and used in fabricating new fuel rods. The remaining material is typically dried, mixed with glass frit, melted, and poured into metal cylinders. Many countries that rely heavily on nuclear power either reprocess their own used nuclear fuel or send it to other countries that have reprocessing facilities. The USA does not reprocess used fuel from commercial nuclear power plants.

The reprocessing method currently used in most countries is the PUREX method which was developed in the USA to reprocess fuel from government-run reactors to recover plutonium for use in nuclear weapons. A small amount of used fuel from commercial nuclear power plants was reprocessed at a facility in West Valley, New York, between 1966 and 1972, but the facility was shut down because it was not economical. Since the USA decided not to reprocess used nuclear fuel in 1977, no additional reprocessing of commercial nuclear fuel has occurred. One objection to use of the PUREX method was that it isolates plutonium from other materials in the used fuel, supposedly making it easier for terrorists to divert the plutonium.

Research is being conducted in the USA on reprocessing methods that would not isolate plutonium. Some of the methods under consideration are for reprocessing used fuel from the light water reactors that are currently operating in the USA. Other methods are being developed for different types of fuel that might be used in the next generation of reactors (commonly referred to as Generation IV) now being designed for use around the world. Reprocessing facilities are complex and expensive to build. Japan completed construction of a nuclear fuel recycling facility in Rokkasho at a cost of approximately $20 billion [15]. It is likely that US policy makers will want more information on the types of nuclear power plants that will be operating in the USA over the next century and results of research programs on reprocessing methods in hand before deciding what type of reprocessing facility, if any, to build in the USA.

Since it appears that the USA will not be disposing of used nuclear fuel or reprocessing it in the near future, storage of used nuclear fuel at a central facility (or facilities) is being studied. Central storage is not a new concept. The Nuclear Waste Policy Act of 1982 called for establishing a Monitored Retrievable Storage (MRS) facility, and the Nuclear Waste Policy Amendments Act of 1987 provided for a person to seek a community willing to host the MRS. No MRS has been sited. A consortium of utilities, called Private Fuel Storage, negotiated with the Skull Valley Band of the Goshute Indian Tribe to establish a central used fuel storage facility on the Tribe's land in Utah. An application was submitted on the NRC for

a license to construct and operate the storage facility, and on February 21, 2006, the NRC granted a license, but said that construction could not begin until it obtained "necessary approvals from other agencies, including the Bureau of Land Management, the Bureau of Indian Affairs, and the Surface Transportation Board" [16]. Neither the Bureau of Land Management nor the Bureau of Indian Affairs has approved the site. At the request of Senators Barbara Boxer, Harry Reid, and John Ensign, the US General Accountability Office did a study of a central storage facility option and an on-site storage facility option, along with the Yucca Mountain repository. The study, which was issued in November 2009, concluded that while a centralized interim storage facility could be built relatively quickly, finding a site could be difficult, and since the facility would not be a final disposal site, any waste going to the centralized storage facility would have to be transported twice [17]. The Blue Ribbon Commission on America's Nuclear Future is also likely to consider options for a central storage facility.

Eventually, the used nuclear fuel currently stored at the nuclear power plants must be transported to a central storage facility, a processing facility, or a permanent disposal site. Some used nuclear fuel has been transported in the USA, for example, between nuclear power plants owned by the same company or from a power plant to a government research facility. Both the NRC and the US Department of Transportation have regulations governing transportation of used nuclear fuel. The NRC regulation is Title 10, Part 71 of the Code of Federal Regulations (10 CFR Part 71) [18], which specifies requirements for the packages that carry the highly radioactive material, called Type B packages. The regulation also specifies how packages for transporting used nuclear fuel are to be approved. Each Type B package must have a Radioactive Material Package Certificate of Compliance from the NRC. Procedures for applying for the Certificate of Compliance can be found in NUREG-1617, "Standard Review Plan for Transportation Packages for Spent Nuclear Fuel" [24]. Packages for used nuclear fuel are designed for transportation by truck and by rail.

To receive a Certificate of Compliance, a Type B package, which is often called a shipping cask, must undergo a series of tests that simulate accident conditions a cask might encounter en route. The first four tests, conducted sequentially on a single cask, are:

1. Drop test. Drop the cask from 30 ft onto a hard, unyielding surface in an orientation most likely to damage the cask.
2. Puncture test. Drop the cask from 40 in. onto a 6-in. diameter shaft in an orientation most likely to result in damage.
3. Fire test. Engulf the cask fully in a fire at least 1,475°F for 30 min.
4. Immersion test. Place the cask under 3 ft of water for 30 min [19].

In order to receive the Certificate of Compliance, the cask must not release any radioactive materials during or following the series of tests. A new, undamaged cask must pass a fifth test, immersion in water at a pressure equivalent to that exerted by water 50 ft deep, before the Certificate can be issued.

Several different shipping casks have been designed to be transported by truck. Those casks carry between 1 and 9 used fuel assemblies. A typical rail cask carries 36 fuel assemblies, but the number varies because there are different sizes of fuel assemblies. The shipping casks are usually cylindrical with their walls made of several layers of different materials. The innermost and outermost layers are usually steel to provide structural strength. One layer of material between the steel shells is designed to absorb gamma rays emitted by the used fuel. Steel, lead, and depleted uranium are some materials that are used to absorb gamma rays. Another layer is made of a material that slows down and absorbs neutrons. *The Radioactive Materials Packaging Handbook*, [20] written at the Oak Ridge National Laboratory in 1998 contains detailed information required to design and manufacture a shipping cask for used nuclear fuel.

NRC regulations govern routes to be used for transporting used nuclear fuel and physical protection for the shipments. The Department of Transportation regulations specify methods for selecting routes (49 CFR 397) and labeling of the shipping casks (49 CFR 172). In addition, drivers of trucks transporting radioactive materials must meet training and experience requirements and undergo a background investigation.

Low-level Radioactive Waste

Low-level radioactive waste is defined in the Low Level Radioactive Waste Policy Act of 1980 as radioactive waste that is not high-level radioactive waste, spent nuclear fuel, or mill tailings [21]. There are four classes of low-level radioactive waste (LLW) based on the concentration of radioisotopes with short half-lives and the concentration of radioisotopes with longer half-lives in the waste. The classes are designated as A, B, C, and Greater Than Class C (GTCC). Tables 1 and 2 in 10 CFR Part 61 are used to determine the class of LLW in a particular container.

LLW is generated by almost any activity that involves radioactive material. Some examples of LLW are lab coats and shoe covers worn when working with radioactive materials, medical equipment involved in treating a patient with radiopharmaceuticals, and laboratory supplies and equipment used in experiments involving radioactive tracers. Radioactive tracers are very commonly used. They are radioactive isotopes that move through a system (e.g., the human body, a growing plant, or an ecosystem) along with the material being studied. Since small amounts of radiation can be detected, the researchers can measure radiation from the tracer to determine how the substance of interest is moving through the system. For example, tracers are used in the development of virtually all new medicines to study how the medicine or its metabolites move through the body. Hospitals, universities, and research laboratories operated by corporations or government agencies often generate LLW.

The largest amount of commercial LLW is generated by industry, including the nuclear power industry. Equipment and materials from power plant maintenance

activities, samples collected during environmental monitoring, and protective clothing are disposed of as LLW. In addition, LLW is generated during the various stages of nuclear fuel fabrication.

Often LLW is initially in liquid form. For example, it is sometimes more cost-effective to wash protective clothing than to dispose of it. Likewise, it may be more economical to decontaminate some equipment using a solvent than to dispose of the equipment. In these cases, the wash water and the solvent become LLW. Environmental samples are routinely dissolved in a liquid for analysis, yielding liquid LLW. Since LLW disposal facilities will not accept large amounts of liquid wastes, most liquid LLW must be solidified. Several methods can be used including evaporation, ion exchange, flocculation, and filtration. The liquid waste could simply be mixed with a solidifying agent such as concrete. However, since the cost of disposal is determined, in part, by the volume of the waste, methods that minimize the volume are usually preferred.

Dry LLW is typically treated to reduce its volume prior to packaging for shipment to a disposal facility. Compaction, which results in a volume reduction to one half or one third of the initial volume, or super-compaction, which can result in a volume reduction to one tenth of the original volume are commonplace. Incineration can reduce the volume to 1% of the original and is especially useful for combustible materials like wood that cannot be compacted easily.

Three disposal facilities for commercial LLW are currently operating in the USA. They are in Barnwell, South Carolina, Richland, Washington, and Clive, Utah. Another one has been proposed in Texas. LLW disposal sites have been available since the early 1960s. Four early sites have been closed. They were in Sheffield, Illinois, Maxey Flats, Kentucky, West Valley, New York, and Beatty, Nevada.

While LLW disposal facilities have been operating in the USA since the 1960s, the law which currently governs LLW disposal was not passed by the US Congress until 1980. The Low-Level Radioactive Policy Act of 1980 made each state responsible for arranging for disposal of its own LLW. States were encouraged to form compacts, groups of states that could collaborate to build one LLW disposal facility to serve all of the compact's members. If a state within a compact built a LLW disposal facility, that facility would not be required to accept LLW from any state outside of the compact. States that did not belong to a compact and chose to build their own disposal facility would not be able to exclude waste from other states. The law required states to form compacts by 1986. States did not meet that deadline, and in 1985, the Low Level Radioactive Waste Policy Amendments Act was passed. It gave the states until 1992 to form compacts. At one time, all states have belonged to a compact. Some have left the compact, and some compacts have been reconstituted. However, no compact has built a new LLW disposal facility.

Until 2008, the lack of new disposal facilities did not impact LLW generators' ability to dispose of their waste. The Richland, Washington, facility accepted Class A, B, and C waste from the Northwest and Rocky Mountain compacts, and the Barnwell, South Carolina, facility accepted Class A, B, and C waste from the rest of the country. The Clive, Utah, facility accepted only Class A waste, but it had

applied for a revised license to accept Class B and C waste. The Barnwell facility announced that after July 1, 2008, it would not accept Class B and C waste from states outside of the Atlantic Compact. As of early 2010, the Clive, Utah, facility did not yet have a license to accept Class B and C waste. Thus, as of July 2008, the 36 states that had previously been served by the Barnwell facility have had no place to send their Class B and C wastes. Since nearly 99% of commercial LLW is Class A waste and can be sent to a disposal facility, most generators have only small amounts of Class B and C waste and will have space to store that waste until a new facility can be built or some other solution can be found [22].

Packaging requirements are specified for each class of LLW in 10 CFR Title 61.56. Some requirements for Class A waste are: no cardboard or fiberboard containers may be used, wastes cannot be explosive or pyrophoric, emit toxic gases, or contain biological pathogens or infectious material and if the package contains liquids, it must also have enough absorbent material to absorb twice the volume of liquid present. Packing for Class B waste must meet all of the requirements for Class A waste packaging plus a stability criterion which ensures that packages will remain intact when other packages are stacked on top of them. Class C waste packaging must meet all of the requirements of Class B waste packaging plus provide a barrier to inadvertent intrusion.

Low-level radioactive waste is typically disposed of in shallow land burial facilities. A facility must be designed to minimize contact of the buried waste with water. A trench about 30 ft deep and 100 ft wide is excavated in soil that drains well. Containers are placed in the trench in a way that minimizes void space, and any voids that are created are filled with sand. When a portion of the trench is full, it is covered with a cap that is designed to divert any water that falls on it away from the waste.

Transuranic Waste

Transuranic wastes are defined in 40 CFR 191, Environmental Standards for the Management and Disposal of Spent Nuclear fuel, High Level and Transuranic Waste, as wastes that are not classified as high-level waste but contain more than 100 nCi/g of alpha-emitting transuranic isotopes (materials with $Z > 92$) with half-lives of more than 20 years. Transuranic isotopes are generated in a reactor when U-238 absorbs neutrons. Most transuranic waste in the USA has been generated during weapons production when used nuclear fuel from government-operated reactors was reprocessed to recover plutonium for weapons. If the USA begins to reprocess used nuclear fuel from commercial nuclear power plants, transuranic wastes will be generated at the commercial fuel reprocessing facilities as well.

Most transuranic (TRU) waste is solid. Typical wastes are protective clothing or equipment that has been contaminated with transuranic isotopes. TRU waste is packaged in steel, concrete, or wooden boxes. Since most of the transuranic isotopes

emit alpha particles which cannot penetrate a sheet of paper, most TRU waste (about 97%) is referred to as Contact Handled TRU, meaning that people can handle the packages. Only 3% of the TRU must be handled remotely [23].

Transuranic waste is disposed of in the Waste Isolation Pilot Plant (WIPP). WIPP is a deep geologic repository in salt located near Carlsbad, New Mexico. It has been accepting and disposing of TRU waste since 1999. The US Department of Energy Report DOE-WIPP-069, Waste Acceptance Criteria for the Waste Isolation Pilot Plant, outlines requirements for TRU waste shipped to the facility for disposal. They include specifications for the container, data to accompany the package, and radiologic, physical, chemical, and gas generation properties of the waste.

TRU waste is transported to WIPP in Type B packages which are certified by the Nuclear Regulatory Commission after undergoing the rigorous tests described in the section on used nuclear fuel.

Future Directions

Future directions for radioactive waste management in the USA vary depending on the type of radioactive waste. Transuranic wastes are likely to continue to be shipped to the Waste Isolation Pilot Plant (WIPP) for disposal. For decades, low-level radioactive wastes have been disposed of in shallow land burial facilities. Currently, several states do not have a location for disposal of Class B and C wastes, but those constitute only about 1% of the low-level wastes and can be stored at the generation site until a disposal facility is available. Efforts to open new or expand existing low-level waste disposal facilities are ongoing.

High-level radioactive waste disposal policy in the USA is being reviewed. The Blue Ribbon Commission on America's Nuclear Future has been established (2010) to consider the alternatives. Meanwhile, used nuclear fuel is being stored at reactor sites and can be kept there for several decades while the federal government adopts a policy for its disposal and constructs the facilities required to carry out the policy. The nation has experience with all of the components of the system required to treat and dispose of HWL. Transportation casks for HLW have been built, certified, and used to transport that material. Used nuclear fuel belonging to the federal government and some used commercial fuel have been reprocessed. Research on advanced reprocessing methods is being conducted at national laboratories and universities. Research done at Yucca Mountain and experience at WIPP have provided extensive data on deep geologic repositories, which are the type of facility in which used nuclear fuel or reprocessing waste is likely to be placed. Several other countries that rely heavily on nuclear power for their electricity are currently reprocessing used nuclear fuel and conducting research on geologic repositories. Technical information related to treatment, storage, transportation, and disposal of high-level radioactive waste will be available when the policy decisions are made.

Bibliography

Primary Literature

1. US Energy Information Administration (2009) United States percent of electricity from nuclear. http://www.eia.doe.gov/cneaf/electricity/epm/epm_sum.html. Accessed 15 Mar 2010
2. World Nuclear Association (2008) World nuclear power reactors & uranium requirements. http://www.world-nuclear.org/info/reactors.html. Accessed 15 Mar 2010
3. World Nuclear Association (2008) Nuclear shares of electricity generation. http://www.world-nuclear.org/info/nshare.html. Accessed 15 Mar 2010
4. Murray RL (1988) Nuclear energy. Pergamon Press, Oxford
5. Ryskamp JM (2003) Nuclear fuel cycle. http://nuclear.inel.gov/docs/papers-presentations/nucle_fuel_CYCLE_3-5-03.PDF. Accessed Jun 2008
6. US Nuclear Regulatory Commission (2007) Spent fuel pools. http://www.nrc.gov/waste/spent-fuel-storage/pools.html.Accessed Mar 2010
7. US Nuclear Regulatory Commission (2010) Nuclear power plant license extensions. http://www.nrc.gov/reactors/operating/licensing/renewal/applications.html#completed. Accessed Mar 2010
8. PBS Frontline (2010) Carter nuclear fuel reprocessing. http://www.pbs.org/wgbh/pages/frontline/shows/reaction/readings/keeny.html. Accessed Mar 2010
9. Nuclear Waste Policy Act of 1982 as amended (2010) http://www.nrc.gov/reading-rm/doc-collections/nuregs/staff/sr0980/v2/sr0980v2.pdf#pagemode=bookmarks&page=141. Accessed Apr 2010
10. Board on Radioactive Waste Management (2006) Safety and security of commercial spent nuclear fuel storage: public report. National Academies Press, Washington
11. How many tons of spent nuclear fuel on hand – in what year http://epw.senate.gov/public/index.cfm?FuseAction=Minority.PressReleases&ContentRecord_id=f2cbe309-802a-23ad-4925-643845f220b5&Region_id=&Issue_id
12. Waste Confidence Decision, 49 FR 34694, August 31, 1984, as amended at 55 FR 38474, September 18, 1990; 72 FR 49509, August 28, 2007, Federal Register
13. Congressional Budget Office Testimony on the Federal Government's Liabilities under the Nuclear Waste Policy Act (2007) Nuclear waste fund balance. http://www.cbo.gov/doc.cfm?index=8675&type=0. Accessed Mar 2010
14. US Nuclear Regulatory Commission (1981) 10 CFR Part 60, disposal of high-level radioactive wastes in geologic repositories
15. vonHippel F (2009) Why reprocessing persists in some counties and not in others: the costs and benefits of reprocessing – for the Non-Proliferation Education Center.www.npec-web.org/.../vonhippel%20-%20TheCostsandBenefits.pdf. Accessed Mar 2010
16. US Nuclear Regulatory Commission press release No. 06-028 (2006) Private Fuel Storage license application. http://www.nrc.gov/reading-rm/doc-collections/news/2006/06-028.html. Accessed Mar 2010
17. US General Accountability Office (2009) Nuclear waste management: key attributes, challenges, and costs for the Yucca mountain repository and two potential alternatives. GAO-10-48
18. US Code of Federal Regulations (CFR) (2010) 10 CFR Part 71 http://www.nrc.gov/reading-rm/doc-collections/cfr/part071. Accessed Mar 2010
19. Kutz M (2009) Environmentally conscious materials handling. Wiley, Hoboken
20. Arnold ED, Shappert LB, Bowman SM (1998) Radioactive materials packaging handbook: design, operations, and maintenance. Department of Energy, Oak Ridge National Laboratory, Oak Ridge

21. Low-level Radioactive Waste Policy Amendments Act of 1985. http://www.nrc.gov/reading-rm/doc-collections/nuregs/staff/sr0980/v2/sr0980v2.pdf#pagemode=bookmarks&page=15. Accessed Apr 2010
22. US General Accounting Office (2004) Low-level radioactive waste: disposal availability adequate in the short term but oversight needed to identify any future shortfalls. GAO-04-604
23. Saling JH, Fentiman AW (2002) Radioactive waste management. Taylor & Francis, New York
24. US Nuclear Regulatory Commission (2000) NUREG-1617 Standard Review Plan for Transportation Packages for Spent Nuclear Fuel. http://www.nrc.gov/reading-rm/doc-collections/nuregs/staff/sr1617/. Accessed Mar 2010

Books and Reviews

Office of Civilian Radioactive Waste Management Website (2010). http://www.ocrwm.doe.gov/. Accessed Mar 2010

Ohio State University Extension (2010) Low-level radioactive waste fact sheets. http://ohioline.osu.edu/rer-fact/index.html. Accessed Mar 2010

US Department of Energy (2002) Final environmental impact statement for a geologic repository for the disposal of spent nuclear fuel and high-level radioactive waste at Yucca mountain, Nye County, Nevada. DOE/EIS-0250

US General Accountability Office (2008) Low-level radioactive waste: status of disposal availability in the United States and other countries. GAO-08-813T

US General Accountability Office (2007) Low-level radioactive waste management: approaches used by foreign countries may provide useful lessons for managing US Radioactive Waste. GAO-07-221

US Nuclear Regulatory Commission Website, Radioactive Waste (2010). http://www.nrc.gov/waste.html. Accessed Mar 2010

Waste Isolation Pilot Plant Website (2010). http://www.wipp.energy.gov/index.htm. Accessed Mar 2010

Chapter 11
Nuclear Power, Economics of

M.R. Deinert

Glossary

c	Onetime costs [$]
E_c	Cost of electricity [$]
FV	Future value [$]
HM	Heavy metal, refers to the uranium and or transuranic component of fuel
kg	Kilogram
kW	Kilowatt
kWh	Kilowatt hour
kWh(e)	Kilowatt hour electric
mill	$0.001
n	Number of years
MOX	Mixed oxide fuel
MWh(e)	Megawatt hour electric
p(t)	Distributed costs [$/year]
Pu	Plutonium
PV	Present value [$]
r	Yearly rate of return in discrete discounting
$r(x_i,x_j)$	Correlation coefficient
SD	Standard deviation
SF	Spent fuel
SW	Separative work

This chapter was originally published as part of the Encyclopedia of Sustainability Science and Technology edited by Robert A. Meyers. DOI:10.1007/978-1-4419-0851-3

M. Deinert (✉)
Department of Mechanical Engineering, The University of Texas at Austin,
Austin, TX 78705, USA
e-mail: mdeinert@mail.utexas.edu

N. Tsoulfanidis (ed.), *Nuclear Energy: Selected Entries from the Encyclopedia of Sustainability Science and Technology*, DOI 10.1007/978-1-4614-5716-9_11,

t	Time [year]
U	Uranium
UOX	Uranium dioxide fuel
VHLW	Vitrified high-level waste
x_i	Denotes a cost component
α	Linear cost escalation rate [\$/year^2]
β	Linear cost escalation intercept [\$/year]
δ	Delta function
ρ	Discount or interest rate [1/year]

Definition of the Subject

Financial viability is an important consideration when deciding whether to proceed with any large-scale engineering project. Many studies of nuclear power economics have been undertaken in an attempt to predict its overall costs or competitiveness (e.g., [1–4]). While these studies tend to differ in their assumptions about construction and operating expenses, they all use similar frame works for the analysis. In essence, the idea is to predict the total cost of producing electric power over the lifetime of a facility and compare that to the market value of the electricity produced. All other things being equal, the larger the ratio of revenue to cost the better the project.

Introduction

Economic assessments of nuclear power tend to be complicated, and not just because of the number of components that have to be factored in, Fig. 11.1. The costs of any large project also depend on how it is financed, and whether this is done through the issuing of bonds by the entity undertaking the project, borrowed money, allocation of liquid assets, and/or the use of complex financial instruments such as derivatives. Tax rates, both federal and local, can also play an important role. The revenue stream from a nuclear power facility itself depends on whether the markets into which the electricity is fed are regulated or unregulated and whether arrangements exist that involve the sale of electricity at fixed rates to municipalities where the facilities reside. The effect of hard to predict market forces can affect the price of electricity itself.

In addition, nuclear power has some peculiarities that are unique to the industry. Among these is the need to safely store the radioactive waste products that are contained in spent nuclear fuel, for extended periods of time. At present, only the US Waste Isolation Pilot Plant, in Carlsbad NM, is actively used for this purpose,

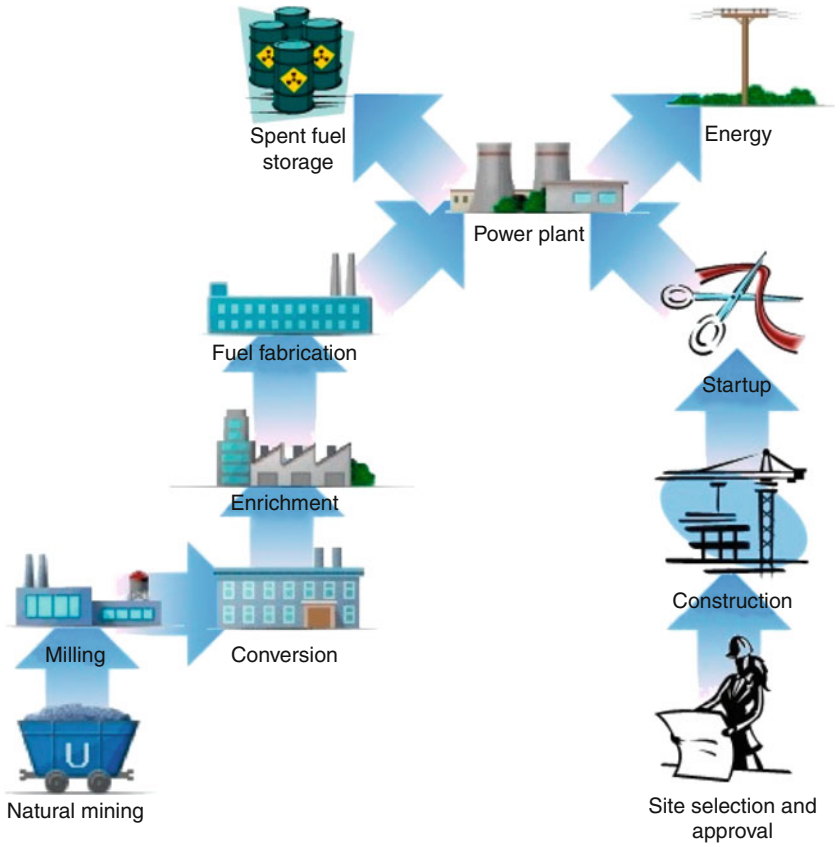

Fig. 11.1 *Components of a nuclear power facility*. Construction of a nuclear power facility begins with site selection and approval. Facility construction (reactor and related facilities) comes next, with final startup typically coming 6–12 years after the start of construction activities. The process of producing uranium fuel typically starts 2 years prior to fuel placement in a reactor with uranium mining, milling, conversion enrichment, and fuel fabrication. Finally, fuel is transported to the reactor site. The fuel pipeline will function continuously as the reactor operates. Interim on-sight storage is common until permanent storage facilities are established (Figure courtesy of Robert Bell, The University of Texas at Austin)

and then only for transuranics (a very specific class of high-level waste) from the US nuclear weapons program. Because of this, *interim* storage facilities exist at civilian nuclear power facilities to handle spent nuclear fuel, but the final disposal costs remain uncertain (e.g., [2]). In addition, most modern reactors run on a uranium fuel that has been enriched to contain more of the uranium 235 isotope than is present in natural uranium (natural uranium is made up of two isotopes: ^{238}U and ^{235}U. The ^{238}U isotopes comprises 99.3% of the uranium atoms and ^{235}U 0.7%. It is the ^{235}U isotope that readily undergoes fission in the thermal reactors that dominate the civilian nuclear power industry.). Because this isotope can also be used in the manufacture of nuclear weapons, concerted efforts have been

Table 11.1 *Life-cycle cost estimates for electricity produced from nuclear, coal, and gas.* The different costs of electricity reflect different life-cycle assumptions between the two studies [4, 11]. Costs were adjusted to $2,007

Production	MIT [4] [cents/kWh(e)]	University of Chicago [11] [cents/kWh(e)]
Nuclear	8.4	5.6
Coal	6.2	4.5
Gas	6.5	3.4

undertaken to limit the development of enrichment facilities outside of a few highly industrialized countries (e.g., [5, 6]). This of course has the effect of forcing nuclear power facilities in less industrialized countries to buy fuel from external sources. Consequently, a common concern is that the fuel supply could be restricted for political reasons (e.g., [7]).

Uncertainties in fuel availability and spent fuel disposal introduce an element of financial risk that is difficult to quantify. Another potential complication comes from uncertainty in whether construction of a nuclear power plant will actually lead to an operational facility. It has in fact happened that facilities have been undertaken whose construction has been halted, or which have been completed but closed before becoming commercially operational. The Shoreham Nuclear Power Plant in Long Island, NY, is an example of this. The facility was completed in the mid-1980s, but public protest resulted in its closure before it produced commercial power.

Because of the above factors, and others, it is difficult to make blanket statements about the economics of nuclear power, and facilities need to be evaluated on an individual basis. However, several recent studies have taken a look at nuclear power relative to competing technologies, see Table 11.1, with somewhat mixed results that reflect the different assumptions that went into the analyses. In the current article, the focus is largely on a discussion of how the cost of a nuclear power facility would be computed when taking into consideration factors such as its construction, operation, maintenance, and decommissioning.

Many of the elements that contribute to the life-cycle cost of a nuclear power plant are common to other types of facilities as well. These include:

Capital costs – The costs associated with building the plant and its components.
O&M – The cost to operate and maintain facilities.
Depreciation – This is a charge recorded against earnings that takes into consideration the lifetime of capital components and the fact that they must be replaced as a part of operating expenses. Depreciation of capital components is typically added to the yearly operations and maintenance costs.
Interest – The money paid for the use of borrowed capital or for bonds that have been issued.
Taxes – Both federal and local may apply.
Interest rate – The annual amount of money paid to a lender or bond holder for the use of capital as a percentage of the amount to be repaid.

Discount rate – Effectively the same as the interest rate, see section on discount rates.

Several other factors that affect the cost of nuclear power are particular to the industry. These include:

Fuel costs – A peculiarity of nuclear power facilities is that they do not always buy the fuel that is used to run them. Instead, they will often lease it, sometimes from a company that was created explicitly for the purpose of doing this. The reason has to do with accounting practices, and it is sometimes cost effective for a utility to acquire its fuel in this way [8].

Nuclear waste fund fee – This is a fee levied in the United States to cover the Federal Government's obligation to take possession of spent nuclear fuel and dispose of it [8]. The current rate is \$0.001/kWh of electricity produced, which is paid into the Nuclear Waste Fund (The Nuclear Waste Fund was established under US Code Title 42, Chapter 108, Subchapter III, 10222 – i.e., The Nuclear Waste Policy Act of 1983). This monetary unit is so common within the utility industry that it is often given a special unit called a "mill," where 1 mill = \$0.001 [8].

On site spent fuel storage cost – The cost to store spent nuclear fuel on site.

Decommissioning costs – The costs associated with removing the power plant and its components along with returning the site to an unrestricted use.

By far the dominant cost for a typical nuclear power plant is that of constructing the facility itself [4]. From the perspective of the people who are building a facility, the cash flows that are required for construction depend not only on the facility cost, and the time required to build it, but also on how it is financed. For example, cash flows associated with a facility financed with cash will be different than those for one financed with a loan that is to be paid back over a fixed period of time, or a bond. Once a facility is built, there are operation and maintenance charges to keep it in working order, and these are spread out over the operating life of the facility. Taxes on property begin as soon as land is acquired, and those on the facility itself depend on the location and municipality, but are likely to be yearly as are taxes on income. Depreciation too is spread out over the operating life of a component (a discussion of common depreciation methods can be found in [4]), and decommissioning costs are incurred at the end of a facility's life. However, it is typical that money must be set aside for decommission costs well in advance of them.

Present and Future Value of Money

The variable nature of the cash inflows and outflows complicates the cost analysis for any industrial facility, but especially those with long lifetimes as is typical with nuclear power plants. When undertaking a life-cycle cost study, it is also important to recognize that not all money is equivalent. Specifically, a dollar paid or earned today has a different value than does one paid or earned a year from now.

The reason for this stems from the fact that money can devalue due to inflation, but also because money held today can be invested and earn interest. Conversely, money received in the future has less value, both because it may have devalued but also because of the inability to invest it until it is received. These concepts are captured in what is often referred to as the "time value of money" [9]. For example, $100 invested today, at a yearly return of 5%, will yield $105 in 1 year. In the parlance of financial engineering, $100 invested this way has a *future value* of $105, and $105 received in 1 year has a *present value* of $100. From the perspective of an investor who expects a yearly return of 5%, both are equivalent.

The relationship between *future value* (FV) and *present value* (PV) is simple:

$$\mathrm{FV} = \mathrm{PV}(1+r)^n \tag{11.1}$$

Here r is the yearly rate of return, and n is the number of years over which the investment takes place (not necessarily an integer), and PV is said to be *compounded* over n years. Conversely, the *present value* of FV (received in n years) is given by:

$$\mathrm{PV} = \mathrm{FV}/(1+r)^n \tag{11.2}$$

An important point that is often overlooked is that PV = FV when the expected rate of return is zero. This situation can effectively arise in environments, where the rate of return is equal to the inflation rate. Equation 11.2 is an example of *discounting*. When the effects of inflation are taken into consideration Eqs 11.1, 11.2 become:

$$\mathrm{FV} = \mathrm{PV}(1+r-i)^n \tag{11.3}$$

and

$$\mathrm{PV} = \mathrm{FV}/(1+r-i)^n \tag{11.4}$$

Here i is the yearly inflation rate. Equations 11.3, 11.4 give the present and future values in constant, or inflation adjusted, dollars. The quantity $\rho = r–i$ is referred to as the "real rate of return" as opposed to the "nominal rate of return" r, and ρ, r, and i all range between 0 and 1. Most economic analyses are done assuming a real rate of return, and that convention is adopted here.

Equations 11.1–11.4 are discrete representations of simple compounding and discounting, and there are several very good descriptions of how they can be extended to more complex situations in general (e.g., [10]), and to the nuclear power industry in particular [1, 8]. However, as these references quickly show, applying discrete financial models becomes cumbersome when the system being analyzed is complex. An alternative is to use continuous approximations to Eqs 11.3, 11.4, which then become:

$$FV = PVe^{\rho t} \tag{11.5}$$

and

$$PV = FVe^{-\rho t} \tag{11.6}$$

Here ρ is again the rate of real rate of return per unit time t.

Levelized Costs

Nuclear power facilities typically operate over extended time periods, and some in the United States are even in the process of receiving license extensions that will bring their operating life spans to 60 years (e.g., [11]). As a result, the present value of funds that are used to build, maintain, fuel, or decommission a nuclear facility will depend significantly on when the costs occur. Therefore, the only way to accurately estimate the total cost of a facility is to compute its total *present value* relative to a specific date (usually the date of startup of the facility). This process is called *levelizing*. In fact, in the United States, all large-scale government projects are required to perform this type of levelized cost analysis [12]. Expenses that take place before the reference date have what is called a *lead time* as they happen *ahead of* the reference time. Expenses that take place after the reference time have a *lag time* as they happen behind the reference time [1, 13]. A framework for how to levelize the costs for nuclear power facilities in terms of lead and lag times was given in a study done by the Organization for Economic Cooperation and Development (OECD) in collaboration with the Nuclear Energy Agency (NEA) [1]. Continuous discounting can be used within this framework to levelize all costs, as well as the revenue from electricity production, to the date at which fresh fuel is loaded into a reactor. Continuous discounting is mathematically simpler than its discrete alternative and often introduces negligible error relative to the large variances for unit cost predictions.

With this approach, levelized costs are easily obtained by multiplying the time-dependent costs, $p(t)$, by the discounting factor, $e^{-\rho(t)t}$, and integrating the product:

$$PV = \int_{t_1}^{t_2} p(t)e^{-\rho(t)t}dt \tag{11.7}$$

where PV [$] is again the present value of a cash outflow, $p(t)$ [$/year], ρt is the real interest or discount rate [1/year], and t is time [year]. It is common in many studies to assume that ρt is constant, though this is not necessary. The total cost of a system over its life is given by the sum over the costs incurred from its construction to its decommissioning:

$$E_c = \sum_i PV_i \tag{11.8}$$

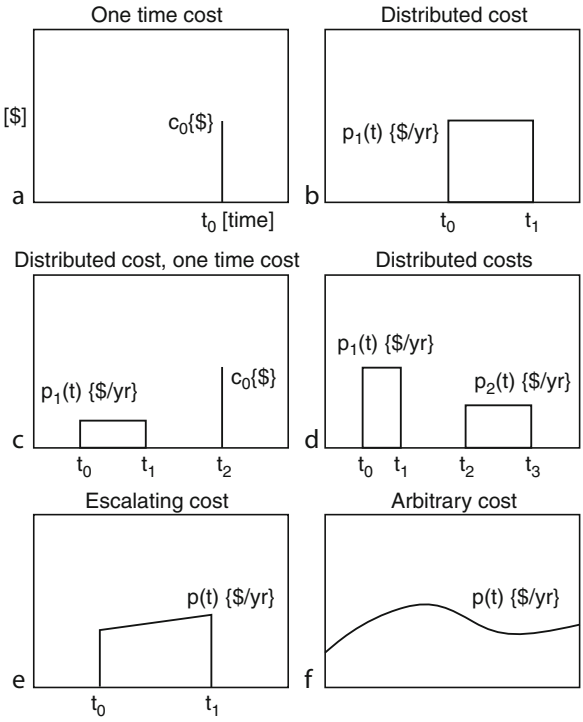

Fig. 11.2 *Common payment, cost, and revenue distributions*. Common distributions for $p(t)$ applicable to Eq. 11.7 are shown. In the figure, c_0 stands for one time cost, and $p(t)$ for distributed cost. The left-hand side of the time axis is assumed to represent $t = 0$

The life-cycle cost in \$/kWh(e) is calculated by dividing E_c by the total kWh's of electricity produced. Some economists argue that the electricity production should itself be discounted using Eq. 11.7 to factor in the temporal nature of the revenue stream (e.g., [14]). It might seem counter intuitive that a unit of energy, being immutable, should be discounted. However, economists who advocate this approach argue that energy (like money) can be viewed as having greater value when it is available in the near term than if its availability is off in the distance. Another interpretation was given by Hannon [14] who suggested that the energy discount rate reflects a society's desire to convert "a present surplus energy into an energy-transformation process so that a greater surplus of energy can be created in the future, rather than consuming the energy now." While energy discounting is used (e.g., [4, 8]), the approach is not universal.

Examples. Fig. 11.2 shows several distributions for $p(t)$ that are relevant to nuclear power systems and out of which any cost or revenue distribution can be built. Equation 11.7 is easy to apply to each situation when it is done systematically.

(a) The present value of a onetime cost, c_0, that occurs at time, t_0, is easy to derive using Eq. 11.7. One starts by noting that:

$$\begin{aligned} p &= 0 \quad 0 \le t < t_0 \\ p &= c_0 \quad t = t_0 \\ p &= 0 \quad t > t_0 \end{aligned} \tag{11.9}$$

Assuming a constant discount rate, Eq. 11.7 becomes:

$$\mathrm{PV} = \int_0^{t_0} c_0 \delta(t_0) \mathrm{e}^{-\rho t} \mathrm{d}t \tag{11.10}$$

where $\delta(t_0)$ is the delta function (zero everywhere but t_0). Equation 11.10 then just gives:

$$\mathrm{PV} = c\mathrm{e}^{-\rho t_0} \tag{11.11}$$

which is just Eq. 11.6 again.

(b) The present value of a uniformly distributed cost is only slightly more complicated to calculate. Here:

$$\begin{aligned} p &= 0 \quad 0 \le t < t_0 \\ p &= c_1 \quad t_0 \le t \le t_1 \\ p &= 0 \quad t > t_1 \end{aligned} \tag{11.12}$$

Equation 11.7 then becomes:

$$\mathrm{PV} = \int_{t_0}^{t_1} c_1 \mathrm{e}^{-\rho t} \mathrm{d}t \tag{11.13}$$

which has the simple solution:

$$\mathrm{PV} = \frac{c_1 \left[\mathrm{e}^{-\rho t_0} - \mathrm{e}^{-\rho t_1}\right]}{\rho} \tag{11.14}$$

(c) The present value of a distributed cost *and* a onetime cost is just the sum of the results given in Eqs. 11.11, 11.14:

$$\mathrm{PV} = c_0 \mathrm{e}^{-\rho t_2} + \frac{c_1 \left[\mathrm{e}^{-\rho t_0} - \mathrm{e}^{-\rho t_1}\right]}{\rho} \tag{11.5}$$

It is implicit in Eq. 11.15 that the discount rate is the same for both distributions; however, this is not always the case, and not a necessary restriction.

(d) The present value of *two* uniformly distributed costs is just obtained using the result in Eq. 11.14 twice:

$$\mathrm{PV} = \frac{c_1 \left[\mathrm{e}^{-\rho t_0} - \mathrm{e}^{-\rho t_1}\right]}{\rho} + \frac{c_2 \left[\mathrm{e}^{-\rho t_2} - \mathrm{e}^{-\rho t_3}\right]}{\rho} \tag{11.16}$$

Here c_1 and c_2 are the uniform cost rates for the respective distributions. It is again implicit that the discount rate is the same for both distributions, though this is again not a necessary restriction.

(e) Linearly escalating costs are also easy to deal with. Here the cost function is given by:

$$\begin{aligned} p &= 0 \qquad && 0 \le t < t_0 \\ p &= \alpha t + \beta \qquad && t_0 \le t \le t_1 \\ p &= 0 \qquad && t > t_1 \end{aligned} \tag{11.17}$$

where α has units of [\$/year^2] and β [\$/year]. In this case, Eq. 11.7 becomes:

$$\mathrm{PV} = \int_{t_0}^{t_1} (\alpha t + \beta) \mathrm{e}^{-\rho t} \mathrm{dt} \tag{11.18}$$

Equation 11.18 has the simple solution:

$$\mathrm{PV} = \alpha\left(\frac{\mathrm{t}}{\rho} - \frac{1}{\rho^2}\right)\left(\mathrm{e}^{-\rho \mathrm{t}_1} - \mathrm{e}^{-\rho \mathrm{t}_0}\right) + \frac{\beta}{\rho}\left(\mathrm{e}^{-\rho \mathrm{t}_1} - \mathrm{e}^{-\rho \mathrm{t}_0}\right) \tag{11.19}$$

In general, Eq. 11.7 is integrable as long as $p(t)$ is known. While the formulas above may seem at first glance to be complicated, they are far simpler and more compact than their discrete discounting alternatives.

Lead and Lag Times in Cost Calculations

A critical factor in using the above equations, and when performing economic analyses in general, is to know when costs occur relative to a specified date. As already pointed out, this is captured in what are referred to as "lead" and "lag" times, and the reference time is typically taken to be the date of the facilities' first operation. Components that affect the cost of nuclear power are shown schematically in Fig. 11.1. In very general terms, the costs associated with nuclear power production can be broken into *capital costs* (which include the construction of physical infrastructure such as the reactor plant, spent fuel storage facilities, or facilities involved in producing nuclear fuel, etc.), *operating costs* (which include operations and maintenance costs, taxes, fuel costs, as well as spent nuclear fuel disposal costs), and *decommission costs* (which include dismantling of physical infrastructure and site remediation).

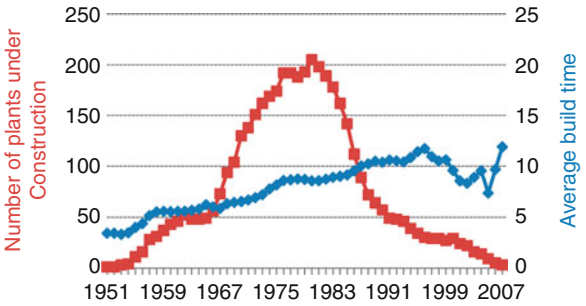

Fig. 11.3 *Reactors under construction and build times*. The total number of nuclear power facilities under construction and the time for facility completion (from start of construction to date of first operation) are shown (The data are from the International Atomic Energy Agency Data Center)

Power Facility Construction

Historically, this has been by far the dominant factor affecting the cost of nuclear power (e.g., [3, 4]). The lead time is highly variable, Fig. 11.3, but 8 years or more is typical for modern large-scale facilities. How this cost is distributed depends on how a facility is financed, Fig. 11.2f.

Power Facility O&M

Operations and maintenance costs for the facilities are usually computed on a yearly basis and can be approximated with a uniform distribution as in Fig. 11.1b. Large capital outlays for replacement of major components can often be assumed to be onetime costs as in Fig. 11.2a (e.g., [3, 4]).

Cooling Water

Availability of cooling water has become a potential constraint for nuclear power plants in some locations. A facility's water use depends on its efficiency, as well as how it is cooled (open loop, closed loop, evaporation pond, etc.). A typical range of water withdrawals for modern Rankine cycle power plants is 2,000–4,000 l/MWh (e), for closed loop systems, and 100,000–220,000 l/MWh(e) for open-loop systems. Water consumption rates are considerably smaller. In this context, water consumption describes water that is taken from a source (ground or surface water), used, and not returned to that source. A cooling tower consumes water through

evaporation for example. Water withdrawal describes water that is taken from a source, used, and then returned to that source. Cost estimates for water vary widely, but \$25 per 1,000 m^3 has been reported and can be based on consumption, or withdrawal, rates and will depend on local water markets and regulatory structures (e.g., [15]).

Uranium Mining

The extraction of uranium ore typically occurs 2 years prior to its use as fuel in a reactor. Uranium is mined as U_3O_8 and is typically sold in this form. Modeled as a onetime cost that would recur with the refueling schedule of a reactor.

Uranium Conversion

The U_3O_8 requires conversion into UF_6 if the uranium is to be enriched to a higher ^{235}U content that occurs in natural uranium. Uranium must be enriched for use as fuel in most commercial light water reactors worldwide [16]. The lead time for conversion is typically 1.5 years. Modeled as a onetime cost that would recur with the refueling schedule of the reactor.

Enrichment

Enrichment typically occurs 1 year before fuel placement in the reactor. Modeled as a onetime cost that would recur with the refueling schedule of the reactor.

Fuel Fabrication

Most reactors worldwide use uranium dioxide fuel that is surrounded by a protective "cladding" and configured in assemblies that can be placed into a reactor. Fabrication usually takes place 0.5 years before fuel emplacement. Modeled as a onetime cost that would recur with the refueling schedule of the reactor.

Leasing or Buying Nuclear Fuel

Not all nuclear utilities buy their fuel. Instead, many lease it, and sometimes from a company or trust that has been created specifically for the purpose of doing this. The lease company covers all expenses for the fuel (mining, conversion, enrichment, fuel manufacture transportation and storage) until it is onsite to be loaded into the core. During this time, the utility pays nothing. Once the fuel begins producing power, the utility will pay the lease company a prorated amount that covers the lease company's expenses plus some degree of profit. In some situations, this arrangement is financially advantageous, though this depends on the accounting practices of the utility and possible constraints from regulatory agencies. Typically, the total cost obligation is met when the fuel has been used to completion. The cost function for the leased fuel can be linearly decreasing, Fig. 11.2e, or of some other shape [8].

Interim Spent Fuel Storage

When the fuel reaches the end of its useful life, it is discharged from the core and is stored on site either under water or in air-cooled vaults until it is removed for final disposal or reprocessing. The residence time in interim storage is highly variable, and the spent fuel from some US reactors has remained in this type of onsite storage for decades. Spent fuel storage is typically calculated per unit time and per unit mass, and it is therefore a linearly increasing cost, Fig. 11.2e, at most reactor facilities, (e.g., [3, 4]).

Spent Fuel Recycle

Some countries, notably France, reprocess spent nuclear fuel and use the plutonium that it contains to manufacture what is called *mixed oxide fuel* (MOX – a mixture of plutonium oxide and uranium oxide) that can be used in addition to standard enriched uranium fuel, Fig. 11.4. In countries where this is done, spent fuel will cool in storage pools for 6–12 years before being sent to reprocessing. The distribution of this cost depends on whether funds are continuously set aside to meet this obligation or whether it is considered to be a series of onetime costs that occur as spent fuel is sent to recycle.

Spent Fuel Disposal

Most countries with domestic nuclear power assume that long-lived nuclear waste products will go into some form of geological storage. At present, only the US Waste Isolation Pilot Plant, in Carlsbad NM, is actively used for this purpose, and then only on a scale sufficient to handle transuranic waste from past US nuclear

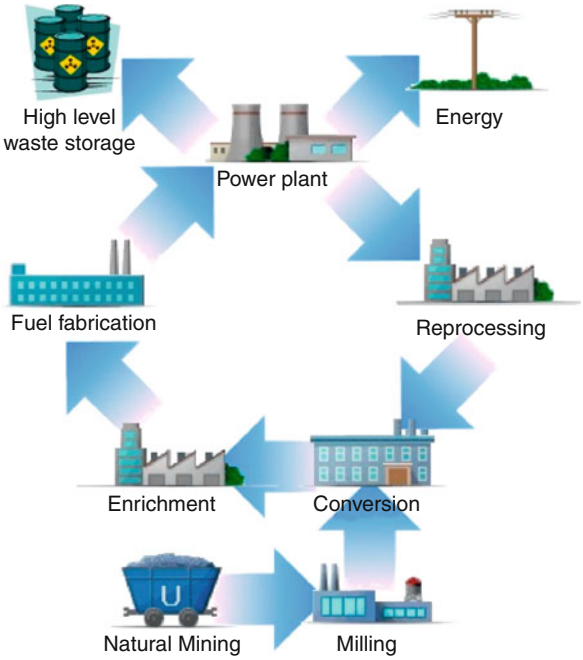

Fig. 11.4 *Recycle-based fuel cycle*. A schematic representation of a reprocessing-based fuel cycle is shown. Instead of spent fuel going to storage, it is sent to reprocessing, and the plutonium, and possibly other *transuranic* elements (such as neptunium, americium, and curium) are recycled to make new fuel. The recycled transuranics would not, however, require enrichment. The high-level waste is comprised of byproducts of reprocessing (Figure courtesy of Robert Bell, The University of Texas at Austin)

weapons efforts. As a result, the actual time at which spent fuel will leave interim storage for final disposal is unclear at most power plants (the final disposal of high-level waste from reprocessing is similarly unclear in countries where this is undertaken). Many reactor facilities whose spent fuel pools are nearing capacity have begun to transition fuel assemblies to onsite dry storage. In the United States, the Nuclear Waste Policy Act of 1987 gives responsibility for the disposal of spent nuclear fuel to the Federal government [17]. In order to cover the associated expenses, US nuclear power facilities pay 1 mill/kWh(e) into the Nuclear Waste Fund for the purpose of covering the final disposal costs [17, 18]. The cost is incurred quarterly and, as a result, constitutes a series of recurrent one time costs for nuclear utilities in the United States, i.e., Fig. 11.2a.

Estimating Uncertainties

Equation 11.8 has the convenient feature of being linear with respect to the total cost of each fuel-cycle component. As a result, E_c can be scaled to account for

changes in unit cost, provided that time points for the integral in Eq. 11.7 remain fixed. Uncertainty in unit costs causes a corresponding uncertainty in the prediction of E_c. These effects can be accounted for by using the well-known formula for error propagation, where the variance of $E_c(x_i)$ is given by:

$$\begin{aligned}\mathrm{var}(\mathrm{E_c}) = &\sum_i \left(\frac{\partial \mathrm{E_c}}{\partial x_i}\right)^2 \mathrm{var}(x_i) \\ &+2\sum_i \sum_{j\neq i} \left(\frac{\partial \mathrm{E_c}}{\partial x_i}\right)\left(\frac{\partial \mathrm{E_c}}{\partial x_j}\right)\sqrt{\mathrm{var}(x_i)}\sqrt{\mathrm{var}(x_j)}\mathrm{r}(x_i,x_j)\end{aligned} \tag{11.20}$$

Here the inputs, x_i, represent the PV_i in Eq. 11.8 with respective variances $\mathrm{var}(x_i)$. The term $r(x_i,x_j)$ is the correlation coefficient, 1 for fully correlated, –1 for anticorrelated and 0 for uncorrelated. The maximum and minimum variances are given by assuming that $r = 1,–1$ respectively with uncorrelated, $r = 0$, typically giving a variance that falls into the midrange. Equation 11.20 is much simplified in the case of $r = 0$. The electricity cost is assumed to have a Gaussian distribution which can be justified by the Central Limit Theorem [19], with the standard deviation of E_c being the square root of the variance. It should also be pointed out that Eq. 11.20 can be used for cost-sensitivity studies.

Costs and Their Uncertainties

Numerous studies have investigated the economics of nuclear power, notably the series of reports produced between 1987 and 2002 by the Organization for Economic Cooperation and Development and the Nuclear Energy Agency (OECD/NEA) [1, 13, 20–22] along with recent reports from groups at MIT and the University of Chicago. The 1994 OECD/NEA study [1], in particular, developed a framework for assessing the economics of nuclear fuel cycles. The study derived the expected levelized cost of a fuel cycle over the lifetime of a reactor, including transients (at startup and shutdown). The fuel cycle was divided into front-end components (uranium ore requirements, conversion to UF_6, enrichment, fuel fabrication and transport) and back-end components (spent fuel transport, reprocessing, direct disposal, or high-level waste (HLW) vitrification and disposal). Cash outflows to meet these obligations were discounted to a reference date using a discrete model as was revenue from electricity, and the subsequent expected cost in $/kWh(e) was calculated.

The 1994 study [1] gave the most comprehensive cost estimates available at the time. Data were obtained from the literature and through survey of OECD member states and gave reliable results where industries were well established. Because no actual disposal facility existed for SF or vitrified HLW, these estimates were considered to be particularly uncertain [1]. The cost data were updated in the 2002 OECD/NEA study and estimated standard deviations were added [13]. Because no

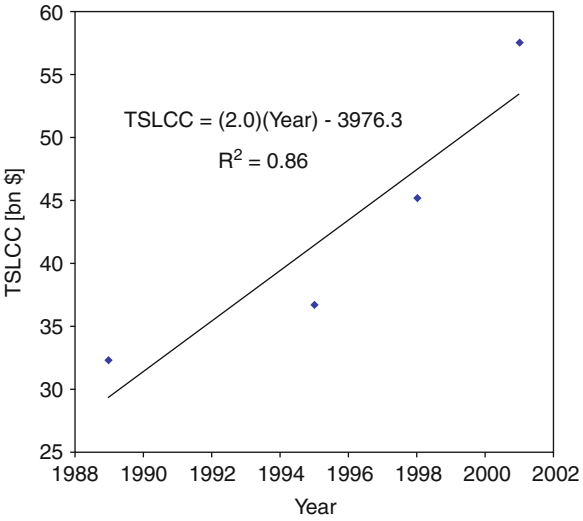

Fig. 11.5 *Yucca Mountain Life Cycle Cost over time*. The Total System Life Cycle Cost (TSLCC) predicted for Yucca Mountain is shown over the period between 1985 and 2001 in year 2000 dollars (inflation adjustment done using GDP deflator). In that time, the predicted cost has nearly doubled from $32.2 to $57.5 billion in constant dollars, with the repository intended to hold 86,000 metric tons of spent fuel heavy metal [18, 23–26]. In this context, "heavy metal" refers only to the mass of uranium and transuranics within the spent uranium dioxide fuel

permanent repository is in operation, it is difficult to estimate what it would cost. However, the experience and cost studies at Yucca Mountain in the United States provides some indication. Here the cost estimates for the repository rose in constant dollars from $32.2 billion to $57.5 billion between 1989 and 2001, Fig. 11.5 [18, 23–26], for a repository that was designed to hold 86,000 metric tons of spent nuclear fuel. Representative costs, lead/lag times, and standard deviations for nuclear power systems are given in Table 11.2.

Discount and Interest Rates

The values of ρ that are used in discounting will have a significant effect on an economic analysis. As a result, discount rates have been widely discussed in the context of decision theory, and in cost-benefit analyses of things that can have intergenerational effects such as environmental damage, resource allocation, or nuclear waste disposal. For economic comparisons, or cost studies, discounting accounts for the fact that payments made could instead have been invested and earned a rate of return. Alternately, future payments could be met by setting aside a smaller amount of money today and letting compound interest make up the difference. In both cases, the appropriate discount rate would be one that reflects

Table 11.2 *Unit costs of various components of the fuel cycle for a light water reactor with and without spent fuel recycle.* For the variables listed U denotes uranium; Pu – plutonium; HM – heavy metal; SD – standard deviation; SW – separative work; % loss – the percentage of material lost during a particular fuel cycle step; SF – spent fuel; MOX – mixed oxide fuel; VHLW – vitrified high-level waste; and led/lag refers to the time at which a particular cost is incurred relative to loading of a fuel batch into the reactor. The lead time for construction is relative to the first startup of the reactor. References are given for each data column in order from *left to right*, NA designates "not applicable." All costs are adjusted to year 2000 dollars. The standard deviation for the reactor facility construction cost was calculated from the cost data for seven reactors whose capital costs were given in [3]. It should be noted that many of the above costs are highly speculative, and other estimates are given in other studies, see for example [31]. Lag times for spent fuel recycle were estimated by assuming that SF_{UOX} remained in storage for 5 years and that fuel reprocessing occurred 1.5 years prior to MOX placement in the reactor. All other times are obtained by applying the time line for UOX fuel. The data in Fig. 11.4 suggests that the standard deviation for SF disposal is larger than that given in [13]

Fuel cycle component	Basis	$	SD (%)	% loss	lead/lag (years)	References
Reactor facility construction	$/kW(e) installed	3,560	15		–12 > –8	[11], [13], NA, see text
Reactor operations and maintenance	$/kW installed/year	142	15			[13], same as capital costs, NA, NA
Uranium mining and milling	$/kgU	30	33		–2.0	[13], [13], NA, [1]
U_3O_8 to UF_6 conversion	$/kgU	5	40	0.5	–1.5	[13], [13], [29], [1]
Enrichment	$/kgSW	80	37.5	0.5	–1.0	[13], [13], [29], [1]
UOX fabrication	$/kgU	250	20	0.5	–0.5	[13], [13], [29], [1]
Onsite interim SF_{UOX} storage	$/kgHM/year	30	5		+5	[13], [13], NA, NA
SF_{UOX} conditioning and disposal	$/kgHM	668	24		+40	[13], [13], NA, [1]
Spent fuel recycle						
SF_{UOX} transport to reprocessing	$/kgHM	50	20		+10.5	[13], [13], NA, see caption
SF_{UOX} reprocessing	$/kgHM	800	12.5	2.0	+11	[13], [13], [13], see caption
MOX Fabrication	$/kgHM	1,100	18	1.0	+12.5	[13], [13], [30], see caption
Onsite interim SF_{MOX} storage	$/kgHM/year	30	5		+17.5	[13],[13], NA, NA
SF_{MOX} transport to disposal site	$/kgHM/	50	20		+22.5	[13], [13], NA, see caption
SF_{MOX} conditioning and disposal	$/kgHM	668	24		+57.5	Same as UOX, [13], NA, see caption
VHLW conditioning and disposal	$/kgHM	288	12.5		+56	[13], [13], NA, see caption

what one could obtain by investing the funds in bonds, stocks, or other investments, and receiving the market rate of return.

There is no single discount rate that is accepted for near-term analysis of utilities, nuclear power included, but values between 5% and 10% (in real terms) are common and reflect the historical range of return by the US utility sector (e.g., [4]). However, there are problems in using this discount rate for projects that run on intergeneration time scales. The dominant concerns are well summarized in several different studies (e.g., [27, 28]), but the main point is that a discount rate that is this high would suggest that money so invested would eventually grow to be larger than the domestic product of any country where the investment was made. As a result, some economists suggest that discount rates appropriate for intergenerational projects would have to tend toward a country's real rate of GDP growth and can be assumed to be around 1–2% (e.g., [27, 28]).

The question of which discount rate to use in evaluating nuclear power facilities is far from academic. Cost studies are often used to compare different systems or management strategies. A high discount rate can make the present value of far-off costs appear negligible. In other words, using a high discount rate in a costs-benefit study of a politically divisive issue, such as spent fuel disposal, can have the perverse effect of suggesting that it would always be cheaper to delay action. In fact, this type of argument has been advanced in the United States to advocate for pushing off the development of reprocessing or permanent geological disposal.

Cost Comparisons and External Costs

Using Eq. 11.8, or similar, one can calculate the cost associated with the generating electricity by various means. Results of such studies are shown in Tables 11.1 and 11.2. However, making true comparisons for the "cost" of generating electricity between different types of power systems can be complicated by the effect of externalities that are often difficult to capture in an economic analysis. Factoring in the true cost of carbon dioxide emissions would be an example. Carbon dioxide emissions from fossil-fueled plants are obvious. They are not so obvious for nuclear, wind, or solar power facilities. While nuclear power facilities have no direct emissions, there are carbon signatures associated with the materials out of which they are made, the processes involved in facility construction, as well as for operations, maintenance, and decommissioning. The same is true for wind and solar power systems. Where one draws the boundary for an analysis (i.e., does one include the carbon dioxide needed to produce, say, the machinery for the processing of facility materials) can have a significant effect on the total carbon signature that is associated with a specific power source, and through this, its total potential cost. Because of the complexity of handling externalities (and the cost of carbon emissions is only one example), how best to do this remains an area of active research and debate.

Future Directions

Electricity demand varies with location, time of day, and time of year. The minimum demand at any point within a year is referred to as *base load*. The utility industry typically gauges demand requirements with what are called *load demand* and *load duration curves*, Figs. 11.6 and 11.7. Commercial nuclear power plants

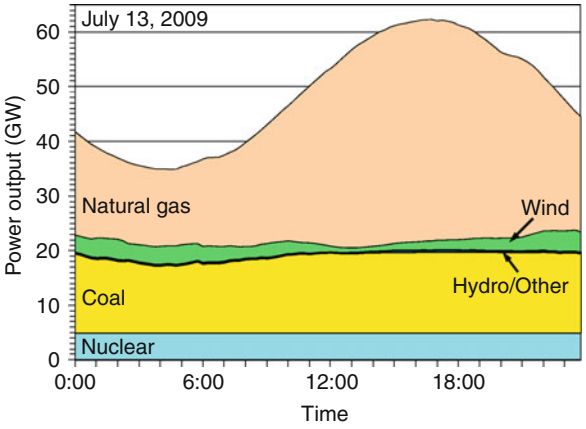

Fig. 11.6 *Electricity load curve and generation source*. The figure shows the variation in electricity demand over a 24 h period, and the sources used to meet that demand (The data are from the Electricity Reliability Council of Texas, for July 13, 2009) (Figure courtesy of Stuart Cohen, The University of Texas at Austin)

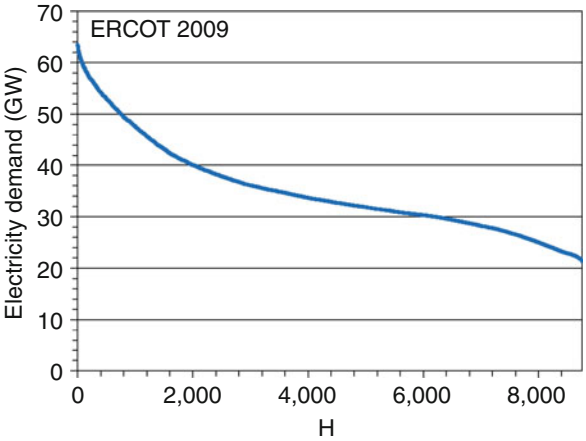

Fig. 11.7 *Load duration curve*. The figure shows the number of hours during 2009 during which a given electric demand needed to be met. The base load for the year is shown at the far *right* (The data are from the Electricity Reliability Council of Texas, for July 13, 2009) (Figure courtesy of Stuart Cohen, The University of Texas at Austin)

have historically been designed to operate at their maximum licensed power. The fraction of time that these facilities are in operation has also increased steadily over the years to an industry average of around 90%. As a result, commercial nuclear power is used to meet base-load requirements, along with coal, hydroelectric, and to a smaller extent wind. Additional load requirements are met with smaller-scale facilities (called *peaking power plants*) that typically run on oil or gas.

Because of perceived economies of scale, nuclear power plants have been built on an increasingly large scale. Recently though, this idea has begun to be been revisited, and there are calls for the development of smaller-scale facilities with peak power outputs of as little as a few tens of megawatts. Such plants, known as *Small Modular Reactors*, could be used to meet local base-load requirements or as peaking plants. A shift in the industry to include smaller-scale facilities could have dramatic effects on the economics of nuclear power. Smaller facilities would likely have shorter build times and far lower capital costs. Many utilities also charge different rates, depending on when electricity is used, and this too would affect the economics of nuclear package plants that might be used to meet peak load requirements. (The first-generation light water reactors were designed for power outputs of 300–600 MWE. In the United States, today most nuclear power facilities are rated for 800–1,000 MWe, but it expected that the next generation of reactor will produce between 1,100 and 1,400 MWe.)

Acknowledgments Special thanks to Andrew Osborne, Brady Stoll, and Geoff Recktenwald for editorial comments. Thanks to Eric Bickel and Michael Webber for useful discussions and to Nick Tsoulfanidis for editorial comments and for acting as Editor for this series.

Bibliography

1. OECD/NEA (1994) The economics of the nuclear fuel cycle. Technical report, OECD/NEA, Paris
2. Bunn M, Fetter S, Holdren JP, van der Zwaan B (2003) The economics of reprocessing vs. direct disposal of nuclear fuel. Technical report DE-FG26-99FT4028, Harvard University, Boston
3. Anolabehere S, Deutch J, Driscoll J, Holdren PE, Joskow PL, Lester RK, Moniz EJ, Todreas NE, Beckjord ES (2003) The future of nuclear power. MIT Press, Boston (Technical report)
4. Tolley GS, Jones DW (2004) The economic future of nuclear power. Technical report 2004, University of Chicago, Chicago
5. Garwin RL, Charpak G (2002) Megawatts and megatons – the future of nuclear power and nuclear weapons. The University of Chicago Press, Chicago
6. Goldschmidt P (2010) Multilateral nuclear fuel supply guarantees & spent fuel management: what are the priorities? Daedalus 139:7–19
7. Stern R (2007) The Iranian petroleum crisis and United States national security. PNAS 104:377–382
8. Cochran R, Tsoulfanidis N (1990) The nuclear fuel cycle: analysis and management, 1st edn. American Nuclear Society, La grange Park
9. Brealey R, Myers S, Allen F (2002) Principles of corporate finance, 9th edn. McGraw-Hill Higher Education, New York

10. Schneider EA, Deinert MR, Cady B (2009) The cost impact of delaying the US spent nuclear fuel reprocessing facility. Energy Econ 31:627–634
11. Deutch J, Forsberg C, Kadak A, Kazimi M, Moniz E, Parsons J (2009) Update of the MIT 2003 future of nuclear power. MIT Press, Cambridge
12. White House (1993) Executive order #12866: regulatory planning and review. Washington, DC
13. OECD/NEA (2002) Accelerator driven systems and fast burner reactors in advanced nuclear fuel cycles. Technical report, OECD/NEA, Paris
14. Hannon B (1982) Energy discounting. Technological Forecasting Soc Change 21:281–300
15. Stillwell AS, King CW, Webber ME, Duncan IJ, Hardberger A (2011) The energy-water nexus in texas. (Special feature: the energy-water nexus: managing the links between energy and water for a sustainable future), Ecol Soc 16(1):2. http://www.ecologyandsociety.org/vol16/iss1/art2/
16. Benedict M, Pigford TH, Levi HW (1981) Nuclear chemical engineering, 2nd edn. McGraw-Hill, New York
17. Nuclear Waste Policy Amendments Act (1987)
18. DOE (2002) Nuclear waste fund fee adequacy: An assessment. DEO/RW-0534, DOE, Office of Civilian Radioactive Waste Management, Washington, DC
19. Shapiro SS (1990) Selection, fitting, and testing statistical models. In: Wadsworth HW (ed) Handbook for statistical methods for scientists and engineers. McGraw Hill, New York
20. OECD/NEA (1987) Nuclear Energy and its fuel cycle-prospects to 2025. Technical report, OECD/NEA, Paris
21. OECD/NEA (1993) The cost of high-level waste disposal in geological repositories – An analysis of factors affecting cost estimates. OECD/NEA, Paris
22. OECD/NEA (1996) Future financial liabilities of nuclear activities. Technical report, OECD/NEA, Paris
23. GAO (1990) Changes needed in DOE user-fee assessments to avoid funding shortfall. Technical report RCED- 90-65, United States General Accounting Office, Washington, DC
24. DOE (1995) Analysis of the total system life cycle cost of the civilian radioactive waste management program. Technical report DOE/RW 0479, DOE, Office of the Civilian Radioactive Waste Management Program, Washington, DC
25. DOE (1998) Analysis of the total system life cycle cost for the civil radioactive waste management program. Technical report DOE/RW-0510, DOE, Office of Civilian Radioactive Waste Management Program, Washington, DC
26. DOE (2001) Analysis of the total system life cycle cost of the civilian radioactive waste management program. Technical report DOE/RW-0533, DOE, Office of Civilian Radioactive Waste Management, Washington, DC
27. Rabl A (1996) Discounting of long term costs: what would future generations prefer us to do? Ecol Econ 17:137–145
28. Arrow K (1999) Discounting, morality, and gaming. In: Portney PR, Weyant JP (eds) Discounting and intergenerational equity. RFF Press, Washington, DC
29. Rasmussen N, Burke T, Choppin G, Croff G, Garrick J, Grunder H, Hebel L, Hunter T, Kazimi M, Kintner E et al (1996) Nuclear wastes: technologies for separations and transmutation. National Academy, Washington, DC
30. Shropshire D, Williams K, Boore W, Smith J, Dixon B, Dunzik-Gougar M, Adams R, Gombert D (2007) Advanced fuel cycle cost basis. US DOE, The Idaho national laboratory INL/EXT-07-12107

Chapter 12
Nuclear Fusion

Thomas J. Dolan

Glossary

COE	Cost of electricity
EAST	Experimental Advanced Superconducting Tokamak
ECRH or ECH	Electron cyclotron resonance heating – heats plasma electrons at the natural rotation frequency of electrons in a magnetic field
EFDA	European Fusion Development Agreement
FRC	Field-reversed configuration
ICRH or ICH	Ion cyclotron resonance heating – heats plasma ions at the natural rotation frequency of ions in a magnetic field
ICF	Inertial confinement fusion
IFMIF	International Fusion Materials Irradiation Facility
ITER	International Thermonuclear Experimental Reactor
LHCD or LH	Lower hybrid resonance wave heating or current drive – Microwaves injected into the plasma induce a plasma current
Magnetic shear	Variation of magnetic field direction from one layer to the next – helps to preserve plasma stability
MHD	Magnetohydrodynamic model – treats plasma as a conducting fluid
MTF	Magnetized target fusion
NBI	Neutral beam injection – injection of high-energy neutral atoms into plasma to heat it, and to help control the plasma current and rotation

This chapter was originally published as part of the Encyclopedia of Sustainability Science and Technology edited by Robert A. Meyers. DOI:10.1007/978-1-4419-0851-3

T.J. Dolan (✉)
Department of Nuclear, Plasma, and Radiological Engineering, University of Illinois, 216 Talbot Laboratory, Urbana, IL 61801, USA
e-mail: dolantj@illinois.edu

N. Tsoulfanidis (ed.), *Nuclear Energy: Selected Entries from the Encyclopedia of Sustainability Science and Technology*, DOI 10.1007/978-1-4614-5716-9_12,

OH	Ohmic heating – resistive heating caused by a current flowing through the plasma
PF	Poloidal magnetic field – The magnetic field component that runs the short way around the torus (donut-shaped vessel). See Fig. 12.6
Q	Fusion energy gain ratio or fusion power gain ratio = (fusion energy)/(input energy) or (fusion power)/(input power)
RF, rf	Radiofrequency
SC	Superconducting magnet coils – Coils that have zero resistance at very low temperature ($T \sim 4$ K), usually made of Nb_3Sn or NbTi in a copper matrix
TF	Toroidal magnetic field – The magnetic field component that runs the long way around the torus (donut-shaped vessel). See Fig. 12.6

Symbols

Symbol	Units	Meaning
a	m	Minor plasma radius at plasma edge (for circular plasma cross section) (Fig. 12.4)
B	T	Magnetic field
beta, β	None	Ratio of (plasma pressure)/(magnetic field pressure)
D		Deuterium or deuteron
I_p	MA	Maximum plasma current
L	m	Plasma length
m_e	kg	Electron mass
m_i	kg	Ion mass
n	m^{-3}	Plasma electron density (electrons per m^3)
r	m	Minor plasma radius (Fig. 12.4)
R, R_0	m	Major plasma radius, and its value at the center of the plasma (Fig. 12.4)
T	C, K, or keV	Temperature. 1 keV = 11.6 MK (Mega-Kelvin)
T		Tritium or triton
T_e	keV	Electron temperature
T_i	keV	Ion temperature
$v_{\|\|}$	m/s	Particle velocity component along B field direction
$v_\perp$	m/s	Particle velocity component perpendicular to B field

Definition of the Subject

Nuclear Fusion of hydrogen isotopes into helium and heavier elements is the energy source of our sun and the other stars. The goal of nuclear fusion research is to build "miniature suns" on earth that will provide clean energy for electricity generation, production of hydrogen for fuel, and industrial applications.

Table 12.1 Potential benefits of fusion reactors

- Abundant fuels (deuterium and lithium) – enough for millions of years
- Cheap fuel
  - D fuel cost $\approx 3 \times 10^{-14}$ \$/J (assuming D at \$10,000/kg)[a]
  - Lithium fuel cost $\approx 10^{-12}$ \$/J (assuming Li at \$300/kg)[a]
  - Coal cost $\approx 2 \times 10^{-9}$ \$/J (assuming \$150/t)
  - Gasoline cost $\approx 2 \times 10^{-8}$ \$/J (assuming 1.00 \$/l)
- Fuel available to all nations, could reduce conflicts over fossil fuels
- Fuel has low mass, easy to transport
- Clean – avoids pollutant emissions, less waste than fission or coal
- Safe – no supercriticality hazard or meltdown hazard
- Does not require expensive energy storage
- No high-level radioactive waste
- Neutrons from fusion reactors could be used to de-activate high-level radioactive waste from fission reactors or to breed fission reactor fuel

[a]Assuming a price of \$10,000/kg of D and an energy yield of 7.2 MeV per deuteron in a catalyzed DD fuel cycle (described below), this corresponds to a fuel cost of 3×10^{-14} \$/J. Early fusion reactors will use lithium to breed tritium, because it greatly enhances the fusion reaction rate. In 2008, the average price of lithium carbonate was about 4–6 \$/kg in the USA, so the cost of the lithium itself was about 20–40 \$/kg [1]. Future demand for lithium batteries might escalate this price as high as 300 \$/kg. Assuming 17.6 MeV released from each tritium bred from lithium, this corresponds to a fuel cost of about 10^{-12} \$/J, as shown in the table

Introduction

The joining together of two light elements to produce a heavier element is called a "nuclear fusion reaction." For example, a deuteron plus a triton can produce ^{4}He plus a neutron

$$\mathrm{D} + \mathrm{T} \rightarrow {}^4\mathrm{He}\ (3.5\mathrm{MeV}) + n\ (14.1\mathrm{MeV}),$$

where D = deuteron, T = triton, n = neutron, the reaction product kinetic energies are given in parentheses, and 1 MeV = 1.602×10^{-13} J. (Deuterium and tritium are isotopes of hydrogen having one neutron or two neutrons, respectively.)

The positively charged atomic nuclei repel each other, so they must have high speeds in order to approach close enough for reactions to occur, which correspond to high temperatures. Temperatures are usually expressed in keV, where 1 keV = 11.6 MK (Mega-Kelvin).

One liter of water contains 0.034 g of deuterium. When burned in a nuclear fusion reactor, this deuterium could yield as much energy as burning 300 liters of gasoline. Thus, there is enough deuterium in the rivers, lakes, and oceans of the world to provide the world's energy needs for millions of years. The first generation of fusion power plants will use deuterium and tritium fuels. Tritium is unavailable on earth, but it can be bred by neutron absorption in lithium, so deuterium and lithium are the primary fuels. Table 12.1 lists some potential benefits of such fusion reactors.

Although the fuel for fusion reactors would be cheap, the reactor capital costs would be very high, so the cost of electricity could still be expensive (to be discussed later).

Fusion Reactions

Tritium has negligible abundance on earth, but it can be bred from lithium via the reactions

$$n + {}^{6}\mathrm{Li} \rightarrow \mathrm{T}(2.73\,\mathrm{MeV}) + 4\mathrm{He}(2.05\,\mathrm{MeV}) \cdots \quad (\text{exothermic} - \text{energy is released}) \tag{12.1}$$

$$n + {}^{7}\mathrm{Li} \rightarrow \mathrm{T} + {}^{4}\mathrm{He} + n - 2.47\,\mathrm{MeV} \cdots \quad (\text{endothermic} - \text{high neutron energy input is required}) \tag{12.2}$$

The fusion reactions with the highest probabilities at $T < 80$ keV are

$$\mathrm{D} + \mathrm{D} \rightarrow \mathrm{H}(3.02\ \mathrm{MeV}) + \mathrm{T}(1.01\ \mathrm{MeV}) \tag{12.3}$$

$$\mathrm{D} + \mathrm{D} \rightarrow \mathrm{n}(2.45\ \mathrm{MeV}) + {}^{3}\mathrm{He}(0.82\ \mathrm{MeV}) + \tag{12.4}$$

$$\mathrm{D} + \mathrm{T} \rightarrow {}^{4}\mathrm{He}(3.52\ \mathrm{MeV}) + \mathrm{n}(14.1\ \mathrm{MeV}) \tag{12.5}$$

$$\mathrm{D} + {}^{3}\mathrm{He} \rightarrow {}^{4}\mathrm{He}(3.66\ \mathrm{MeV}) + \mathrm{H}(14.7\ \mathrm{MeV}) \tag{12.6}$$

where H = proton, D = deuteron, T = triton (distinguish from T meaning temperature), n = neutron, and the energies of the reaction products are shown in parentheses. The TT reaction has a probability similar to those of the DD reactions. The two branches of the DD reaction have roughly equal probabilities. If the ^{3}He and T produced by the DD reactions are recycled as fuel in the other two reactions (dashed arrows), the sum of these four reactions yields

$$6\mathrm{D} \rightarrow 2{}^{4}\mathrm{He} + 2\mathrm{H} + 2n + 43.2\ \mathrm{MeV} \tag{12.7}$$

which is called the "catalyzed DD" fuel cycle, having an average energy yield of 7.2 MeV per deuteron. The only fuel input would be deuterium, avoiding the need to breed tritium from lithium, but the fusion power density would be much lower than from the DT fuel cycle using tritium bred from lithium.

Other reactions, such as H + ^{6}Li and H + ^{11}B, have lower reaction probabilities at $T < 100$ keV, so they are more difficult to use, but they would have the potential advantage of emitting fewer (or no) neutrons, which lead to the production of radioactive materials.

Table 12.2 Plasma heating methods

Ohmic heating	OH	Ohmic heating power density $P_{oh} = \eta J^2$ (W/m^3), where J = current density (A/m^2) and η = plasma resistivity (ohm-m). At high temperatures η is very low, and ohmic heating is ineffective.
Neutral beam injection	NBI	Ions accelerated to high energies (typically 0.04–1 MeV) pass through a gas cell where some of them are neutralized. The neutral atoms can then penetrate across the magnetic field into the plasma, where they become ionized and trapped, depositing their energy in the plasma.
Ion cyclotron resonance heating	ICRH	Radio waves are injected into the plasma at approximately the frequency of the ion spiral motion around the magnetic field lines, accelerating their motion. Frequency $f = eB/2\pi m_i$ (Hz), where e = electronic charge, B = magnetic field, m_i = ion mass.
Electron cyclotron resonance heating	ECRH	Microwaves injected into the plasma with near the frequency of electron spiral motion around the magnetic field lines. $f = eB/2\pi m_e$ (Hz), where m_e = electron mass.
Lower hybrid wave heating	LH	Waves are injected at the lower hybrid frequency, which is between the ECRH and ICRH frequencies.
Compression		If the plasma is compressed, such as by increasing the magnetic field or by squeezing a metallic shell around the plasma, its temperature and pressure increase.

Fusion Reactor Requirements

In order to build a fusion reactor two requirements must be met, heating and confinement:

Heating Requirement

The fuel must be heated to $T \sim 15$ keV (170 Million Kelvin) for the D + T reaction, and $T \sim 40$ keV (460 MK) for the D + D fuel cycle. Ions with more positive charge, such as lithium and boron, repel each other more strongly, so higher temperatures would be required to use them as fuels. (At such high temperatures, hydrogen is in the *plasma state* [a sea of positive ions and negative electrons]. The five states of matter are solid, liquid, gas, plasma, and "dark matter." Other familiar forms of plasmas [some of them only partially ionized gases] include lightning, welding arcs, hot flames, and fluorescent lights.)

Table 12.2 lists some plasma heating methods.

Confinement Requirement

The fuel must be confined long enough for part of it to "burn" (to fuse) before it is lost or cools off.

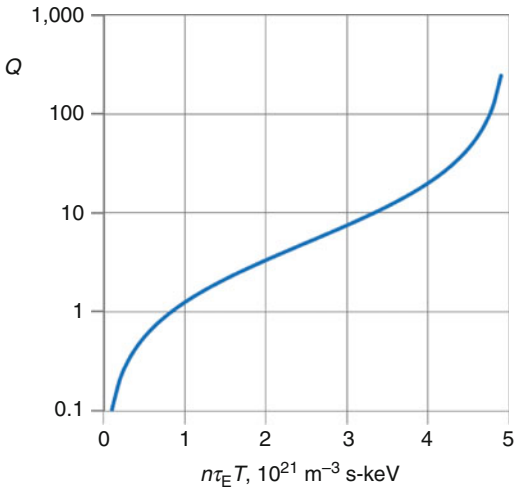

Fig. 12.1 Energy gain ratio Q versus triple product

The heating and confinement requirements for a DT reactor may be expressed in the "triple product" parameter

$$n\tau_E T > 4 \times 10^{21} \mathrm{m}^{-3}\mathrm{s\ keV} \tag{12.8}$$

where n is fuel ion density (ions/m^3), τ_E is their energy confinement time (s), and T is their temperature (keV). (The required product of density and confinement time is often referred to as the "Lawson criterion.") The energy gain ratio is defined to be

$$Q = (\text{fusion energy per pulse})/(\text{input energy per pulse})$$

or

$$Q = (\text{fusion power})/(\text{input power})$$

if the reactor operates steady state.

For the DT fusion reaction Q is given approximately by the equation [2]

$$Q \approx 5(n\tau_E T)/[5 \times 10^{21} - n\tau_E T] \tag{12.9}$$

which is illustrated in Fig. 12.1.

Thus, to attain $Q > 10$, values of $n\tau_E T \sim 4 \times 10^{21}$ m^{-3} s-keV are needed. (This equation and graph are only approximate, varying with the type of plasma confinement system.)

When confinement is very good, the alpha particles (^{4}He ions) produced by fusion reactions can deposit enough energy in the plasma to sustain its temperature.

Then the input power for heating may be turned off. (Some input power may still be needed to drive a plasma electrical current.) This self-sustainment condition, called "ignition," corresponds to the right side of Fig. 12.1, where Q reaches very high values. The precise value of the triple product that produces ignition varies from one type of confinement system to another and with plasma impurity content.

For DD reactions, higher values of $n\tau_E T$ are required, so the DT reaction will probably be used in the first generation fusion power plants.

Everything in nature tends toward a state of *thermodynamic equilibrium*, in which the temperatures of various bodies are uniform and equal to each other. Since we want to keep the chamber wall temperature below about 1,200 K and the fuel ion temperature $>10^8$ K, the plasma confinement system must retard the establishment of thermodynamic equilibrium. Coulomb collisions and plasma instabilities bring the plasma closer to thermodynamic equilibrium, so avoiding it is a difficult problem.

Plasma Confinement Methods

Plasma confinement methods are listed in Table 12.3.

Magnetic Confinement

Magnetic fields may be either "open" (Figs. 12.2 and 12.3) or "closed" (Fig. 12.4).

A plasma ion starting out at the center with velocity components $v_{\|o}$ parallel to magnetic field and $v_{\perp o}$ perpendicular to the magnetic field would experience a higher magnetic field as it moves toward the magnet coil. In the higher field, its rotational velocity component $v_\perp$ would increase, and its parallel velocity component $v_\|$ could decrease gradually to zero, where it would be reflected back toward the center (hence, the name "magnetic mirror"). The ion would oscillate back and forth between points a and b, restrained by a magnetic field gradient force

$$F = -(m_i v_\perp{}^2/2B)\nabla B \tag{12.10}$$

Electrons would also be confined in the same way. Although electrons and ions are reflected by high magnetic fields, those with high velocities $v_{\|o}$ along the field lines will escape, and confinement is limited by the time it takes for Coulomb collisions to increase their parallel velocities. The end loss problem can be eliminated by using a closed magnetic field, Fig. 12.4.

It might appear that electrons and ions could be confined forever as they spiral along the closed magnetic field lines, but the magnetic field gradient and curvature cause a drift velocity across the magnetic field. This drift can be compensated by

Table 12.3 Plasma confinement methods

Solid walls	Low-temperature plasmas, such as fluorescent lights, may be contained by glass or metal tubes. Hot plasma confinement in magnetic fields may be augmented by solid walls for brief periods of time, but prolonged contact cools the plasma rapidly by heat conduction and may overheat the wall.
Gravity	Although stellar plasmas, such as the sun, are confined by gravity, the mass of a laboratory plasma is far too small for self-gravitational attraction to be significant. (The mass density and temperature at the center of the sun are about 150 g/cm^3 and 1.3 keV).
Inertia	If a DT fuel pellet is quickly compressed to ultrahigh densities, significant fusion burn can occur before the compressed pellet expands. The inertia of the pellet limits the expansion rate of the internal plasma. At $n = 10^{30}$ m^{-3}, and $T = 10$ keV, a confinement time $\tau_E \sim 4 \times 10^{-10}$ s would yield a triple product $n\tau_E T \sim 4 \times 10^{21}$ m^{-3} s-keV. The compression may be produced by laser beams or by particle beams.
Radiofrequency waves	Radiofrequency waves and microwaves can confine low-pressure plasma, but enormous power inputs would be required to confine high-pressure plasmas. These waves can augment magnetic confinement.
Electrostatic fields	Electrostatic potential peaks can be established with high-voltage grids or by creating local regions of higher plasma density. Positive peaks can inhibit ion motion, and negative peaks can inhibit electron motion. Purely electrostatic plasma confinement has only succeeded in confining low-pressure plasmas, but such electrostatic potential peaks can be used to augment magnetic confinement.
Magnetic fields	Confinement by strong magnetic fields is the most promising means for prolonged containment of high-pressure plasmas. It is based on the fact that ions and electrons cannot travel across a magnetic field easily. Instead, they tend to travel in helical paths along the field lines.

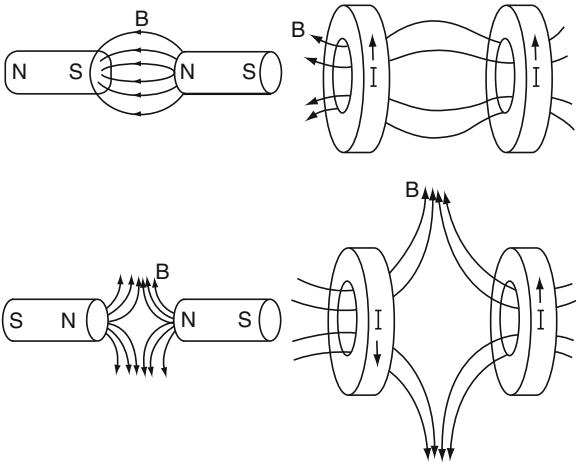

Fig. 12.2 Simple magnetic "mirror" fields **B** (*top*) and "spindle cusp" fields (*bottom*) produced by bar magnets (*left side*) or by a pair of circular magnet coils carrying currents I (*right side*). Plasma could be confined in the central regions

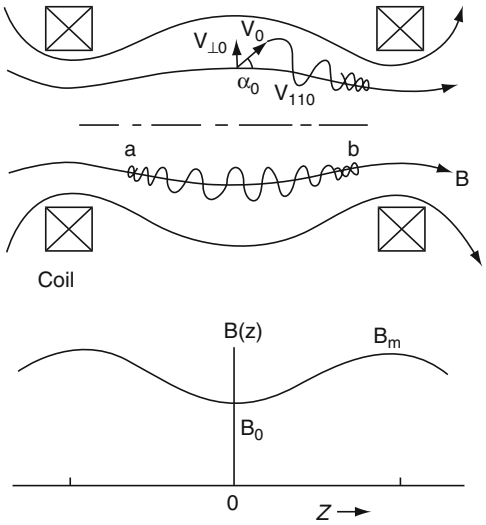

Fig. 12.3 A simple magnetic mirror (*top*) and axial variation of magnetic field strength (*bottom*)

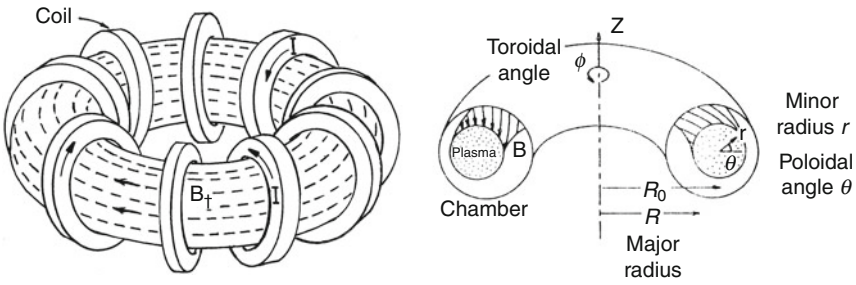

Fig. 12.4 "Closed" (toroidal) magnetic field lines B_t (*dashed lines*) generated by circular magnet coils carrying currents I, and the definitions of "major radius *R*" and "minor radius *r*." The value of *r* at the plasma edge is called "a", and the value of *R* at the plasma center is called "R_o"

twisting the magnetic field lines, producing a helical closed magnetic field, Fig. 12.5.

This twisting of the magnetic field, called "rotational transform," may be produced by inducing a plasma electrical current in the toroidal direction (a "tokamak"), or by using specially shaped magnetic field coils (a "stellarator").

There are many processes that cause plasma energy loss, Table 12.4.

In what follows, we describe tokamaks, stellarators, compact toroids, and open magnetic confinement systems, then inertial confinement systems, other fusion concepts, plasma theory issues, fusion technology issues, and fusion reactor design studies.

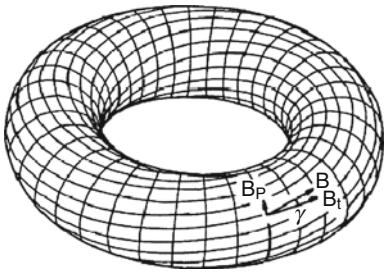

Fig. 12.5 A helical magnetic field. The field lines B have components B_t in the "toroidal" direction (the long way around the torus) and B_p in the "poloidal" direction (the short way around the torus). Twisting the magnetic field compensates for the tendency of particles to drift across the magnetic field

Table 12.4 Plasma energy loss mechanisms

1.	Particle and energy *loss along magnetic field lines* (open magnetic systems) In simple magnetic mirrors, the loss time is roughly the time for collisions to increase the ion velocity along the field lines. If electrostatic potential barriers are used, then the loss time is roughly the time for collisions to increase the particle energies over the barriers.
2.	Particle *driftvelocities* across the magnetic field, driven by magnetic field gradient and curvature and by an electric field.
3.	*Magnetohydrodynamic (MHD) plasma instabilities*, whereby the plasma boundary, affected by gradients of pressure, current density, and magnetic field, pushes through the magnetic field toward the chamber wall.
4.	*Radiation losses* from line radiation, bremsstrahlung radiation (radiation from electrons during deceleration by collisions), cyclotron radiation, and recombination radiation. Radiation losses can be high when the plasma contains many impurity ions (such as iron), when the temperature is very high, or when the magnetic field is very strong (cyclotron radiation).
5.	*Energy transport* across the magnetic field by heat conduction and convection.
6.	Interaction of electrons and ions with plasma waves can enhance energy transport. Such "*microinstabilities*" have required many decades of plasma theory, experiment, and computer simulation to be understood.
7.	Ion energy loss by *charge exchange*. (A hot ion grabs an electron from an atom, becomes neutralized, and is no longer confined by the magnetic field, which does not confine neutral atoms.)

Tokamaks

The name "tokamak" is an acronym for the Russian "т**о**роидальная к**а**мера с м**а**гнитными катушками" (**to**roidal'naya **ka**mera s **ma**gnitnymi **k**atushkami – toroidal chamber with magnetic coils). Fig. 12.6 shows the main components of a tokamak.

Pulsing a current in the primary winding of the transformer induces a high current in the plasma, which generates the poloidal magnetic field. (Although this figure shows an iron core transformer, most modern tokamaks use air core transformers.) When the transformer saturates, the current gradually dies away.

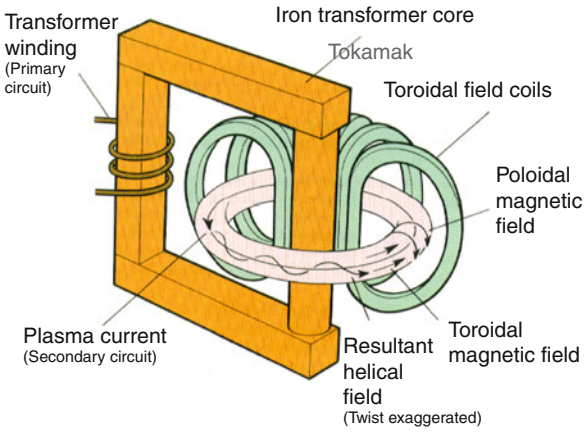

Fig. 12.6 Simplified diagram of a tokamak with circular plasma cross section (Courtesy of Culham Centre for Fusion Energy, UK)

A "current drive" system, such as electromagnetic waves or neutral beam injection, is needed to sustain the current for long periods. Although Fig. 12.6 shows a plasma with circular cross section, most modern tokamaks have noncircular cross sections, in order to facilitate higher beta values (ratios of plasma pressure to magnetic field pressure).

Over 200 tokamaks have been built worldwide. Table 12.5 shows the parameters of a few of them.

Fig. 12.7 shows the interior of the European Fusion Development Agreement (EFDA) Joint European Torus (JET), which has a noncircular cross section.

The walls are lined with refractory tiles to withstand high heat fluxes. Using DT fuel JET briefly generated 16 MW of heat from fusion reactions. JET has also demonstrated the feasibility of using beryllium tiles on the walls.

The National Spherical Torus Experiment (NSTX) and Mega Ampere Spherical Torus (MAST) are smaller, with very low aspect ratios $R_o/a \sim 1.4$, which facilitates high values of β (the ratio of plasma pressure to magnetic field pressure). They are called "spherical tokamaks."

In order to attain higher triple product values, larger experiments are needed. The International Thermonuclear Experimental Reactor (ITER) Joint Project began construction in 2008 with an estimated cost of about 5 billion Euro. It is to begin operation in about 2019, reaching full power operation in about 2027. Fig. 12.8 shows how the experimentally attained values of the triple product have increased over the years of fusion research.

ITER should demonstrate a power gain ratio $Q > 10$ for hundreds of seconds, and $Q > 5$ for longer periods. The next step planned after ITER will be a technology demonstration fusion power plant called "DEMO" that generates electricity for commercial use.

Table 12.5 Parameters of some tokamaks. SC means superconducting coils. Parameters of future experiments are planned values [3]

Name	Country	Years	R_0/a, m/m	B, T	I_p, MA	ECRH + ICRH + LH, MW	NBI, MW	Remarks
TFTR	USA	1982–1997	2.4/0.8	6	3	11	39	Circular cross section plasma; achieved 10 MW fusion power for fraction of a second
DIII-D	USA	1986–	1.66/0.67	2.2	3	11	20	Beta = 12%, graphite walls, plasma shaping
Tore Supra	France	1988–	2.25/0.7	4.5 SC	2	16	1.7	Pulses lasting many minutes
T-15	Russia	1988–1995, 2009–	2.43/0.42	3.5 SC	1	11	9	5 s pulses
JT 60U	Japan	1991–2010	3.4/1.0	4.2	5	24	50	Record fusion triple product, would yield $Q = 1.2$ if DT fuel were used
JET	UK	1992–	3/1.25	4	6	29	24	Generated 22 MJ of DT fusion energy in 4 s. Has used Be wall tiles
MAST	UK	1999–	0.85/0.6	0.5	1.4	1	4	Spherical tokamak
NSTX	USA	1999–	0.85/0.6	0.6	1.4	3	7	Spherical tokamak
EAST	China	2006–	1.75/0.43	5 SC	0.5	8		First fully superconducting tokamak with noncircular cross section
KSTAR	Korea	2008–	1.8/0.5	3.5 SC	2	13	14	Fully superconducting coils
SST-1	India	2012–	1.1/0.2	3 SC	0.2	3	0.8	1,000 s pulses
JT 60 SA	Japan	2014–	3.16/1.02	2.7 SC	5.5	7	34	100 s pulses, startup 2014
ITER	France	2019–	6.2/2.0	5.3 SC	15	40	33	Startup 2019. 400 MW, 400 s pulses in 2023

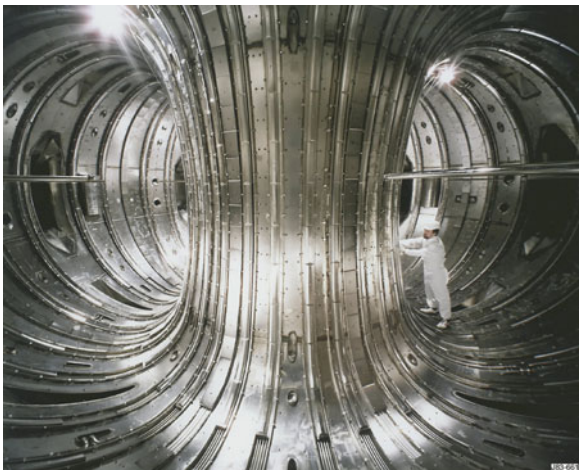

Fig. 12.7 The interior of the Joint European Torus (JET) (Courtesy of Culham Centre for Fusion Energy, UK)

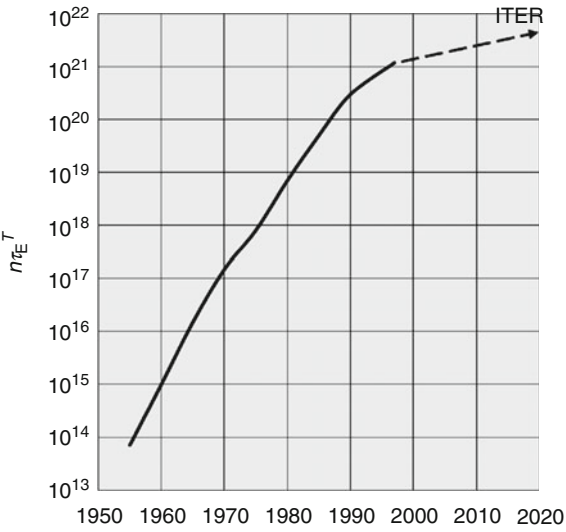

Fig. 12.8 Triple product $n\tau_E T$ (m^{-3} s-keV) attained by tokamak experiments versus year. The dashed arrow points to planned ITER values [4]

Stellarators

Stellarators (including "heliotrons" and "torsatrons") produce rotational transform by shaping the magnet coils, Figs. 12.9 and 12.10.

The Large Helical Device at the National Institute for Fusion Sciences in Japan, Fig. 12.11, is a "heliotron" (torsatron) with two helical coils.

Fig. 12.12 shows the Wendelstein 7-X experiment, which uses modular coils to achieve a magnetic field shape suitable for plasma confinement.

Table 12.6 shows some parameters of these stellarators.

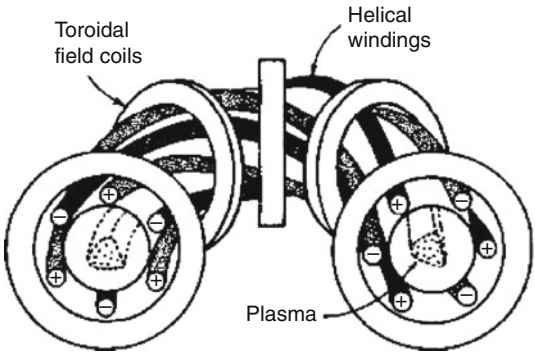

Fig. 12.9 Magnet coils of a stellarator with three pairs of helical windings, which have currents in alternating directions (indicated by + and – signs). Other numbers of helical windings are also possible

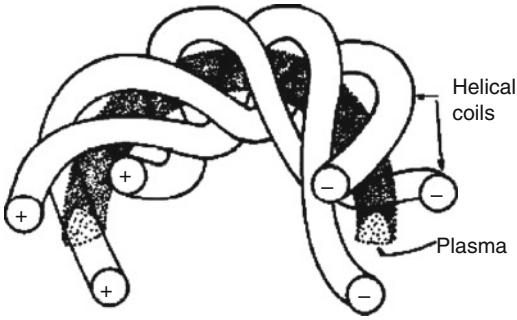

Fig. 12.10 A torsatron with three helical coils and no toroidal field coils

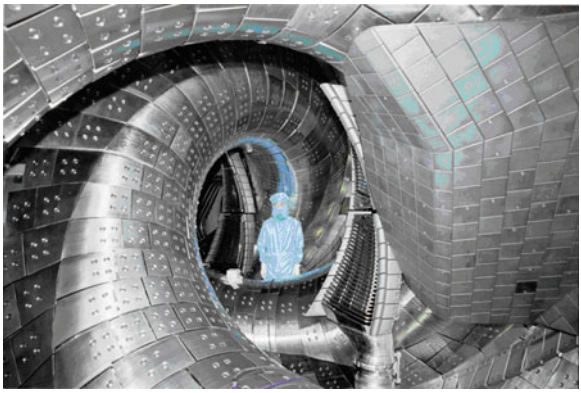

Fig. 12.11 The two helical superconducting coils inside the Large Helical Device, operating since 1998 (Courtesy of the National Institute for Fusion Science, Japan)

Since stellarators do not require a strong plasma current, they have the following advantages over tokamaks:

- No strong disruptions of the plasma.
- Current drive is not required, so the input power is lower, and the energy gain ratio Q can be higher.
- Potentially less plasma turbulence and better energy confinement.

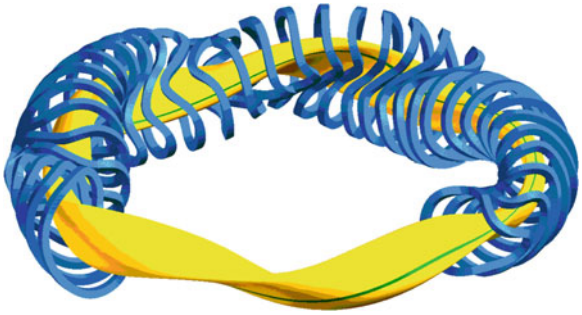

Fig. 12.12 The coils (*blue*) of the Wendelstein 7-X experiment in Greifswald, Germany, and the resulting plasma shape (*orange*), expected to begin operation in 2014 (Courtesy of the Max-Planck-Institut fuer Plasmaforschung, Greifswald, Germany)

Table 12.6 Main parameters of the LHD and Wendelstein 7-X experiments. The LHD values shown here were not all attained simultaneously. The Wendelstein 7-X parameters are planned values

Parameter	Units	LHD	Wendelstein 7-X
Startup		1998	2014
Major radius R	m	3.7	5.5
Approximate minor radius a	m	0.64	0.53
Magnetic field on axis	T	2.8	3
Heating power	MW	20	15
Average plasma density n	m^{-3}	4×10^{19}	$\sim 10^{20}$
Ion temperature	keV	13.6	(Several)
Electron temperature	keV	10	(Several)
Energy confinement time	s	0.36	0.15
Beta	%	5	

One the other hand, the coils of stellarators are difficult to wind, join, support, and align, and space for energy recovery blankets is limited.

Reversed Field Pinch (RFP)

A reversed field pinch is a toroidal plasma with a relatively weak toroidal field and a strong plasma current. The plasma currents evolve into a stable configuration in which the direction of the toroidal component of the magnetic field at the plasma edge is in the opposite direction from the internal toroidal field, Fig. 12.13.

This strong variation of magnetic field direction with radius, called magnetic shear, helps preserve plasma stability. This type of experiment has been operated in Italy, Japan, the UK, the USA, and elsewhere. It offers the potential of a compact

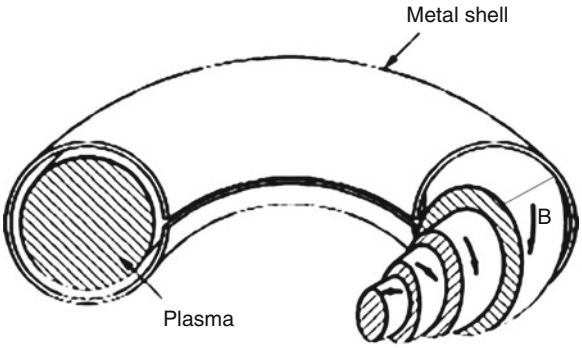

Fig. 12.13 A reversed field pinch, showing how the direction of the magnetic field varies with radius [5]

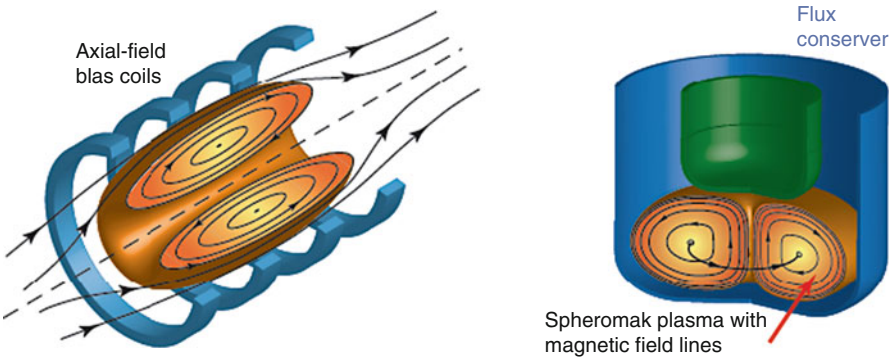

Fig. 12.14 A field-reversed configuration (*left*) and a spheromak. Neither has any structure on the axis of the torus [6]

reactor with a simpler toroidal field system than tokamaks, but plasma energy confinement times may be shorter, and efficient current drive to sustain the RFP is difficult to achieve.

Compact Toroids

Fig. 12.14 compares a field-reversed configuration (FRC) and a spheromak.

The FRC has only poloidal magnetic field components, with zero (or nearly zero) toroidal field. The spheromak is a naturally stable configuration having both toroidal and poloidal magnetic field components. Fig. 12.15 illustrates one way of generating a spheromak, by using a coaxial plasma gun.

In step (1). A coil (black) generates a magnetic field (blue). (2) A puff of hydrogen is admitted into the vacuum (pink cloud). (3) A high voltage is applied

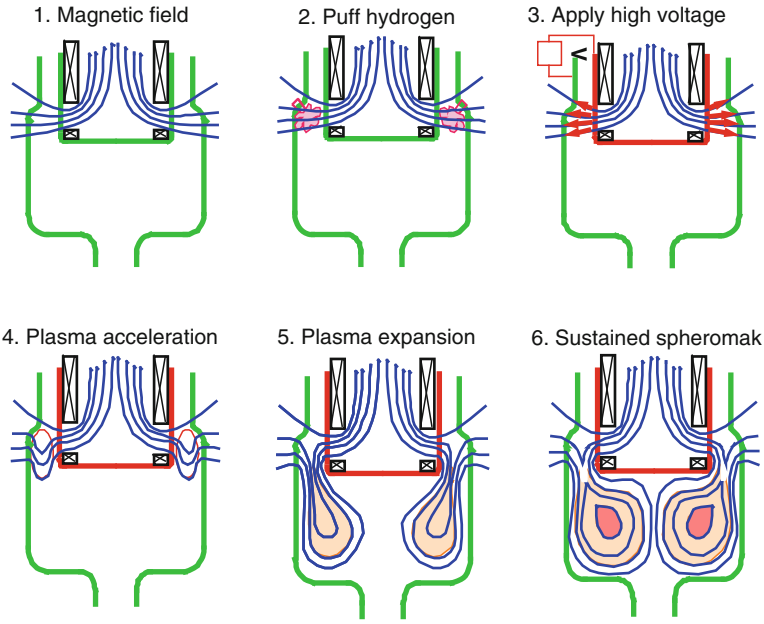

Fig. 12.15 Formation of a spheromak by coaxial plasma gun injection into a flux conserving chamber (Courtesy of Lawrence Livermore National Laboratory)

between the inner and outer cylinders, ionizing the gas. (4) The plasma current flowing interacts with the magnetic field to produce a thrust that accelerates the plasma downward. (5) The plasma (pink) expands into the metal chamber (green). (6) Image currents in the walls create an opposing magnetic field that retards the plasma penetration into the wall. This is called a "sustained spheromak" configuration with quasi-closed field lines similar to tokamaks. The plasma has both toroidal and poloidal magnetic fields without the need for toroidal field coils. It is therefore simpler than tokamaks, and potentially less expensive. Some parameters of the Sustained Spheromak Physics Experiment (SSPX) are shown in Table 12.7.

Spheromak experiments generally last only a few milliseconds, with electron temperatures less than 1 keV. Larger spheromak experiments with more heating auxiliary power and longer duration would be needed to test this concept adequately.

Field-Reversed Configuration (FRC)

A field-reversed configuration may be formed by a theta pinch coil, as shown in Fig. 12.16.

Table 12.7 Typical SSPX parameters (SSPX is now decommissioned) (Courtesy of Lawrence Livermore National Laboratory)

Flux conserver radius and height	0.5 m × 0.5 m
Radius of magnetic axis	0.31 m
Plasma minor radius	0.17 m
Peak discharge current	0.45 MA
Toroidal current	0.6 MA
Peak toroidal field	0.6 T
Edge poloidal field	0.35 T
Plasma duration	4.5 ms
Plasma density	5×10^{19} m^{-3}
Peak electron temperature	0.35 keV

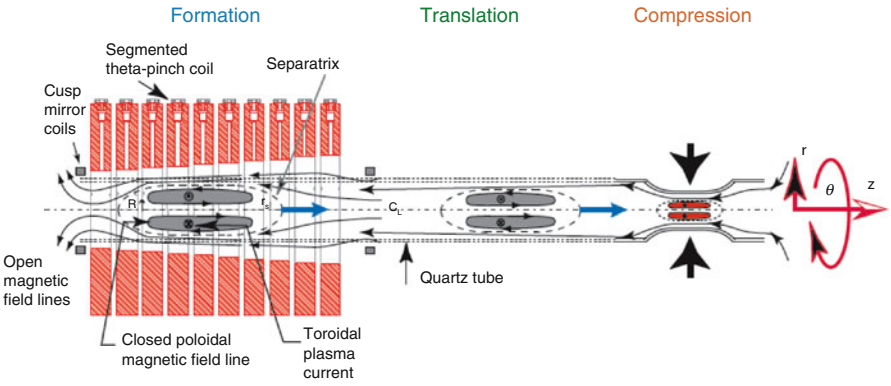

Fig. 12.16 Formation of an FRC by a theta pinch coil, translation to another chamber, and compression by a metallic liner (Courtesy of Los Alamos National Laboratory)

A theta pinch coil is usually a one-turn coil with a sudden current flowing in the theta (azimuthal) direction. The coil current may rise to its peak value in microseconds, squeezing the plasma, hence the name "pinch." With careful programming of the coil current, the plasma may form into an elongated torus with the internal magnetic field in the opposite direction from the external magnetic field (indicated by the small arrows in Fig. 12.16), hence the name "field reversed." FRC plasmas can also be generated and sustained by rotating magnetic fields. They appear to be stable, in spite of their weak or zero toroidal magnetic fields. After formation, an FRC plasma may be moved axially to another chamber, where it can be compressed by a converging magnetic field or by an imploding metallic liner [7]. FRC experiments have been conducted at Los Alamos National Laboratory, University of Tokyo, Osaka University, University of Washington, and TRINITI Laboratory (Troitsk, Russia).

Magnetized Target Fusion (MTF)

MTF target plasma parameters could be $n \sim 10^{23}$ m^{-3}, $T \sim 0.3$ keV, $B \sim 3$ T, and duration $t \sim 10$ μs before compression. The target plasma could be moved axially into another chamber (Fig. 12.16), where a metallic liner would compress it to thermonuclear temperature ($T \sim 10$ keV). Intense DT fusion burn could occur until the configuration disassembled, and it might be possible to achieve energy gain ratios $Q > 5$ in a less expensive device than tokamaks or stellarators.

Pulsed, High-Density Fusion

A similar concept would accelerate an FRC axially to very high velocity, then inject it into a converging magnetic field, which would compress the plasma up to thermonuclear burn conditions. It would flow through the burn chamber, then continue on into an expansion and exhaust chamber [8].

Open Magnetic Confinement Systems

Open magnetic confinement systems can avoid MHD instabilities if the magnetic field pressure is lower in the plasma confinement region than around the outside, a so-called "minimum-B" confinement system.

Tandem Mirror

Due to rapid particle loss along the magnetic field lines, a simple magnetic mirror can only achieve a power gain ratio $Q \sim 1$, which is inadequate for a power plant. This loss can be reduced by creating an electrostatic potential variation along the magnetic field with hills and valleys, as illustrated in Fig. 12.17.

The positive peaks ϕ_c confine ions in the central cell, and the negative wells ϕ_b confine electrons. The plasma density, temperature, and electrostatic potential in tandem mirrors can be controlled by injection of neutral atom beams, by electron cyclotron resonance heating (ECRH), and by radiofrequency (RF) wave heating at selected axial locations. Such electrostatic potential control could make it possible to reduce the required length of a power plant with $Q \sim 10$ from kilometers to less than 200 m. There have been tandem mirror experiments in Japan, Russia, Korea, and the USA. The Gamma-10 experiment in Japan with length $L = 6$ m, $a = 0.36$ m, and central cell $B = 0.41$ T has confined plasma with $n \sim 10^{18}$ m^{-3}, $T_e \sim 0.3$ keV, $T_i \sim 1$ keV. It has achieved values of $\phi_c > 2$ kV [9].

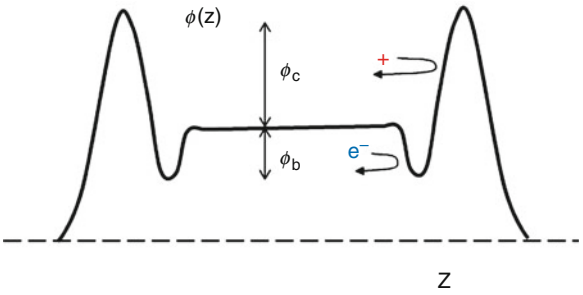

Fig. 12.17 Electrostatic potential versus axial position in a tandem mirror

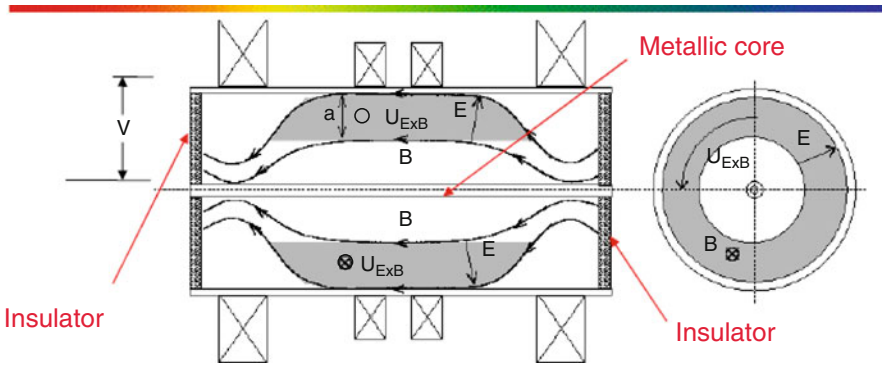

Fig. 12.18 The Maryland centrifugal experiment (Courtesy of the University of Maryland)

Electrostatically Plugged Cusps

High-voltage electrodes can also produce electrostatic potential hills and valleys along magnetic field lines, similar to those of a tandem mirror. The electrons are confined by the magnetic field and the negative electrodes, and the ions are confined in a negative electrostatic potential well created by the electrons' negative charge. For example, the Jupiter-IIM electrostatically plugged magnetic cusp experiment in the Ukraine demonstrated low diffusion rates of plasma across the magnetic field [10].

Rotating Plasmas

Rotating plasmas can be formed by putting high-voltage electrodes in the ends of a magnetic mirror to create a strong radial electric field, which causes the plasma to rotate azimuthally at high speed. This rotation can accelerate ions up to keV energies, and the angular momentum reduces end losses from the magnetic mirror. Fig. 12.18 shows the Maryland Centrifugal Experiment

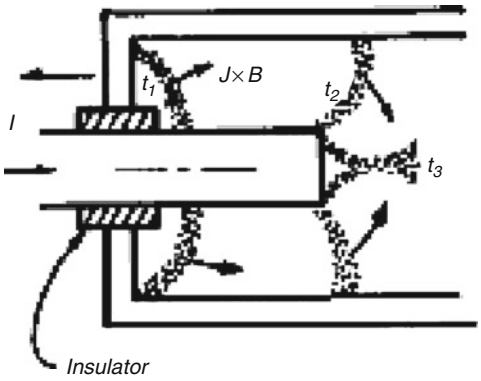

Fig. 12.19 Plasma acceleration by a coaxial gun

This experiment has a central $B \sim 0.3$ T, $a \sim 0.2$ m, $L \sim 1.4$ m, $n \sim 3 \times 10^{20}$ m^{-3}, $T \sim 20$–60 eV, applied voltage 5–20 kV, pulse length 1–10 ms, and has achieved rotational speeds of 100 km/s.

Other Concepts

Plasma Focus

The plasma focus uses a coaxial plasma gun to accelerate a blob of plasma to high velocities, as illustrated in Fig. 12.19.

At time t_1, high voltage breakdown along the insulator forms a plasma that is accelerated axially by the $J \times B$ force. At t_2 the plasma reaches the end of the gun, and at t_3 electromagnetic forces cause it to collapse into a high-density blob, causing a brief burst of fusion reactions before the plasma expands and cools. At low currents (<0.3 MA), the fusion yield increases proportional to I^4, where I is the plasma current, but this favorable scaling saturates at high currents, and economical power production appears to be unlikely at reasonably attainable currents (~ 10 MA). Plasma focus devices are useful as sources of neutrons and x-rays, and many have been built around the world.

Levitated Dipole Experiment

The Levitated Dipole Experiment magnetically levitates a superconducting coil ring, Fig. 12.20.

The resulting magnetic surfaces are good for plasma confinement. This experiment has a low-density background plasma plus a hot electron plasma produced by

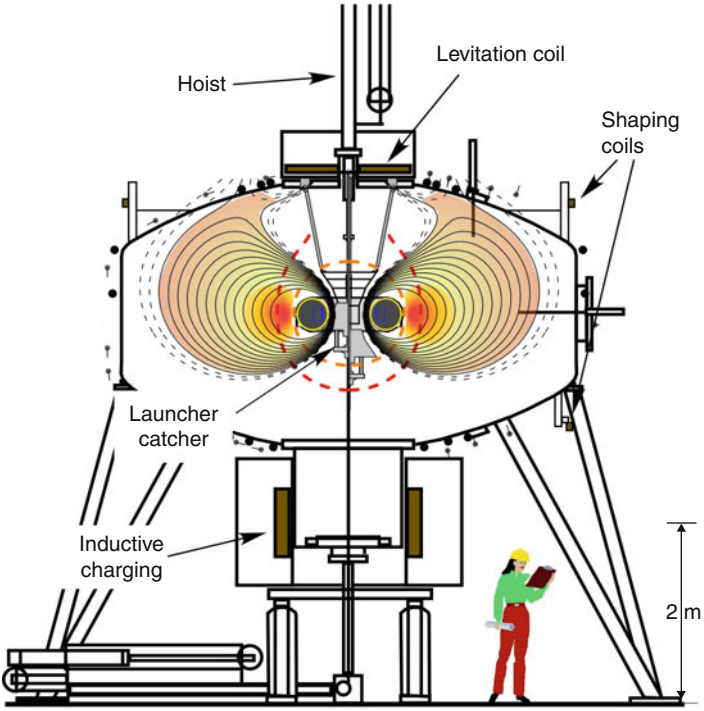

Fig. 12.20 The Levitated Dipole Experiment, showing the magnetic surfaces surrounding the levitated coil. The dotted curves indicate the resonant surfaces for ECRH with frequencies 2.45 and 6.4 GHz (Courtesy of Columbia University and Massachusetts Institute of Technology [11]

absorption of microwaves. The superconducting ring gradually absorbs heat, so it must be periodically shut down and recooled. If this scheme were used for a fusion reactor, heating and radiation damage to the ring would be significant issues.

Inertial Electrostatic Confinement (IEC)

Plasma may also be confined by concentric spherical grids, Fig. 12.21.

With tens of kilovolts applied and deuterium plasma, small devices of this type have produced DD fusion reaction neutron emission rates $\sim 10^7$ neutrons/s. In a high-power fusion reactor, however, the electrodes would tend to melt. IEC devices are useful as sources of neutrons and energetic charged particles.

RF Plasma Confinement

Potential wells in standing radiofrequency (rf) fields can contain low-pressure plasmas effectively, but for high-pressure plasmas of a fusion reactor excessively

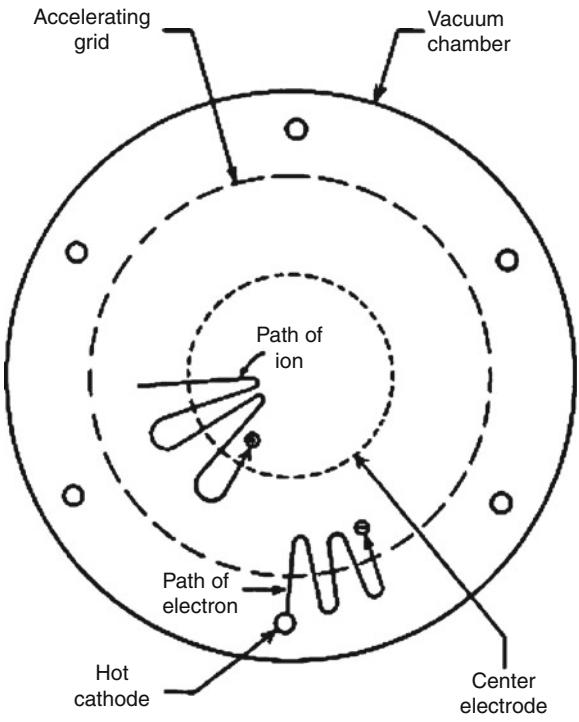

Fig. 12.21 Plasma confinement by spherical grids. In this configuration, the accelerating grid is positive, and the center electrode is negative

high rf power levels would be required. Rf fields have been used to reduce end losses from open magnetic confinement systems, as in the RFC-XX experiment in Japan. High-voltage rf electrodes accelerated ions to higher rotational energies, which inhibited their ability to escape through the point cusps and line cusps.

Polywell

The Polywell concept has a spherical array of six or more point cusps, with electron injection creating a negative potential well that focuses ions into the center of the sphere. It is a form of electrostatic plugging of a cusped magnetic field. Good ion focusing to small radii would be required to achieve satisfactory fusion power density.

Muon-Catalyzed Fusion

Negative mu mesons (muons) produced by accelerators can bind to deuterons to form atoms. Since the muon is 207 times heavier than an electron, the radius of its orbit is 207 times smaller. This small atomic size allows the shrunken deuterium atom to approach very close to another deuteron or triton, close enough for

a nuclear fusion reaction to occur. After a fusion reaction occurs the muon is released, and it can bind to another deuteron (or triton) and catalyze a second fusion reaction. The muon may also be captured by other nuclei, such as by an alpha particle (^{4}He nucleus), which stops the reaction chain. This "helium sticking" problem has limited the number of experimentally attained fusion reactions to about 100 per muon, which is not enough to achieve an energy gain, since about 6 GeV energy are required to generate each muon by an accelerator, and the DT fusion reaction yields only 17.6 MeV.

Cold Fusion

Evidence for low-energy nuclear reactions (LENR) has been reported from many types of experiments: electrolysis of water, gas discharges, gas diffusion through thin films, electron beam impact, exploding wires, and laser irradiation. The evidence includes apparent heat generation, x-rays, and transmutations. Such phenomena were once called "cold fusion" after the 1989 hypothesis by Fleischmann and Pons that the energy generation by their electrolysis cell was a result of nuclear fusion reactions [12]. Many theories have been proposed to explain the LENR phenomena, but so far, no theory has gained widespread acceptance.

Inertial Confinement Fusion (ICF)

Target Compression

Fig. 12.22 shows the general idea of an inertial confinement fusion (ICF) power plant.

The goal is to ignite frequent small explosions in a blast chamber. The target injector shoots fuel capsules ("targets") into the chamber several times per second. When the target reaches the center of the chamber laser beams ablate its surface, which causes an inwards force that compresses the target to ultrahigh density. Then a high-power laser pulse raises part of the compressed target to ignition temperature, and a thermonuclear burn wave causes a miniature explosion. The explosion energy is deposited in the chamber walls and absorbed in a blanket and coolant, which could be liquid metal, molten salt, or helium gas. The hot coolant boils water in a steam generator, and the steam drives a turbine to generate electricity. (Helium gas coolant could drive a gas turbine directly without needing to make steam.) Instead of using laser beams, the target compression could also be done with heavy ion beams or exploding wires and x-rays. Fig. 12.23 shows the steps of target compression and burn.

The laser beam heats the plasma surrounding the target shell (Step a of Fig. 12.23). The plasma ablates the target surface away, causing an inward pressure

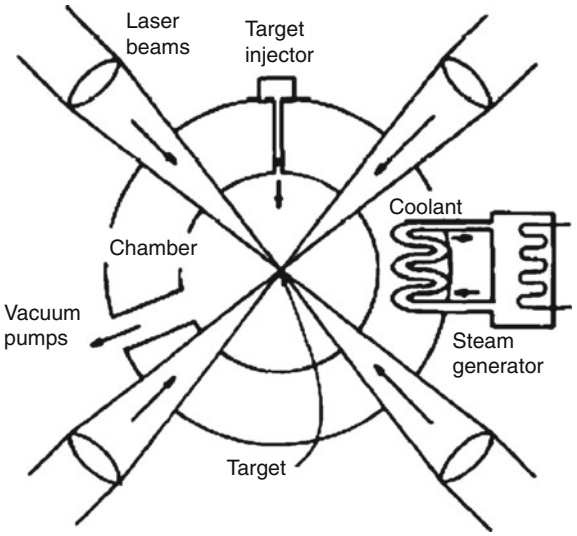

Fig. 12.22 The general idea of a laser ICF power plant

similar to the forward thrust of a rocket caused by rearward expulsion of burning fuel (Step b). The heating to ignition (Step c) may be done by a shock wave to the center of the volume (Step c) or by a sudden PetaWatt laser beam impact on the outside ("fast ignition"), which requires less heating energy. Then a thermonuclear burn wave can spread to surrounding fuel (Step d).

The National Ignition Facility at Lawrence Livermore National Laboratory, California; the Laser MegaJoule facility in France; and the GEKKO-XII in Japan are all large laser facilities approaching ignition of targets. Fig. 12.24 shows the National Ignition Facility (NIF) in Livermore, California.

Fig 12.25 shows a man inside the spherical NIF target chamber.

The NIF experiment is expected to demonstrate target ignition and energy gain $Q > 5$ in 2010–2011. It uses glass lasers with low efficiency, and it requires hours between shots to replace the target, which is suspended on a thin quartz fiber. For "ignition campaign" experiments, the target holder must also provide cryogenic refrigeration. The repetition rate is limited by replacement of the target, by evacuation of the chamber, and by cooling of the walls.

If the target capsule irradiation is not extremely uniform, a Rayleigh-Taylor instability [13] can break up the shell before compression is complete, as in Fig. 12.26.

Target pellets may be irradiated directly by the laser beams, or they may be mounted inside a hollow cylinder, called a "Hohlraum," Fig. 12.27, to achieve more uniform compression.

The laser beams would enter through holes in the ends of the cylinder and irradiate the inside walls of the Hohlraum, causing them to emit intense x-rays. The x-rays would illuminate the 2.2 mm diameter target capsule, ablating its surface and compressing the frozen DT fuel to ultrahigh density. This "indirect drive" may provide better compression than the "direct drive," where the laser

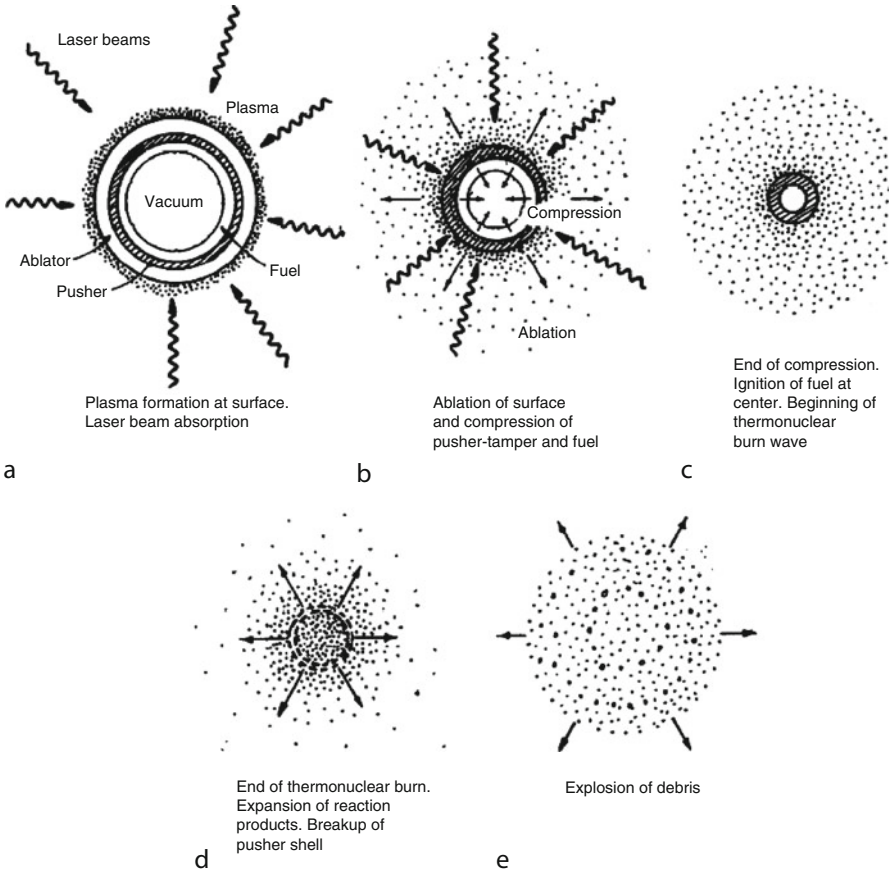

Fig. 12.23 Ablation, compression, and burn of an ICF target

beams interact directly with the target surface, but the Hohlraum targets are more complex and more difficult to inject into a chamber and align with the laser beams.

Table 12.8 shows that many issues must be resolved before ICF reactors can become practical.

Potential solutions are available for most issues, but technology development has not yet been completed, especially for efficient, reliable, cost-effective drivers.

Table 12.9 lists some issues of target design and manufacture.

Laser Development

Great improvements are needed in laser efficiency, pulse repetition rate, and target injection rates. In the USA, two experiments are aimed at high average power lasers: Electra and Mercury.

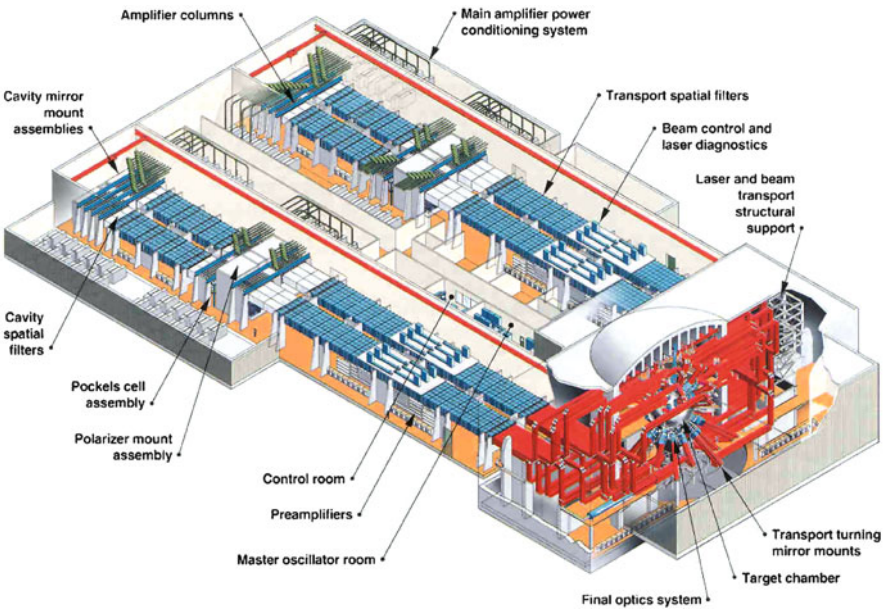

Fig. 12.24 The National Ignition Facility, USA. 192 laser beams (in *red* tubes) go to the target chamber (Courtesy of Lawrence Livermore National Laboratory)

Fig. 12.25 The NIF target chamber, with holes where the laser beams enter. (The wide angle photo makes the 10-m diameter chamber appear to be larger.) (Courtesy of Lawrence Livermore National Laboratory)

The *Electra KrF laser* experiment at the Naval Research Laboratory is illustrated in Fig. 12.28.

Electron beams in vacuum from the cathode pass through the foil into the Kr and F_2 gases in the laser cell, where they cause excitation, resulting in a laser beam that exits through the amplifier window. Electra will run at 5 Hz with a laser output of

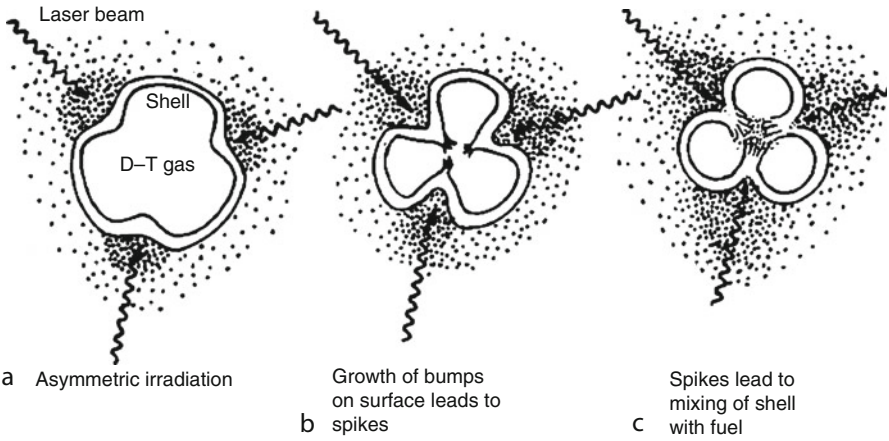

Fig. 12.26 Growth of the Rayleigh-Taylor instability, causing breakup of the target shell (exaggerated for clarity)

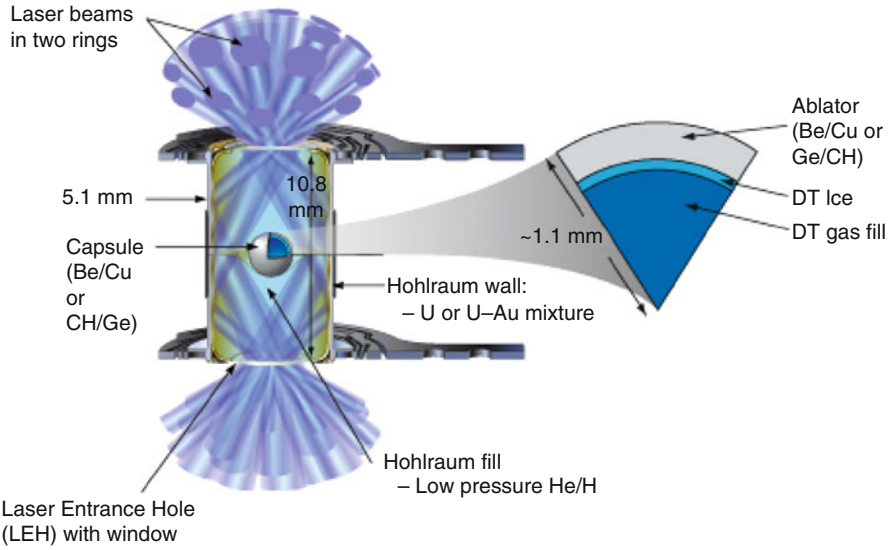

Fig. 12.27 A Hohlraum target (Courtesy of Lawrence Livermore National Laboratory)

400–700 J. This will be large enough to develop technologies that can be scalable to the 50–150 kJ needed for a fusion power plant beam line.

Fig. 12.29 shows the *Mercurydiode-pumped solid state laser*.

The material in which light amplification occurs is crystalline strontium fluoro-apatite doped with ytterbium (Yb:S-FAP), which has a long excited state lifetime

Table 12.8 Technical issues of ICF reactor development

Theory	Understand the physics of energy absorption, reflection, heat transport, compression, instabilities ignition, and burn
Experiments	Attain satisfactory values of the critical elements for high energy gain • Beam-to-fuel coupling efficiency • Avoiding fuel preheating before compression is complete • Implosion symmetry • Driver energy per unit fuel mass
Target manufacture	Develop an automated system to manufacture high-gain spherical targets accurately and cheaply. Select target materials to avoid production of long-lived radioisotopes. Use cryogenic refrigeration to keep the DT fuel frozen.
Target shelf life	Tritium decay heat can damage the cryogenic target, so targets have a finite shelf life.
Target injection	Develop a target injection and guidance system to ensure that the target is at the focus of the beams when the driver is fired.
Diagnostics	Measure the parameters of experiments, such as implosion velocity, density distributions, energy distributions, ablated matter, laser beam reflection, implosion symmetry, and fusion reaction products, with fine spatial and temporal resolution.
Chambers	Develop reactor chambers to withstand repeated ($>3 \times 10^8$) explosions without failure. (A 1,000 MJ yield has the explosive energy of 240 kg of TNT, but less momentum).
Chamber Clearing	Remove debris and gases rapidly between explosions, in order to avoid attenuating the incident driver beams.
Drivers	Develop laser or ion beams with high-energy (l–10 MJ), high-pulse repetition rate (l–10 Hz), proper pulse shape (duration 10–20 ns), suitable wavelength (lasers), good efficiency ($\geq$8%), and low enough cost.
Reliability	Develop power supplies, power conditioning equipment, diodes, and optical components to operate reliably for $>10^9$ shots.

Table 12.9 Target design and manufacture issues

Hydrodynamic stability and high compression
Good sphericity
Fast fill and layering
Uniform thickness shells
Very smooth surfaces
Minimum preheat of fuel
High-Z material to stop electrons and x-rays
Minimum production of long-lived radioisotopes
Easy handling and storage
Capable of high-velocity acceleration and injection without damage
Cheap materials, like plastics
Simple, inexpensive fabrication
Target cost goal typically <10 cents per target

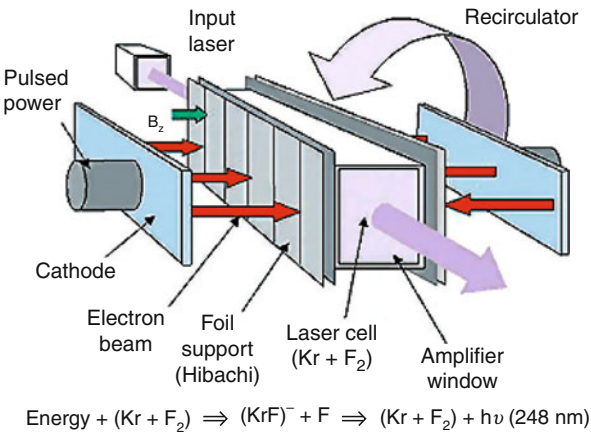

Fig. 12.28 The Electra KrF laser (Courtesy of Naval Research Laboratory)

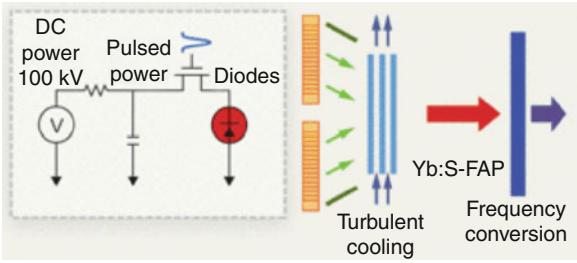

Fig. 12.29 The Mercury diode-pumped solid state laser (Courtesy of the Lawrence Livermore National Laboratory)

and high saturation fluence. High-power diodes inject 900 nm wavelength light into the Yb:S-FAP, which emits near 1,047 nm. About 15–20% of the diode energy is dissipated as heat in the Yb:S-FAP, which is removed by turbulently flowing helium gas [14]. The Mercury laser should deliver 100 J pulses at a rate of 10 Hz. If successful, this could be scaled up by using many units to MJ energies for a power plant. With mass production of diodes, their cost may fall to pennies per Watt, as needed for an economical power plant.

Hypervelocity Impact Fusion

Small pellets (mass ~ 1 g) would be accelerated to velocities $>10^5$ m/s and shot at a solid target. Either the projectile or the target would contain DT fuel. During impact, intense compression and shock heating would occur, igniting some of the fuel. The compression could be made nearly three-dimensional by shaping the projectile and target, Fig. 12.30.

If compression is great enough, a high energy gain ratio $Q > 30$ may be attained. The fusion yield should be low enough that the blast chamber is not destroyed and high enough for economical power generation. The required projectile energy is about 25 MJ. Possible means of acceleration include electromagnetic rail guns,

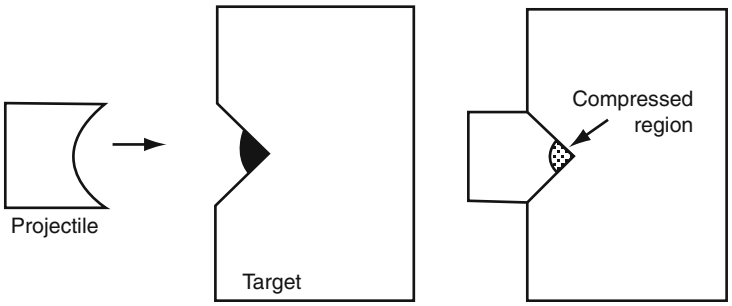

Fig. 12.30 Hypervelocity impact projectile and target shaped to provide good compression

electrostatic accelerator, light gas guns, traveling electromagnetic wave accelerator, and laser ablation.

Challenges of Plasma Theory

In order to model fusion reactor behavior plasma physics theory must take into account many phenomena, Table 12.10.

Many of these models are based on simplifications of the Boltzmann transport theory and Maxwell's equations. Because these phenomena are diverse and often involve nonlinear differential equations, there is no unified theory that encompasses all of them. Instead, these phenomena may be modeled separately and the models stitched together to get an approximate picture of plasma behavior. Analytic theories are useful to understand how individual phenomena vary with input parameters, but are limited by the simplifying assumptions that are needed to make the equations solvable.

Large-scale computer simulations are widely used to model these effects. Three-dimensional models can be used to predict plasma behavior. The successful modeling of many phenomena lends confidence to predictions of the behavior of future experiments, such as ITER, but experimental data will still be needed to confirm the predictions.

Fusion Technology Issues

Many areas of technology are required for successful development of fusion power, Table 12.11.

Most of these issues have been successfully resolved during the 6 decades of fusion research. The ITER experiment should demonstrate the successful

Table 12.10 Some phenomena to be modeled by plasma theory

Magnetohydrodynamic (MHD) instabilities	Motion of plasma boundary, driven by plasma pressure and Lorentz force
Radiation losses	Line radiation, bremsstrahlung, cyclotron radiation
Coulomb collision effects on velocity distributions	Boltzmann or Fokker-Planck equation
Plasma wave generation, cutoffs, and resonances	Maxwell equations coupled to plasma current density and magnetic field
Wave-particle interactions and microinstabilities	Anisotropic or non-Maxwellian distributions; kinetic theory (based on Boltzmann equation)
Nuclear fusion reactions	Cross sections averaged over ion velocity distributions
Particle and energy transport	Transport coefficients in conservation equations; scaling laws derived from experimental data
Plasma–wall interactions	Sputtering, vaporization
Impurity transport and control	Edge plasma and divertor theory
Plasma heating and current drive	Neutral beam injection, wave heating

combination of many of these technologies, but will not demonstrate much tritium breeding, durable wall materials, high availability, or electrical power generation.

ITER must deal with transient heat loads caused by "edge localized modes" (ELMs) and disruptions, which can potentially damage the first wall or divertor. A robotic system to replace damaged wall tiles will be tested under high radiation levels in ITER. Development of first wall or divertor materials that can resist high heat fluxes and are resistant to damage by 14-MeV neutrons will not be completed by ITER, which uses more conventional structural materials.

In parallel with the ITER project, the International Fusion Materials Irradiation Facility (IFMIF), planned to be built in Japan, will bombard a flowing lithium target with 40 MeV deuteron beams to produce an intense flux of energetic neutrons for testing small samples of candidate fusion reactor materials. Fig. 12.31 shows a drawing of IFMIF [15].

Use of high-temperature superconductors is becoming feasible for fusion devices [16]. They could operate near liquid nitrogen temperature (77 K), instead of near liquid helium temperature (4 K). This would simplify the design of the coils, cryostats, and instrumentation, and greatly reduce the refrigeration power and cost of refrigeration systems.

Coating the plasma chamber walls with lithium may help improve plasma performance. Usually, many of the deuterons escaping from the plasma hit the wall, where they are neutralized. Some of them re-emerge from the wall as cold neutral gas, which keeps the plasma edge temperature low, making a steep temperature gradient, which causes rapid heat conduction. Lithium absorbs escaping deuterium, reducing backflow of cold deuterium gas, and flattening the temperature profile, which can reduce plasma electron turbulence and heat conduction rates [17].

Table 12.11 Fusion technology issues

Component	Issues
Magnet coil systems	High magnetic field, superconducting cable, stresses, quench protection
Plasma heating, fueling, current drive	Plasma compression
	Magnetic induction
	Electromagnetic waves
	Particle beam injection
	Plasma guns
First wall	Low-Z (atomic number), high heat flux, heat removal, radiation damage, tritium trapping
Blanket, shield	Tritium breeding ratio, neutron and gamma shielding, heat removal, radiation damage
Divertors (channels that remove plasma impurities)	High heat flux, sputtering, vaporization, tritium trapping, vacuum pumping
Energy conversion	Efficient conversion of fusion energy into electrical energy, such as with a steam cycle or helium gas turbine. High efficiency requires high coolant temperature, which causes materials problems
Materials issues	Stress, embrittlement, swelling, creep, fatigue, tritium trapping
Vacuum systems	Pumping speed, conductance, cryopanels
Cryogenic systems	Coolant flow, refrigeration, liquefaction, heat shields
Plasma diagnostic systems	Space-time mapping of magnetic field, electric field, plasma density, temperature, impurities, waves
Control systems	Plasma control, heating, current drive, magnets, fusion burn, electrical power plant
Maintenance	Magnets, first wall, heating systems, diagnostics, heat transfer systems
Safety and environmental systems	Routine emissions, accident scenarios, decommissioning, waste disposal
Power plant designs	Criteria for attractive power plants
	Reliability, availability, and maintenance
	Economics
	Fusion–fission hybrids

Fusion Reactor Design Studies

Electric power utility companies have many criteria for power plant selection and siting [18] including:

- Output of power plant, compatibility with power grid
- Grid stability
- Required transmission lines
- Capital cost per kW
- Simplicity of plant
- Construction time
- Reliability and availability of power plant
- Ease and speed of maintenance

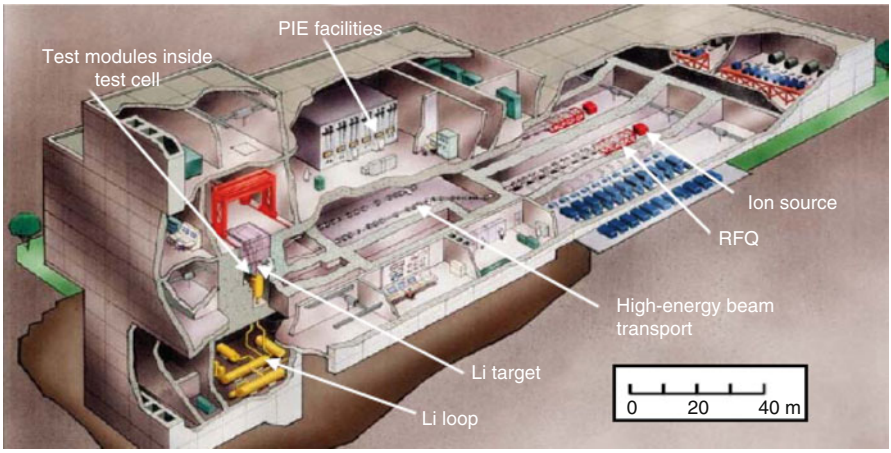

Fig. 12.31 The international fusion materials irradiation test facility (Courtesy of the International Energy Agency)

- Plant lifetime
- Load-following (ability to vary output to meet demand)
- Seismic activity and flood danger
- Availability of fuel, and fuel cycle costs
- Decommissioning costs
- Adequacy of resources, such as helium, lithium, and niobium
- Feasibility of shipping large, heavy components
- Staff numbers, skills, and costs
- Security requirements and costs
- Government laws and regulations
- Ease of licensing
- Intervener lawsuits
- Safety
- Environmental issues
- Plant emissions and waste products
- Willingness of financial institutions to invest
- Public acceptance

The availability of fusion power plants is difficult to predict, because current experiments often have equipment failure rates that would be unacceptable to utilities. The availability of some systems can sometimes be improved by providing redundant components, with slight increases in cost. Repair of large superconducting magnets would be difficult, if not impossible, so designers try to ensure that they will last for the life of the plant.

Fusion reactors have an economy of scale, which means that a 3,000 MWe power plant would probably have a much lower COE than a 300 MWe plant,

but utilities may not wish to build very large power plants, to avoid large grid perturbations during outages [19].

The electricity from a fusion power plant could also be used to make hydrogen by high-temperature electrolysis. The hydrogen could be used as fuel for transportation and industrial processes. If the fusion reactor blanket could operate at $T > 800°C$, then the heat could be used directly for hydrogen production by a thermo-chemical system, such as one using a sulfur-iodine cycle [20].

Fusion–Fission Hybrids

Present light water fission reactors burn mainly the fissile isotope ^{235}U, which is only 0.711% of natural uranium. ("Fissile" means that it can be fissioned easily by slow neutrons.) The other 99.27% is mostly ^{238}U, which does not fission easily. A strong neutron source is needed in order to convert the ^{238}U into ^{239}Pu, which is another fissile fuel, if we are to generate energy from the other 99% of the uranium resources.

That strong neutron source could be a "fast" fission reactor, such as a liquid metal fast breeder reactor, but it takes years for such a reactor to generate enough fuel to start up a second reactor. The neutron source could be a high-power accelerator beam (like IFMIF), but fusion plasma neutron sources would be better where large quantities of materials are to be irradiated.

A fusion–fission hybrid would use uranium or thorium in the fusion reactor blanket, in addition to lithium. The blanket could be optimized either to produce more heat and electricity from the hybrid plant or to breed fissile fuel (^{239}Pu or ^{233}U) for use in satellite fission reactors. Hybrid blanket design studies indicate that one hybrid reactor could provide fuel for about five light water reactors. An "Energy Park" could have a fusion reactor plus several fission reactors and a fission reactor fuel reprocessing plant. With modern reactor designs, much of the spent fuel radioactive wastes could be recycled in the fission reactors or "incinerated" (transmuted to stable isotopes) in the fusion reactor blanket [21].

Future Directions

Most past magnetic fusion experiments have had small minor radii, so energy confinement times were short (<0.1 s), and impurities from the wall prevented optimum performance. The fusion research field needs bold investment to build large, high-power devices, such as ITER, in several other areas:

- Large compact toroid experiments (FRC and spheromak)
- A high-power accelerator neutron source for materials testing
- A plasma-based volumetric neutron source for materials testing

- Tokamak demonstration power plant construction during ITER operation
- Two reactor-sized stellarators following LHD and W 7-X
- A reactor-sized tandem mirror following Gamma-10
- Rapid-pulse, high-gain laser fusion demonstration power plants
- Full-scale heavy ion beam driver demonstration

Fusion reactor design teams in Europe, Japan, and the USA have done many design studies of tokamaks, stellarators, inertial fusion, and other types of fusion power plants. The capital costs of most fusion reactors are very high, but the fuel costs are very low. The resulting cost of electricity (COE) is typically predicted to be about 1.5–2 times as high as the COE from coal plants and nuclear fission reactors. Fusion power plants could become competitive

- If cheaper fusion reactors were developed, such as from compact toroids
- If fusion–fission hybrids were developed
- If carbon emissions were taxed
- If public opposition made it difficult to build new fission reactors or coal power plants

Acknowledgments The following provided helpful comments on this article: Ralph Moir, Chan Choi, Lee Cadwallader, Nicholas Tsoulfanidis, Alex Parrish, and the Institute for Plasma Research (Gandhinagar, India). Charlou Dolan drew many of the figures.

Bibliography

Primary Literature

1. Jaskula BW (2010) Lithium. USGS 2008 Minerals Yearbook, United States Geological Survey
2. Freidberg J (2006) Plasma physics and fusion energy. Cambridge University Press, Cambridge
3. "All-the-world's tokamaks" (2010) http://www.toodlepip.com/tokamak
4. Bolt H (2001) Materials for Fusion. European White Book on Fundamental Research in Materials Science, Max-Planck-Gesellschaft, Munich, Section 2.9, Fig 12.2.17. (See also http://www.mpg.de/bilderBerichteDokumente/dokumentation/europWhiteBook/)
5. Hazeltine R et al (2009) Research needs for magnetic fusion energy sciences. Report of the Research Needs Workshop (ReNeW), Bethesda, 8–12 June, 2009, U.S. Department of Energy, p 203
6. Hazeltine R et al (2009) Research needs for magnetic fusion energy sciences. Report of the Research Needs Workshop (ReNeW), Bethesda, 8–12 June, 2009, U.S. Department of Energy, p 213
7. Tacetti JM et al (2003) FRX-L: a field-reversed configuration plasma injector for magnetized target fusion. Rev Sci Instrum 74(10):4314–4323
8. Slough J et al (2007) The pulsed high density experiment: concept, design, and initial results. J Fusion Energy 26:199–205
9. Ichimura M et al (2006) CRF experiments and potential formation on the GAMMA 10 tandem mirror. Plasma Sci Technol 8(1):87–90
10. Dolan TJ (1994) Magnetic electrostatic plasma confinement. Plasma Phys Controlled Fusion 36:1539–1593

11. Boxer AC et al (2010) Turbulent inward pinch of plasma confined by a levitated dipole magnet. Nature-Physics 6:207–212, Supplementary Information
12. Storms E (2007) The science of low energy nuclear reaction: a comprehensive compilation of evidence and explanations. World Scientific, Hackensack
13. Dolan TJ (1982) Fusion research. Pergamon, Elmsford, Chapter 15
14. Ebbers C, Caird J, Moses E (2009) Laser Focus World 45, No. 3, March 1
15. IFMIF International Team (2004) International Fusion Materials Irradiation Facility (IFMIF) Comprehensive Design Report. International Energy Agency, Paris
16. Hazeltine R et al (2009) Research needs for magnetic fusion energy sciences. Report of the Research Needs Workshop (ReNeW), Bethesda, 8–12 June, 2009, U.S. Department of Energy, Thrust 7, pp 285–293
17. Zakharkov LE et al (2004) Ignited spherical tokamaks. Fusion Eng Des 72:149–168
18. Kaslow J et al (1994) Criteria for practical fusion power systems: report from the EPRI fusion panel. J Fusion Energy 13(2/3):181–183
19. Dolan TJ (1993) Fusion power economy of scale. Fusion Technol 24:97–111
20. Terada A et al (2007) Development of hydrogen production technology by thermochemical water splitting IS process, pilot test plan. J Nucl Sci Technol 44(3):477–482
21. Freidberg J et al (2009) Research needs for fusion-fission hybrid systems. Report of the Research Needs Workshop (ReNeW), Gaithersburg, Maryland, September 30–October 2, 2009, U.S. Department of Energy

Books and Reviews

Braams CM, Stott PE (2002) Nuclear fusion: Half a century of magnetic confinement fusion research. Institute of Physics, Philadelphia

Chen FF (1984) Introduction to plasma physics and controlled thermonuclear fusion. Plenum, New York

Dinklage A et al (2005) Plasma physics – confinement, transport, and collective effects. Springer, Berlin

Dolan TJ (1982) Fusion research. Pergamon, Elmsford

Freidberg J (2006) Plasma physics and fusion energy. Cambridge University Press, Cambridge

Chapter 13
Radiation Sources

Richard E. Faw and J. Kenneth Shultis

Glossary

Absorbed dose	A general term for the energy transferred from radiation to matter. Specifically, the absorbed dose is the amount of energy absorbed in a unit mass of matter from ionizing radiation. Units are the gray (Gy) and rad, respectively, equivalent to 1 J/kg and 100 ergs/g. Thus, 1 Gy equals 100 rad.
Activity	The decay rate (expected number of nuclear transformations per unit time) in a radioactive sample. Units are the becquerel (Bq) equal to one decay per second, and the curie (Ci) equal to 3.7×10^{10} decays per second.
Alpha particle	The nucleus of a ^{4}He atom, composed of two neutrons and two protons and denoted by α.
Committed dose	The dose equivalent accumulated over the rest of a person's life following the ingestion or inhalation of radioactive material into the body.

This chapter was originally published as part of the Encyclopedia of Sustainability Science and Technology edited by Robert A. Meyers. DOI:10.1007/978-1-4419-0851-3

R.E. Faw (✉)
Department of Mechanical & Nuclear Engineering, Kansas State University,
132 Brooks Landing Drive, Winston Salem, NC 27106, USA
e-mail: fawre@triad.rr.com

J.K. Shultis
Department of Mechanical & Nuclear Engineering, Kansas State University,
Ward Hall, Manhattan, KS 66506-2503, USA
e-mail: jks@ksu.edu

N. Tsoulfanidis (ed.), *Nuclear Energy: Selected Entries from the Encyclopedia of Sustainability Science and Technology*, DOI 10.1007/978-1-4614-5716-9_13,

Coulomb force	The electrostatic force between two charges. It is proportional to the product of the charges and inversely proportional to the square of the distance between them. The force is attractive if the charges are of opposite sign, and repulsive if of like sign.
Dose equivalent	A measure of the health risk associated with the absorption of radiation locally in the human body. It equals the local absorbed dose multiplied by a *quality factor* to correct for the relative biological effect associated with different radiations. Units are the sievert (Sv) or rem.
Effective dose	An overall measure of the risk of cancer or hereditary illness associated with radiation exposure. It is a weighted average dose to multiple organs and tissues of the body, with weighting over both quality factor and the relative sensitivity of each organ or tissue. Units are the sievert (Sv) or rem for the dose in grays and rads, respectively.
Hadron	A subatomic particle that reacts via strong nuclear forces. Hadrons include mesons (e.g., pions and kaons) and baryons (e.g., protons and neutrons). Hadrons do not include bosons (e.g., photons) and leptons (e.g., electrons, muons, and neutrinos).
Meson	A subatomic particle, a subclass of hadrons, composed of an even number of other subatomic particles called quarks. Most important are the pi meson (pion) and K meson (kaon).
Nuclide	A term used to refer to a particular atom or nucleus with a specific neutron number N and atomic (proton) number Z. The nuclide with N neutrons and Z protons and electrons is denoted as ${}^{A}_{Z}\mathrm{X}$ where X is the chemical symbol (determined by Z) and $A = Z + N$ is the mass number. If the nuclide is radioactive, it is called a *radionuclide*.
Photon	A quantum of electromagnetic radiation with energy $E = h\nu$ where h is Planck's constant and ν is the frequency. Photons produced by changes in the structure of a nucleus are called *gamma photons*, and those produced by atomic electron rearrangement are called *x-rays*.
Positron	The antiparticle of the electron with the same mass m_e but with a positive charge equal in magnitude to the negative charge of the electron. A positron, denoted by β^+, quickly after its formation annihilates with an ambient electron converting the two electron masses into two photons each with energy $m_e c^2 = 0.511$ MeV.

Definition of the Subject

This entry treats sources of only ionizing radiation, such as electrons, protons, high-energy photons, neutrons, and similar radiations that have the ability to cause ionization, either directly or indirectly, and, thus, to induce chemical and physical changes along their passages through materials. Not included are sources of relatively lower frequency electromagnetic radiation from radio waves to ultraviolet light.

Characterization of sources requires characterization of radiations as well. Many sources encountered are radioactive isotopes of elements in the periodic table. These sources, as they decay radioactively, emit ionizing radiation. Some of the ionizing radiation is in the form of alpha particles, gamma rays, and x-rays, all characteristically monoenergetic in nature. Some is in the form of beta particles, distributed in energy but with well-defined maxima. Other sources are not directly associated with radioisotopes. X-ray machines and accelerators release ionizing radiation generally distributed in energy but with some monoenergetic components. The radiation belts surrounding the earth are composed of electrons and protons distributed in energy. Solar radiation and galactic cosmic rays are ionizing radiations widely distributed in type and energy. The nuclear fission process results in prompt emission of gamma rays and neutrons very widely distributed in energy. Fission also yields an extremely wide range of *fission products*, which radioactively decay over long periods of time.

Characterization of sources, to be meaningful, also begs discussion of radiation doses and radiation effects. There are acute effects accompanying high exposures. There are also known carcinogenic effects of human exposure and suspected mutational and hereditary effects. Therefore, a portion of this entry is devoted to examination of health effects associated with exposure to ionizing radiation.

This entry is divided into two parts. In the first several sections, the quantitative technical characterization of physical processes that produce ionizing radiation are reviewed. In latter sections, a qualitative examination is given of the various types of radiation sources encountered in the environment, workplace, laboratory, or medical facility.

Introduction

Throughout our lives, ionizing radiation is ever present, though rarely sensed. Radioactive sources are present in the food we eat, in the water we drink, and in the air we breathe. Most of these sources have but brief sojourns in our bodies, but some are taken up in bone and permanently retained. These sources, isotopes of elements in the periodic table, decay radioactively, emitting ionizing radiation most often in the form of gamma and x-rays, alpha particles, beta particles, and electrons. The ionization taking place in the body accounts for biological effects, good and bad.

Radiation also reaches us from sources outside our bodies. Radioactivity is present in our soils and minerals, and in our construction materials. Electromagnetic radiation of all wavelengths, including radio waves, microwaves, radar, and light, of both man-made and natural origins, constantly, bombard us. Photons are far more prevalent in number than atoms in our universe; for every nucleon there are about 10^9 photons. Cosmic rays and the subatomic debris they create during interactions in the atmosphere also impinge on us. Neutrinos from fusion reactions in our sun reach us in such numbers that tens of billions per second pass through every square centimeter of our skin. Most of this radiation, for example, neutrinos and radio waves, fortunately, passes harmlessly through us. Other radiation such as light and longer wavelength electromagnetic radiation usually interacts harmlessly with our tissues. However, shorter wavelength electromagnetic radiation, for example, ultraviolet light, x-rays and gamma rays, and charged particles produced by nuclear reactions can cause various degrees of damage to our cells.

The types and sources of radiation just described may be naturally occurring, may be a legacy of the era of nuclear weapons testing, or may be a result of human enterprise, for example, uranium in coal ash, radium in mine tailings, medical wastes, and fission or activation products in wastes from nuclear power production. All vary with latitude, longitude, and altitude – even on a small scale.

There are also population groups especially affected, but in different ways, by exposure to ionizing radiation from many sources. First among these in importance are patients and providers of medical radiation exposures. In the USA, as of 2006, collective effective doses to patients accruing from medical exposure, about 900,000 person-Sv annually, amount to almost half the total for the entire population. Computed tomography and nuclear medicine procedures dominate the exposure, with fluoroscopy and radiology accounting for about 230,000 person-Sv annual effective dose. Interventional fluoroscopy, while of great value to the patient, contributes in a major way to provider dose. Brachytherapy and beam therapy using photons, electrons, and protons lead to high therapeutic radiation exposures to patients, of course. Modern beam therapy utilizes exquisite beam shielding techniques to minimize doses to off-target patient tissues. Of all occupational groups, medical workers are greatest in number and accrue the highest collective doses, namely, 549 person-Sv annually in the USA. However, recordable individual worker annual doses are about 0.75 mSv as compared to 1.87 mSv for the fewer workers in commercial nuclear power.

Another population group consists of astronauts and aviation flight crews especially in high-altitude, international flights. Radiation from solar and galactic sources lead to high occupational radiation exposures. For astronauts, the life-threatening risk of solar-flare radiation exposures is a major concern.

Radiation sources used in industry affect another significant occupational group. Industrial radiography using x-ray, gamma-ray, or even neutron sources is an important component of occupational exposure. Other sources find wide use in measurement devices and sensor appliances.

For radiation to produce biological damage, it must first interact with tissue to alter molecular bonds and change the chemistry of the cells. Likewise, for radiation to produce damage in structural and electrical materials, it must cause interactions

that disrupt crystalline and molecular bonds. Such radiation must be capable of creating ion–electron pairs and is termed *ionizing* radiation. Fast-moving charged particles, such as alpha particles, beta particles, and fission fragments, can directly ionize matter. Neutral particles, such as photons and neutrons, cannot interact directly with the electrons of the matter through they pass; rather they cause interactions that transfer some of their energy to charged secondary particles, which in turn produce ionization as they slow.

Radiation-Producing Reactions

Origins of Ionizing Radiation

Ionizing radiation is invariably the consequence of physical reactions, involving subatomic particles, at the atomic or nuclear level. The possible radiation-producing reactions are many, and usually, although not always, involve altering the configuration of neutrons and protons in an atomic nucleus or the rearrangement of atomic electrons about a nucleus. These reactions can be divided into two categories:

Radioactive decay. In the first type of radiation-producing reaction, the nucleus of an atom spontaneously changes its internal arrangement of neutrons and protons to achieve a more stable configuration. In such spontaneous *radioactive* transmutations, ionizing radiation is almost always emitted. The number of known different atoms, each with a distinct combination of Z and A is about 3,200. Of these, only 266 are stable and 65 are long-lived radioisotopes all of which are found in nature. The remaining nuclides have been made by humans and are radioactive with lifetimes much shorter than the age of the solar system. Both naturally occurring and manufactured radionuclides are the mostly commonly encountered sources of ionizing radiation.

Binary reactions. The second category of radiation-producing interactions involves two impinging atomic or subatomic particles that react to form one or more reaction products. Examples include neutrons interacting with nuclei of atoms, or photons interacting with nuclei or atomic electrons. Many binary reactions, in which an incident subatomic particle x strikes an atom or nucleus X, produce only two reaction products, typically a residual atom or nucleus Y and some subatomic particle y. These binary two-product reactions are often written as $X(x,y)Y$, for example, ${}^{14}_{7}\mathrm{N}(\alpha, p){}^{17}_{8}\mathrm{O}$.

Energetics of Radiation-Producing Reactions

In any nuclear reaction, total energy must be conserved. The total energy (kinetic plus rest-mass energy) of the initial particles must equal the total energy of the final products, that is, $\sum_i [E_i + m_i c^2] = \sum_i \left[E'_i + m'_i c^2\right]$, where E_i (E'_i) is the kinetic

energy of the ith initial (final) particle with a rest mass m_i (m'_i), and c is the speed of light.

Any change in the total kinetic energy of particles before and after the reaction, ΔE, must be accompanied by an equivalent change in the total rest mass of the particles before and after the reaction, Δm, that are related by Einstein's famous equation $\Delta E = \Delta m c^2$. To quantify this change in the kinetic or rest-mass energies, a so-called Q-value is defined as

$$\begin{aligned} Q &= (\text{rest mass of initial particles})c^2 - (\text{rest mass of final particles})c^2 \\ &= (\text{KE of final particles}) - (\text{KE of intial particles}) \end{aligned}$$

The Q value of a nuclear reaction may be either positive or negative. If the rest masses of the reactants exceed the rest masses of the products, the Q value of the reaction is positive with the decrease in rest mass being converted into a gain in kinetic energy. Such a reaction is *exoergic*. Radioactive decay is such a spontaneous exoergic nuclear reaction in which the Q-value energy is converted into the kinetic energy of the products.

Conversely, if Q is negative, the reaction is *endoergic*. For this case, kinetic energy of the initial particles is converted into rest-mass energy of the reaction products. The kinetic energy decrease equals the rest-mass energy increase. Such reactions cannot occur unless the colliding particles have at least a certain amount of kinetic energy, the so-called *threshold energy* for the reaction. For the binary, two-product reaction $X(x,y)Y$, the threshold kinetic energy of x incident on a stationary X is, neglecting Coulombic barrier effects, given approximately by

$$E_{th} \simeq -\left(1 + \frac{m_x}{m_X}\right) Q.$$

In any reaction, linear momentum must also be conserved. Thus, the momentum of the reaction products must equal that of the reactants. For two-product nuclear reactions, conservation of linear momentum requires that the products, depending on their recoil directions, have very definite amounts of kinetic energy. By contrast, for reactions with three or more products, there is no unique division of the reaction energy, and the products generally have a continuous distribution of kinetic energies.

Physical Characterization of Sources

The most fundamental type of source is a *point source*. Clearly, no real source can have zero size, but a real source can be approximated as a point source provided (1) that the volume is sufficiently small, that is, with dimensions much smaller than

the dimensions of the attenuating medium between source and detector, and (2) that there is negligible interaction of radiation with the matter in the source volume. The second requirement may be relaxed if source characteristics are modified to account for source self-absorption and other source–particle interactions.

In general, a point source may be characterized as depending on energy, direction, and time. In almost all cases, time is not treated as an independent variable because the time delay between a change in the source and the resulting change in the radiation field is usually negligible. Therefore, the most general characterization of a point source used here is in terms of energy and direction. Most radiation sources treated in shielding practice are isotropic, so that source characterization requires only knowledge of energy dependence. Radioisotope sources are certainly isotropic, as are fission sources and capture gamma-ray sources.

A careful distinction must be made between the activity of a radioisotope and its source strength. *Activity* is precisely defined as the expected number of atoms undergoing radioactive transformation per unit time. It is *not* defined as the number of particles emitted per unit time. Decay of two very common laboratory radioisotopes illustrate this point. Each transformation of ^{60}Co, for example, results in the emission of two gamma rays, one at 1.173 MeV and the other at 1.333 MeV. Each transformation of ^{137}Cs, accompanied by a transformation of its decay product ^{137m}Ba, results in emission of a 0.662-MeV gamma ray with probability 0.85.

The SI unit of activity is the becquerel (Bq), equivalent to one transformation per second. In medical and health physics, radiation source strengths are commonly calculated on the basis of *accumulated activity*, Bq s. Such time-integrated activities account for the cumulative number of transformations in some biological entity during the transient presence of radionuclides in the entity. Of interest in such circumstances is not the time-dependent dose rate to that entity or some other nearby region, but rather the total dose accumulated during the transient. Similar practices are followed in dose evaluation for reactor transients, solar flares, nuclear weapons, and so on.

Radiation sources may be distributed along a line, over an area, or within a volume. Source characterization requires, in general, spatial and energy dependence. Occasionally, it is necessary to include angular dependence. This is especially true for effective area sources associated with computed angular flows across certain planes. Energy dependence may be discrete, such as for radionuclide sources, or continuous, as for bremsstrahlung or fission neutrons and photons.

Radioactivity

Radioactive Decay Dynamics

The decay of a radioactive nuclide is a stochastic phenomenon. The time an individual radionuclide decays cannot be predicted; rather, only the probability of decay in a specified time interval can be predicted. The rate at which a sample of

a large number of identical radionuclides decays is determined by the *radioactive decay constant* λ for the nuclide. This constant is the probability, per unit time, that a radionuclide decays in an infinitesimal time interval. That λ is constant for a given radionuclide species implies that the expected number of radionuclides, $N(t)$, at time t is $N(t) = N(0)e^{-\lambda t}$, where $N(0)$ is the initial number of radionuclides in the sample. The exponential decay of radionuclides is sometimes called the *radioactive decay law*.

Generally, the number of radionuclides in a sample is not of interest. Rather the *activity* $A(t)$ or rate at which a radionuclide sample decays, $\mathrm{d}N(t)/\mathrm{d}t$, is desired since this quantity determines the rate of radiation emission from the sample. From the radioactive decay law, it is found that $\mathrm{d}N(t)/\mathrm{d}t = \lambda N(t) \equiv A(t)$, so that the activity of a radionuclide sample also decays exponentially, that is, $A(t) = A(0)e^{-\lambda t}$. The standard unit of activity is the becquerel (Bq) equal to one radioactive decay per second. The traditional unit is the curie (Ci) = 3.7×10^{10} Bq (approximately the activity of 1 g of ^{226}Ra).

The rate at which a radioactive sample decays is commonly described by its *half-life* $T_{1/2}$. The half-life is the time required for half of the sample to decay, or, equivalently, for the sample activity to halve. From the radioactive decay law, it is found $T_{1/2} = \ln 2/\lambda \simeq 0.693/\lambda$.

Types of Radioactive Decay

There are several types of spontaneous changes (or *transmutations*) that can occur in radioactive nuclides. In each transmutation, the nucleus of the parent atom ${}^{A}_{Z}\mathrm{P}$ is altered in some manner and one or more particles of radiation are emitted. If the number of protons in the nucleus is changed, then the number of orbital electrons in the daughter atom D must subsequently also be changed, either by releasing an electron to or absorbing an electron from the ambient medium. The most commonly encountered types of radioactive decay are

Gamma decay (γ) ${}^{A}_{Z}\mathrm{P}^{*} \rightarrow {}^{A}_{Z}\mathrm{P} + \gamma$: An excited nucleus decays (usually within 10^{-8} s) to its ground state by the emission of one or more gamma photons. The excited parent is often the product of radioactive decay or a binary nuclear reaction.

Isomeric transition (IT) ${}^{Am}_{Z}\mathrm{P}^{*} \rightarrow {}^{A}_{Z}\mathrm{P} + \gamma$: This is a special case of gamma decay, in which the excited parent has a lifetime much greater than usual nuclear lifetimes (10^{-8} s), ranging from seconds to thousands of years. Such a long-lived excited nucleus is said to be *metastable* and is called an *isomer*.

Internal conversion (IC) ${}^{A}_{Z}\mathrm{P}^{*} \rightarrow \left[{}^{A}_{Z}\mathrm{P}\right]^{+1} + \mathrm{e}^{-}$: The excitation energy of a nucleus is used to eject an orbital electron (usually a K-shell electron).

Alpha decay (α) ${}^{A}_{Z}\mathrm{P} \rightarrow {}^{Z-4}_{Z-2}\mathrm{D} + \alpha$: An α particle is emitted leaving the daughter with 2 fewer neutrons and 2 fewer protons than the parent. The transition often is to an

excited nuclear state of the daughter which decays by emission of one or more gamma photons.

Beta decay (β^-) ${}^{A}_{Z}\mathrm{P} \rightarrow {}^{A}_{Z+1}\mathrm{D} + \beta^- + \bar{\nu}$: In effect, a neutron in the nucleus decays to a proton. An electron (β^-) and antineutrino ($\bar{\nu}$) are emitted, which share the decay energy. The daughter is often produced in an excited nuclear state and subsequently emits gamma photons.

Positron decay (β^+) ${}^{A}_{Z}\mathrm{P} \rightarrow {}^{A}_{Z-1}\mathrm{D} + \beta^+ + \nu$: In effect, a proton in the nucleus changes into a neutron. A positron (β^+) and neutrino (ν) are emitted, which share the decay energy. If the daughter is produced in an excited state, gamma decay results. The emitted positron, after slowing in the ambient medium, annihilates with an ambient electron producing two 0.511-MeV gamma rays.

Electron capture (EC) ${}^{A}_{Z}\mathrm{P} \rightarrow {}^{A}_{Z-1}\mathrm{D}^* + \nu$: An orbital electron is absorbed by the nucleus, converts a nuclear proton into a neutron, emits a neutrino (ν), and, generally, leaves the nucleus in an excited state, which decays by the emission of one or more gamma photons.

Spontaneous fission (SP) ${}^{A}_{Z}\mathrm{P} \rightarrow {}^{A_H}_{Z_H}\mathrm{D}_H + {}^{A_L}_{Z_L}\mathrm{D}_L + n({}^{1}_{0}\mathrm{n}) + m(\gamma)$: A heavy nucleus spontaneously splits or fissions into a heavy (H) and light (L) fission fragment. The fission fragments are produced in highly excited nuclear states and decay by prompt neutron and gamma photon emission within 10^{-13} s of the fission event, releasing, on the average, n neutrons and m γ photons. The resulting *fission products* are usually radioactive and undergo a chain of β^- decays releasing several delayed gamma photons and beta particles until a stable nucleus is reached. In some instances, ternary rather than binary fission takes place, releasing a light product such as tritium.

Many radionuclides decay by more than a single decay mechanism. For example, electron capture is always in competition with positron decay. An example of a radionuclide that decays by three mechanisms is ^{64}Cu whose decay scheme is shown in Fig. 13.1.

In any radioactive decay that alters the proton number Z, electron rearrangements necessarily result. The resulting cascade of orbital electrons to lower energy levels results in emission of x-rays and, in competition, ejection of what are called *Auger electrons*.

Naturally Occurring Radionuclides

Singly Occurring Primordial Radionuclides

Of the many radioactive species present when the earth was formed, only those very few with half-lives comparable to the age of the earth remain in the environment. Of these few primordial radionuclides not belonging to a decay chain, only ^{40}K and ^{87}Rb contribute significantly to human exposure. Of minor consequence

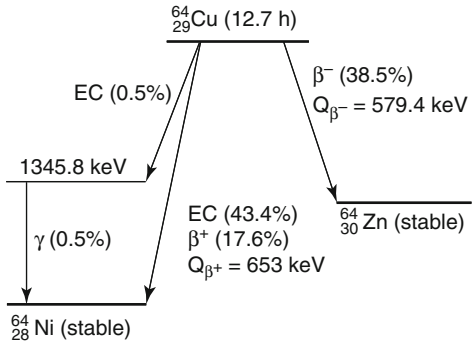

Fig. 13.1 The radioactive decay scheme for ^{64}Cu per decay, on average a beta particle of maximum energy 0.579 MeV is emitted with a probability of 0.385, a positron of maximum energy 0.653 MeV is emitted with a probability of 0.176, and a gamma ray of energy 1.346 MeV is emitted with a probability of 0.005. Source: NUDAT 2.5, National Nuclear Data Center, Brookhaven National Laboratory

are the nuclides ^{138}La, ^{147}Sm, and ^{176}Lu. The radionuclide ^{87}Rb has a half-life of 4.8×10^{10} years and decays by beta-particle emission. In the human body, its main impact is on bone-surface cells. The radionuclide ^{40}K is a major contributor to human exposure from natural radiation. Present in an isotopic abundance of 0.0118%, it has a half-life of 1.227×10^{9} years, decaying both by electron capture and beta-particle emission. Annual human doses are about 140 μGy to bone surface, 170 μGy on average to soft tissue, and 270 μGy to red marrow [1]. ^{40}K also contributes in a major way to external exposure. The population-average specific activity of the nuclide in soil is 420 Bq/kg [2]. Based on a soil density of 1,600 kg/m^3, and dose conversion factors from [3], ^{40}K in the soil contributes 120 μSv effective dose annually.

Decay Series of Terrestrial Origin

Two actinide decay series, identified by the long-lived parents ^{238}U and ^{232}Th contribute appreciably to human exposure to natural radiation. Another series headed by ^{235}U contributes very little. Members of the two important series are listed in Table 13.1. Many of the radionuclides in these series decay by emission of alpha particles with energies from 4 to 6 MeV. Others in the series emit beta particles accompanied by gamma rays. With long-lived parent radionuclides and short-lived daughter products, the chain might be thought to exist in a state of secular equilibrium, that is, each component having the same decay rate per unit volume of the host medium. However, some of the chain members are more soluble than others, and some are gaseous. Thus, unless the host medium is a rigid solid, such as granite, decay rates are far from equilibrium state.

Table 13.1 Principal radioisotopes in two naturally occurring primordial decay series. Source: NUDAT 2.5, National Nuclear Data Center, Brookhaven National Laboratory

Thorium series			Uranium series		
Nuclide and decay mode		Half-life[a] $T_{1/2}$	Nuclide and decay mode		Half-life[a] $T_{1/2}$
$^{232}_{90}$Th	α	**14.05 Gy**	**$^{238}_{92}$U**	α	**4.468 Gy**
$^{228}_{88}$Ra	β	5.75 years	$^{234}_{90}$Th	β	24.10 days
$^{228}_{89}$Ac	β	6.15 h	$^{234m}_{91}$Pa	β	1.159 min
$^{228}_{90}$Th	α	1.912 years	$^{234}_{92}$U	α	245.5 ky
$^{224}_{88}$Ra	α	3.66 days	$^{230}_{90}$Th	α	75.4 ky
$^{220}_{86}$Rn	α	55.6 s	$^{226}_{88}$Ra	α	1,600 years
$^{216}_{84}$Po	α	0.145 s	$^{222}_{86}$Rn	α	3.8235 days
$^{212}_{82}$Pb	β	10.64 h	$^{218}_{84}$Po	α, β	3.098 min
$^{212}_{83}$Bi	α, β	60.55 min	$^{214}_{82}$Pb	β	26.8 min
$^{212}_{84}$Po	α	0.299 μs	$^{214}_{83}$Bi	α, β	19.9 min
$^{208}_{81}$Ti	β	3.053 min	$^{214}_{84}$Po	α, β	164 μs
$^{208}_{82}$Pb		∞	$^{210}_{82}$Pb	β	22.2 years
			$^{210}_{83}$Bi	α, β	5.012 days
			$^{210}_{84}$Po	α	138.4 days
			$^{206}_{82}$Pb		∞

[a]Gy = 10^9 years, ky = 10^3 years, μs = 10^{-6} s

Table 13.2 Annual intake and effective dose from ingestion of uranium, thorium, and daughters. For population weighted averages, apply 5% infants, 30% children, and 65% adults

	Activity intake (Bq/year)			Committed effective dose (μSv/year)		
Nuclide	Infants	Children	Adults	Infants	Children	Adults
^{238}U	1.9	3.8	5.7	0.23	0.26	0.25
^{234}U	1.9	3.8	5.7	0.25	0.28	0.28
^{230}Th	1.0	2.0	3.0	0.42	0.48	0.58
^{226}Ra	7.8	15	22	7.5	12	8.0
^{210}Pb	11	21	30	40	40	28
^{210}Po	21	39	58	180	100	85
^{232}Th	0.6	1.1	1.7	0.26	0.32	0.36
^{228}Ra	5.5	10	15	31	40	21
^{228}Th	1.0	2.0	3.0	0.38	0.30	0.25
^{235}U	0.1	0.2	0.2	0.011	0.011	0.011
Total				260	200	110

Source: Reference [2].

Ingestion of elements in the uranium and thorium decay chains is unavoidable. Table 13.2 illustrates the consequences in terms of the committed effective dose incurred by ingestion but perhaps experienced long thereafter.

The portions of the series headed by the gases ^{220}Rn and ^{222}Rn are of special importance in public health. The gases escape from soil and rock into the atmosphere and into the airspace within homes. Their daughter products, some of which

Table 13.3 Cosmogenic radionuclides and consequential mean doses to the population

Nuclide	Half-life	Global inventory (PBq)	Troposphere conc. (mBq/m^3)	Annual effective dose (μSv/year)
^{3}H	12.32 years	1,275	1.4	0.01
^{7}Be	53.22 days	413	12.5	0.03
^{14}C	5,700 years	12,750	56.3	12
^{22}Na	2.602 years	0.44	0.0021	0.15

Source: Reference [2].

emit alpha particles, may be inhaled, with risk of radiation damage to radiation-sensitive cells in the lungs potentially leading to lung cancer. ^{222}Rn and its daughters ordinarily present a greater hazard than ^{220}Rn (thoron) and its daughters, largely because the much shorter half-life of ^{220}Rn makes decay more likely prior to release into the atmosphere. Globally, the mean annual effective dose equivalent due to ^{222}Rn daughters is about 1 mSv (100 mrem) while that due to ^{220}Rn daughters is estimated to be about 0.2 mSv (20 mrem).

Cosmogenic Radionuclides

Cosmic-ray interactions with constituents of the atmosphere, sea, or earth, but mostly with the atmosphere, lead directly to radioactive products. Capture of secondary neutrons produced in primary interactions of cosmic rays, leads to the formation of many more radionuclides. Of the nuclides produced in the atmosphere, only ^{3}H, ^{7}Be, ^{14}C, and ^{22}Na contribute appreciably to human radiation exposure.

Over the past century, combustion of fossil fuels and the emission of carbon dioxide not containing ^{14}C has diluted the cosmogenic content of ^{14}C in the environment. Moreover, since World War II, artificial introduction of ^{14}C, ^{3}H, and other nuclides into the environment by human activity has been significant, especially as a result of atmospheric nuclear tests. Consequently, these radionuclides no longer exist in natural equilibria in the environment.

The tritium ^{3}H nuclide is produced mainly from interactions of neutrons with nitrogen and oxygen. Tritium has a half-life of 12.3 years and, upon decay, releases one low-energy beta particle of mean energy 5.7 keV. Tritium exists in nature almost exclusively in water form (HTO) but, in foods, may be partially incorporated into organic compounds. The nuclide ^{14}C is produced mainly from the interactions of neutrons with nitrogen in the atmosphere. It exists in the atmosphere as CO_2, but the main reservoir is the ocean. It has a half-life of 5,700 years and decays by beta particle emission of mean energy 49.5 keV.

^{7}Be is also produced by cosmic ray interactions with nitrogen and oxygen in the atmosphere. It decays by electron capture, 10.4% of which events yield a 0.478-MeV gamma ray. ^{22}Na decays by positron emission (90%) and electron capture (10%). The positron emission yields two annihilation photons as well as a positron of mean energy 215 keV. Both the positron emission and electron capture yield a 1.275-MeV gamma ray. Table 13.3 lists natural inventories, atmospheric concentrations, and effective doses to populations. Note that 1 PBq = 10^{15} Bq.

Sources of Neutrons

Fission Neutrons

Many heavy nuclides fission after the absorption of a neutron, or even spontaneously, producing several energetic fission neutrons. Almost all of the fast neutrons produced from a fission event are emitted within 10^{-14} s of the fission event, and are called *prompt neutrons*. Generally, less than 1% of the total fission neutrons are emitted as *delayed neutrons*, which are produced by the neutron decay of fission products at times up to many seconds or even minutes after the fission event. As the energy of the neutron which induces the fission in a heavy nucleus increases, the average number of fission neutrons also increases. For example, the fission of ^{235}U by a thermal neutron (average energy 0.025 eV) produces, on the average, 2.43 fission neutrons. A fission caused by a 10-MeV neutron, by contrast, yields 3.8 fission neutrons. For ^{239}Pu, fission by thermal or 10 MeV neutrons yield 2.87 or 4.2 neutrons. The fission of ^{238}U is induced only by fast neutrons, a 10-MeV neutron yielding 3.9 fission neutrons.

Since the advent of fission reactors, many transuranic isotopes have been produced in significant quantities. Many of these isotopes have appreciable spontaneous fission probabilities, and consequently they can be used as very compact sources of fission neutrons. For example, 1 g of ^{252}Cf releases 2.3×10^{12} neutrons per second, and very intense neutron sources can be made from this isotope, limited in size only by the need to remove the fission heat through the necessary encapsulation. Almost all spontaneously fissioning isotopes decay much more frequently by α emission than by fission.

The energy dependence of the fission neutron spectrum has been investigated extensively, particularly for the important isotope ^{235}U. All fissionable nuclides produce prompt-fission neutrons with energy frequency distributions that go to zero at low and high energies, reaching a maximum at about 0.7 MeV, and have an average energy of about 2 MeV. The fraction of prompt fission neutrons emitted per unit energy about E, $\chi(E)$, can be described quite accurately by a Watt distribution

$$\chi(E) = ae^{-E/b}\sinh\sqrt{cE},$$

where the parameters a, b, and c depend on the fissioning isotope. For example, a = 0.5535 MeV, b = 1.0347 MeV, and c = 1.6214 MeV^{-1} for thermal-neutron fission of ^{235}U, whose fission-neutron spectrum is often used as an approximation for other fissioning isotopes.

Fusion Neutrons

Neutrons can be produced as products of nuclear reactions in which energetic charged particles hit target atoms. Most such reactions require accelerators to produce the energetic charged particles and, hence, such neutrons are to be encountered only near accelerator targets.

One major exception to the insignificance of charged-particle-induced reactions are those in which light elements fuse exoergically to yield a heavier nucleus and which are accompanied quite often by the release of energetic neutrons. The resulting fusion neutrons are usually the major source of radiation to be shielded against. The two neutron-producing fusion reactions of most interest in the development of thermonuclear fusion power are

$$^2\mathrm{H} + {}^2\mathrm{H} \rightarrow {}^3\mathrm{He}(0.82\ \mathrm{MeV}) + {}^1n(2.45\ \mathrm{MeV})$$

$$^2\mathrm{H} + {}^3\mathrm{H} \rightarrow {}^4\mathrm{He}(3.5\ \mathrm{MeV}) + {}^1n(14.1\ \mathrm{MeV}).$$

When these reactions are produced by accelerating one nuclide toward the other, the velocity of the center of mass must first be added to the center-of-mass neutron velocity before determining the neutron energy in the laboratory coordinate system. In most designs for fusion power, the velocity of the center of mass is negligible, and the concern is with monoenergetic 2.45- or 14.1-MeV fusion neutrons. The 14.1-MeV fusion neutrons are also produced copiously in a thermonuclear explosion.

A beam of relatively low-energy deuterons (100–300 keV) incident on a deuterium or tritium target can produce a significant number of thermonuclear neutrons. Thus, these D–D or D–T reactions are used in relatively compact accelerators, called *neutron generators*, in which deuterium ions are accelerated through a high voltage (100–300 kV) and allowed to fall on a thick deuterium- or tritium-bearing target. Typically, in such devices, a 1-mA beam current produces up to 10^9 14-MeV neutrons per second from a thick tritium target.

Photoneutrons

A gamma photon with energy sufficiently large to overcome the neutron binding energy (about 7 MeV in most nuclides) may cause a (γ,n) reaction. Very intense and energetic photoneutron production can be realized in an electron accelerator where the bombardment of an appropriate target material with the energetic electrons produces intense bremsstrahlung (see "Sources of X-rays") with a distribution of energies up to that of the incident electrons. The probability a photon will cause a (γ,n) reaction increases with the photon energy, reaching a maximum over a broad

energy range of approximately 20–23 MeV for light nuclei ($A \lesssim 40$) and 13–18 MeV for medium and heavy nuclei. The peak energy of this broad (often called *giant*) nuclear resonance can be approximated by $80\,A^{-1/3}$ MeV for $A > 40$. The width of the resonance varies from about 10 MeV for light nuclei to 3 MeV for heavy nuclei. Consequently, in medical or accelerator facilities that produce photons with energies above about 15 MeV, neutron production in the surrounding walls can lead to a significant neutron field.

However, the gamma photons produced in radioactive decay of fission and activation products in nuclear reactors generally have energies too low, and most materials have a photoneutron threshold too high for photoneutrons to be of concern. Only for the light elements ^{2}H, ^{6}Li, ^{7}Li, ^{9}Be, and ^{12}C are the thresholds for photoneutron production sufficiently low that these secondary neutrons may have to be considered. In heavy-water- or beryllium-moderated reactors, the photoneutron source may be very appreciable, and the neutron field deep within an hydrogenous shield is often determined by photoneutron production in deuterium, which constitutes about 0.015 atom percent of the hydrogen. Capture gamma photons arising from neutron absorption have particularly high energies, and thus may also cause a significant production of energetic photoneutrons.

The photoneutron mechanism can be used to create laboratory neutron sources by mixing intimately a beryllium or deuterium compound with a radioisotope that decays with the emission of high-energy photons. Alternatively, the encapsulated radioisotope may be surrounded by a beryllium- or deuterium-bearing shell. A common reactor photoneutron source is an antimony–beryllium mixture, which has the advantage of being rejuvenated by exposing the source to the neutrons in the reactor to transmute the stable ^{123}Sb into the required ^{124}Sb isotope (half-life of 60.2 days).

One very attractive feature of such (γ,n) sources is the nearly monoenergetic nature of the neutrons if the photons are monoenergetic. However, in large sources, the neutrons may undergo significant scattering in the source material and thereby degrade the nearly monoenergetic nature of their spectrum. These photoneutron sources generally require careful use because of their inherently large photon emission rates. Because nominally only one in a million high-energy photons actually interacts with the source material to produce a neutron, these sources generate gamma rays that are of far greater biological concern than are the neutrons.

Alpha-Neutron Sources

Many compact laboratory neutron sources use energetic alpha particles from various radioisotopes (*emitters*) to induce (α,n) reactions in appropriate materials (*converters*). Although a large number of nuclides emit neutrons if bombarded with alpha particles of sufficient energy, the energies of the alpha particles from radioisotopes are capable of penetrating the potential barriers of only the lighter nuclei.

Of particular interest are those light isotopes for which the (α,n) reaction is exoergic ($Q > 0$) or, at least, has a low threshold energy. For endoergic reactions ($Q > 0$), the threshold alpha energy is $-Q\,(1 + 4/A)$. Thus, for an (α,n) reaction to occur, the alpha particle must (1) have enough energy to overcome the repulsive Coulombic force field of the nucleus, and (2) exceed the threshold energy for the reaction. Converter materials used to make practical (α,n) sources include lithium, beryllium, boron, carbon, fluorine, and sodium.

The converter nuclides ^{18}O and ^{19}F are responsible for neutron production in many areas of the nuclear fuel cycle. Alpha particles emitted by uranium and plutonium range between 4 and 6 MeV in energy and can cause (α,n) neutron production when in the presence of oxygen or fluorine. In particular, (α,n) neutrons often dominate the spontaneous fission neutrons in UF_6 or in aqueous mixtures of uranium and plutonium such as found in nuclear waste.

A neutron source can be fabricated by mixing intimately a light converter element, such as lithium or beryllium, with a radioisotope that emits energetic alpha particles. Most of the practical alpha emitters are actinide elements, which form intermetallic compounds with beryllium. Such a compound, for example, $PuBe_{13}$, ensures both that the emitted alpha particles immediately encounter converter nuclei, thereby producing a maximum neutron yield, and that the radioactive actinides are bound into the source material, thereby reducing the risk of leakage of the alpha-emitting component.

The neutron yield from an (α,n) source varies strongly with the converter material, the energy of the alpha particle, and the relative concentrations of the emitter and converter elements. The degree of mixing between converter and emitter and the size, geometry, and source encapsulation may also affect the neutron yield. For example, a ^{239}Pu/Be source has an optimum neutron yield of about 60 neutrons per 10^6 primary alpha particles.

The energy distributions of neutrons emitted from (α,n) sources are continuous below some maximum neutron energy with definite structure at well-defined energies determined by the energy levels of the converter and the excited product nuclei. The use of the same converter material with different alpha emitters produces similar neutron spectra with different portions of the same basic spectrum accentuated or reduced as a result of the different alpha-particle energies. Average energies of neutrons typically are several MeV. For example, the neutrons produced by a ^{239}Pu/Be source have an average energy of 4.6 MeV.

Activation Neutrons

A few highly unstable nuclides decay by the emission of a neutron. The delayed neutrons associated with fission arise from such decay of the fission products. However, there are nuclides other than those in the fission-product decay chain which also decay by neutron emission. Only one of these nuclides, ^{17}N, is of

importance in nuclear reactor situations. This isotope is produced in water-moderated reactors by an (*n,p*) reaction with ^{17}O (threshold energy, 8 MeV). The decay of ^{17}N by beta emission (half-life 4.4 s) produces ^{17}O in a highly excited state, which in turn decays rapidly by neutron emission. Most of the decay neutrons are emitted within ± 0.2 MeV of the most probable energy of about 1 MeV, although neutrons with energies up to 2 MeV may be produced.

Spallation Neutron Sources

In a spallation neutron source, pulses of very energetic protons (up to 1 GeV), produced by an accelerator, strike a heavy metal target such as mercury or liquid bismuth. Such an energetic proton when it strikes a target nucleus "spalls" or knocks out neutrons. Additional neutrons boil off as the struck nucleus heats up. Typically, 20–30 neutrons are produced per spallation reaction. These pulses of neutrons are then slowed down or thermalized by passing them through cells filled with water, or even liquid hydrogen if very slow neutrons are needed.

Sources of Gamma Photons

Radioactive Decay

Radioactive sources serve a wide variety of purposes in educational, medical, research, industrial, governmental, and commercial activities. The radionuclides in these sources almost always leave their decay daughters in excited nuclear states whose subsequent transitions to lower-energy states usually result in the emission of one or more gamma photons.

Prompt Fission Photons

The fission process produces copious gamma photons either within the first 6×10^{-8} s after the fission event (the *prompt fission gamma photons*) or from the subsequent decay of the fission products. These photons are of extreme importance in the shielding and gamma-heating calculations for a nuclear reactor. Consequently, much effort has been directed toward determining their nature.

Most investigations of prompt fission gamma photons have centered on the thermal-neutron-induced fission of ^{235}U. For this nuclide, it has been found that the number of prompt fission photons is 8.13 ± 0.35 photons per fission over the

energy range 0.1–10.5 MeV, and the energy carried by this number of photons is 7.25 ± 0.26 MeV per fission. The energy spectrum of prompt gamma photons from the thermal fission of ^{235}U between 0.1 and 0.6 MeV is approximately constant at 6.6 photons MeV^{-1} fission^{-1}. At higher energies, the spectrum falls off sharply with increasing energy. The measured energy distribution of the prompt fission photons can be represented by the following empirical fit over the range 0.1–10.5 MeV:

$$N(E) = \begin{cases} 6.6 & 0.1 < E < 0.6 \text{ MeV} \\ 20.2e^{-1.78E} & 0.6 < E < 1.5 \text{ MeV} \\ 7.2e^{-1.09E} & 1.5 < E < 10.5 \text{ MeV}, \end{cases}$$

where E is in MeV and $N(E)$ is in units of photons MeV^{-1} fission^{-1}.

Investigation of ^{233}U, ^{239}Pu, and ^{252}Cf indicates that the prompt fission photon energy spectra for these isotopes resembles very closely that for ^{235}U, and hence for most purposes, it is reasonable to use the ^{235}U spectrum for other fissioning isotopes.

Fission-Product Photons

With the widespread application of nuclear fission, an important concern is the consideration of the very long lasting gamma activity produced by the decay of fission products.

In the fission process, most often two fragments are produced (*binary fission*) with a distribution in mass shown in Fig. 13.2. About 0.3% of the time, a third light fragment is produced (*ternary fission*), most often ^{3}H. As seen in Fig. 13.2, the mass distribution or *fission-product chain yield* is bimodal, with many products having atomic mass number around 95 and around 140. Among the former are the important long-lived radionuclide ^{90}Sr, several isotopes of the halogen bromine, and various isotopes of the noble gas krypton. Among the heavy fragments are the important long-lived radionuclide ^{137}Cs, radioisotopes of halogen iodine, notably ^{131}I, and isotopes of the noble gas xenon. The fission-products are neutron-rich and decay almost exclusively by β^- emission, often forming long decay chains. From the range of mass numbers produced (see Fig. 13.2), about 100 different decay chains are formed. An example of a short chain is

$$^{140}_{54}\text{Xe} \xrightarrow[16\,\text{s}]{\beta^-} {}^{140}_{55}\text{Cs} \xrightarrow[66\,\text{s}]{\beta^-} {}^{140}_{56}\text{Ba} \xrightarrow[12.8\,\text{days}]{\beta^-}$$
$$^{140}_{57}\text{La} \xrightarrow[40\,\text{h}]{\beta^-} {}^{140}_{58}\text{Ce}(\text{stable}).$$

The total gamma-ray energy released by the fission product chains is comparable to that released as prompt fission gamma photons. The gamma-ray energy release rate declines rapidly in the time after fission. About three-fourths of the delayed

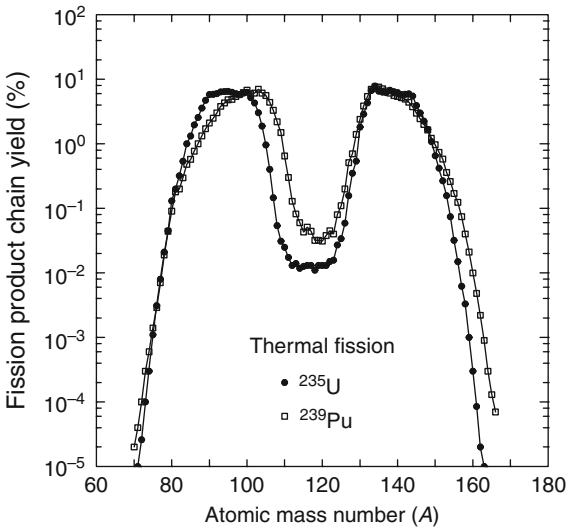

Fig. 13.2 The probability (%) that a fission product with mass number A is produced in the thermal-neutron-induced fission of ^{235}U and ^{239}Pu

gamma-ray energy is released in the first 1,000 s after fission. In most calculations involving spent nuclear fuel, the gamma activity at several months or even years after removal of fuel from the nuclear reactor is of interest and only the long-lived fission products need be considered.

It has been found that the gamma energy released from fission products is relatively independent of the energy of the neutrons causing the fissions. However, the gamma-ray energy released and the photon energy spectrum depend significantly on the fissioning isotope, particularly in the first 10 s after fission. Generally, fissioning isotopes having a greater proportion of neutrons to protons produce fission-product chains of longer average length, with isotopes richer in neutrons and hence with greater available decay energy. Also, the photon energy spectrum generally becomes less energetic as the time after fission increases.

For very approximate calculations, the energy spectrum of delayed gamma photons from the fission of ^{235}U, at times up to about 500 s, may be approximated by the proportionality $N(E) \sim e^{-1.1E}$, where $N(E)$ is the delayed gamma yield (photons MeV^{-1} fission^{-1}) and E is the photon energy in MeV. The time dependence for the total gamma photon energy emission rate $F(t)$ (MeV s^{-1} fission^{-1}) is often described by the simple decay formula $F(t) = 1.4\, t^{-1.2}$, 10 s $< t < 10^7$ s, where t is in seconds. More complicated (and accurate) expressions for $F(t)$ have been obtained from fits to experimental data; but for preliminary calculations the simpler result is usually adequate. It is observed that both ^{235}U and ^{239}Pu have roughly the same total gamma-ray-energy decay characteristics for up to 200 days after fission, at which time ^{235}U products begin to decay more rapidly until at 1 year after fission, the ^{239}Pu gamma activity is about 60% greater than that of ^{235}U.

For accurate calculations involving fission products, the variation with time after fission of the energy spectra of the photons must be taken into account. Often the energy spectra are averaged over discrete energy intervals and the energy emission

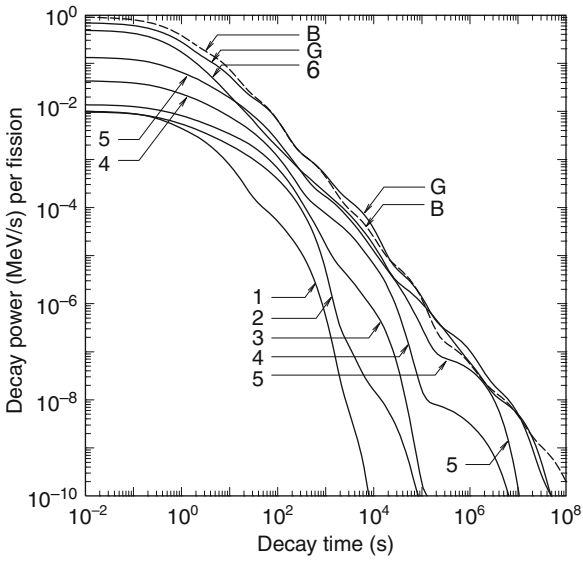

Fig. 13.3 Total gamma-ray (G) and beta-particle (B) energy emission rates as a function of time after the thermal fission of ^{235}U. The curves identified by the numbers 1–6 are gamma emission rates for photons in the energy ranges 5–7.5, 4–5, 3–4, 2–3, 1–2, and 0–1 MeV, respectively

rate in each energy group is considered as a function of time after fission. Computer codes, based on extensive libraries of radionuclide data, have been developed to compute the abundances and decay rates of the hundreds of fission-product radionuclides. An example of such calculations is shown in Fig. 13.3.

Capture Gamma Photons

The compound nucleus formed by neutron absorption is initially created in a highly excited state with excitation energy equal to the kinetic energy of the incident neutron plus the neutron binding energy, which averages about 7 MeV. The decay of this nucleus, usually within 10^{-12} s, and usually by way of intermediate states, typically produces several energetic photons. Generally, the probability a neutron causes an (n,γ) reaction is greatest for slow-moving *thermal neutrons*, that is, neutrons whose speed is in equilibrium with the thermal motion of the atoms in a medium. At high energies, it is more likely that a neutron scatters, thereby losing some of its kinetic energy, and then slows toward thermal energies.

Capture photons may be created intentionally by placing a material with a high thermal-neutron (n,γ) cross section in a thermal neutron beam. The energy spectrum of the resulting capture gamma photons can then be used to identify trace elements in the sample. More often, however, capture gamma photons are an undesired secondary source of radiation.

Inelastic Scattering Photons

The excited nucleus formed when a neutron is inelastically scattered decays to the ground state within about 10^{-14} s, with the excitation energy being released via one or more photons. Because of the constraints imposed by the conservation of energy and momentum in all scattering interactions, inelastic neutron scattering cannot occur unless the incident neutron energy is greater than $(A + 1)/A$ times the energy required to excite the scattering nucleus to its first excited state. Except for the heavy nuclides, neutron energies above about 0.5 MeV are typically required for inelastic scattering.

The detailed calculation of secondary photon source strengths from inelastic neutron scattering requires knowledge of the fast-neutron fluence, the inelastic scattering cross sections, and spectra of resultant photons, all as functions of the incident neutron energy. The cross sections and energy spectra of the secondary photons depend strongly on the incident neutron energy and the particular nuclide. Such inelastic scattering data are known only for the more important structural and shielding materials, and even the known data require extensive data libraries. Fortunately, in most situations, these secondary photons are of little importance compared to the capture photons. Although inelastic neutron scattering is usually neglected with regard to its secondary-photon radiation, it is a very important mechanism in the attenuation of fast neutrons, better even than elastic scattering in some cases.

Activation Photons

For many materials, absorption of a neutron produces a radionuclide with a half-life ranging from a fraction of a second to many years. The radiation produced by the subsequent decay of these activation nuclei may be very significant for materials that have been exposed to large neutron fluences, especially structural components in a reactor or accelerator. Many radionuclides encountered in research laboratories, medical facilities, and industry are produced as activation nuclides from neutron absorption in some parent material (see Table 13.4). Such nuclides decay, usually by beta emission, leaving the daughter nucleus in an excited state, which usually decays quickly to its ground state with the emission of one or more gamma photons. Thus, the apparent half-life of the photon emitter is that of the parent (or activation nuclide), while the number and energy of the photons are characteristic of the nuclear structure of the decay daughter.

Although most activation products of concern in shielding problems arise from neutron absorption, there is one important exception in water-moderated nuclear reactors. The ^{16}O in the water can be transmuted to ^{16}N in the presence of fission neutrons by an (n,p) reaction with a threshold energy of 9.6 MeV. ^{16}N decays with a 7.4-s half-life emitting gamma photons of 6.13 and 7.10 MeV (yields of 0.69 and 0.05 per decay). This gamma-ray source is very important in coolant channels of power reactors.

Table 13.4 Important radioisotopes produced by reactors and accelerators for use in medical, research, and industrial applications. Those isotopes commercially available for medical use are shown in bold. Decay data from NUDAT 2.5, National Nuclear Data Center, Brookhaven National Laboratory

Nuclide	Half-life	Decay modes[a]	Nuclide	Half-life	Decay modes[a]
^{3}H	12.33 years	β^- *	^{81m}Kr	13.1 s	EC IT
^{11}C	20.39 min	β^+ EC	^{85}Kr	10.76 years	β^-
^{13}N	9.965 min	β^+ EC	**^{82}Sr**[b]	25.6 days	EC *
^{14}C	5,730 years	β^- *	**^{89}Sr**	50.5 days	β^-
^{15}O	122.2 s	β^+ EC	**^{90}Sr**[c]	28.90 years	β^- *
^{18}F	109.8 min	β^+ EC	**^{99}Mo**[d]	65.94 h	β^-
^{22}Na	2.602 years	β^+ EC	^{103}Pd	16.99 days	EC
^{26}Al	7.17E5 years	β^+ EC	^{110m}Ag	249.8 days	β^- IT
^{28}Mg	20.91 h	β^-	**^{111}In**	2.80 days	EC
^{32}Si	153 years	β^- *	^{113m}In	99.48 min	IT
^{32}P	14.26 days	β^- *	**^{123}I**	13.27 h	EC
^{33}P	25.3 days	β^- *	**^{125}I**	59.40 days	EC
^{35}S	87.51 days	β^- *	**^{131}I**	8.025 days	β^-
^{36}Cl	3.01E5 years	$\beta^\pm$ EC	**^{133}Xe**	5.243 days	β^-
^{46}Sc	83.79 days	β^-	^{137}Cs[e]	30.1 years	β^- *
^{51}Cr	27.70 days	EC	^{140}La	1.679 days	β^-
^{54}Mn	312.1 days	β^- EC	^{148}Gd	70.9 years	α *
^{57}Co	271.7 days	EC	**^{153}Sm**	46.3 h	β^-
^{57}Cu	196 ms	β^+ EC	^{159}Gd	18.48 h	β^-
^{57}Cr	21.1 s	β^- *	^{169}Yb	32.02 days	EC
^{59}Fe	44.50 days	β^-	^{170}Tm	128.6 days	β^- EC
^{60}Co	5.271 years	β^-	^{186}Re	89.25 h	β^- EC
^{64}Cu	12.70 h	$\beta^\pm$ EC	^{191}Os	15.4 days	β^-
^{65}Zn	244.1 days	β^+ EC	^{192}Ir	73.83 days	β^- EC
^{67}Ga	3.261 days	EC	^{198}Au	2.696 days	β^-
^{68}Ga	67.71 min	β^+ EC	**^{201}Tl**	73 h	EC
^{75}Se	119.8 days	EC	^{204}Tl	3.78 years	β^- EC *
^{81}Rb	4.570 h	β^+ EC	^{210}Pb	22.2 years	$\alpha\beta^-$
^{82}Rb	1.273 min	β^+ EC	^{241}Am	432.6 years	α

[a]Decays without any gamma photon emission are denoted by *
[b]In equilibrium with decay product ^{32}Rb (1.273 min, β^+ EC)
[c]In equilibrium with decay product ^{90}Y (64 h, β^-)
[d]In equilibrium with decay product ^{99m}Tc (6.01 h, IT)
[e]In equilibrium with decay product ^{137m}Ba (2.552 min, IT)
Source: References [4, 5].

Positron Annihilation Photons

Positrons, generated either from the positron decay of radionuclides or from pair production interactions induced by high-energy photons, slow down in matter within about 10^{-10} s and are subsequently annihilated with electrons. With rare exception, the rest-mass energy of the electron and positron is emitted in the form of two annihilation photons, each of energy $m_e c^2$ (= 0.511 MeV).

Sources of X-rays

The interaction of photons or charged particles with matter leads inevitably to the production of secondary x-ray photons. The x-rays in many applications have energies $\lesssim$100 keV, and hence are easily attenuated by any shield adequate for the primary radiation. Consequently, the secondary x-rays are often completely neglected in analyses involving higher-energy photons. There are many cases, though, when the energies of x-rays and Auger electrons must be accounted for as well as those of the x-rays. An example is the evaluation of radiation dose to the total body, or an organ of the body, after a radionuclide intake. This is a situation in which the source and receiver volumes may be the same.

There are important situations in which x-ray production is the only source of photons. To estimate the intensity, energies, and doses from the x-ray photons, it is necessary to understand how the x-rays are produced and some characteristics of the production mechanisms. There are two principal methods whereby secondary x-ray photons are generated: the rearrangement of atomic electron configurations leads to characteristic x-rays, and the deflection of charged particles in the nuclear electric field results in bremsstrahlung.

Characteristic X-rays and Fluorescence

The electrons around a nucleus are arranged in shells or layers, each of which can hold a maximum number of electrons. The two electrons in the innermost shell (K shell) are the most tightly bound, the six electrons in the next shell (L shell) are the next most tightly bound, and so on outward for the M, N,... shells. If the normal electron arrangement around a nucleus is altered, say by ejection of an inner electron, the electrons begin a complex series of transitions to vacancies in the inner shells (thereby acquiring higher binding energies) until the unexcited state of the atom is achieved. In each electronic transition, the difference in binding energy between the final and initial states is either emitted as a photon, called a *characteristic x-ray*, or given up to another electron which is ejected from the atom, called an *Auger electron*. The discrete electron energy levels and the transition probabilities between levels vary with the Z number of the atom, and thus the characteristic x-rays provide a unique signature for each element.

The number of x-rays with different energies is greatly increased by the multiplicity of electron energy levels available in each shell (1, 3, 5, 7, ... distinct energy levels for the K, L, M, N, ... shells, respectively). To identify the various characteristic x-rays for an element, many different schemes have been proposed. One of the more popular uses the letter of the shell whose vacancy is filled together with a numbered Greek subscript to identify a particular electron transition (e.g., $K_{\alpha 1}$ and $L_{\gamma 5}$).

Production of Characteristic X-Rays

There are several methods whereby atoms may be excited and characteristic x-rays produced. A photoelectric absorption leaves the absorbing atom in an ionized state. If the incident photon energy is sufficiently greater than the binding energy of the *K*-shell electron, which ranges from 14 eV for hydrogen to 115 keV for uranium, it is most likely (80–100%) that a vacancy is created in the *K* shell and thus that the *K* series of x-rays dominates the subsequent secondary radiation. These x-ray photons produced from photoelectric absorption are often called *fluorescent radiation* and are widely used to identify trace elements in a sample by bombarding the sample with low-energy photons from a radioactive source or with x-rays from an x-ray machine and then observing the induced fluorescent radiation.

Characteristic x-rays can also arise following the decay of a radionuclide. In the decay process known as *electron capture*, an orbital electron, most likely from the *K* shell, is absorbed into the nucleus, thereby decreasing the nuclear charge by one unit. The resulting *K*-shell vacancy then gives rise to the *K* series of characteristic x-rays. A second source of characteristic x-rays which occurs in many radionuclides is a result of *internal conversion*. Most daughter nuclei formed as a result of any type of nuclear decay are left in excited states. This excitation energy may be either emitted as a gamma photon or transferred to an orbital electron which is ejected from the atom. Again, it is most likely that a *K*-shell electron is involved in this internal conversion process.

X-Ray Energies

To generate a particular series of characteristic x-rays, an electron vacancy must be created in an appropriate electron shell. Such vacancies are created only when sufficient energy is transferred to an electron in that shell so as to allow it to break free of the atom or at least be transferred to an energy level above all the other electrons. The characteristic x-rays emitted when electrons fill a vacancy in a shell always have less energy than that required to create the vacancy. The most energetic x-rays arise from an electron filling a *K*-shell vacancy and, since the binding energy of *K*-shell electrons increases with the atomic number *Z*, the most energetic x-rays are *K*-shell x-rays from heavy atoms. For example, the K_α x-ray energy varies from only 0.52 keV for oxygen ($Z = 8$) to 6.4 keV for iron ($Z = 26$) to 98 keV for uranium ($Z = 92$). By comparison, the *L* series of x-rays for uranium occurs at energies around 15 keV. Thus, in most shielding situations, only the *K* series of x-rays from heavy elements are sufficiently penetrating to be of concern.

X-Ray Yields

The *fluorescent yield* of a material is the fraction of the atoms with a vacancy in an inner electron shell that emit an x-ray upon the filling of the vacancy. The fluorescent yield increases dramatically with the *Z* number of the atom.

For example, the fluorescent yield for vacancies in the K shell increases from 0.0069 for oxygen ($Z = 8$) to 0.97 for uranium ($Z = 92$). Thus, the secondary fluorescent radiation is of more concern for heavy materials.

Bremsstrahlung

A charged particle gives up its kinetic energy either by collisions with electrons along its path or by photon emission as it is deflected, and hence accelerated, by the electric fields of nuclei. The photons produced by the deflection of the charged particle are called *bremsstrahlung* (literally, "braking radiation"). For a given type of charged particle, the ratio of the rate at which the particle loses energy by bremsstrahlung to that by ionizing and exciting the surrounding medium is

$$\frac{\text{Radiation loss}}{\text{Ionization loss}} \simeq \frac{EZ}{700}\left(\frac{m_e}{M}\right)^2,$$

where E is in MeV, m_e is the electron mass, and M is the mass of the charged particle. From this result, it is seen that bremsstrahlung is more important for high-energy particles of small mass incident on high-Z material. In shielding situations, only electrons ($m_e/M = 1$) are ever of importance for their associated bremsstrahlung. All other charged particles are far too massive to produce significant amounts of bremsstrahlung. Bremsstrahlung from electrons, however, is of particular radiological interest for devices that accelerate electrons, such as betatrons and x-ray tubes, or for situations involving radionuclides that emit only beta particles.

Energy Distribution of Bremsstrahlung

The energy distribution of the photons produced by the bremsstrahlung mechanism is continuous up to a maximum energy corresponding to the maximum kinetic energy of the incident charged particles. The exact shape of the continuous bremsstrahlung spectrum depends on many factors, including the energy distribution of the incident charged particles, the thickness of the target, and the amount of bremsstrahlung absorbed in the target and other masking material.

For monoenergetic electrons of energy E_o incident on a target thick compared to the electron range, the number of bremsstrahlung photons of energy E, per unit energy and per incident electron, emitted as the electron is completely slowed down can be approximated by the Kramer distribution

$$N(E_o, E) \simeq 2kZ\left(\frac{E_o}{E} - 1\right), \qquad E \leq E_o,$$

where $k \simeq 0.0007\ \text{MeV}^{-1}$ is a normalization constant. The fraction of the incident electron's kinetic energy that is subsequently emitted as bremsstrahlung can then be calculated from this approximation as kZE_o, which is usually a small fraction. For example, about 10% of the energy of a 2-MeV electron, when stopped in lead, is converted into bremsstrahlung.

Angular Distribution of Bremsstrahlung

The angular distribution of bremsstrahlung is generally quite anisotropic and varies with the incident electron energy. Bremsstrahlung induced by low-energy electrons ($\lesssim$100 keV) is emitted over a relatively broad range of directions around the direction of the incident electron. As the electron energy increases, the direction of the peak intensity shifts increasingly toward the forward direction until, for electrons above a few MeV, the bremsstrahlung is confined to a very narrow forward beam. The angular distribution of radiation leaving a target is very difficult to compute since it depends on the target size and orientation. For thin targets, the anisotropy of the bremsstrahlung resembles that for a single electron–nucleus interaction, while for thick targets multiple electron interactions and photon absorption in the target must be considered.

X-ray Machines

The production of x-ray photons as bremsstrahlung and fluorescence occurs in any device that produces high-energy electrons. Devices that can produce significant quantities of x-rays are those in which a high voltage is used to accelerate electrons, which then strike an appropriate target material. Such is the basic principle of all x-ray tubes used in medical diagnosis and therapy, industrial applications, and research laboratories.

Although there are many different designs of x-ray sources for different applications, most designs for low-to-medium voltage sources ($\lesssim$180 kV) place the electron source (cathode) and electron target (anode) in a sealed glass tube. The glass tube acts as both an insulator between the anode and cathode and a chamber for the necessary vacuum through which the electrons are accelerated. The anodes of x-ray tubes incorporate a suitable metal upon which the electrons impinge and generate the bremsstrahlung and characteristic x-rays. Most of the electron energy is deposited in the anode as heat rather than being radiated away as x-rays, and thus heat removal is an important aspect in the design of x-ray tubes. Tungsten is the most commonly used target material because of its high atomic number and because of its high melting point, high thermal conductivity, and low vapor pressure. Occasionally, other target materials are used when different characteristic x-ray energies are desired. For most medical and dental diagnostic units, voltages

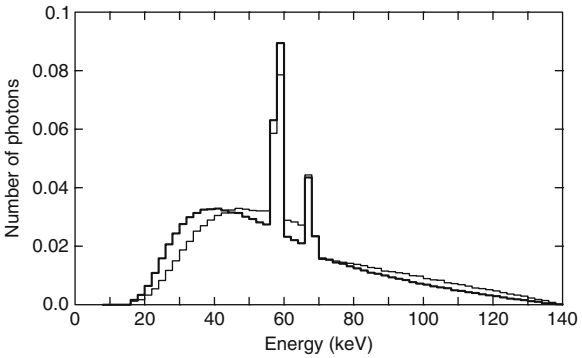

Fig. 13.4 Measured photon spectra from a Machlett Aeromax x-ray tube (tungsten anode) operated at a constant 140 kV potential. This tube has an inherent filter thickness of 2.50-mm aluminum equivalent and produces the spectrum shown by the thick line. The addition of an external 6-mm aluminum filter hardens the spectrum shown by the thin line. Both spectra are normalized to unit area. Data are from [6]

between 40 and 150 kV are used, while medical therapy units may use 6–150 kV for superficial treatment or 180 kV to 50 MV for treatment requiring very penetrating radiation.

The energy spectrum of x-ray photons emitted from an x-ray tube has a continuous bremsstrahlung component up to the maximum electron energy, that is, the maximum voltage applied to the tube. If the applied voltage is sufficiently high as to cause ionization in the target material, there will also be characteristic x-ray lines superimposed on the continuous bremsstrahlung spectrum. Absorbing filters are used to minimize low-energy x-rays, which are damaging to skin. As the beam filtration increases, the low-energy x-rays are preferentially attenuated and the x-ray spectrum *hardens* and becomes more penetrating. These phenomena are illustrated in Fig. 13.4. Calculated exposure spectra of x-rays are shown for the same operating voltage but for two different amounts of beam filtration. As the filtration increases, lower energy x-rays are preferentially attenuated; the spectrum hardens and becomes more penetrating. Readily apparent in these spectra are the tungsten $K_{\alpha 1}$ and $K_{\alpha 2}$ characteristic x-rays.

The characteristic x-rays may contribute a substantial fraction of the total x-ray emission. For example, the *L*-shell radiation from a tungsten target is between 20% and 35% of the total energy emission when voltages between 15 and 50 kV are used. Above and below this voltage range, the *L* component rapidly decreases in importance. However, even a small degree of filtering of the x-ray beam effectively eliminates the low-energy portion of the spectrum containing the *L*-shell x-rays. The higher-energy *K*-series x-rays from a tungsten target contribute a maximum of 12% of the x-ray emission from the target for operating voltages between 100 and 200 kV.

Synchrotron Photons

When a charged particle moving in a straight line is accelerated by deflecting it in an electromagnetic field, the perturbation in the particle's electric field travels away from the particle at the speed of light and is observed as electromagnetic radiation (photons). Such is the origin of bremsstrahlung produced when fast electrons (beta particles) are deflected by the electric field of a nucleus.

This same mechanism can be used to produce intense photon radiation by deflecting an electron beam by magnetic fields. In a special accelerator called a *synchrotron*, highly relativistic electrons are forced to move in a circular path inside a storage ring by placing *bending magnets* along the ring. Photons are emitted when the beam is accelerated transversely by (1) the bending magnets (used to form the circular electron beam), and by (2) insertion device magnets such as *undulators*, *wigglers*, and *wavelength shifters*.

Because the electrons are very relativistic, the synchrotron radiation is emitted in a very narrow cone in the direction of electron travel as they are deflected. Undulators cause the beam to be deflected sinusoidally by a weak oscillatory magnetic field, thereby producing nearly monochromatic photons. By contrast, a wiggler uses a strong oscillatory magnetic field which, because of relativistic effects, produces distorted sinusoidal deflections of the electron beam and synchrotron radiation with multiple harmonics, that is, a line spectrum. If very strong magnetic fields are used, many harmonics are produced that merge to yield a continuous spectrum ranging from the infrared to hard x-rays. By placing undulators or wigglers at a specific location in the storage ring, very intense and narrowly collimated beams of photons with energies up to a few keV can be produced to use, for example, in x-ray diffraction analysis.

Cosmic Rays, Solar Radiation, and Trapped Radiation Belts

The earth is subjected continuously to radiation with sources in our sun and its corona, from sources within our galaxy, and from sources beyond our galaxy. In addition, surrounding the earth are belts of trapped particles with solar origins. Radiation reaching the earth's atmosphere consists of high-energy electrons and atomic nuclei. Hydrogen nuclei (protons) constitute the major component, with heavier atoms decreasing in importance with increasing atomic number. The highest energy particles originate in our galaxy and more distant galaxies and are referred to as galactic cosmic radiation (GCR). Cascades of nuclear interactions in the atmosphere give rise to many types of secondary particles. Of much lower energy are particles of solar origin, which are highly variable in time and are associated with solar activity. Sources of these particles are sometimes associated with solar flares but are more generally identified with solar particle events (SPE) or coronal mass ejections (CME). The number of solar flare events and SPE emissions

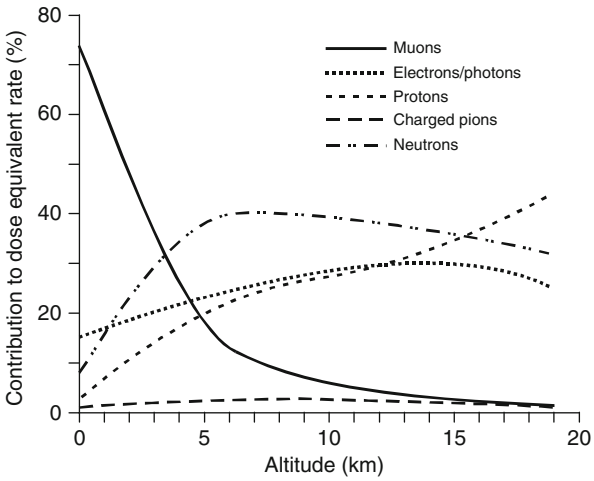

Fig. 13.5 Components of the dose equivalent rate from cosmic rays in the atmosphere (Reproduced from [2], derived from [5])

fluctuate with the 11-year cycle associated with solar activity. GCR intensity is modulated by SPE emissions, being minimal when solar activity is maximal.

Galactic Cosmic Radiation

At the earth's surface, cosmic radiation dose rates are largely due to muons and electrons. The intensity and angular distribution of galactic radiation reaching the earth is affected by the earth's magnetic field and perturbed by magnetic disturbances generated by solar flare activity. Consequently, at any given location, cosmic ray doses may vary in time by a factor of 3. At any given time, cosmic ray dose rates at sea level may vary with geomagnetic latitude by as much as a factor of 8, being greatest at the pole and least at the equator. Cosmic ray dose rates also increase with altitude. At geomagnetic latitude 55°N, for example, the absorbed dose rate in tissue approximately doubles with each 2.75 km (9,000 ft) increase in altitude, up to 10 km (33,000 ft). Fig. 13.5 illustrates the relative importance, in terms of dose rate, for cosmic rays and their reaction products in the atmosphere. Cosmic ray dose rates affecting populations vary strongly with latitude. Table 13.5 describes this variation. The outdoor and indoor average effective dose rates for space radiation in the most heavily populated urban areas in the USA are 45 and 36 nSv/h [7]. Population averaged annual doses are about the same in the northern and southern hemispheres, and globally amount to 31 nSv/h for charged particles plus 5.5 nSv/h for neutrons. GCR energies span a vast range and there is no way of shielding astronauts from GCR effects. On the earth's surface, the GCR presence results in a source of steady low-dose-rate radiation.

As a result of nuclear reactions of cosmic rays with constituents of the atmosphere, secondary neutrons, protons, and pions, mainly, are produced. Subsequent

Table 13.5 Cosmic ray dose rate variation at sea level as a function of latitude for the northern and southern hemispheres

		Effective dose rate (nSv/h)	
Latitude (deg N–S)	Population% in latitude band (N–S)	Charged particles	Neutrons
60–70	0.4–0	32	10.9
50–60	13.7–0.5	32	10
40–50	15.5–0.9	32	7.8
30–40	20.4–13	32	5.3
20–30	32.7–14.9	30	4
10–20	11–16.7	30	3.7
0–10	6.3–54	30	3.6

Source: Reference [2].

pion decay results in electrons, photons, and muons. Muon decay, in turn, leads to secondary electrons, as do scattering interactions of charged particles in the atmosphere. Cosmic ray debris that reaches the surface of the earth consists mainly of muons and electrons with a few neutrons. Except for short-term influences of solar activity, galactic cosmic radiation has been constant in intensity for at least several thousand years. The influence of solar activity is cyclical and the principal variation is on an 11-year cycle. The geomagnetic field of the earth is responsible for limiting the number of cosmic rays that can reach the atmosphere thus accounting for the strong effect of latitude on cosmic-ray dose rates.

Solar Particle Events

Both SPE and CME emissions are mainly hydrogen and helium nuclei, that is, protons and alpha particles, predominantly the former. Electrons are thought to be emitted as well, but with energies less than those of protons by a factor equal to the ratio of the rest masses. Energy spectra are highly variable, as are temporal variations of intensity. A typical course of events for a flare is as follows. Gamma and x-ray emission takes place over about 4 h as is evidenced by radio interference. The first significant quantities of protons reach the earth after about 15 h and peak proton intensity occurs at about 40 h after the solar eruption.

Solar particle events are closely related to solar flares associated with sunspots with intense magnetic fields linking the corona to the solar interior. CME emissions are not directly connected to flares, but originate in the corona driven by the energy of the sun's magnetic field. While of too low energy to contribute to radiation doses at the surface of the earth, these radiations, which fluctuate cyclically with an 11-year period, perturb earth's magnetic field and thereby modulate galactic cosmic-ray intensities with the same period. Maxima in solar flare activity lead to minimal GCR intensity. SPE and CME emissions, in comparison to galactic cosmic rays, are of little significance as a hazard in aircraft flight or low orbital space travel. On the other hand, these radiations present considerable, life-threatening risk to personnel

and equipment in space travel outside the earth's magnetic field. Protection of astronauts in space missions beyond low-earth orbit is addressed in [8].

Trapped Radiation Belts

Released continuously from the sun, as an extension of the corona, is the solar wind, a plasma of low-energy protons and electrons. The solar wind does not present a radiation hazard, even in interplanetary space travel. However, it does affect the interplanetary magnetic field and the shape of the geomagnetically trapped radiation belts. These radiation belts are thought to be supplied by captured solar-wind particles and by decay into protons and electrons of neutrons created by interactions of galactic cosmic rays in the atmosphere. The trapped radiation can present a significant hazard to personnel and equipment in space missions.

The earth's geomagnetically trapped radiation belts are also known as Van Allen belts in recognition of James A. Van Allen and his coworkers who discovered their existence in 1958. There are two belts. The inner belt consists of protons and electrons, the protons being responsible for radiation doses in the region. The outer belt consists primarily of electrons. The particles travel in helical trajectories determined by the magnetic field surrounding the planet. They occur at maximum altitude at the equator and approach the earth most closely near the poles. At the equator, the inner belt extends to about 2.8 earth radii. The center of the outer belt is at about 5 earth radii. The solar wind compresses the trapped radiation on the sunny side of the earth and the compression is enhanced by solar flare activity. In the earth's shadow, the belts are distended as the solar wind sweeps the magnetosphere outward. In a plane through the earth, perpendicular to the earth–sun axis, the proton and electron belts are maximum in intensity at altitudes of about 3,000 and 18,000 km, respectively.

In the southern Atlantic Ocean, there is an eccentricity of the geomagnetic field with respect to the earth's center, and magnetic field lines dip closer to earth. This region, the South Atlantic Anomaly, is the primary source of radiation exposure to astronaut crew members in low-altitude and low-inclination missions. Radiation protection guidance for low-earth orbit missions is found in [9] and [10].

Radiation Sources Used in Human Activities

Life on earth is continually subjected to radiation of natural origin. Exposure is from sources outside the body, arising from cosmic radiation and radionuclides in the environment, and from sources inside the body, arising from ingested or inhaled radionuclides retained in the body. Natural sources are the major contributors to human radiation exposure and represent a reference against which exposure to

Table 13.6 Summary of US annual doses from natural background radiation

	Average annual dose equivalent (mrem)				
Radiation source	Bronchial epithelium	Other soft tissues	Bone surfaces	Bone marrow	Effective dose equivalent
Cosmic radiation	27	27	27	27	27
Cosmogenic nuclides	1	1	1	3	1
External terrestrial	28	28	28	28	28
Inhaled nuclides	2,400				200
Nuclides in the body	36	36	110	50	39
Totals (rounded)	2,500	90	170	110	300

Source: Reference [11].

man-made sources may be compared. Table 13.6 summarizes radiation doses to man resulting from natural sources. Listed in the table are both doses to individual organs or tissues of the body and the effective dose equivalent, which is a composite dose weighted by the relative radiation sensitivities of many organs and tissues of the body.

Since the early 1980s, there has been negligible change in exposure to naturally occurring radiation, an increase estimated from 3 to 3.1 mSv annually. However, in the USA, medical diagnostic exposures have increased by a factor of 5.5 by 2006, an increase from 0.53 to 3 mSv annually. Of the 3 mSv total, 1.47 mSv is from computed tomography (CT) scans, 0.43 mSv for interventional fluoroscopy, 0.77 mSv for nuclear medicine procedures, and 0.33 mSv for conventional radiography and fluoroscopy (10).

Sources in Medicine

Very shortly after their discoveries at the end of the nineteenth century, radium and x-rays were used for medical purposes – radium sources being concentrated from natural materials and x-rays being generated using new technology. These were the only radiation sources seeing significant use until the 1930s, when research into nuclear fission began and when high-energy particle accelerators were developed for nuclear research. In the first half of the twentieth century, x-rays revolutionized diagnostic medicine. In the second half, accelerator radiation and radionuclides produced by accelerators and nuclear reactors established radiography, radiation therapy, and nuclear medicine, both diagnostic and therapeutic, as mature medical sciences. Table 13.4 lists the radioisotopes commonly used in medicine and industry. Some of these radionuclides are produced in nuclear reactors, either as products

of fission or as products of neutron absorption. Nuclei of these isotopes are rich in neutrons and tend to decay by emission of negative beta particles, thereby becoming more positive in charge and more stable. Other isotopes are produced in accelerators. These generally have nuclei deficient in neutrons and tend to decay either by emission of a position or capture of an electron, either process leaving the nucleus more negative and more stable.

There are three broad categories of medical procedures resulting in human radiation exposure: (1) diagnostic x-ray examinations, including mammography and computed tomographic (CT) scans, (2) diagnostic nuclear medicine, and (3) radiation therapy.

Diagnostic X-Rays

Of all the radiation exposures to the general public arising from human activity, the greatest is due to medical procedures, and collective exposures from diagnostic x-rays dominate all other medical exposures. Also, the population subgroup receiving diagnostic x-rays is not small. In the USA, about 250 million medical x rays are delivered annually, as are about 70 million CT scans. About 900 thousand persons receive radiation therapy annually [2, 7].

Diagnostic Nuclear Medicine

Internally administered radionuclides are used medically for imaging studies of various body organs and for non-imaging studies such as thyroid uptake and blood volume measurements. Such uses present hazards for both patients and medical staff. Radiopharmaceuticals are also used for in vitro studies such as radioimmunoassay measurements and thus are of potential hazard to medical staff. Frequencies of procedures, while steadily increasing, vary widely from country to country. As of 2000, in industrialized countries, about 10–40 examinations involving radiopharmaceuticals are carried out annually per 1,000 population. In developing countries, annual frequencies are on the order of 0.2–2 examinations per 1,000 population. In the USA in 2006, for example, some 18 million radionuclide administrations were performed annually for diagnostic purposes [2, 7].

Radiation Therapy

There are three broad categories of radiation therapy– teletherapy, brachytherapy, and therapy using administered radiation sources. *Teletherapy* involves external beams from sources such as sealed ^{60}Co sources, x-ray machines, and accelerators that generate electron, proton, neutron, or x-ray beams. *Brachytherapy* involves sources placed within body cavities (*intracavitary* means) or placed directly within tumor-bearing tissue (*interstitial* means). In the USA, Europe, and Japan, the

frequencies for teletherapy and brachytherapy procedures exceed 2,000 annually per million population.

Thyroid disorders, including cancer, for many years have been treated by ^{131}I, usually by oral administration. Introduced about 1980, in association with the development of techniques for producing monoclonal antibodies, were new cancer diagnosis and treatment methodologies called radioimmunoimaging and radioimmunotherapy. The therapy involves administration of large doses of antibodies tagged with radionuclides and selected to bind with antigens on the surfaces of tumor cells. Imaging involves administration of very much smaller doses, with the goal of detecting the presence of tumor cells using standard camera and scanner imaging techniques. Imaging requires the use of radionuclides such as ^{99m}Tc, which emit low-energy gamma rays. Therapy involves the use of radionuclides emitting beta particles and electrons, with minimum emission of gamma rays, thus limiting radiation exposure, to the extent possible, to tumor cells alone. Among radionuclides used in radioimmunotherapy are ^{75}Se, ^{90}Y, ^{111}In, ^{125}I, ^{186}Re, and ^{191}Os.

Occupational Medical Exposure

A world survey conducted by the United Nations for the years 1990–1994 reports the annual average effective dose 1.39 mSv to some 550,000 workers receiving measurable doses (2.3 million total). Of this group, the greatest number were involved in diagnostic radiology (350,000 at 1.34 mSv). Overall, exposures were in the range of 0.9–1.7 mSv annually [2].

Accelerator Sources

The earliest particle accelerators were the x-ray tubes of the late nineteenth century. Indeed, the radio and television (cathode-ray) tubes of the twentieth century are low-voltage electron accelerators. As electrons beams are stopped, x-rays are produced, inadvertently in the case of radio tubes, and deliberately in the case of x-ray generators.

Modern charged-particle accelerators date from the early 1930s, when Cockroft and Walton in England, and Lawrence and Livingston in America developed particle accelerators for research purposes using beams of electrons or ions. Over the years, steady advances have been made in types of accelerators, in the energies of the particles accelerated, and in the magnitude of the current carried by the charged particle beams. Accelerators continue to serve at the frontiers of atomic and nuclear physics as well as the materials sciences. Moreover, accelerators play an ever more important role in diagnostic and therapeutic medicine and in industrial production processes such as radiography, analysis of materials, radiation processing, and radioisotope production.

Particle accelerators may be classified technologically as direct (potential drop) accelerators and indirect (radio-frequency, plasma) accelerators. Among the former are the Van de Graaff and Cockroft-Walton devices. Among the latter are linear accelerators, betatrons, cyclotrons, and synchrotrons. In the linear accelerator, the particles travel in straight lines, accelerated by the electric fields along their paths. In cyclic accelerators, magnets are used to direct particles into approximately circular paths, along which they may pass through the same accelerating electric fields many times along their paths. The ultimate energies reached by the accelerated particles have increased from about 10^6 eV in the accelerators of the 1930s to 10^{12} eV in modern research accelerators.

By their very nature and function, accelerators are intense radiation sources. In certain applications, accelerated beams of charged particles are extracted from accelerators and directed onto external receivers. Medical applications and radiation processing see this use of accelerators. In other applications, charged particle beams impinge on internal target receivers designed to act as desired sources of secondary radiations such as x-rays or neutrons. In all cases, beams are stopped by targets within which secondary x-rays, neutrons, and other particles such as mesons may be produced as undesirable but unavoidable by-product radiations. Radiation shielding integral with the accelerator as well as structural radiation shielding surrounding the accelerator are necessary for personnel protection.

The production of secondary radiations arises mainly from three phenomena, direct nuclear reactions of ions or electron with accelerator components, electromagnetic cascades, and hadronic cascades. Among the secondary radiations are neutrons, which in turn may be absorbed in accelerator and structural materials thereby leading to capture gamma rays and radioactive reaction products.

Representative of the direct nuclear reactions are those of relatively low-energy proton or deuteron beams in light-element targets. A popular method of generating energetic neutrons, for example, involves interactions of deuterons accelerated to 150 keV with tritium atoms in a target. The resulting reaction, $^3\mathrm{H}(d,n)^4\mathrm{He}$, produces an approximately isotropic and monoenergetic source of 14-MeV neutrons. Other such reactions include $^3\mathrm{H}(p,n)^3\mathrm{He}$, $^2\mathrm{H}(d,n)^3\mathrm{He}$, and $^7\mathrm{Li}(p,n)^7\mathrm{Be}$.

The electromagnetic cascade involves exchanges of the kinetic energy of an electron to electromagnetic energy of multiple photons in the bremsstrahlung process, followed by creation of the rest-mass and kinetic energies of an electron–positron pair in the pair-production process experienced by the photons. As the positrons and electrons lose kinetic energy radiatively, more photons are produced, and the cascade continues. The cascade is quenched when photons have insufficient energy to generate the rest masses of the electron–positron pair and when electron radiative energy losses fall below collisional energy losses.

In high-energy electron or proton accelerators, hadronic cascades may be produced when particles collide with atoms in the accelerator target or, inadvertently, with some other accelerator component, giving rise to many reaction products, including pions, kaons, protons, and neutrons. There is also exchange with the electromagnetic cascade via photodisintegration reactions and by production of energetic gamma rays upon decay of π^0 mesons. Propagation of the hadronic

cascade occurs through reactions of the secondary protons and neutrons, and is especially important for nucleon energies of 150 MeV or greater. The cascade process produces most of the induced radioactivity at high-energy accelerators. Many reaction-product nuclei are in highly excited nuclear states and relax by emission of neutrons, whose subsequent absorption leads, in many cases, to radioactive by-products.

Water, plastics, and oils in the radiation environs of high-energy accelerators yield ^{7}Be and ^{11}C. Aluminum yields these same radionuclides plus ^{18}F, ^{22}Na, and ^{24}Na. Steel, stainless steel, and copper yield all the aforementioned, plus a very wide range of radionuclides, especially those of V, Cr, Mn, Co, Fe, Ni, Cu, and Zn. Neutron absorption in structural concrete also leads to a wide range of radionuclides, among which ^{24}Na is a major concern. This nuclide has a half-life of 15 h and, in each decay, emits high-energy beta particles and gamma rays.

Industrial Isotope Sources

Radionuclides used in industry contribute very little to collective population doses, although individual occupational exposures may be significant. The largest sources are those used in radiography, typically comprising 10–100 Ci of ^{192}Ir, ^{137}Cs, ^{170}Tm, or ^{60}Co. Borehole logging is accomplished using somewhat lower activity gamma-ray sources and neutron sources such as mixtures of plutonium, americium, or californium with beryllium. Much lower activity sources, often ^{90}Sr – ^{90}Y beta-particle sources, are used for various instrumentation and gaging applications.

There are many consumer products containing radiation sources. While these sources are very weak and no one individual receives significant radiation exposure, many persons are involved. For example, the soil, water supplies, and building materials contain low concentrations of naturally occurring radionuclides. Electronic devices emit very low levels of x-rays, and devices ranging from luminous timepieces to smoke detectors contain weak radiation sources. Even the use of tobacco exposes smokers to alpha particles from naturally occurring ^{210}Po in the tobacco leaf.

Various modern technologies have led to human radiation exposures in excess of those which would have occurred in the absence of the technologies. For example, the mining of coal and other minerals and their use is responsible for increased releases of naturally occurring radionuclides to the environment. World production of coal is about 4 billion tonnes annually. About 70% is used in generation of electricity, the balance mainly in domestic heating and cooking. Coal contains ^{40}K, and the ^{238}U and ^{232}Th decay chains in widely varying concentrations. Depending on the nature of combustion, radionuclides are partitioned between fly ash and bottom ash. The smaller-sized fly ash particles are more heavily enriched with radionuclides, particularly ^{210}Pb and ^{210}Po. The average ash content of coal is about 10% by weight, but may be as high as 40%. Efficiency of ash removal in power

plants is quite variable– from only 80% removal to as much as 99% removal, the average being about 97.5%. In domestic use of coal, as much as 50% of the total ash is released into the atmosphere. In terms of doses to individual tissues, the main impact of atmospheric releases during combustion is the dose to bone surface cells accruing from inhalation of ^{232}Th present in the downwind plumes of particulates from plants.

Annually, some 1.4 billion tonnes of phosphate rock are mined and processed for use in production of fertilizers and phosphoric acid. By-product (phospho)gypsum finds wide use in the construction industry. The USA produces about 38% of the phosphate rock, the former Soviet Union 19%, and Morocco 14%. Sedimentary phosphate rock contains high concentrations of radionuclides in the ^{238}U decay chain. Most airborne radioactivity releases are associated with dust produced in strip mining, grinding, and drying of the ore. Utilization of the phosphates leads to both internal and external radiation exposure, the greatest exposure resulting from use of by-product gypsum in construction.

The Nuclear Power Industry

In mid-2008, there were 439 nuclear power plants operating around the world, with a total electrical generating capacity of 372,000 MW. An additional 42 nuclear plants were under construction in 15 countries. Most of the generating capacity consisted of pressurized-water and boiling-water reactors, which use ordinary water as coolant. Gas-cooled reactors, heavy-water reactors, light-water graphite reactors, and sodium-cooled reactors provided the balance of the capacity.

Nuclear Power Reactors

The fission process and production of neutrons associated with reactor operation lead to a wide array of radioactive fission products and activation products arising from neutron absorption. Moreover, large quantities of uranium and plutonium are fissioned in modern nuclear power plants (typically 3 kg/day) to produce the thermal energy needed to produce electricity. Consequently, large quantities of fission products are produced and accumulate in the fuel. Also contained within the fuel are actinides produced by cumulative neutron absorption in uranium, thorium, and plutonium fuels. The actinides are characterized by spontaneous fission in competition with alpha-particle decay, and require sequestration to the same degree as the fission products.

One way of categorizing the generated radionuclides is by their physical–-chemical behavior, namely, (1) noble gases (2) ^{3}H and ^{14}C, (3) halogens, and (4) particulates. These divisions are based on the relative ease of isolation of the radionuclides from airborne effluents. The noble gases include the many isotopes of

the krypton and xenon fission products as well as the activation product ^{41}Ar. These elements cannot be removed from a gas stream by filtration. Halogens include the many isotopes of the bromine and iodine fission products. If they are present in a gas stream, they are likely to be in a chemical form unsuitable for filtration, and effective removal requires adsorption on a material such as activated charcoal. Other radionuclides and the halogens in ionic form may be removed from a gas stream by filtration. In aqueous liquids, the particulates may be isolated by evaporation, filtration, or ion exchange. The halogens, unless in ionic form, cannot be isolated by evaporation or filtration, nor can noble gases. Special cases are ^{3}H in the form of tritiated water and ^{14}C as carbon dioxide. The tritium can be isolated only with very great difficulty, and CO_2 removal requires chemical treatment.

There are two sources of radionuclides in reactor coolant, leakage from defective fuel rods and activation products produced by neutron interactions in the coolant itself or with fuel and structure in contact with the coolant. Activation product sources are inevitable, and include a number of radionuclides which may be produced in the coolant. For example, ^{16}N is produced as a result of neutron interactions with oxygen, ^{41}Ar as a result of neutron absorption in naturally occurring argon in the atmosphere and ^{3}H as a result of neutron absorption in deuterium and, especially in pressurized-water reactors, by neutron-induced breakup of ^{10}B. Of course, in a sodium-cooled fast reactor, activation of natural sodium to short-lived ^{24}Na is an important consideration for in-plant radiation protection. Other activation products include isotopes of iron, cobalt, chromium, manganese, and other constituents of structural and special-purpose alloys. The radionuclides are leached into the coolant stream. They then may be adsorbed on surfaces or trapped as particulates in the boundaries of coolant streams within the plant, only later to be resuspended in the coolant. These sources can be minimized by carefully specifying the alloy and trace-element concentrations in plant components.

Uranium Mining and Fuel Fabrication

In the preparation of new fuel for nuclear reactors, the radiation sources encountered are natural sources associated with the uranium and thorium decay chains.

The principal release of radiation sources associated with uranium mining, underground or open pit, is release of natural ^{222}Rn to the atmosphere. Airborne particulates containing natural uranium daughter products also arise from open pit mining and from ore crushing and grinding in the milling process. Mill tailings can also become a long-term source of radiative contamination due to wind and water erosion, leaching, and radon release, the degree depending on the tailing-stabilization program followed. Mining and milling operations are generally conducted in remote areas, and liquid releases containing dissolved uranium daughter products are of little impact on human populations.

The product of milling is U_3O_8 “yellow cake” ore concentrate. In this phase of the nuclear fuel cycle, the concentrate is purified and most often converted to UF_6

for enrichment in ^{235}U via gaseous diffusion or centrifuge processes. Prior to fuel fabrication, the uranium is converted to the metallic or the ceramic UO_2 form suitable for use in fuel elements. Large quantities of uranium depleted in ^{235}U are by-products of the enrichment process. Under current practice, the depleted uranium is held in storage as being potentially valuable for use in breeder reactors. In this stage of the nuclear fuel cycle, there are relatively minor liquid and gaseous releases of uranium and daughter products to the environment.

Fuel Reprocessing

As nuclear fuel reaches the end of its useful life in power generation, there remain within the fuel recoverable quantities of uranium and plutonium which may be extracted for reuse in the fuel reprocessing stage of the nuclear fuel cycle. Whether or not the fuel is reprocessed is governed by economic and political considerations. Among the former are costs of reprocessing as compared to costs of mining, milling, conversion, and enrichment of new stocks of uranium. Among the latter are concerns over the potential diversion of plutonium to nuclear-weapons use.

In the reprocessing of oxide fuels, the spent fuel is first dissolved in nitric acid. Plutonium and uranium are extracted into a separate organic phase from which they are ultimately recovered and converted into the oxide form. The aqueous phase containing fission and activation products is then neutralized and stored in liquid form pending solidification and ultimate disposal. Because one reprocessing plant may serve scores of power plants, inventories of radionuclides in process may be very great and extraordinary design features and safety procedures are called for. Because of the time delays between removal of fuel from service and reprocessing, concerns are with only relatively long-lived radionuclides, notably ^{3}H, ^{14}C, ^{85}Kr, ^{90}Sr, ^{106}Ru, ^{129}I, ^{134}Cs, and ^{137}Cs.

During the dissolution step of reprocessing, all the ^{85}Kr, the bulk of the ^{14}C (as CO_2), and portions of the ^{3}H and ^{129}I appear in a gas phase. This gas is cleaned, dried, and released through a tall stack to the atmosphere. All the ^{85}Kr is thus released; however, the major part of the ^{3}H is removed in the drying process and the bulk of the ^{129}I and ^{14}C is removed by reaction with caustic soda. The ^{14}C may then be precipitated and held as solid waste. Depending on the degree of liquid-effluent cleanup, some of the ^{129}I and other fission products subsequently may be released to the environment.

Waste Storage and Disposal

Wastes generated in the nuclear fuel cycle fall into the broad categories of high-level wastes (HLW) and low-level wastes (LLW). The former, comprising unprocessed spent fuel or liquid residues from fuel reprocessing, accounts for only about 1–5% of the waste volume, but about 99% of the waste activity. The latter is comprised of in-reactor components, filter media, ion-exchange resins,

Table 13.7 Collective doses incurred by the public and workers from the nuclear fuel cycle, normalized to unit electrical energy generation

	Committed dose (person Sv) per GWy(e)		
	General population		
Operation	Local/regional	Waste/global[a]	Occupational
Mining	0.19	–	1.72
Milling	0.008	–	0.11
Mine tailings	0.04	7.5	–
Fuel fabrication	0.003	–	0.1
Reactor operation	0.44	0.5	3.9
Fuel reprocessing	0.13	0.05	3.0
Transportation	<0.1	–	–
Global dispersion	–	40	–
Research	–	–	1.0
Enrichment	–	–	0.02
Total	0.91	50	9.8

[a]For solid waste and global dispersion, committed dose is for 10,000 years
Source: Reference [2]: (1995–1997 general, 1990–1994 occupational).

contaminated clothing and tools, and laboratory wastes. For the most part, LLW consists of short-lived beta-particle and gamma-ray emitters. Wastes of low specific activity, but containing long-lived alpha-particle emitters, for example, ^{239}Pu, require special handling more in the nature of that required for HLW.

In the USA, fuel elements from commercial reactors are presently not processed. By the year 2000, the cumulative spent fuel reached about 16,000 m^3, amounting to 40,000 t of uranium and fission products. Most of this spent fuel will be stored at the plant sites where it is generated which are primarily in eastern states.

Nuclear Power and Occupational Exposure

Table 13.7 summarizes a United Nations survey of occupational exposures as well as public exposures based on nuclear power operations in the 1990s. Improvements continue to be made and US occupational annual committed occupational doses have by 2007 declined from about 3 to 1.1 person Sv per GWy(e).

Nuclear Explosives

Large fractions of radioactive debris from atmospheric nuclear weapons tests are distributed globally, and the radionuclides remain in the biosphere indefinitely. The hazard is better characterized by the long-term dose commitment than by the dose rate at any instant and location. The fusion and fission energy released in

a nuclear-weapon explosion is usually measured in units of megatons (Mt). One megaton refers to the release of 10^{15} cal of explosive energy– approximately the amount of energy released in the detonation of 10^6 metric tons of TNT. The quantity of fission products produced in a nuclear explosion is proportional to the *weapon fission yield*. For a 1-Mt weapon fission yield, there must be the complete fissioning of about 56 kg of uranium or plutonium. The quantities of ^{3}H and ^{14}C, which are produced in the atmosphere by interactions of high-energy fission neutrons, are also proportional to the *weapon fusion yield*. There are several fusion reactions used in thermonuclear devices, with a 1-Mt weapon fusion yield requiring, for example, the fusion of 7.4 kg of tritium with 4.9 kg of deuterium.

The disposition of weapon debris may be divided into three categories, local fallout, tropospheric fallout, and stratospheric fallout. Local fallout, comprising as much as 50% of the debris and consisting of large particles, is defined as that deposited within 100 miles of the detonation site. Depending on detonation altitude and weather conditions, a portion of the weapon's debris is injected into the stratosphere and a portion remains in the troposphere. These two atmospheric regions are separated by the tropopause (about 16 km altitude at the equator and 9 km at the poles). Temperature decreases with elevation in the troposphere. This hydrodynamically unstable condition leads to the development of convective weather patterns superimposed upon generally westerly winds. In the stratosphere, temperature is more nearly constant or, in equatorial regions, even rises with elevation. Vertical convective motion is relatively slight and the tropical temperature inversion restricts transfer of material in the stratosphere from hemisphere to hemisphere.

Debris in the troposphere is distributed in longitude but remains within a band of about 30° of latitude. The mean lifetime of radioactive debris in the troposphere is about 30 days and tropospheric fallout is important for radionuclides with half-lives of a few days to several months. Over the years, the bulk of the radioactive debris from weapons tests has been injected into the stratosphere in the northern hemisphere and at altitudes less than 20 km. Mechanisms for transfer of the debris to the troposphere and thence to fallout on the earth's surface are complex. At elevations less than 20 km, the half-life for transfer of aerosols between hemispheres is about 60 months, while the half-life for transfer to the troposphere is only about 10 months, with little material crossing the tropopause in equatorial regions. Consequently, the bulk of the fallout from any one test occurs over the hemisphere of injection and in temperate regions. In terms of the megatons of fission energy, in the period prior to 1980, 78% of the debris was injected into the stratosphere– 70% into the northern hemisphere and 8% into the southern.

Eight radionuclides contribute significantly to the committed effective dose equivalent to the population. These are ^{137}Cs, ^{131}I, ^{14}C, ^{239}Pu, ^{90}Sr, ^{106}Ru, ^{144}Ce, and ^{3}H. Because of its long half-life, 5,730 years, the commitment from ^{14}C extends over many human generations. The collective effective dose equivalent commitment into the indefinite future due to weapons tests to date is equivalent to about four extra years of exposure of the current world population to natural background radiation.

High-level radioactive wastes generated in the USA in the production of nuclear weapons have accumulated for decades. The wastes are stored at three sites, one in the state of Washington, one in Idaho, and one in South Carolina. The approximately 9,000 t of waste has a volume of 380,000 cubic meters and there are plans to dispose of this waste in a repository used also for disposal of spent fuel for nuclear power plants.

Future Directions

Accelerators

Research, materials processing, and teletherapy accelerators employ higher and higher energy beams and beam currents. The production of secondary radiations associated with beam interactions with targets and structure lead to radiation sources of new types and increased magnitudes. Proton-beam accelerators grow in use for specialized radiation therapy. Synchrotrons deliver beams of protons with energies up to 250 MeV, with increased demands for new and better radiation surveillance, shielding, and dosimetry. Minimization of radiation damage to accelerator components calls for more precise beam simulation in the design process as well as more robust components.

Space Activities

In low-earth orbit, galactic cosmic rays (GCR) properties are well known except for short-term enhancements caused by solar particle events (SPE), especially in polar regions [10]. Consequences may be important in extravehicular activities (EVA) outside the Space Shuttle or International Space Station. There is a need for real-time measurement of instantaneous absorbed dose and effective dose rates as well as cumulative doses. Improved modeling of the space environment is needed so that longer-term predictions may be of conditions in orbit.

For activities beyond low-earth orbit, there is also a need for improved forecasting capabilities [8] for SPE. There is also a need for development and validation of space radiation transport codes, accounting for neutrons, protons, light and heavy ions, mesons, and electromagnetic cascades. Radiation spectrometers are needed for combined measurements of neutron doses and doses from high-energy charged particles. As to biological effects, there is need for more sophisticated risk assessment methodology – at one extreme addressing late somatic and carcinogenic effects – at the other extreme addressing thresholds for symptoms affecting mission requirements, namely, central nervous system effects, dermal and immune issues.

Nuclear Power

Extending the operating lives of nuclear power plants brings on the need for increased attention to maintenance, corrosion control, and surveillance of piping and components. Similarly, extending the in-core operating life of individual fuel assemblies places intense demands on design, manufacturing, and quality assurance. Likewise, greater fuel "burnup" requires increased attention to actinide source inventories and secondary neutron production in spent fuels. Plant operating lives of 60 or more years need support of strong technical and manufacturing infrastructure.

No doubt the future will also see new generations of plants operating with radically advanced designs, with breeding capability, and using mixed $^{235}U/^{239}Pu$ fuels as well as fuels utilizing the ^{232}Th fuel cycle. These changes will bring on new design and operational challenges as well as the continued support of the physics community in broadening the evaluated nuclear data files (ENDF) and the evaluated nuclear structure data files (ENSDF).

Methods of storage and disposal of spent nuclear fuel continues to involve a complex mixture of technical, economic, political, and emotional issues. Resolution of the political and emotional issues seems to be the more demanding challenge.

Medical Applications

Challenges in nuclear medicine vary from nation to nation, but a recent survey [4] identified a number of universal concerns.

Hybrid imaging, employing dual use of CT, PET, MRI, and SPECT methods, introduces new combinations of radiation sources – positron emitters for PET, x-rays for CT, and gamma ray emitters for SPECT. Accounting for these mixed sources brings new challenges in facility design, treatment planning, patient and staff protection, as well as management of wastes. The same is true for radionuclides used in nuclear-medicine therapy such as delivery of radionuclides to malignant tumor cells using monoclonal antibody and related techniques.

In many countries, there is a need for improvement of domestic medical radionuclide production to alleviate the shortage of accelerator- and nuclear reactor–produced medical radionuclides available for research, diagnosis, and treatment. Finally, improvements in detector technology, image reconstruction algorithms, and advanced data processing techniques are needed to facilitate translation from research laboratory to the clinic.

Industrial and Commercial Activities

Sources of ionizing radiation find use in a very broad array of applications, examples being radiography and tracer techniques in manufacturing and density

and moisture gauging in highway construction. Sources find their way into the home via ^{241}Am in smoke detectors and into public buildings via ^{3}H in exit signs. There is a very sad history of injury and death caused by the loss, abandonment, and theft of such sources. Better control of inventory, use, storage, and disposal of such sources is badly needed as well as better oversight by regulatory bodies.

Bibliography

Primary Literature

1. UN (1982) Sources and effects of ionizing radiation. Reports of the United Nations Scientific Committee on the effects of atomic radiation. United Nations, New York
2. UN (2000) Sources and effects of ionizing radiation. Reports of the United Nations Scientific Committee on the effects of atomic radiation. United Nations, New York
3. Eckerman KF, Ryman JC (1993) External exposure to radionuclides in air, water, and soil. Federal guidance report 12, EPA-402-R-93-081. U.S. Environmental Protection Agency, Washington, DC
4. National Research Council (2007) Advancing nuclear medicine through innovation. Committee on State of the Science of Nuclear Medicine. National Academy of Sciences, Washington, DC
5. World Nuclear Association (2006) Radioisotopes in industry (Information paper). www.world-nuclear.org/info/inf56.html
6. Fewell TR, Shuping RE, Hawkins KR (1981) Handbook of computed tomography and X-ray spectra. Report HHS (FDA) 81-8162
7. NCRP (2009) Ionizing radiation exposure of the population of the United States. Report no 160. National Council on Radiation Protection and Measurements, Bethesda
8. NCRP (2006) Information needed to make radiation protection recommendations for space missions beyond low-earth orbit. Report no 153. National Council on Radiation Protection and Measurements, Bethesda
9. NCRP (2000) Radiation protection guidance for activities in low-earth orbit. Report no 132. National Council on Radiation Protection and Measurements, Bethesda
10. NCRP (2002) Operational radiation safety program for astronauts in low-earth orbit. Report no 142. National Council on Radiation Protection and Measurements, Bethesda
11. NCRP (1987) Exposure of the population in the United States and Canada from natural background radiation. Report no 94. National Council on Radiation Protection and Measurements, Bethesda

Books and Reviews

Cohen BL (1986) A national survey of ^{222}Rn in U.S. homes and correlating factors. Health Phys 51:175–183

Cohen BL, Shah RS (1991) Radon levels in United States homes by states and counties. Health Phys 60:243–259

Eisenbud M (1987) Environmental radioactivity, 3rd edn. Academic, Orlando

Faw RE, Shultis JK (1999) Radiological assessment: sources and doses. American Nuclear Society, La Grange Park
Firestone RB, Shirley VS (eds) (1996) Table of isotopes, 8th edn. Wiley-Interscience, Malden
Haffner JW (1967) Radiation and shielding in space. Academic, New York
Glasstone S, Dolan PJ (eds) (1977) The effects of nuclear weapons. United States Departments of Energy and Defense, Washington, DC
ICRP (1987) Radiation dose to patients from radiopharmaceuticals. ICRP publication 53. Annals of the ICRP 18(1–4). International Commission on Radiological Protection, Pergamon Press, Oxford
Kocher DC (1981) Radioactive decay tables. Report DOE/TIC-11026. National Technical Information Service, Springfield
NAS (1971) Radioactivity in the marine environment. Report of the panel on radioactivity in the marine environment. Committee on Oceanography, National Research Council, National Academy of Sciences, Washington, DC
NAS (1988) Health risks of radon and other internally deposited alpha-emitters. Report of the BEIR Committee [The BEIR-IV Report]. National Research Council, National Academy of Sciences, Washington, DC
NAS (1990) Health effects of exposure to low levels of ionizing radiation. Report of the BEIR Committee [The BEIR-V Report]. National Research Council, National Academy of Sciences, Washington, DC
NCRP (1975) Natural background radiation in the United States. Report no 45. National Council on Radiation Protection and Measurements, Washington, DC
NCRP (1977) Radiation protection design guidelines for 0.1–100 MeV particle accelerator facilities. Report no 51. National Council on Radiation Protection and Measurements, Bethesda
NCRP (1984) Exposures from the Uranium Series with Emphasis on Radon and its Daughters. Report no 77. National Council on Radiation Protection and Measurements, Washington, DC
NCRP (1987a) Ionizing radiation exposure of the population of the United States. Report no 93. National Council on Radiation Protection and Measurements, Washington, DC
NCRP (1987b) Radiation exposure of the U.S. population from consumer products and miscellaneous sources. Report no 95. National Council on Radiation Protection and Measurements, Bethesda
NCRP (1989a) Exposure of the U.S. population from diagnostic medical radiation. Report no 100. National Council on Radiation Protection and Measurements, Bethesda
NCRP (1989b) Exposure of the U.S. population from occupational radiation. Report no 101. National Council on Radiation Protection and Measurements, Bethesda
NCRP (1989c) Radiation protection for medical and allied health personnel. Report no 105. National Council on Radiation Protection and Measurements, Bethesda
NCRP (2003) Radiation protection for particle accelerator facilities. Report no 144. National Council on Radiation Protection and Measurements, Bethesda
Shultis JK, Faw RE (2000) Radiation shielding. American Nuclear Society, La Grange Park
Slaback LA Jr, Birky B, Schleien B (1997) Handbook of health physics and radiological health. Lippincott Williams & Wilkins, Hagerstown
UN (1977/1982/1988/1993/2000) Report of the United Nations Scientific Committee on the effects of atomic radiation. United Nations, New York
Weber DA, Eckerman KF, Dillman LT, Ryman JC (1989) MIRD: radionuclide data and decay schemes. Society of Nuclear Medicine, New York

Chapter 14
Radiation Shielding

J. Kenneth Shultis and Richard E. Faw

Glossary

Albedo	A quantity describing how neutrons or photons incident on the surface of some medium (e.g., a wall) are reflected or reemitted from the surface.
Buildup factor	A factor to account for production of secondary photons in a shield. The transmitted dose from only uncollided photons times the buildup factor equals the dose from all photons, uncollided plus secondary photons.
Dose	A general term for the energy transferred from radiation to matter. Specifically, the absorbed dose is the amount of energy imparted to matter from ionizing radiation in a unit mass of that matter. Units are the gray (Gy) and rad, respectively, equivalent to 1 J/kg and 100 ergs/g.
Flux	A measure of the intensity of a radiation field. Specifically, it equals the number of radiation particles entering, in a unit time, a sphere of cross-sectional area ΔA divided by ΔA, as $\Delta A \rightarrow 0$. The flux, integrated over a specified time interval is called the *fluence*.

This chapter was originally published as part of the Encyclopedia of Sustainability Science and Technology edited by Robert A. Meyers. DOI:10.1007/978-1-4419-0851-3

J.K. Shultis (✉)
Department of Mechanical & Nuclear Engineering, Kansas State University,
Ward Hall, Manhattan, KS 66506-2503, USA
e-mail: jks@ksu.edu

R.E. Faw
Department of Mechanical & Nuclear Engineering, Kansas State University,
132 Brooks Landing Drive, Winston Salem, NC 27106, USA
e-mail: fawre@triad.rr.com

N. Tsoulfanidis (ed.), *Nuclear Energy: Selected Entries from the Encyclopedia of Sustainability Science and Technology*, DOI 10.1007/978-1-4614-5716-9_14,

Interaction coefficient	A quantity, denoted by μ, describing how readily a photon or neutron interacts with a given medium. Specifically, it is the probability a radiation particle of energy E will interact in a specified manner per unit distance of travel, for infinitesimal distances. It thus has units of inverse length. The total interaction coefficient $\mu = \sum_i \mu_i$ where μ_i is the coefficient for the ith type of interaction (e.g., scattering, absorption).
Neutron	A neutral subatomic particle that collectively with positively charged protons forms an atomic nucleus. Although both are composite particles composed of quarks and gluons, for the energies considered in this entry they can be viewed as fundamental unchangeable particles.
Photon	A quantum of electromagnetic radiation with energy $E = h\nu$, where h is Planck's constant and ν is the frequency. Photons produced by a change in the structure of the nucleus are called *gamma photons* and those produced by atomic electron rearrangement are called *x-rays*.
Skyshine	A term for the radiation that reaches some point of interest after being scattered by the atoms in the atmosphere back to the point of interest.
Transport equation	Also known as the linearized Boltzmann equation, it describes rigorously the spatial, energy, and angular distribution of neutrons or photons in any medium with arbitrary source distributions. From its solution, the radiation flux or dose anywhere in the medium can be determined.

Definition of the Subject

We live in a world that abounds in radiation of all types. Many radiations, such as the neutrinos or visible light from our sun present little risk to us. Other radiations, such as medical x-rays or gamma rays emitted by radioactive materials, have the potential to cause us harm. In this entry, only the transport of *indirectly ionizing radiation* is considered. These radiations consist of chargeless particles such as neutrons or photons that, upon interacting with matter, produce energetic secondary charged particles called *directly ionizing radiation*. It is these secondary charged particles that, through ionization and excitation of ambient atoms along their paths, cause radiation damage to biological tissues or other sensitive materials.

To mitigate radiation damage, a *shield* is often interposed between a source of ionizing radiation and the object to be protected so that the radiation levels near the object are reduced to tolerable levels. Typically, a shield is composed of matter that

effectively diminishes the radiation that is transmitted. (However, there are noncorporeal shields such as magnetic fields that deflect moving charged particles. The earth's magnetic field serves as such a shield to protect us from charged particles reaching earth from outer space.) The term *radiation shielding* refers usually to a system of shields constructed for a specific radiation protection purpose. The term also refers to the study of shields – the topic of this entry.

Introduction

The origins of shielding go back to the science of optics in which the exponential attenuation of light was long recognized. The exponential attenuation of radiation rays is still widely used for neutron and photon shielding. Also the governing field equation that describes how radiation migrates through matter was introduced in 1872 by Ludwig Boltzmann who used it to study the kinetic theory of gas. All this occurred before the discovery of ionizing radiation! The *radiation transport equation* is just a special case of the Boltzmann equation applied to situations in which radiation particles do not interact among themselves.

The study of shielding has many aspects: transport of (deeply penetrating) indirectly ionizing radiation in the shield, the production of very slightly penetrating secondary (directly ionizing) radiation in the shield and its surroundings, the radiation levels in the vicinity of the shield, deposition of heat in the shield, radiation penetration through holes in the shield, radiation scattered around the shield, selection of shielding materials, optimization of the shielding configuration, and the economics of shield design. It also involves understanding of related matters such as radiation source characteristics, radiation protection standards, and the fundamentals of how radiation interacts with matter.

The restriction of this entry to indirectly ionizing radiation is of a practical nature. Sources of charged particles, such as the alpha and beta particles emitted in some types of radioactive decay, can and do cause biological damage, particularly if the radioactive material is ingested. Here, however, it is assumed that the radiation sources are external to the body or the sensitive material of interest. Such external sources also usually emit far more penetrating indirectly ionizing radiation, and any shield that is effective against indirectly ionizing radiation is usually more than adequate to stop the directly ionizing radiation.

History of Shielding

To appreciate better the current state of shielding practice, it is important to understand how the discipline developed and what were the driving forces that caused it to mature. In this section, a brief overview of the history of shielding is presented. (A greatly expanded version of the following synopsis is provided by Shultis and Faw [1].)

Early History

The hazards of x-rays were recognized within months of Roentgen's 1895 discovery, but dose limitation by time, distance, and shielding was at the discretion of the individual researcher until about 1913. Only then were there organized efforts to create groups to establish guidelines for radiation protection. And it was not until about 1925 that instruments became available to quantify radiation exposure.

In 1925, Mutscheller [2] introduced important concepts in x-ray shielding. He expressed the erythema dose (An *ED* value of unity represents a combination of time, distance, and beam current just leading to a first-degree burn) *ED* quantitatively in terms of the beam current i (mA), exposure time t (min), and source-to-receiver distance r (m), namely, $ED = 0.00368it/r^2$, independent of x-ray energy. Mutscheller also published attenuation factors in lead as a function of lead thickness and x-ray average wavelength.

Evolutionary changes to x-ray shielding were made during the decades preceding World War II. These included consideration of scattered x-rays, refinements in shielding requirements in terms of x-ray tube voltages, recommendations for use of goggles (0.25-mm Pb equivalent) and aprons (0.5-mm Pb equivalent) for fluoroscopy, and specifications for tube-enclosure shielding and structural shielding for control rooms.

The other major source of ionizing radiation before World War II was the medical and industrial use of radioactive radium discovered by Marie and Pierre Curie in 1898. Not until 1927 were lead shielding standards recommended for radium applicators, solutions, and storage containers. For example, the International X-Ray and Radium Protection Committee recommended that tubes and applicators should have at least 5 cm of lead shielding per 100 mg of radium. It was not until 1941 that a tolerance dose for radium, expressed in terms of a maximum permissible body burden of 0.1 μCi, was established. This was done largely in consideration of the experiences of early "radium-dial" painters and the need for standards on safe handling of radioactive luminous compounds [3].

Manhattan Project and the Early Postwar Period

Early reactor shielding. During World War II, research on nuclear fission, construction of nuclear reactors, production of enriched uranium, generation of plutonium and its separation from fission products, and the design, construction, testing, and deployment of nuclear weapons all were accomplished at breakneck speed in the Manhattan Project. Radiation sources new in type and magnitude demanded not only protective measures such as shielding but also examination of biological effects and establishment of work rules.

The construction of nuclear reactors for research and for plutonium production required shield designs for both gamma rays and neutrons. However, with only

sparse empirical data and large uncertainties about how neutrons and gamma rays migrate through shields, shield designers acted very conservatively. For example, shielding for both Fermi's 1943 graphite pile in Chicago and the 1947 X-10 research reactor at what is now Oak Ridge National Laboratory was adequate for gamma rays and overdesigned for neutrons. Operation of the X-10 reactor, built to provide data for the design of plutonium-production reactors, revealed problems with streaming of gamma rays and neutrons around access holes in the shield. The water-cooled graphite plutonium-production reactors at Hanford, Washington used iron thermal shields and high-density limonite and magnetite concrete as biological shields.

By the 1940s, the importance of scattered gamma rays was certainly known from measurements, and use of the term *buildup factor* to characterize the relative importance of scattered and unscattered gamma rays had its origin during the days of the Manhattan Project. Neutron diffusion theory and Fermi age theory were established, but shielding requirements for high-energy neutrons were not well understood. Wartime radiation shielding was an empirical, rule-of-thumb craft.

Nuclear reactors for propulsion. The Atomic Energy Act of 1946 transferred control of nuclear matters from the Army to the civilian Atomic Energy Commission (AEC). That same year, working with the AEC, the US Navy began development of a nuclear powered submarine and the US Air Force, a nuclear powered aircraft. Both of these enterprises demanded minimization of space and weight of the nuclear-reactor power source. Such could be accomplished only by minimizing design margins and that required knowledge of mechanical, thermal, and nuclear properties of materials with greater precision than known before.

Research reactors were constructed at various national laboratories in the USA and Britain to provide the much needed shielding data. The first such research program was begun in 1947 at Oak Ridge National Laboratory with the construction of the X-10 graphite reactor. The X-10 graphite reactor had a 2-ft square aperture in its shielding from which a neutron beam could be extracted, the intensity being augmented by placement of fuel slugs in front of the aperture. Attenuation of neutrons could then be measured within layers of shielding materials placed against the beam aperture. Early measurements revealed the importance of capture gamma rays produced when neutrons were absorbed. Improved experimental geometry was obtained by using a converter plate containing enriched uranium instead of relying on fission neutrons from fuel slugs. A broadly uniform beam of thermal neutrons incident on the plate generated a well-defined source of fission neutrons. A water tank was adjacent to the fission source, with shielding slabs and instrumentation within the tank. This *Lid Tank Shielding Facility*, LTSF, was the precursor of many so-called *bulk-shielding facilities* incorporated into many water-cooled research reactors.

Although a nuclear powered aircraft never flew, the wealth of information gained on the thermal, mechanical, and shielding properties of many special materials is a valuable legacy. To obtain shielding data in the absence of ground reflection of radiation, several specialized facilities were constructed. A test reactor

was suspended by crane for tests of ground reflection. Then an aircraft shield test reactor was flown in the bomb-bay of a B-36 aircraft to allow measurements at altitude. The Oak Ridge tower shielding facility (TSF) went into operation in 1954, and remained in operation for almost 40 years. Designed for the aircraft nuclear propulsion program, the facility allowed suspension of a reactor hundreds of feet above grade and separate suspension of aircraft crew compartments. In its long life, the TSF also supported nuclear defense and space nuclear applications.

Streaming of radiation through shield penetrations and heating in concrete shields due to neutron and gamma-ray absorption were early shielding studies conducted in support of gas-cooled reactor design. Additional efforts were undertaken soon thereafter at universities as well as government and industrial laboratories. Shielding material properties, neutron attenuation, the creation of capture and inelastic scattering gamma rays, reflection and streaming of neutrons and gamma rays through ducts and passages, and radiation effects on materials were major research topics.

The Decade of the 1950s

This era saw the passage in the USA of the Atomic Energy Act of 1954, the Atoms for Peace program, and the declassification of nuclear data. During this decade, many simplified shielding methods were developed that were suitable for hand calculations. The first digital computers appeared and were quickly used for radiation transport calculations. The US Air Force also started a short-lived nuclear rocket program.

Advances in neutron shielding methods. These advances resulted from measurements at the LTSF and other bulk-shielding facilities. One advancement was the measurement of point kernels, or Green's functions, for attenuation of fission neutrons in water and other hydrogenous media. The other was the discovery that the effect of water-bound oxygen, indeed the effect of homogeneous or heterogeneous shielding materials in hydrogenous media, could be modeled by exponential attenuation governed by effective "removal" cross sections for the non-hydrogen components. The LTSF allowed measurement of removal cross section for many materials.

Advances in gamma-ray shielding methods. As the decade began, researchers at the National Bureau of Standards investigated electron and photon transport. Much of this effort dealt with the moments method for solving the transport equation describing the spatial, energy, and angular distributions of radiation particles emitted from fixed sources. From such calculations, *buildup factors* to account for scattered photons were determined for various shielding media and shield thicknesses. Various empirical formulas were also developed to aid in the interpolation of the buildup-factor data.

Advances in Monte Carlo computational methods. The Monte Carlo method of simulating radiation transport computationally has its roots in the work of John von Neumann and Stanislaw Ulam at Los Alamos in the 1940s. Neutron-transport calculations were performed in 1948 using the ENIAC digital computer which had commenced operations in 1945. In this decade, major theoretical advances in Monte Carlo methods were made and many clever algorithms were invented to allow Monte Carlo simulations of radiation transport through matter. Little did the pioneers of this transport approach realize that Monte Carlo techniques would become indispensable in modern shielding practice.

The Decade of the 1960s

The 1960s saw the technology of nuclear-reactor shielding consolidated in several important publications. Blizard and Abbott [4] edited and released a revision of a portion of the 1955 Reactor Handbook as a separate volume on radiation shielding, recognizing that reactor shielding had emerged from nuclear-reactor physics into a discipline of its own. In a similar vein, the first volume of the Engineering Compendium on Radiation Shielding [5] was published. These two volumes brought together contributions from scores of authors and had a great influence on both practice and education in the field of radiation shielding.

This exciting decade also saw the beginning of the Apollo program, the start of the NASA NERVA (Nuclear Engine for Rocket Vehicle Application) program, the deployments in space of SNAP-3, a radioisotope thermoelectric generator in 1961, and SNAP-10A nuclear-reactor power system in 1965. It also saw the Cuban missile crisis in October 1962 and a major increase in the cold-war apprehension about possible use of nuclear weapons. The Apollo program demanded attention to solar flare and cosmic radiation sources and the shielding of space vehicles. Cold-war concerns demanded attention to nuclear-weapon effects, particularly structure shielding from nuclear-weapon fallout. Reflection of gamma rays and neutrons and their transmission through ducts and passages took on special importance in structure shielding. The rapid growth in access to digital computers allowed introduction of many computer codes for shielding design and fostered advances in solving various approximations to the Boltzmann transport equation for neutrons and gamma rays. Similar advances were made in treating the slowing down and transport of charged particles.

Space shielding. Data gathered over many years revealed a very complicated radiation environment in space. Two trapped-radiation belts had been found to surround the earth, an inner proton belt and an outer electron belt. Energy spectra and spatial distributions in these belts are determined by the earth's magnetic field and by the solar wind, a plasma of low-energy protons and electrons. The radiations pose a risk to astronauts and to sensitive electronic equipment. Uniform intensities of very-high-energy galactic cosmic rays demand charged-particle shielding for

protection of astronauts in long duration missions. The greatest radiation risk faced by Apollo astronauts was from solar flare protons and alpha particles with energies as great as 100 MeV for the former and 400 MeV for the latter. The overall subject of space radiation shielding is treated by Haffner [6].

Structure shielding. Structure shielding from nuclear-weapon fallout required careful examination of the atmospheric transport of gamma rays of a wide range of energies and expression of angular distributions and related data in a manner easily adopted to analysis of structures. There was a need to assess, at points within a structure, the ratios of interior dose rates to that outside the building, called *reduction factors*. These factors were measured experimentally and also calculated with the transport moments method which had been used so successfully in calculation of buildup factors.

Other shielding advances. Of great importance to structure shielding, but also of interest in reactor and nuclear plant shielding, were the development of simplified methods to quantify neutron and gamma-ray streaming through ducts and voids in shields. This decade saw the development of removal-diffusion methods to describe quite accurately the penetration and slowing down of fast fission neutrons in shields. Finally, a simplified approach was developed to describe how gamma rays or neutrons incident on some material are scattered back. The central concept in this approach is the *particle albedo*, a function that describes how radiation incident on a thick medium, a concrete wall for example, is reemitted or reflected back from the surface. Measurements, theoretical calculations, and approximating formulas for both neutron and gamma-ray albedos were developed in this decade.

Digital computer applications. Radiation transport calculations are by nature very demanding of computer resources. The community of interest in radiation transport and shielding has been served magnificently for more than 4 decades by the Radiation Safety Information Computational Center (RSICC). Established in 1962 as the Radiation Shielding Information Center (RSIC) at Oak Ridge National Laboratory, RSICC's mission is to provide in-depth coverage of the radiation transport field to meet the needs of the international shielding community.
The 1960s saw many new "mainframe" computer codes developed and disseminated. Among these codes were gamma-ray "point-kernel" codes such as ISOSHLD and QAD, with versions of both still in use after almost 4 decades. The discrete-ordinates method of solving the Boltzmann transport equation was devised in the 1950s and put into practice in the 1960s in a series of computer codes, such as DTF, DOT, and ANISN. The spherical harmonics method of treating neutron spatial and energy distributions in shields was advanced by Shure [7] in one-dimensional P_3 calculations. Progress in Monte Carlo methods advanced in pace with discrete-ordinates methods, and the multigroup Monte Carlo code for neutron and gamma-ray transport, MORSE, was introduced at the end of the decade. The continuous energy Monte Carlo code, now known as MCNP, also began in this decade at Los Alamos National Laboratory. A general-purpose particle-transport code MCS was written in 1963 to be followed by the MCN code for three-dimensional calculations written in 1965.

The Decade of the 1970s

The Nuclear Non-Proliferation Treaty (NPT) of 1968 and the National Environmental Policy Act (NEPA) of 1969 had major impacts on the radiation shielding field in the 1970s and succeeding decades. The NPT precluded nuclear fuel reprocessing and led to ever-increasing needs for on-site storage of spent fuel at nuclear power plants. NEPA required exhaustive studies of off-site radiation doses around nuclear power plants and environmental impacts of plant operations. Early in the 1970s, there were major disruptions in oil supplies caused by the OPEC embargo. The response in the USA was an energy policy that forbade electricity production using oil or natural gas. The result was placement of many orders for nuclear power plants despite NPT and NEPA constraints. In the field of radiation shielding, special attention was given to plant design issues such as streaming of neutrons and gamma rays through voids, passageways, and shield penetrations, and to operational issues such as fission-product inventories in fuels and gamma-ray skyshine, particularly associated with ^{16}N sources.

Information essential for plant design, fuel management, and waste management is data tracking radionuclide activities in reactor fuel and process streams, and corresponding strengths and energy spectra of sources, including fission products, activation products, and actinides. To accomplish this, the ORIGEN codes were developed at Oak Ridge National Laboratory and the CINDER code was developed at Los Alamos National Laboratory. Assessment of radiation doses from airborne beta-particle emitters was also studied for the first time. Although the ETRAN Monte Carlo code for electron transport was available at the National Bureau of Standards, work began in the mid-1970s at Sandia Laboratory on the TIGER code and at Stanford Linear Accelerator Center on the EGS code, both for coupled photon and electron transport by the Monte Carlo method.

Design needs brought new attention to buildup factors and to attenuation of broad beams of neutrons and gamma rays. Definitive compilations were made of buildup factors and also the attenuation and reflection by shields obliquely illuminated by photons. Detailed results were also obtained for transmission of neutrons and secondary gamma rays through shielding barriers. This decade also saw the publication of two important NCRP reports [8,9] dealing with neutron shielding and dosimetry and with design of medical facilities that protected against effects of gamma rays and high-energy x-rays.

Design and analysis needs also fostered continuing attention to computer codes for criticality and neutron-transport calculations. A series of more robust discrete-ordinates transport codes were developed. Advances in Monte Carlo calculations were also made. The MCN code was merged with the MCG code in 1973 to form the MCNG code for treating coupled neutron–photon transport. Another merger took place with the MCP code in 1977, allowing detailed treatment of photon transport at energies as low as 1 keV. This new code was known, then and now, as MCNP.

The 1980s and 1990s

These years saw the consolidation of resources for design and analysis work. In the 1980s, personal computers allowed methods such as point-kernel calculations to be programmed. In the 1990s, personal computers took over from the mainframe computers in even the most demanding shielding design and analysis. Comprehensive sets of fluence-to-dose conversion factors became available for widespread use. Radionuclide decay data became available in databases easily used for characterizing sources. Gamma-ray buildup factors were computed with precision and a superb method of data fitting was devised. All these carried point-kernel as well as more advanced shielding methodology to a new plateau.

Databases. Kocher [10] published radioisotope decay data for shielding design and analysis that largely supplanted earlier compilations. Then a new MIRD compendium [11] and ICRP-38 database became the norms, with the latter especially useful for characterizing low-energy x-ray and Auger electron emission. Today a wealth of nuclear structure and decay data is available on the web from the National Nuclear Data Center at Brookhaven National Laboratory (http://www.nndc.bnl.gov/index.jsp).

Advances in buildup factors. Refinements in the computation of buildup factors continued to be made over the years. Computer codes now could account for not only Compton scattering and photoelectric absorption, but also positron creation and annihilation, fluorescence, and bremsstrahlung. Calculation of buildup factors incorporating all these sources of secondary photon radiation was made leading to a comprehensive set of precise buildup factors standardized for use in design and analysis [12]. Also a new five-parameter buildup-factor formulation, called the *geometric progression* formula, was introduced. Although difficult to use for hand calculations, it is an extraordinarily precise formula and is today used in most modern point-kernel codes. Both the calculated buildup factors and the coefficients for the geometric progression buildup factors are tabulated in the design standard [12].

Cross sections and dose conversion factors. Authoritative cross-section data are now available in the ENDF/B (evaluated nuclear data file) (http://www.nndc.bnl.gov/exfor/endf00.htm) database containing evaluated cross sections, spectra, angular distributions, fission product yields, photo-atomic and thermal scattering law data, with emphasis on neutron-induced reactions. The National Institute of Science and Technology (NIST) has long been the repository for gamma-ray interaction coefficients. The Institute also sponsors the XCOM cross-section code, which may be executed on the NIST Internet site (http://physics.nist.gov/PhysRefData/Xcom/Text/XCOM.html) or downloaded for personal use.

Gamma-ray fluence-to-dose conversion factors for local values of exposure or kerma may be computed directly from readily available energy transfer or energy absorption coefficients for air, tissue, etc. Neutron conversion factors for local values of tissue kerma were computed by Caswell et al. [13]. As the second century of radiation protection begins, there are two classes of fluence-to-dose conversion factors in use for neutrons and gamma rays. One very conservative class is to be used for

operational purposes at doses well below regulatory limits. This class is based on doses at fixed depths in 30-cm diameter spherical phantoms irradiated in various ways. The other class is to be used for dose assessment purposes, and not for personnel dosimetry. This class is based on the anthropomorphic human phantom and weight factors for effective dose equivalent [14] or effective dose [15].

Computer applications. The 1980s and 1990s were decades of revolution for the computational aspects of radiation shield design and analysis. The advent of inexpensive personal computers with rapidly increasing speeds and memory freed the shielding analyst from dependence on a few supercomputers at national laboratories. Many shielding codes that could previously run only on large mainframe computers were reworked to run on small personal computers, thereby, allowing any shielding analysts to perform detailed calculations that only a privileged few were able to do previously.

At the same time, many improvements were made to the transport codes and their algorithms. MCNP has gone through a series of improvements adding new capabilities and improvements, such as new variance reduction methods, tallies, and physics models. It has also spun off a second version MCNPX with a capability of treating 34 types of particles with energies up to 150 MeV. Also in these decades many other Monte Carlo transport codes were developed by researchers in many nations. Each version has unique features and capabilities. General-purpose discrete-ordinates codes were also extensively improved with many novel acceleration schemes introduced to improve their speeds. An excellent review of many such improvements is given by Adams and Larsen [16].

Practice of Radiation Shielding

Shielding design and shielding analysis are complementary activities. In design, the source and maximum target dose are specified, and the task is to determine the type and amount of the shielding required to reduce the target dose to that specified. In analysis, the source and shielding are identified and the task is to determine the dose at some point(s) of interest. Whether one is engaged in a hand calculation or in a most elaborate Monte Carlo simulation, one is faced with the tasks of (1) characterizing the source, (2) characterizing the nature and attenuating properties of the shielding materials, (3) evaluating at a target location the radiation intensity and perhaps its angular and energy distributions, and (4) converting the intensity to a dose or response meaningful in terms of radiation effects.

Source Characterization

Source geometry, energy, and angular distribution are required characteristics. Radionuclide sources, with isotropic emission and unique energies of gamma and x-rays are relatively easy to characterize. Activity and source strength must be

carefully distinguished, as not every decay results in emission of a particular gamma or x-ray. Careful consideration must be given to a low-energy limit below which source particles may be ignored, else computation resources may be wasted. Similarly, when photons of many energies are emitted, as in the case of fission-product sources, one is compelled to use a group structure in source characterization, and much care is needed in establishing efficient and appropriate group energy limits and group average energies. When the source energies are continuously distributed, as is the case with fission neutrons and gamma rays, one option is to use a multigroup approach, as might be used in point-kernel calculations. Another option, useful in Monte Carlo simulations, is to sample source energies from a mathematical representation of the energy spectrum.

A point source is very often an appropriate approximation of a physical source of small size. It is also appropriate to represent a line, plane, or volume source as a collection of point sources, as is done in the point-kernel method of shielding analysis. Radionuclide and fission sources are isotropic in angular distribution; however, there are cases for which it is efficient to identify a surface and to characterize the surface as a secondary source surface. Such surface sources are very often non-isotropic in angular distribution. For example, consider the radiation emitted into the atmosphere from a large body of water containing a distributed radiation source. The interface may be treated approximately, but very effectively, as a plane source emitting radiation not isotropically, but with an intensity varying with the angle of emission from the surface.

Attenuating Properties

The total microscopic cross section for an element or nuclide, $\sigma(E)$, multiplied by the atomic density, is the linear interaction coefficient $\mu(E)$, also called the macroscopic cross section, the probability per unit (differential) path length that a particle of energy E interacts with the medium in some way. Its reciprocal, called the *mean free path*, is the average distance traveled before interaction. Usually, the ratio μ/ρ, called the mass interaction coefficient, is tabulated because it is independent of density. Various subscripts may be used to designate particular types of interactions, for example, $\sigma_{\mathrm{a}}(E)$ for absorption or $\sigma_{\mathrm{f}}(E)$ for fission. Likewise, additional independent variables may be introduced, with, for example, $\sigma_{\mathrm{s}}(E, E')\mathrm{d}E'$ representing the cross section for scattering from energy E to an energy between E' and $E' + \mathrm{d}E'$. Information resources for attenuating properties are described in this entry's historical review, as are resources for radionuclide decay data.

Intensity Characterization

The intensity of a neutron or photon field is usually described in terms of radiation crossing the surface of a small spherical volume V. The *fluence* Φ is defined, in the limit $V \to 0$, as the expected or average sum of the path lengths in V traveled by

entering particles divided by the volume V. Equivalently, Φ is, again in the limit $V \to 0$, the expected number of particles crossing the surface of V divided by the cross-sectional area of the volume. The time derivative of the fluence is the fluence rate or *flux density* Φ. Note that the fluence, though having units of reciprocal area, has no reference area or orientation. Note too that the fluence and flux are point functions. The fluence, a function of position, may also be a distribution function for particle energies and directions. For example, $\Phi(r, E, \Omega)\, \mathrm{d}E\mathrm{d}\Omega$ is the fluence at $\mathbf{r}$ of particles with energies in $\mathrm{d}E$ about E and with directions in solid angle $\mathrm{d}\Omega$ about the direction Ω. When a particular surface, with outward normal $\mathbf{n}$, is used as a reference, it is useful to define radiation intensity in terms of the flow $J_n(\mathbf{r}, E, \Omega)\, \mathrm{d}E\mathrm{d}\Omega \equiv \mathbf{n} \cdot \Omega\Phi(\mathbf{r}, E, \Omega)\, \mathrm{d}E\mathrm{d}\Omega$ across the reference surface.

Fluence-to-Dose Conversion Factors

Whether the shield designer uses the simplest of the point-kernel methods or the most comprehensive of the Monte Carlo or discrete-ordinates methods, fluence-to-dose conversion factors generally have to be used. The radiation attenuation calculation deals with the particle fluence, the direct measure of radiation intensity. To convert that intensity into a measure of radiation damage or heating of a material, to a field measurement such as *exposure*, or to a measure of health risk, conversion factors must be applied.

The shielding analysis ordinarily yields the energy spectrum $\Phi(\mathbf{r}, E)$ of the photon or neutron fluence at a point identified by the vector $\mathbf{r}$. Use of a Monte Carlo code normally yields the energy spectrum as a function of energy, whence the dose or, more generally, response $R(\mathbf{r})$ is given by the convolution of the fluence with the fluence-to-dose factor, here called the response function $\mathcal{R}(E)$, so that

$$R(\mathbf{r}) = \int_E \mathrm{d}E\mathcal{R}(\mathbf{r}, E)\Phi(\mathbf{r}, E). \tag{14.1}$$

Point-kernel, or other energy-multigroup methods yield the energy spectrum at discrete energies, or in energy groups, and the dose convolution is a summation rather than an integration.

While the fluence is most always computed as a point function of position, the response of interest may be a dose at a point (called a *local* dose) or it may be a much more complicated function such as the average radiation dose in a physical volume such as an anthropomorphic phantom. Local and phantom-related doses are briefly discussed later.

Suppose the local dose of interest is the kerma, defined as the expected sum of the initial kinetic energies of all charged particles produced by the radiation field in a mass m, in the limit as $m \to 0$. Then the response function is given by

$$\mathcal{R}_K(E) = \kappa \sum_i \frac{N_i}{\rho} \sum_j \sigma_{ji}(E)\epsilon_{ji}(E). \tag{14.2}$$

in which ρ is the mass density, N_i is the atoms of species i per unit volume (proportional to ρ), $\sigma_{ji}(E)$ is the cross section for the jth interaction with species i, and $\epsilon_{ji}(E)$ is the average energy transferred to secondary charged particles in the jth interaction with species i. A units conversion factor κ is needed to convert from, say, units of MeV cm^2/g to units of rad cm^2 or Gy cm^2. For neutrons, a quality factor multiplier $Q(E)$ is needed to convert to units of *dose equivalent* (rem or Sv). For photons, Eq. 2 reduces to

$$\mathcal{R}_{\mathcal{K}}(E)\ (\text{Gy cm}^2) = 1.602 \times 10^{-10} E[\mu_{\text{tr}}(E)/\rho], \tag{14.3}$$

where E is in MeV and μ_{tr}/ρ is the mass energy transfer coefficient in units of cm^2/g for the material to which energy is transferred.

More related to radiation damage is the local *absorbed dose*, defined as the expected energy imparted, through ionization, excitation, chemical changes, and heat, to a mass m, in the limit as $m \to 0$. Under conditions of *charged-particle equilibrium*, the neutron or gamma-ray kerma equals the absorbed dose, less the energy radiated away as bremsstrahlung. Such equilibrium is approached in a region of homogeneity in composition and uniformity in neutron or photon intensity. Then the absorbed dose is given by Eq. 3 with μ_{tr} replaced by the energy absorption coefficient μ_{en} to account for any bremsstrahlung losses.

The second type of response function or dose is that related to the local dose within a simple geometric phantom or some sort of average dose within an anthropomorphic phantom. The phantom dose, in fact, is a point function and serves as a standardized reference dose for instrument calibration and radiation protection purposes. Even though the radiation fluence, itself a point function, may have strong spatial and angular variation as well as energy variation, it is still possible to associate with the radiation fluence a phantom-related dose. The procedure is as follows. The fluence is treated, for example, as a very broad parallel beam of the same intensity as the actual radiation field, incident in some fixed way on the phantom. This is the so-called expanded and aligned field. For a geometric phantom, the dose is computed at a fixed depth. For an anthropomorphic phantom, the dose is computed as an average of doses to particular tissues and organs, weighted by the susceptibility of the tissues and organs to radiation carcinogenesis or hereditary illness. Many phantoms have been used with various directions of incident radiation. The calculated response functions are then tabulated as a function of the radiation energy. Additional details of phantom doses and their tabulations are given by Shultis and Faw [17].

Basic Analysis Methods

To say modern shielding practice has been reduced to running large "black-box" codes is very misleading. Randomly varying model parameters, such as shield dimensions, placement, and material, is a very inefficient way to optimize shielding

for a given situation. Using the concepts and ideas behind the earlier simplified methods often allows a shield analyst to select materials and geometry for a preliminary design before using large transport codes to refine the design. In this section, fundamental methods for estimating neutron or photon doses are reviewed. Such indirectly ionizing radiation is characterized by straight-line trajectories punctuated by "point" interactions. The basic concepts presented here apply equally to all particles of such radiation.

It should be noted that throughout this entry, calculated doses are the *expected* or *average* value of the stochastic measured doses, that is, the mechanistically calculated dose represents the statistical average of a large number of dose measurements which exhibit random fluctuations as a consequence of the stochastic nature of the source emission and interactions in the detector and surrounding material.

Uncollided Radiation Doses

In many situations, the dose at some point of interest is dominated by particles streaming directly from the source without interacting in the surrounding medium. For example, if only air separates a gamma-ray or neutron source from a detector, interactions in the intervening air or in nearby solid objects, such as the ground or building walls, are often negligible, and the radiation field at the detector is due almost entirely to uncollided radiation coming directly from the source.

In an attenuating medium, the uncollided dose at a distance r from a point isotropic source emitting S_p particles of energy E is

$$D^\mathrm{o}(r) = \frac{S_\mathrm{p}\mathcal{R}}{4\pi r^2}\mathrm{e}^{-l}, \tag{14.4}$$

where l is the total number of mean-free-path lengths of material a particle must traverse before reaching the detector, namely, $\int_0^r \mathrm{d}s\,\mu(s)$. Here $\mathcal{R}$ is the appropriate response function. The $1/(4\pi r^2)$ term in Eq. 4 is often referred to as the *geometric* attenuation and the e^{-l} term the *material* attenuation. Equation 4 can be extended easily to a source emitting particles with different discrete energies or a continuous spectrum of energies.

Point Kernel for Uncollided Dose

Consider an isotropic point source placed at $\mathbf{r}_\mathrm{s}$ and an isotropic point detector (or *target*) placed at $\mathbf{r}_\mathrm{t}$ in a homogeneous medium. The detector response depends not on $\mathbf{r}_\mathrm{s}$ and $\mathbf{r}_\mathrm{t}$ separately, but only on the distance $|\mathbf{r}_\mathrm{s} - \mathbf{r}_\mathrm{t}|$ between the source and detector. For a unit strength source, the detector response is (cf. Eq. 4)

$$\mathcal{G}^{\mathrm{o}}(\mathbf{r}_{\mathrm{s}}, \mathbf{r}_{\mathrm{t}}, \mathcal{E}) = \frac{\mathcal{R}(\mathcal{E})}{\triangle\pi|\mathbf{r}_{\mathrm{s}} - \mathbf{r}_{\mathrm{t}}|^{\in}} \mathrm{e}^{-\mu(\mathcal{E})|\mathbf{r}_{\mathrm{s}} - \mathbf{r}_{\mathrm{t}}|}. \tag{14.5}$$

Here $\mathcal{G}^{\mathrm{o}}(\mathbf{r}_{\mathrm{s}}, \mathbf{r}_{\mathrm{t}}, E)$ is the *uncollided dose point kernel* and equals the dose at $\mathbf{r}_{\mathrm{t}}$ per particle of energy E emitted isotropically at $\mathbf{r}_{\mathrm{s}}$. This result holds for any geometry or medium provided that the material through which a ray from $\mathbf{r}_{\mathrm{s}}$ to $\mathbf{r}_{\mathrm{t}}$ passes has a constant interaction coefficient μ.

With this point kernel, the uncollided dose due to an arbitrarily distributed source can be found by first decomposing (conceptually) the source into a set of contiguous effective point sources and then summing (integrating) the dose produced by each point source.

Applications to Selected Geometries

The results for the uncollided dose from a point source can be used to derive expressions for the uncollided dose arising from a wide variety of distributed sources such as line sources, area sources, and volumetric sources [4, 5, 18, 19]. An example to illustrate the method is as follows:

An isotropic disk source of radius a emitting isotropically S_a particles per unit area at energy E is depicted in Fig. 14.1. A detector is positioned at point P a distance h above the center of the disk. Suppose the only material separating the disk source and the receptor at P is a slab of thickness t with a total attenuation coefficient μ.

Consider a differential area $\mathrm{d}A$ between distance ρ and $\rho + \mathrm{d}\rho$ from the disk center and between ψ and $\psi + \mathrm{d}\psi$. The source within $\mathrm{d}A$ may be treated as an effective point isotropic source emitting $S_a \mathrm{d}A = S_a \rho \mathrm{d}\rho \mathrm{d}\psi$ particles which produces an uncollided dose at P of $\mathrm{d}D^{\mathrm{o}}$. The ray from the source in $\mathrm{d}A$ must pass through a slant distance of the shield $t\sec\theta$ so that the dose at P from particles emitted in $\mathrm{d}\rho$ about ρ is

$$\mathrm{d}D^{\mathrm{o}}(P) = \frac{\mathcal{R} S_a \rho \mathrm{d}\rho \mathrm{d}\psi}{4\pi r^2} \exp[-\mu t \sec\theta], \tag{14.6}$$

where $\mathcal{R}$ and μ generally depend on the particle energy E. To obtain the total dose at P from all differential areas of the disk source, one then must sum, or rather integrate, $\mathrm{d}D^{\mathrm{o}}$ over all differential areas. Thus, the total uncollided dose at P is

$$D^{\mathrm{o}}(P) = \frac{S_a \mathcal{R}}{4\pi} \int_0^{2\pi} \mathrm{d}\psi \int_0^a \mathrm{d}\rho \frac{\rho exp[-\mu t \sec\theta]}{r^2}. \tag{14.7}$$

Because h is fixed, $\rho \mathrm{d}\rho = r\mathrm{d}r$, and from Fig. 14.1 it is seen that $r = h\sec\theta$. Integration over ψ and changing variables yields

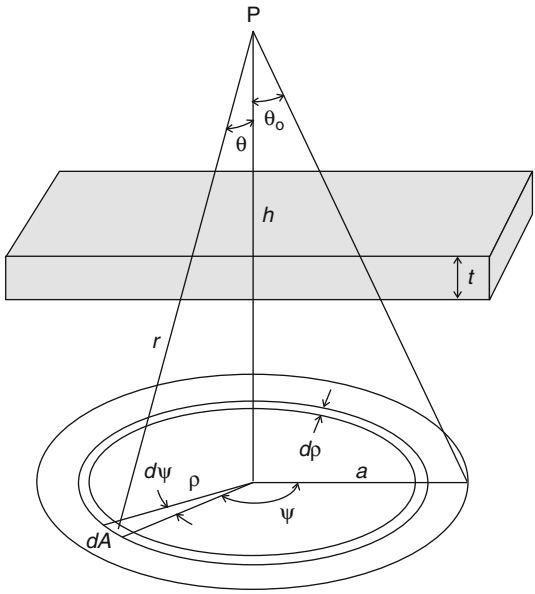

Fig. 14.1 An isotropic disk source is shielded by a parallel slab shield of thickness t

$$D^{\mathrm{o}}(P) = \frac{S_a \mathcal{R}}{2} \int_h^{h\sec\theta_{\mathrm{o}}} \mathrm{d}r\, r^{-1} \mathrm{e}^{-\mu r t/h} \tag{14.8}$$

$$= \frac{S_a \mathcal{R}}{2} \int_{\mu t}^{\mu t \sec\theta_o} \mathrm{d}x\, x^{-1} \mathrm{e}^{-x} \tag{14.9}$$

$$= \frac{S_a \mathcal{R}}{2} [E_1(\mu t) - E_1(\mu t \sec\theta_{\mathrm{o}})], \tag{14.10}$$

where the *exponential integral function* E_n is defined as $E_n(x) \equiv x^{n-1} \int_x^\infty \mathrm{d}u\, u^{-n} \mathrm{e}^{-u}$ and is tabulated in many compilations [4, 5, 17].

Intermediate Methods for Photon Shielding

In this section, several special techniques are summarized for the design and analysis of shielding for gamma and x-rays with energies from about 1 keV to about 20 MeV. These techniques are founded on very precise radiation transport calculations for a wide range of carefully prescribed situations. These techniques, which rely on buildup factors, attenuation factors, albedos or reflection factors, and line-beam response functions, then allow estimation of photon doses for many frequently encountered shielding situations without the need of transport calculations.

Buildup-Factor Concept

The total photon fluence $\Phi(\mathbf{r}, E)$ at some point of interest $\mathbf{r}$ is the sum of two components: the *uncollided* fluence $\Phi^{\mathrm{o}}(\mathbf{r}, E)$ of photons that have streamed to $\mathbf{r}$ directly from the source without interaction, and the fluence of *scattered* and *secondary* photons $\Phi^{\mathrm{s}}(\mathbf{r}, E)$ consisting of source photons scattered one or more times, as well as secondary photons such as x-rays and annihilation gamma rays.

The buildup factor $B(\mathbf{r})$ is defined as

$$B(\mathbf{r}) \equiv \frac{D(\mathbf{r})}{D^{\mathrm{o}}(\mathbf{r})} = 1 + \frac{D^{\mathrm{s}}(\mathbf{r})}{D^{\mathrm{o}}(\mathbf{r})}, \tag{14.11}$$

where $D(\mathbf{r})$ is the total dose equal to the sum of the uncollided dose $D^{\mathrm{o}}(\mathbf{r})$ and the scattered or secondary photon dose $D^{\mathrm{s}}(\mathbf{r})$. For a monoenergetic source this reduces to

$$B(E_{\mathrm{o}}, \mathbf{r}) = 1 + \frac{1}{\Phi^{\mathrm{o}}(\mathbf{r})} \int_0^{E_{\mathrm{o}}} \mathrm{d}E \frac{\mathcal{R}(E)}{\mathcal{R}(E_{\mathrm{o}})} \Phi^{\mathrm{s}}(\mathbf{r}, E). \tag{14.12}$$

In this case, the nature of the dose or response is fully accounted for in the ratio $\mathcal{R}(E)/\mathcal{R}(E_{\mathrm{o}})$. By far the largest body of buildup-factor data is for point, isotropic, and monoenergetic sources of photons in infinite homogeneous media. Calculation of buildup factors for high-energy photons requires consideration of the paths traveled by positrons from their creation until their annihilation. Such calculations have been performed by Hirayama [20] and by Faw and Shultis [21] for photon energies as great as 100 MeV. Because incoherent scattering was neglected in many buildup-factor calculations, coherent scattering should also be neglected in calculating the uncollided dose, a significant consideration only for low-energy photons at deep penetration.

Buildup-Factor Geometry

Generally, buildup factors depend on the source and shield geometries. For a given material thickness between source and detector, buildup factors are slightly different for point isotropic sources in (a) an infinite medium, (b) at the surface of a bare sphere, and for a slab shield between source and detector. However, the use of buildup factors for a point isotropic source is almost always conservative, that is, the estimated dose is greater than that for a finite shield [17]. Adjustment factors for buildup factors at the surface of a finite medium in terms of the infinite-medium buildup factors is illustrated in Fig. 14.2.

Buildup factors are also available for plane isotopic (PLI) and plane monodirectional (PLM) gamma-ray sources in infinite media. Indeed, Fano et al. [22], Goldstein [23], and Spencer [24], in their moments-method calculations,

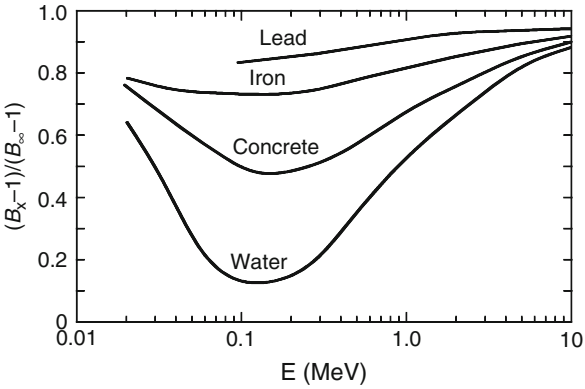

Fig. 14.2 Adjustment factor for the buildup factor B_x at the boundary of a finite medium in terms of the infinite-medium buildup factor B_∞ for the same depth of penetration (EGS4 calculations courtesy of Sherrill Shue, Nuclear Engineering Department, Kansas State University)

obtained buildup factors for plane sources first and, from these, buildup factors for point sources were derived. Buildup factors at depth in a half-space shield are also available for the PLM source, that is, normally incident photons [20, 25, 26]. The use of buildup factors for a point isotropic source in an infinite medium is conservative, that is, overpredictive, for the PLI and PLM geometries.

Buildup Factors for Stratified Shields

Sometimes shields are stratified, that is, composed of layers of different materials. The use of the buildup-factor concept for such heterogeneous shields is, for the most part, of dubious merit. Nevertheless, implementation of point-kernel codes for shielding design and analysis demands some way of treating buildup when the ray from source point to dose point is through more than one shielding material. However, certain regularities do exist, which permit approximate use of homogeneous-medium buildup factors for stratified shields. Many approximate buildup methods have been suggested, as described by Shultis and Faw [17]; however, they are of little use in most point-kernel codes and are not needed at all for shielding analysis based on transport methods.

Point-Kernel Computer Codes

There are many codes in wide use that are based on the point-kernel technique. In these codes, a distributed source is decomposed into small but finite elements and the dose at some receptor point from each element is computed using the uncollided dose kernel and a buildup factor based on the optical thickness of material between the source element and the receptor. The results for all the source elements are then added together to obtain the total dose. Some that have been widely used are MicroShield [27], the QAD series [28], QADMOD-GP [29], QAD-CGGP [30], and G^3 [31].

Broad-Beam Attenuation

Often a point radionuclide or x-ray source in air is located sufficiently far from a wall or shielding slab that the radiation reaches the wall in nearly parallel rays. Further, the attenuation in the air is usually quite negligible in comparison to that provided by the shielding wall. Shielding design and analysis for such broad-beam illumination of a slab shield are addressed by NCRP Report 49 [9], Archer [32], and Simpkin [33]. The dose at the surface of the cold side of the wall can be computed as

$$D = D^{\mathrm{o}} A_{\mathrm{f}}. \tag{14.13}$$

For a radionuclide source of activity $\mathcal{A}$, the dose D^{o} without the wall can be expressed in terms of the source energy spectrum, response functions, and distance r from the source to the cold side of the wall. Then,

$$D = D^{\mathrm{o}} A_{\mathrm{f}} = \frac{\mathcal{A}}{r^2} \Gamma A_{\mathrm{f}}, \tag{14.14}$$

where Γ, called the *specific gamma-ray constant*, is the dose rate in vacuum at a unit distance from a source with unit activity, and A_{f} is an *attenuation factor* which depends on the nature and thickness of the shielding material, the source energy characteristics, and the angle of incidence θ (with respect to the wall normal). Values for Γ and A_{f} are provided by NCRP [9].

Oblique Incidence

Attenuation factors for obliquely incident beams are presented in NCRP Report 49 [9]. For such cases, special three-argument slant-incidence buildup factors should be used [17]. For a shield wall of thickness t mean free paths, slant incidence at angle θ with respect to the normal to the wall, and source energy E_{o}, the attenuation factor is in function form $A_{\mathrm{f}}(E_{\mathrm{o}}, t, \theta)$. However, a common, but erroneous, practice has been to use a two-argument attenuation factor based on an infinite-medium buildup factor for slant penetration distance $t\sec\theta$, in the form $A_{\mathrm{f}}(E_{\mathrm{o}}, t\sec\theta)$. This practice can lead to severe underprediction of transmitted radiation doses.

X-ray Beam Attenuation

For x-ray sources, the appropriate measure of source strength is the electron-beam current i, and the appropriate characterization of photon energies, in principle, involves the peak accelerating voltage (kVp), the wave form, and the degree of

filtration (e.g., beam half-value thickness). If i is the beam current (mA) and r is the source-detector distance (m), the dose behind a broadly illuminated shield wall is

$$D(P) = \frac{i}{r^2} K_o A_f, \tag{14.15}$$

in which K_o, called the *radiation output (factor)*, is the dose rate in vacuum (or air) per unit beam current at unit distance from the source in the absence of the shield. Empirical formulas for computing A_f are available for shield design [34, 35].

Intermediate Methods for Neutron Shielding

Shielding design for fast neutrons is generally far more complex than shielding design for photons. Not only does one have to protect against the neutrons emitted by some source, one also needs to protect against primary gamma rays emitted by most neutron sources as well as secondary photons produced by inelastic neutron scattering and from radiative capture. There may also be secondary neutrons produced from $(n, 2n)$ and fission reactions. In many instances, secondary photons produce greater radiological risks than do the primary neutrons. Fast-neutron sources include spontaneous and induced fission, fusion, (α, n) reactions, (γ, n) reactions, and spallation reactions in accelerators, each producing neutrons with a different distribution of energies.

Unlike photon cross sections, neutron cross sections usually vary greatly with neutron energy and among the different isotopes of the same element. Comprehensive cross-section databases are needed. Also, because of the erratic variation of the cross sections with energy, it is difficult to calculate uncollided doses needed in order to use the buildup-factor approach. Moreover, buildup factors are very geometry dependent and sensitive to the energy spectrum of the neutron fluence and, consequently, point-kernel methods can be applied to neutron shielding only in very limited circumstances.

Early work led to kernels for fission sources in aqueous systems and the use of removal cross sections to account for shielding barriers. Over the years, the methodology was stretched to apply to nonaqueous hydrogenous media, then to non-hydrogenous media, then to fast-neutron sources other than fission. Elements of diffusion and age theory were melded with the point kernels. Today, with the availability of massive computer resources, neutron shielding design and analysis is largely done using transport methods. Nevertheless, the earlier methodologies offer insight and allow more critical interpretation of transport calculations.

Also, unlike ratios of different photon response functions, those for neutrons vary, often strongly, with neutron energy. Hence, neutrons doses cannot be converted to different dose units by simply multiplying by an appropriate constant. The energy spectrum of the neutron fluence is needed to obtain doses in different units. Consequently, many old measurements or calculations of point kernels,

albedo functions, transmission factors, etc., made with obsolete dose units cannot be converted to modern units because the energy spectrum is unknown. In this case, there is no recourse but to repeat the measurements or calculations.

Capture Gamma Photons

A significant, often dominant, component of the total dose at the surface of a shield accrues from capture gamma photons produced deep within the shield and arising from neutron absorption. Of lesser significance are secondary photons produced in the inelastic scattering of fast neutrons. Secondary neutrons are also produced as a result of (γ, n) reactions. Thus, in transport methods, gamma-ray and neutron transport are almost always coupled.

Historically, capture gamma-ray analysis was appended to neutron removal calculations. Most neutrons are absorbed only when they reach thermal energies, and, consequently, only the absorption of thermal neutrons was considered. (Exceptional cases include the strong absorption of epithermal neutrons in fast reactor cores or in thick slabs of low-moderating, high-absorbing material.) For this reason, it is important to calculate accurately the thermal neutron fluence $\Phi_{\text{th}}(\mathbf{r})$ in the shield. The volumetric source strength of capture photons per unit energy about E is then given by

$$S_\gamma(\mathbf{r}, E) = \Phi_{\text{th}}(\mathbf{r})\mu_\gamma(\mathbf{r})f(\mathbf{r}, E), \tag{14.16}$$

where $\mu_\gamma(\mathbf{r})$ is the absorption coefficient at $\mathbf{r}$ for thermal neutrons and $f(\mathbf{r}, E)$ is the number of photons produced in unit energy about E per thermal neutron absorption at $\mathbf{r}$.

Once the capture gamma-ray source term $S_\gamma(\mathbf{r}, E)$ is known throughout the shield, point-kernel techniques using exponential attenuation and buildup factors can be used to calculate the capture gamma-ray dose at the shield surface.

Neutron Shielding with Concrete

Concrete is probably the most widely used shielding material because of its relatively low cost and the ease with which it can be cast into large and variously shaped shields. However, unlike that for photon attenuation in concrete, the concrete composition, especially the water content, has a strong influence on its neutron attenuation properties. Other important factors that influence the effectiveness of concrete as a neutron shield include type of aggregate, the dose–response function, and the angle of incidence of the neutrons.

Because concrete is so widely used as a shield material, its effectiveness for a monoenergetic, broad, parallel beam of incident neutrons has been extensively studied, both for normal and slant incidence, and many tabulated results for shields of various thickness are available [36–40]. These results, incorporated into design and manufacturing standards (standards are available from professional societies such as the American Nuclear Society and the American Society of Mechanical Engineers) are extremely useful in the preliminary design of concrete shields.

Gamma-Ray and Neutron Reflection

Until now only shielding situations have been considered in which the radiation reaching a target contains an uncollided component. For these situations, point-kernel approximations, in principle, may be used and concepts such as particle buildup may be applied. However, in many problems encountered in shielding design and analysis, only scattered radiation may reach the target. Radiation doses due to reflection from a surface are examples that arise in treatment of streaming of radiation through multi-legged ducts and passageways. Treatment of radiation reflection from surfaces of structures is also a necessary adjunct to precise calibration of nuclear instrumentation. Skyshine, that is, reflection in the atmosphere of radiation from fixed sources to distant points is another example of this class of reflected-radiation problems. All such reflection problems are impossible to treat using elementary point-kernel methods and are also very difficult and inefficient to treat using transport-based methods. For reflection from a surface of radiation from a point source to a point receiver, the *albedo function* has come to be very useful in design and analysis. The same can be said for use of the *line-beam response function* in treatment of skyshine. Both are discussed below.

Albedo Methods

There are frequent instances for which the dose at some location from radiation reflected from walls and floors may be comparable to the line-of-sight dose. The term *reflection* in this context does not imply a surface scattering. Rather, gamma rays or neutrons penetrate the surface of a shielding or structural material, scatter within the material, and then emerge from the material with reduced energy and at some location other than the point of entry.

In many such analyses, a simplified method, called the *albedo method*, may be used. The albedo method is based on the following approximations. (1) The displacement between points of entry and emergence may be neglected. (2) The reflecting medium is effectively a half-space, a conservative approximation. (3) Scattering in air between a source and the reflecting surface and between the reflecting surface and the detector may be neglected.

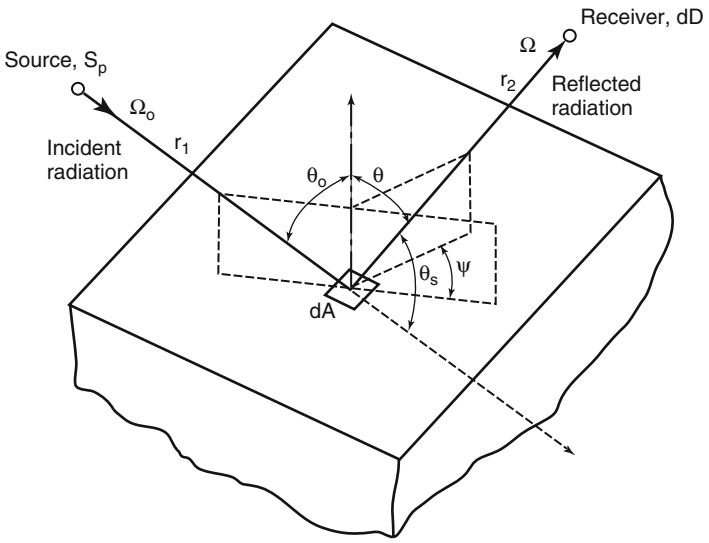

Fig. 14.3 Angular and energy relationships in the albedo formulation

Application of the Albedo Method

Radiation reflection may be described in terms of the geometry shown in Fig. 14.3. Suppose that a point isotropic and monoenergetic source is located distance r_1 from area dA along incident direction Ω_o and that a dose point is located distance r_2 from area dA along emergent direction Ω. Suppose also the source has an angular distribution such that $S(\theta_o)$ is the source intensity per steradian evaluated at the direction from the source to the reflecting area dA. Then the dose dD_r at the detector from particles reflected from dA can be shown to be [17]

$$\mathrm{d}D_r = D_o \alpha_D(E_o, \theta_o; \theta, \psi) \frac{\mathrm{d}A \cos\theta_o}{r_2^2}, \tag{14.17}$$

in which D_o is the dose at dA due to incident particles. Here $\alpha_D(E_o, \theta_o; \theta, \psi)$ is the *dose albedo*. Determination of the total reflected dose D_r requires integration over the area of the reflecting surface. In doing so one must be aware that, as the location on the surface changes, all the variables $\theta_o, \theta, \psi, r_1$, and r_2 change as well. Also, it is necessary to know $\alpha_D(E_o, \theta_o; \theta, \psi)$ or, more usefully, to have some analytical approximation for the dose albedo so that numerical integration over all the surface area can be performed efficiently.

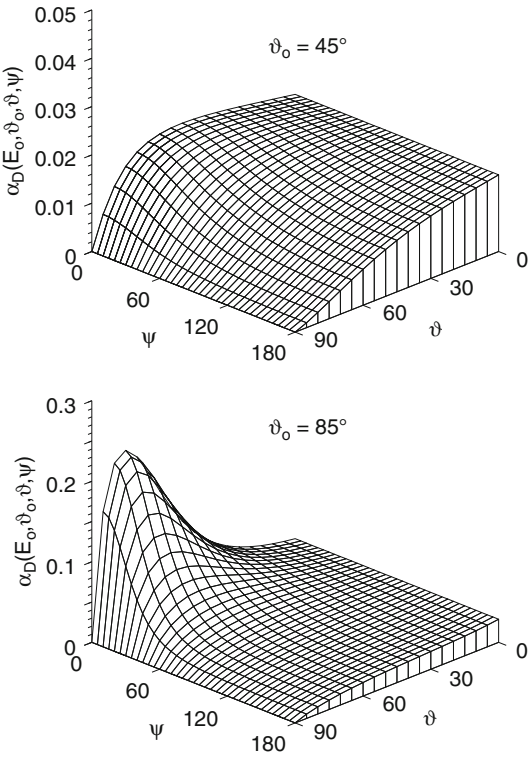

Fig. 14.4 Ambient-dose-equivalent albedos for reflection of 1.25-MeV photons from concrete, computed using the seven-term Chilton–Huddleston approximation

Gamma-Ray Dose Albedo Approximations

A two-parameter approximation for the photon dose albedo was first devised by Chilton and Huddleston [41] and later extended by Chilton et al. [42]. Chilton [43] later proposed a more accurate seven-parameter albedo formula for concrete. Brockhoff [44] published seven-parameter fit data for albedos from water, concrete, iron, and lead. Two examples of this dose albedo approximation are shown in Fig. 14.4.

Neutron Dose Albedo Approximations

The dose albedo concept is very useful for streaming problems that involve "reflection" of neutrons or photons from some material interface. However, unlike photon albedos, the neutron albedos are seldom tabulated or approximated for monoenergetic incident neutrons because of the rapid variation with energy of neutron cross sections. Rather, albedos for neutrons with a specific range of energies (energy group) are usually considered, thereby, averaging over all the

cross-section resonances in the group. Also unlike photon albedos, neutron albedos involve reflected dose from both neutrons and secondary capture gamma rays.

There are many studies of the neutron albedos in the literature. Selph [45] published a detailed review. Extensive compilations of neutron albedo data are available, for example, SAIL [46] and BREESE-II [47]. Of more utility are analytic approximations for the albedo based on measured or calculated albedos. Neutrons albedos are often divided into three types: (1) fast-neutron albedos ($E \geq 0.2$ MeV), (2) intermediate-energy albedos, and (3) thermal-neutron albedos. Selph [45] reviews early approximations for neutron albedos, among which is a 24-parameter approximation developed by Maerker and Muckenthaler [48]. Newly computed and more accurate fast-neutron albedos, based on different 24-parameter approximations, have been computed by Brockhoff [44] for several shielding materials.

For neutrons with energy less than about 100 keV, the various dose equivalent response functions are very insensitive to neutron energy. Consequently, the dose albedo α_D is very closely approximated by the number albedo α_N. Thus, for reflected dose calculations involving intermediate or thermal neutrons, the number albedo is almost always used. Coleman et al. [49] calculated neutron albedos for intermediate-energy neutrons (200 keV to 0.5 eV) incident monodirectionally on reinforced concrete slabs and developed a nine-parameter formula for the albedo.

Thermal neutrons entering a shield undergo isotropic scattering that, on the average, does not change their energies. For one-speed particles incident in an azimuthally symmetric fashion on a half-space of material that isotropically scatters particles, Chandrasekhar [50] derived an exact expression for the differential albedo. A purely empirical and particularly simple formula, based on Monte Carlo data for thermal neutrons, has been proposed by Wells [51] for ordinary concrete, namely,

$$\alpha_N(\theta_o; \theta, \psi) = 0.21 \cos\theta (\cos\theta_o)^{-1/3}. \tag{14.18}$$

Radiation Streaming Through Ducts

Except in the simplest cases, the analysis of radiation streaming requires advanced computational procedures. However, even within the framework of Monte Carlo transport calculations, albedo methods are commonly used, and special data sets have been developed for such use [46, 47, 52].

Elementary methods for gamma-ray streaming are limited to straight cylindrical ducts, with incident radiation symmetric about the duct axis and uniform over the duct entrance. Transmitted radiation generally may be subdivided into three components: line-of-sight, lip-penetrated, and wall scattered. The first two may be treated using point-kernel methodology. The last requires use of albedo methods to account for scattering over the entire surface area of the duct walls. Selph [45]

reviews the methodology of duct transmission calculations and LeDoux and Chilton [53] devised a method of treating two-legged rectangular ducts, important in analysis of structure shielding.

Neutron streaming through gaps and ducts in a shield is much more serious for neutrons than for gamma photons. Neutron albedos, especially for thermal neutrons, are generally much higher than those for photons, and multiple scattering within the duct is very important. Placing bends in a duct, which is very effective for reducing gamma-ray penetration, is far less effective for neutrons. Fast neutrons entering a duct in a concrete shield become thermalized and thereafter are capable of scattering many times, allowing the neutrons to stream through the duct, even those with several bends. Also, unlike gamma-ray streaming, the duct need not be a void (or gas filled) but can be any part of a heterogeneous shield that is "transparent" to neutrons. For example, the steel walls of a water pipe embedded in a concrete shield (such as the cooling pipes that penetrate the biological shield of a nuclear reactor) act as an annular duct for fast neutrons.

There is much literature on experimental and calculational studies of gamma-ray and neutron streaming through ducts. In many of these studies, empirical formulas, obtained by fits to the data, have been proposed. These formulas are often useful for estimating duct-transmitted doses under similar circumstances. As a starting point for finding such information, the interested reader is referred to Rockwell [18], Selph [45], and NCRP [54].

Gamma-Ray and Neutron Skyshine

For many intense localized sources of radiation, the shielding against radiation that is directed skyward is usually far less than that for the radiation emitted laterally. However, the radiation emitted vertically into the air undergoes scattering interactions and some radiation is reflected back to the ground, often at distances far from the original source. This atmospherically reflected radiation, referred to as *skyshine*, is of concern both to workers at a facility and to the general population outside the facility site.

As alternatives to rigorous transport-theory treatment of the skyshine problem several approximate procedures have been developed for both gamma-photon and neutron skyshine sources [54]. This section summarizes one approximate method, which has been found useful for bare or shielded skyshine sources. The *integral line-beam skyshine method*, is based on the availability of a *line-beam response function* $\mathcal{R}(E, \phi, x)$, which gives the dose (air kerma or ambient dose) at a distance x from a point source emitting a photon or neutron of energy E at an angle ϕ from the source-to-detector axis into an infinite air medium. The air–ground interface is neglected in this method. This response function can be fit over a large range of x to the following three-parameter empirical formula, for a fixed value of E and ϕ [55]:

$$\mathcal{R}(E, \phi, x) = \kappa(\rho/\rho_o)^2 E[x(\rho/\rho_o)]^b \exp[a - cx(\rho/\rho_o)], \tag{14.19}$$

in which ρ is the air density in the same units as the reference density $\rho_o = 0.001\ 2\ \mathrm{g/cm^3}$. The constant κ depends on the choice of units.

The parameters a, b, and c in Eq. 19 depend on the photon or neutron energy and the source emission angle. These parameters have been estimated and tabulated, for fixed values of E and ϕ, by fitting Eq. 19 to values of the line-beam response function, at different x distances, usually obtained by Monte Carlo calculations. Gamma-ray response functions have been published by Lampley [56] and Brockhoff et al. [57]. Neutron and secondary gamma-ray response functions have been published by Lampley [56] and Gui et al. [58]. These data and their method of application are presented by Shultis and Faw [17].

To obtain the skyshine dose $D(d)$ at a distance d from a bare collimated source, the line-beam response function, weighted by the energy and angular distribution of the source, is integrated over all source energies and emission directions. Thus, if the collimated source emits $S(E, \Omega)$ photons, the skyshine dose is

$$D(d) = \int_0^\infty \mathrm{d}E \int_{\Omega_s} \mathrm{d}\Omega\, S(E, \Omega)\mathcal{R}(E, \phi, d), \tag{14.20}$$

where the angular integration is over all emission directions Ω_s allowed by the source collimation. Here, ϕ is a function of the emission direction Ω. To obtain this result, it has been assumed that the presence of an air–ground interface can be neglected by replacing the ground by an infinite air medium. The effect of the ground interface on the skyshine radiation, except at positions very near a broadly collimated source, has been found to be very small.

The presence of a shield over a skyshine source, for example, a building roof, causes some of the source particles penetrating the shield to be degraded in energy and angularly redirected before being transported through the atmosphere. The effect of an overhead shield on the skyshine dose far from the source can be accurately treated by a two-step hybrid method [59,60]. First a transport calculation is performed to determine the energy and angular distribution of the radiation penetrating the shield, and then, with this distribution as an effective point, bare, skyshine source, the integral line-beam method is used to evaluate the skyshine dose.

The integral line-beam method for gamma-ray and neutron skyshine calculations has been applied to a variety of source configurations and found to give generally excellent agreement with benchmark calculations and experimental results [59]. It has been used as the basis of the microcomputer code *MicroSkyshine* [61] for gamma rays. A code package for both neutron and gamma-ray calculations is available from the Radiation Safety Computation Information Center. (Code package CCC-646: SKYSHINE-KSU: Code System to Calculate Neutron and Gamma-Ray Skyshine Doses Using the Integral Line-Beam Method, and data library DLC-188: SKYDATA-KSU: Parameters for Approximate Neutron and Gamma-Ray Skyshine Response Functions and Ground Correction Factors.)

Transport Theory

For difficult shielding problems in which simplified techniques such as point kernels with buildup corrections cannot be used, calculations based on transport theory must often be used. There are two basic approaches for transport calculations: *deterministic* transport calculations in which the linear Boltzmann equation is solved numerically, and *Monte Carlo* calculations in which a simulation is made of how particles migrate stochastically through the problem geometry. Both approaches have their advantages and weaknesses. Because of space limitations, it is not possible to give a detailed review of the vast literature supporting both approaches. What follows is a brief explanation of the basic ideas involved and some general references are supplied.

Deterministic Transport Theory

The neutron or photon flux $\phi(\mathbf{r}, E, \Omega)$ for particles with energy E and direction Ω is rigorously given by the linear Boltzmann equation or, simply, the transport equation

$$\Omega \cdot \nabla\phi(\mathbf{r}, E, \Omega) + \mu(\mathbf{r}, E)\phi(\mathbf{r}, E, \Omega) = S(\mathbf{r}, E, \Omega) + \int_0^\infty \mathrm{d}E' \int_{4\pi} \mathrm{d}\Omega' \, \mu_s(\mathbf{r}, E', \Omega' \to E, \Omega)\phi(\mathbf{r}, E', \Omega'), \tag{14.21}$$

where S is the volumetric source strength of particles. This equation can be formally integrated to yield the integral form of the transport equation, namely,

$$\phi(\mathbf{r}, E, \Omega) = \phi(\mathbf{r} - R\Omega, E, \Omega)f(R) + \int_0^R \mathrm{d}R' q(\mathbf{r} - R'\Omega, \Omega)f(R'), \tag{14.22}$$

where $f(x) \equiv \exp\left[-\int_0^x \mu(\mathbf{r} - R''\Omega, E)\,\mathrm{d}R''\right]$ and q is given by

$$q(\mathbf{r}, E, \Omega) \equiv S(\mathbf{r}, E, \Omega) + \int_0^\infty \mathrm{d}E' \int_{4\pi} \mathrm{d}\Omega' \mu_s(\mathbf{r}, E', \Omega' \to E, \Omega)\phi(\mathbf{r}, E', \Omega'). \tag{14.23}$$

Unfortunately, neither of these formulations of the transport equation can be solved analytically except for idealistic cases, for example, infinite medium with monoenergetic particles or a purely absorbing medium. Numerical solutions must be used for all practical shielding analyses. Many approximations of the transport equation are used, such as diffusion theory, to allow easier calculations. Also the

energy region of interest is usually divided into a few or even hundreds of contiguous energy subintervals and average cross sections are calculated for each group using an assumed energy spectrum of the radiation. In this manner, the transport equation is approximated by a set of coupled equations in which energy is no longer an independent variable. Even with an energy-multigroup approximation, numerical solutions are still computationally formidable.

The most widely used deterministic transport approach is the discrete-ordinates method. In this method, a spatial and directional mesh is created for the problem geometry, and the multigroup form of the transport equation is then integrated over each spatial and directional cell. The solution of the approximating algebraic equations is then accomplished by introducing another approximation that relates the cell-centered flux densities to those on the cell boundaries, and an iterative procedure between the source (scattered particles and true source particles) and flux density calculation is then used to calculate the fluxes at the mesh nodes. For details of this method, the reader is referred to Carlson and Lathrop [62], Duderstadt and Martin [63], and Lewis and Miller [64].

Discrete-ordinates calculations can be computationally expensive because of the usually enormous number of mesh nodes and the fact that the convergence of an iterative solution is often very slow. A subject of great interest in the last 30 years has been the development of numerous methods to accelerate convergence of the iterations. Without convergence acceleration schemes, discrete-ordinate solutions would be computationally impractical for many shielding problems. An excellent description of the various acceleration schemes that have been used is provided by Adams and Larsen [16].

Mature computer codes based on the discrete-ordinates method are widely available to treat one-, two-, and three-dimensional problems in the three basic geometries (rectangular, spherical, and cylindrical) with an arbitrary number of energy groups [65,66].

Although discrete-ordinates methods are widely used by shielding analysts, these methods do have their limitations. Most restrictive is the requirement that the problem geometry must be one of the three basic geometries (rectangular, spherical, or cylindrical) with boundaries and material interfaces placed perpendicular to a coordinate axis. Problems with irregular boundaries and material distributions are difficult to solve accurately with the discrete-ordinates method. Also, in multidimensional geometries, the discrete-ordinates method often produces spurious oscillations in the flux densities (the *ray effect*) as an inherent consequence of the angular discretization. Finally, the discretization of the spatial and angular variables introduces numerical truncation errors, and it is necessary to use sufficiently fine angular and spatial meshes to obtain flux densities that are independent of the mesh size. For multidimensional situations in which the flux density is very anisotropic in direction and in which the medium is many mean-free-path lengths in size, typical of many shielding problems, the computational effort to obtain an accurate discrete-ordinates solution can become very large. However, unlike Monte Carlo calculations, discrete-ordinates methods can treat

very-deep-penetration problems, that is, the calculation of fluxes and doses at distances many mean-free-path lengths from a source.

Monte Carlo Transport Theory

In Monte Carlo calculations, particle tracks are generated by simulating the stochastic nature of the particle interactions with the medium. One does not even need to invoke the transport equation; all one needs are complete mathematical expressions of the probability relationships that govern the track length of an individual particle between interaction points, the choice of an interaction type at each such point, the choice of a new energy and a new direction if the interaction is of a scattering type, and the possible production of additional particles. These are all stochastic variables, and in order to make selections of specific values for these variables, one needs a complete understanding of the various processes a particle undergoes in its lifetime from the time it is given birth by the source until it is either absorbed or leaves the system under consideration.

The experience a particle undergoes from the time it leaves its source until it is absorbed or leaves the system is called its *history*. From such histories expected or average values about the radiation field can be estimated. For example, suppose the expected energy $\langle E \rangle$ absorbed in some small volume V in the problem geometry is being sought. There is a probability $f(E)\mathrm{d}E$ that a particle deposits energy in $\mathrm{d}E$ about E. Then the expected energy deposited is simply $\langle E \rangle = \int Ef(E)\mathrm{d}E$. Unfortunately, $f(E)$ is not known *a priori* and must be obtained from a transport calculation. In a Monte Carlo analysis, $f(E)$ is constructed by *scoring* or tallying the energy deposited E_i in V by the ith particle history. Then in the limit of a large number of histories N

$$\langle E \rangle \equiv \int Ef(E)\mathrm{d}E \simeq \overline{E} \equiv \frac{1}{N}\sum_{i=1}^{N} E_i. \tag{14.24}$$

The process of using a computer to generate particle histories can be performed in a way completely analogous to the actual physical process of particle transport through a medium. This direct simulation of the physical transport is called an *analog* Monte Carlo procedure. However, if the tally region is far from the source regions, most analog particle histories will make zero contribution to the tally, and thus a huge number of histories must be generated to obtain a statistically meaningful result. To reduce the number of histories, *nonanalog* Monte Carlo procedures can be used whereby certain biases are introduced in the generation of particle histories to increase the chances that a particle reaches the tally region. For example, source particles could be emitted preferentially toward the tally region instead of with the usual isotropic emission. Of course, when tallying such biased histories, corrections must be made to undo the bias so that a correct score is

obtained. Many biasing schemes have been developed, and are generally called *variance reduction* methods since, by allowing more histories to score, the statistical uncertainty or variance in the average score is reduced.

The great advantage of the Monte Carlo approach, unlike discrete-ordinates, is that it can treat complex geometries. However, Monte Carlo calculations can be computationally extremely expensive, especially for deep-penetration problems. The stochastic contribution a single history makes to a particular score requires that a great many histories be simulated to achieve a good estimate of the expected or average score. If a tally region is many mean-free-path lengths from the source, very few histories reach the tally region and contribute to the score. Even with powerful variance reduction techniques, enormous numbers of histories often are required to obtain a meaningful score in deep-penetration problems.

Those readers interested in more comprehensive treatments of the Monte Carlo method will find rich resources. A number of monographs address Monte Carlo applications in radiation transport. Those designed for the specialists in nuclear-reactor computations are Goertzel and Kalos [67], Kalos [68], Kalos et al. [69], and Spanier and Gelbard [70]. More general treatments will be found in the books by Carter and Cashwell [71] Lux and Koblinger [72], and Dunn and Shultis [73]. Coupled photon and electron transport are addressed in the compilation edited by Jenkins et al. [74]. A very great deal of practical information can be gleaned from the manuals for Monte Carlo computer codes. Especially recommended are those for the EGS4 code [75], the TIGER series of codes [76], and the MCNP code [77].

Future Directions

In many respects, radiation shielding is a mature technological discipline. It is supported by a comprehensive body of literature and a diverse selection of computational resources. Indeed, the present availability of inexpensive computer clusters and the many sophisticated transport codes incorporating the most detailed physics models, modern data, and the ability to model complex geometries has reduced shielding practice in many cases to brute force calculation. Many shielding problems require such a computer approach; however, there are many routine shielding problems that can be effectively treated using the simplified techniques developed in the 1940s–1970s. Point-kernel methods are still widely used today. However, there are shielding problems for which no simplified approach is effective and transport methods must be employed. These include transmission of radiation through ducts and passages in structures, reflection of gamma rays from shielding walls and other structures, and transmission of beams of radiation obliquely incident on shielding slabs.

Despite the relative maturity of the discipline, one must not become complacent. There will continue to be advances in many areas. Undoubtedly, new computational resources will allow much more detailed 3-D graphical modeling of the shielding geometries and their incorporation into the transport codes. Likewise 3-D displays

of output will allow much better interpretations of results. New capabilities will be added to Monte Carlo and discrete-ordinates codes. Hybrid codes employing both Monte Carlo and deterministic techniques will also be developed. More nuclear data will become available that will, for example, allow detailed analysis of actinides in spent fuel and correlation effects in nuclear data will allow better sensitivity analyses of results. Likewise, more information on material properties, especially in radiation resistance, will become known. Advances in microdosimetry will provide better understanding of cellular responses to single radiation particles and the effects of low-level radiation doses. A better understanding of radiation hormesis effects may lead to changes in radiation standards that will better reflect health effects of radiation. New sources of radiation in research and medicine will include energetic protons and neutrons. These developments require continuing attention and adoption into the radiation-shielding discipline.

Bibliography

Primary Literature

1. Shultis JK, Faw RE (2005) Radiation shielding technology. Health Phys 88:297–322
2. Mutscheller A (1925) Physical standards of protection against Roentgen-ray dangers. Am J Roentgenol Radiat Ther 13:65–70
3. National Council on Radiation Protection and Measurements (1941) Safe handling of radioactive luminous compounds. NBS handbook 27. NCRP report 5. US Government Printing Office, Washington, DC
4. Blizard EP, Abbott LS (eds) (1962) Reactor handbook, vol III, Part B, Shielding. Wiley, New York
5. Jaeger RH (ed) (1968) Engineering compendium on radiation shielding, vol 1, Shielding fundamentals and methods. Springer, New York
6. Haffner JW (1967) Radiation and shielding in space. Academic, New York
7. Shure K (1964) P-3 multigroup calculations of neutron attenuation. Nucl Sci Eng 19:310
8. National Council on Radiation Protection and Measurements (1971) Protection against neutron radiation. NCRP report 38. National Council on Radiation Protection and Measurements, Washington, DC
9. National Council on Radiation Protection and Measurements (1976) Structural shielding design and evaluation for medical use of x-rays and gamma rays of energies up to 10 MeV. NCRP report 49. National Council on Radiation Protection and Measurements, Washington, DC
10. Kocher DC (1981) Radioactive decay tables. Technical Information Center, U.S. Department of Energy; DOE/TIC 11026, Washington, DC
11. Weber DA, Eckerman KE, Dillman LT, Ryman JC (1989) MIRD: radionuclide data and decay schemes. Society of Nuclear Medicine, Medical Internal Radiation Dose Committee, New York
12. ANS (American Nuclear Society) (1991) American national standard gamma-ray attenuation coefficients and buildup factors for engineering materials. ANSI/ANS-6.4.3-1991. American Nuclear Society, La Grange Park
13. Caswell RS, Coyne JJ, Randolph ML (1980) Kerma factors for neutron energies below 30 MeV. Radiat Res 83:217–254

14. International Commission on Radiological Protection (1987) Data for use in protection against external radiation. Publication 51. Annals of the ICRP 17(2/3). Pergamon, Oxford
15. International Commission on Radiological Protection (1996) Conversion coefficients for use in radiological protection against external radiation. Publication 74. Annals of the ICRP 26(3/4). Pergamon, Oxford
16. Adams ML, Larsen EW (2002) Fast iterative methods for discrete-ordinates particle transport calculations. Prog Nucl Energy 40(1):3–159
17. Shultis JK, Faw RE (2000) Radiation shielding. American Nuclear Society, La Grange Park
18. Rockwell T III (ed) (1956) Reactor shielding design manual. Van Nostrand, Princeton
19. Schaeffer NM (1973) Historical background. In: Schaeffer NM (ed) Reactor shielding. TID-25951. US Atomic Energy Commission, Washington, DC
20. Hirayama H (1987) Exposure buildup factors of high-energy gamma rays for water, concrete, iron, and lead. Nucl Technol 77:60–67
21. Faw RE, Shultis JK (1993) Absorbed dose buildup factors in air for 10–100 MeV photons. Nucl Sci Eng 114:76–80
22. Fano U, Spencer LV, Berger MJ (1959) Penetration and diffusion of x rays. In: Encyclopedia of physics, vol 38, Part 2. Springer, Berlin
23. Goldstein H (1959) Fundamental aspects of reactor shielding. Addison-Wesley, Reading
24. Spencer LV (1962) Structure shielding against fallout radiation from nuclear weapons. Monograph 42. National Bureau of Standards, Washington, DC
25. Takeuchi K, Tanaka S, Kinno M (1981) Transport calculation of gamma rays including bremsstrahlung by the discrete ordinates code PALLAS. Nucl Sci Eng 78:273–283
26. Takeuchi K, Tanaka S (1984) Buildup factors of gamma rays, including bremsstrahlung and annihilation radiation for water, concrete, iron, and lead. Nucl Sci Eng 87:478–489
27. Negin CA, Worku G (1998) Microshield v.5 user's manual. Grove Software, Lynchburg
28. Malenfant RE (1967) QAD: a series of point kernel general-purpose shielding programs. LA-3573. Los Alamos National Laboratory, Los Alamos
29. Price JH et al (1979) Utilization instructions for QADMOD-G. RRA-N7914. Radiation Research Association, Fort Worth. Available from RSICC as CCC565/QADMOD-GP
30. Litwin KA et al (1994) Improvements to the point kernel code QAD-CGGP: a code validation and user's manual. RC-1214 COG-94-65. AECL Research, Canada. Available from RSICC as CCC-645/QAD-CGGP-A
31. Malenfant RE (1990) G^3: a general purpose gamma-ray scattering code. LA-5176. Los Alamos National Laboratory, Los Alamos. Available from RSICC as CCC-564/G33-GP
32. Archer BR (1995) History of the shielding of diagnostic x-ray facilities. Health Phys 69:750–758
33. Simpkin DJ (1989) Shielding requirements for constant-potential diagnostic x-ray beams determined by a Monte Carlo calculation. Health Phys 56:151–154
34. Archer BR, Conway BJ, Quinn PW (1994) Attenuation properties of diagnostic x-ray shielding materials. Med Phys 21:1499–1507
35. Simpkin DJ (1995) Transmission data for shielding diagnostic x-ray facilities. Health Phys 68:704–709
36. Chilton AB (1971) Effect of material composition on neutron penetration of concrete slabs. Report 10425. National Bureau of Standards, Washington, DC
37. Roussin RW, Schmidt FAR (1971) Adjoint Sn calculations of coupled neutron and gamma-ray transport through concrete slabs. Nucl Eng Des 15:319–343
38. Roussin RW, Alsmiller RG Jr, Barish J (1973) Calculations of the transport of neutrons and secondary gamma rays through concrete for incident neutrons in the energy range 15 to 75 MeV. Nucl Eng Des 24:250–257
39. Wyckoff JM, Chilton AB (1973) Dose due to practical neutron energy distributions incident on concrete shielding slabs. Proceedings of 3rd international congress IRPA, American Nuclear Society, La Grange Park

40. Wang X, Faw RE (1995) Transmission of neutrons and secondary gamma rays through concrete slabs. Radiat Prot Dosim 60:212–222
41. Chilton AB, Huddleston CM (1963) A semi-empirical formula for differential dose albedo for gamma rays on concrete. Nucl Sci Eng 17:419–424
42. Chilton AB, Davisson CM, Beach LA (1965) Parameters for C-H albedo formula for gamma rays reflected from water, concrete, iron, and lead. Trans Am Nucl Soc 8:656
43. Chilton AB (1967) A modified formula for differential exposure albedo for gamma rays reflected from concrete. Nucl Sci Eng 27:481–482
44. Brockhoff RC (2003) Calculation of albedos for neutrons and photons. Ph.D. dissertation, Department of Mechanical and Nuclear Engineering, Kansas State University, Manhattan
45. Selph WE (1973) Albedos, ducts, and voids. In: Schaeffer NM (ed) Reactor shielding. TID-25951. US Atomic Energy Commission, Washington, DC
46. Simmons GL, Albert TE, Gritzner DM (1979) The SAI/EPRI information library. Report SAI-013-79-525-LJ. Science Applications Inc, La Jolla
47. Cain VR, Emmett MV (1979) BREESE-II: auxiliary routines for implementing the albedo option in the MORSE Monte Carlo code. ORNL/TM-6807. Oak Ridge National Laboratory, Oak Ridge
48. Maerker RE, Muckenthaler FJ (1966) Measurements and single-velocity calculations of differential angular thermal-neutron albedos for concrete. Nucl Sci Eng 26:339
49. Coleman WA, Maerker RE, Muckenthaler FJ, Stevens PJ (1967) Calculation of doubly differential current albedos for epicadmium neutrons incident on concrete and comparison of the subcadmium component with experiment. Nucl Sci Eng 27:411–422
50. Chandrasekhar S (1960) Radiative transfer. Dover, New York
51. Wells MB (1964) Reflection of thermal neutrons and neutron capture gamma rays from concrete. USAEC report RRA-M44. Radiation Research Associates, Fort Worth
52. Gomes IC, Stevens PN (1991) MORSE/STORM: a generalized albedo option for Monte Carlo calculations. ORNL/FEDC-91/1, TN. Oak Ridge National Laboratory, Oak Ridge
53. LeDoux JC, Chilton AB (1959) Gamma ray streaming through two-legged rectangular ducts. Nucl Sci Eng 11:362–368
54. National Council on Radiation Protection and Measurements (2003) Radiation protection for particle accelerator facilities. NCRP report 144. National Council on Radiation Protection and Measurements, Washington, DC
55. Lampley CM, Andrews MC, Wells MB (1988) The SKYSHINE-III procedure: calculation of the effects of structure design on neutron, primary gamma-ray, and secondary gamma-ray dose rates in air. RRA-T8209A. Radiation Research Associates, Fort Worth
56. Lampley CM (1979) The SKYSHINE-II procedure: calculation of the effects of structure design on neutron, primary gamma-ray, and secondary gamma-ray dose rates in air. RRA-T7901. Radiation Research Associates, Fort Worth
57. Brockhoff RC, Shultis JK, Faw RE (1996) Skyshine line-beam response functions for 20- to 100-MeV photons. Nucl Sci Eng 123:282–288
58. Gui AA, Shultis JK, Faw RE (1997) Response functions for neutron skyshine analysis. Nucl Sci Eng 125:111–127
59. Shultis JK, Faw RE, Bassett MS (1991) The integral line-beam method for gamma skyshine analysis. Nucl Sci Eng 107:228–245
60. Stedry MH (1994) A Monte Carlo line-beam calculation of gamma-ray skyshine for shielded sources. MS thesis, Kansas State University, Manhattan
61. Negin CA (1987) The microskyshine manual. Grove Software, Lynchburg
62. Carlson BG, Lathrop KD (1968) Transport theory, the method of discrete ordinates. In: Greenspan H, Kelber CN, Okrent D (eds) Computing methods in reactor physics. Gordon and Breach, New York
63. Duderstadt JJ, Martin WR (1979) Transport theory. Wiley, New York
64. Lewis EE, Miller WF (1984) Computational methods of neutron transport theory. Wiley, New York

65. Rhoades WA, Childs RL (1987) The TORT three-dimensional discrete ordinates neutron/photon transport code. ORNL-6268. Oak Ridge National Laboratory, Oak Ridge
66. Alcouffe RE, Baker RS, Dahl JA, Turner SA (2002) PARTISN user's guide. CCS-4, LA-UR-02-5633. Los Alamos National Laboratory, Transport Methods Group, Los Alamos
67. Goertzel G, Kalos MH (1958) Monte Carlo methods in transport problems. In: Progress in nuclear energy, ser 1, vol 2. Pergamon, New York
68. Kalos MH (1968) Monte Carlo integration of the adjoint gamma-ray transport equation. Nucl Sci Eng 33:284–290
69. Kalos MH, Nakache NR, Celnik JC (1968) Monte Carlo methods in reactor computations. In: Greenspan H, Kelber CN, Okrent D (eds) Computing methods in reactor physics. Gordon and Breach, New York
70. Spanier J, Gelbard EM (1969) Monte Carlo principles and neutron transport problems. Addison-Wesley, Reading
71. Carter LL, Cashwell ED (1975) Particle-transport simulation with the Monte Carlo method. TID-26607. Los Alamos National Laboratory, Los Alamos
72. Lux I, Koblinger LK (1991) Monte Carlo particle transport methods: neutron and photon calculations. CRC Press, Boca Raton
73. Dunn WL, Shultis JK (2011) Exploring the Monte Carlo method. Elsevier, Amsterdam
74. Jenkins TM, Nelson TM, Rindi A (1988) Monte Carlo transport of electrons and photons. Plenum, New York
75. Nelson WR, Hirayama H, Rogers DWO (1985) The EGS4 code system. SLAC-265. Stanford Linear Accelerator Center, Menlo Park
76. Halbleib JA, Kensek RP, Mehlhorn TA, Valdez GD, Seltzer SM, Berger MJ (1992) ITS Version 3.0: the integrated TIGER series of coupled electron/photon Monte Carlo transport codes. SAND91-1634. Sandia National Laboratories, Albuquerque
77. X-5 Monte Carlo Team (2003) MCNP—a general Monte Carlo n-particle transport code, version 5. LA-UR-03-1987 (vol 1: Overview and theory), LA-UR-03-0245 (vol 2: User's guide). Los Alamos National Laboratory, Los Alamos

Books and Reviews

Blizard EP, Abbott LS (eds) Reactor handbook, vol 3, Part B, Shielding. Wiley, New York
Faw RE, Shultis JK (1999) Radiological assessment: sources and doses. American Nuclear Society, La Grange Park
Goldstein H (1959) Fundamental aspects of reactor shielding. Addison-Wesley, Reading
Haffner JW (1967) Radiation and shielding in space. Academic, New York
ICRP (2007) The 2007 recommendations of the international commission on radiological protection. Report 103. Annals of the ICRP 37:2–4
ICRP (2008) Nuclear decay data for dosimetric calculations. Report 107. Annals of the ICRP 38(3):1–96
ICRU (1993) Quantities and units in radiation protection dosimetry. Report 51. International Commission on Radiation Units and Measurements, Bethesda
ICRU (1998) Fundamental quantities and units for ionizing radiation. Report 60. International Commission on Radiation Units and Measurements, Bethesda
Jaeger RG (ed) (1968–1975) Engineering compendium on radiation shielding. Shielding materials and design, vol 1; Shielding materials and designs, vol 2; Shield design and engineering, vol 3. Springer, New York
NCRP (2003) Radiation protection for particle accelerator facilities. Report 144. National Council on Radiation Protection and Measurements, Bethesda

NCRP (2005) Structural shielding design for medical x-ray imaging facilities. Report 147. National Council on Radiation Protection and Measurements, Bethesda

NCRP (2005) Structural shielding design and evaluation for megavoltage x- and gamma-ray radiotherapy facilities. Report 151. National Council on Radiation Protection and Measurements, Bethesda

Rockwell T III (ed) (1956) Reactor shielding design manual. Van Nostrand, Princeton

Schaeffer NM (ed) (1973) Reactor shielding. TID-25951, U.S. Atomic Energy Commission, Washington, DC

Shultis JK, Faw RE (2000) Radiation shielding. American Nuclear Society, La Grange Park

UN (1977, 1982, 1988, 1993, 2000) Reports of the United Nations Scientific Committee on the Effects of Atomic Radiation, New York. http://www.unscear.org/unscear/en/publications.html

Chapter 15
Ionizing Radiation Detectors

Wm. David Kulp, III

Glossary

Alpha particle	A particle emitted during radioactive decay that is comprised of two protons and two neutrons, equivalent to the nucleus of a ^{4}He atom.
Beta particle	An electron or a positron (the positively charged antimatter twin of an electron) emitted during radioactive decay.
Electron volt (eV)	A unit of energy measurement defined by the kinetic energy gained by a free electron when accelerated through a potential difference of 1 V; approximately equivalent to 1.602×10^{-19} joule.
Gamma radiation	Highly energetic electromagnetic radiation (energy greater than approximately 100 keV) emitted from the nucleus during radioactive decay.
Ionizing radiation	Particles or light with sufficient energy to remove an electron from an atom or molecule.
Nuclide	A species of atomic nuclei, defined by the number of protons and neutrons present in the nucleus; nuclides are represented by the chemical symbol and atomic mass number. Two examples are ^{14}C (carbon-14, six protons and eight neutrons) and ^{235}U (uranium-235, 92 protons and 143 neutrons).
Radioactive	Describes an unstable atomic nucleus that releases energy through ionizing radiation.

This chapter was originally published as part of the Encyclopedia of Sustainability Science and Technology edited by Robert A. Meyers. DOI:10.1007/978-1-4419-0851-3

W.D. Kulp, III (✉)
Mechanical Engineering, Georgia Institute of Technology, Atlanta, GA, USA
e-mail: david.kulp@gatech.edu

N. Tsoulfanidis (ed.), *Nuclear Energy: Selected Entries from the Encyclopedia of Sustainability Science and Technology*, DOI 10.1007/978-1-4614-5716-9_15,

Scintillator	A type of detector that uses fluorescence to detect radiation.
Spectroscopy	The measurement of radiation intensity as a function of radiation energy; a device or system of detectors capable of spectroscopy is referred to as a spectrometer.

Definition of the Subject

Equipment to detect, identify, and measure radioactivity is a key component in the safe and responsible development of nuclear science and technology. Whether designed to monitor radioactive processes, provide an alert, or characterize the radiation measured, these systems "see" what is undetectable to human senses. Used in nuclear power, industry, medical imaging, nuclear medicine, scientific exploration, and nuclear security, radiation detectors provide information about the radiation present and can be used to interpret what the source of the radioactivity is.

Experimental data exist for about 2,900 nuclides, or species of atomic nuclei, characterized in the laboratory. Yet less than 300 nuclides are found in measurable abundance in the environment. Most of these naturally occurring nuclides are stable nuclei, meaning that they do not decay to other nuclei over time. However, some unstable, or radioactive, nuclei are found in everyday objects. Examples of naturally occurring radioactive material (NORM) are ^{40}K in bananas and the nuclides in the uranium and thorium decay series that are found in cat litter. The identification of radioactive nuclides is accomplished through detection and measurement of the radiation emitted during the decay of the unstable nucleus.

The decay of a radioactive atomic nucleus results in energy being released in the form of particles or electromagnetic radiation. Particles emitted during radioactive decay include alpha particles, beta particles, neutrons, and photons. Alpha and beta radiation are electrically charged particles ejected from the decaying nucleus. Alpha particles are positively charged helium nuclei. Beta particles are electrons or positrons (the antiparticle of an electron), which carry negative and positive charges, respectively. Neutrons have no electric charge. Photons, X and gamma rays, are electromagnetic radiation; treated as particles, they have zero charge, zero rest mass, and travel at the speed of light.

Introduction

The detection and characterization of radiation originated with Wilhelm Conrad Röntgen, who was awarded the first Nobel Prize in Physics in 1901 [1]. This work was continued and led to the discovery of spontaneous radioactivity, for which

Antoine Henri Becquerel, Pierre Curie, and Marie Curie shared the 1903 Nobel Prize in Physics [1]. The mature nature of the field is demonstrated by the many textbooks available on nuclear physics and radiation detection. Suggested reading for in-depth study with focused discussion on radiation detection are Glasstone [2], Kantele [3], Knoll [4], Krane [5], Leo [6], and Tsoulfinidis [7].

Nuclear radiation ranges in energy from a few thousand electron volts (kilo-electron volts, or keV) to millions of electron volts (mega-electron volts, or MeV). Particles in the keV or MeV energy range are energetic enough that as they pass through matter they can cause the ejection of one or more electrons from a neutral atom in the material, ionizing the atom. Because of this interaction, nuclear radiation is also referred to as ionizing radiation. The physical processes that lead to ionization as radiation passes through matter depend upon the kind of radiation. Charged particles, photons, and neutral particles all interact with matter in different ways.

Alpha particles and other heavy, charged particles interact with matter through a variety of mechanisms, but the primary reaction is simply Coulomb scattering, an interaction between charged particles that is kinematic in nature. When energy is imparted to a target atom in the material, an inelastic collision has occurred with atomic electrons. Where no energy is transferred to the target material, the incident particle has elastically scattered from a target nucleus. These interactions have two basic results for the incident particle: (1) the particle loses energy, and (2) the particle is deflected from its initial trajectory.

Electrons and positrons also lose energy through Coulomb scattering in matter. However, they are more easily deflected in the electric field near an atomic nucleus due to the small mass of these particles or in collisions with atomic electrons (same mass). When electrons collide, energy is directly transferred to the atomic electrons. When electrons are accelerated or decelerated, electromagnetic energy is emitted in a process known as bremsstrahlung. Above a few MeV in energy, this mechanism is the predominant interaction for high-energy electrons and positrons.

Gamma rays and X rays are very different from the charged particles discussed above. They are electromagnetic radiation, called photons; a photon has zero electric charge and zero rest mass. Photons have three main interactions with matter:

1. The photoelectric effect, where an atomic electron is ejected from an atom after the absorption of the photon
2. Compton scattering, the scattering of photons by free electrons
3. Pair production, where a photon is transformed into an electron-positron pair

Neutrons are similar to photons in that they lack electric charge and will not interact with matter through Coulomb scattering. Instead, a neutron interacts with nuclei through the strong force. This is a relatively rare occurrence due to the short range of the strong force (effective only within 10^{-15} m). The result of interaction may be:

1. Elastic scattering from nuclei, so that no nuclear reaction takes place.
2. Inelastic scattering, where the target nucleus is left in an excited state.

3. Neutron capture, where the target nucleus is transformed through absorption of the neutron; most of the time the new nucleus is radioactive and decays by emitting beta particles and/or gamma rays (and neutrons, too, in a few cases).
4. Nuclear reactions with the emission of a charged particle.
5. Fission, the splitting of a heavy atomic nucleus.

Radiation detectors make use of these interactions with matter to produce a measurable effect that signals the presence of radioactivity. In general, a radiation detector can be characterized through three traits: (1) the radiation absorber (the materials of which the detector is made), (2) an observable that signals the interaction with radiation, and (3) a way to measure the signal.

The radiation absorber may be gas, liquid, or solid and can be made from a range of materials. The choice of detection medium phase depends on the type of radiation to be measured. Heavy charged particles have a range of less than about 100 μm (0.01 cm or 0.004 in.) in a solid absorber, but the resulting signals may be hard to distinguish from electronic noise. Neutrons and gamma rays, on the other hand, may penetrate centimeters of solid matter without producing any observable response. For detecting neutrons, the use of enriched isotopes may be used in order to take advantage of specific nuclear reactions that have higher probabilities of occurring.

The choice of observable effect produced by the detector is usually more dependent upon the application and the material used as the radiation absorber, rather than the type of radiation. Early researchers Henri Becquerel and Marie and Pierre Curie recorded data on photographic plates. While this method of observation provided long-lasting visible evidence of radiation, other detection methods such as electronic signals, scintillation light emissions, and changes in temperature are more advantageous for modern radiation detection. For example, light emissions produce the fastest detector response, thus a scintillation detector is the best choice for a measurement that requires precision timing. On the other hand, semiconductor detectors provide excellent energy resolution with good timing resolution, and are used for detailed nuclear spectroscopy.

If the radiation detection application requires only a qualitative measure of the presence of radiation, then an effective method of measurement would be an audible alarm that sounds when a threshold radiation level is reached, measured as a current generated within the detector volume. Nuclear science, however, requires quantitative analysis of the number and energy of individual particles emitted by atomic and nuclear transitions. For nuclear spectroscopy, it is therefore necessary to measure each electronic pulse registered in the detector, amplify the pulses and perhaps shape the signals as necessary, and record these signals for later analysis.

Given the different types of radiation and the range of energies, no single detector will be sensitive to all nuclear radiations at all applicable energies. Further, the diverse applications for radiation detection preclude a general list of radiation detectors that could be considered comprehensive. In the sections that follow, the most common detector types will be discussed and some recent advancements in the field will be introduced.

Gas-Filled Detectors

Ionizing radiation produces pairs of positively charged ions and negatively charged electrons as it passes through matter. It follows that a simple way to measure radioactivity is to apply an electric field across the radiation-absorbing material and count the ion-electron pairs produced in the detector. Such a detector can be envisioned as a parallel-plate capacitor filled with a gas. An electric potential applied across the capacitor creates an electric field that separates the electrons and ions. The electrons drift toward the positively charged anode plate, while the ions drift in the opposite direction toward the negatively charged cathode. This separation prevents the electrons and ions from recombining and enables measurement of the electronic signal produced by the ionizing radiation.

Ionization Chambers

The applied voltage across the capacitor influences how quickly charged particles move in the ionization chamber. Electrons and ions tend to recombine to form neutral atoms at low voltages, with the result that only a weak signal is collected. This recombination region is indicated in the range where $V < V_1$ as in Fig. 15.1. Above some threshold potential, the electric field prevents recombination. This is indicated in the region where $V_1 < V < V_2$, where the total charge detected is insensitive to the applied voltage, as all of the electron-ion pairs that are created by the initial ionizing event are collected. A detector operating in this region collects only the charge produced directly by the incident radiation and is thus called an ionization chamber.

How big is the output electronic signal from an ionization chamber? The average energy required to produce an ion in dry air is about 30 electron volts (eV). An ionization chamber consisting of two square plates, each 10 cm long on a side, separated by a 1-cm air gap has a capacitance of 9×10^{-12} farads. Based on the energy to produce one ion in air, a 1-MeV gamma ray that deposits all of its energy in this detector would produce a maximum of about 3×10^4 electron-ion pairs, and a 2-MeV gamma ray would produce twice as many pairs. The voltage pulse resulting from these events would be about 0.5 or 1 mV, respectively.

To analyze individual pulses, the small signals produced by the direct radiation interaction require amplification. The two curves illustrated in Fig. 15.1 correspond to radiations that deposit different energies in the detector, e.g., an alpha particle and a beta particle or two gamma rays of different energies. The more energetic radiation produces more electron-ion pairs, resulting in a larger output signal.

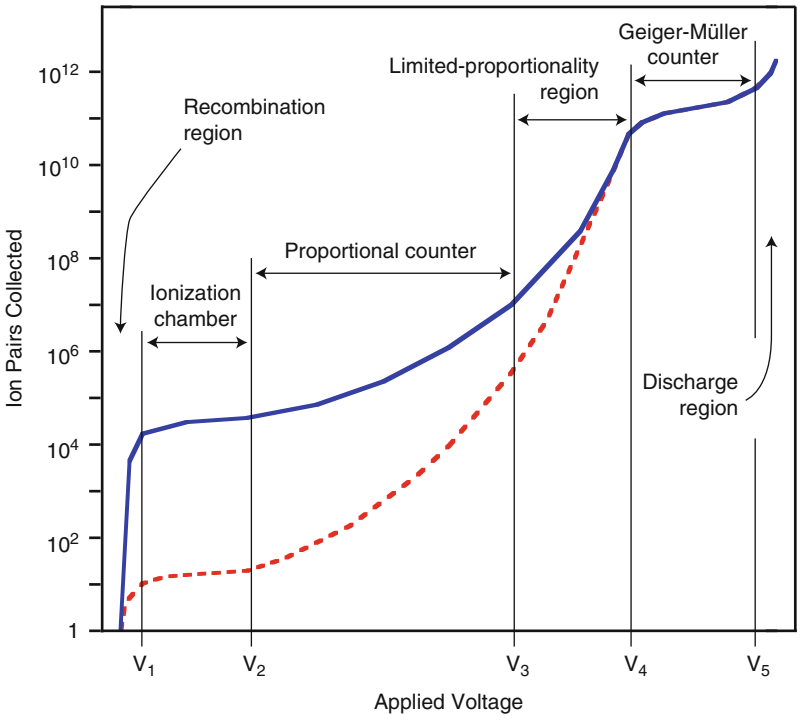

Fig. 15.1 The number of ion-electron pairs collected in a gas-filled detector depends on the applied voltage and on the energy deposited in the active volume of the detector

Proportional Counters

A larger output signal can also be generated by increasing the applied voltage across the capacitor. The increased electric field accelerates the ions and electrons in the chamber to higher kinetic energy. Above a second threshold voltage, indicated as V_2 in Fig. 15.1, free electrons, produced by the incident radiation, are accelerated to sufficient energy such that they ionize additional gas atoms during collisions and produce more free electrons. This process is known as *gas multiplication* and results in a larger output signal.

The electrons produced in the knock-on reactions are called *secondary electrons*. The secondary electrons accelerate and produce additional ionization, resulting in a *Townsend avalanche*, where 10^3–10^5 secondary events occur for each original ion produced. As shown in region $V_2 < V < V_3$, the number of electron-ion pairs is proportional to the number of pairs produced in the primary event. Detectors operating in this range are called *proportional counters*. Using such a detector, the measurement of the incident particle energy is possible because the final signal is proportional to the energy deposited in the detector.

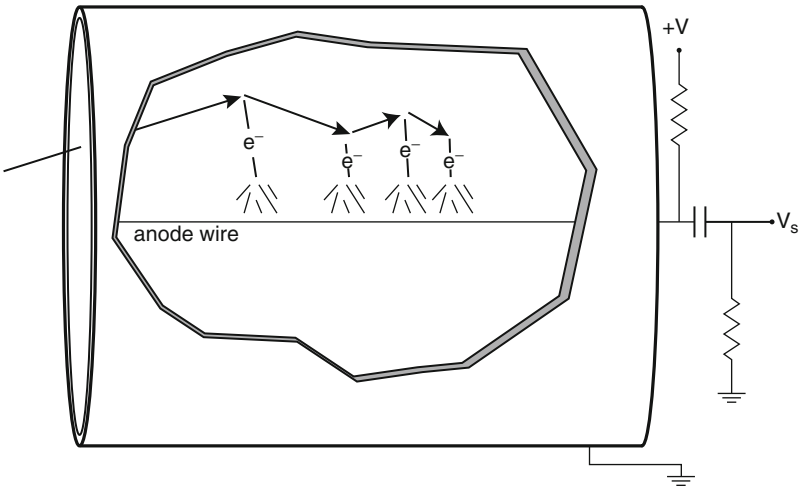

Fig. 15.2 Radiation enters a proportional counter through a thin window and interacts with the gas within the cylinder, creating electron-ion pairs. The electrons accelerate toward the anode wire and produce avalanches of secondary electrons

Proportional counters are typically cylindrical in shape, as shown in Fig. 15.2. This geometry results in an electric field that has an inversely proportional 1/r dependence, where r is the distance from the distance from the center of the detector. The site of the original interaction is not critical in such a detector. However, as an electron accelerates closer to the central anode wire, the field becomes very intense, resulting in a Townsend avalanche, indicated as a shower of electrons in Fig. 15.2. Because this occurs near the anode, the secondary electrons created are highly localized and no additional cascades form.

Increasing the applied voltage beyond $V = V_3$, the total ionization produced through gas multiplication continues to increase, but with reduced proportionality. This is the result of the creation of clouds of ions near the anode wire that have significantly lower drift speeds than the electrons. As a result, as the voltage increased in the region $V_3 < V < V_4$, the ions build up a space charge that shields the anode and changes the effective electric field.

Further increasing the voltage beyond V_4 results in a discharge occurring in the gas. Instead of a single, localized avalanche for each original electron-ion pair, *secondary avalanches* occur all along the anode wire. The secondary avalanches are the result of photons emitted by de-exciting gas molecules in the detector causing further ionization and avalanches elsewhere in the detector. A saturation effect thus takes place in the region indicated by $V_3 < V < V_4$: the discharge always has the same output, independent of the energy of the initial event.

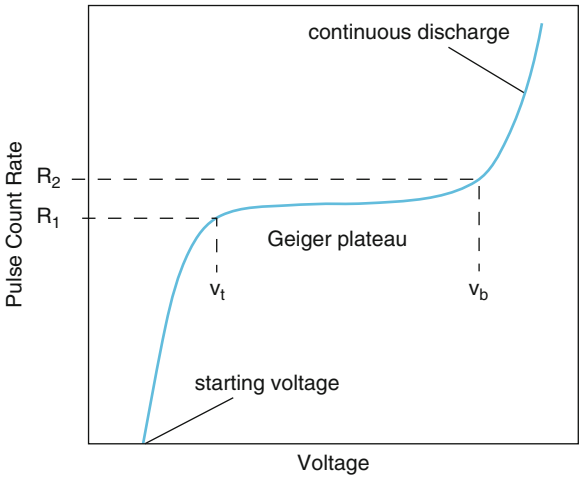

Fig. 15.3 The operating point of a Geiger-Müller tube is the middle of a region between a threshold voltage, V_t, and a breakdown voltage, V_b. In this region, called the *Geiger plateau*, the count rate changes very little as a function of the applied voltage. Beyond the breakdown voltage, the tube discharges continuously

Geiger-Müller Counters

Detectors operating in the $V_4 < V < V_5$ region are called *Geiger-Müller counters*. As shown in Fig. 15.1, there is no difference in count rate due to the energy initially deposited in the detector. Moreover, while the measured pulse size changes because the charge collected increases with increasing voltage, the pulse count rate does not change significantly, as shown in Fig. 15.3.

What is happening here is that the potential difference is so large in the active region of the detector that secondary avalanches cause a chain reaction of avalanches and total breakdown occurs. The discharge ends only when a large number of slow-moving secondary ions are formed near the anode wire. This localized concentration of ions represents a *space charge* that reduces the magnitude of the electric field, diminishing the attractive force accelerating the secondary electrons, and quenching the breakdown so that all radiation interacting with the detector produces the same current, regardless of particle type or initial energy.

Increasing the voltage to $V > V_5$ results in continuous breakdown in the gas, producing a steady current, whether radiation is present or not. This discharge region should be avoided in order to prevent damage to the detector. For this reason, Geiger-Müller tubes are typically operated at a voltage in the middle of the Geiger plateau.

In general, gas-filled detectors are the simplest detectors to operate, but have relatively low radiation detection efficiency. For electrons, ions, and low-energy

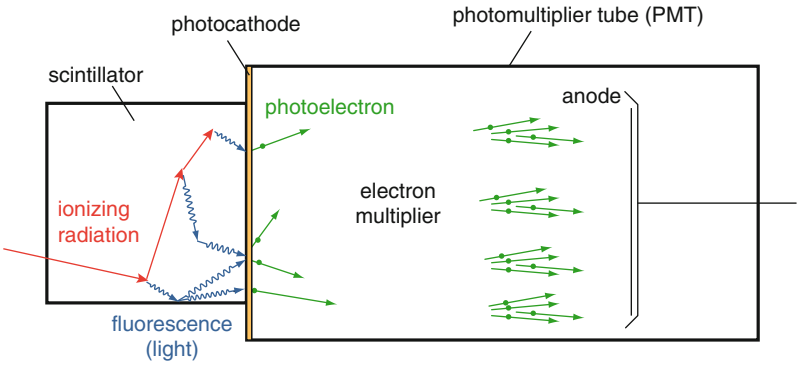

Fig. 15.4 Ionizing radiation produces flashes of light in a scintillation detector. This light is focused to produce photoelectrons, which are multiplied to produce a measurable signal

X rays and gamma rays, the low density of matter in the active volume of the detector is sufficient. However, for high-energy photons, gas-filled detectors lack sufficiently high density to stop the radiation effectively. Practically, this is demonstrated using a rule of thumb: the thickness of material required to attenuate by half the intensity of a beam of 1 MeV photons is $\sim$10 g/cm^2. To halve the intensity of a 1 MeV source of gamma rays using air (density = 0.00129 g/cm^3 at standard temperature and pressure) would require a detector 78 m thick. In comparison, only 2.7 cm thickness of sodium iodide (density = 3.667 g/cm^3) is needed to reduce the beam intensity by half.

Scintillation Detectors

The principle of operation for a scintillation detector is very different from that of a gas-filled detector. Rather than collecting the electrons produced directly in the ionizing event in the radiation absorber, scintillation detectors use light as the observable that signals radiation detection.

The basic principle of operation of a scintillation detector, illustrated in Fig. 15.4, is as follows:

1. Incident radiation ionizes an atom in the scintillator material.
2. The excited atom *fluoresces*, i.e., produces light, as it relaxes to its initial state.
3. The light strikes the front surface of a *photomultiplier tube* (*PMT*) called a *photocathode* that yields a *photoelectron* through the photoelectric effect.
4. The photoelectrons are accelerated and multiplied through a series of electrodes (called *dynodes*) to produce a shower of secondary electrons.
5. The secondary electrons are collected at the anode as an output signal pulse.

The scintillator medium may be a solid, liquid, or gas. Scintillator material may be selected from organic crystals, organic liquids, plastics, glasses, inorganic

crystals, glasses, and gases. With the exception of the crystalline detectors, organic scintillators are referred to using manufacturer designations. For example, a common liquid scintillator used in fast neutron detection is known as NE-213 (Nuclear Enterprises), BC-501A (Bicron/St. Gobain), and EJ-301 (Eljen). Plastic scintillation detectors, such as NE-102A (alternatively marketed as BC-400 or EJ-212), are manufactured by dissolving organic scintillators in a solvent such as styrene or polyvinyltoluene (PVT) that can be polymerized. These detectors have a notable advantage in that they may be cut or shaped as needed and are fairly durable, but the choice of material ultimately depends on the detection application.

The characteristics of a good scintillator are:

1. Efficient *luminescence*, i.e., it converts most of the energy deposited in the material into light.
2. Transparent to its own light output to enable light transmission through the absorbing material.
3. Has an index of refraction approximately that of glass ($n = 1.5$) to allow coupling to a light sensor.
4. Emits light within a wavelength range that matches existing light sensors.
5. Emits light pulses with a short decay time constant (τ).

Organic detectors are characterized by the shortest decay time constants; however, these lighter compounds lack the efficiency of detectors made using materials of higher atomic number. Inorganic crystals can be made from materials as heavy as bismuth (atomic number, Z = 83), and typically have better energy resolution than organic detectors. Scintillators in common use are:

- Anthracene ($C_{14}H_{10}$), an organic crystal with a short decay constant ($\tau = 30$ ns) used in general radiation detection
- Stilbene ($C_{14}H_{12}$), a very fast ($\tau < 5$ ns) organic crystal used in neutron detection
- NE-102A, a general-purpose plastic scintillator ($\tau = 2.4$ ns)
- NE-213, an organic liquid used in neutron detection ($\tau = 3.7$ ns)
- NaI(Tl) (sodium iodide activated with a thallium dopant), an inorganic crystal in wide use in radiation detection ($\tau = 230$ ns)
- LiI(Eu) (lithium iodide doped with europium), an inorganic crystal used in neutron detection ($\tau = 1{,}200$ ns)
- $Bi_4Ge_3O_{12}$ (bismuth germanate, or BGO), used in PET scanners and in nuclear spectroscopy ($\tau = 300$ ns)
- BaF_2 (barium fluoride), used for fast timing in nuclear spectroscopy (two components to the pulse $\tau = 0.6$ and 630 ns, respectively)

Semiconductor Detectors

Semiconductor detectors are essentially solid-state ionization chambers. With higher mass density, and requiring less energy per charge generated (on the order

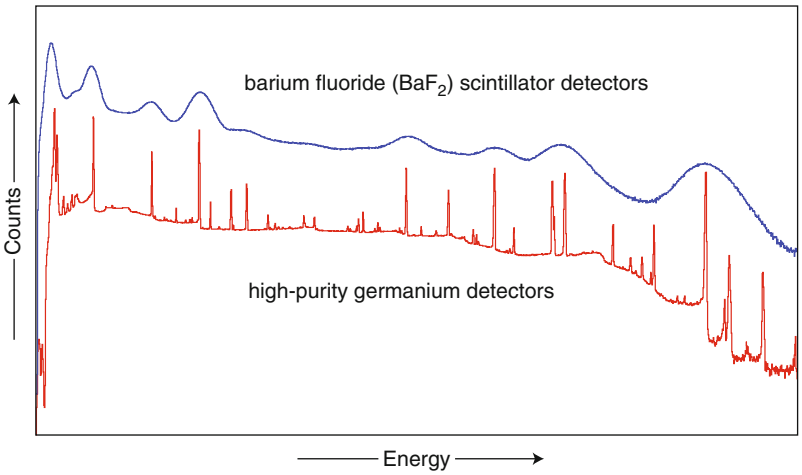

Fig. 15.5 Gamma-ray spectra from the radioactive decay of ^{152}Eu demonstrate the difference in energy resolution between that of a barium fluoride (BaF_2) scintillator detector array (*top*) and that of a high-purity germanium semiconductor detector array (Spectra courtesy of D. Cross)

of 3 eV, compared with about 30 eV in gaseous detectors), however, semiconductor detectors provide both increased detection efficiency and superior energy resolution compared with gaseous detectors. Ionizing radiation excites electrons into the conduction band of the semiconductor crystal. These electrons and the positively charged *holes* left behind in the valence band of the semiconductor migrate under the influence of the applied electric field, which is on the order of a few thousand volts.

The band gap in a semiconductor is on the order of about 1 eV. Such a small energy difference results in a measurable output signal from semiconductor detectors at room temperature. To reduce this thermal noise, some semiconductor detectors are operated at cryogenic temperatures.

The two operational constraints on semiconductor detectors, high voltage and cryogenic temperatures, limit widespread use of these devices. However, semiconductor detectors typically have significantly better energy resolution than scintillator detectors. This is illustrated in the gamma-ray spectrum measured during the decay of ^{152}Eu, shown in Fig. 15.5.

The upper pulse-height spectrum in Fig. 15.5 shows the response of an array of barium fluoride (BaF_2) scintillation detectors, while the lower spectrum is that collected using an array of high-purity germanium (HPGe) semiconductor detectors. Individual lines resolved by the HPGe detector appear as a continuum with mound-like features in the BaF_2 spectrum. This difference makes semiconductor detectors the tool of choice in nuclear spectroscopy. With a higher atomic number (Z = 32), germanium detectors are typically used for gamma-ray spectroscopy, while silicon detectors (Z = 14) are used in X-ray spectroscopy and in charged particle spectroscopy.

Neutron Detectors

The absence of an electric charge complicates neutron detection. Neutrons do not directly produce ionization in matter. However, neutrons interact with atomic nuclei through absorption or scattering, and are thus detected through reaction products that do produce ionization.

Absorption through neutron-induced nuclear reactions is most probable at very low energies (eV); the probability of a reaction occurring increases with decreasing neutron energy with a 1/v relationship, i.e., inversely proportional to the neutron velocity. Most nuclear power reactors are designed to work at thermal energies (on the order of 0.025 eV), where a neutron has a speed of 2,200 m/s, and the probability is high for neutron-induced fission in uranium. The 1/v relationship implies that nuclear reactions will be most useful for detecting *slow* neutrons, categorized by a neutron energy < 0.5 eV. Neutrons with an energy above this threshold are more effectively detected through scattering in the detector material.

Slow Neutron Detectors

Nuclear reactions used to detect slow neutrons (neutron energy <0.5 eV) typically produce heavy charged particles such as protons and alpha particles. These reactions are referred to as activation reactions, because they usually leave the product nucleus in an excited state, which subsequently decays through gamma-ray emission. Two common reactions used in detectors are the (n,p) and (n,α) activation reactions. In the (n,p) reaction a neutron, n, is absorbed and a proton, p, is emitted. Similarly, in the (n,α) reaction an alpha particle, α, is emitted. These reactions release considerable energy (approximately 1 MeV or more), so that the incident neutron energy (< 0.5 eV) cannot be determined from the reaction. Subsequently, detectors designed for slow neutrons are used only for indicating the presence of neutrons, and not for neutron spectroscopy.

The primary reactions used to detect slow neutrons are:

- $^{10}B(n,\alpha)^{7}Li$, where the detector requires enriched boron that is >90% ^{10}B (boron is naturally found in ratios of 19.8% ^{10}B and 80.2% ^{11}B)
- $^{6}Li(n,\alpha)^{3}$ H, which uses ^{6}Li enriched to over 90% (the natural abundance of lithium is 7.59% ^{6}Li and 92.41% ^{7}Li)
- $^{3}He(n,p)^{3}$ H, where the detector relies on rare ^{3}He gas that has a natural abundance of 0.00137% and is very expensive to produce
- $^{157}Gd\ (n,\gamma)^{158}Gd$, used in liquid scintillator detectors

Because the nuclear reactions require the use of specific isotopes, the availability of enriched isotopes contributes to the cost of fabrication for these detectors. In the case of ^{3}He, this cost is significant, if sufficient quantities of the material can be

acquired at all. Helium-3 is not only for neutron detection, but also for cryogenics and is in high demand in many fields of research. Manufactured through the decay of tritium produced in a nuclear reactor, ^{3}He was available in greater quantities during the Cold War, because tritium is a critical component in thermonuclear weapons.

Fast Neutron Detectors

Neutron-induced nuclear transformations such as the ^{6}Li(n,α) and ^{3}He(n,p) reactions may be used to detect fast neutrons. Unlike the case for slow neutrons, where the incident neutron energy is negligible compared with the reaction energy, it is possible to measure the neutron energy. However, the efficiency of these detectors is limited because the reaction probability decreases rapidly with increasing neutron energy. More commonly, scattering reactions are used to detect and measure the energy of fast neutrons.

Kinematics limit the energy that may be transferred in the neutron-nucleus collision. Because the mass of the neutron and the mass of the proton are nearly the same, it is only possible to transfer all of the neutron energy in a single collision in the (n,p) reaction. As the mass of the recoil nucleus increases, the fraction of energy transferred decreases. For the case of a deuterium recoil nucleus (atomic mass A = 2), a maximum of 88.9% of the energy can be transferred. In the case of ^{3}He, this maximum value falls to 75%. It is evident that a radiation absorber made from light nuclei is preferred, as it is possible to transfer more energy to the detector nuclei in fewer collisions. To provide higher efficiency, a solid-state detector is preferable, and materials with relatively high concentrations of hydrogen are desired.

The *proton recoil scintillation detector* takes advantage of kinematics and the high availability of scintillators that contain hydrogen. The kinematic advantage of these detectors is that the energy distribution of the recoil protons does not depend on the collision angle, resulting in a rectangular-shaped distribution in an ideal case. The shape of the detector output pulse may be used to separate gamma rays from neutrons, and the energy of the incident neutrons may be determined by comparing the response of the detector with calibration spectra obtained using a monoenergetic neutron source.

The availability of organic scintillators in many forms, including plastic and liquid detectors, provides a broad range of available materials for detector construction. The hydrogen in the aromatic compounds provides an efficient mechanism for energy transfer in the absorbing medium, but the response of the detector is complicated by the presence of other elements such as carbon and oxygen. If the source of neutrons is pulsed, such as at an accelerator facility, then the energy may be extracted using a *time-of-flight* method. This method relates the detection time to the pulse structure of the beam used to create the neutrons and extracts the neutron energy from the amount of time it takes for the neutron to travel to the detector.

Moderating Detectors

A third type of neutron detector uses a layer of hydrogen-containing material to slow down, or *moderate*, neutrons in order to use neutron-induced nuclear reactions as the detection method. Called *moderating detectors*, these systems are useful if there is a broad range of neutron energies to be detected or if the neutron energy distribution is unknown. This type of detector has a relatively slow response time due to the moderating process. This is unsuitable for situations where the neutron energy distribution changes with time or when it is desirable to relate the neutron with another event, such as the detection of a gamma ray.

Examples of moderating detectors include *Bonner sphere spectrometers* and *spherical neutron dosimeters*. Used to detect fast neutrons, the Bonner sphere spectrometer consists of a set of different-diameter solid polyethylene moderating spheres that slow incident neutrons and a thermal neutron detector such as a lithium iodide scintillator. The spheres are placed over the detector in turn, and the count rate is recorded for each sphere. The neutron energy spectrum is then interpreted from this data using calibration data.

A spherical neutron dosimeter is essentially the same construction as a Bonner sphere spectrometer, but only uses a single sphere. The sphere is modified to provide a response that coincidentally resembles the neutron dose equivalent delivered curve as a function of energy. This detector is often used for neutron monitoring to provide neutron dose estimates.

Future Directions

Advances in radiation detection may result from the development of new radiation absorber materials, the refinement of methods to signal radiation interactions, and innovations in signal measurement. Some recent advances are discussed in the following section. The impact of these new developments and future directions may have an effect on the ability to detect small quantities of nuclear materials for safety and security, provide better tools for medicine and medical imagining, characterize the rarest nuclei in the cosmos, provide key data for understanding astronomical interests such as supernovas and neutron stars, and investigate dark matter and the nature of neutrinos.

Advancements in Detector Materials (Radiation Absorbers)

It is the interaction of radiation with matter which provides a signal to be measured. Perhaps because of this, and because of the limitations of current radiation detectors, it may be presumed that the primary need in radiation detection is in

the characterization of new materials that are sensitive to radiation. Indeed, the physical characteristics of some of these materials in use are not optimal. Some examples are found in gamma-ray detectors: HPGe crystals require cryogenics temperatures for operation and the hygroscopic nature of NaI(Tl) leads to performance degradation as water is absorbed in the crystal. In other cases, the optimal materials are simply difficult to acquire: the scarcity of ^{3}He for cryogenics and for neutron detectors since the reduction of tritium production is a case in point [8].

There are many open areas of research, including applications in nanotechnology and crystal growth. Suspension of nanoparticles in liquid scintillators may lead to improved scintillation detectors or detectors based on novel new materials. Development of crystal growth techniques for newer CdZnTe-based detectors [9] may reduce the defects found in these detectors and enable the growth of larger crystals. It is important to note, however, that the common materials already in use have been selected through years of research, and that a breakthrough in detector materials may take decades to come to fruition.

Near-term improvements may come from refining methods to make detectors, as in the case of the high-purity germanium crystal. Originally, germanium semiconductors required a lithium dopant in the crystal matrix. This dopant would degrade as the lithium migrated out of the crystal, unless the detector was constantly kept at liquid nitrogen temperature. By refining the technique for growing germanium crystals, the lithium dopant is no longer used in these detectors.

Simply modifying compounds already in use can advance the field as well. A case in point is in the use of deuterated benzene scintillators for neutron detection. Benzene (C_6H_6) is commonly used in neutron scintillation detectors. In neutron spectroscopy, neutron energy is generally extracted using the time-of-flight method. This is because the detector response is essentially featureless, as shown in Fig. 15.6a, 15.6b taken with NE-213 scintillators. On the other hand, Fig. 15.6c, 15.6d are from deuterated benzene scintillators measured at the same energies. The peaks in these spectra appear due to the kinematics of scattering from deuterium. By combining these detectors with advanced pulse-shape analysis electronics, the energy information may be extracted in addition to the time-of-flight method, allowing for fast neutron spectroscopy in laboratory experiments.

Advancements in Detection Methods (Observables)

The types of detectors discussed here, gas-filled ionization detectors, scintillation detectors, semiconductor detectors, and neutron detectors, represent the majority of radiation detectors currently in use. The primary observables have been the electronic signals or light output based on direct or indirect ionization to signal the interaction of radiation in the detector. These represent the basic interactions which can be measured in common detectors.

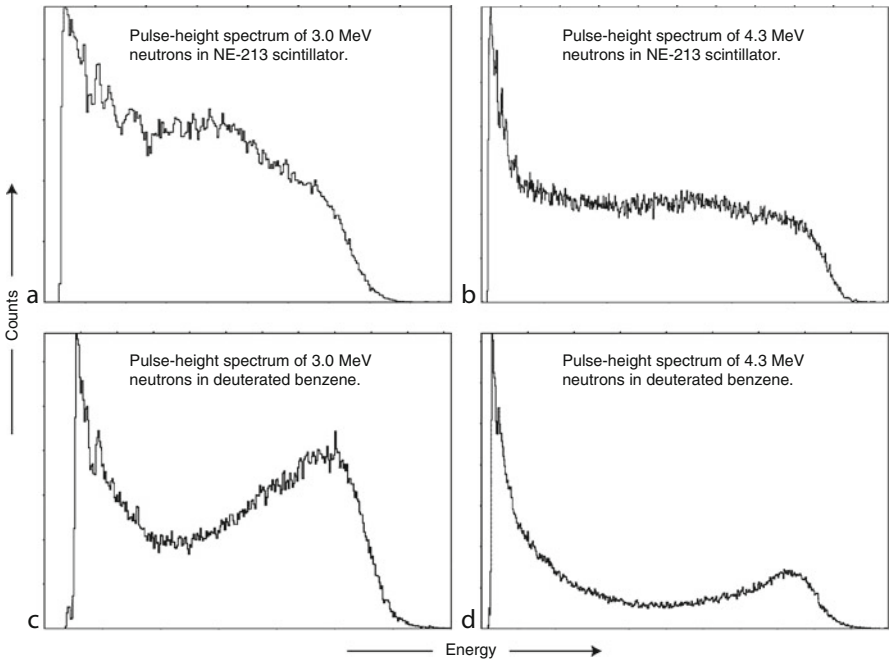

Fig. 15.6 Pulse-height spectra of monoenergetic neutrons collected using NE-213 scintillators and deuterated benzene scintillators. Neutron energy may be extracted from the deuterated benzene detectors using pulse-shape discrimination electronics (Spectra courtesy of P. E. Garrett)

Another possible observable is to measure temperature changes in a material to indicate radiation detection. Such a detector is called a *bolometer*, and the radiation absorber in this kind of detector is a material that has electric resistance that is highly dependent upon the material temperature. These detectors are at the forefront of dark matter and neutrinoless double-beta decay experiments [10] and are typically small metal, semiconductor, or even superconductor devices. The size is limited in order to maximize the temperature rise and the measured change in resistance. A drawback to this kind of detector is the need to maintain a consistent temperature.

One simple advancement in this area is to combine multiple types of detectors to filter the signal that is recorded for later use. An example of this is found in the *Compton-suppressed* germanium detector [11]. A germanium semiconductor detector is surrounded by high-efficiency scintillation detectors that act as an anticoincidence shield. If a gamma ray is detected only in the HPGe detector, but not in the surrounding detectors, it is presumed to have deposited the full energy in the germanium crystal. However, when signals are detected in coincidence with the surrounding scintillators, this indicates that the gamma ray has scattered out of the HPGe detector, and a full-energy pulse will not be detected. By suppressing these Compton scattering events using nanosecond coincidence timing circuits, the

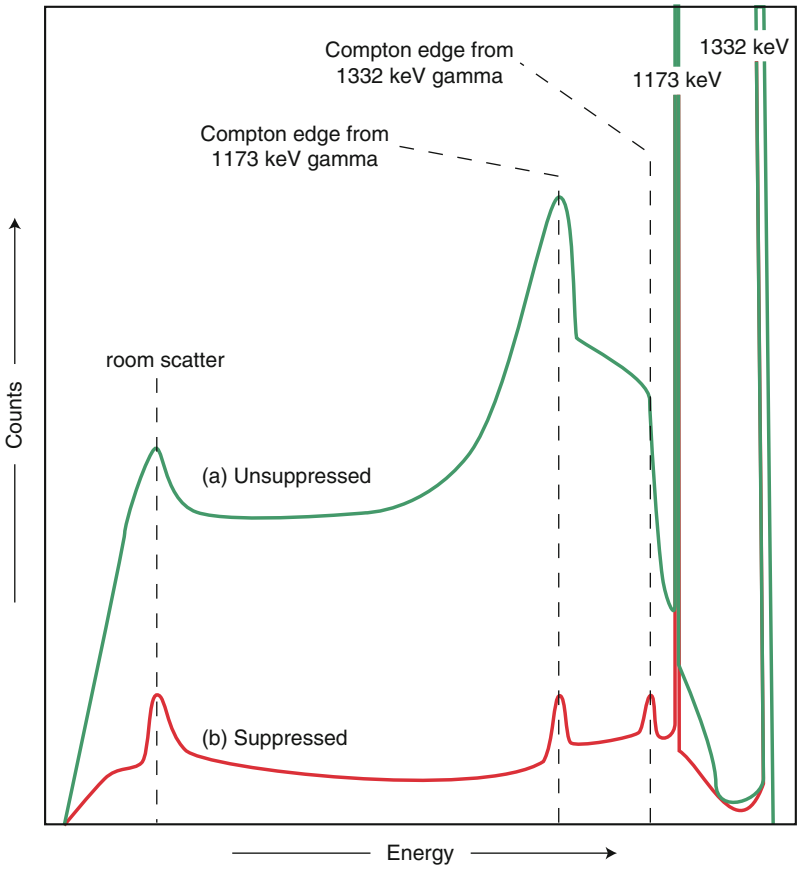

Fig. 15.7 The spectrum of a ^{60}Co source with characteristic gamma-ray lines at 1,173 and 1,332 keV collected using (**a**) a high-purity Ge semiconductor (HPGe) detector, and (**b**) the same HPGe detector operated in anticoincidence with a Compton-suppression shield of scintillators

background spectrum of the detector can be greatly reduced, as shown in Fig. 15.7. This enables the detection of much lower intensity peaks than would normally be visible with an unsuppressed detector.

Advancements in Signal Measurement

The basic method for radiation spectroscopy is to measure signal outputs and record the data to build up statistics for interpretation. Typically, each signal is passed through electronic circuits comprised of amplifiers, discriminators, and analog-to-digital convertors in order to electronically record each event as it is detected.

Computer analysis is later used to scan the recorded data, sort out events that fit requisite criteria, and fit the data for interpretation.

In some cases, such as in neutron detection, pulse-shape discrimination is used to distinguish between the types of radiation detected. This is typically done off-line during the computer analysis in order to separate the neutrons from gamma rays. An advancement to this technique is to use a computer in the data acquisition system in order to fit and digitize pulses during the data collection, and record only the signals of interest.

Very advanced gamma-ray spectrometers GRETA (Gamma-Ray Energy Tracking Array) [12] and AGATA (Advanced GAmma Tracking Array) [13] are being constructed in the United States and in Europe, respectively, to follow gamma-ray interactions as they scatter in germanium detectors. These *gamma-ray tracking spectrometers* use segmented germanium crystals connected by electronic contacts to determine where gamma rays interact in the detector. Off-line computer analysis is used to reconstruct the history of interaction. The full energy of the gamma ray is determined by summing up the energy of the individual interactions, and the first point of interaction in the detector may be determined for use in analysis based on angular distributions.

The GRETA and AGATA spectrometers are the most advanced research-class systems in gamma-ray spectroscopy and come with multimillion dollar (euro) price tags. Such systems are in development to support large groups of scientists at national laboratories, and as such are of specialized interest, rather than directly applicable to the general field of radiation detection. However, the future in this area will be closely tied to computational power and to the development of specialized electronics and programs for signal processing and data analysis. Adoption of better in-line and off-line computational power may overcome some of the inherent barriers in radiation detection and open opportunities for the development of new materials and new observables for detectors.

Bibliography

1. Nobel Lectures, Physics 1901–1921. Elsevier, Amsterdam, 1967
2. Glasstone S (1958) Sourcebook on atomic energy. D. Van Nostrand, Princeton
3. Kantele J (1995) Handbook of nuclear spectroscopy. Academic, San Diego
4. Knoll GF (2010) Radiation detection and measurement. Wiley, New York
5. Krane KS (1988) Introductory nuclear physics. Wiley, New York
6. Leo WR (1994) Techniques for nuclear and particle physics experiments. Springer, New York
7. Tsoulfanidis N (1995) Measurement and detection of radiation. Taylor & Francis, Washington, DC
8. Kouzes RT et al (2010) Nucl Instr Meth A 623:1035
9. Erickson JC, Yao HW, James RB, Hermon H, Greaves M (2000) J Electron Mater 29:699
10. Arnaboldi C et al (2008) Phys Rev C 78:035502
11. Nolan PJ, Gifford DW, Twin PJ (1985) Nucl Instr Meth A 236:95
12. Deleplanque MA et al (1999) Nucl Instr Meth Phys Res A 430:292
13. Eberth J, Simpson J (2008) Prog Part Nucl Phys 60:283

Chapter 16
Dosimetry

John W. Poston, Sr.

Glossary

Absorbed dose	The amount of energy deposited by ionizing radiation per unit mass of the material. Usually expressed in the special radiologic unit rad or in the SI unit the gray (Gy). One Gy equals 1 J/kg or 100 rad.
Dosimeter	Any device worn or carried by an individual to establish total exposure, absorbed dose, or equivalent (or the rates) in the area or to the individual worker while occupying the area.
Equivalent dose	(Formally the dose equivalent) The product of the absorbed dose and the radiation-weighting factor (formerly the quality factor) for the type of radiation for which the absorbed dose is measured or calculated. The equivalent dose is used to express the effects of radiation-absorbed dose from many types of ionizing radiation on a common scale. The special radiologic unit is the rem or in the SI unit the sievert (Sv). One sievert is equal to 1 J/kg or 100 rem.
Exposure	A quantity defined as the charge produced in air by photons interacting in a volume of air of known mass. An old quantity that is generally no longer used. Also, a general term used to indicate any situation in which an individual is being irradiated.
Ionization	The process of removing one or more electrons from an atom or a molecule. The positively charged atom and the negatively charged electron are called an *ion pair*.

This chapter was originally published as part of the Encyclopedia of Sustainability Science and Technology edited by Robert A. Meyers. DOI:10.1007/978-1-4419-0851-3

J.W. Poston, Sr. (✉)
Department of Nuclear Engineering, Texas A & M University, College Station, TX 77843-3133, USA
e-mail: poston@ne.tamu.edu; j-poston@tamu.edu

N. Tsoulfanidis (ed.), *Nuclear Energy: Selected Entries from the Encyclopedia of Sustainability Science and Technology*, DOI 10.1007/978-1-4614-5716-9_16,

Isotope	One of two or more atoms with the same number of protons but a different number of neutrons in their nuclei. A radioisotope is an isotope of a chemical element that is unstable and transforms by emission of nuclear particles and electromagnetic radiation to reach a more stable state. This term is often misused because unless the materials are the same element this term should not be used (see radionuclide below).
Nuclide	A general term to indicate an atomic nucleus characterized by its atomic number (number of protons), number of neutrons, atomic mass, and energy state.
Radiation	Used in this section to mean ionizing radiation. That is, particles or electromagnetic radiation emitted from the nucleus with sufficient energy to cause ionization of atoms and molecules composing the material with which the radiation is interacting.
Radionuclide	A nuclide that is radioactive and, upon decaying, emits ionizing radiation.

Definition

Dosimetry is best defined as "the theory and application of principles and techniques associated with the measurement of ionizing radiation" [1].

Introduction

The term "dosimetry" can be best explained by assuming it was derived from combining two words: "dose" and "measurement." The word dose is shorthand for several quantities associated with the profession of health physics (i.e., radiation protection and safety). The terms include the "absorbed dose," which is a measure of the energy deposited per unit mass of material, and the "equivalent dose," which includes consideration of the biological effects of different radiations, when the same absorbed dose is delivered to matter. The term "equivalent dose" is now used instead of the older term dose equivalent to signify changes in the ICRP recommended radiation and tissue weighting factors. There are many other "dose terms" used in health physics but these will not be included here because the fundamental quantity associated with dosimetry is the absorbed dose. Of course, the term measurement implies the use of some sort of detector that is sensitive to the ionizing radiation being measured. These "detectors" can take many forms from photographic film, first used more than 100 years ago, to sophisticated solid-state detectors being introduced today.

Scientists have been detecting radiation for more than a century using a wide variety of detectors. Initially, the detectors were either photographic film or simple ionization chambers filled with air. Crude scintillation systems led to the invention of detectors such as the Geiger–Mueller counter and more sophisticated proportional counters and detectors designed for specific applications and/or to detect a specific radiation. A discussion of these detectors would fill a textbook [2–5] and see also entry C. Radiation Detection Devices (in this encyclopedia). For this reason, this discussion of dosimetry will focus on two of the more modern dosimeters used to monitor the absorbed dose to occupationally exposed workers in nuclear facilities across the United States.

As indicated above, *Dosimetry* is best defined as "the theory and application of principles and techniques associated with measurement of ionizing radiation" [1]. In reality, two basic areas encompass the term "dosimetry." These are called external dosimetry and internal dosimetry. Again, these terms are shorthand descriptions of the more complex exposure conditions being considered. External dosimetry simply means the measurement of radiation that exists outside the human body. Basically, this type of dosimetry uses radiation detection devices and instrumentation to establish the characteristics of the radiation field. These measurements provide information in many forms, for example, the energy or energy spectrum of the radiation, the radiation intensity, the types of radiation present, and other useful information. In many cases, the radiation detectors used for these measurements are called "dosimeters"; an indication that the sole purpose is to measure the radiation-absorbed dose and which leads to an estimate of the equivalent dose. It is important to remember that, because the radiation source and the dosimeters are both outside the body, the measurement does not provide a direct measurement of the absorbed dose to the organs of the body. Methods used to provide estimates of the absorbed doses to organs and tissues of the body will be discussed later.

When a radionuclide or radionuclides are taken into the body, through inhalation, ingestion, injection, or assimilation through the intact skin, there is a completely different set of challenges facing the dosimetrist. Internal dosimetry is defined as "a process of measurement and calculation that results in an estimate of the absorbed dose to organs and tissues of the body from an intake of radioactive material" [1]. Internal dosimetry is primarily confined to the use of mathematical models and calculational techniques based on an internationally agreed upon set of standard assumptions. The dose estimate relies on mathematical models that describe the uptake, distribution, and retention of the radioactive material in the body. However, the calculations may be based on a set of measurements, such as the concentration of airborne radioactivity in a work area, the activity of radioactive material deposited in the body or specific organs in the body, or measurement of the concentration of radioactivity in excreta, such as urine or feces. Even with these measurements as initial input, internal dosimetry must rely on models of a reference human and calculational techniques. These aspects will not be discussed here.

This section will focus on a discussion of external dosimetry methods, which are primarily used to monitor radiation exposures of occupationally exposed workers conducting licensed activities in the US. Radiation dosimeters that are no longer widely used, such as film badges and pocket ionization chambers will not be discussed.

Thermoluminescence Dosimetry

In 1950, Daniels suggested that the thermoluminescence (TL) phenomenon could be used as a radiation dosimeter [3]. This suggestion came late in the development of radiation dosimeters even though it was known that Henri Becquerel, as well as his father, had mentioned this phenomenon in his scientific papers. In addition, the relation between X-ray exposure and thermoluminescence was observed as early as 1904. Nevertheless, after many struggles and failures in the research of Cameron and his colleagues, thermoluminescence and thermoluminescence dosimetry (TLD) became a reality and flourished in the late 1960s and 1970s [3]. For a very long time, TLD has been the most popular method of personnel monitoring.

In these dosimeters, the absorbed dose is determined by observing the emitted light from an inorganic crystal after exposure to radiation. The light is released from the crystal as it is heated under controlled conditions. The heat energy originally was provided by electrical heating but subsequent developments in TLD led to the use of high-intensity light as an alternate method. Regardless of the method of heating, the amount of light emitted is directly proportional to the radiation energy deposited in the TL material. This light is normally measured with a photomultiplier tube sensitive to the wavelength of the emitted light. It must be remembered that the TLDs are not "absolute dosimeters" and, therefore, require proper calibration in the radiation fields to which the dosimeters will be exposed.

Detailed explanations of the TL phenomenon have been offered by a number of scientists but a simple bandgap model can be used to explain the basic mechanism. The usual procedure is to refer to the energy-level diagram in an insulating crystal. In a pure crystal, radiation impinging on the crystal would free electrons and these electrons would pass from the valence band to the conduction band. These electrons would not remain in the conduction band for a long period and would return to the valence band releasing the energy acquired in the form of light. In a pure crystal, this light would be absorbed and would not escape the crystal. In TLDs, dopants (impurities) are added to the crystal and these impurities reside in the forbidden or bandgap between the valence and conduction bands. When these crystals are exposed to radiation, the loss of electrons from the valence band creates positively charged atoms ("holes"). The electrons and holes may migrate through the crystal until they recombine or are "trapped" by the impurity atoms (dopants) residing in the bandgap. Thus, the energy absorbed by the crystal is stored until it is released, in the form of light, through heating the crystal (thus, thermoluminescence). This light, which is now characteristic of the impurity sites, can escape the crystal and can be measured with an external detector (i.e., a photomultiplier tube).

It is important to realize that these trapping sites may exist at many different levels in the bandgap and it is not correct to assume that all electrons (or holes) are trapped at exactly the same energy level. Thus, the light intensity may vary as a function of temperature and the plot of the light intensity as a function of

Table 16.1 Summary of characteristics of thermoluminescence dosimetry (TLD) materials

TLD material	Effective atomic number (Z_{eff})	Temperature of main peak
$CaSO_4$:Mn	15.3	110°C
$CaSO_4$:Dy	15.5	220°C
CaF_2:Mn	16.3	260°C
CaF_2:Dy	16.3	180°C
LiF:Mg,Ti[a]	8.2	195°C
$Li_2B_4O_7$:Mn	7.4	200°C
Al_2O_3:C	10.2	185°C

[a]LiF:Mg,Ti is the standard material to which all other TLD materials are compared

Table 16.2 Summary of dosimetric characteristics of TLD materials

TLD material	Efficiency to Co-60	Energy response	Useful dose range	Fading
$CaSO_4$:Mn	70	~10	0.2 μGy–10^2 Gy	50% in 24 h
$CaSO_4$:Dy	20	~12.5	0.2 μGy–10^3 Gy	2% in 1 month 8% in 6 months
CaF_2:Mn	10	~13	10 μGy–3 × 10^3 Gy	10% in 16 h 15% in 2 weeks
CaF_2:Dy	30	~12.5	0.1 μGy–10^4 Gy	10% in 24 h 16% in 2 weeks
LiF:Mg,Ti	1.0	1.25	10 μGy–3 × 10^3 Gy	5% in 1 year
$Li_2B_4O_7$:Mn	0.15	0.9	0.5 μGy–10^4 + Gy	<5% in 3 months
Al_2O_3:C	70	2.9	0.5 μGy–10 Gy	<3% in 1 year

temperature (called a "glow curve") may exhibit a number of peaks and valleys depending on the number of trapping levels in the crystal. Either the total light emitted or the height of a particular peak may be used to determine the absorbed dose (upon proper calibration). It is also important that the heating cycle be very reproducible to avoid causing fluctuations in the peak heights.

There are a large number of inorganic materials that have been studied for use as TLDs. Table 16.1 presents a summary of the characteristics of some of the most popular materials (but there are many other possible TLD materials). In dosimetry, it is common to use materials that are "tissue equivalent" in terms of the interactions of photons or other radiations with the dosimeters. Thus, the closer the effective atomic number of the material is to that of tissue (~7.6), the more tissue equivalent is the material. For historical reasons, LiF is the standard to which all other TLD materials are compared. The standard LiF is the natural form of lithium with the normal concentrations of the isotopes of Li-6 (7.4%) and Li-7 (92.6%). Also in this table are listed the temperatures of the "main peak." This designation is the peak in the TLD glow curve that is used to determine the absorbed dose. One big disadvantage of TLDs is that the dosimeter can only be read (evaluated) once. Heating the crystal essentially releases all the electrons or holes that are trapped and an opportunity to confirm the reading is not possible.

Table 16.2 compares other characteristics of the TLD materials. These include the "light output" of the material when exposed to ^{60}Co radiation compared to the

light output for the standard, that is, LiF. The data for $Li_2B_4O_7$:Mn are somewhat misleading because the measurements quoted in this table were made with the standard photomultiplier tube used for all other TLD materials. However, because the wavelength of light from the $Li_2B_4O_7$:Mn is different, the output can be improved significantly by replacing the normal photomultiplier with one with a photocathode sensitive to the correct wavelength of light. The energy response is the ratio of the light output at energy of 30 keV to that from irradiation with ^{60}Co. Except for $Li_2B_4O_7$:Mn, most materials overrespond to low-energy photon radiation.

As can be seen in Table 16.2, the usual TLD materials are very sensitive to radiation with lower limits of detection in the range of tenths of microgray. Upper limits range from only 10 Gy to more than 10^4 Gy. The term "fading" is an indication of the ability of the TLD material to retain the stored energy and thus the stored information necessary to assign the absorbed dose from the wearing of the dosimeter. As is shown, LiF:Mg,Ti, $Li_2B_4O_7$:Mn, and Al_2O_3:C have good energy storage capability, which has led to a focus on these three materials.

Estimates of Absorbed Doses to Organs of the Body

In the United States, federal regulations require the reporting of three quantities for all occupationally exposed workers who are anticipated to receive doses in excess of 10% of the federal limits. These quantities are the "deep-dose equivalent," the "eye-dose equivalent," and the "shallow-dose equivalent." The deep-dose equivalent is defined as the dose at 1-cm depth in the body, which produces an overestimate of the absorbed doses because most organs and tissues of the body are located deeper than 1 cm (or 1,000 mg/cm^2). The eye-dose equivalent considers the dose to the lens of the eye, which is assumed to be at a depth of 300 mg/cm^2. Finally, the shallow-dose equivalent (or more properly the skin-dose equivalent) is assumed to be at a depth of 7 mg/cm^2.

Now the question arises, "How does one measure these absorbed doses, and the subsequent equivalent doses, with radiation dosimeters located outside the body of the worker?" The approach taken has been used for many years and is not new. It has been applied since the Manhattan Project era and is an accepted method to provide these dose estimates. The technique involves using multiple detector elements, that is, typically four TLDs, and covering these TLDs with different thicknesses of materials (called filters) to represent these depths. So, the TLD designated to measure the deep-dose equivalent is covered with a material having a density thickness of 1,000 mg/cm^2. The eye-dose equivalent is determined by covering the TLD with material with a density thickness of 300 mg/cm^2. Usually, there are two different materials of this density thickness in the dosimeter. Finally, there is a thin filter included to allow extrapolation to the depth of 7 mg/cm^2. It is very difficult to provide a direct measurement at such an extremely shallow depth.

Thermoluminescence Dosimetry for Neutron Radiations

TLDs have their primary application in dosimetry for X-ray and gamma-ray fields. In addition, the TLDs have limited sensitivity to beta radiation. Because certain materials in the TLDs interact with neutrons, TLDs can be used to measure both thermal and fast neutron dose – with proper calibrations. Table 16.3 lists the pertinent information regarding three types of LiF TLDs as these are applied to neutron dosimetry. As can be seen in this table, the natural LiF TLD has the normal concentrations on Li-6 and Li-7. This material is designated as TLD-100. The other two materials are designated TLD-600 and TLD-700. TLD-600 contains a high concentration of the isotope Li-6 with less that 5% Li-7. TLD-700 contains essentially all the isotope Li-7 with a very small amount of Li-6. Notice also the differences in the thermal neutron cross sections (probability to absorb neutrons) for these two isotopes. These differences play a role in the dosimetry of both thermal and fast neutrons.

Thermal neutron dosimetry is based on the "difference technique" used to separate the photon and thermal neutron dose from each other. This technique is similar in some ways to the standard method using bare and cadmium-covered gold foils to measure the thermal neutron fluence in a nuclear reactor core. Basically, the LiF TLD-600 is sensitive to photon radiation as well as to thermal neutron radiation. The LiF TLD-700 has the same photon sensitivity but essentially no sensitivity to thermal neutrons. Thus, when used in a mixed photon and thermal neutron field the TLD-600 will provide the absorbed dose for both the photons and the thermal neutrons. The TLD-700 will provide only the absorbed dose from the photon radiation and the difference between the doses indicated by the two dosimeters is the thermal neutron dose.

Fast neutron dosimetry uses a similar technique but to obtain the fast neutron dose the "albedo technique" is used. The albedo technique relies upon the dosimeter being held closely to the body and the fast neutron dose is measured as the fast neutrons enter the body, are moderated there by tissue, are subsequently reflected from the body and hit the dosimeter. There are many designs of albedo fast neutron dosimeters but the concept is the same as that outlined above. The fast neutron dose is obtained by using the difference technique as before.

Note that using TLDs to measure either thermal neutron or fast neutron dose require very careful calibration of the dosimeters in radiation fields approximating those in which the exposures are anticipated. In addition, in very high photon radiation fields with a low percentage of thermal or fast neutrons, these dosimeters may provide data that is highly suspect. This is often the consequence of subtracting two very large

Table 16.3 Characteristics of lithium fluoride TLDs for neutron dosimetry

TLD type	Li-6 percentage	Li-7 percentage	Thermal neutron cross section
Natural (TLD-100)	7.4%	92.6%	N/A
TLD-600	95.62%	4.38%	950 barns
TLD-700	0.007%	99.993%	0.033 barns

numbers (large photon dose) to obtain an estimate of the very low thermal or fast neutron dose. Other methods of neutron dosimetry, for example, track-etch detectors, may be preferred in these situations.

Optically Stimulated Luminescence

Currently, the dosimetry method of choice for dosimetry appears to be optically stimulated luminescence (OSL). Even though film and TLD are still used to some extent, many facilities are switching over to this newer technology. OSL may be used, not only for personnel monitoring, but also for environmental monitoring and medical dosimetry. Basically, OSL is very similar to TLD in terms of the basic physics associated with the energy deposition, storage, and release. The major difference is that, instead of using heat, laser light is used to release ("detrap") the electrons. The laser is pulsed at a rate of 4,000 times per second and is directed to only a small area on the material. This provides an opportunity for multiple readings on the same dosimeter, if necessary, as the laser can be focused on another region of the crystal. In a similar fashion to the development of TLDs in the latter part of the twentieth century, many materials have been studied for possible use as OSL dosimeters. These materials include halides, sulfates, sulfides, and oxides [6].

However, the material of choice is an Al_2O_3:C crystalline detector. Single crystals of Al_2O_3:C are ground into a powder and mixed with a polyester base. This mixture is deposited on a polyester film about 0.03 cm thick, which can be fabricated in a thin strip for incorporation into a dosimeter. This material has a good response to photon radiation as well as a response to beta radiation. Copper (0.18 g/cm^2) and tin (0.39 g/cm^2) filters, as well as an open area, are used in the dosimeter (as described above) to provide the dosimetry quantities of interest. Commercially available dosimeters have a dose measurement range for photons of 1 mrem to 1,000 rem (10 μSv to 10 Sv) over an energy range from 5 keV to more than 40 MeV. For beta radiation, the dose measurement range is from 10 mrem to 1,000 rem (100 μSv to 10 Sv) over an energy range of 150 keV to 10 MeV (average energy). The commercially available OSL dosimeters may be used for up to 1 year. If the packaging is not compromised, the dosimeter is unaffected by heat, moisture, and pressure [7].

Electronic Dosimeters

Currently, in many situations, such as in a nuclear power plant, it is common to wear two types of dosimeters. One of these dosimeters is usually a TLD or an OSL-type. This dosimeter is usually designated as the "dosimeter of record." That is, these dosimeters

are worn for long periods of time (i.e., 1 month, 3 months, or perhaps 1 year) and provide a measure of the total dose received by the exposed worker over the wearing period. It is these doses that are reported annually to the US Nuclear Regulatory Commission, as required by the federal regulations. The second dosimeter is a modern, electronic dosimeter that may contain as many as three small detector elements (usually solid-state detectors such as silicon diodes). Electronic dosimeters are used to monitor the work and may be worn for short periods of time. The primary function of these dosimeters is work and dose control. The dosimeters feature adjustable alarm points that may be set by a computer, before use, based on the anticipated total dose received or maximum dose rate encountered. Workers are trained to recognize the alarms and understand the proper response to these alarms.

There are many different electronic dosimeters but most have similar characteristics. A typical dosimeter would use small silicon diode detectors, which would be sensitive to both photons (50 keV to 6 MeV) and beta radiation (>60 keV up to more than 2 MeV). Doses from 0.1 mrem (1 μSv) to 10 Sv can be measured with dose rates ranging from 0.01 mrem/h (0.1 μSv/h) to 1,000 rem/h (10 Sv/h). Most dosimeters feature both audible and visible alarms. Typically, these dosimeters are lightweight, from 50 g up to perhaps 200 g. A unique feature of some of these dosimeters, and a good radiation protection practice, is the use of permanent stations throughout the plant that interrogate the dosimeters as the worker passes by the station and transmits this information to a central station. Other types of dosimeters contain small transmitters that transmit the accumulated dose (or dose rates) to central locations, which are monitored by the radiation safety staff. As technology moves forward, it is difficult to predict what the future holds in terms of the next generation of dosimeters.

Summary

The measurement of radiation energy deposited in material, that is, the measurement of the absorbed dose, is the primary goal of the practice of dosimetry. Over the last 100 years or more, dosimetry has taken many forms as science and technology have made significant progress. Many of the techniques have been relegated to the history books as other more advanced techniques have been introduced. This short discussion of dosimetry was intended to present the basic concepts and to provide two examples of modern dosimeters used to monitor personnel that are occupationally exposed to ionizing radiation, as well as to introduce the use of electronic dosimeters, which are used widely in nuclear utilities.

Future Directions

Approaches to dosimetry have changed rapidly with developments in electronics and computers. The last decade or so has seen the design and manufacture of dosimeters that are small but incorporate computer capabilities. These dosimeters allow the setting of dose and dose rate alarms, remote interrogation of the dosimeters to monitor worker exposure, and many other features. It appears these trends will continue as the demand for "smarter" dosimeters, with many more capabilities, for use in nuclear facilities as well as in emergency response continues to increase.

Bibliography

1. Poston JW Sr (1987) Dosimetry. In: Encyclopedia of physical science and technology, vol 6. Academic, New York
2. Knoll GF (2000) Radiation detection and measurements, 3rd edn. Wiley, New York
3. Eichholz GG, Poston JW (1979) Principles of nuclear radiation detection. Ann Arbor Science Publishers, Ann Arbor
4. Tsoulfanidis N (1995) Measurement & detection of radiation, 2nd edn. Taylor & Francis, Washington, DC
5. Kase KR, Bjarngard BE, Attix FH (eds) (1985) The dosimetry of ionizing radiation, vol I–III. Academic, New York
6. Boetter-Jensen L, McKeever SWS, Wintle AG (2000) Optically stimulated luminescence dosimetry. Elsevier, Maryland Heights
7. R. S. Landauer, Inc. (2010) http://www.osldosimetry.com/luxel/. Accessed 9 May 2010

Chapter 17
Health Physics

John W. Poston, Sr.

Glossary

Absorbed dose	The amount of energy deposited by ionizing radiation per unit mass of the material. Usually expressed in the special radiologic unit the rad or in the SI unit the gray (Gy). One Gy equals 1 J/kg or 100 rad.
Dosimeter	Any device worn or carried by an individual into a radiation area to establish total exposure, absorbed dose, or equivalent dose (or the rates) in the area or to the individual worker while occupying the area.
Dosimetry	The theory and application of principles and techniques associated with the measurement of ionizing radiation.
Epilation	Loss of hair due to damage to the follicles in the skin. Temporary epilation occurs for acute exposures in the range of 300 to 500 rad with permanent epilation occurring above about 700 rad.
Equivalent dose	(Formally the dose equivalent) The product of the absorbed dose and the radiation-weighting factor (formerly the quality factor) for the type of radiation for which the absorbed dose is measured or calculated. The equivalent dose is used to express the effects of radiation-absorbed dose from many types of ionizing radiation on a common scale. The special radiologic unit is the rem or in the SI unit the sievert (Sv). One Sv is equal to 1 J/kg or 100 rem.

This chapter was originally published as part of the Encyclopedia of Sustainability Science and Technology edited by Robert A. Meyers. DOI:10.1007/978-1-4419-0851-3

J.W. Poston, Sr. (✉)
Department of Nuclear Engineering, Texas A & M University, College Station, TX 77843-3133, USA
e-mail: poston@ne.tamu.edu; j-poston@tamu.edu

N. Tsoulfanidis (ed.), *Nuclear Energy: Selected Entries from the Encyclopedia of Sustainability Science and Technology*, DOI 10.1007/978-1-4614-5716-9_17,

Erythema	Reddening of the skin due to exposure to radiation, similar to sunburn or thermal burns depending on the severity of exposure; occurs for acute exposures in the range 600–800 rad.
Exposure	A quantity defined as the charge produced in air by photons interacting in a volume of air of known mass. An old quantity that is generally no longer used. Also, a general term used to indicate any situation in which an individual is being irradiated.
Ionization	The process of removing one or more electrons from an atom or a molecule. The positively charged atom and the negatively charged electron are called an *ion pair*.
Isotope	One of two or more atoms with the same number of protons (same atomic number Z) but a different number of neutrons (N) in their nuclei. A radioisotope is an isotope of a chemical element that is unstable and transforms by emission of nuclear particles and electromagnetic radiation to reach a more stable state. This term is often misused because unless the materials are the same element this term should not be used (see radionuclide below).
Nuclide	A general term that indicates an atomic nucleus that is characterized by its atomic number (number of protons), number of neutrons, atomic mass, and energy state.
Radiation	Used in this section to mean ionizing radiation. That is, particles or electromagnetic radiation emitted from the nucleus with sufficient energy to cause ionization of atoms and molecules, either directly or indirectly, composing the material with which the radiation is interacting.
Radionuclide	A nuclide that is radioactive and upon decaying, emits ionizing radiation.

Definition

Health Physics: The theory and practice of radiation protection [1].

Introduction

The term health physics probably has a large number of definitions because it means many things to many practitioners of nuclear technology. As indicated above, health physics basically means radiation protection or radiation safety. The term itself has its origins in the Manhattan Engineering District (MED) days during World War II. Dr. Arthur Holly Compton and his deputy, Dr. Robert S. Stone, recognized the need for a group of individuals whose sole responsibilities

were to protect the workers from the potential harmful effects of radiation while allowing the MED work to move forward as rapidly as possible. However, such individuals did not exist at the time and the decision was made to select individuals from the medical physics profession, who understood radiation exposures and biological effects of radiation, and those with expertise in measuring low levels of radiation exposure. The former group of individuals was recruited from the ranks of those in hospitals and cancer therapy clinics across the country while the latter group was recruited from cosmic-ray physicists (Compton himself was a cosmic-ray physicist). There was a need to select a name for these individuals and a number were considered. It was important that the name selected did not reveal the work of those involved in the MED activities. Since Dr. Stone was in charge of the Health Division at the Chicago Lab and the members of the group were physicists, the name health physics seemed to come naturally. There was also a clear intent to hide from those without the need to know exactly what was going on at the Lab. Thus, the term health physics was selected with the full intent that it be somewhat nebulous.

Dr. K. Z. Morgan, a cosmic-ray physicist and one of the original eight health physicists, defined health physics as the study and practice of radiation protection [2]. In a lighter moment, he also defined health physics as "what health physicist do." Health physicists are professionals dedicated to the protection of the human race and the environment from the harmful effects of radiation, while recognizing that there are enormous benefits to be derived from the use of nuclear technology [3, 4]. A health physicist is constantly balancing the risk of radiation exposure with the benefit from the use of the nuclear technology. In simple terms, health physicists strive to keep the radiation risk as small as possible and the benefit as large as possible. If one visualizes an old-fashioned balance or scale, the risk would be very small and the benefit would be large. It is not their intent to balance the scale but to have "benefit pan" outweigh the "risk pan" so that the scale is tilted significantly.

Current approaches to health physics (i.e., radiation protection) are based on three principles, summarized in three words: justification, optimization, and limitation. First, there should not be any unnecessary radiation exposures: the benefit must exceed the risk from the exposure. Second, all exposures to radiation should be kept As Low As is Reasonably Achievable (this is called the ALARA principle but, in other countries, this is called "optimization"). Finally, no radiation exposures should exceed the recommended regulatory limits on radiation exposures.

Those facilities licensed by either the US Nuclear Regulatory Commission (USNRC) or by agreement states generally apply an exposure limit of 5 rem/year (0.05 Sv/year) for occupationally exposed workers. But health physicists use the three principles to drive exposures as far below the regulatory limits as is possible. The ALARA principle has not only kept exposures below the regulatory limits, but also has resulted in a significant reduction in the collective doses and average worker doses at nuclear utilities in the United States. The average doses to workers at both pressurized water reactors (PWRs) and boiling water reactors (BWRs) in the United States have been reduced to levels of only a few hundred mrem per worker per year. In 2007, the average dose equivalent to a worker in the US nuclear power plant was 130 mrem [5].

Early History and Development

Even though the terms health physics and health physicist were not used until the early 1940s, the need to protect individuals from harmful radiation exposure dates back to just after the discovery of X-rays by Wilhelm Roentgen in 1885 and natural radioactivity by Henri Becquerel in 1896. With such amazing discoveries, many scientists began to investigate these phenomena for themselves and many were perhaps unnecessarily exposed to radiation. Many researchers took things into their own hands and established exposure guidelines and restrictions for use in their laboratories. However, often these exposure guidelines were based on observable effects such as the production of erythema and even evidence of epilation. Even with these informal and unified guidelines, there were still individuals who experienced harm from excessive radiation exposures.

In 1899, the British Roentgen Society formed a committee to collect data on the effects of X-rays. These efforts were hampered by the general belief that X-rays were harmless [6]. Later, the British X-ray and Radium Protection Committee adopted recommendations in 1921. It is important to notice the name of this committee because it indicates the limited nature of the early use of radioactivity and radiation-producing machines. In the United States, the American Roentgen Ray Society established a standing committee on radiation protection in 1920 and recommendations of this committee were adopted at the annual meeting of the Society in 1922 [2].

It was not until 1925, at the First International Congress on Radiology, that there was an international effort to begin to control radiation exposure. This effort resulted in the formation of the International Committee on X-ray and Radium Protection in 1928 at Second International Congress held in Stockholm [7]. These efforts resulted in two current organizations, the International Commission on Radiological Protection (ICRP) and the International Commission on Radiation Units and Measurements (ICRU). These international activities were paralleled by similar efforts in the United States. In 1929, the Advisory Committee on X-ray and Radium Protection was formed as an outgrowth of discussions between the American Roentgen Ray Society, the Radiological Society, and the Radium Society. This committee ultimately became the National Council on Radiation Protection and Measurements (NCRP) and was chartered by Congress in 1964 to provide advice and counsel on these matters to the federal government [7]. General overviews of the profession as well as discussion of the early development of the profession can be found in the bibliography provided at the end of this section [8–10].

The International Commission on Radiological Protection (ICRP) is responsible for making general recommendations on approaches to radiation protection. These recommendations are intended to provide the basic framework for radiation protection for those nations with nuclear technology programs, but it is the responsibility of each country to adapt these recommendations to the current state of their nuclear technology program. In the United States, the National Council on Radiation Protection and Measurements (NCRP) reviews the recommendations of the ICRP

and provides a set of recommendations that are intended for use in the United States. The Environmental Protection Agency is responsible for establishing the general recommendations for all federal agencies and this guidance is signed into law by the President of the United States. Then, each federal agency is required to promulgate a set of regulations to govern their activities. For example, the USNRC regulations are found in Title 10 Code of Federal Regulations part 20 (10CFR20) and the Department of Energy regulations are in 10CFR835.

But, in the United States, things are not so simple. In the federal government, at least one agency has not revised their recommendations in response to the 1987 EPA guidance and is still functioning under the 1959 version of the Code of Federal Regulations. Most agencies are using the 1977 recommendations of the ICRP in compliance with the EPA guidance. The 35 agreement states in United States have promulgated regulations that are in compliance with the EPA guidance. However, the Department of Energy has instructed their contractors to implement the newer recommendations published by the ICRP in 1990. Even though these recommendations are similar, some significant differences must be recognized and understood. But, the situation in the United States is not currently very simple.

The Health Physics Profession

Health physicists are found in essentially all activities involving the use of ionizing radiation, including research, education, medical uses, industrial applications, consulting services, and state and federal regulatory agencies [3, 4]. Although most health physicists are involved in only one of these areas, it is common for the professional health physicist to become active in many of the above areas. There is always a need to train employees and educate the general public concerning the hazards of radiation and the appropriate methods of protection. A health physicist must ensure that the state and federal regulations regarding radiation exposure are followed and that legal limits are not exceeded. In addition, it is the health physicist's responsibility always to seek better ways of accomplishing tasks so that exposures to ionizing radiation are kept as low as reasonably achievable, releases to the environment are controlled and appropriate, and all uses of radiation or radioactivity result in a positive benefit.

Health physics is a course of study in a number of universities across the country; both at the baccalaureate and graduate levels. Many universities grant advanced degrees in health physics and related fields (physics, radiobiology, radiochemistry, etc.). The courses of study are found in colleges of engineering, schools of public health, physics departments, biology departments, and chemistry departments. There seems to be no official "home" for these programs. However, this situation provides a certain interdisciplinary flavor to the profession, because each academic program is different and students can find an institution that best satisfies their interests and needs.

Health physics is an exciting, interesting, and challenging profession. Controlling radiation exposures to the lowest possible levels, while allowing the use of nuclear technology for the benefit of society, requires a broad background in a number of technical areas. This broad general understanding includes physics, chemistry, biology, anatomy, physiology, ecology, electronics, and a number of other disciplines. Opportunities for employment exist within a number of allied professional activities, such as medicine, cancer therapy, research, education, and regulatory affairs. Health physics and its related fields present the individual with daily challenges that require the application of sound professional judgment so that other work can proceed safely.

Opportunities within the profession have increased dramatically over the past few years. Projections indicate that the demand for health physicists will exceed to supply for the foreseeable future. Many of the early leaders of the profession have retired and a large number of those active in the profession have more than 30 years of experience. The demands for qualified health physicists will likely stay high for a very long time as the use of nuclear technology continues to increase.

Radiation Exposure to the US Population

Health physicists have the responsibility to protect the general population from unnecessary radiation exposure, just as they do with occupationally exposed workers. A question that often arises is, "what if the average radiation exposure to members of the public?" The NCRP has answered this question in a series of reports over a number of years. In 1987, the NCRP estimated that the average dose equivalent to a member of the US population was 360 mrem/year [11]. A large majority of this exposure was due to naturally occurring radiation sources such as cosmic rays, solar radiation, internally deposited radionuclides, and, especially, radon gas (200 mrem/year). In the most recent NCRP report [12], the average equivalent dose was estimated to be 620 mrem/year (6.2 mSv/year). The significant increase in this average was due to the use of medical technology involving radioactivity (nuclear medicine) and radiation-producing devices used in diagnosis and in cancer therapy (48%). Occupational exposures to radiation were estimated to be $<0.1\%$ of the total average equivalent dose. This is perhaps a testament to the dedication of health physicists to keep these exposures ALARA.

Future Directions

The practice of radiation safety and control (health physics) will continue to evolve as more and more challenges are added to the daily routine of the professionals. Revisions of dose/risk estimates continue to result in lower recommended radiation exposures limits. Some of these may be unjustified but, nevertheless, place an

increased burden on those responsible for occupational exposures. One big challenge in the United States is the impact of the use of radiation-producing machines and radioactive materials in medicine. The increase in the average annual exposure to the general population is astounding and is a concern to those dedicated to the profession of health physics and the concept that all exposures should be justified.

Bibliography

1. Poston JW Sr (1987) Health physics. In: Encyclopedia of physics science and technology, vol 6. Academic, New York
2. Morgan KZ, Turner JE (1973) Principles of radiation protection. Robert E. Kreiger, Huntington
3. Health Physics Society, Health physics: a profession of the nuclear age, Health Physics Society, 1313 Dolley Madison Blvd., Suite 402, McLean, VA 22101
4. Health Physics Society, Prospectus, Health Physics Society, 1313 Dolley Madison Blvd., Suite 402, McLean, VA 22101
5. Nuclear Energy Institute (2009) Radiation safety at nuclear power plants, June 2009. http://www.nei.org/keyissues/safetyandsecurity/factsheets/safetystudiespublicworkers. Accessed 20 May 2010
6. Kathren RL, Tarr NE (1974) The origins of the Health Physics Society. Health Phys 27:419–428
7. Taylor LS (1971) Radiation Protection Standards. CRC, Cleveland
8. Taylor LS (1958) Brief history of the National Committee on Radiation Protections and Measurements (NCRP) covering the period 1929–1946. Health Phys 1:3–10
9. Taylor LS (1958) History of the International Commission on Radiological Protections (ICRP). Health Phys 1:97–104
10. Claus WD (1958) What is health physics? Health Phys 1:56–61
11. National Council on Radiation Protection and Measurements (1987) Ionizing radiation exposure of the population of the United States. National Council on Radiation Protection and Measurements, Bethesda
12. National Council on Radiation Protection and Measurements (2009) Ionizing radiation exposure of the population of the United States. National Council on Radiation Protection and Measurements, Bethesda, NCRP Report 160

Chapter 18
Uranium and Thorium Resources

J. Stephen Herring

Glossary

Cross section	Probability of neutron interaction with a nucleus, expressed in terms of area, in units of barns (b). One barn equals 1.0×10^{-24} cm^2.
Enrichment	The fraction of an isotope, usually fissile ^{235}U, in a mass of uranium. Enrichment is commonly quoted as the weight percent of the particular isotope. Natural uranium has an enrichment of 0.711 wt%, commercial reactor fuel is 3–5% enriched, and depleted uranium is 0.2–0.3% ^{235}U.
Enrichment tails (also depleted uranium)	The uranium remaining after the enrichment of natural uranium into fuel, today about 0.3% ^{235}U, earlier 0.2–0.25% ^{235}U.
Fractionation	Crystallization from a magma in which the initial crystals are prevented from equilibrating from the parent liquid, resulting in a series of residual liquids of more extreme composition than would have resulted from continuous reaction [1].
Highly enriched uranium (HEU)	Uranium containing more that 20 wt% ^{235}U.
J_{th}	Joule (i.e., Watt-second) thermal. One British thermal unit (BTU) equals 1,055 J_{th}.
Log-normal distribution	Distribution of the form $f(x) = e^{-(\ln x)^2}$. In the present usage, the tonnage of an element available at concentration c, $T(c)$, is

This chapter was originally published as part of the Encyclopedia of Sustainability Science and Technology edited by Robert A. Meyers. DOI:10.1007/978-1-4419-0851-3

J.S. Herring (✉)
Idaho National Laboratory, Idaho Falls, ID, USA
e-mail: J.Herring@inl.gov

N. Tsoulfanidis (ed.), *Nuclear Energy: Selected Entries from the Encyclopedia of Sustainability Science and Technology*, DOI 10.1007/978-1-4614-5716-9_18,

	given by $T(c) = C_1\, e^{-(\ln c_o - \ln c)^2}$, where c_o is the average crustal abundance and C_1 is a constant.
Low-enriched uranium (LEU)	Uranium containing less than 20 wt% ^{235}U.
Mafic	Composed chiefly of dark ferromagnesian minerals.
MOX	Mixed oxide fuel, usually consisting of a ceramic mixture of uranium dioxide and plutonium dioxide.
MSWU	Mega-separative work unit, a million separative work units. A separative work unit is the separative work that must be done to one kilogram of a mixture of isotopes to change its separation potential by one unit. The separation potential, a dimensionless function, is defined by $\phi\ (x_k) = (2x_k - 1) \ln \frac{x_k}{1-x_k}$, where x_k is the atomic fraction of the isotope, k. See Benedict 1981, p. 667 for a more complete definition [2].
Pegmatite	An exceptionally coarse-grained igneous rock, with interlocking crystals, often found at the margins of batholiths.
Placer	A mineral deposit at the surface formed by sedimentary concentration of heavy mineral particles from weathered debris.
Quad	Quadrillion (i.e., 10^{15}, also written 1E15) British thermal units. One quad = 1.055×10^{18} J_{th}.
t	Metric ton, also used in *Mt*, million metric tons, and *Tt*, trillion metric tons (teratons).
Unconformity	A break or gap in the geologic record, such as an interruption in the normal sequence of deposition of sedimentary rocks, or a break between eroded metamorphic rocks and younger sedimentary strata [1].
Yellowcake	A concentrate of uranium ore, containing 80–90% U_3O_8. Yellowcake ranges from yellow to black, depending on impurities, processing temperature, and degree of hydration [3]. Although uranium prices are sometimes colloquially cited as "dollars per pound of yellowcake," the actual prices are $ per lb of U_3O_8, where all of the uranium is assumed to be present in the yellowcake as that oxide.

Definition of the Subject

Uranium is a widely distributed element which is essential, at least in the near term, to the use of nuclear fission as a source of energy. Uranium is ubiquitous in the earth because of the wide variety of minerals in which it can occur, and because of the variety of geophysical and geochemical processes that have transported it since the primordial formation of the earth from the debris of supernovae. Uranium is

approximately as common in the earth's crust as tin or beryllium, and is a minor constituent in most rocks and in seawater. The average crustal abundance of uranium is 2.76 weight parts per million (wppm), higher than the average concentrations of such economically important elements as molybdenum (1.5 wppm), iodine (0.5 wppm), mercury (0.08 wppm), silver (0.07 wppm), and gold (0.004 wppm).

Introduction

Beginning with the discovery of nuclear fission, uranium has been seen as a valuable but scarce resource. Uranium-235 (^{235}U) is the only naturally occurring isotope that can be made to fission with thermal neutrons. Consequently, the resources of uranium have been believed to inherently limit the sustainability of nuclear energy. There have been two periods of extensive exploration for uranium, in the 1950s and in the 1970s, both followed by long periods of severe contraction in the market and in exploration activity. With the peak of uranium prices to about $350/kg in 2007, there was an increased effort in exploration. However, that exploration quickly resulted in increased known reserves in several deposits and the return of prices to about $140/kg. Today, exploration activity is at a moderate level for several reasons: (1) deposits found during earlier exploration periods have proven to be larger than initially estimated, (2) nuclear energy is growing, but not as rapidly as earlier forecast, (3) improved nuclear fuel management techniques and materials are allowing higher burnup and longer operating cycles, and (4) the conversion ("downblending") of highly enriched uranium of military origin to civilian purposes has postponed the need for large amounts of newly mined natural uranium.

Concern that uranium would soon be exhausted was one of the driving forces in the development of fast breeder reactors, particularly in the 1960s and 70s. Fast breeder reactors convert the fertile isotope ^{238}U into the fissile isotope ^{239}Pu. These concerns also led to the development of thermal breeder reactors capable of converting thorium into the fissile, but not naturally occurring, isotope ^{233}U. Thorium, consisting almost entirely of the isotope ^{232}Th, is about four times more abundant than uranium and thus may represent a source of nuclear fuel in the distant future.

Estimates of Uranium Reserves

The importance of the overall uranium and thorium resource is demonstrated by the attention given to the estimates by such international agencies as the International Atomic Energy Agency (IAEA) and the Nuclear Energy Agency (NEA) of the Organisation for Economic Co-operation and Development (OECD). The estimates of these organizations are based on information provided by the member states and backed by research from others. The results are regularly compiled in the "Red Book" [4].

However, the estimates of uranium resources in the Red Book are based on the known and expected reserves that can be economically extracted using present or near-future technology. Because of the wide range of uranium concentrations in various minerals, the cost of extraction serves as the independent variable against which resources are estimated. Any reported amount of reserves/resources should be accompanied by the estimated cost of recovery of those reserves.

The Red Book [4] estimates the economically recoverable uranium reserves based on current and prospective mining projects ("Total Identified Resources Reasonably Assured and Inferred") as of January 2009 are 5.4 million metric tons (Mt) of uranium of the best-proven category recoverable worldwide at a marginal cost of <$130/kg of uranium metal. When the high-cost category (between $130/kg and $260/kg of U metal) is added, the total identified resources are estimated to be 6.3 Mt. Total undiscovered resources (prognosticated resources and speculative resources) as of January 2009 were estimated to be 10.4 Mt. The 2008 consumption of natural uranium by the 438 reactors worldwide was 59,065 t, and consequently, these total identified resources could be expected to last about 100 years at current rates and 250 years if speculative resources are included. These ratios of identified and speculative resources to consumption rate are longer than those for nearly all metals and fossil fuels, with the exception of coal.

Low market prices, the slow growth of nuclear power, and the downblending of highly enriched uranium (HEU) have in the past resulted in both very low levels of exploration and little effort in the development of advanced extraction technologies. Downblending agreements with the Russian Federation are due to expire in 2013. The discovery of additional total identified resources has shown a strong correlation with exploration expenditures, averaging 0.65 kg of additional resources per exploration dollar from 1987 to 2005 and 0.32 kg/exploration dollar from 2005 to 2009, following the uranium price increases after 2005 [5]. Those transient price increases led to an increase in the average annual expenditures for exploration from $127 million/year for 1987–2005 to $1.1 billion/year for 2005–2009.

It is important to note that uranium today is used overwhelmingly in the light water reactor fuel cycle, where only about 1.1–1.5% of the ultimate energy of the mined uranium is extracted via fissioning of ^{235}U and the small amounts of ^{239}Pu bred in situ. The rest of the uranium remains either in the used fuel or in the depleted uranium tails remaining after enrichment. Of the 1.8 Mt of uranium mined worldwide since 1945, the location of all but about 1,500 t is known. Only the location of that uranium dispersed either in nuclear explosions or as armor-piercing projectiles is not known. The inventory of used fuel and of depleted uranium represents a very significant resource that could become fuel for fast breeder reactors.

While uranium is an essential input for the production of nuclear energy, the costs of natural uranium are a minor component of the overall cost. Today, at uranium prices of about $140/kg U ($53/lb of U_3O_8), the natural uranium required for the light water reactor (LWR) fuel cycle is responsible for only about 2.5–3% of generating costs. The fuel cost is 15–20% of the generating costs, but those costs include conversion of the uranium ore to UF_6, enrichment of the natural uranium,

production of the ceramic UO_2 fuel pellets, and fabrication of the fuel assemblies. A tenfold increase in the cost of natural uranium would not be welcome, but would not fundamentally change the economics of nuclear power. A tenfold increase in uranium prices would, at first estimate, be expected to increase the cost of nuclear electricity by 25–30%. However, a more detailed calculation, optimizing the ^{235}U content of the depleted uranium tails and adjusting fuel management for a higher priced resource, would result in an increase in the cost of electricity significantly less than 20%.

This entry discusses uranium resources in a global sense, beyond the official estimates of the IAEA and the OECD. As an introduction to that discussion, the origins of the earth's present inventory of uranium, the geophysical and geochemical processes that serve to concentrate uranium into economically viable deposits, and the technologies now being used for the extraction and concentration of uranium ores are described. Finally, the potential impacts of technologies now under development and the overall impact of the cost of uranium on the cost of energy from nuclear fission will be reviewed.

Thorium as a Nuclear Fuel

For the foreseeable future, uranium will probably continue to be the only source of nuclear energy. Nevertheless, for completeness, thorium resources should also be considered because of thorium's unique characteristics as a nuclear fuel. There are basically four reasons for considering thorium resources within the overall discussion of nuclear fuel resources. First, thorium is about 3.9 times more abundant than uranium, on a mass basis, as indicated both by samples of the continental crust and by spectroscopy of supernova debris, from which planets are formed. Secondly, because similarities of the geochemistry and mineralogy of thorium and the lanthanides, thorium and the lanthanides (often called the "rare earth elements") are often found in the same ore bodies. Since the lanthanides are of increasing technical and strategic importance due to their widespread use in magnets and electronics, thorium is often treated as a waste since it has only a small market and since it is radioactive. Thus research on the efficient separation and purification of thorium could enhance both rare earth and thorium resources. Third, thorium can be directly substituted in the UO_2 crystal, making it a long-term supplement for uranium for in situ ^{233}U breeding. Thorium, as ThF_4, can also be used in the molten salt reactor in combination with UF_4, where the uranium would be a mixture of ^{233}U, ^{235}U, and ^{238}U. Finally, because thorium has only one oxide, ThO_2, which has high thermal stability, it can serve as a very robust matrix for actinide transmutation, after which the ThO_2 would serve as the waste form for the transmutation targets.

Thorium averages 12 parts per million in the earth's crust, and is the 39th most abundant of the 78 crustal elements. Soil commonly contains an average of 6 wppm of thorium. When thorium is used as a nuclear fuel, much less plutonium and other

minor transuranics (i.e., neptunium, americium, curium, berkelium, ...) are produced than are produced in uranium fuel cycles. The reduced production of transuranics occurs for two reasons. First, the fissile product of neutron absorption by ^{232}Th is ^{233}U, which is further down the actinide series from plutonium and the minor actinides, and secondly, the fission to capture ratio of ^{233}U is approximately nine, while that of ^{239}Pu is about three, thus resulting in lower production of the transuranics.

The generation of thorium deposits occurs in a fundamentally different manner from deposits of uranium. Uranium has some nine oxides and is dissolved or precipitated depending on the oxygen content and pH of the groundwater. Thus deposits are often formed where there is a decrease in the oxygen content of groundwater. Thorium, on the other hand, has only one oxide, ThO_2, which is very refractory and insoluble. Thus thoria (along with many of the lanthanide oxides) is not dissolved in erosion by groundwater and flowing rivers. The surviving grains, containing the thoria from the base rock, form into alluvial deposits of monazite sands.

Thorium occurs as the ores thoriatite (ThO_2), thorite ($ThSiO_4$) and mainly as monazite ($(Ce, La, Nd, Th)PO_4$). Thorium and its compounds have been produced primarily as a by-product of the recovery of titanium, zirconium, tin, and rare earths from monazite, which contains 6–8.5 wt% thorium oxide. Only a small portion of the thorium produced is consumed. Limited demand for thorium, relative to the demand for rare earths, has continued to create a worldwide oversupply of thorium compounds and mining residues. Most major rare-earth processors have switched feed materials to thorium-free intermediate compounds to avoid the handling of radioactive thorium. Excess thorium not designated for commercial use is either disposed of as a radioactive waste or stored for potential use as a nuclear fuel or other applications. Increased costs to comply with environmental regulations and potential legal liabilities and costs to purchase storage and waste disposal space were the principal deterrents to its commercial use. Health concerns associated with thorium's natural radioactivity have not been a significant factor in switching to alternative nonradioactive materials. US consumption of thorium, all for nonenergy uses, has decreased from 11.4 t (thorium content) to 0.7 t since 1997. The principal applications of thorium today make use of the very high melting point of ThO_2 (3,300°C, the highest of all binary oxides) and of the electron emitting capability of thorium when alloyed with tungsten for use in filaments for high-powered magnetrons for radar.

In the short term, thorium is available for the cost of extraction from rare-earth processing wastes. In the longer term, large resources of thorium are available in known monazite deposits in India, Brazil, China, Malaysia, and Sri Lanka. The world total thorium resources identified and prognosticated amounts to 3.6 million tons Th. Though reported values vary because of the difficulty in measuring such low concentrations, ^{232}Th is present in seawater at only about 0.050 wppb, due primarily to the insoluble nature of its only oxide, ThO_2. Thus the recovery of thorium from seawater is not a realistic option.

Because ^{232}Th is the only isotope of natural thorium, there are no enrichment plant tails from thorium nuclear fuel. Therefore, the cost of thorium in a mixed

thorium-uranium LWR fuel or in a pure thorium-^{233}U fuel cycle is relatively small. However, the cost of chemically processing of ThO_2-based fuel and the separation of ^{233}U is significant.

Energy Content of Uranium and Thorium

Uranium has 18 known isotopes, none of which are stable and only two of which have half-lives longer than a million years, ^{235}U (704 Ma) and ^{238}U (4.47 billion years). Only ^{235}U, which is about 0.711 wt% (0.720 atom%) of natural uranium, is fissile, i.e., will fission using thermal (i.e., low velocity) neutrons. Uranium-238, which is by far the dominant isotope at 99.2745 wt%, will fission if struck by high-energy neutrons. However, ^{235}U is the only naturally occurring isotope of any element capable of sustaining a neutron chain reaction in a suitably designed reactor.

^{238}U is a fertile isotope and can be transformed into ^{239}Pu through the capture of a neutron and two subsequent beta decays, as shown in the following reaction:

$$^{238}\mathrm{U}(n,\gamma)^{239}\mathrm{U} \xrightarrow[\beta^- t_{1/2} = 23.5\ \text{min}]{}$$

$$^{239}\mathrm{Np} \xrightarrow[\beta^-\ \ t_{1/2} = 2.35\,\text{days}]{}$$

$$^{239}\mathrm{Pu} \xrightarrow[\sigma_{f\ \text{thermal}} = 750b]{} \text{fission}$$

where β^- indicates a beta decay with electron emission and $\sigma_{\text{f thermal}}$ is the fission cross section in barns at a neutron energy of 0.025 eV.

Thorium has 25 isotopes, of which only the non-fissile isotope ^{232}Th is long-lived, with a half-life of 14 billion years. However, in the reaction shown below, ^{232}Th can be transmuted into ^{233}U, a fissile isotope:

$$^{232}\mathrm{Th}(n,\gamma)^{233}\mathrm{Th} \xrightarrow[\beta^- t_{1/2} = 22.3\ \text{min}]{}$$

$$^{233}\mathrm{Pa} \xrightarrow[\beta^-\ \ t_{1/2} = 27.0\ \text{days}]{}$$

$$^{233}\mathrm{U} \xrightarrow[\sigma_{f\ \text{thermal}} = 531\,b]{} \text{fission}$$

The fission energy of ^{233}U is 190 MeV and that of ^{239}Pu is 200 MeV. If 1 kg of thorium were bred into ^{233}U, the fission energy available would be 78.9×10^{12} $J_{thermal}$ (78.9 TJ_{th}). The fission energy in 1 kg of natural uranium, bred to ^{239}Pu, is 80.4 TJ_{th}. Thus thorium and uranium are quite similar in maximum energy content, but uranium is far more important in the near term because ^{235}U is a naturally occurring fissile isotope.

Global Estimates of Overall Uranium and Thorium Resources

Uranium and thorium have two unique characteristics when compared with other fuels. First, their energy is contained in the nucleus, rather than in the chemical bonds between the atoms, as is the case with fossil fuels. Thus, chemical reactions within the earth, due to pressure, high temperatures, or the presence of oxygen, have no effect on the nuclear energy available from uranium or thorium. In contrast, exposure of fossil fuels to the oxygen in the atmosphere or to volcanic activity releases the energy stored in their chemical bonds. The vast majority of the solar energy originally stored in fossil fuels through photosynthesis of the source biomass has been lost in chemical reactions with the atmosphere, groundwater, and lava.

A second, less obvious, characteristic of uranium and thorium is that they are constantly signaling their presence via the products of radioactive decay. Everyone is familiar with pictures of the prospector with a Geiger counter searching for uranium. Gamma rays and beta particles can be detected with a handheld instrument if the uranium ore is at the surface. However, even as little as a meter of overlying soil will shield the gammas and beta particles from the counter. Therefore, any ore deposits more than a meter below the surface will have to be detected through well logs or core samples or via their gravitational or magnetic signatures, rather than through their radiation.

Astrophysical Origins of Uranium

Uranium, thorium, and all other elements heavier than nickel result from the sudden collapse of massive stars as supernovae. The lifetime of stars and the results of these gravity-driven implosions are very dependent on the stars' initial mass. A star having the mass of our sun lasts for about ten billion years but can only produce elements up to iron. A star having ten solar masses lasts for only 10 Ma until it explodes as a supernova, producing all the elements in the periodic table.

The groundbreaking work by Burbidge, Burbidge, Fowler, and Hoyle [6] led to the realization that all of the elements heavier than nickel are the result of less than a minute of tremendous neutrino and neutron fluxes during the collapse and explosion of a supernova [7]. The nuclide distribution as a function of time in a supernova has been simulated [8] and indicates that isotopes with the maximum

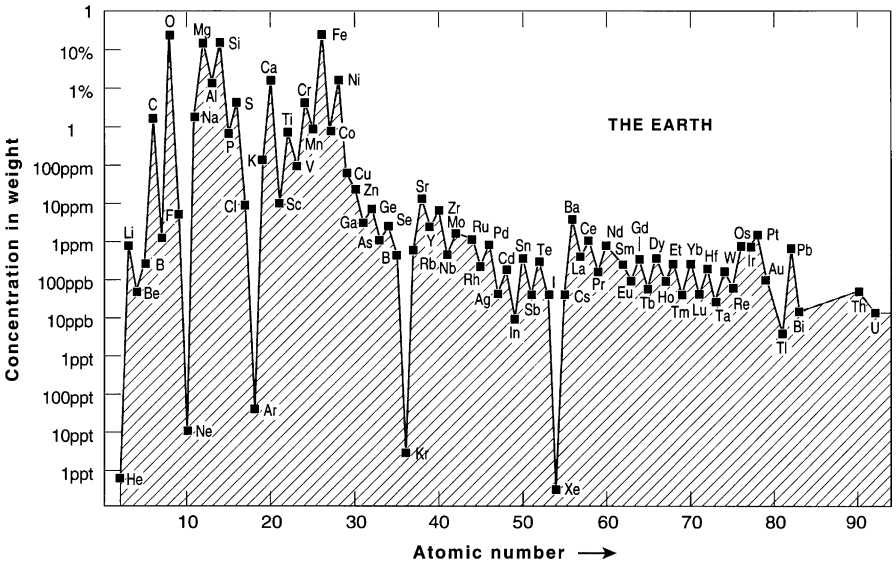

Fig. 18.1 Composition of the bulk silicate Earth

number of neutrons ("the neutron drip edge") form during few seconds of intense activity at the center of the imploding supernova. From this nuclear modeling of a supernova explosion, it can be inferred that uranium and thorium are about seven orders of magnitude below silicon in the composition of the supernova debris – the material from which planets are formed. This is in rough agreement with Bulk Silicate Earth model, shown in Fig. 18.1.

Earlier studies are also in agreement. Urey cites estimates by Goldschmidt of the primordial abundance of 41 weight parts per billion (wppb) for uranium and 106 wppb for thorium. Alpher's theoretical curves and Harrison S. Brown's observed astrophysical data show uranium approximately 6.5 orders of magnitude less abundant than silicon, resulting in a primordial abundances of 57 wppb. Deffeyes, accounting for the decay of uranium since the expansion of the primordial neutron gas, estimates global uranium abundance at 10.5 wppb [9].

Recent work on the physics of supernova collapse offers some insight into the expected global inventories of uranium and thorium. These two elements, and all other elements heavier than nickel, are formed in a few seconds of extremely violent conditions during the collapse and explosion of massive stars. During the last few minutes of such a massive star's evolution, hydrogen, helium, and all of the elements lighter than nickel at the center of the star are depleted through fusion reactions. With no more energy available for continued fusion reactions, the center cannot withstand the outer shells of material, and the matter in the center is compressed to a degenerate state in which matter is broken into the constituent particles, primarily neutrons and neutrinos. The torrent of neutrons from the center of the supernova irradiates the infalling outer layers of stellar material, producing

heavier isotopes at a rate faster than the radioactive decay of those isotopes. The result is the production of isotopes stretching from nickel through uranium and beyond, all saturated with neutrons.

This type of supernova explosion is estimated to occur, somewhere in the universe, at the rate of one per second. Obviously, most such explosions are too distant or masked by dust clouds and are not detected from the earth. Since the beginning of the universe, some interstellar material has gone through multiple cycles of collapse, explosion, dispersal, and accretion into new stars.

The hydrodynamic instabilities of the implosion result in a wide variation in the shapes of the resulting nebulae. Nevertheless, neutron transport and reaction codes have been developed to estimate the distribution of isotopes resulting from a supernova implosion. Wanajo and others [8] have modeled the first few seconds of isotope production and shown that the uranium mass should be about seven orders of magnitude less than that of silicon. Since the chemical and planetary accretion characteristics of silicon, uranium, and thorium are similar, and since the earth is about 10% silicon, one would expect that the overall concentration of uranium in the earth is about 10 wppb. The geoneutrino data from KamLAND and from newer detectors indicate that the global uranium inventory is, in fact, about 10 wppb.

Therefore, based on these astrophysical models, it is fairly clear that the earth taken as uniform body contains about 10 wppb uranium and about 40 wppb thorium. Stated in other terms, the present global inventory is thus 63 Tt (63×10^{12} t) of uranium and approximately 400 Tt of thorium. Although this inventory is a vast amount of both elements, if uranium and thorium had a uniform distribution throughout the earth, as assumed in the cold accretion model, concentrations of uranium and thorium would be far too small to be economically extracted.

Geoneutrino Estimates of Uranium and Thorium

In the last 20 years, however, another decay product of the 4.5 billion year half-life of ^{238}U and the 14.2 billion year half-life of ^{232}Th has been used to estimate the total global inventory of uranium and thorium. These particles, called neutrinos, are extremely difficult to detect and most neutrinos pass completely through the earth without interacting. Thus neutrino detectors are usually a thousand tons in mass and must be located deep underground to avoid unwanted signals caused by cosmic rays.

Neutrinos occur in three types: electron, muon, and tau. Each of the three types has a corresponding antineutrino. Neutrinos originating within the earth, termed *geoneutrinos*, are actually electron antineutrinos primarily resulting from the decay of ^{40}K, ^{238}U, and ^{232}Th. Geoneutrinos provide a means for estimating the total uranium and thorium content of the earth and also may provide limited information on the location of those resources. These elementary particles have been measured over the past decade by massive detectors in Japan, Canada, and Europe in an effort

to differentiate the radiogenic and gravitational components of the total geothermal energy flux through the earth's surface [10]. Neutrino and antineutrino fluxes have also been measured to understand neutrino oscillations, to investigate solar fusion processes, and as a first signal of supernova events. Neutrinos (and antineutrinos) travel close to the speed of light, have a small mass (<2 eV), and lack an electric charge. When an electron antineutrino collides with a proton, the result is a neutron and a positron (i.e., an antielectron). This reaction, known as the neutron inverse β decay, was used in the first detection of the neutrino in the Cowan–Reines experiment of 1956. Following the neutron inverse β decay, the positron reacts with a nearby electron to produce two 511 keV gamma rays. The neutron is absorbed by a hydrogen nucleus, releasing a characteristic 2.2 MeV gamma with a mean delay of ~200 μs. Circuitry in the detector registers a neutrino event through the delayed emission of a 2.2 MeV gamma following two 511 keV gammas.

The KamLAND (the Kamioka Large Antineutrino Detector), in central Japan, consists of a 18 m diameter spherical vessel which in turn contains a 13 m diameter nylon balloon. The balloon contains approximately 1,000 t of a liquid scintillator (mineral oil, benzene, and fluorescent compounds). The volume between the balloon and the spherical vessel contains highly purified oil which shields the balloon from external radiation and provides buoyancy to support the liquid scintillator. About 1,900 photomultiplier tubes are mounted on the inner surface of the spherical vessel. Surrounding the spherical vessel is a water Cherenkov detector which provides additional shielding and acts as a muon veto counter.

The decay chain of ^{238}U into ^{206}Pb results in six antineutrinos, one antineutrino for each beta decay. Similarly, the decay of ^{232}Th in ^{208}Pb results in four antineutrinos [11]. Because the neutron inverse β decay requires an electron antineutrino threshold energy of 1.80 MeV, KamLAND cannot detect ^{40}K antineutrinos, but antineutrinos from both ^{238}U and ^{232}Th are within the range of this instrument.

The overall results of the KamLAND geoneutrino study [12] show that the sum of the global U and Th inventory is approximately 30×10^{16} kg. Since the global Th/U mass ratio is 3.9, the global U inventory is about 6×10^{16} kg or ~10 ppb of the mass of the earth. The geoneutrino signal also indicates that the majority of the uranium is in the upper continental crust (UCC) and that relatively little of the inventory is in the oceanic crust, the mantle, or the core. The partitioning of the uranium among the upper, middle, and lower continental crust and the upper mantle occurs via geochemical processes [13].

Thermal models of the earth point to inevitable melting of the earth soon after its accretion due to gravitation energy and due to radioactive decay of uranium, thorium, and potassium. Because of its large ionic size and heating due to radioactive decay, uranium is transferred into low melting temperature fractions and out of the earth's core and mantle into the crust. These geochemical and geophysical models predict that two thirds of initial 63 Tt of uranium present in the earth are now concentrated in the crust, which constitutes only 0.4% of the earth's total mass. The low uranium and high iron concentrations predicted for the earth's mantle and core have been supported by concentrations in iron meteorites and in mantle issuing

Table 18.1 The main properties of geoneutrinos

Decay	Q (MeV)	$\tau_{½}$ (10^9 year)	E_{max} (MeV)	ε_H (W/kg)	$\epsilon_{\bar{\nu}_e}$ (kg^{-1} s^{-1})
$^{238}U \rightarrow {}^{206}Pb + 8\,{}^4He + 6\,e + 6\,\bar{\nu}_e$	51.7	4.47	3.26	0.95×10^{-4}	7.41×10^7
$^{232}Th \rightarrow {}^{208}Pb + 6\,{}^4He + 4\,e + 4\,\bar{\nu}_e$	42.7	14.0	2.25	0.27×10^{-4}	1.63×10^7
$^{40}K \rightarrow {}^{40}Ca + e + \bar{\nu}_e$	1.32	1.28	1.31	0.36×10^{-8}	2.69×10^4

$\bar{\nu}_e$ denotes electron antineutrinos
where:
Q is the energy release for the overall decay chain
$\tau_{½}$ is the half-life of the parent isotope
E_{max} is the maximum antineutrino energy in the decay chain
ε_H is the heating rate, per kg of the parent isotope
$\epsilon_{\bar{\nu}_e}$ is the electron antineutrino source rate, per kg of the parent isotope

Table 18.2 U, Th, and K global inventories, radiogenic heating, and neutrino luminosities according to the Bulk Silicate Earth (BSE) model

	m (10^{17} kg)	H_R (10^{12} W)	L_ν (10^{24} s^{-1})
U	0.8	7.6	5.9
Th	3.1	8.5	5.0
^{40}K	0.8	3.3	21.6

from oceanic spreading zones (0.1 ppm U), compared with U concentrations in magma and crust in subduction zones, (2 ppm U).

Preliminary results from the newer antineutrino detector Borexino at Gran Sasso in the Apennines [14] generally confirm the KamLAND results but indicate a geoneutrino flux 60% higher. Because of very low radioactive contamination in the materials of construction for Borexino, a signal-to-noise ratio of 50:1 was achieved. This greater sensitivity allowed the Borexino researchers to place an upper bound on the power of any critical fissioning zones in the core at 3 TW, significantly below the indicated global radiogenic heat production of about 18 TW. Collection of geoneutrino data by Borexino is continuing.

Geoneutrino data collected to date indicates that the uranium content of the earth is several orders of magnitude greater than conventional resource estimates. Limited geoneutrino data and an understanding of geochemical processes suggest that most of that uranium content is in the upper continental crust. This data provides some confidence that, with further local exploration or advanced extraction technologies, sufficient uranium could be found for several centuries of expanded nuclear power (Tables 18.1 and 18.2).

The overall results of the KamLAND geoneutrino study [10, 12] show that the sum of the U and Th inventory is 3E17 kg and since the global Th/U mass ratio is 3.9, the global U inventory is 6E16 kg or 10 ppb of the mass of the earth, in agreement with the supernova production ratio with silicon. Further note that the

geoneutrino signal indicates that the majority of the uranium is in the upper continental crust and that relatively little of the inventory is in the oceanic crust. The partitioning of the uranium into the UCC via geochemical process is discussed in the next section.

Mechanisms for the Concentration of Uranium

Unlike other energy resources such as coal or petroleum, the resources of uranium are not fundamentally changed by geological processes. Whereas petroleum might be lost through evaporation or combustion or a natural gas reservoir may vent into the atmosphere, uranium is lost only through radioactive decay or through the relatively rare formation of a natural reactor. Therefore the primordial inventory of uranium, reduced by radioactive decay, remains present somewhere in the earth. The crucial question is "where?"

The natural distribution of elements in the earth's crust is controlled by two major factors. The first is the set of ambient geological fractionating processes that leads to regions of depletion and concentration of the element. The second factor includes the overall geochemical characteristics of the element. Elements that are concentrated by a small number of fractionation processes can be expected to have a multimodal distribution, with a peak in the tonnage versus grade curve for each of the modes of geochemical concentration. For elements having a large number of applicable concentration processes, the peaks overlap and the resulting tonnage versus grade curve takes on a log-normal characteristic. For example, the element chromium, whose distribution at high concentrations is solely governed by fractional crystallization in mafic magmas (i.e., high in magnesium and iron), one would expect a bimodal distribution of concentrations, with one peak at the average crustal abundance and the high concentration peak at the mafic fractionation concentration. On the other hand, most elements, uranium included, can undergo a wide variety of fractionating processes, and deposits would be expected over a wide range of concentrations. In this latter case, the tonnage versus grade distribution would be expected to be log-normal. Bear in mind that geological conditions change over time and therefore the distribution patterns have varied with time.

In considering uranium in particular, it is important to examine the tectonic and igneous processes that have redistributed the uranium within the crust. In the past four billion years, the most important processes are continental accretion and plate tectonics. In the accretion process, crust formed into masses of continental dimensions. In the second, continuing, process, the continental crust and the oceanic crust have taken on quite different characteristics in terms of uranium concentration.

Igneous Processes

Igneous processes begin with the melting of mantle rocks at depths of 60–200 km, followed by the migration of less dense liquids to the surface. The migration of these less dense minerals to the surface is a predominant process in the formation of the continental crust. The extruded liquid forms crust in two general locations, at mid-oceanic ridges, where the upwelling material forms new oceanic crust and in subduction zones, where the oceanic crust plunges back into the mantle, usually passing under the edge of a continent.

The behavior of uranium in igneous processes is dominated by two characteristics of the element. In the +4 oxidation state, the condition expected in the earth's mantle, the U^{+4} ion has an ionic radius of 97×10^{-12} m (picometers, pm) about the same as Na^{+1} ion (97 pm). Other ions common in the core and mantle are significantly smaller in radius: Fe^{+2}, 74 pm; Ni^{+2}, 69 pm, Mg^{+2}, 66 pm; and Al^{+3}, 51 pm. Thus, like sodium and the other large ions, uranium ions selectively enter partial melts within the mantle and are transported to the surface.

The second characteristic of uranium is its radioactivity, serving as a source of heat for melting the mantle and core. Like Th^{+4} (ionic radius 102 pm) and K^{+1}(133 pm), these heat-producing elements are readily fractionated out of the mantle and toward the surface. Deffeyes notes that the earth would be a radically different place if the heat-producing elements had small radii, since the geothermal energy source would then be located deep within the core and the convection currents driving plate tectonics would be much stronger [15].

The rocks forming the oceanic crust at mid-oceanic ridges are characterized by a uniform uranium concentration of about 0.1 wppm. Conversely, the crust formed above subduction zones is characterized by uranium concentrations of about 2 wppm. The wide difference in concentration is due to the differences in the source materials and to the different chemistry. The upwelling mantle at the oceanic ridge has a uranium concentration of about 0.005 wppm, while the subduction zones have as their source material oceanic crust and bits of continental crust, with an average uranium concentration of about 0.1 wppm. The continuous upwelling at the oceanic ridges serves as a mechanism for depleting the core and mantle of uranium and incorporating that uranium in the oceanic crust. The relatively low concentration of uranium in the oceanic crust is augmented with uranium from continental runoff, which subsequently precipitates in the ocean basins. At the subduction zones, the oceanic crust is again subjected to partial melting and the uranium is again fractionated in the melt and transported to the surface.

Average Vertical Distribution of Uranium and Thorium

As a result of the various igneous processes, the average concentration of uranium is highest at the surface of the continental crust and decreases approximately exponentially with depth.

Table 18.3 Sources of heat in the upper continental crust

Isotope	Thermal output
U-238	0.095 mW/kg
Th-232	0.027 mW/kg
K-40	3.6 nW/kg

Table 18.4 Temperature distribution depth parameter

Location	h_r (m)
Sierra Nevada	10,000
Eastern USA	7,500
Norway and Sweden	7,200 ± 700
Eastern Canadian Shield	7,100 ± 1,700
Canadian Appalachians	10,000 ± 2,000
US Appalachians	8,100 ± 1,300

In the other references the depth parameter is denoted as D, rather than h_r

The anticipated variation of uranium concentration with depth is given by the equation $U(z) = U(z = 0)\, e^{(-z/h_r)}$, where z is the depth in m, h_r is the depth parameter (discussed below), and *U(z)* is the concentration at depth z, in wppm. *U(z = 0)* is the average continental crustal abundance of uranium at the surface, 2.76 wppm.

This approximation is based on the presence of heat-producing elements, U-238, Th-232, and K-40, in the continental crust, measurements of the thermal conductivity of the crustal materials, and the linear temperature distribution with depth measured at many locations. The heat produced in the crust is divided about evenly between U-238 and Th-232, since the crustal abundance mass ratio between Th and U is 3.9. K-40 is about four orders of magnitudes lower, although potassium has a crustal abundance of 2.1%, since K-40 is only 117 ppm of natural potassium and the thermal energy output of K-40 is about four orders of magnitude below U-238 and Th-232, as shown by Lachenbruch, below [16] [17] (Table 18.3).

Obviously, this method assumes one-dimensional heat transport and a fairly uniform thermal conductivity, without a significant contribution from flowing fluids. A more recent review by Brady et al. [18] provides more details on the technique.

Several measured values of the depth parameter are listed in Table 18.4. [19].

If a depth parameter of 8,500 m is assumed, based on the above data, then 11% of the crustal uranium inventory would be expected to be within 1,000 m of the surface and 21% within 2,000 m.

Geochemical Beneficiation Processes

Uranium occurs in ores such as uraninite [UO_2, pitchblende], carnotite [$K_2(UO_2)_2V_2O_8{\cdot}3(H_2O)$], autunite [$Ca(UO_2)_2(PO_4){\cdot}11(H_2O)$], uranophane [$Ca(UO_2)_2$

$(HSiO_4)_2{\cdot}5H_2O$), davidite [Ce0.75La0.25Y 0.75U0.25$Ti_{15}Fe_3$ + 5O38 and $La_{0.7}Ce_{0.2}Ca_{0.1}Y_{0.75}$ $U_{0.25}Ti_{15}Fe_3$ + 5O38], torbernite [$Cu(UO_2)_2(PO_4)_2{\cdot}$ $12H_2O$], and other minerals containing U_3O_8 (actually a stable complex oxide of $U_2O_5{\cdot}UO_3$).

The governing characteristic in the geochemical transport of uranium is the fact that uranium is highly soluble in oxidizing environments and essentially insoluble in reducing environments. The change in the earth's atmosphere from a reducing to an oxidizing condition about 1.8 billion years ago is thus responsible for a fundamental change in the dominant processes in uranium transport. In the earlier age, igneous processes and fractionation of uranium in partial melts due to its large ionic size were dominant. In the last 1.8 billion years the transport of uranium by means of groundwater oxygenated at the surface has been dominant.

Thus, in the period more than 1.8 billion years ago, uranium was primarily concentrated in placer deposits as a chemically inert and physically dense phase. Because of the low solubility of uranium in reducing environments, rivers, lakes, groundwater, and thus the sea contained very low uranium concentrations. The placer deposits at Elliott Lake, Canada and at Witwatersrand, South Africa are typical of the deposits formed during this period.

With the dominance of photosynthesis in the last 1.8 billion years, the atmospheric and groundwater conditions have been oxidizing and uranium minerals have been highly soluble in the sedimentary weathering cycle. Placer deposits no longer formed and, in fact, began to dissolve. The uranium content of rivers, lakes, and groundwater increased and gradually, the uranium concentration in the oceans also increased. Nevertheless, the uranium concentration remained well below saturation.

In a few isolated locations, however, oxidation of organic-rich beds by groundwater led to locally reducing conditions. In these locations, the uranium ions or their complexes would reach supersaturation and re-precipitate. An important example of this re-precipitation is in the Mesozoic sandstones of the Colorado Plateau. The uranium ores are found in organic-rich zones where the oxygen in groundwater was removed by carbon-rich debris. Precipitation of uranium has also occurred where restricted circulation in the oceans and organic-rich sediments led to anoxic conditions. Good examples are the black Chatanooga Shale and the phosphorite shale of the Phosphoria Formation [9].

Specific Deposit Types

Before the discovery of the McArthur River deposit, the highest grade uranium ores were obtained from igneous sedimentary deposits such as Great Bear Lake in Canada, Joachimsthal in the Czech Republic, and Katanga in the Congo. The deposits at Oklo in the Gabon Republic in Africa were of high enough concentration and the uranium, 1.7 billion years ago, contained 3% ^{235}U rather than the present 0.711% such that several critical natural reactors occurred in the deposit.

The reactor zones released about 15,000 MW-years of fission energy over the course of about 250,000 years. These deposits were formed by the movement of hot water through fractures in blocks of rock heated by their own uranium and thorium content.

Precambrian sandstones overlie much older Precambrian granites and metamorphic rocks. At the interface, there is a discontinuity in the age of the rocks. This type of discontinuity is termed an unconformity. Unconformity deposits, such as those in Saskatchewan and northern Australia occur where uranium from the sandstone, has formed into veins in the open spaces of the interface, and has been heated to temperatures of several hundred degrees Celsius.

Roll-Front Deposits

As mentioned earlier, uranium oxide precipitates when the solution enters a reducing environment. The uranium oxide can be redissolved in situ by oxygenated leach solutions. In sandstone deposits, the uranium minerals have been deposited in the interstices between the sand grains. The deposits are often moving very slowly through the sandstone because of the flow of groundwater, much like the movement of a front through a liquid chromatography column. Oxygenated water from the surface enters the sandstone where reducing agents, such as sulfides or organic matter, are located in the interstitial spaces. The organic carbon in one pore volume of sandstone can remove all the oxygen dissolved in 50,000 pore volumes of oxygenated groundwater.

Therefore, the front between the oxygenated groundwater and oxygen-free groundwater moves slowly through the sandstone. Uranium dissolved at the surface and uranium dissolved from the sandstone by the oxygenated groundwater is swept along and precipitated at the front. Upstream of the front the uranium is present in the groundwater as the soluble hexavalent uranyl carbonate complex. As the oxygen is removed from the groundwater at the front, the soluble hexavalent uranium is reduced to the insoluble quadrivalent state.

The quadrivalent uranium precipitates in the form of the mineral uraninite (UO_2). Thus the location of ore bodies is often associated with deposits of carbonaceous materials where the carbon, in much larger quantities compared with the uranium, has removed the oxygen from the groundwater.

Based on the various modes for the formation of uranium ore bodies, reviewing the large body of prior research, Deffeyes and MacGregor estimated the uranium content of the various crustal regimes in a report for the USDOE in 1978 [9].

The distribution of mass versus grade for the various types of uranium deposits is shown in Fig. 18.2 with additional data [9, 15]. The three gray bars on the left (grade $>$1,000 ppm U) indicate deposits of the type now mined for uranium alone. The expected log-normal distribution is shown and the mass and grade of two Canadian mines discovered since 1978 are also indicated: (1) the McArthur River deposit, 137,000 t U of proven reserves averaging 18 wt% U and (2) the Cigar Lake deposit,

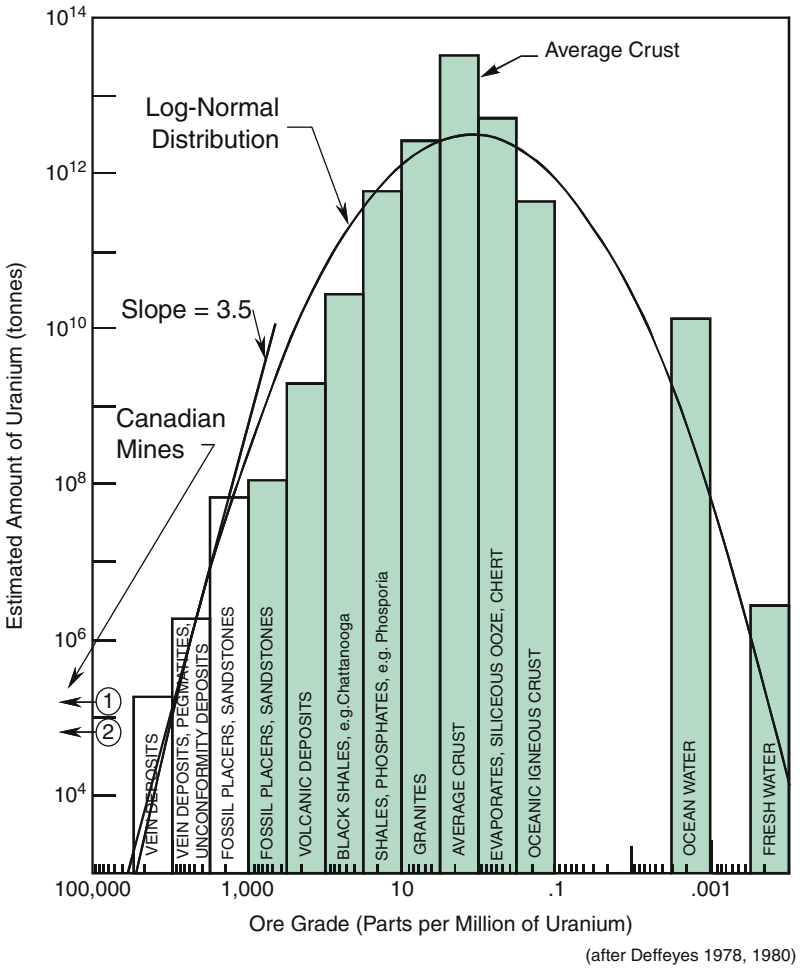

Fig. 18.2 Distribution of uranium in the Earth's crust

90,000 t U at an average grade of 17 wt% U. Other known larger, but lower grade deposits, such as Olympic Dam in Australia, have not been shown.

Present mining activities are recovering uranium at market prices of $150/kg from ores containing 0.027–20% U_3O_8. Given the log-normal distribution and the known quantities of the various uranium mineralizations, a tenfold increase in the price of uranium (and thus a tenfold decrease in economically viable ore grade) would result in a 300-fold increase in the amount of uranium available. Equivalently, the World Nuclear Association (formerly the Uranium Institute) estimates that a doubling of uranium prices would result in a tenfold increase in supply [5] (WNA 2010).

'The slope of the log-normal curve at presently mined grades is also shown in Fig. 18.2. This slope, about +3.5, indicates that for a doubling of the cost of mining

(i.e., mining ore at half the present concentration), the economically available resources of uranium would increase by more than an order of magnitude $(2^{3.5} \approx 11)$. This estimate presumes a continuation of present mining techniques and does not consider the increased using of in situ leaching and recovery of uranium as a by-product in gold, copper, and phosphate mining.

Unconventional Resources

Existing Enrichment Tails

Another potential source of uranium is the re-enrichment of depleted uranium by using today's overcapacity of enrichment. Because of low price of natural uranium in recent years, many enrichment plants have been operating with tails assays of up to 0.3% ^{235}U. The 1.18 million tons of depleted uranium currently stored at enrichment plants could therefore supplant a few hundred thousand tons of natural uranium if demand required. The inventory of depleted uranium is expected to increase by about 51,400 t U/year though at least 2010. The enrichment capacity in 2010 was reported to be 57 MWSU/year compared with an annual demand of 49 MWSU/year. The present spare capacity in enrichment plants in the world, around 8 MSWU/year, theoretically represents an equivalent of around 3,000 tons/year of natural uranium if this spare capacity was utilized for enrichment of depleted uranium with an assay of 0.3% and a new tails assay of 0.1%.

The economics of re-enrichment depend on the ^{235}U assay of the depleted uranium and the relationship between the price of uranium and the cost of enrichment services. A tails assay of above 0.3% is preferable if re-enrichment of depleted uranium is to be considered a possibility. Re-enrichment of depleted uranium for the production of low-enriched uranium (LEU) in the Russian Federation has taken place for several years in times of excess enrichment capacity. However, decreasing amounts of excess enrichment capacity makes re-enrichment a marginal source of light water reactor fuel. On the other hand, the eventual use of enrichment tails as breeding blankets for fast reactors, as will be discussed shortly, represents a large long-term source of fuel.

Gold and Phosphate Tailings

In addition to the discovery of new resources through increased exploration, improvements in mining technology are also lowering the cost of previously high-cost deposits. In particular, in situ leaching (ISL) is of growing significance and could be applied to existing gold and phosphates tailings piles. The resource base of 16.2 million tons U does not include uranium in gold and phosphate tailings. The phosphate deposits are estimated at 22 million t U.

Uranium from Seawater

The recovery of uranium from seawater places an upper limit on the cost of uranium. Uranium is dissolved in seawater at 3 mg/m^3 (3 wppb) and represents a well-known resource of 4.2 billion tons, 250 times the known land-based resource. The uranium content of the oceans is relatively constant and large-scale extraction can be done without local depletion of the resource. Since only about 3% of global population lives in landlocked countries, extraction of uranium from seawater is truly the bounding cost for uranium.

New Technologies for Uranium Extraction

The current prices for uranium provide little motivation for the development of new extraction technologies. However, regulations to minimize the impact of mining on the environment and radiation exposure to workers have led to the use of technologies where uranium is extracted in situ or where ores previously mined for another element are processed for uranium extraction. In addition, the technologies described above for the extraction of uranium from seawater could have a major impact in minimizing environmental impact and radiation exposure.

In Situ Leaching

During conventional mining, the rock of the ore body is removed from the ground, transported to a mill, and treated to remove the minerals of economic value. The opening of the mine, the transport of the ore, the milling and the disposal of remaining treated rock can create severe environmental impacts. In situ leaching (ISL), sometimes known as solution mining, involves the use of liquids to dissolve the desired elements from the ore body without removing it from the ground. The liquid is pumped through the ore body and returned to the surface, where the desired elements are removed from the solution by precipitation, by electrochemistry, or other means. The leaching liquid is then returned to the ore body and the process is repeated. ISL eliminates the need to remove large quantities of ore from ground and to transport it to the mill, thus minimizing surface disturbance. ISL also eliminates the need to dispose of the tailings or waste rock. However, for ISL to be effective, the ore body must be permeable to the flow of the leaching liquid. Furthermore, the ISL site must be located so as not to contaminate ground water away from the ore body.

Today, because of its reduced surface impact and lower cost, ISL is used for 85% of US uranium production. Most of the operations in Wyoming, Nebraska, and Texas are less than 10 years old. Worldwide, about 16% of world uranium production uses ISL, including all the production in Uzbekistan and Kazakhstan.

ISL can be used to extract uranium from deposits below the water table in permeable sand or sandstone, provided that the deposit is confined above and below by impermeable strata. Suitable candidates are often roll-front deposits as described earlier. The uranium mineral are usually uranium oxide or uranium silicate coatings on the individual sand grains. The ISL process replicates, in a few months, the conditions that led to the formation of the roll-front deposit in the sandstone initially.

There are two types of ISL, depending on the chemistry of the deposit and groundwater. When the ore body is limestone or gypsum, i.e., containing significant amounts of calcium, then an alkaline leaching agent such as sodium bicarbonate and CO_2 must be used. Otherwise an acid leaching agent, such as weak sulfuric acid plus oxygen at a pH of 2.5–2.8 (about the same as vinegar) is preferred. ISL in Australia is primarily acid, while ISL in the USA is primarily alkaline.

Generally the uranium is extracted by progressively drilling wells into the deposit on a rectangular grid with ~30-m spacing. The leaching fluid is pumped into four wells surrounding a central extraction well, into which a submersible pump has been lowered. The wells are cased to assure that the fluids do not enter strata above the deposit. In the USA the production life of an individual alkaline ISL well is typically 6–10 months. The most successful operations have extracted 80% of the uranium from the ore. Production life is often limited when the sandstone is plugged by mobilized clay and silt. Sometimes the blockages can be dislodged by reversing the flow through the field or by increasing the injection pressure.

The uranium is recovered from the extracted solution in an ion exchange or solvent extraction process. Solvent extraction is preferred if the groundwater is saline, while ion exchanges is most effective if the chloride content is below 3,000 ppm. With alkaline leaching, ion exchange is effective until the total dissolved solids reach 3,000 ppm. The uranium is then stripped from the resin or solution for further processing [20].

Before the process solution is reinjected, it is reoxygenated or recharged with sulfuric acid, for alkaline or acidic processes respectively. About 1% of the process solution is bled off to maintain a pressure gradient toward the wellfield. The pressure gradient ensures that groundwater from any surrounding aquifer flows into the wellfield and that ISL mining solutions does not enter the aquifer.

Recovery of Uranium from Seawater

The recovery of uranium from seawater is highly speculative and may never prove to be economic. One cubic meter of seawater contains 3 mg of natural uranium,

which can deliver 244 MJ_{th} in a breeder or about 2.5 MJ_{th} in a present day LWR. Simple calculations show that the pumping energy needed in an extraction plant could easily consume all the energy available, particularly in the LWR case. Thus seawater extraction conceptual designs relying on ion exchange or adsorption have utilized ocean currents or wave action to move the seawater past the uranium-collecting surfaces.

However, the magnitude of the seawater resource places an upper limit on the cost of uranium for several reasons. First, seawater is available to nearly all countries of the world at virtually the same uranium concentration and without local depletion due to the extraction of uranium. Secondly, because no group of countries can form a cartel over the uranium supply if seawater extraction is practiced, the price of uranium is unlikely to be driven artificially high through market manipulation. Furthermore, the only present limitation on the extraction of uranium from seawater is knowledge of the technology and resins. Thus one would expect that, if conventional sources of uranium become limiting, a healthy competition in research and development would drive down the cost of extraction.

Uranium recovery from seawater has been studied in Japan for a very long term or to face a very strong development of fission energy. In a laboratory scale experiment performed by the Japan Atomic Energy Agency (JAEA) where uranium is trapped by an amidoxime adsorbent which has been prepared on nonwoven polyethylene material with the aid of radiation-induced cografting. This experiment, 7 km offshore from Sekine-Hama in Aomori Prefecture, Japan, produced more than 1 kg of U on 350 kg of nonwoven fabric during a total submersion time of 240 days [21]. However, at this stage of the study, it is difficult to predict the practical application of uranium recovery from seawater. An economic assessment has been reported indicating a possible cost for this uranium process in a 1,000-t U/year commercial plant of approximately $600/kgU [22].

Impact of Uranium Scarcity and Higher Extraction Costs

Table 18.5 shows the approximate impact of increases in the price of natural uranium on the cost of electricity from a light water reactor. In this set of calculations, the cost of natural uranium is set at $140/kg U (approx. average price of domestic U to US utilities, 2011), $500/kg U, representing an optimistic cost of extraction from seawater and $1,000/kg U, representing a more pessimistic (or perhaps more realistic) cost for extraction from seawater. Two burnups are shown for each uranium price, 45 MW-day (thermal) per kg of initial uranium (MW-day/kg) and 60 MW-day/kg. The specific power of the fuel remains constant at 37.9 kWth/kg of initial uranium, as does the interest charged on the fuel during the fuel cycle. In the cases with higher cost uranium, the tails assay ("Tails U-235 content") to optimize the balance between raw materials and enrichment costs. As shown in the last two lines of the table, an increase in the cost of natural uranium from $140/kg U to $1,000/kg U results in an increase in the cost of electricity of

Table 18.5 Impact of uranium costs on the cost of electricity

Impact of uranium costs on the cost of electricity							
			Uranium from unconventional sources				
	Current uranium prices		Optimistic: $500/kg		Pessimistic: $1,000/kg		
	UO_2 fuel 45 MWd/kg	UO_2 fuel 60 MWd/kg	UO_2 fuel 45 MWd/kg	UO_2 fuel 60 MWd/kg	UO_2 fuel 45 MWd/kg	UO_2 fuel 60 MWd/kg	Units
Specific power	37.9	37.9	37.9	37.9	37.9	37.9	kWth/kg
Cycle parameters							
Total cycle length	3.6	4.8	3.6	4.8	3.6	4.8	years
Capacity factor	90%	90%	90%	90%	90%	90%	
Effective full power days	1183	1578	1183	1578	1183	1578	efpd
Burnup	45	60	45	60	45	60	MWd/kg ihm
Feed U-235 content	0.711%	0.711%	0.711%	0.711%	0.711%	0.711%	wt%
Product U-235 enrichment	4.00%	5.34%	4.00%	5.34%	4.00%	5.34%	wt%
Tails U-235 content	0.25%	0.25%	0.20%	0.20%	0.10%	0.10%	wt%
Separative work	5.874	8.692	6.546	9.636	8.953	13.020	kg-SWU/kg fuel
Natural uranium	8.089	10.964	7.439	10.050	6.385	8.569	kg/kg fuel
	0.180	0.183	0.166	0.168	0.142	0.143	kg/MWd
Rates							
Interest rate	5.0%	5.0%	5.0%	5.0%	5.0%	5.0%	/year
Natural uranium	$140	$140	$500	$500	$1,000	$1,000	/kg U
Conversion U3O8 to UF6	$54	$54	$193	$193	$385	$385	/lb U3O8
	$11	$11	$11	$11	$11	$11	/kg natural U
Separative work	$150	$150	$150	$150	$150	$150	/kg-SWU
Costs							
Natural uranium	$1,132	$1,535	$3,719	$5,025	$6,385	$8,569	/kg fuel

(continued)

Table 18.5 (continued)

Impact of uranium costs on the cost of electricity							
			Uranium from unconventional sources				
	Current uranium prices		Optimistic: $500/kg		Pessimistic: $1,000/kg		
	UO_2 fuel 45 MWd/kg	UO_2 fuel 60 MWd/kg	UO_2 fuel 45 MWd/kg	UO_2 fuel 60 MWd/kg	UO_2 fuel 45 MWd/kg	UO_2 fuel 60 MWd/kg	Units
Separative work	$881	$1,304	$982	$1,445	$1,343	$1,953	/kg fuel
Conversion	$89	$121	$82	$111	$70	$94	/kg fuel
Fabrication	$500	$500	$500	$500	$500	$500	/kg fuel
Total cost	$2,602	$3,459	$5,283	$7,081	$8,298	$11,116	/kg fuel
Interest during use	$234	$415	$475	$850	$747	$1,334	/kg fuel
Total fuel cost	$2,837	$3,874	$5,758	$7,931	$9,045	$12,450	/kg fuel
	$63.19	$64.73	$128.27	$132.50	$201.48	$208.00	/MWth-day
	$0.772	$0.790	$1.566	$1.618	$2.460	$2.540	/million BTU
	$7.81	$8.00	$15.86	$16.38	$24.91	$25.72	/MWe-h
COE increase due to high uranium prices			$8.05	$8.38	$16.91	$17.71	/MWe-h
			0.8	0.84	1.69	1.77	cents/kWe-h

about $0.018/kW-h. For comparison, an increase in the prices of natural gas of $2.80 per million BTU, as has occurred five times since 2005, also results in an increase in the cost of electricity of $0.018/kW-h.

Uranium Compared with Future Energy Needs

A simple calculation is needed to place the magnitude of current uranium mining in perspective. If it is assumed that the world population reaches a steady-state level of 10 billion and each of those people consumes energy at the average rate of a US resident in 2011, then the total annual world consumption of energy would be about 3.7×10^{21} J_{th}. While that high rate of consumption would probably not be sustainable for a variety of other reasons, the required natural uranium input to a system of fast reactors to produce 3.7×10^{21} J_{th} would be about 45,000 t U. Average worldwide uranium usage, from both mining and the downblending of HEU, is now about 59,000 t U/year [4].

The Need for Fast Reactors

The early development of fast breeder reactors and of thermal breeder reactors using thorium was driven in part by the apparent global scarcity of fissile isotopes to fuel a rapidly growing set of nuclear reactors. Slow growth in nuclear power and large discoveries of natural uranium in a few regions of the world have reduced the global urgency for breeding more fissile material. In those regions of the world lacking known uranium resources, particularly Europe and Japan, there has been continuing interest in the development of sodium-cooled fast breeder reactors. Such reactors reduce the need for natural uranium by a factor of ~50, compared with light water reactors and thus the cost and availability of natural uranium is a much smaller consideration.

However, beyond the breeding of fissile isotopes, the use of a fast neutron spectrum offers unique capabilities for the consumption of the long-lived actinides, particularly plutonium, neptunium, americium, and curium.

In the long term, the capability of a fast reactor to make use of both ^{238}U and ^{235}U will be critical in meeting future energy needs. However, in the next century, fast reactors will be crucial for the management of actinides and the reduction of the long-term radiotoxicity of the nuclear fuel cycle by at least two orders of magnitude.

Table 18.6 Comparison with fossil reserves

Coal		909	Billion tons
	=	2.01E + 22	Jth
	=	19,089	Quadrillion BTU (quad)
Petroleum		1340	Billion barrels
	=	8.20E + 21	Jth
	=	7,772	Quad
Natural gas		6261	Trillion cubic feet
	=	6.84E + 21	Jth
		6,480	Quad
Total fossil reserves		3.52E + 22	Jth
	=	33,341	Quad
Uranium		5.404	Million t natural U
	+	1.2	Million t depleted U
	=	2.33E + 21	Jth in LWRs
	=	2211	Quad in LWRs
	=	5.36E + 23	Jth in fast reactors
	=	508,000	Quad in fast reactors

Comparison of Fossil Fuel and Uranium Reserves

It is interesting to compare the cited uranium known reserves and the inventory of depleted uranium with the estimated reserves of coal, oil, and natural gas. In Table 18.6, the reserves of fossil fuels and uranium are compared on the basis of known, economically recoverable reserves.

Fossil fuel reserves are those of the World Energy Council, the *Oil & Gas Journal*, and *World Oil* [23]. In the use of Table 18.6, the caveat cited above applies. Resources of both fossil fuels and of uranium are undoubtedly much larger than the reserves cited. Nevertheless, it is noteworthy that the uranium resources are energetically equivalent to about 20% of natural gas or oil resources, even with the use of LWRs only. The 1.2 million tons of depleted uranium currently in storage itself represents an energy source larger than the fossil reserves if used in a fast reactor.

Future Directions

Uranium is ubiquitous in the continental crust and concentrated in economically recoverable deposits by several relatively well-understood processes. Today uranium is being mined from the richest and most convenient of the deposits though little exploration has taken place in the last 20 years. Uranium and thorium are often being extracted as by-products of mining for other elements. It is likely that other similarly rich deposits exist in relatively unexplored regions of Asia and Africa.

Prices in the present uranium market are dominated by large discoveries in the last 20 years and by the conversion of military HEU to civilian purposes.

The continued use of nuclear energy and the end of downblending can be expected to raise uranium prices, encourage exploration, and return the uranium to a slightly higher-priced equilibrium.

However, because of the wide range of igneous and geochemical processes that are responsible for the formation of uranium deposits, it can be expected that uranium will be found in significant quantities with renewed exploration.

Emerging technologies for the extraction of uranium, particular in situ leaching, will make resources in sandstone and shale economically recoverable and minimize the surface disruption due to open pit mining and the occupational radiation exposures of underground mining.

In more distant future, the extraction of uranium from seawater will make this fuel available to virtually every nation. While extraction from seawater is likely to be five to ten times more expensive than uranium is today, the overall increase in the cost of electricity or other energy products would be minimal.

Therefore, the need for fast reactors in the near term, with a global view in mind, is not driven by a scarcity of uranium but rather by a need to effectively manage the long-lived actinides in spent fuel. A fast neutron spectrum is uniquely capable of fissioning the higher actinides and reducing the long-term radiotoxicity and volume of the nuclear fuel cycle. Likewise, although thorium is more abundant than uranium, the primary use of thorium will probably not be for the breeding of ^{233}U, but rather as a host material for the transmutation of the higher actinides in fast neutron spectrum reactors.

There are many challenges in the development of safe, proliferation-resistant, and economical reactors and fuel cycles. Fortunately, the uranium and thorium resources do not appear to be a near-term limitation.

Bibliography

1. Bates RL, Jackson JA, American Geological Institute (eds) (1984) Dictionary of geological terms, 3rd edn. Anchor Books, New York
2. Benedict M, Pigford TH, Levi HW (1981) Nuclear chemical engineering. McGraw-Hill, New York
3. NRC Glossary (2011) Yellowcake. http://www.nrc.gov/reading-rm/basic-ref/glossary/yellowcake.html. Updated 27 May 2011
4. OECD Nuclear Energy Agency, International Atomic Energy Agency (2010) Uranium 2009: resources, production and demand: a joint report. OECD, Paris
5. World Nuclear Association (2010) Supply of uranium, Dec 2010. www.world-nuclear.org/info/inf75.html
6. Burbidge EM, Burbidge GR, Fowler WA, Hoyle F (1957) Synthesis of the elements in stars. Rev Mod Phys 29(4):547
7. Burrows A (2000) Supernova explosions in the Universe. Nature 403:727–733, 17 Feb 2000
8. Wanajo S et al (2003) The r-process in supernova explosions from the collapse of O-Ne-Mg cores. Astrophys J 593:968–979, 20 Aug 2003
9. Deffeyes KS, MacGregor ID (1978) Uranium distribution in mined deposits and in the Earth's crust: final report. GJBX–1(79). Dept of Geological and Geophysical Sciences, Princeton University, Princeton. Prepared for the USDOE, Grand Junction Office, Aug 1978

10. Araki T et al (2005) Experimental investigation of geologically produced antineutrinos with KamLAND. Nature 436:499–503, 28 Jul 2005
11. Fiorentini G, Lissia M, Mantovani F, Vannucci R (2004) Geo-Neutrinos: a short review. arXiv: hep-ph/0409152v1, 14 Sep 2004
12. Enomoto S, Ohtani E, Inoue K, Suzuki A (2005) Neutrino geophysics with KamLAND and future prospects. arxiv.org/ftp/hep-ph/papers/0508/0508049.pdf
13. Herring JS (2004) Uranium and thorium resources. In: Cleveland CJ (ed) The encyclopedia of energy. Academic, Amsterdam/Boston
14. Borexino Collaboration (2010) Observation of geo-neutrinos. Phys Lett B 687:299–304
15. Deffeyes KS, MacGregor ID (1980) World uranium resources. Sci Am 242(1):66–76
16. Lachenbruch AH (1968) Preliminary geothermal model of the Sierra Nevada. J Geophys Res 73(22):6977–6989, 15 Nov 1968
17. Lachenbruch AH (1970) Crustal temperature and heat production: implications of the linear heat-flow relation. J Geophys Res 75(17):3291–3300, 10 June 1970
18. Brady RJ, Ducea MN, Kidder SB, Saleeby JB (2006) The distribution of radiogenic heat production as a function of depth in the Sierra Nevada Batholith, California. Lithos 86:229–244
19. Schubert G, Turcotte DL, Olson P (2001) Mantle convection in the Earth and planets. Cambridge University Press, Cambridge/New York, p 146
20. World Nuclear Association (2010) In situ leach (ISL) mining of uranium. http://www.world-nuclear.org/info/inf27.html. Updated Mar 2010
21. Seko N et al (2003) Aquaculture of uranium in seawater by fabric-adsorbent submerged system. Nucl Technol 144:274–278
22. Joint Nuclear Energy Action Plan, Fuel Cycle Technology Working Group (2010) Uranium extraction from seawater, 1st information exchange meeting. Lawrence Berkeley National Laboratory, Berkeley, Meeting record, 24–25 June 2010
23. EIA (2010) Annual energy review 2009, DOE/EIA-0384(2009). Energy Information Administration, US Department of Energy, Washington, DC, Aug 2010

Chapter 19
Nuclear Safeguards and Proliferation of Nuclear Weapons Materials

Michael C. Baker

Glossary

Calorimetry	Calorimetry is a nondestructive assay technique for determining the thermal power output of heat-producing nuclear materials. Calorimeter systems are used to determine the power output (Watts) of various radionuclides over a broad range of power levels and sample types (Pu, highly enriched uranium, and Tritium).
Destructive assay	Destructive Assay (DA) aims at the measurement of the nuclear material content, the isotopic composition, or other chemical properties of a sample. The analysis introduces a significant change to the physical form of the test sample.
Detection time	The maximum time that may elapse between diversion of a given amount of nuclear material and detection of that diversion by a safeguards authority.
Direct-use material	Nuclear material that can be used for the manufacture of nuclear explosive devices without transmutation or further enrichment. It includes plutonium containing less than 80% ^{238}Pu, highly-enriched uranium, and ^{233}U.
Diversion	The undeclared removal of nuclear material from a safeguarded facility or the use of a safeguarded facility for the production or processing of undeclared nuclear material.

This chapter was originally published as part of the Encyclopedia of Sustainability Science and Technology edited by Robert A. Meyers. DOI:10.1007/978-1-4419-0851-3

M.C. Baker (✉)
Advanced Nuclear Technology Group, Nuclear Nonproliferation Division, Los Alamos National Laboratory, Los Alamos, NM 87545, USA
e-mail: mcbaker@lanl.gov

N. Tsoulfanidis (ed.), *Nuclear Energy: Selected Entries from the Encyclopedia of Sustainability Science and Technology*, DOI 10.1007/978-1-4614-5716-9_19,

Dual-use technology	Technology that can be used for both military and peaceful purposes.
Highly enriched uranium (HEU)	Uranium containing 20% or more of the isotope uranium-235.
Holdup	The amount of nuclear material remaining in process equipment and facilities after the in-process material, stored materials, and product have been removed.
Nondestructive assay	Nondestructive Assay (NDA) techniques allow analysis of a sample in its own physical/chemical form without any modification of its properties and characteristics. The most common NDA techniques applied in nuclear safeguards include gamma spectroscopy, neutron counting, and calorimetry.
Nuclear material (NM)	Any source or special fissionable material.
Safeguards	An integrated, layered system of physical protection, material accounting, and material control measures designed to deter, prevent, detect, and respond to unauthorized possession, use, or sabotage of nuclear materials.
Significant quantity (SQ)	The approximate amount of nuclear material for which the possibility of manufacturing a nuclear explosive device cannot be excluded. The International Atomic Energy Agency uses 8 kg of plutonium, 25 kg of ^{235}U in highly enriched uranium, and 75 kg of ^{235}U in low enriched or natural uranium.
Source material	Uranium containing the mixture of isotopes occurring in nature; uranium depleted in the isotope 235; thorium; or ore concentrate.
Special fissionable material	Plutonium-239; uranium-233; uranium enriched in the isotopes 235 or 233; and any material containing one or more of the foregoing; and such other fissionable material as the International Atomic Energy Agency Board of Governors shall from time to time determine; but the term "special fissionable material" does not include source material.
Special nuclear material (SNM)	Plutonium, uranium-233, uranium enriched in the isotope 235, and any other material which, pursuant to Section 51 of the United States Atomic Energy Act of 1954, as amended, has been determined to be special nuclear material, but does not include source material; it also includes any material artificially enriched by any of the foregoing, not including source material.

Definition of the Subject

Nuclear technology, by its very nature, may be used for peaceful or harmful ends. From its birth, efforts have existed to control access to, as well as the spread of, nuclear technology for destructive purposes, while at the same time attempting to provide access to its multitude of beneficial applications. Nuclear safeguards refers to the system of legal, institutional, and technical mechanisms used to control the use of nuclear materials, detect nuclear material misuse, and if the material is misused, to provide domestic and international responses in a timely fashion. Proliferation refers to the spread of weapons usable or direct-use materials, nuclear weapons technology, and the knowledge and skills necessary for the design and manufacture of such weapons. Nonproliferation policy and technology, including nuclear safeguards, has traditionally been centered on the spread between nation states. In the past decade, that focus has broadened to include the spread of materials, technology, and knowledge to criminal and terrorist entities. Nuclear safeguards must be viewed as a multilayered system, no single layer being self-sufficient, which as a whole, provides deterrence, detection, and response to theft, diversion, or misuse of nuclear material and nuclear weapons knowledge and skills.

Introduction: Historical Development of Nuclear Safeguards and Nonproliferation Policy

Before the end of World War II, diplomats and scientists familiar with nuclear weapons technology and its early development during the war were struggling with how to control the technology while sharing its benefits. Early efforts were largely focused on international control and the development of an international authority for management of the control regime and nuclear materials. In June 1946, following the formation of the United Nations Atomic Energy Commission (UNAEC) in January, the US representative, Bernard Baruch, proposed a plan for such an international control regime. The Soviet Union and other countries opposed the significant transfer of state authority to an international body, as would be required, and the Baruch plan quickly came to pass. However, it did provide the conceptual framework and foundation for subsequent discussions between nation states.

By mid 1953, three nations (USA, United Kingdom, and Soviet Union) had conducted nuclear tests, Dwight Eisenhower had been elected President of the USA, and Joseph Stalin had died. These events set the stage for President Eisenhower's address to the United Nations on December 8, 1953. This address outlined the President's Atoms for Peace initiative, which included the creation of an international agency responsible for the peaceful expansion of nuclear technology and the control of nuclear materials that in accordance with the President's plan would be contributed by nation states. The President's initiative also called for states receiving assistance with the peaceful application of nuclear technology to

allow inspections that would ensure that the technology and materials were not used for military purposes. The President's speech was the genesis of the International Atomic Energy Agency (IAEA).

In 1956, 81 nations unanimously approved the charter of the IAEA. At the same time, international cooperation related to the peaceful application of nuclear technology was rapidly expanding. By the end of 1959, the USA had cooperative bilateral agreements with 42 countries for collaborative nuclear technology development. Within the next decade, the Soviet Union would have similar agreements with another 26 countries. In most cases, both the USA and Soviet Union included at least a minimal acknowledgement of the dual-use capabilities of the nuclear technologies to be shared. The Soviet cooperative agreements typically required the return of spent nuclear fuel to the Soviet Union as a nuclear material control measure, as well as a pledge to use the material only for peaceful purposes. Most of the US agreements foresaw the need for nuclear safeguards to be applied by the USA that would eventually be turned over to the IAEA. The safeguards experience gained as a result of these bilateral agreements, as well as that obtained following the establishment of Euratom safeguards by the European community in 1957, provided a useful experience base and context for the establishment of specific IAEA safeguards agreements and protocols. In 1959, IAEA safeguards were applied for the first time at the Japanese JRR-3 research reactor running on natural uranium fuel from Canada. [1]

The political history of the early 1960s included France and China joining the club of countries that had conducted nuclear tests and the Cuban Missile Crisis in 1962. This later event, one of the major confrontations of the Cold War, is the closest the world has come to a nuclear war. During the crisis, US armed forces were at their highest state of readiness and Soviet commanders were prepared to use nuclear weapons to defend Cuba against an invasion [2]. As a result, both superpowers came to the realization that greater cooperation on nuclear arms and nuclear safeguards were necessary for their mutual national security and that of their allies. This recognition and associated efforts to seek common ground were also seen in other countries. For example, in 1967, the Treaty for the Prohibition of Nuclear Weapons in Latin America was signed. By 1968, negotiations regarding the Treaty on the Non-Proliferation of Nuclear Weapons (NPT) were well underway. Although the idea of such a treaty had been proposed ten years earlier by Ireland, the NPT was not opened for signature until 1970. This marked a major milestone in the evolution of nonproliferation policy and nuclear safeguards. One of the significant requirements that resulted from the NPT is that nonnuclear weapons states place all of their peaceful nuclear programs under IAEA safeguards. As of 2007, the NPT had been ratified by 189 nations.

After the NPT had established a legal framework for international safeguards in 1970, the next twenty years saw the rapid development of both destructive and nondestructive measurement technology in support of nuclear safeguards, as well as the continued development of procedures and protocols used for international inspections. Formal training programs were established in multiple countries, as well as by the IAEA, to train and develop a cadre of professional safeguards inspectors. Some would argue that safeguards programs, personnel, and international policy had reached a state of maturity by the mid 1980s. However, in 1991,

the international community was shocked with the revelation of a clandestine nuclear weapons program in Iraq. This program had developed under the noses of international inspectors that had been reviewing the declared activities in Iraq but were unaware of the clandestine program.

The international community responded with a reevaluation of safeguards and nonproliferation policy that included an acknowledgment of the need for IAEA safeguards to be significantly strengthened. Specifically, the IAEA needed the capability to detect undeclared nuclear activities in countries that were parties to the NPT. In 1997, the IAEA Board of Governors approved the "Additional Protocol" which allows for the use of environmental sampling to detect clandestine activities, earlier provision of design information on nuclear facilities to the IAEA, complementary access to additional locations within a country, and a broader use of open source, satellite imagery, and third party information to access nonproliferation performance in a particular nation. As of 2009, implementation of the Additional Protocol was complete or at a minimum underway in countries with significant nuclear programs.

Until the terror attacks on September 11, 2001, the diversion of nuclear material for a nation state's weapon program was the primary threat that nuclear safeguards programs were designed to mitigate and international policy experts had been focused. Those attacks demonstrated a higher level of sophistication than previously expected and brought the realization to international security professionals that nuclear terrorism sponsored by substate actors must also be considered as a significant threat to be addressed by nuclear security programs. In the last decade, the proliferation of nuclear materials and nuclear weapons to substate groups has replaced a potential nuclear confrontation between dominant superpowers as the preeminent global security concern. This has shifted emphasis in the nuclear security community to border monitoring, event attribution, and consequence management. In 2009, with the election of a new President in the USA, focus of international security policy and programs is returning to the threat from nations with large nuclear arsenals; however, it is certain that the terrorist threat will remain a greater concern than it was before 2001. Significant events that impacted the development of international nonproliferation and safeguards policy are shown in Table 19.1.

Technologies for Safeguarding Nuclear Materials

To properly secure nuclear materials, a state must know how much material it possesses and where it is located. This baseline is used to plan protection strategies, which mitigate the risks from both insider and outsider threats. The fundamental system that both provides this baseline information and allows the tracking and maintenance of the information as it changes over time is the nuclear material accounting system. To be effective, this system must be supported by a nuclear material measurement program, which provides accurate and precise information on the material being protected.

Table 19.1 Influential events in the development of international safeguards and nonproliferation policy

Date	Event
1945	USA's first nuclear test at the Trinity Site.
	Nuclear bombing of Hiroshima and Nagasaki.
1946	Formation of the United Nations Atomic Energy Commission (UNAEC).
	Baruch Plan presented.
1949	Soviet nuclear test.
	UNAEC dissolves.
1952	United Kingdom nuclear test.
1953	President Eisenhower presents Atoms for Peace.
1955	USA and Turkey conclude the first "Atoms for Peace" cooperative agreement for the peaceful uses of nuclear energy.
1956	International Atomic Energy Agency (IAEA) charter is approved.
1957	European Atomic Energy Community (Euratom) is established.
1959	First application of IAEA safeguards.
1960	French nuclear test.
1962	Cuban Missile Crisis.
1964	Chinese nuclear test.
1967	Treaty for the Prohibition of Nuclear Weapons in Latin America established.
1968	Treaty for the Non-Proliferation of Nuclear Weapons (NPT) established.
1974	Indian nuclear test.
1979	Three Mile Island nuclear accident.
1986	Chernobyl nuclear accident.
1991	Iraqi clandestine nuclear weapons program discovered.
1995	NPT is made permanent.
1997	IAEA approves the Additional Protocol.
1998	Pakistan's nuclear test.
2001	September 11, 2001 terrorist attacks in the USA.
2003	Disclosure of the A. Q. Kahn clandestine nuclear trade network.
2006	North Korean nuclear test.

Nuclear material accounting and nuclear material measurements must be closely coupled with a physical protection system that ensures that access to the material is controlled and the materials stay in their intended locations. The physical protection system consists of people, procedures, and technology, which are designed and implemented following a careful evaluation of system vulnerabilities against predicted threats. Each facility is unique; therefore, a systematic planning effort is required to manage risks appropriately.

Nuclear Material Accounting

Nuclear material accounting is not that different from managing inventory for a complicated manufacturing and warehouse operation or the accounting involved in today's banking systems. Matter of fact, initial nuclear materials accounting

developed from procedures and tools, which had been developed for financial and materials management. Today, nuclear material accounting is defined as the use of statistical and accounting measures to maintain knowledge of the quantities of SNM present in each area of a facility. It includes the use of physical inventories and material balances to verify the presence of material or to detect the loss of material after it occurs.

The quality of nuclear material accounting data and therefore the quality of the entire safeguards system is dependent on

- A measurement system that provides accurate, repeatable data on nuclear material quantities involved in both storage and internal or external transfers;
- Operating records that document nuclear material movements, locations, item identities, item histories, and links to the measurement data; and
- Accounting control procedures that include frequent cross-checking of data to detect inconsistencies, which may be indications of human error, unidentified measurement errors, or an attempt to divert or steal material.

The accounting system may divide a facility or process into sections, which are frequently called material balance areas (MBA) for monitoring and tracking of nuclear material (NM). Measurement, storage, and transfer records are maintained for each MBA. The choice of MBA boundaries will impact detection probabilities and should be carefully considered. The MBA will include defined key measurement points (KMP), where NM is in a form that can be measured to determine material flow or inventory. KMPs include, but are not limited to, all of the inputs and outputs to the MBA. Selection of appropriate KMPs is a fundamental requirement for timely detection of diversion or theft attempts. Ideally these KMPs would be identified during facility or process design to optimize their effectiveness while minimizing the impact on operational efficiency.

One of the primary goals of an accounting system is to monitor the inventory difference (ID) or material unaccounted for (MUF) within a facility or a specific area within a facility, such as an MBA, over a given period of time. The period of time used is typically the time between physical inventories of SNM within the facility, usually one or two months. The ID for SNM over this time period of interest, represented by t, is defined as:

$$ID_t = BI_t + R_t - EI_t - S_t \tag{19.1}$$

where BI is the beginning inventory of SNM, R is receipts of SNM during the inventory period, EI is the ending physical inventory of SNM, and S is shipments out of SNM during the inventory period. Note that all terms may have multiple individual components and include some uncertainty due to measurement and sampling errors. IDs are charted as a function of time and monitored for trends that may indicate a loss of nuclear material. If the safeguards practitioner understands the uncertainties in the components of each of the inputs to equation 3.1, the practitioner may propagate these uncertainties to determine the variance of the ID, σ_{ID}. The monthly ID may then be compared to statistical limits to

determine whether or not an indicator of theft or diversion may exist. An ID in excess of a significant quantity (SQ) indicates an abrupt loss of NM. Trends including systematic, smaller losses of NM over a period of time indicate a protracted loss of material. In some cases, protracted losses may be referred to as a trickle diversion.

A common performance measure for an accounting program is the magnitude of the ID variance, σ_{ID}. IDs must be maintained at a level sufficiently small to detect abrupt diversions, while a sequential test or alternative statistical test for trend detection may be used to detect both abrupt and protracted diversions [3–6]. Specific statistical tests are well documented in the literature and beyond the scope of this section. Safeguards practitioners must understand several issues that complicate the evaluation of IDs, including (1) the impact of holdup on σ_{ID}; (2) serial correlation in successive IDs; (3) poorly characterized measurement quality and its impact on estimates of σ_{ID}; and (4) time delays in the measurement results that are input components to the terms in equation 3.1. Without a detailed understanding of these effects, the practitioner will not be sensitive to the subtle variations and trends, the impact of nuclear process changes, or the impact of safeguards policy changes.

Nuclear Material Measurement Technology

The accurate quantification of nuclear material is essential to nuclear safeguards and as noted previously, the minimization of precision and bias in these measurements of NM is vital to the system's ability to detect abrupt and protracted diversion attempts. Measurement of NM is typically accomplished by either destructive wet chemistry techniques or nondestructive measurement of radiation or heat output. Nuclear material is found in multiple chemical forms, a wide range of quantities, and a variety of packaging configurations. Each of these variables introduces uncertainty into measurement results that must be carefully managed and considered when determining whether or not nuclear material is present and accounted for appropriately without evidence of diversion, theft, or misuse.

Destructive Analysis

Analytical chemistry typically provides the most accurate techniques for the quantification of pure metals and compounds of safeguards interest. These techniques require the destruction of a small sample of the nuclear material item, which must be homogenous to prevent the introduction of significant uncertainties from a sample that is not representative of the bulk item. The nature of these destructive analysis (DA) techniques requires ready access to the material to be analyzed. Finished material, such as a fuel rod, is not a candidate for DA for this reason. Some

of the more common techniques, which are described below, are gravimetry, titrimetry, and mass spectrometry [7, 8].

Mass spectrometry is a mature technology used for the determination of the isotopic composition of nuclear material samples. Samples to be analyzed in a thermal ionization mass spectrometer (TIMS) are deposited on a filament that is then inserted into the spectrometer and slowly heated by an electrical current. This results in ions of the sample "boiling off" after which they are accelerated by an electric field through a magnetic field, which is orthogonal to their trajectory. This results in a deflection of the ions, the magnitude of which is a function of the weight of the ion. Following the deflection, ions are collected at positions of interest that allow the analyst to infer the isotopic mass of each ion. The precision of this technique for the analysis of plutonium or uranium isotopics is better than 0.05% [7, 8]. Gas mass spectrometers and Isotope Dilution Mass Spectrometers (IDMS) are also in use and in many cases may lead to even better precision than TIMS.

Plutonium or Uranium can be burned to PuO_2 and $U_3O_{8,}$ respectively, and then accurately weighed. This technique, called gravimetry, can be performed in the laboratory with random and systematic errors of less than 0.05% [7, 8]. Nonvolatile impurities must be accurately determined and the gravimetric results then corrected accordingly.

Titration procedures are used to assay the amount of uranium or plutonium in solution through the careful addition of a reagent that reacts with the nuclear material. The measured amount of reagent to produce a particular endpoint is then related to the amount of NM. A typical endpoint is detected by a color change or electrical response of the solution. One of the most common techniques in use by the IAEA and other laboratories is the Davies–Gray method [7]. The precision for these techniques can be as good as 0.02% for uranium and 0.04 % for plutonium [7, 8].

DA techniques in use by the IAEA's Safeguards Analytical Laboratory (SAL) and its network of approved analytical laboratories are summarized in Table 19.2. In addition to requiring access to the material and destruction of a sample, DA techniques, in general, are more costly and time consuming than nondestructive techniques.

Nondestructive Assay

Many nuclear materials that one may encounter, such as a fuel assembly or a radioisotopic heat source, are technologically complex and have high economic value. Nevertheless, to adequately track and account for these materials, they must be quantified accurately. This necessitates the use of methods that do not alter their physical form or integrity of the item. Nondestructive assay (NDA) techniques can provide the necessary information and, although the precision and accuracy is generally poorer than DA, NDA is usually less expensive and can be performed within quicker time periods. DA and NDA should be viewed as complimentary techniques that are both necessary for a quality safeguards measurement program.

Table 19.2 IAEA destructive analysis techniques [7]

Technique	NM	Material Type	Random Error (%)	Systematic Error (%)
Davies–Gray	U	U, MOX	0.05	0.05
MacDonald–Savage	Pu	Pu materials	0.1	0.1
Controlled Potential Coulometry	Pu	Pure Pu	0.1	0.1
Ignition Gravimetry	U, Pu	Oxides	0.05	0.05
K X-ray Flouresence	Pu	Pu materials	0.2	0.2
Isotope Dilution Mass Spectrometry (IDMS)	U, Pu	Pu, MOX, spent fuel	0.1	0.1
Pu(IV) Spectrophotometry	Pu	Pu, MOX	0.2	0.2
Alpha Spectrophotometry	Np, Am, Cm	Spent fuel	5.0	5.0
Thermal Ionization Mass Spectrometry (TIMS)	U, Pu	Pure U, Pu	0.05	0.05

Most NDA techniques measure spontaneous or stimulated radiation or heat generated as a result of the radioactive decay process. Passive NDA methods measure radiation that is spontaneously emitted, while active techniques measure radiation that is stimulated by external neutron or gamma ray irradiation. Of the principal radiations, alpha and beta particles do not penetrate bulk material sufficiently to be of use to the NDA professional. On the other hand, x-rays, gamma rays, and neutrons are all electrically neutral, penetrate bulk materials, and are regularly used for NDA applied to nuclear safeguards.

Gamma rays and x-rays are photons with energies above that of the visible light spectrum. X-rays are emitted as result of changes in the electronic structure of the atom, while gamma rays are emitted when there is a change in the state of the nucleus. In commonly assayed nuclear materials, x-rays in the energy range 80–120 keV or gamma rays from 60–2,600 keV may be used for quantitative measurements. Since every isotope emits radiations at very precise energies and at well-characterized intensities, it provides a signature that is unique to that specific isotope and related to the amount of material present.

One of the most common NDA measurements is to determine the isotopic composition of plutonium or uranium by measuring the intensity of specific gamma rays produced by one isotope of interest relative to those from other isotopes present in the sample. For example, Fig. 19.1 shows spectra from two types of plutonium. If the spectra are carefully examined, one can see that the characteristics of each spectrum are highly dependent on the isotopic composition of the plutonium. Common instruments for the measurement of gamma ray spectra are scintillators, such as NaI, or semiconductors, such as high-purity germanium. Scintillators are materials that produce optical light pulses when the detector material interacts with a gamma-ray photon. The production of light is proportional to energy deposited in the detector material by the interacting gamma ray. Alternatively, when a gamma photon interacts with a semiconductor (solid-state) material,

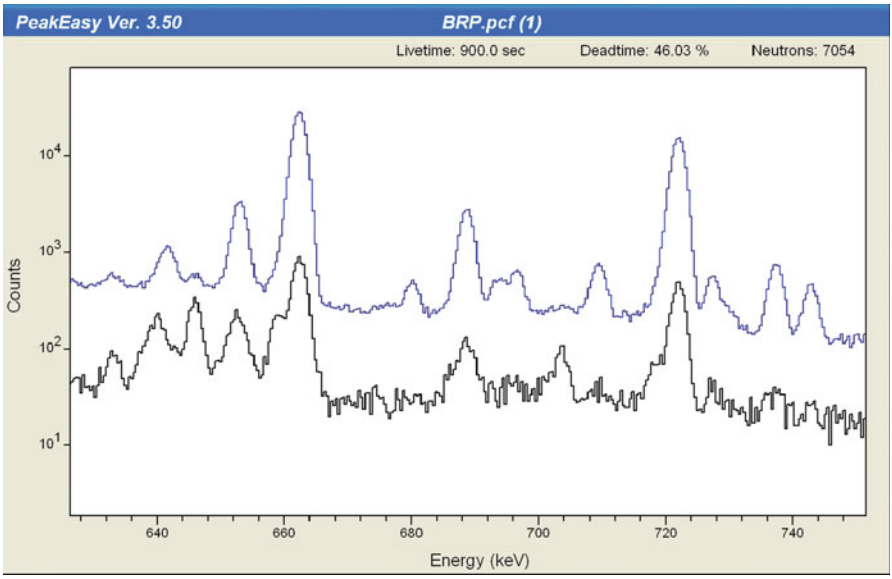

Fig. 19.1 Simulated High Purity Germanium spectra for weapons-grade and reactor-grade plutonium [9]

Table 19.3 Commonly used gamma detector materials [10]

Material	Type	Average Z	Density (g/cm^3)	Resolution % FWHM @ 662 keV	Resolution % FWHM @ 122 keV
$Bi_4Ge_3O_{12}$ (BGO)	Scintillator	28	7.1	12	28
NaI:Tl	Scintillator	32	3.7	7	13
$LaCl_3$:Ce	Scintillator	28	3.9	3.3	8
$LaBr_3$:Ce	Scintillator	41	5.3	2.8	7
Xe	Gas	54	0.4–0.5	2	7
CdZnTe	Solid-state	49	6.0	3.2	6.3
CdTe	Solid-state	49	6.1	0.6	1.5
Ge (thick planar)	Solid-state	32	5.3	0.2	0.4

it creates electron–hole pairs in proportion to the deposited energy. The characteristics of commonly used detector materials are delineated in Table 19.3. Resolution describes how well a given spectrometer can distinguish one gamma ray from another as a function of energy.

Under some conditions, the measurement of gamma rays may be used to determine the mass of NM present. Most nuclear materials have high atomic numbers and densities and therefore readily scatter and absorb their own radioactive emissions. By measuring the transmission of known gamma-ray intensities at one or more energies, the NDA professional may calculate correction factors to

account for the scatter and absorption in the item. It is common practice to use the 413.7 keV gamma ray from plutonium or the 185.7 keV gamma ray from uranium for mass measurements. It should be noted that the self-attenuation factor for plutonium is smaller than that for uranium, since the plutonium gamma ray of interest has a higher energy. This means that self-attenuation corrections for mass measurements of plutonium items are generally smaller than those required for uranium items.

Since many items to be assayed may have the nuclear material dispersed nonuniformly in a matrix that may also be nonuniform, systems that make attenuation correction frequently have to divide the measured item up into a number of elements that are measured individually and have attenuation correction factors determined for each individual element. Early systems used a technique called Segmented Gamma Scanning (SGS) [11]. The SGS measured the item as a series of horizontal slices; each slice was characterized individually and then summed to arrive at an overall result. With the powerful computers that became economically available in the early 1990s, a tomographic gamma scanner (TGS) was developed that divides an item up into a large number of volume elements [12]. The techniques used to calculate the absorption-corrected mass of nuclear material following the TGS measurement are similar to those used in computed tomography for medical applications. The accuracy of assay results for low-density matrices, such as combustible waste, is as good as 2–3%, but may be as high as 15–18% for higher density matrices such as sludge.

Like gamma rays, neutrons are electrically neutral, but they penetrate high-Z, high-density materials further than a gamma ray of the same energy. Therefore, the measurement of neutrons for the assay of special nuclear material is advantageous for large items and items in high-density matrices. At this point in time, neutron detectors in use around the world do little to distinguish one neutron from another of a different energy. However, neutron intensity and the time correlation of multiple neutron detections provide information that can be used to determine the amount of nuclear material present in a sample if the isotopic composition of the sample is already known. Most nuclear material assay applications in use today using neutrons, measure coincident neutrons that result from induced or spontaneous fission.

Most neutron detectors use ^{3}He gas proportional counters embedded in polyethylene. The ^{3}He has a large cross section (probability) for capturing thermal neutrons. The polyethylene acts as a moderator to slow down the neutrons, produced by fission or (α, n) reactions, to thermal energies where they have a higher probability of interaction with the ^{3}He gas. The capture interaction then results in the release of a triton and proton that share 765 keV of energy, which then ionize the gas and create an associated electronic pulse that can be measured. Passive detector systems developed using this basic technique have been installed in nuclear facilities for nuclear safeguards of plutonium that have demonstrated precisions of better than 2% [8, 13]. Plutonium measurement is the primary application of passive neutron counting since plutonium has a high rate of spontaneous fission from the decay of its even-numbered isotopes. Counters using higher-order

coincident neutrons from fission have also been developed and are in widespread use [14, 15]. Such multiplicity counters are advantageous for the measurement of impure plutonium-bearing items [16]. In general, the precision and accuracy of the measurements using multiplicity counting can be as good as 1–3% [8].

Uranium, due to its long radioactive decay half-lives, emits very few neutrons from spontaneous fission or (α, n) reactions, unlike plutonium. Therefore, effective assay of uranium via neutron measurement requires that the fission rate in the item be externally enhanced. By placing an external neutron source near the item, fissions will be induced in the sample. If the external source used to interrogate the sample produces uncorrelated neutrons, such as those from an AmLi source, they can be distinguished from those produced by the induced fissions in the sample, since these later neutrons will be correlated in time. Alternatively, one can use an external fission source, such as a small ^{252}Cf source, that can be moved away from the sample after inducing fissions or be turned off, such as a small accelerator. In these later two cases, the measurement of neutrons from the induced fissions is then conducted after the external source is no longer present.

The Active Well Coincidence Counter (AWCC), which is in common use around the world, uses AmLi sources to induce fissions in a uranium sample [17]. Its precision and accuracy have been reported to be better than 5% for the measurement of uranium [8]. Another advantage of using AmLi sources is that it produces neutrons with a mean energy of 0.5 MeV, which is below the fission threshold of ^{238}U. This allows the effective assay of ^{235}U in a sample of uncertain enrichment.

The Californium Shuffler is an example of an instrument that rapidly moves a spontaneous fission source away from a sample to allow subsequent measurement of the induced fissions [18, 19]. This instrument measures the delayed neutrons from fission. Approximately 1.6% of neutrons from fission reactions are produced a few seconds to minutes after the fission. For materials that are well represented with appropriate calibration standards, the shuffler technique has been reported to accuracy as good as 1–2%.

The differential die-away technique (DDT) was developed to use a pulsed accelerator producing 14 MeV neutrons as the external source. This technique has been successfully applied to the assay of both uranium- and plutonium-bearing wastes [20–22]. The combined thermal epithermal neutron (CTEN) method is similar to the DDT method, but interrogates the sample with both thermal and epithermal neutrons [23]. This is achieved partly by the addition of ^{4}He detectors, which have a faster response than the ^{3}He detectors and can detect fast fission neutrons in the presence of the epithermal interrogating flux. ^{4}He detectors rely on the recoil of light nuclei to ionize the gas in the detector tube, which is dependent on the elastic scattering cross section. Because epithermal neutrons are more penetrating in fissile material than thermal neutrons, the differential response can be analyzed to detect the occurrence of self-shielding by fissile material and measure the size of the effect. Self-shielding occurs when discrete lumps of fissile material are present, and can result in assay errors of several hundred percent. The DDT and CTEN methods have been applied to the measurement of SNM in waste containers and for the detection of the potentially smuggled SNM in packages [24].

Many nuclear materials, including plutonium and to some extent uranium, emit heat produced as a result of alpha particle absorption in the sample following radioactive decay. Plutonium produces 2–12 W of heat for each kilogram of material in the sample depending on the specific isotopic composition of the plutonium. Radiometric calorimeters measure the heat output of nuclear materials [25]. This method has seen wide application to plutonium and tritium samples, as well as large (kilogram) quantities of uranium and neptunium [26, 27]. Calorimetry is generally considered the most accurate and precise NDA technique for plutonium measurement since it is not subject to many of the biases that effect both gamma-ray and neutron measurements. Accuracy and precisions better than 1% are generally reported in the literature [28]. As is required for neutron-based NDA, the calorimetry data must be combined with isotopic data from gamma-ray or mass spectroscopy to obtain the total amount of plutonium in a specific item. Although calorimeters are the most accurate technique, it usually requires long measurement times (typically 4–8 h) and is not generally portable. These disadvantages make the application of calorimeters to international safeguards and inspection efforts very limited.

Detection of Nuclear Proliferation and Treaty Verification

There is a well-established historical record of states pursuing nuclear weapon development, even after accepting international obligations through treaties not to develop weapons. In recent years, those countries have included Iraq, Libya, and North Korea. It is likely that such trends will continue in the future. This necessitates that the international community have the capability to detect, deter, and even dismantle undeclared nuclear capabilities. It should be noted that Libya agreed to abide by the NPT in 2003 and following negotiations with the USA and Great Britain, the USA airlifted out of Libya components of the abandoned nuclear weapons program in 2004.

Open Source Information and Satellite Imagery

The analysis of open source information and commercial satellite imagery are two methods currently in use by the IAEA and state intelligence assets. Open sources of information include such things as publically available data, media reports, published scientific literature, business reports, information on technical conferences and meetings, and patent applications. Open sources of information are numerous and continuously changing. Each type of information must be assessed in relationship to the others in an attempt to establish an integrated picture of a state's legal nuclear programs, undeclared activity, and potential to breakout and quickly establish a nuclear weapons capability. The open source analyst, which

should have a broad technical background, must understand the potential quality pitfalls from the large volume of data available and then formulate useful search, query, and analysis strategies. This type of analysis requires sustained efforts over time, personnel with excellent research skills, and teams with multidisciplinary backgrounds [29].

Another open source is commercial satellite imagery, which has recently become available for anyone with modest computer access to view, identify, and monitor facilities that may be used in a nuclear weapons program. Commercial satellite images have been available since the 1970s, although at that time resolution was as poor as 80 m. Today, commercial images with resolution better than 0.5 m are becoming widely available for panchromatic data [30, 31]. Commercial satellites typically acquire images in the visible and/or near-infrared parts of the electromagnetic spectrum. Multispectral satellites, which collect data from more than one electromagnetic band, generally have poorer resolution (~2.5 m) than those collecting panchromatic data (black and white). An image that results from the fusion of the multispectral data and a panchromatic overlay is generally the best for facility and infrastructure analysis.

Imagery analysis is the process of identifying, analyzing, and attaching significance to the image data. An analyst's effectiveness requires

- Size – an ability to assess true and relative size of the objects being imaged
- Shape – an ability to determine physical characteristics
- Shadows – an ability to use the sun angle and orientation on the imaged objects
- Shade – an ability to use tonal brightness and contrast of objects of interest
- Surroundings – an ability to use context and setting of the objects including topographic and geographic information
- Signatures – an ability to use cultural or manmade features to help separate objects from their surroundings and to uniquely identify them
- Time – an ability to monitor temporal changes to provide insight on functionality, operating histories, or facility changes [32]

These techniques have been used multiple times in the detection and monitoring of clandestine nuclear activities. They are complementary to direct access inspections, open source analysis, and traditional nuclear safeguards (nuclear material accounting and measurements) in the detection and deterrence of nuclear weapons development.

Seismic and Hydroacoustic Monitoring

As a nation tries to develop new nuclear weapons, whether or not it already possesses one or more earlier generation nuclear weapons, they are likely to test new designs. It is probable that such tests would be conducted underground to both contain the fission products and conceal the exact nature of the test from other

countries. Hence, seismic monitoring is an important tool in the nonproliferation regime [33]. Monitoring requires the detection of the signal, separation of the signal from background and natural events (earthquake vs. explosion), as well as estimating the location and size of the event. There are more than 200,000 seismic events that are similar in magnitude to a small nuclear explosion every year. These events are either earthquakes or chemical explosions associated with peaceful applications, such as mining.

The energy released by a sudden movement of the earth's crust produces two types of elastic body-waves. The first to arrive at a monitoring station are the high velocity P-waves, which move in a direction parallel to the direction of the wave energy. S-waves move as transverse waves with motion perpendicular to the direction of wave propagation and arrive at the monitoring station at a later time relative to the P-wave. An explosion produces little S-wave energy relative to that produced by an earthquake. Therefore, the shape of the wave recorded by a monitoring station can be used to distinguish between an explosion and earthquake. The Comprehensive Test Ban Treaty, which was opened for signature in 1996, specifies a minimum detection level for explosions of 1 kiloton. This level, which is currently exceeded by international monitoring capabilities, corresponds to a seismic event of approximately 4.0 on the Richter scale. At some locations around the globe, monitoring capability is better than 2.5 on the Richter scale. How this relates to the size of a nuclear explosion is dependent on the geology between the event and the monitoring stations [34, 35].

Since more than 65% of the earth's surface is water, it is also important to monitor for explosive events in the world's oceans. Underwater explosions produce extremely powerful broadband acoustic signals. A sensitive hydrophone either suspended from a moored buoy or anchored to the ocean floor can be used to monitor low frequencies (1–100 Hz). Such low-frequency monitoring is optimal for detecting explosions over long distances. Today's hydrophones can detect signals more than 15,000 km from their source. The waveform detected can be used to differentiate explosions from underwater earthquakes or volcanoes.

Environmental Surveillance and Monitoring

Another tool that can be used to monitor treaty compliance or breakout activity by a proliferant is the surveillance of radionuclides present in the environment [36]. The fission products produced by nuclear fission and their isotopic ratios are an unambiguous and well-characterized indicator. However, unlike seismic or acoustic monitoring, it is not done in real time. Atmospheric and underwater explosions release particles carrying radionuclides as well as noble gases, while underground explosions release noble gases. In either case, the nuclides are then transported by air or water to monitoring stations. At that point in time, which may be several days or even weeks following the event, the analysis of the sample can confirm the nuclear event but not pinpoint the location. Combining seismic and acoustic monitoring with the atmospheric

surveillance, with meteorological data, can provide definitive evidence of a nuclear explosion and its location.

Most of the energy of a nuclear explosion is transformed into the immediate blast or the radiation released during the blast. Approximately 10% of the energy is released as residual radiation, which is emitted over time, through the decay of fission products generated during the nuclear blast. Fission products are produced in both gaseous and particulate form and most are radioactive. Following an atmospheric explosion, solid fission products attach to dust particles, which may then be propagated by winds over significant distances. Underwater explosions also release particles into the atmosphere. Underground explosions may be conducted in such a way that particles carrying radionuclides are contained. However, some fission products, particularly xenon, are noble gases that are much more difficult to contain and can be collected and analyzed by monitoring stations thousands of kilometers from the explosion site [37].

A radionuclide particulate monitoring station contains an air sampler and detection equipment. At the air sampler, air is forced through a filter, which typically retains 85% or more of all particles that reach it. The used filter is usually first cooled for a period of 24 h and then measured for another 24 h in the detection device at the monitoring station. The result is a gamma ray spectrum that the analyst can use to identify specific radionuclides. The analyst can use the spectrum to determine characteristics of the device tested and the nuclear material used in the device.

Detection and Prevention of Illicit Trafficking and Terrorism

Since the attacks in the USA on September 11, 2001, terrorism's threat against a country's national security has come under increased scrutiny. Although few terrorist organizations will implement acts of such devastation, it is considered by many experts that nuclear terrorism cannot be ruled out, and, because the devastation of a nuclear attack would be unmatched, the risks must be mitigated regardless of the low probability [38–40]. To mitigate these risks, one may increase security at the storage locations (strengthen nuclear safeguards), dispose of the nuclear materials in such a way that they are unavailable to the terrorists, strengthen methods to detect their misuse and transport once they have fallen into the wrong hands, and also develop methods through which illegal activity may be attributed to a particular national or subnational group.

Rigorous nuclear safeguards, which have been described previously, are only one layer in a defensive system against the use of nuclear materials by a subnational or terrorist organization. In addition to nuclear safeguards, the other layers of mature protection system would include monitoring of nuclear material in transit, robust intelligence collection and analysis, consequence management, and a vigorous response capability to a nuclear emergency or event to mitigate it prior to

a detonation. Each of these layers relies on, at least in part, the ability to detect and characterize nuclear or radiological materials at various points in their life cycle.

Nuclear smuggling is difficult to stop due to the small size of the materials required by the terrorist to make a nuclear bomb; the weak radiation many of these materials emit; the large number of smuggling routes; the large amount of legitimate traffic crossing these borders every year; and the existence of established smuggling networks for other contraband, such as illegal drugs. A recent analysis of 174 illicit radiological material trafficking incidents that have occurred since 1991 found little evidence of clear trends that can be used by nuclear security personnel [41]. It did note that the incidents involved a variety of radionuclides; however, approximately 60% of the cases involved Cesium-137, which happens to be an attractive isotope for radiological dispersal devices.

Border and Port Monitoring

Studies of illicit trafficking of nuclear and radiological materials have indicated that whether by auto, bus, train, or air, smugglers have consistently used transportation methods and routes that were most convenient to them, maintaining a close physical proximity to the materials [42]. During the past decade, one of the areas that has received international emphasis for this very reason is the improvement of border and port detection capability and protocols.

In the USA, one such effort is the Second Line of Defense program at the Department of Energy's National Nuclear Security Administration. This program seeks to interdict illicit trafficking of nuclear and radiological material through airports, seaports, and border crossings in Russia and other key transit states. This is to be accomplished by helping other nations install and use radiation detection equipment at these sites and by providing associated training and support. It is worth investing in improved border detection systems, but this line of defense will inevitably be porous, and one should not place undue reliance on it.

Fixed portal monitors have been installed at land, sea, and air facilities with the goal of detecting smuggled radioactive materials. Typically, these detectors use passive gamma measurement, which in its simplest and least expensive configuration utilizes gross gamma counting with little discrimination of the gamma-ray energy. Plastic scintillators are the most common detector material for this application and are inexpensively available in large sizes. Pedestrians, vehicles, or cargo pass through one or more pairs of these detectors. The number of gamma rays detected over the time interval during which the object is between the detectors can be used to trigger an alarm requiring the intervention of a guard or similar security personnel. There is a significant trade-off between the sensitivity of this method and the permissible duration that the object can be measured. Also, if the sensitivity is set such that frequent false alarms occur, security personnel may ignore alarms in order to keep traffic moving efficiently. Most of the radiation emitted by highly

enriched uranium (HEU) is weak, which means it is both easy to shield by the smuggler and difficult to detect through passive means. The detectors being deployed in the Second Line of Defense program simply detect gamma-ray radiation, without attempting to zero in on particular energy levels, and therefore have almost no ability to detect HEU above the background of natural radiation if the terrorist or smuggler uses even modest radiation shielding.

Efforts are underway to develop "advanced spectroscopic portal monitors" (ASPs) that do examine the energy ranges of different gamma rays. This will theoretically allow them to not only detect nuclear or radiological material, but also to identify the type of material. The ASPs are expected to reduce the rates of false alarms caused by naturally radioactive materials in legitimate shipment; however, they are significantly more costly than nonspectroscopic detectors and can only be manufactured with much lower detection probabilities. Thus, substantial controversy exists over whether there is a true benefit to their deployment.

Active detectors, such as neutron sources coupled with detectors to detect induced fission, may offer higher confidence of detecting HEU, even in a shielded configuration. Several methods are under active research and development that have been demonstrated to be highly effective at detecting shielded SNM. These detection methods are based on the active neutron techniques developed for nuclear safeguards discussed previously. Other development efforts are underway to use high-energy photons to induce fission. In both cases, neutron or photon sources, systems are in the developmental stages and not yet ready for wide-spread deployments.

Nuclear Forensics

In response to nuclear smuggling, which was first reported in 1991, a new branch of science was developed: "nuclear forensics" [43]. Analytical methods were initially borrowed from nuclear safeguards and supplemented with techniques developed for material science investigations. Over several ensuing years, techniques were standardized, new methods developed, and extensive databases of nuclear information compiled to guide the analysis and attribution of nuclear materials. As in other forensic fields, the analyst relies on the fact that certain measureable parameters in a sample are characteristic of the nuclear material and can be used to draw conclusions on the intended use or origin of the materials. Such attribution is an important deterrent to a nation state's participation, whether willingly or not, in smuggling activity.

The first category of characteristics to be exploited for nuclear forensics was major elemental and macroscopic composition of the interdicted nuclear material. Physical dimensions and isotopic composition of the major nuclear materials, usually uranium and plutonium, may be used to identify the intended use of the material. For example, plutonium with less than 7% ^{240}Pu is considered to be

weapons grade and likely produced for that purpose. The isotopic composition may also indicate the origin of the material. Since different types of nuclear reactors have different fuel loadings and neutron energy spectra, they generally produce plutonium of differing isotopic composition [44]. The concentration of the nuclear material may indicate stoichiometry of the compound or the presence of impurities, both of which may be indicators of the materials' source or status in a known nuclear fuel cycle. Fuel additives, which are used in the fuel cycle or material processing steps, such as gadolinium as a nuclear reactor burnable poison, may also be used by the analyst to narrow down the type of nuclear material present. In the case of manufactured items, such as nuclear fuel elements or pellets, the physical dimensions may allow the identification of the intended reactor type or design.

Further developments in the nuclear forensics field lead to the use of minor elemental as well as microscopic composition of the nuclear material in investigations initiated in the late 1990s [42]. This included chemical and isotopic analysis of individual particles as part of the forensic toolbox. Techniques such as secondary ionization mass spectrometry and scanning electron microscopy coupled with electron dispersive x-ray analysis allow for the isotopic composition of particles or powders to be determined. With powder samples, the analyst also gains information related to the sample homogeneity with regard to the isotopic composition and the particle size distribution.

In the past decade, analysts have also developed geolocation techniques and methods. Trace elements can be found in uranium at all stages of its mining, milling, and enrichment. Each processing step reduces the concentration of these trace elements and may introduce new trace contaminants. However, it has been noted that the pattern of certain impurities does not vary through the processing and may be used as a characteristic of the starting material. For example, the distribution of lead isotopes in the sample may be used as an indication of the age of the ore body and its initial U/Th ratio. The ratio of $^{18}O/^{16}O$ in a uranium oxide sample may be used to determine the temperature, latitude, and distance to the sea for the water used in the wet processing of the uranium [42].

The challenge in the interpretation of the many data sources discussed above is the accessibility of reference data. Efforts are underway to develop databases of reference forensic information. Data on nuclear materials produced for commercial applications, such as power production, are generally available with the various manufacturers and to some extent in open literature. However, some of the data is commercially sensitive and its availability is limited. Also, similar data on nuclear materials developed for weapons applications is generally protected for national security reasons.

Terrorism Response and Consequence Management

If a terrorist succeeds in smuggling nuclear or radiological material through the layers of nuclear safeguards and security at the source and subsequent national or international monitoring (such as the Second Line of Defense) it may then be

readied for use as a weapon. If monitoring stations, intelligence, or criminal investigations lead to the discovery of the material or weapon, a response is required to mitigate the threat. That response requires personnel familiar with weapons design, device characterization, weapon defusing and disposal, and consequence management.

To assist the response or management of the consequences of the event, small portable instruments are required for identification and quantification of the materials involved. Many responders, including those that may be on the incident scene first, such as police officers, today use hand-held or backpack size instruments called radioisotope identification devices (RIIDs). These instruments have undergone significant advancements over the past several years in both hardware and algorithms.

The algorithm used for isotope identification by a RIID plays a key role in obtaining a correct identification of the radioisotope. Correct ID is perhaps the most essential step in determining whether or not a true threat exists that requires a more extensive response for mitigation. The majority of RIIDs deployed around the world are based on NaI spectrometers. Their performance in isotope identification is generally poor and therefore secondary analysis of spectra by a trained spectroscopist is frequently necessary to resolve problems in the isotope identification. A trained spectroscopist is capable of identifying complicated, multiple-line sources with even the poorest resolution detectors, such as NaI. Many factors in detector performance, such as energy resolution, play an important role in isotope identification and are active areas of research [45–47].

Future Directions

World energy demand continues to grow and along with it does the demand for nuclear power, a carbon-free energy source. Some are predicting that world energy demand growth will exceed 50% over the next 20–25 years [48]. This expansion presents both challenges and opportunities to nuclear safeguards and nonproliferation. Challenges include the timely detection of diversion at large throughput fuel cycle facilities, new types of fuel cycles that may present challenges to accurate measurement of the fuel at appropriate KMPs, and the detection of nuclear material misuse in the background of activity required for a large-scale nuclear fuel cycle. Finally, significant expansion of nuclear power will also include increased nuclear material shipping, which creates its own issues related to continuity of knowledge and monitoring of the material in transit.

Addressing these future challenges will require advances in instrumentation, safeguards system analysis, modeling techniques, and data mining. On-line, near real-time monitoring methods using both radiation and nonradiation signatures will be required as part of integrated process monitoring schemes for new facilities. There will also be opportunities to incorporate nuclear safeguards and physical protection into the design of new facilities. This will allow the efficacy of the

safeguards system to be maximized while minimizing cost and impact to the facility.

Improvements in the detection of shielded nuclear material is one of the most active areas of research to improve border monitoring and other efforts related to illicit nuclear trafficking. As worldwide commerce continues to increase, so will the movement of goods around the world. This will necessitate that the false alarm rates of the current generation of portal monitors be significantly improved to avoid considerable negative impacts to commerce. Although this is another area of active research, implementable solutions are likely still several years away.

Bibliography

Primary Literature

1. Fischer D (1997) History of the International Atomic Energy Agency: the first 40 Years. IAEA, Austria
2. Kennedy RF (1968) Thirteen days: a memoir of the cuban missile crisis. McCall, New York
3. Jaech J (1973) statistical methods in nuclear materials control, U.S. Atomic Energy Commission
4. Burr T, Coulter C, Hakkila E, Ai H, Kadokura I, and Fujimaki K (1995) Statistical methods for detecting loss of materials using near-real time accounting data. 36th Annual Meeting of the Institute of Nuclear Materials Management, Palm Dessert, California
5. Picard R (1987) Sequential analysis of materials balances. J Nuclear Mater Manage 15(2):38–42
6. Zrdecki A, Armstrong J, Longmire V, and Strittmatter R (1997) Inventory difference analysis at Los Alamos Plutonium Facility. 38th Annual Meeting of the Institute of Nuclear Materials Management, Phoenix, Arizona
7. IAEA (2003) Safeguards Techniques and Equipment – 2003 Edition. IAEA/NVS/1 (revised), International Nuclear Verification Series No. 1, Austria
8. Aigner H, Binner R, Kuhn E, Blohm-Hieber U, Mayer K, Guardini S, Pietri C, Rappinger B, Mitterrand B, Reed J, Mafra-Guidicini O, and Deron S (2002) International target values 2000 for Measurement uncertainties in safeguarding nuclear materials. ESARDA Bulletin, No. 31
9. Garner S, (2009) personal communication, July 28, 2009
10. Russo P and Vo D (2005) Gamma-Ray Detectors for Nondestructive Analysis, Los Alamos National Laboratory, LA-UR-05-3813
11. Martin R, Jones D, Speir L, and Walker A (1974) Field assay of plutonium with a new computerized segmented gamma scan instrument, Los Alamos Scientific Laboratory, LA-UR-74–924
12. Estep R, Prettyman T, Sheppard G (1993) Tomographic gamma scanning to assay heterogeneous waste. Nuc Sci Eng 118:145–152
13. Menlove H, Swansen J (1985) A high-performance neutron time correlation counter. Nuclear Technol 71:497–505
14. Krick M, Swansen J (1984) Neutron multiplicity and multiplication measurements. Nucl Inst Methods 219:384–393
15. Langer D, Krick M, Ensslin N, Bosler G, and Dytlewski N (1991) Neutron multiplicity counter development, Proceedings of the 13th Annual ESARDA Symposium, Avignon, France

16. Stewart J, Krick M, Langer D, and Wenz T (1998) Neutron multiplicity assay of impure materials using four different neutron counters, 39th Annual Meeting of the Institute for Nuclear Materials Management, Naples, Florida
17. Menlove H, Foley J, and Bosler G (1980) Application of the active well coincidence counter to the measurement of uranium, 2nd Symposium on Safeguards and Nuclear Material Management, Edinburgh, Scotland
18. MacMurdo K, Bowman W (1977) Assay of fissile materials by a cyclic method of neutron activation and delayed neutron counting. Nucl Inst Methods 141:299–306
19. Menlove H, Crane T (1978) A ^{252}Cf Nondestructive assay system for fissile material. Nucl Inst Methods 152:549–557
20. Kunz W, Atencio J, and Caldwell J (1980) A 1-nCi/g Sensitivity transuranic waste assay system using pulsed neutron interrogation, 21st Annual Meeting of the Institute for Nuclear Materials Management
21. Caldwell J, Hastings R, Herrera G, and Kunz W (1986) The Los Alamos second-generation system for passive and active neutron assays of drum-sized containers, Los Alamos National Laboratory LA-10774-MS
22. Rinard P, Coop K, Nicholas N, Menlove H (1994) Comparison of shuffler and differential die-away technique instruments for the assay of fissile materials in 55-gallon waste drums. J Nuclear Mater Manage 22(3):4–28
23. Coop K and Hollas C (1996) Epithermal interrogation of fissile waste, Institute of Nuclear Materials Management Annual Meeting, Naples, Florida
24. Rooney B, York R, Close D, and Williams H (1998) Active interrogation package monitor, IEEE Nuclear Science Symposium, Toronto, Canada
25. Bracken D, Biddle R, Carillo L, Hypes P, Rudy C, Schneider C, Smith M (2002) Application guide to safeguards calorimetry, Los Alamos National Laboratory LA-13867-M
26. Walsh T, Hamilton R, Baker E, Hurlbut S, Fazzari D, Delegard C, McRae L, Liebetrau A, Lemaire R, and DeRidder P (1996) Plutonium assay for safeguards purposes: material heterogeneity and application of calorimetry, 37th Annual Meeting of the Institute for Nuclear Materials Management, Naples, Florida
27. Thornton M, Vassallo G, Miller J, Mason J (1995) Design and performance testing of a tritium calorimeter. Nucl Inst Methods A363:598–603
28. Guardini S (2003) Performance Values for Nondestructive Assay (NDA) techniques applied to safeguards: The 2002 evaluation by the ESARDA NDA Working Group, ESARDA Bulletin 31
29. Wallace R, Anzelon G, Essner J (2009) Safeguards information from open sources. J Nuclear Mater Manage 37(4):30–40
30. Hitchens T (2006) European eyes in the sky: strategic independence is focus as security comes to the forefront. Imaging Notes 21(3):20–24
31. Niemeyer I (2009) Safeguards information from satellite imagery. J Nuclear Mater Manage 37(4):41–48
32. Pabian F (2008) Commercial satellite imagery: another tool in the nonproliferation verification and monitoring toolkit, Chapter 12 of nuclear safeguards, security, and nonproliferation. Elsevier, New York
33. Hannon W (1985) Seismic verification of a comprehensive test ban. Science 227(4684):251–257
34. Bache T (1982) Estimating the yield of underground nuclear explosions. Bull Seismol Soc Amer 72(6B):S131–S168
35. Taylor S, Dowla F (1991) Spectral yield estimation of NTS explosions. Bull Seismol Soc Amer 81(4):1292–1308
36. Yutaka M, Tetsuzo O, Hiroshi N, Hideo N (1998) Overview of atmospheric radionuclide monitoring techniques for CTBT International Monitoring System, Proceedings of the Annual Meeting of INMM Japan Chapter, 19:129–130

37. Carrigan C, Heinie R, Hudson G, Nitao J, Zucca J (1996) Trace gas emissions on geological fualts as indicators of underground nuclear testing. Nature 382:528–531
38. Ferguson C, Potter W, Sands A, Spector L, Wehling F (2005) The four faces of nuclear terrorism. Routledge, New York
39. Jenkins BM (2008) Will terrorists go nuclear? Prometheus Books, New York
40. Allison G (2005) Nuclear terrorism: the ultimate preventable catastrophe. Holt Paperbacks, New York
41. Kerst R (2009) Trends and patterns in illicit trafficking of radioactive sources, LLNL-GS-0052-2009, Lawrence Livermore National Laboratory
42. Battelle Memorial Institute (2009) Nuclear smuggling handbook: case studies and detection methods
43. Mayer K, Wallenius M, Fanghanel T (2007) Nuclear forensic science – from cradle to maturity. J Alloys Compounds 444–445:50–56
44. Wallenius M, Lutzenkirchen K, Mayer K, Ray I, Aldave de lss Heras L, Betti M, Crombroom O, Hild M, Lynch B, Nicholl A, Ottmar H, Rasmussen G, Schubert A, Tamborini G, Thiele H, Wagner W, Walker C, Suleger E (2007) Nuclear forensic investigations with a focus on plutonium. J Alloys Compounds 444–445:57–62
45. Sullivan C, Garner S, Lombardi M, Butterfied K, Smith-Nelson M (2007) Evaluation of key detector parameters for isotope identification. IEEE Nuclear Sci Symposium Conf Record 2:1181–1184
46. Keyser R, Rwomey T, Upp D (2005) A Comparison of an HPGe-based and NaI-based Radioisotope Identifier (RIID) for radioactive materials. ESARDA Symposium, London
47. Sullivan C, Garner S, Blagoev K, Weiss D (2007) Generation of customized wavelets for the analysis of gamma-ray spectra. Nuclear Instruments Methods A 579(1):275–278
48. Energy Information Administration (2007) International Energy Outlook 2007, DOE/EIA-0484

Books and Reviews

Doyle JE (ed) (2008) Nuclear safeguards, security, and nonproliferation: achieving security with technology and policy. Elsevier, New York
Hakansson A, Jonter T, (2007) An Introduction to Nuclear Non-Proliferation and Safeguards. SKI Report 2007:44
IAEA, (2007) Combating illicit trafficking in nuclear and other radioactive material: reference manual, IAEA Nuclear Security Series No. 6. International Atomic Energy Agency, Vienna
Moody K, Hutcheon I, Grant P (2005) Nuclear forensic analysis. CRC Press, Boca Raton
Mozley RF (1998) The politics and technology of nuclear proliferation. University of Washington Press, Seattle/London

Index

N. Tsoulfanidis (ed.), *Nuclear Energy: Selected Entries from the Encyclopedia of Sustainability Science and Technology*, DOI 10.1007/978-1-4614-5716-9,